US Army Corps of Engineers

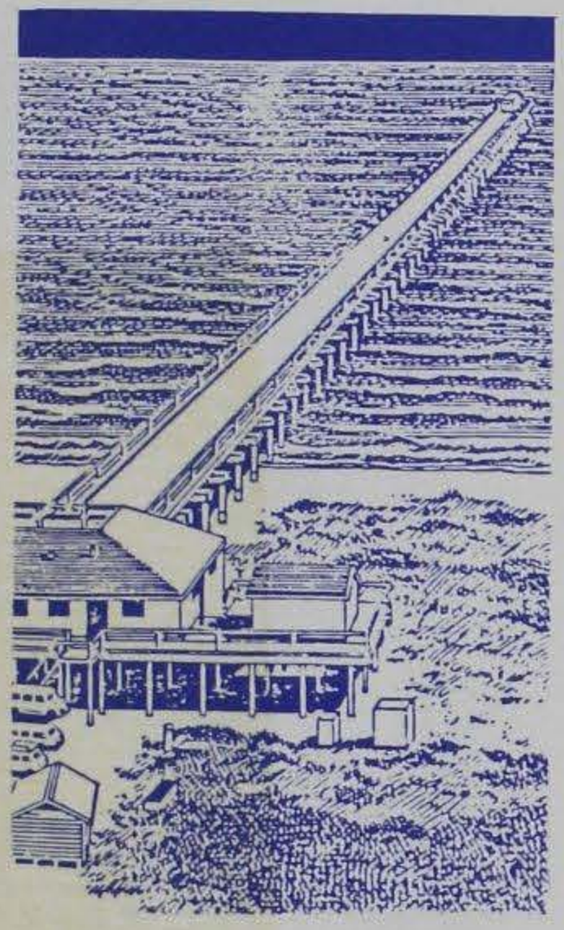

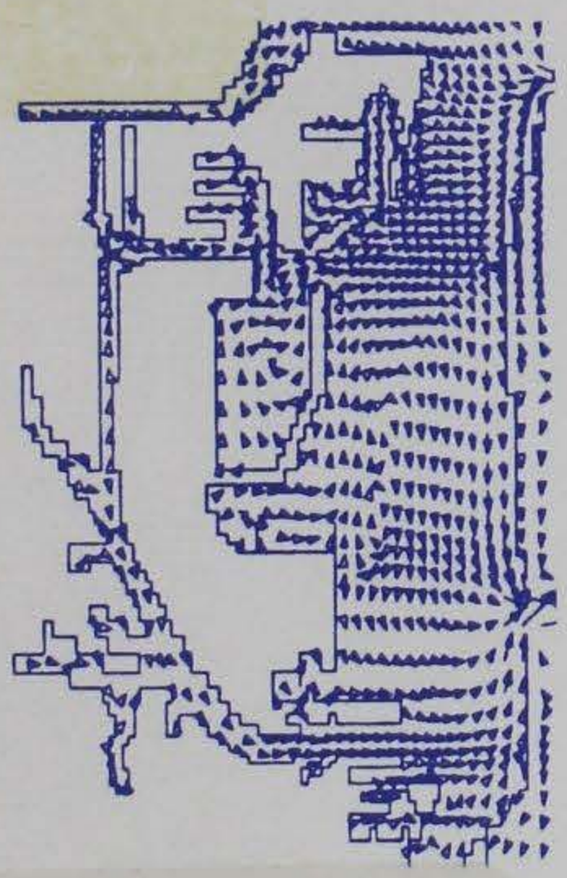

2

TECHNICAL REPORT CERC-90-16

LOS ANGELES AND LONG BEACH HARBORS MODEL ENHANCEMENT PROGRAM

THREE-DIMENSIONAL NUMERICAL MODEL TESTING OF TIDAL CIRCULATION

by

Coastal Engineering Research Center

DEPARTMENT OF THE ARMY
Waterways Experiment Station, Corps of Engineers
3909 Halls Ferry Road, Vicksburg, Mississippi 39180-6199

September 1990
Final Report

Approved For Public Release; Distribution Unlimited

Prepared for US Army Engineer District, Los Angeles
Los Angeles, California 90053-2325

Port of Los Angeles
San Pedro, California 90733-0151

and Port of Long Beach
Long Beach, California 90801-0570

When this report is no longer needed return it to the originator.

The findings in this report are not to be construed as an official Department of the Army position unless so designated by other authorized documents.

The contents of this report are not to be used for advertising, publication, or promotional purposes. Citation of trade names does not constitute an official endorsement or approval of the use of such commercial products.

Unclassified
SECURITY CLASSIFICATION OF THIS PAGE

REPORT DOCUMENTATION PAGE

Form Approved
OMB No. 0704-0188

1a. REPORT SECURITY CLASSIFICATION
Unclassified

1b. RESTRICTIVE MARKINGS

2a. SECURITY CLASSIFICATION AUTHORITY

2b. DECLASSIFICATION / DOWNGRADING SCHEDULE

3. DISTRIBUTION / AVAILABILITY OF REPORT
Approved for public release; distribution unlimited

4. PERFORMING ORGANIZATION REPORT NUMBER(S)
Technical Report CERC-90-16

5. MONITORING ORGANIZATION REPORT NUMBER(S)

6a. NAME OF PERFORMING ORGANIZATION
USAEWES, Coastal Engineering Research Center

6b. OFFICE SYMBOL (*If applicable*)

7a. NAME OF MONITORING ORGANIZATION

6c. ADDRESS (*City, State, and ZIP Code*)
3909 Halls Ferry Road
Vicksburg, MS 39180-6199

7b. ADDRESS (*City, State, and ZIP Code*)

8a. NAME OF FUNDING / SPONSORING ORGANIZATION
See reverse.

8b. OFFICE SYMBOL (*If applicable*)

9. PROCUREMENT INSTRUMENT IDENTIFICATION NUMBER

8c. ADDRESS (*City, State, and ZIP Code*)

10. SOURCE OF FUNDING NUMBERS

PROGRAM ELEMENT NO.	PROJECT NO.	TASK NO.	WORK UNIT ACCESSION NO.

11. TITLE (*Include Security Classification*)
Los Angeles and Long Beach Harbors Model Enhancement Program: Three Dimensional Numerical Model Testing of Tidal Circulation

12. PERSONAL AUTHOR(S)

13a. TYPE OF REPORT	13b. TIME COVERED	14. DATE OF REPORT (*Year, Month, Day*)	15. PAGE COUNT
Final report	FROM _____ TO _____	September 1990	192

16. SUPPLEMENTARY NOTATION
Available from National Technical Information Service, 5285 Port Royal Road, Springfield, VA 22161.

17. COSATI CODES		
FIELD	GROUP	SUB-GROUP

18. SUBJECT TERMS (*Continue on reverse if necessary and identify by block number*)
Harbors; Long Beach Harbor; Tidal circulation; Hydrodynamics; Numerical models; Los Angeles Harbor; Three-dimensional models

19. ABSTRACT (*Continue on reverse if necessary and identify by block number*)

To meet future needs, the Ports of Los Angeles and Long Beach have undertaken a long-range cooperative planning effort known as the 2020 Plan. Under this master plan, a number of phased plans have been determined to accommodate future needs. These plans involve deepening of ship channels and harbors and creation of new landfills. The purpose of the study described in this report was to determine three-dimensional (3-D) hydrodynamics of tidal and wind-driven circulation for existing conditions as well as a plan condition selected by the ports. This goal was accomplished by applying a state-of-the-art, 3-D numerical hydrodynamic model called CH3D. The model results also were used to drive a separate water quality model.

In order to calibrate and verify the CH3D model, comprehensive field data were collected in the summer of 1987. These included surface elevation data measured at eight
(Continued)

20. DISTRIBUTION / AVAILABILITY OF ABSTRACT
☒ UNCLASSIFIED/UNLIMITED ☐ SAME AS RPT. ☐ DTIC USERS

21. ABSTRACT SECURITY CLASSIFICATION
Unclassified

22a. NAME OF RESPONSIBLE INDIVIDUAL

22b. TELEPHONE (*Include Area Code*)

22c. OFFICE SYMBOL

DD Form 1473, JUN 86 *Previous editions are obsolete.*

SECURITY CLASSIFICATION OF THIS PAGE
Unclassified

8a. NAME AND ADDRESS OF FUNDING/SPONSORING ORGANIZATION (Continued).

US Army Engineer District, Los Angeles
Los Angeles, CA 90053-2325;

Port of Los Angeles
San Pedro, CA 90733-0151;

Port of Long Beach
Long Beach, CA 90801-0570

19. ABSTRACT (Continued).

locations, current measurements with in situ current meters deployed at nine stations, current velocity profile measurements taken at major entrances to the harbors and interior channels, and a drogue study.

For the numerical simulation, a variable, rectilinear grid containing 12,032 cells was used in the horizontal. In the vertical, a stretching mechanism was used to represent the bathymetry smoothly. Several sensitivity tests were conducted to determine model response to variation of key model parameters. On the basis of the tests, three cells were used in the vertical. The period from 7 to 11 August 1987 representing a large spring tide was used for model calibration, and the period from 19 to 23 August 1987 representing a mean tide was used for verification. In each case, the model was started from rest and forced with measured surface elevations at the open boundary and wind stresses, computed from measured wind data, at the free surface. Comparison of model results with observed surface elevations and currents indicated the model reproduced prototype behavior throughout the harbor complex and overall calibration and verification were successful.

In order to demonstrate model use in investigating plan conditions, a plan condition known as Scheme B, Phase 1 was tested in the model. Model bathymetry was modified to represent plan conditions. Base conditions adopted for comparing the plan with existing conditions were the two periods used for model calibration and verification. Comparison of model results for plan with existing conditions indicated tidal ranges were maintained and there were no noticeable differences in phase. Discharge into the system was reduced by an amount equivalent to the reduced harbor surface area (about 10 percent). Velocity magnitude and direction were changed at specific locations. Peak flood and ebb velocities at Angel's and Queen's Gates were reduced up to 50 and 40 percent, respectively, for a large spring tide condition. Net circulation in the Inner Harbor showed a tendency to reverse under plan conditions.

PREFACE

This report was prepared by the Coastal Engineering Research Center (CERC) at the US Army Engineer Waterways Experiment Station (WES) and is a product of the Los Angeles and Long Beach Harbors Model Enhancement (HME) Program. The HME Program has been conducted jointly by the Ports of Los Angeles and Long Beach (LA/LB); the US Army Engineer District, Los Angeles (SPL); and WES. The purpose of the HME Program has been to provide state-of-the-art engineering tools to aid in port development. In response to the expansion of oceanborne world commerce, the LA/LB are conducting planning studies for harbor development in coordination with SPL. Ports are a natural resource, and enhanced port capacity is vital to the Nation's economic well-being. In a feasibility study being conducted by SPL, the LA/LB are proposing a well-defined and necessary expansion to accommodate predicted needs in the near future. The Corps of Engineers (CE) will be charged with the responsibility for providing deeper channels and determining the effects of this construction on the local environment. Changes in tidal circulation and harbor flushing need to be examined to determine how expansion and channel deepening will affect water quality in the harbors and local vicinity.

The investigation was conducted during the period February 1987 through September 1988 by personnel of the Coastal Processes Branch (CPB) and Coastal Oceanography Branch (COB), Research Division (RD), and the Wave Processes Branch (WPB), Wave Dynamics Division (WDD). The CPB personnel involved in the study were Dr. S. Rao Vemulakonda, Messrs. Bruce A. Ebersole and David J. Mark, and Mses. Lucia W. Chou and Brenda D. Grimes under the direct supervision of Dr. Steven A. Hughes, former Chief, CPB; Dr. Lyndell Z. Hales, Acting Chief, CPB; and Mr. H. Lee Butler, Chief, RD. Also involved in the study was Mr. Paul D. Farrar of COB, under the direct supervision of Dr. Edward F. Thompson, Chief, COB, and Mr. Butler. The WPB personnel involved were Messrs. Ernest R. Smith and William C. Seabergh under the direct supervision of Mr. Douglas G. Outlaw, Chief, WPB, and Mr. C. E. Chatham, Chief, WDD. Overall CERC management of the HME Program was furnished by Messrs. Outlaw and Seabergh. Personnel of the Prototype, Measurement and Analysis Branch (PMAB), Engineering Development Division (EDD), who provided analyzed prototype data were Messrs. David D. McGehee, Andrew Morang, and James P. McKinney under the direction of Mr. J. Michael Hemsley, Acting Chief, PMAB, and Mr. Thomas W. Richardson, Chief, EDD. This study was under the

general supervision of Dr. James R. Houston, Chief, CERC, and Mr. Charles C. Calhoun, Jr., Assistant Chief, CERC.

During the course of the study, liaison was maintained between WES, SPL, and the Ports. Mr. Dan Muslin, followed by Mr. Angel P. Fuertes, was SPL point of contact. Mr. John Warwar and Ms. Lillian Kawasaki, Port of Los Angeles, and Mr. Michael Burke, followed by Mr. Rich Weeks and Dr. Geraldine Knatz, Port of Long Beach, were LA/LB points of contact and provided invaluable assistance.

Commander and Director of WES during publication of this report was COL Larry B. Fulton, EN. Dr. Robert W. Whalin was Technical Director.

CONTENTS

LIST OF FIGURES

CONVERSION FACTORS, NON-SI TO SI (METRIC)
UNITS OF MEASUREMENT

Non-SI units of measurement used in this report can be converted to SI (metric) units as follows:

Multiply	By	To Obtain
acres	0.00404686	square kilometres
cubic feet	0.028317	cubic metres
degrees (angle)	0.01745329	radians
feet	0.3048	metres
knots	0.5144	metres per second
miles (US statute)	1.6093	kilometres
miles per hour (mph)	0.4470	metres per second
square feet	0.0929	square metres
square miles	2.590	square kilometres

LOS ANGELES AND LONG BEACH HARBORS

MODEL ENHANCEMENT PROGRAM

THREE-DIMENSIONAL NUMERICAL MODEL TESTING OF TIDAL CIRCULATION

PART I: INTRODUCTION

1. Los Angeles and Long Beach (LA/LB) Harbors are located adjacent to each other on the California coast and share a common breakwater system that encloses one of the largest harbor systems in the world (Figure 1). The harbors' history since the 1890's has largely been one of continuous expansion to meet the demands of world commerce and national security. As larger ships were built, channels were deepened to accommodate them. Dredged material could then be used to create additional landfill for facilities. Thousands of acres of landfill have created the harbor complex as it exists today (Figure 2).

2. Once again a dramatic increase in activity is predicted for the Pacific trade routes. To meet the trade needs of the Nation, the Ports of Los Angeles and Long Beach have undertaken a long-range cooperative planning effort known as the 2020 Plan. A special study known as the Operations, Facilities, and Infrastructure (OFI) Study was performed to determine the cargo handling requirements necessary. The study determined a variety of phased plans that could accommodate future needs. Incorporated in the plans are 2,400 acres* of new landfill and 600 acres of new development on existing land. Thirty-eight new terminals are planned along 7 miles of deep-draft ship channels. Also included are systems of highway and rail connectors and intermodal container transfer facilities.

Objective

3. The purpose of the study described in this report is to determine three-dimensional (3-D) hydrodynamics of tidal and wind-driven circulation for the existing harbors and to demonstrate model use in investigating a Phase 1

---

* A table of factors for converting non-SI units of measurement to SI (metric) units is presented on page 5.

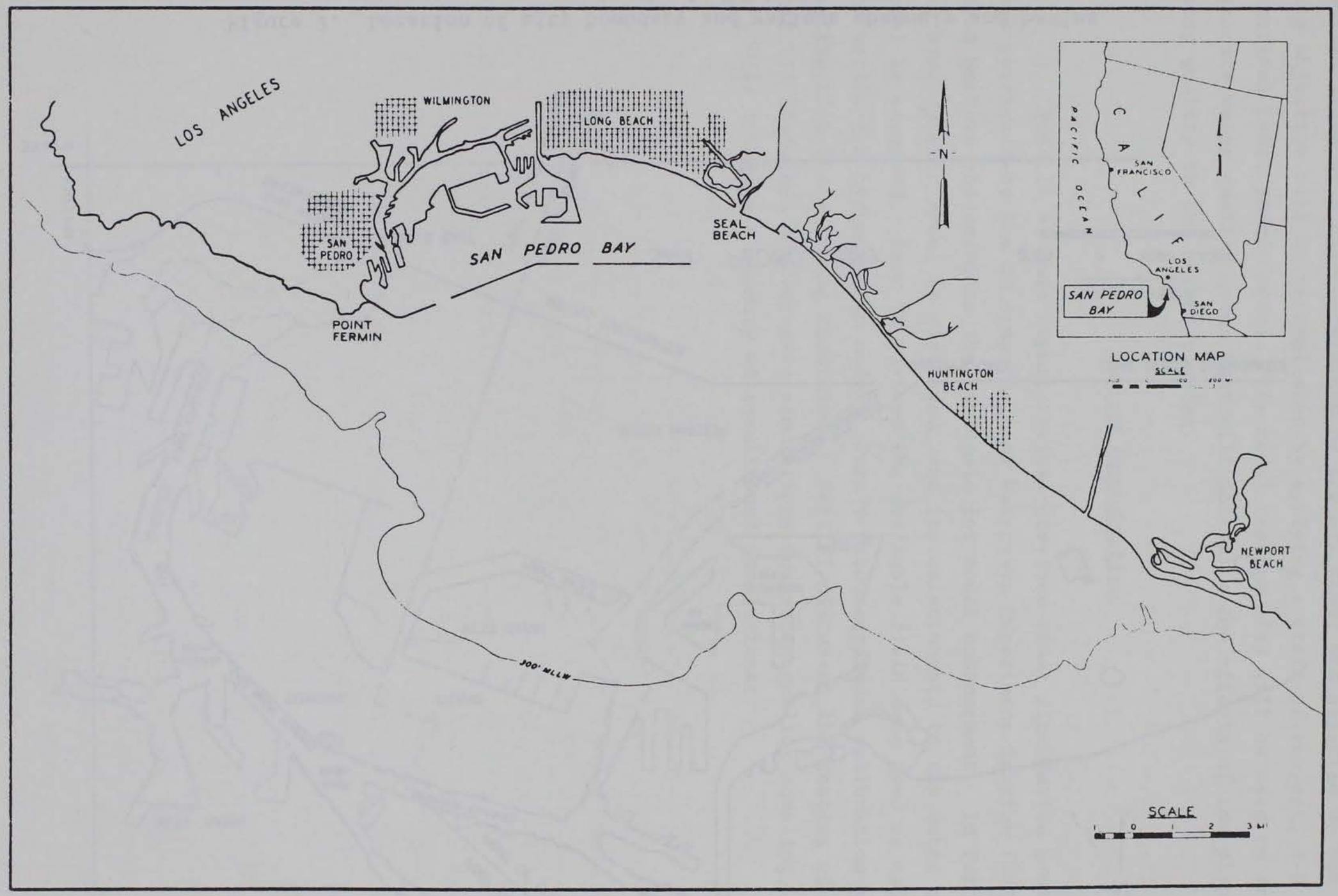

Figure 1. Vicinity map

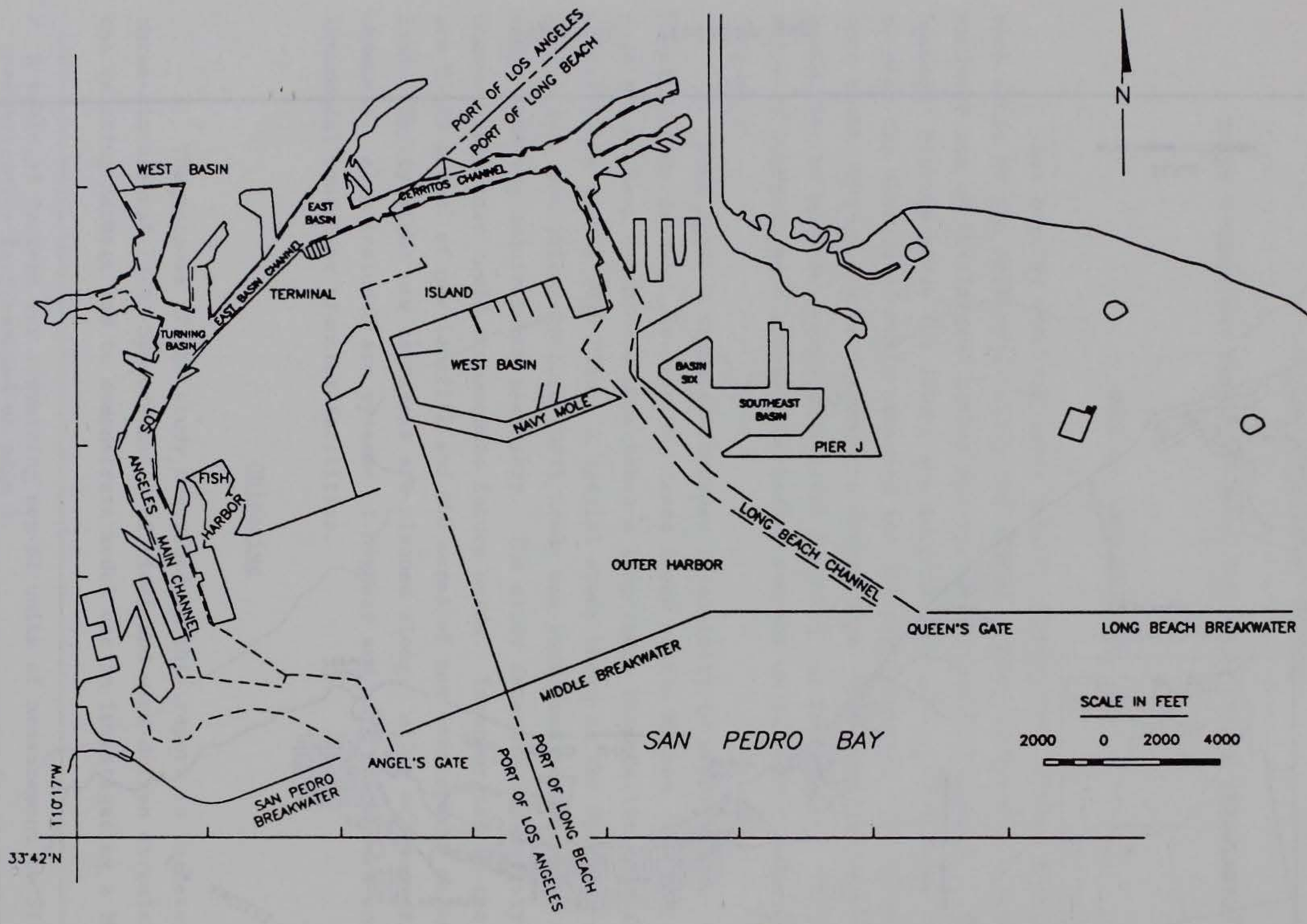

Figure 2. Location of city boundary and various channels and basins in the LA/LB Harbors

configuration of a plan determined by the OFI study and selected by the ports. This objective will be accomplished by applying a state-of-the-art, 3-D numerical hydrodynamic model. The model results also will be used to drive a separate water quality model that will determine the effects of the plan on water quality in the harbor complex.

Report Organization

4. Part II of this report reviews previous tidal circulation modeling work performed by the US Army Engineer Waterways Experiment Station (WES) for LA/LB Harbors and examines the rationale for model enhancement. In Part III, the hydrodynamic model is discussed, and its relationship to the water quality model is examined. Part IV reviews the available field data used to calibrate and verify the hydrodynamic model. Part V discusses model calibration and verification for existing conditions. Part VI discusses the testing of plan, Part VII describes hydrodynamic simulations for water quality modeling, and Part VIII contains a summary of results and conclusions.

PART II: PREVIOUS STUDIES

5. A physical model of the LA/LB Harbors was constructed at WES in 1973 to study tidal circulation and harbor oscillations. The initial tidal circulation test results were reported by McAnally (1975). The 1:400 horizontal scale, 1:100 vertical scale distorted model was calibrated with a limited prototype data set. Some difficulties were encountered in the measurement of the relatively low velocities that normally exist in the harbors inside the breakwaters. A satisfactory calibration was obtained, and the model was tested for a number of plan conditions. However, during the mid-1970's, computer modeling of hydrodynamics was becoming more feasible as computer memory and speed increased. It was felt that computer modeling would be an alternative approach to modeling tidal circulation in harbors with relatively low velocities (normally less than 1 ft/sec). Also, the physical model was heavily used at the time to examine harbor resonance conditions for wave periods in the 30- to 400-sec range.

6. During 1975-76, a numerical model was applied by WES to study tidal circulation in the LA/LB Harbors. The model selected for use was a two-dimensional (2-D), depth-averaged numerical model of the hydrodynamic equations. This model neglected the vertical components of velocity and acceleration, and the general 3-D governing hydrodynamic equations were integrated over the water depth. In this way, 3-D geometry could be considered. The model solved the governing equations using a finite difference approximation of the equations and an alternating direction semi-implicit technique. Application to San Pedro Bay required use of a grid of 20,000 finite difference cells, each cell representing a 300-ft square of the harbor region. The model reproduced a 25-hr prototype tide sequence and was applied by Raney (1976a,b) and by Outlaw and Raney (1979) for plans that included a proposed Outer Harbor oil terminal in the Port of Long Beach in conjunction with a proposed Los Angeles Harbor deepening project. These studies indicated that the plans resulted in only minor overall changes in tidal circulation in LA/LB Harbors and that any changes were very local in nature.

7. Improvements, which increased numerical stability, were implemented in the previously discussed model permitting reproduction of longer prototype scenarios. Also, utilization of a stretched grid having the capability to be smoothly varied permitted simulation of a complex planform by locally increasing resolution. Figure 3 shows the grid as applied to LA/LB Harbors.

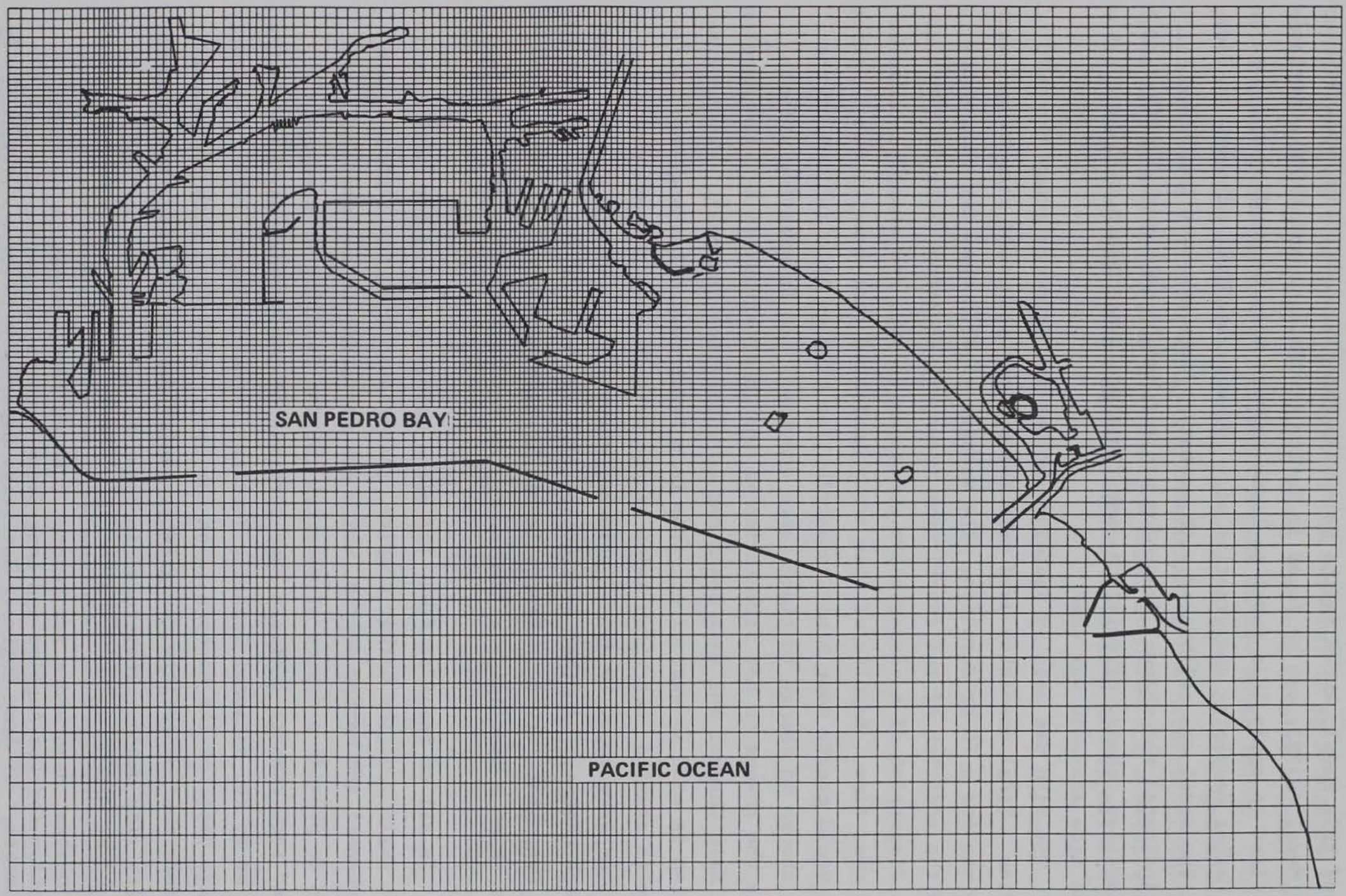

Figure 3. Grid layout over the LA/LB Harbors

Details of this model, known as the Waterways Experiment Station Implicit Flooding Model (WIFM), can be found in Butler (1978a,b,c, and 1980). Outlaw* was the first to apply this model to LA/LB Harbors when he studied the Los Angeles Harbor deepening and creation of a 190-acre landfill adjacent to Fish Harbor. The model was calibrated with prototype data measured in 1972. Results indicated the channel deepening project had no substantial effect on tidal elevation, phase, circulation, and flushing. Once again a 25-hr prototype tide scenario was used.

8. The WIFM was used by Seabergh and Outlaw (1984) to study the 2020 Master Plan. Tidal scenarios used were for spring, mean, and neap tides; each scenario was for a 70-hr duration. The version of WIFM used for this study included the addition of the constituent transport equation (Schmalz 1983) so that the dispersion of a conservative substance (a dye, for example) could be followed over time. Results of this study indicated that a major Outer Harbor landfill would create some minor redistribution of flow into and out of the harbors, though no change in tidal range occurred. An interesting effect noted was the change in net circulation in the Inner Harbor (i.e., Los Angeles Harbor's Main Channel and Long Beach Harbor's Cerritos Channel). Existing net circulation is east to west (i.e., from Long Beach toward Los Angeles), while for the plan studied, net circulation became west to east. These net circulations were about 10 and 17 percent, respectively, of the average flow in the back channel. Another application of WIFM was made for the Port of Los Angeles' Deep Draft Dry Bulk Export Terminal, Alternative No. 6 (Seabergh 1985), in which a landfill was studied on the Los Angeles side of the Outer Harbor.

9. In all of these studies, the plans examined called for landfills in different regions of the harbor complex. Associated with the landfills are greater channel and harbor depths, which are necessary to accommodate larger ships and to provide a source of material for the landfill by dredging. Forecasted requirements indicate some portions of the harbors may have depths as great as 90 ft, National Geodetic Vertical Datum (NGVD) of 1929. Currently the average depth of the harbors is on the order of 40 ft. With increased depths comes the possibility for greater variations in velocity, temperature, and density with depth. Therefore, in order to better evaluate flow

---

* D. G. Outlaw, Memorandum for Record, 5 March 1985, "Analysis of Tidal Circulation for Los Angeles and Long Beach Harbors Navigation Channel Improvements," US Army Engineer Waterways Experiment Station, Vicksburg, MS.

conditions (and thus water quality) in the harbors, it is necessary to advance to a 3-D modeling system, that is, a model that can resolve hydrodynamic and water quality parameters at different depths in the water column. The previous modeling efforts have been performed with depth-averaged models, which have been effective in aiding understanding the harbors' global hydrodynamics but cannot provide the detailed input required for a water quality model study of a deep harbor where vertical variations are significant.

PART III: COMPUTATIONAL MODEL

10. Harbor enhancements may affect water quality in the study area by changing tidal circulation and harbor flushing patterns that presently exist. Furthermore, channel deepening introduces the possibility that transported contaminants will not be well-mixed within the water column. To determine the vertical velocity distribution for investigating water quality, a 3-D hydrodynamic model is necessary. The model selected for simulating hydrodynamics, CH3D, is based on the methodology presented in Sheng (1983).

Hydrodynamic Model

11. Model CH3D is a time-varying, 3-D hydrodynamic model for simulating circulation affected by tide, wind, river inflow, and density currents induced by salinity and/or temperature gradients. Assuming hydrostatic pressure distribution and employing the eddy-viscosity concept, the basic equations can be written for a right-handed coordinate system (Figure 4) as shown in Figure 5. In the governing equations u, v, and w are the velocities in

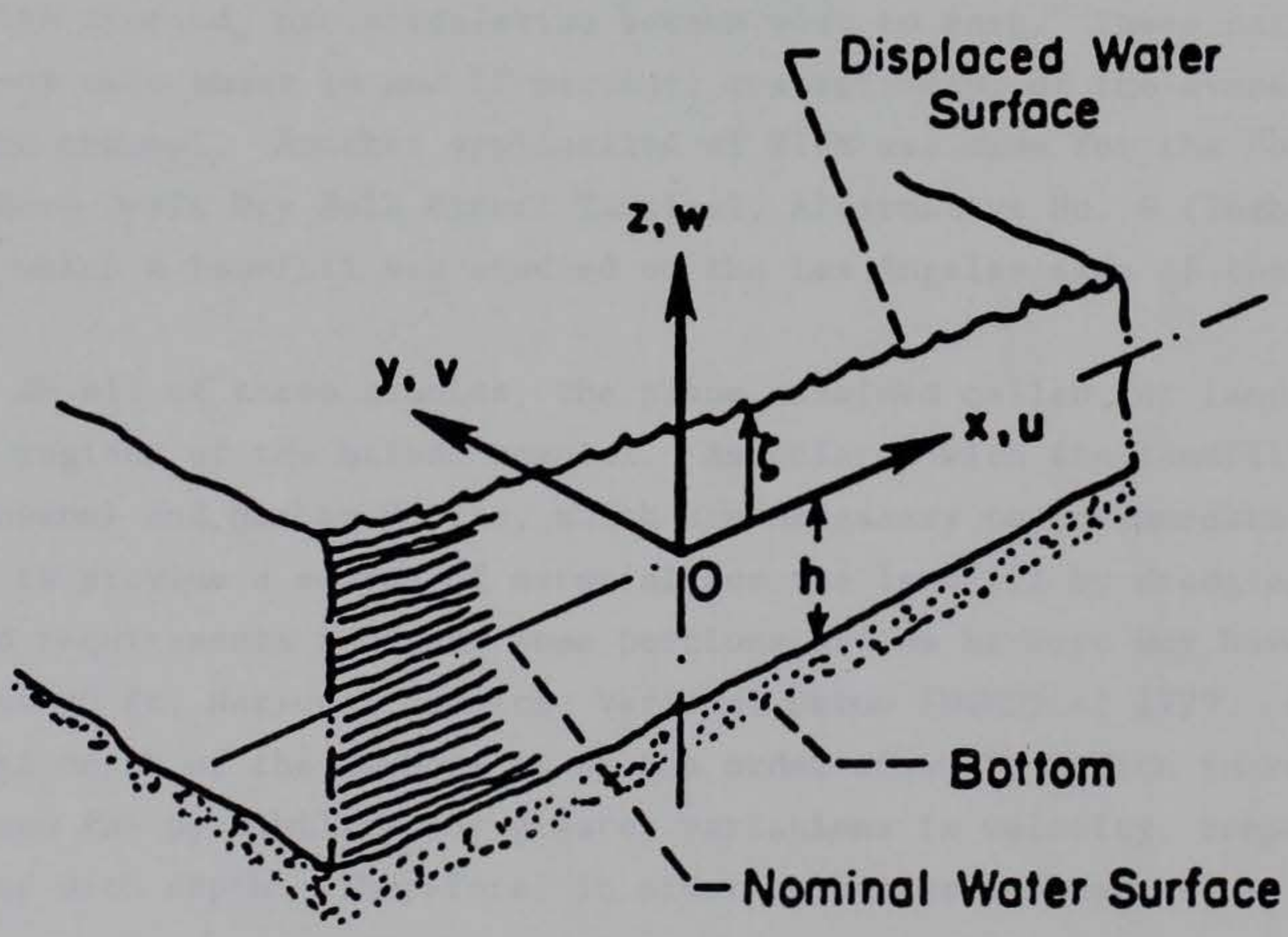

Figure 4. Coordinate system

$$\frac{\partial u}{\partial x} + \frac{\partial v}{\partial y} + \frac{\partial w}{\partial z} = 0 \tag{3.1}$$

$$\frac{\partial u}{\partial t} + \frac{\partial u^2}{\partial x} + \frac{\partial uv}{\partial y} + \frac{\partial uw}{\partial z} = fv - \frac{1}{\rho_o}\frac{\partial p}{\partial x} + \frac{\partial}{\partial x}\left(A_H \frac{\partial u}{\partial x}\right)$$

$$+ \frac{\partial}{\partial y}\left(A_H \frac{\partial u}{\partial y}\right) + \frac{\partial}{\partial z}\left(A_v \frac{\partial u}{\partial z}\right) \tag{3.2}$$

$$\frac{\partial v}{\partial t} + \frac{\partial uv}{\partial x} + \frac{\partial v^2}{\partial y} + \frac{\partial vw}{\partial z} = - fu - \frac{1}{\rho_o}\frac{\partial p}{\partial y} + \frac{\partial}{\partial x}\left(A_H \frac{\partial v}{\partial x}\right)$$

$$+ \frac{\partial}{\partial y}\left(A_H \frac{\partial v}{\partial y}\right) + \frac{\partial}{\partial z}\left(A_v \frac{\partial v}{\partial z}\right) \tag{3.3}$$

$$\frac{\partial p}{\partial z} = - \rho g \tag{3.4}$$

$$\frac{\partial T}{\partial t} + \frac{\partial uT}{\partial x} + \frac{\partial vT}{\partial y} + \frac{\partial wT}{\partial z} = \frac{\partial}{\partial x}\left(K_H \frac{\partial T}{\partial x}\right) + \frac{\partial}{\partial y}\left(K_H \frac{\partial T}{\partial y}\right) + \frac{\partial}{\partial z}\left(K_v \frac{\partial T}{\partial z}\right) \tag{3.5}$$

$$\frac{\partial S}{\partial t} + \frac{\partial uS}{\partial x} + \frac{\partial vS}{\partial y} + \frac{\partial wS}{\partial z} = \frac{\partial}{\partial x}\left(D_H \frac{\partial S}{\partial x}\right) + \frac{\partial}{\partial y}\left(D_H \frac{\partial S}{\partial y}\right) + \frac{\partial}{\partial z}\left(D_v \frac{\partial S}{\partial z}\right) \tag{3.6}$$

Figure 5. Governing equations

x- , y- , and z-directions, respectively; f is the Coriolis parameter defined as $2\Omega \sin \phi$ where ϕ is the latitude; ρ_o is the reference density; p is the pressure; g is the acceleration due to gravity; T is the temperature; S is the salinity; A_H , K_H , and D_H are the horizontal eddy coefficients; and A_v , K_v , and D_v are the vertical eddy coefficients. The nonlinear inertia terms and the advection terms have been written in conservative forms. Source/sink terms may be included in Equations 3.5 and 3.6 (Figure 5) to account for such effects as radiation, precipitation, and evaporation.

12. Boundary conditions at the water surface include specification of the wind stress and heat flux and satisfying the kinematic and dynamic conditions. At the bottom the boundary conditions include specification of heat flux and use of a quadratic stress law.

13. Use of a vertical-stretching relationship (Figure 6) leads to a smooth representation of the topography and the same number of vertical cells in the shallow and deep regions of the water body.

$$\sigma = \frac{z-\zeta}{\zeta+h} \approx \frac{z}{h}$$

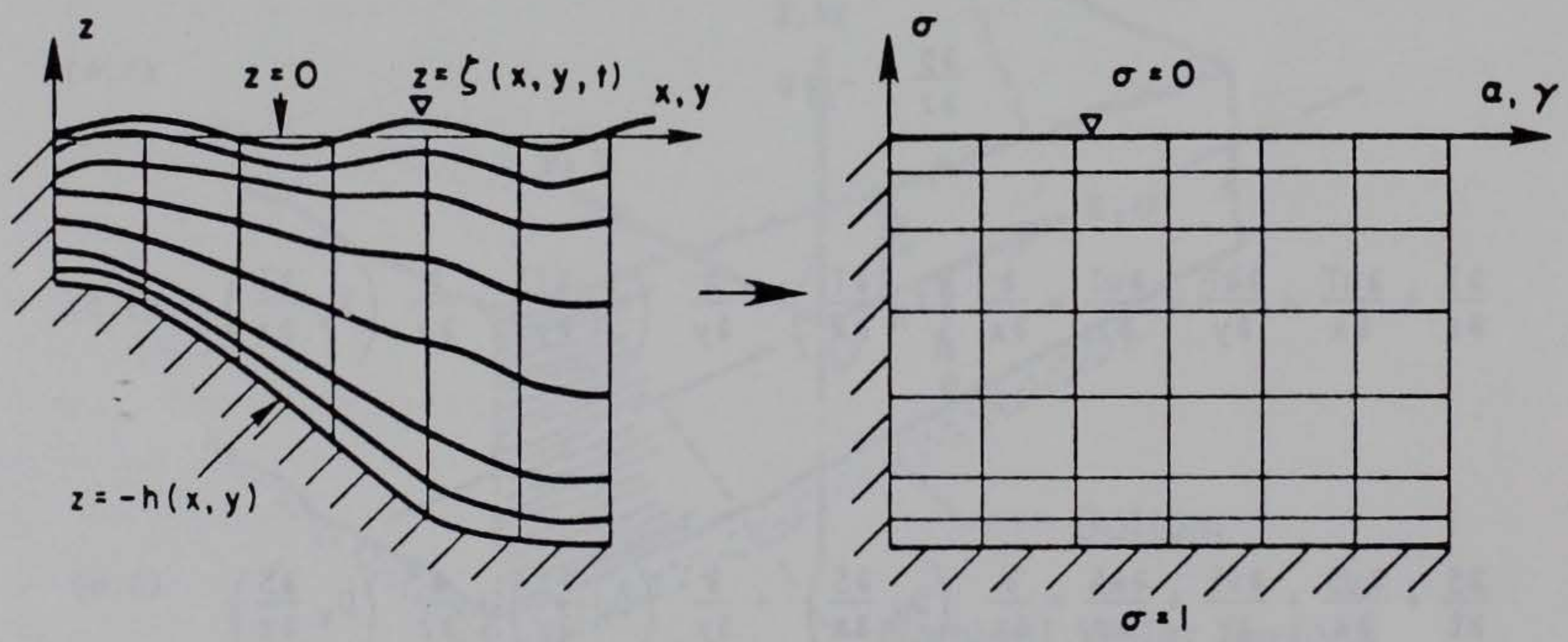

Figure 6. Vertical coordinate transformation

14. The CH3D computer code can be used to simulate 2-D or 3-D unsteady currents in Cartesian or curvilinear grids. To treat curvilinear grids, the governing equations are transformed into a boundary-fitted coordinate system (Figure 7). The resulting equations are very complex and will not be repeated here.* To alleviate various problems experienced in similar model developments, the dependent and independent variables are transformed into the new coordinate system. Equations in transformed coordinates (ξ, η, σ,) are obtained in terms of the contravariant velocity components. These components are locally orthogonal to the grid lines permitting more accurate specification of boundary conditions.

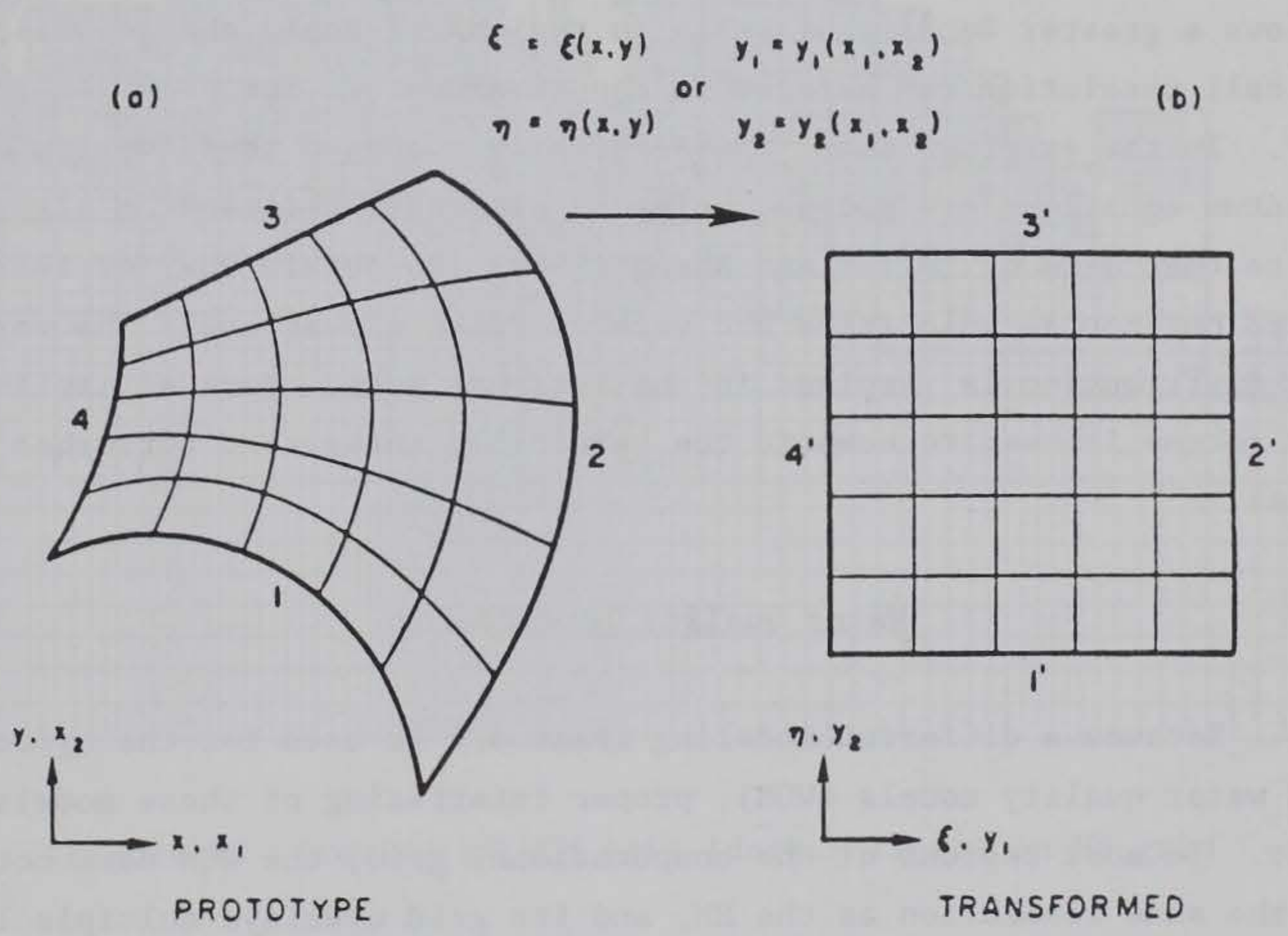

Figure 7. Boundary-fitted coordinate transformation

---

* Y. P. Sheng, 1986, "A Three-Dimensional Mathematical Model of Coastal, Estuarine, and Lake Currents Using Boundary Fitted Grid," Draft Report prepared for the WES, Vicksburg, MS.

15. To facilitate a more efficient numerical scheme, an external-internal mode-splitting technique is used. Numerical computation of the internal mode, which is governed by the slower baroclinic vertical flow structure dynamics, is separated from the computation of the vertically integrated variables (external mode), which are governed by the fast barotropic dynamics.

16. To apply a finite difference solution method, the study area is approximated by a computational grid composed of a 3-D lattice network of cells. Bathymetry and land-water interfaces, such as shorelines and break-waters, are specified for each vertical column of cells. Flow field parameters, such as velocities or surface elevations, are evaluated at each cell. In order to improve model accuracy, mathematical mapping or transformation techniques are applied independently to the horizontal and vertical grid coordinates. The horizontal grid directions are mapped into a general curvilinear system. This allows a greater density of cells in regions of rapid change while coarser cell resolution can be used in the remainder of the grid.

17. In the external mode, the vertically averaged conservation of mass and momentum equations are solved, using an alternating-direction algorithm similar to that used by Butler and Sheng (1982), to obtain the vertically integrated horizontal velocities and water surface elevations. The vertical velocity distribution is resolved in the internal mode. Here an implicit-explicit scheme is used to compute the vertically integrated perturbation velocities.

Water Quality Interfacing

18. Because a different modeling framework is used for the hydrodynamic (HM) and water quality models (WQM), proper interfacing of these models is important. In most regions of the computational grid, the WQM does not require the same resolution as the HM, and its grid overlays multiple layers and lateral segments of the HM (Figure 8). This procedure reduces unnecessary computational expense. When more than one HM cell is overlain by a WQM segment, the flows for those cells are combined in a manner to provide a single flow for each face of the WQM segment.

19. The WQM uses time steps larger than the HM. The fundamental interfacing problem consists of processing the hydrodynamic output so that

advection and diffusion are accurately depicted in the WQM. Testing of the HM/WQM interfacing is required to ensure that transport predicted by the HM is maintained in the WQM. Tests consist of comparisons of the transport of a conservative substance (dye) in both. These tests are reported in a companion report (Hall 1990) to the present study. Supporting hydrodynamic runs will be discussed in a later section of this report.

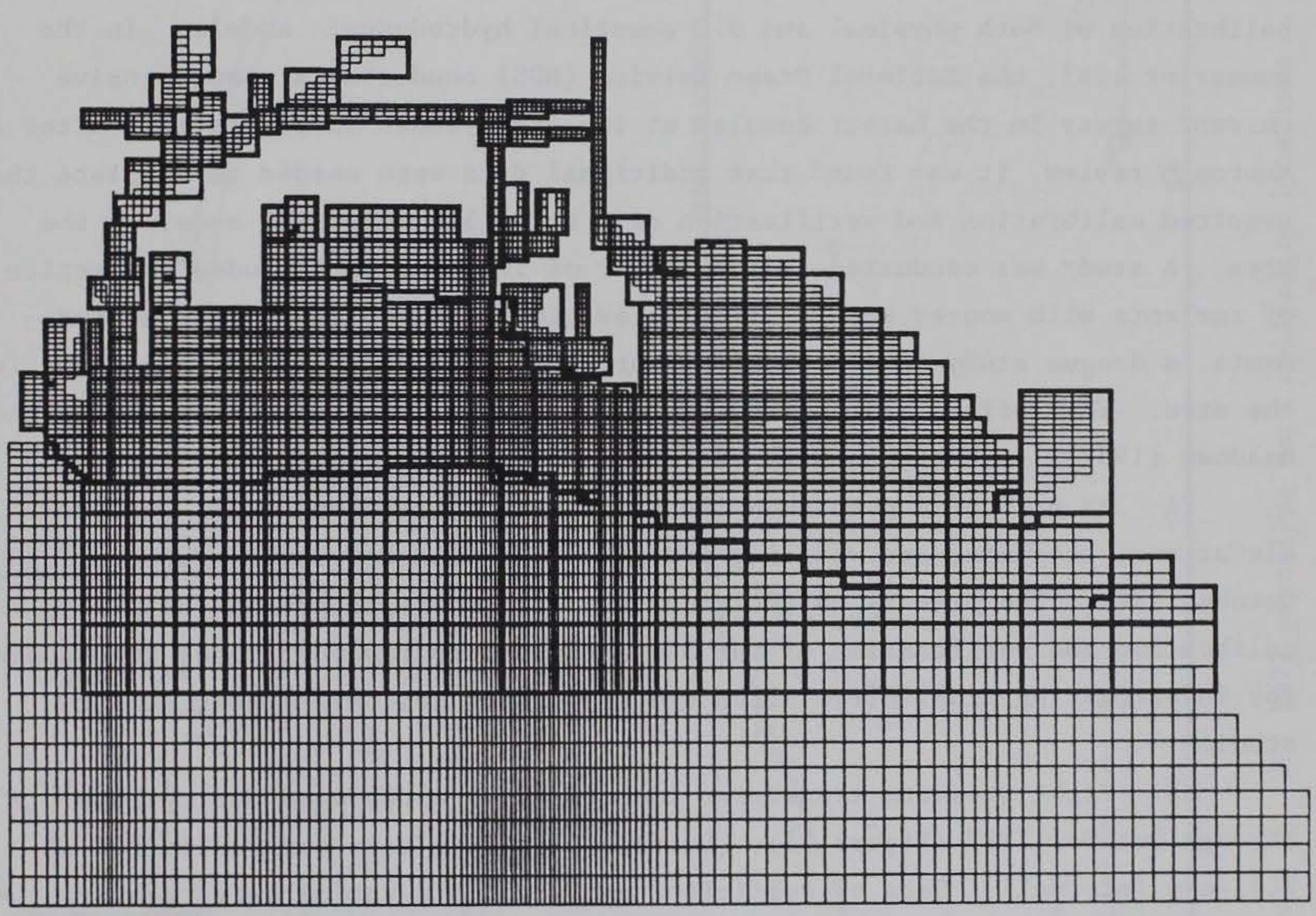

Figure 8. Overlay of WQM grid (darker lines) on HM grid

PART IV: FIELD DATA REVIEW

20. Field data measurements are required for model calibration and verification. Data taken prior to the present study were reviewed for completeness and sufficiency for model validation. The first comprehensive field measurements of tidal circulation in San Pedro Bay were performed in 1971-74 and reported in Pickett et al. (1975). Figure 9 shows locations where tidal velocities and elevations were measured. This data set was used in calibration of both physical and 2-D numerical hydrodynamic models. In the summer of 1983, the National Ocean Service (NOS) conducted a comprehensive current survey in the harbor complex at locations shown in Figure 10. After a thorough review, it was found that additional data were needed to complete the required calibration and verification of a fully 3-D numerical model of the area. A study was conducted in the summer of 1987, which included collection of currents with moored meters, tidal elevations, shipboard profile measurements, a drogue study in the Outer Harbor, and a dye study at two locations in the area. This effort is reported by McGehee, McKinney, and Dickey (1989) and Meadows (1987). A short summary of the field data measurements follows.

21. As part of a comprehensive field data collection study, surface elevations, currents, and velocity profiles were measured during June through October 1987. The primary objective of the effort was to provide data for calibration and verification of the 3-D circulation/transport model to be used for investigating tidal circulation and supporting follow-on water quality studies.

22. Eight pressure transducer tide gages were deployed during June through October 1987 (Figure 11). Surface elevation data were collected at 3.75-min intervals. Data of sufficient quality and duration were recovered from Tide Gages (TG) 1, 2, 3, 6, and 7. Tide Gages 1, 2, and 6, located outside the breakwaters, are used to furnish boundary conditions to drive the hydrodynamic model, whereas, TG 3 and 7, located inside the breakwaters are used to check model results during calibration and verification. Figures 12 through 15 are example plots of tidal measurements at TG 1 and 3 for the entire period of gage deployment as well as for the 2-day period of 7 to 9 August 1987. Figure 15 displays a substantial amount of seiching in the Cerritos Channel gage, evidence of the subtidal 1-hr oscillation occurring in the Inner Harbor. The Inner Harbor acts as a resonance chamber for the oscillations occurring in outer San Pedro Bay (Wilson et al. 1968). These

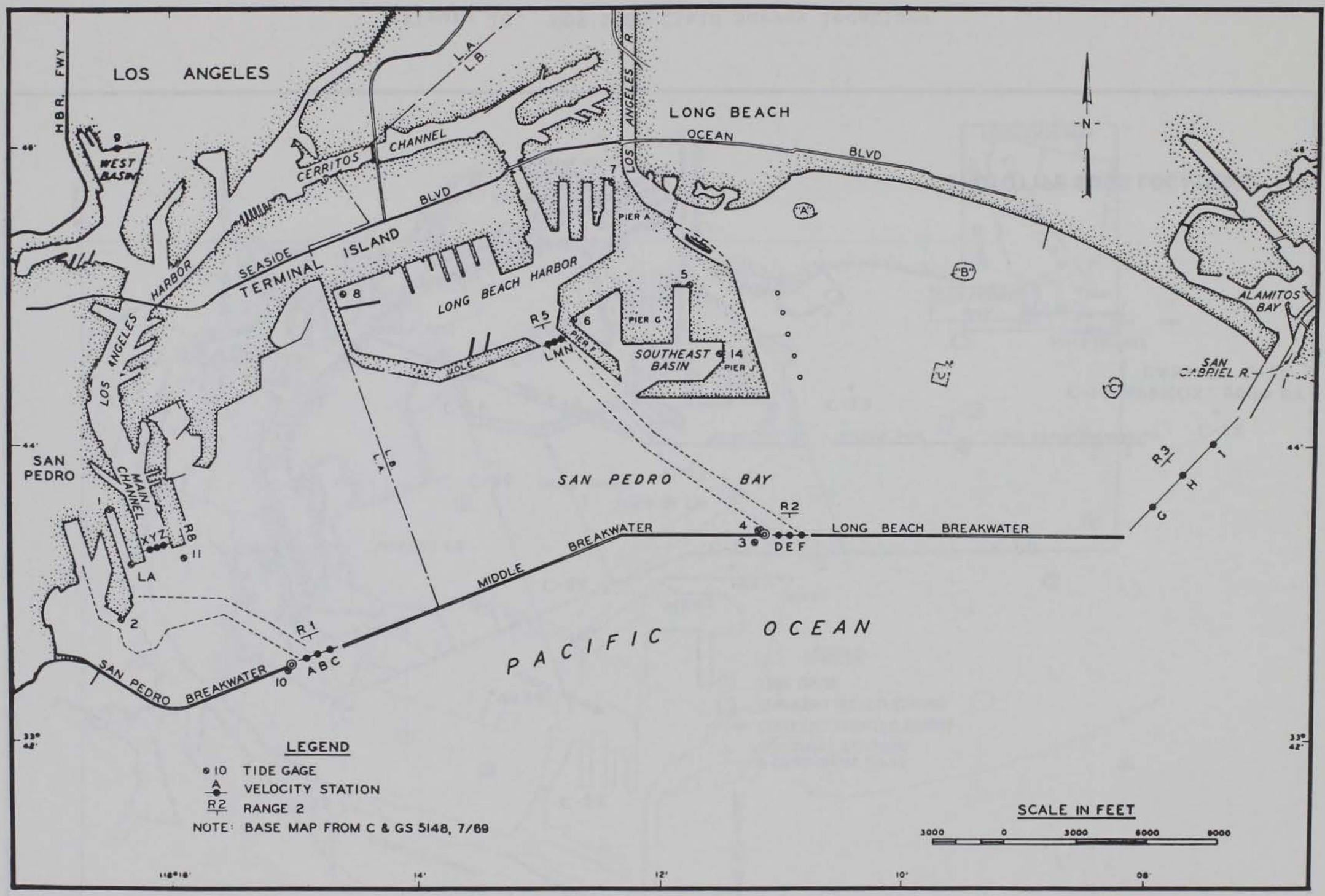

Figure 9. WES 1972 prototype data collection locations

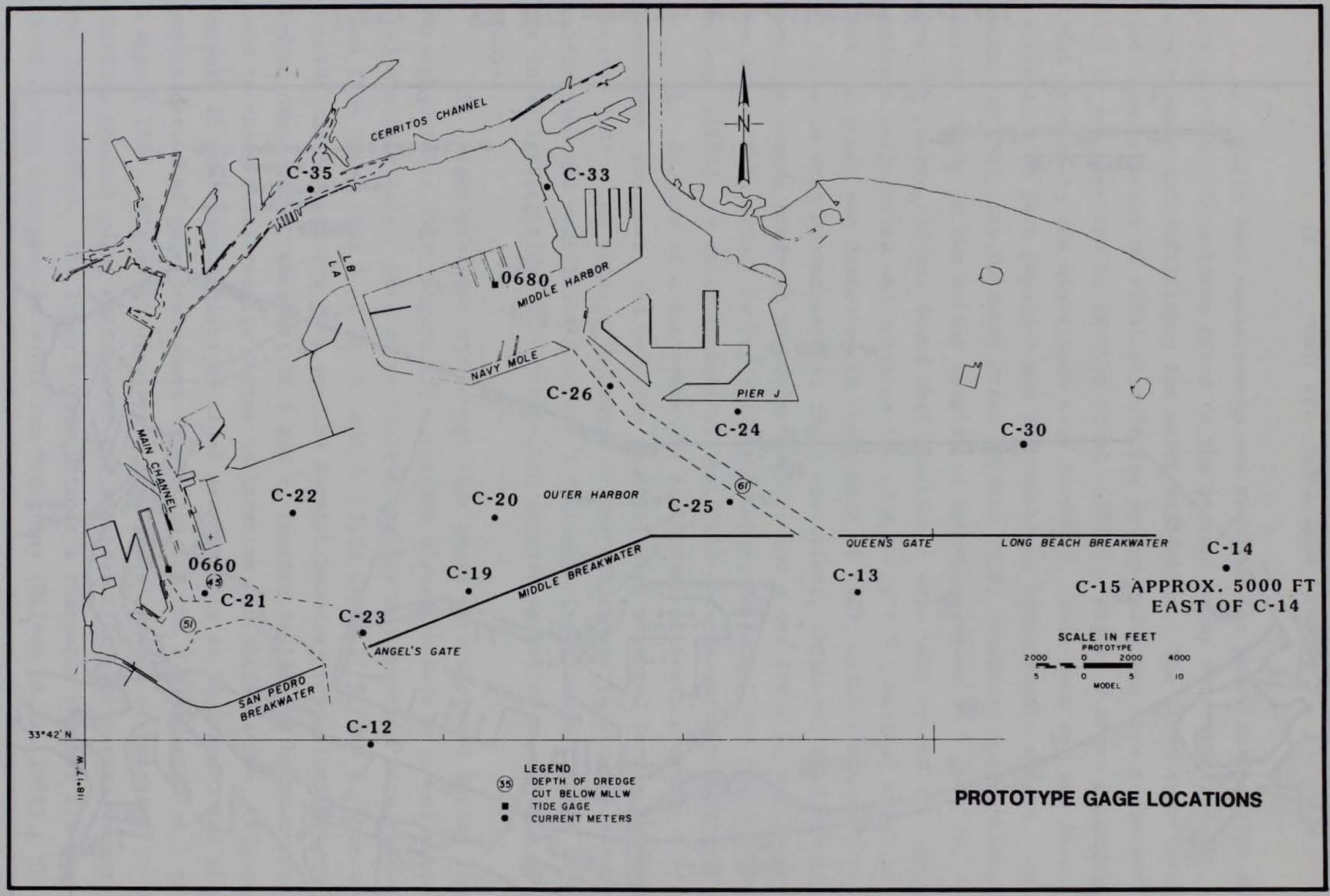

Figure 10. NOS 1983 field survey locations

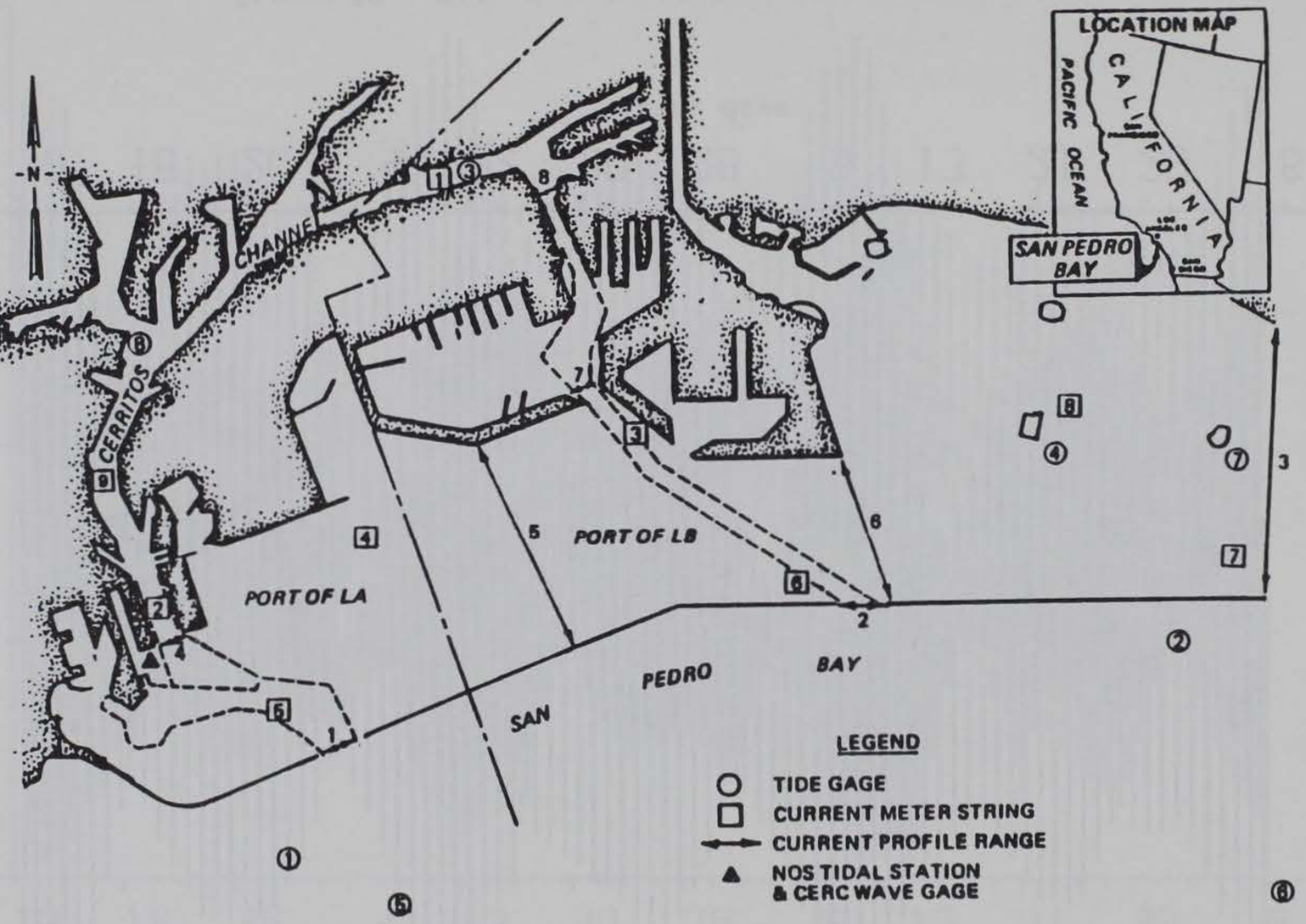

Figure 11. WES 1987 field survey locations

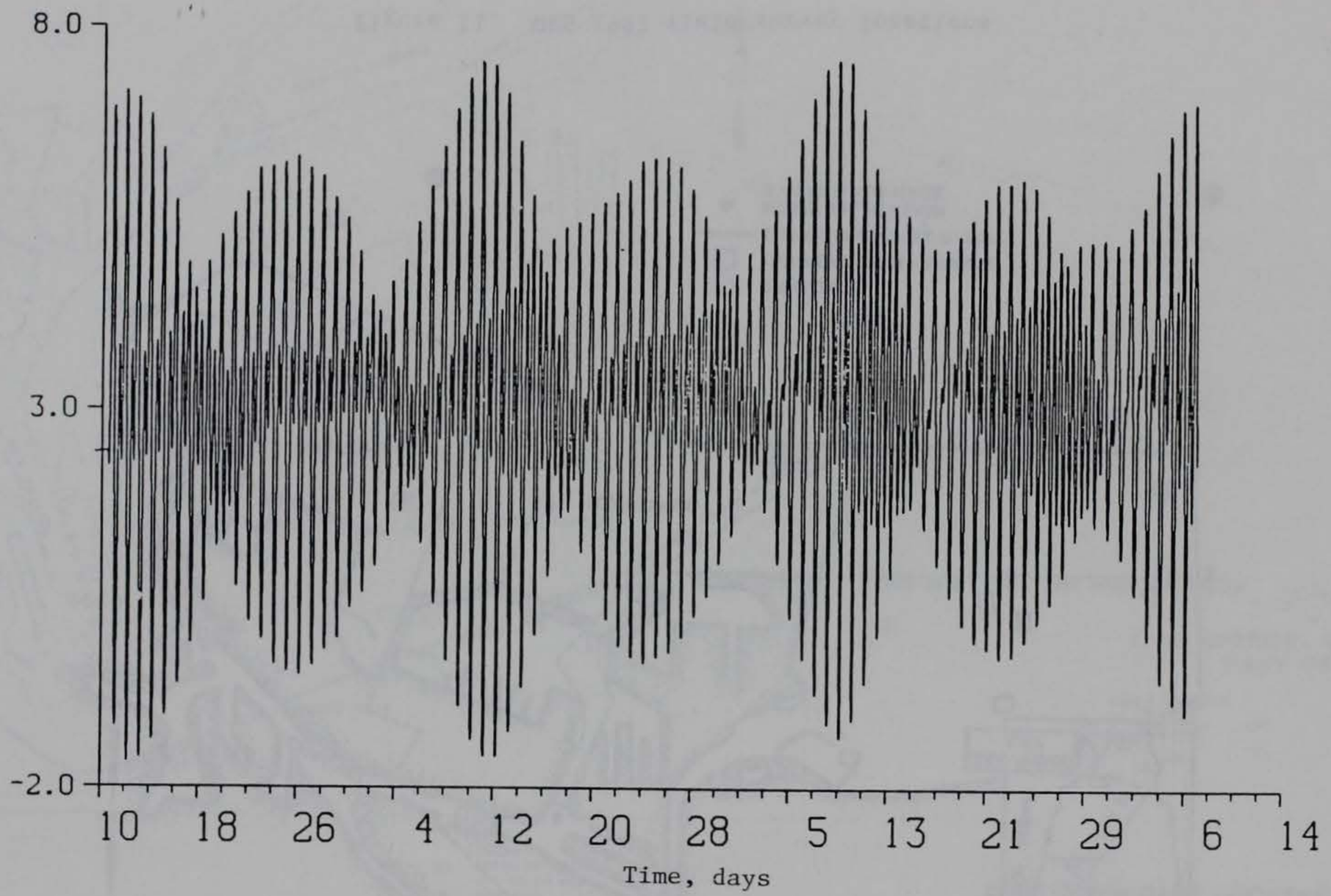

Figure 12. Tide Gage 1, 10 June-14 September 1987

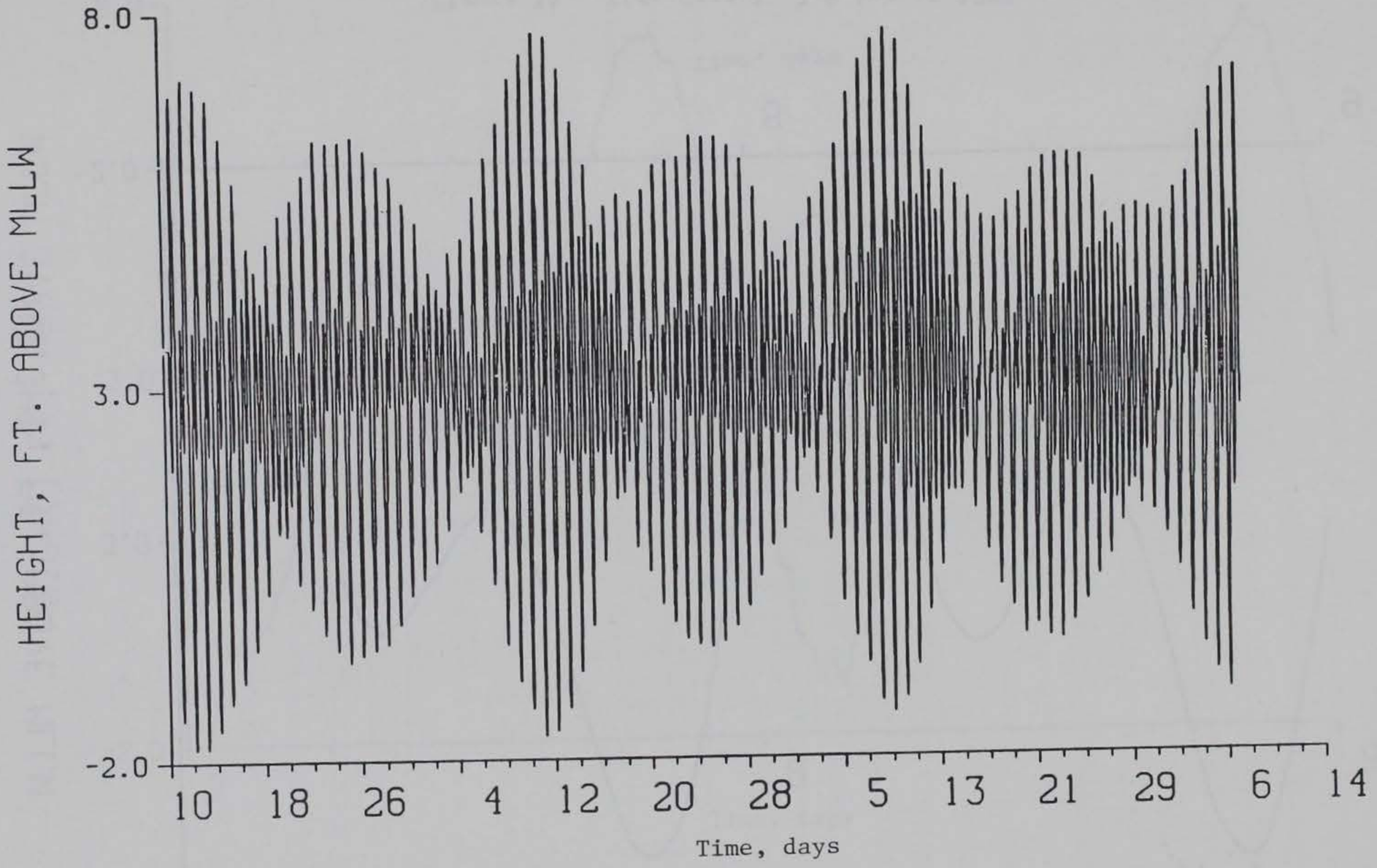

Figure 13. Tide Gage 3, 10 June-14 September 1987

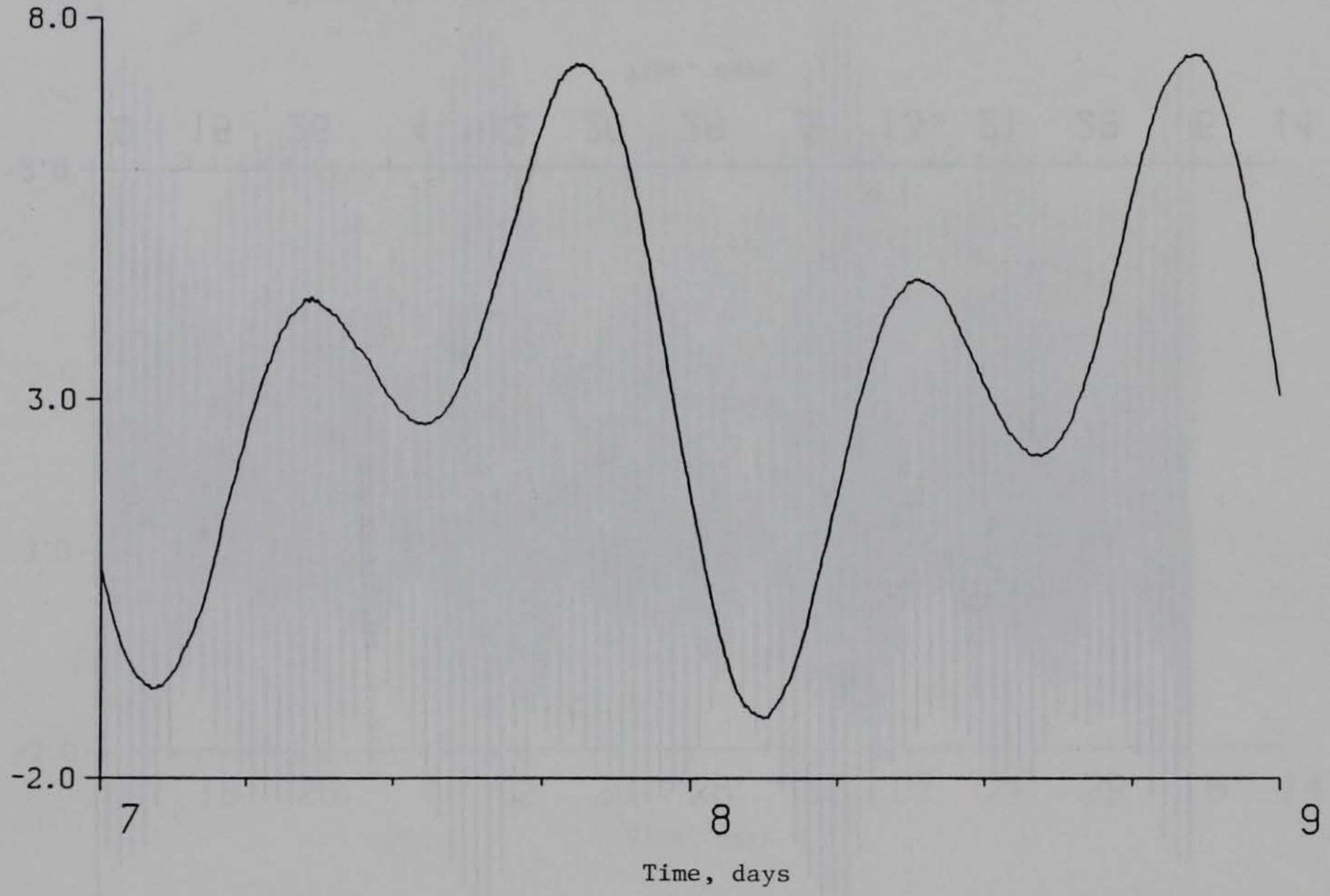

Figure 14. Tide Gage 1, 7-9 August 1987

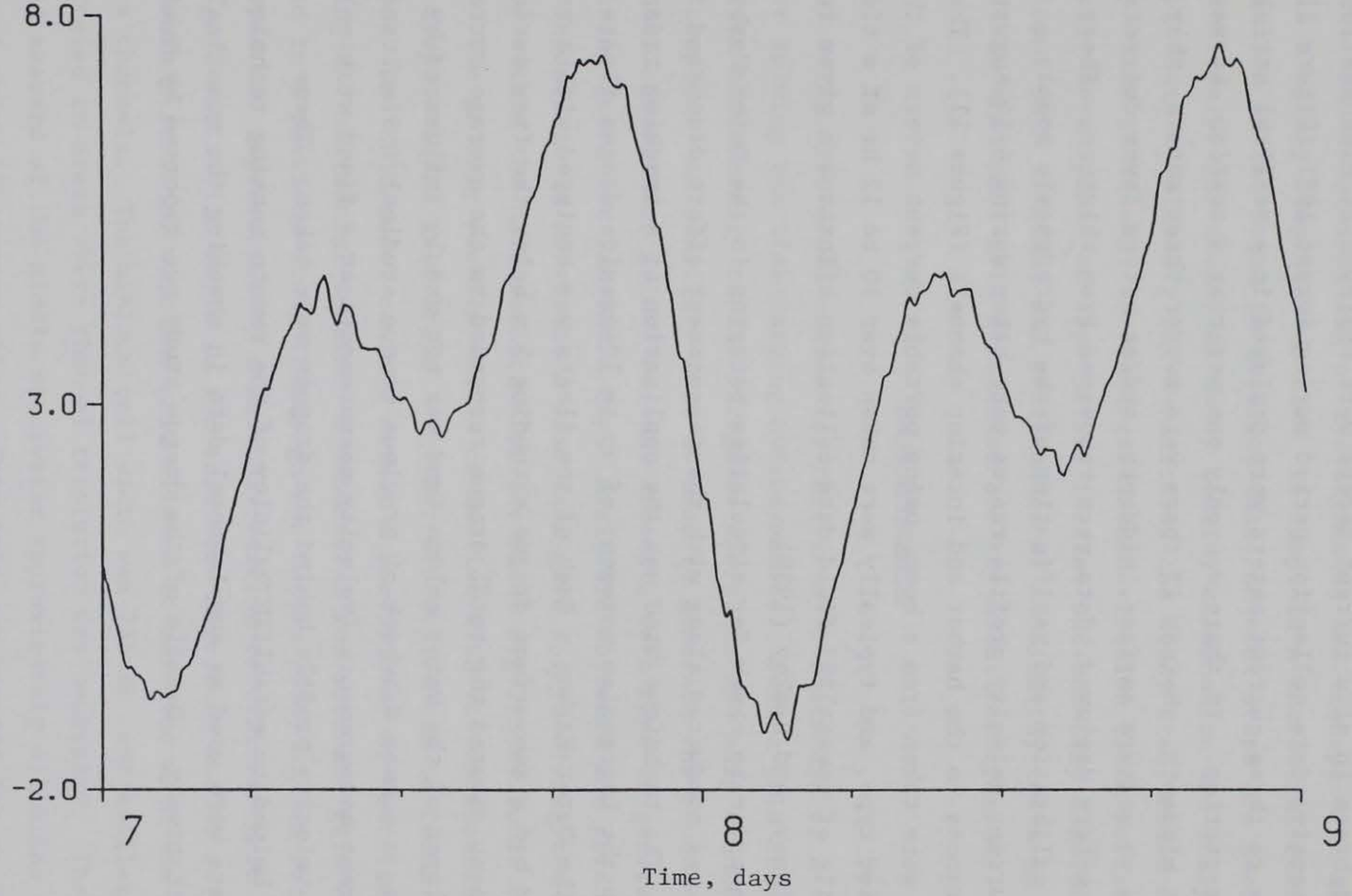

Figure 15. Tide Gage 3, 7-9 August 1987

outer bay oscillations were observed in all open coast gages as seen with careful examination of Figure 14.

23. Eighteen in situ current meters were deployed at nine stations for a 1-month intensive data collection period during August 1987 (Figure 11). Typically one to three current meters were deployed in a vertical string at a current meter station. If there was only one meter at a station, it was positioned at middepth, whereas if there were two or three meters, they were located so as to measure surface, middepth, and/or bottom layer currents. Of the eighteen meters deployed, data were recovered from thirteen. These data were used in calibration and verification of the hydrodynamic model.

24. Current velocity profile ranges were taken during 6-14 August 1987 at major entrances to the harbor and interior channels (Figure 11). These measurements were taken from a boat, using portable current meters of the ducted impeller type, and typically were taken over 10 to 12 hr of a tidal cycle. Details of these 1987 field data collection efforts are given in McGehee, McKinney, and Dickey (1989).

25. In order to check for circulation patterns in the Outer Harbor, a drogue study was conducted along with the measurement effort discussed in paragraph 24. The technique used was the application of a tracking radar system to map the Lagrangian movement of up to 10 passive drogue floats deployed in the Outer Harbor. Each of the floats was equipped with a radar reflector and had a subsurface drogue extending 5 m below the free surface. This arrangement ensured the total drogue responded to the average currents in the top 3-m layer of the water column (and was not unduly influenced by surface winds, a common drawback of previous drogue studies). Simultaneously, Eulerian current measurements (velocity measurements at a fixed station) of the vertical velocity profile behind the drogues were taken. These measurements helped to establish validity of the remote sensing technique. The drogue data were used as supplemental data in checking the numerical model results qualitatively. Details of the drogue study are reported by Meadows (1987).

PART V: MODEL CALIBRATION AND VERIFICATION

26. Numerical modeling of hydrodynamics and transport in three dimensions is a highly complicated task. To complete a successful calibration and verification of the model to observed data, several steps are necessary. These include proper choice of model domain, examination and analysis of available data to classify the dynamics of the study area, model resolution of the important processes, accurate grid schematization (both horizontal and vertical), development of appropriate initial and boundary conditions and model input data streams, and performance of sensitivity tests on model response to choice of grid resolution and key model coefficients.

Grid Selection

27. The CH3D model chosen for this study permits use of a curvilinear grid for solving the time-varying hydrodynamics. Such a grid should be fitted to conform horizontally to the irregular shoreline and ship channels of the harbor complex. An auxiliary code is used to generate the boundary-fitted horizontal curvilinear grid. Several attempts were made to generate accurate engineering grids for San Pedro Bay. Available software for grid generation proved inadequate to construct a practical grid for resolving the complex geometry within the harbors for which the model algorithms would remain stable. The primary problem was in connection with the development of highly skewed computational grid cells. Further discussion can be found in Appendix A.

28. The CH3D model can use either a curvilinear or rectilinear grid for resolving the horizontal domain. A successful and accurate grid (Figure 3) was used in a previous study (Seabergh and Outlaw 1984) of San Pedro Bay. The study area was represented by a smoothly varying rectilinear grid containing 12,032 grid cells (128 cells in the east-west direction and 94 cells in the north-south direction) with the grid aligned to coincide with the Inner Harbor entrance channels. The minimum cell width was 235 ft, and smaller cells were concentrated in areas where channel resolution was necessary. The grid extended seaward of the Middle Breakwater approximately 4.2 miles and covered an area of about 146 square miles. This grid was adopted for use in the present study.

29. In the vertical, a stretching mechanism is used to smoothly represent the bathymetry. It permits the same number of cells in shallow and deep portions of the water body.

Model Input Data

30. Boundary conditions chosen for all model runs were the application of measured or constituent tidal elevations at the seaward and western open boundaries, wind stress on the water surface, and a quadratic bottom stress using the Manning's n coefficient. For astronomic tidal forcing, an elevation computed from tidal constituents was applied along the entire open boundary. This assumption was tested in previous studies (Raney 1976a, b; Outlaw and Raney 1979; and Seabergh and Outlaw 1984) and found to be adequate for reproducing accurate tidal elevations and velocities within San Pedro Bay. When wind stress was applied at the surface, measured tidal elevations were used to drive the open boundary. These data contained the effects of wind stress at the boundary. The adapted boundary condition formulation was tested and is discussed in a following section.

31. Initial conditions for all model runs included setting all internal grid cell velocities to zero and selecting a starting time in the tidal and wind records consistent with the assumption of a quiescent water body. The model requires a large input data stream that includes information relating to physical constants, turbulence/wind/friction parameters, grid characteristics (depth, coordinate locations), and input/output control variables.

Sensitivity Tests

32. In order to successfully calibrate a model, it is important to first obtain a knowledge as to how the model responds to a different selection of key model coefficients. This effort is conducted by applying good engineering judgment for an initial selection of these parameters and running the uncalibrated model several times, varying individual parameters one at a time. Tests conducted during this task included variations of the bottom friction coefficient, wind-stress drag coefficient, horizontal and vertical eddy diffusivity coefficients, vertical grid resolution, and boundary condition sensitivity.

33. Due to different scales and intensities associated with the horizontal and vertical turbulent eddies in large water bodies, the lateral eddy coefficients are typically several orders of magnitude larger than the vertical eddy coefficients. Determination of realistic values is a major and difficult task in modeling the harbor currents. Previous experience (Sheng 1983) with similar applications indicated that use of constant eddy coefficients for both the horizontal and vertical is sufficient for this study. Data are not available to justify spatial or temporal variation of these coefficients.

34. Several types of runs were made with the model: constituent tidal forcing, pure wind-driven forcing, measured tidal forcing with and without wind, and use of varying number of layers. The bottom friction coefficient was varied between a Manning's n of 0.005 and 0.03. Little effect was noticed on the vertically integrated velocities; however, the vertical profile was slightly altered. This behavior was expected due to the relative deepness of the harbors. The friction coefficient was used in future runs to adjust the model for obtaining a better representation of the vertical structure at prototype gage locations.

35. The model permits use of several formulations of the inertia terms in the governing equations. The horizontal eddy coefficient A_H was varied between 0 and 1,000,000 cm^2/sec, depending on the finite difference form of the inertia terms. Values between 10,000 and 100,000 cm^2/sec appeared to give reasonable results, which was consistent with earlier experience (Sheng 1983). The vertical eddy coefficient was varied between 2 and 100 cm^2/sec, and it was found that a value between 5 and 15 cm^2/sec gave reasonable results in the model tests. These ranges for the eddy coefficients are technically appropriate for the San Pedro Bay application.

36. The formulation of the wind drag coefficient is according to Garrat (1977). Data used by Garrat to develop this drag law contain a high degree of variability in the lower range of wind speeds (less than 20 knots). The nearest recording of wind speed and directional data was at the offices of the Port of Los Angeles, north of the entrance to the Main Channel. Data were not obtained during the month of August 1987 from the WES gage located on the San Pedro Breakwater due to instrument malfunction. Therefore, several tests were run to determine the need for including a spatial variation in the wind field, representing the marine-land influence, and adjusting the drag coefficient used by Garrat. These tests resulted in the following conclusions: the Inner

Harbor channels are protected from wind influence by the structural industrialization of the surrounding land; wind influence in the harbor was restricted to those periods when the wind speed exceeded 5 to 10 knots; and the data obtained from the Port of Los Angeles Headquarters Building anemometer were representative of wind behavior over the entire model domain. Artificial adjustment to represent a spatial variation would have been an impossible task and, without any wind data to check the adjustment, could not have been defended. These conclusions resulted in the decision to apply Garrat's drag law without adjustment and to eliminate wind influence on protected Inner Harbor waters.

37. The model was run with three and five layer resolution in the vertical. Results from these runs indicated that three layers were sufficient to resolve the vertical structure in all areas of the domain where measurements were obtained. Vertical resolution planned for the WQM will not exceed three layers; hence further resolution in the hydrodynamics was not warranted. Additional sensitivity tests were performed in support of the WQM application. These included testing dye tracer conservation, length of time to reach a dynamic steady-state condition within the harbor, and tracer studies to assist the WQM calibration. These efforts will be reported in Part VII on Hydrodynamic Simulations for Water Quality Modeling.

38. In conducting these tests, it was evident model results throughout the harbor complex were highly sensitive to a choice in boundary conditions. Figure 16 shows the residual obtained by subtracting observed surface elevations at TG 1 and 6 for 7-9 August. These measurements are typical for the open coast fronting the harbors. Data were not collected along the entire open boundary, and an attempt was made to estimate tidal variation along the seaward boundary by using measurements at TG 1 and 6. These tests improved comparison with observed data at current gage (CM7) near the end of the Long Beach Breakwater, but comparisons of model and observed current data at all other gages in the Outer and Inner Harbors were not as good as those obtained using a constant tidal signal along the seaward boundary. Since proposed plans are limited to modifications of these areas, it is important to pay greater attention to calibrating to gages within the harbors. From the analysis of the tide measurements and model testing, it appears the level of sensitivity is on the same order as the accuracy of the measurements. Hence, the assumption of a constant tidal signal along the open coast boundary was used in all calibration/verification and plan test simulations.

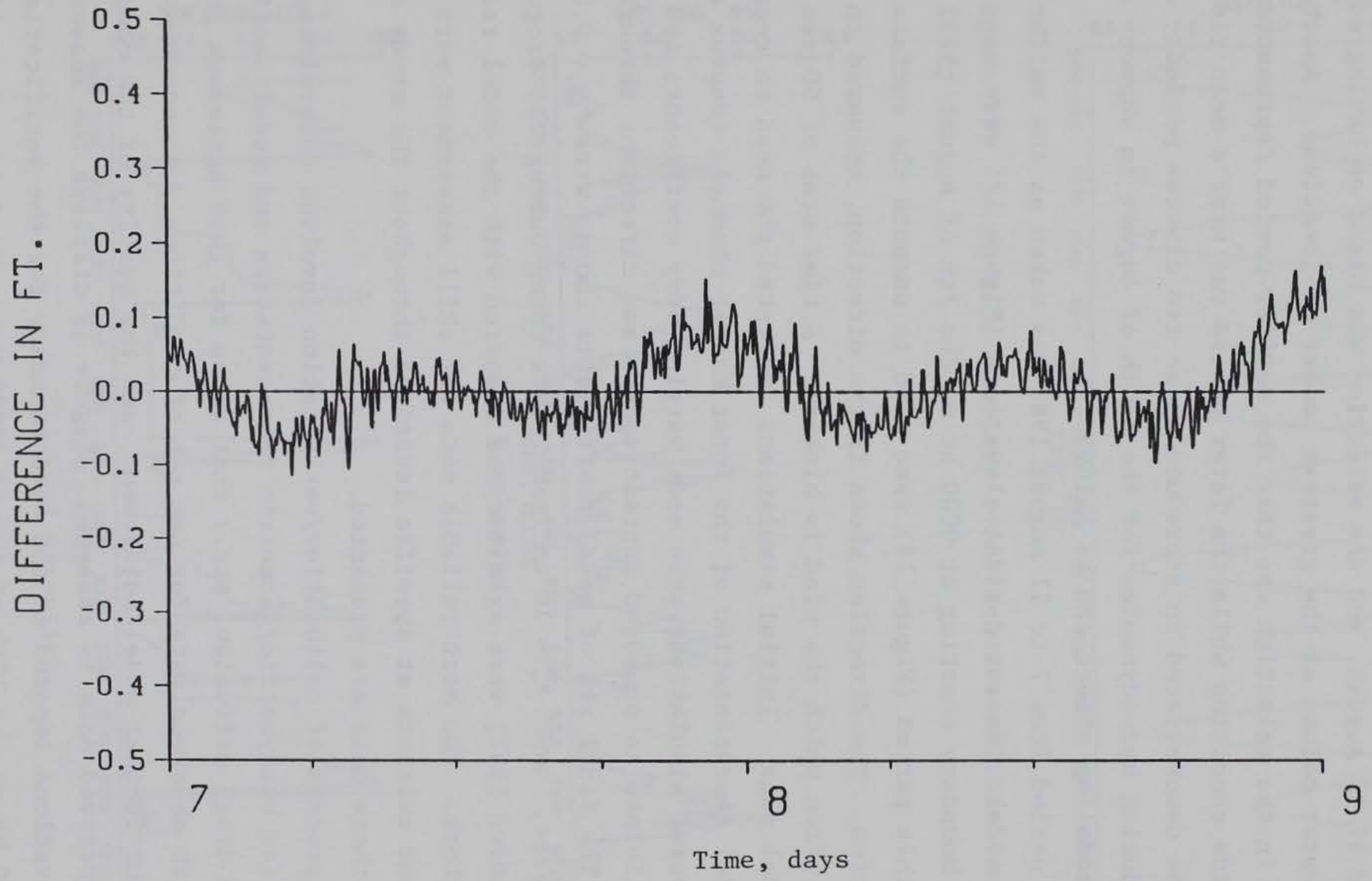

Figure 16. Tide difference between TG1 and TG 6 for 7-9 August 1987

Hydrodynamic Model Calibration/Verification

39. Data collected during the month of August 1987 were reviewed, and two periods for model skill assessment were determined. These periods were 7-11 August and 19-23 August, and the selection was based on having collected data over the water column at the greatest number of locations. Another criterion used in the selection was that the earlier period represented a large spring tide condition while the later period was near a mean tide. If the model can be demonstrated to reproduce these two diverse periods, confidence in reproducing hydrodynamics for the month of August in support of the water quality modeling effort can be gained.

40. The period from 7 to 11 August 1987 was taken as the calibration period for the model. Measured tidal elevations (Figure 17) were used to drive the open boundary starting at 0000 hr on the 7th of August (5232 hr). Wind data for this period (Figure 18) were used to compute the surface stress boundary condition. The direction shown is the direction, measured in degrees from the north, from which the wind is blowing. A time step of 60 sec was used in all model runs. Initial simulations indicated the need to reconfigure some of the model representation of the Inner Harbor channels (depths and geometry). Several simulations were made varying eddy coefficents and bottom friction to calibrate to measured current speeds and directions throughout the water column. The final set of model coefficients chosen were $n = 0.02$, $A_H = 20{,}000\ cm^2/sec$, and $A_v = 10\ cm^2/sec$. Data taken during the drogue experiment (Meadows 1987) were examined and compared with the model results as a consistency check. The most reliable data for skill assessment were measured tide and currents at specific locations throughout the study area. Comparisons to these data are presented.

41. The process of calibration/verification involves determining the best estimates for bathymetric/geometric representation and model coefficients (friction, wind drag, diffusion, etc.) that allow for good agreement in comparing model with observed data for one set of conditions. A second event is simulated without further model adjustment, and the quality of the comparison of model with observed data is assessed. Figure 19 displays the measured and model tidal elevations imposed at the open boundary for the verification period starting at 0000 hr on the 19th of August (5520 hr). Wind data for this period (Figure 20) were used to compute the surface stress boundary condition.

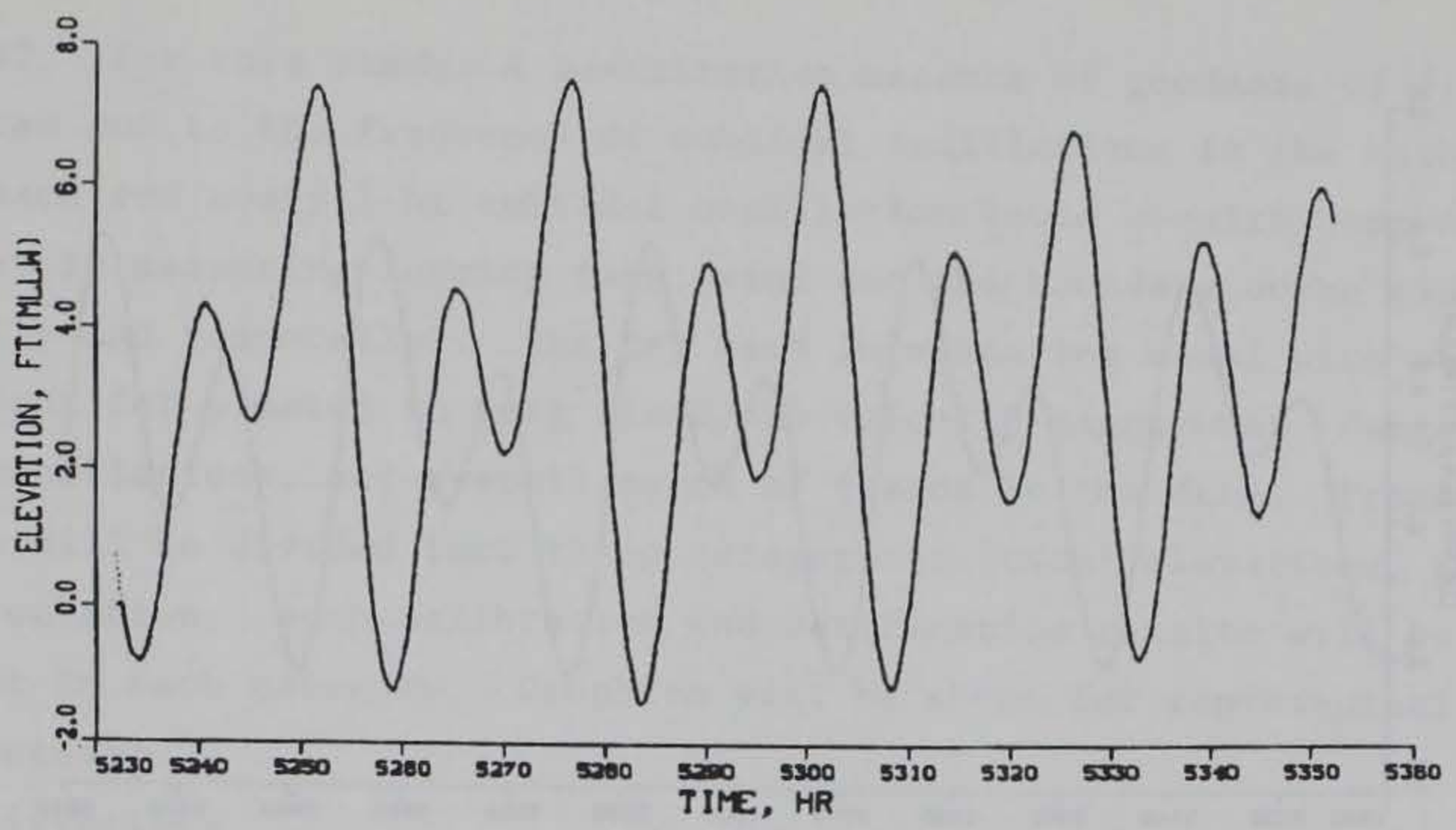

Figure 17. Ocean tide boundary condition for calibration period

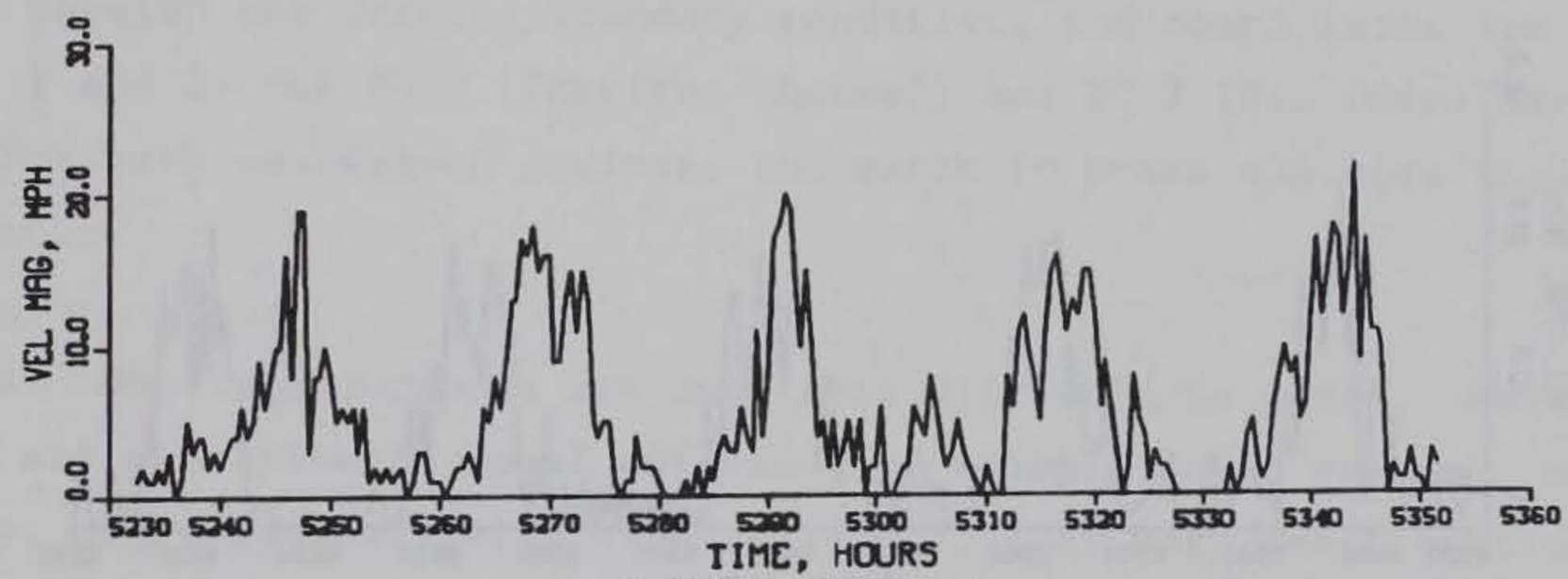

(a) Wind speed

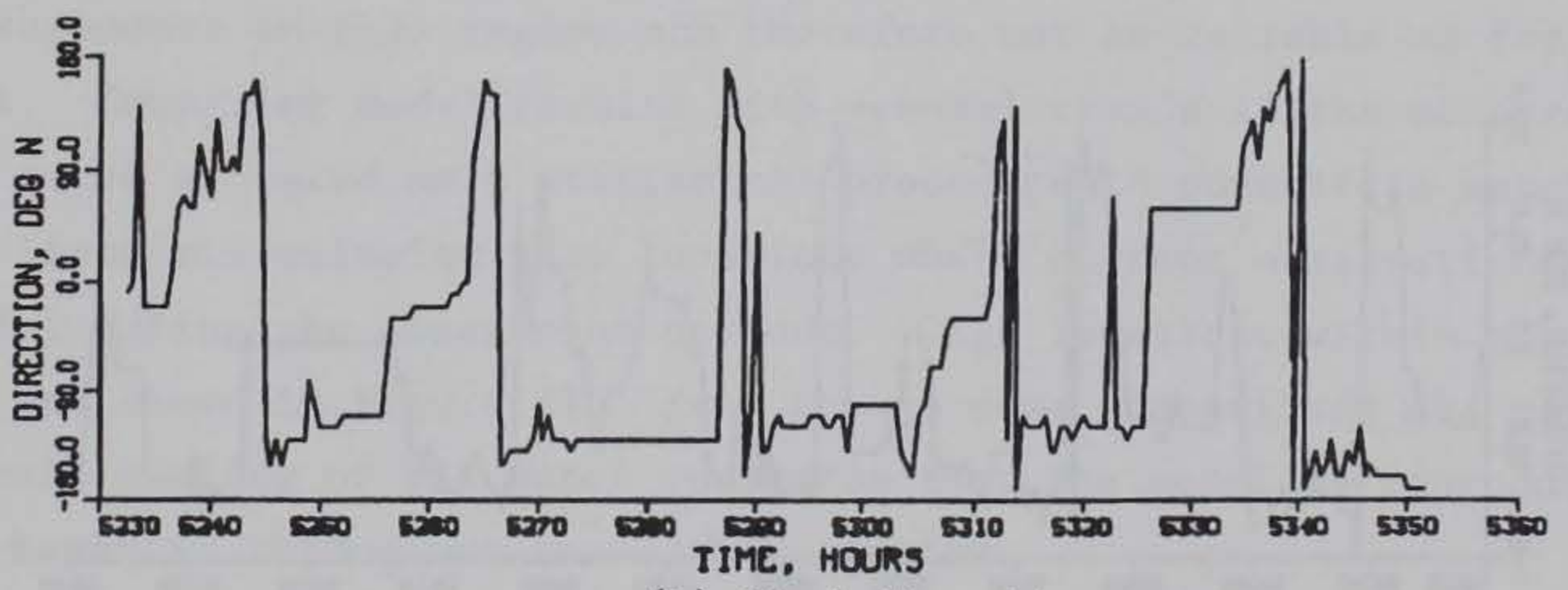

(b) Wind direction

Figure 18. Wind data for calibration period

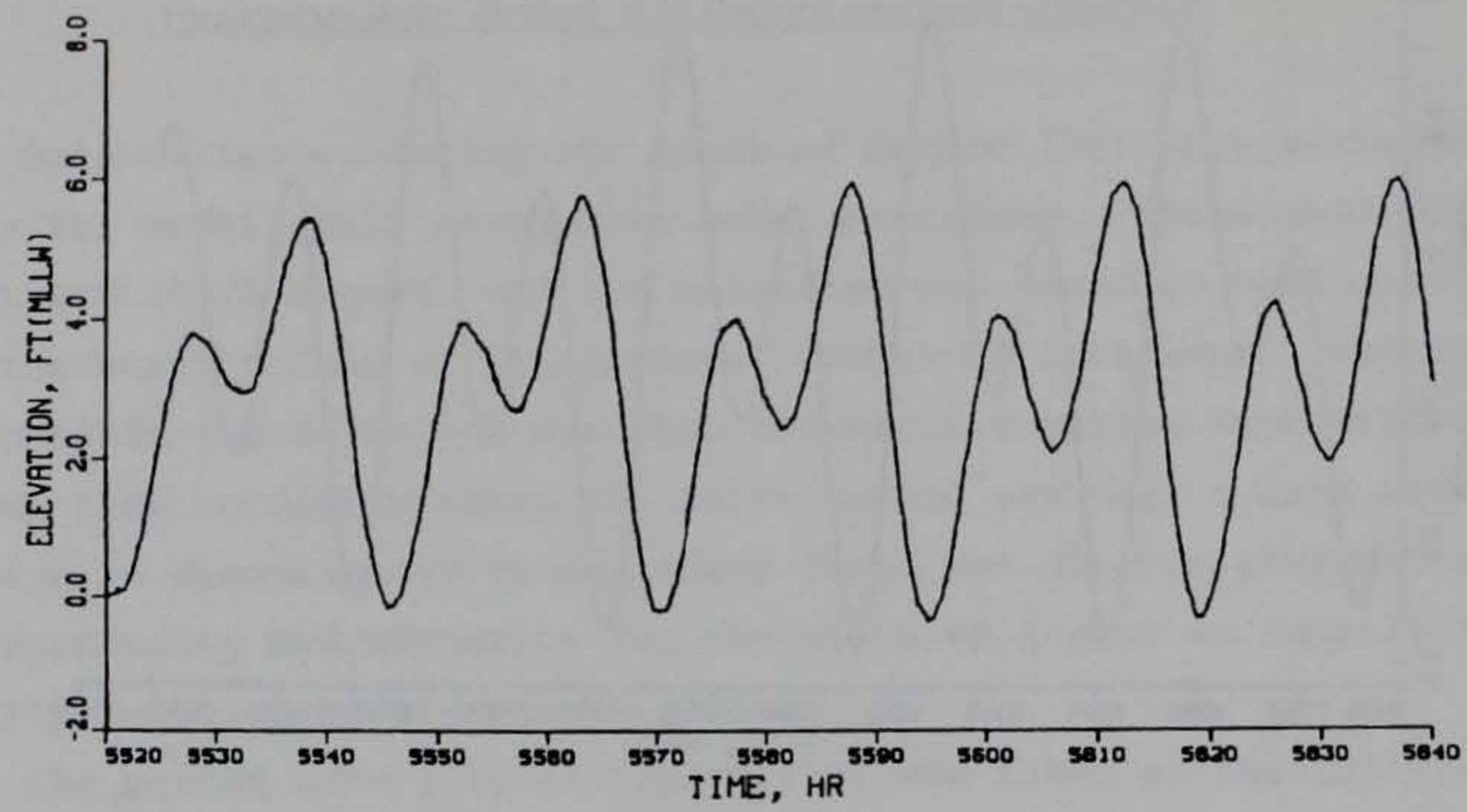

Figure 19. Ocean tide boundary condition for verification period

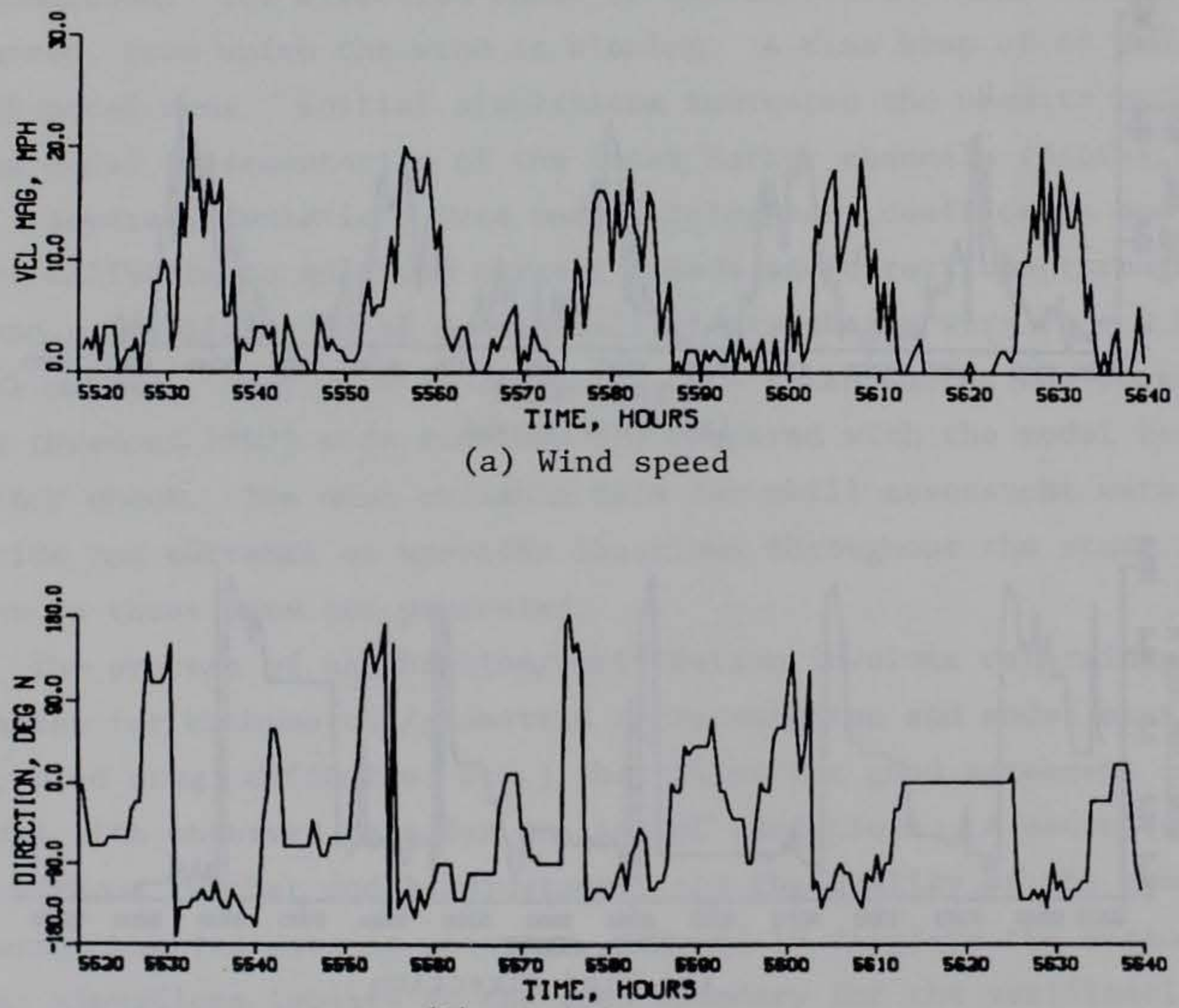

(a) Wind speed

(b) Wind direction

Figure 20. Wind data for verification period

42. For this study, a quantitative measure of goodness of fit was not attempted due to the frequency of subtidal oscillations in the harbors. To match each and every 1-hr subtidal oscillation would require commensurate accuracy in measuring forcing data (wind and the boundary ocean tide both spatially and temporally). The key used in comparing model with observed data is to look for a match in peak flood/ebb velocity magnitudes, range of subtidal oscillations, and overall match of trends in the data. Presentation of results will be divided into three categories: tidal elevations, currents, and circulation. Both calibration and verification results will be presented together in each category. Graphics will be shown for representative gages and processes.

Tidal elevations

43. As mentioned previously, tidal response within San Pedro Bay is almost immediate, and shelf oscillations are present throughout the harbor and are amplified in the Inner Harbor. Gage data taken from open ocean sites were used to develop the forcing boundary condition, and comparisons are presented (Plates 1 and 2) for TG 3 (Cerritos Channel) and TG 7 (San Pedro Bay-East End). For both assessment periods, the match in phase and tide range is excellent.

Currents

44. Observed currents are much more difficult to match. Measurement devices are sensitive to local effects (for example, ship passage, nearby geometry, high-frequency wind effects, etc.). For very small currents, the measured directional data and current magnitudes may exhibit unreasonable values and higher scatter because of inertia and higher noise-to-signal ratio. The measurements in this regime are therefore not as reliable as for higher currents. Comparing model results with general trends in the measured data appears to be as valid as a statistical procedure to quantify a match. Table 1 lists all velocity gage locations where current observations were successful during the assessment periods. Gage locations within the harbor complex are shown in Figure 21. Even though some comparisons are not perfect, the overall quality of the match indicates that the model is reproducing current behavior throughout the harbor complex.

45. In comparing model and observed currents, several factors must be kept in mind. First, model results are averaged over areas between 3 and 30 acres, whereas gage readings are representative of a singular point in the harbor. Second, the model approximates the vertical with three layers, and

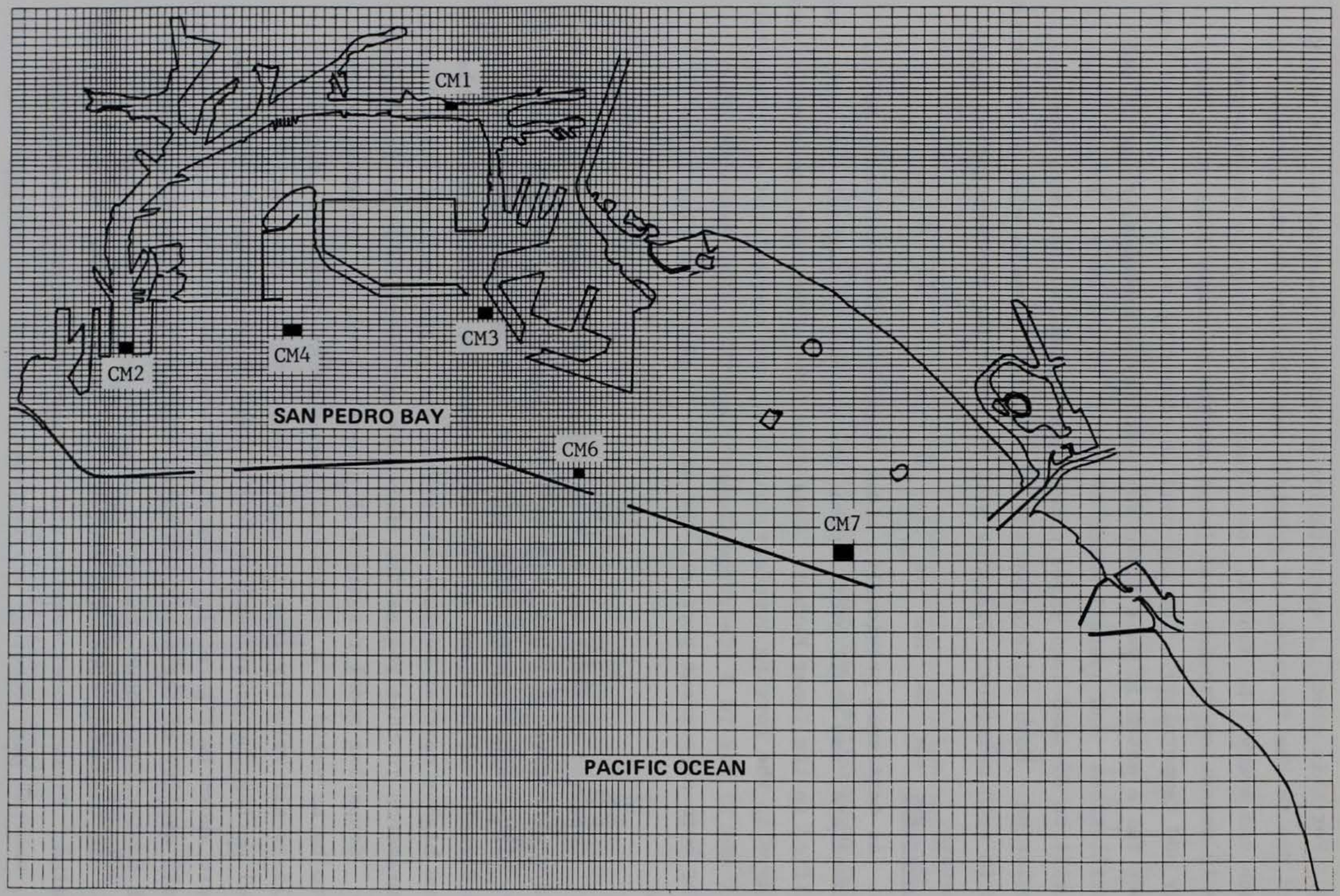

Figure 21. Current meter locations for model validation comparisons

model velocities are an average for an entire layer (usually 10 to 25 ft in height; see Table 1 for meter locations in the vertical). Gage results are taken at specific heights in the water column. Third, but not necessarily inclusive, gage measurements devices have an inherent error, and the forcing boundary condition is not exact.

46. Comments on comparisons at each gage location are as follows:

a. CM1 - Cerritos Channel - Plates 3-10. Measurements were obtained in two layers (surface and bottom). Current direction shown in the plates is in degrees measured from the north and represents the direction in which the current is flowing. Note that directions shown as +180 and -180 deg are the same. In general, all peak flood and ebb currents (magnitudes and directions) were matched in the upper and lower model layers. Ranges of observed subtidal oscillations were replicated. A greater variance between model and observed currents was noted for the upper layer in the calibration run. Somewhat higher subtidal oscillations were noted during day 2 of the verification simulation, which may be caused by an extraneous small oscillation in the forcing tide gage (see Figure 19).

b. CM2 - Main Channel - Plates 11-22. Gage measurements were taken in three layers. A good comparison is noted for all levels (see comments for CM1). Greatest variance is noted for subtidal oscillations during different ebb events in both calibration and verification runs.

c. CM3 - Long Beach/Pier F - Plates 23-34. Gage measurements were made in three layers. Greatest variance is noted in the bottom layer of the calibration run and in the surface layer of the verification run. Directions compared well, and the overall comparison is fair to good.

d. CM4 - Outer Harbor - Plates 35-38. Gage data were recovered at the bottom layer only. Velocities are generally low in this area of the harbor, and circulation patterns are complex and highly sensitive to the boundary forcing. Both magnitude and direction were poorly represented in the calibration run, as if the gage data were in error or results were sensitive to the exact location of the gage. Results from the verification run showed much improvement in magnitude and direction comparisons.

e. CM6 - Queen's Gate/Interior - Plates 39-46. Gage measurements were retrieved for the surface and bottom layers and were accurately modeled in both calibration and verification periods.

f. CM7 - East Entrance/South - Plates 47-54. Data were taken in the surface and bottom layers. Comparisons of model with observed data were good during parts of both calibration and verification periods. High velocities observed in the bottom layer could not be replicated. It is expected current magnitude may be highly sensitive in this area to the specification of the ocean tide at the shallow, eastern end of the open boundary. However, gage data and model results both show an opposing two-layer flow at times during the 5-day runs.

47. Subtidal oscillations are in evidence throughout the harbor complex. To better understand effects of these oscillations, circulation plots (depth-integrated velocity) for a 2-hr period within the verification period were made at 15-min intervals (Figures 22a-22i). These figures clearly indicate reversal of direction in several areas throughout the harbor complex. Significant influence extends beyond the outer breakwaters. However, primary impact is felt within the complex. This effect may be characterized as a pulsating flow pattern. At a given location, the flow may alternately speed up and slow down. As observed in Figures 22b and 22c, flow into the harbors is strong and directed toward the east in the Outer Harbor. Flow is toward the west in the Inner Harbor. Thirty minutes later (Figure 22e), flow into the harbors has diminished, and a circulation gyre has formed in the Outer Harbor. Within the Inner Harbor, flow has reversed and is directed toward the east. Then again, 30 min later (Figure 22g), the pattern for the entire harbor complex has reverted to what was observed an hour earlier (Figure 22c). This behavior of the harbor system is confirmed by analyzing observed data from the 1987 Field Data Survey.

Circulation

48. No definitive data were taken to confirm overall model replication of flow patterns. Circulation data were saved and plotted at 3-hr intervals during one tidal cycle in both calibration and verification periods. Plates 55-60 display flow patterns at near peak flood, peak ebb, and slack water for both calibration (7-11 August) and verification (19-23 August) periods at each level in the vertical. Velocity vectors were plotted at every third grid cell, and their length is proportional to current magnitude. Comparisons of model results with gage, boat survey, and drogue data indicate model flow patterns are reasonable. Circulation gyres are noted to exist near the breakwater entrances and in the Outer Harbor, as expected. Range discharge computations (discussed in a later section) confirm a net circulation to the west in Cerritos Channel as modeled in previous studies (Raney 1976a, b; Seabergh and Outlaw 1984; Seabergh 1985). For most of the harbors, flow is well-mixed. Additional discussion on circulation patterns is presented in a later section comparing plan with existing conditions.

49. In summary, the overall calibration and verification of the model was successful. Complex low flows and subtidal effects were well represented. More accurate comparisons could not be achieved without the necessary detailed

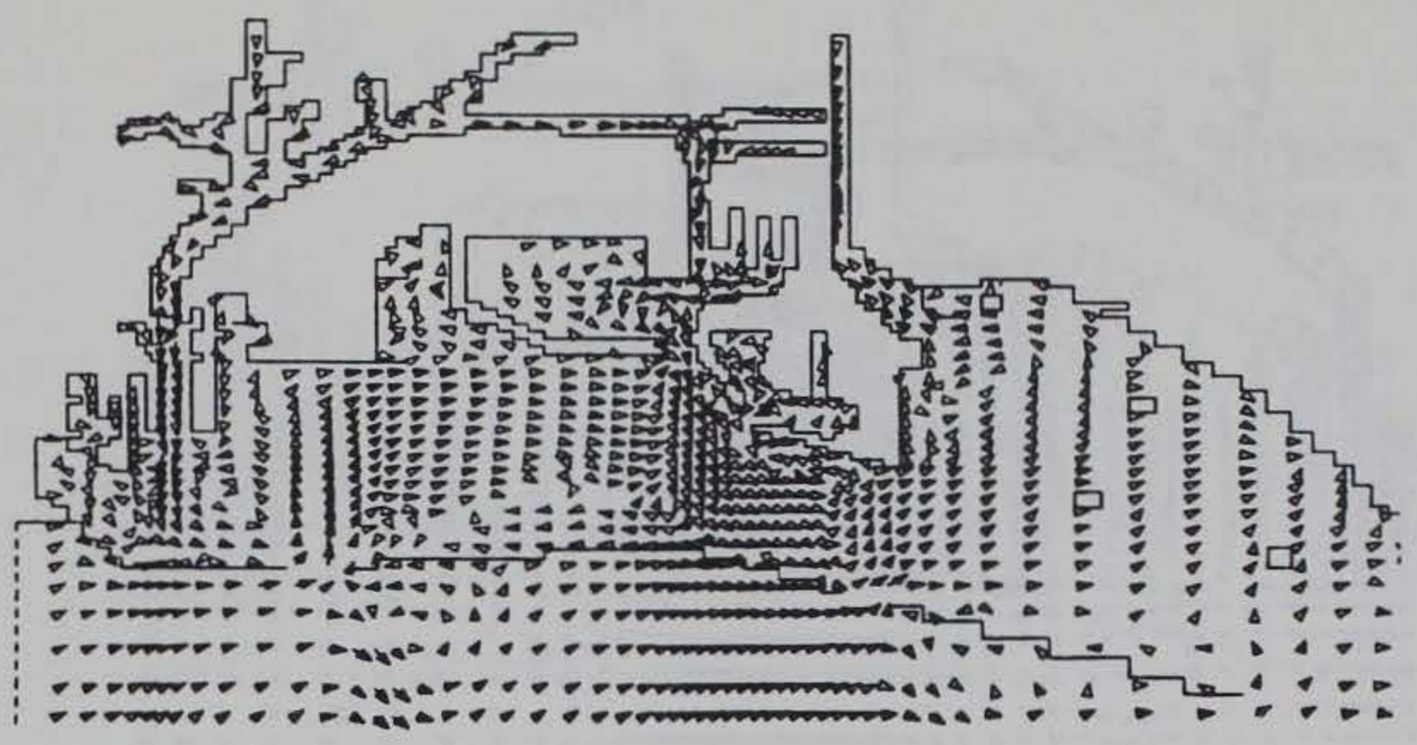

(a) Hour 5548.00

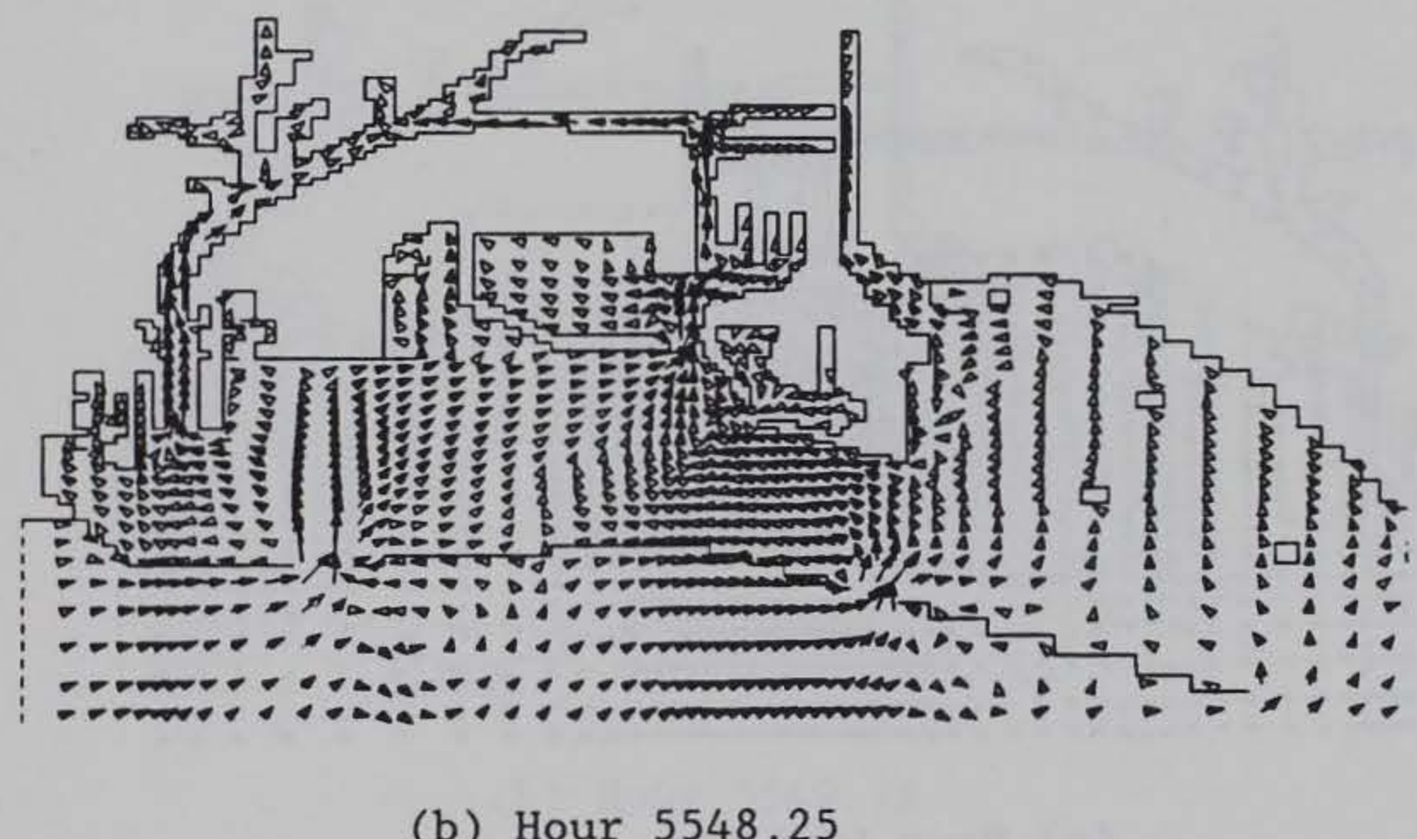

(b) Hour 5548.25

→ 1 FT/SEC

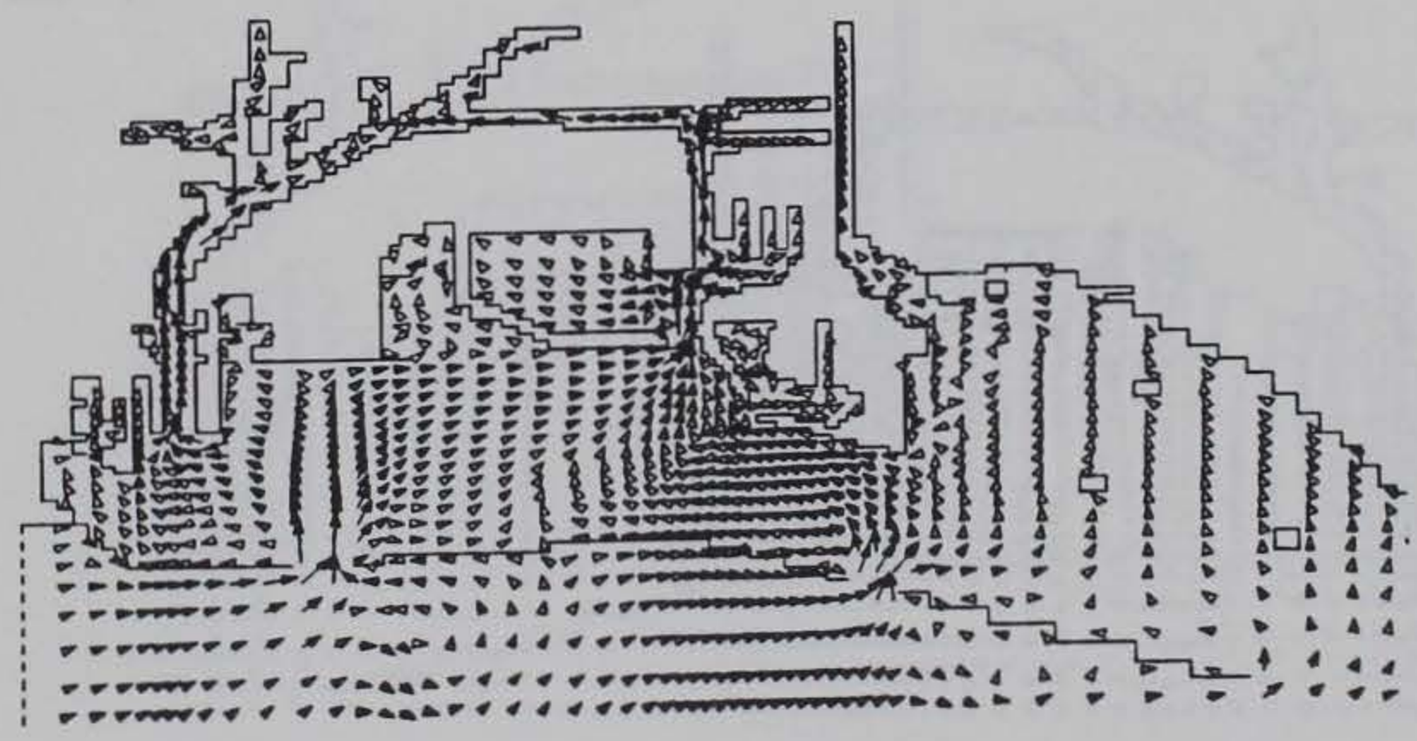

(c) Hour 5548.50

Figure 22. Circulation patterns of depth-integrated velocities for a 2-hr interval (Sheet 1 of 3)

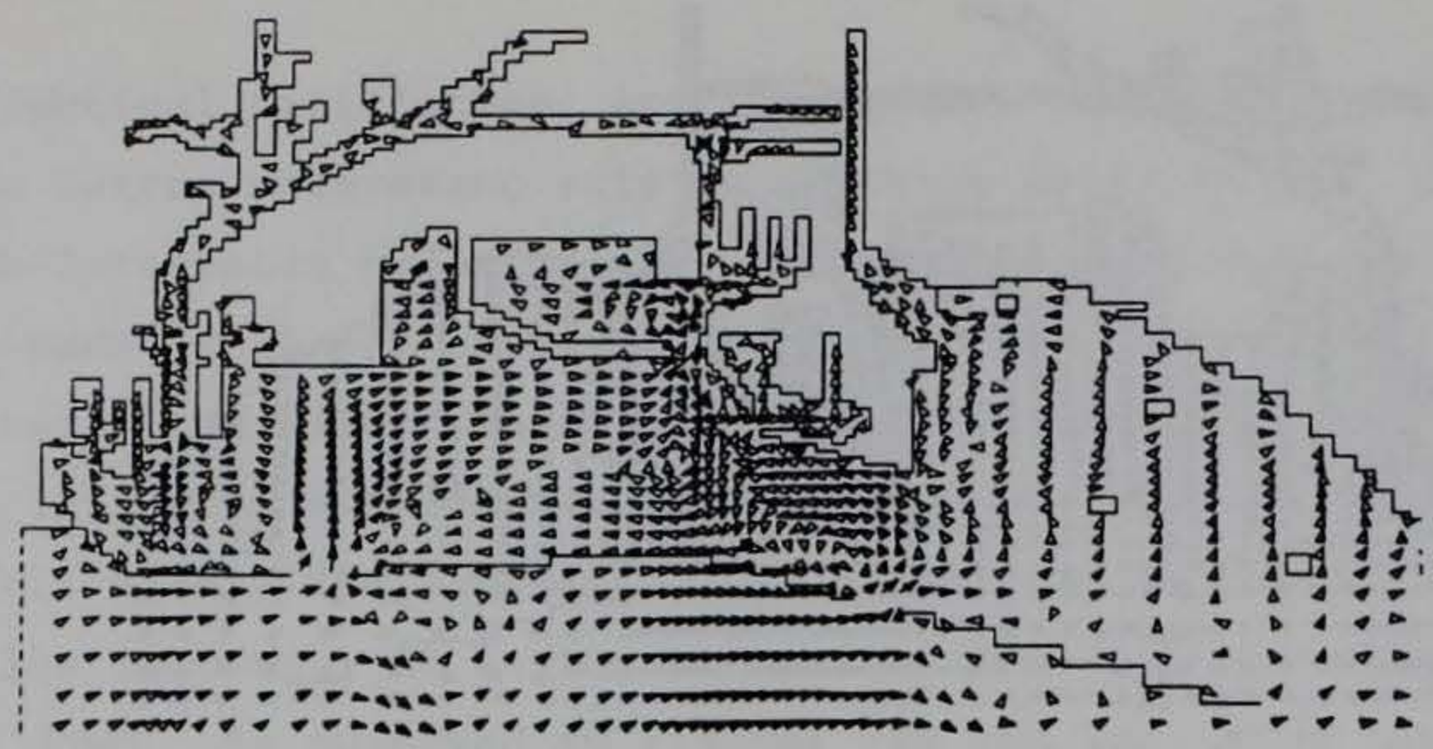

(d) Hour 5548.75

(e) Hour 5549.00

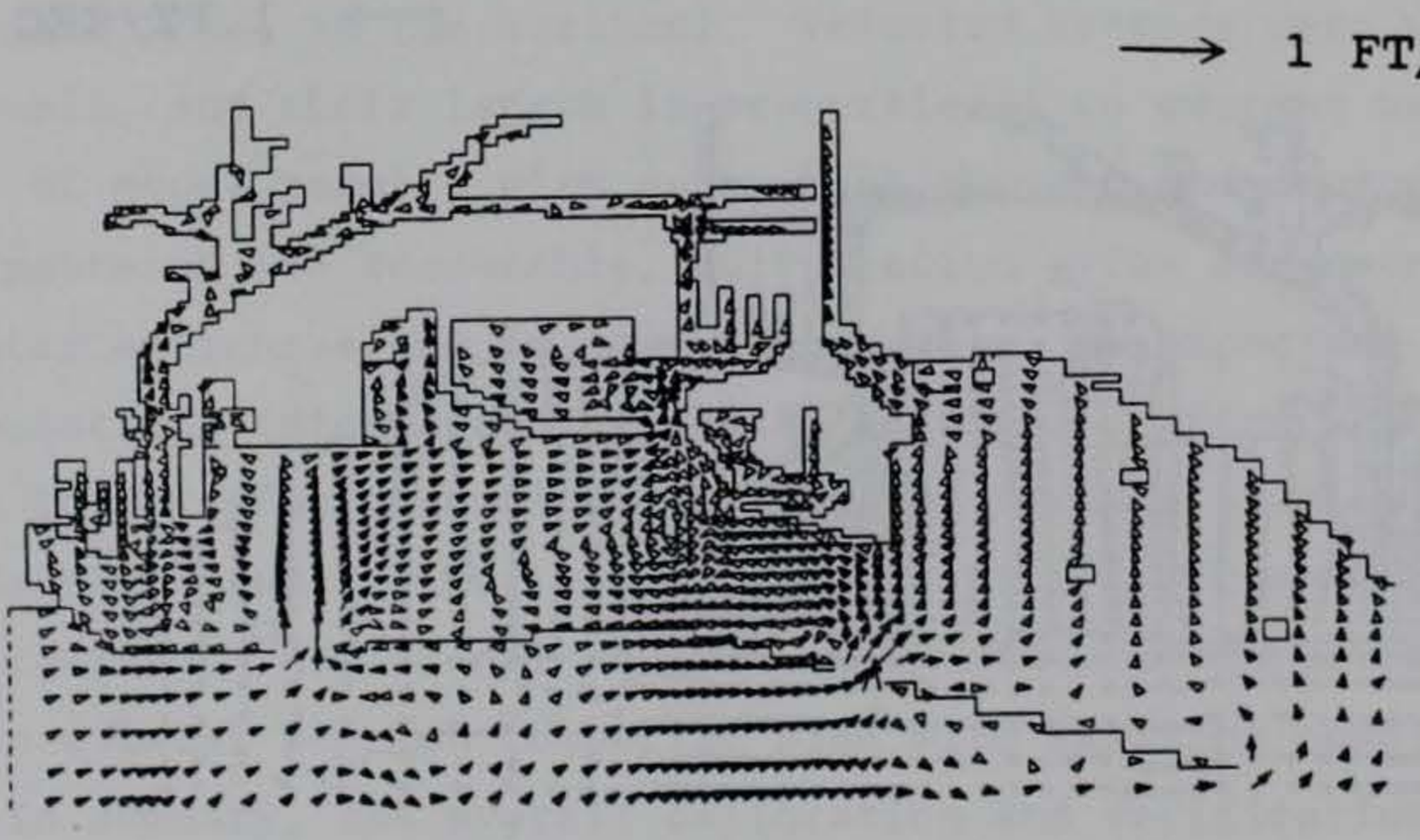

(f) Hour 5549.25

Figure 22. (Sheet 2 of 3)

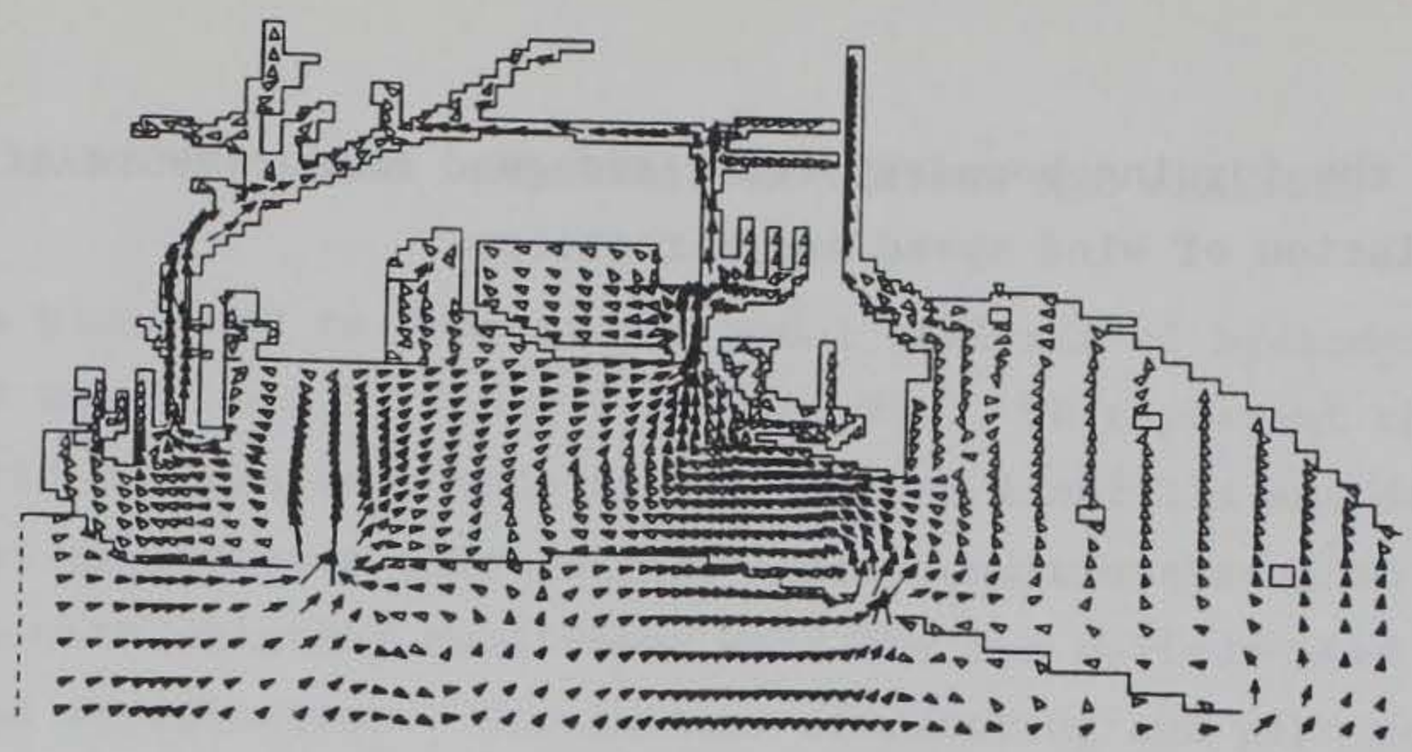

(g) Hour 5549.50

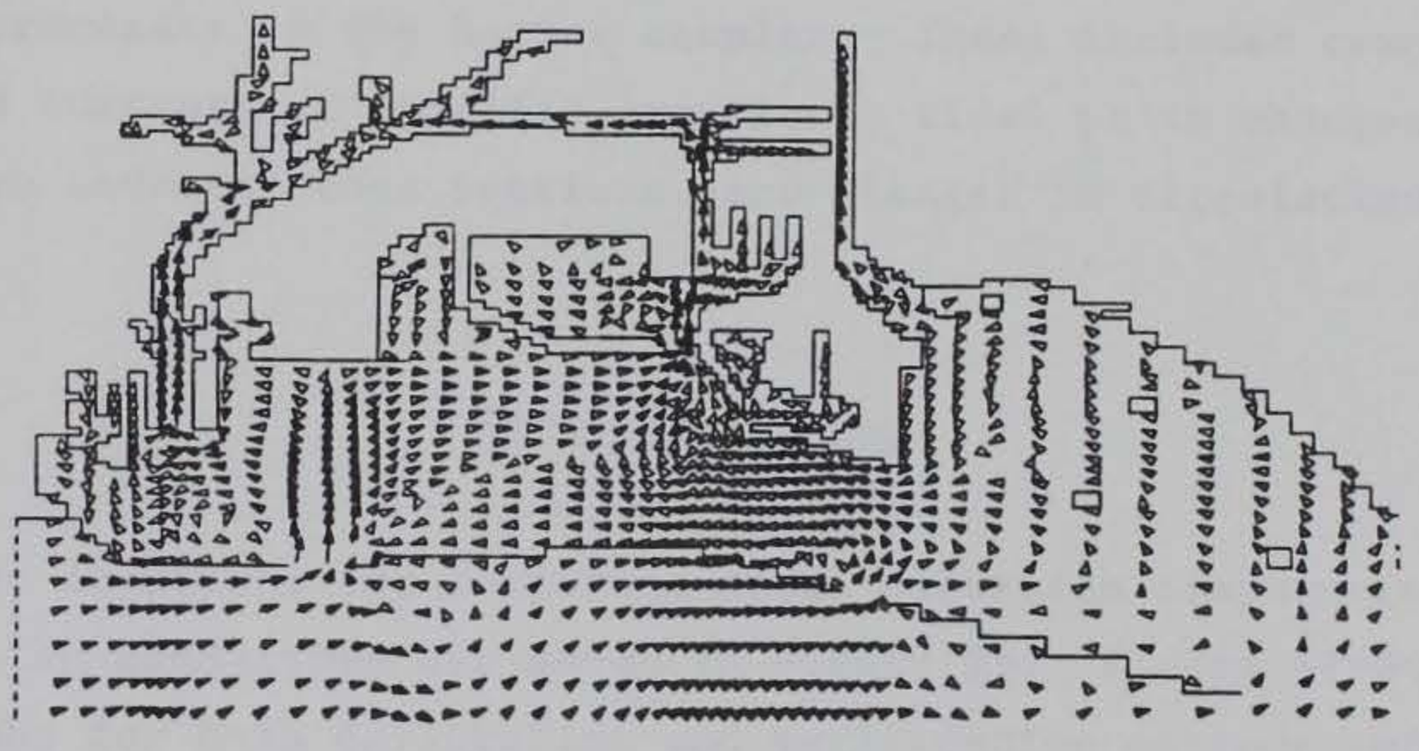

(h) Hour 5549.75

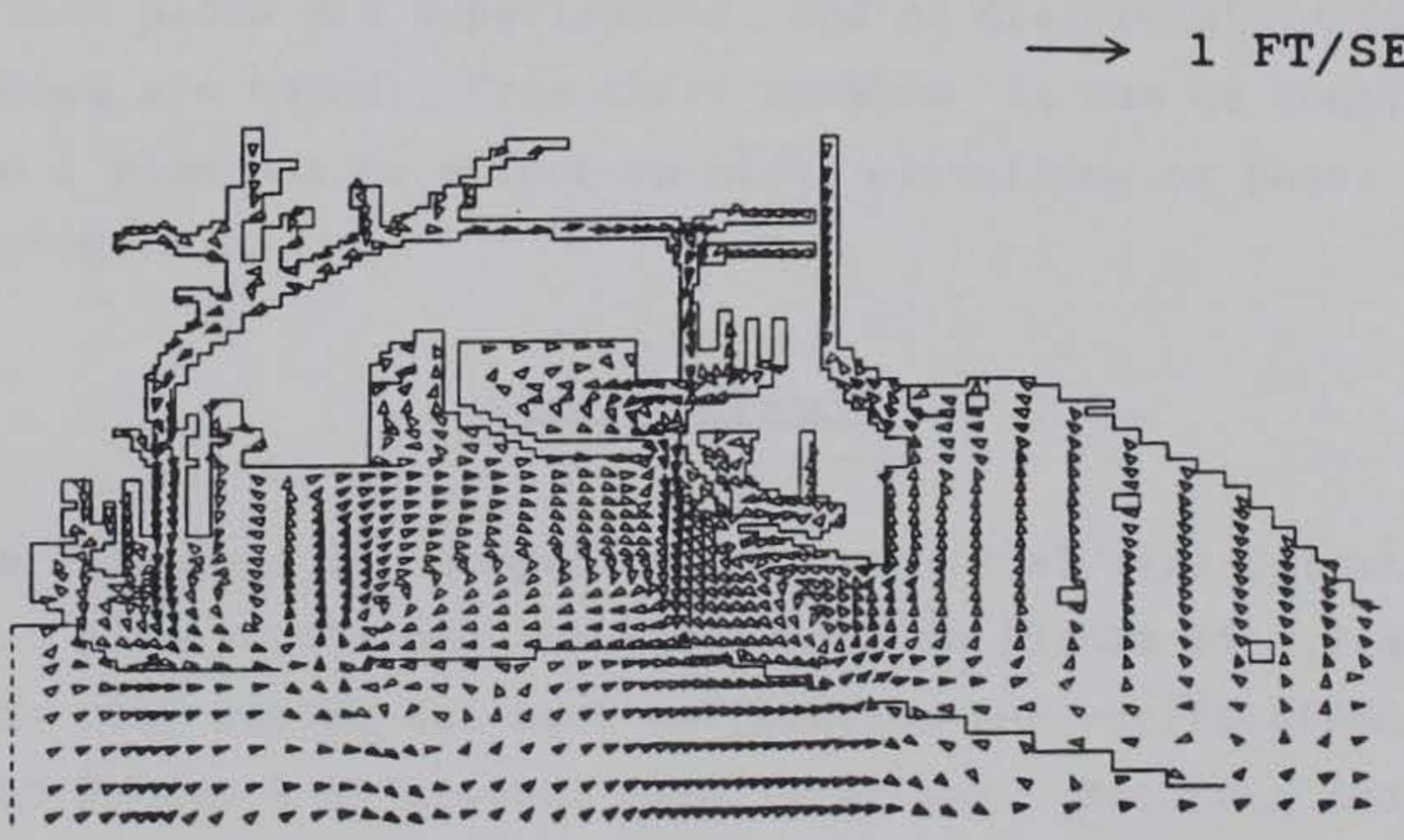

(i) Hour 5550.00

Figure 22. (Sheet 3 of 3)

knowledge of the forcing boundary tides and good measurements of spatial and temporal variation of wind speed and direction.

PART VI: PLAN DEMONSTRATION TESTING AND ANALYSIS

50. The plan used to demonstrate model analysis of hydrodynamic/water quality impact was Scheme B, Phase 1 (Figure 23). To represent this plan, appropriate grid changes were made to approximate landfills and dredged depths for all channel alterations (Figure 24). Base conditions adopted for comparing plan with existing conditions were the two periods used for model calibration and verification. Simulations of existing and plan conditions for the month of August 1987 were also made to support water quality modeling efforts.

51. Several methods were used to analyze the impacts of Scheme B on hydrodynamic processes in the harbor complex. These included comparisons of elevations and currents at specific locations, tidal prism changes, flow changes through several cross sections, and changes in circulation patterns of the harbor.

Tidal Elevations

52. Gage locations for comparing tidal elevation computations for existing and plan conditions are shown in Figure 25. Plates 61-64 display tide hydrographs for both calibration and verification periods, with and without Scheme B at gage locations TC1, TC3, TC5, TC14, and TC17. Existing and plan condition plots are superimposed, and no discernible differences in amplitude or phase are noted. From these results, it can be concluded the Scheme B, Phase 1 plan has no effect on tidal elevations or phase throughout the harbor complex.

Tidal Currents

53. Gage locations for comparing computed tidal/wind-driven currents for existing and plan conditions are also shown in Figure 25. Plates 65-104 display velocity time series for both calibration and verification periods, with and without Scheme B at several gage locations. Existing and plan condition plots are superimposed to permit easy visual inspection of impact.

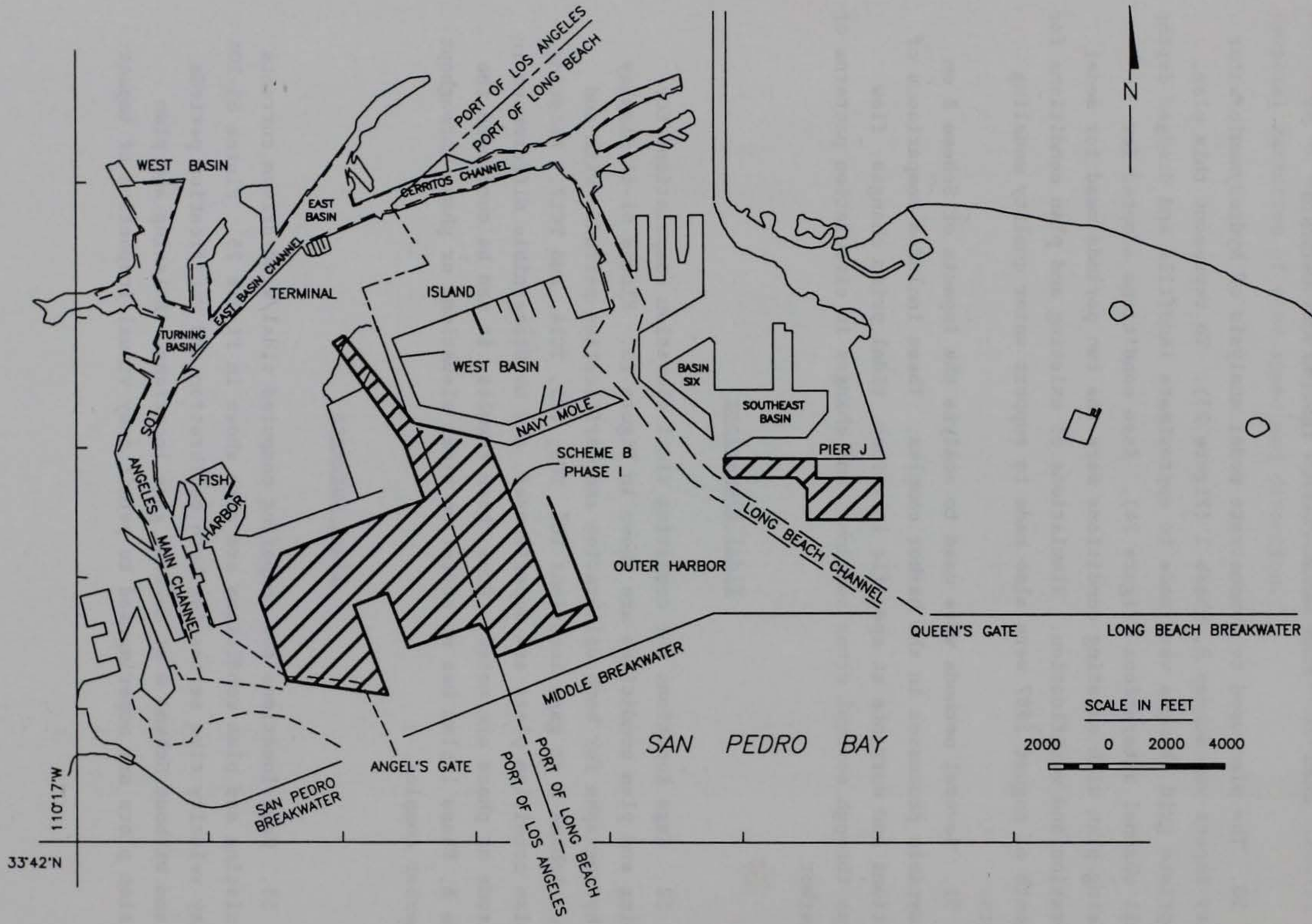

Figure 23. Harbor layout for Scheme B, Phase 1

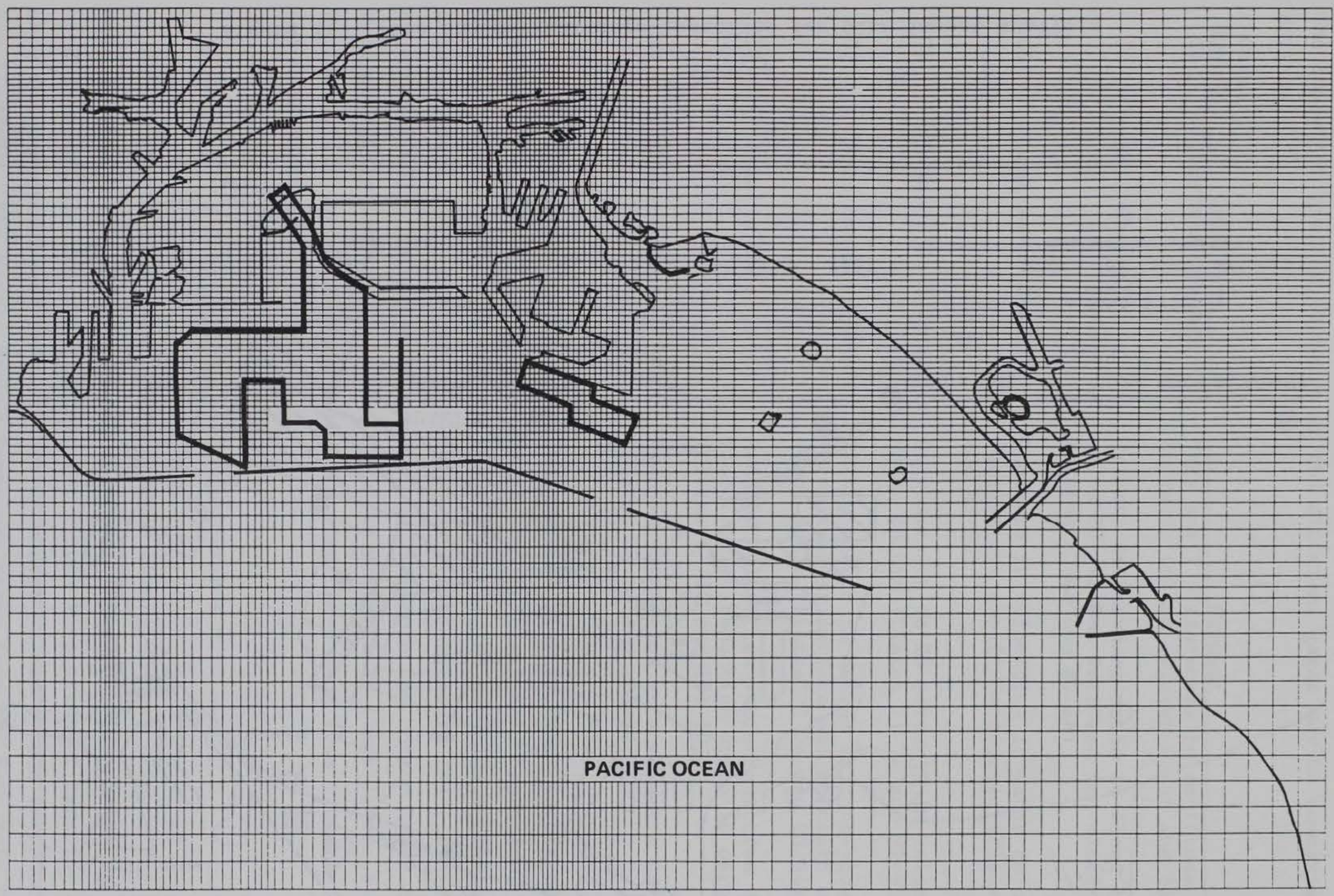

Figure 24. Representation of Scheme B, Phase 1 landfill in computational grid

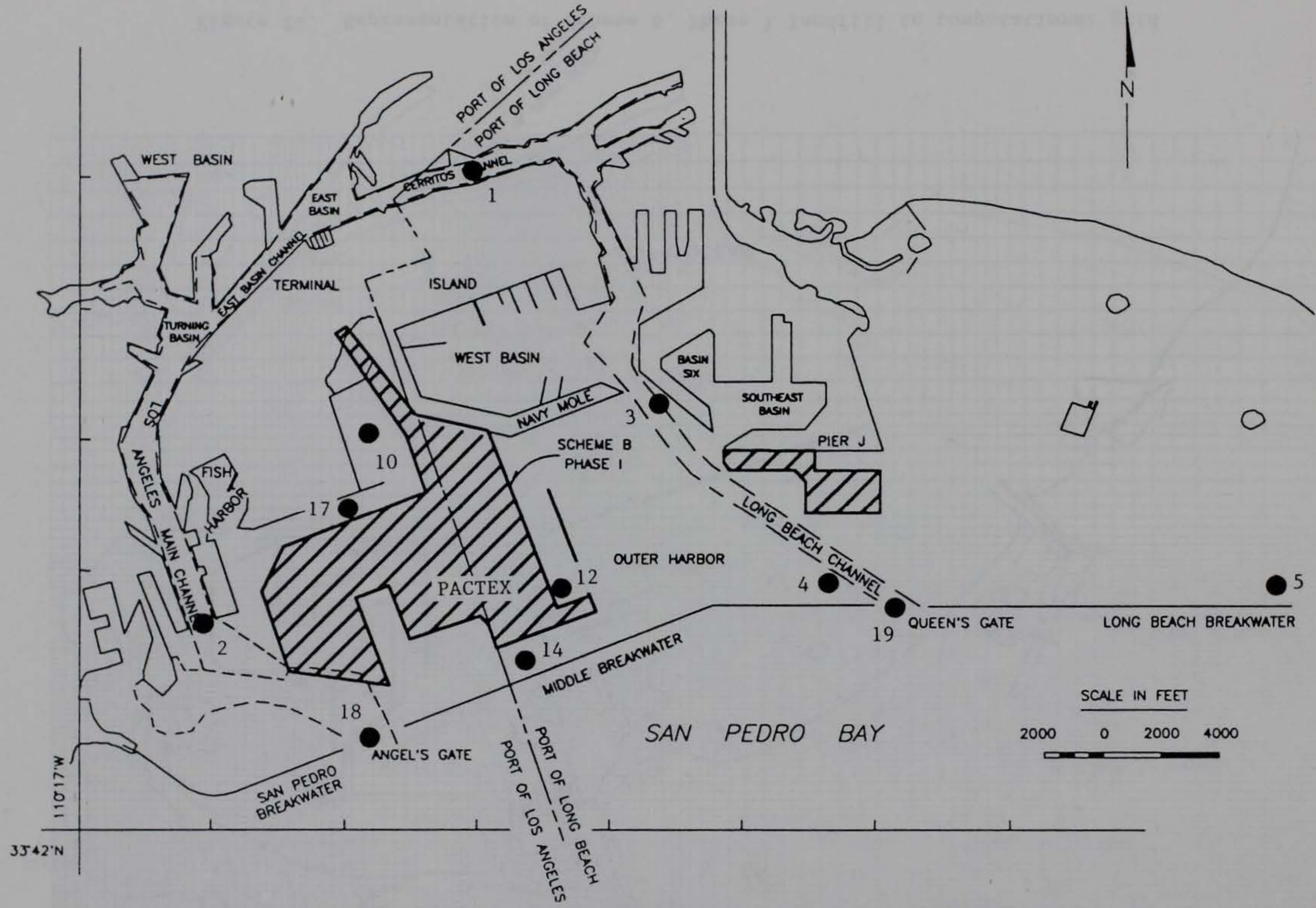

Figure 25. Tide and current gage locations for plan impact analysis

The impact of plan on currents at the different gages may be summarized as follows:

Gage Number	Gage Name	Comment
C1	Cerritos Channel	Very small differences in amplitude and phase in water column (Plates 65-66 and 85-86)
C2	Main Channel	Primary differences noted in flood cycle--up to 20-percent increase in velocity (Plates 67-68 and 87-88)
C3	Long Beach-Pier F	Decrease in velocities in water column--oscillation amplitude reduced (Plates 69-70 and 89-90)
C4	Queen's Gate-Interior	Decrease (up to 25 percent) in velocities in water column (Plates 71-72 and 91-92)
C5	East Entrance-South	Little change in bottom current--lower velocities at surface and middepth during flood cycle (Plates 73-74 and 93-94)
C18	Angel's Gate	Reduced velocities--more reduction during flood cycle--reduction up to 50 percent (Plates 81-82 and 101-102)
C19	Queen's Gate	Reduced velocities as at Angel's Gate (Plates 83-84 and 103-104)

54. For both test periods, current behavior in newly constructed slips (PACTEX, Long Beach Dike (Plates 77-78 and 97-98), Pier J Expansion) exhibited opposing directions from surface to bottom. In the new Middle Breakwater Channel (Gage C14), surface velocities were higher toward the east (Plates 79-80 and 99-100). For existing conditions, middepth and bottom layer currents were primarily toward the west. For plan conditions, these layers exhibited typical tidal cycle behavior with directions reversing from flood to ebb phase and vice versa.

Tidal Discharges

55. Total tidal discharges through several ranges (Figure 26) established in the model grid are shown in Plates 105-112. Existing and plan condition results are superimposed for visual inspection of impact. Results show the expected small reduction in discharge caused by the introduction of new landfill. The Middle Harbor Range was taken from the Navy Mole to the

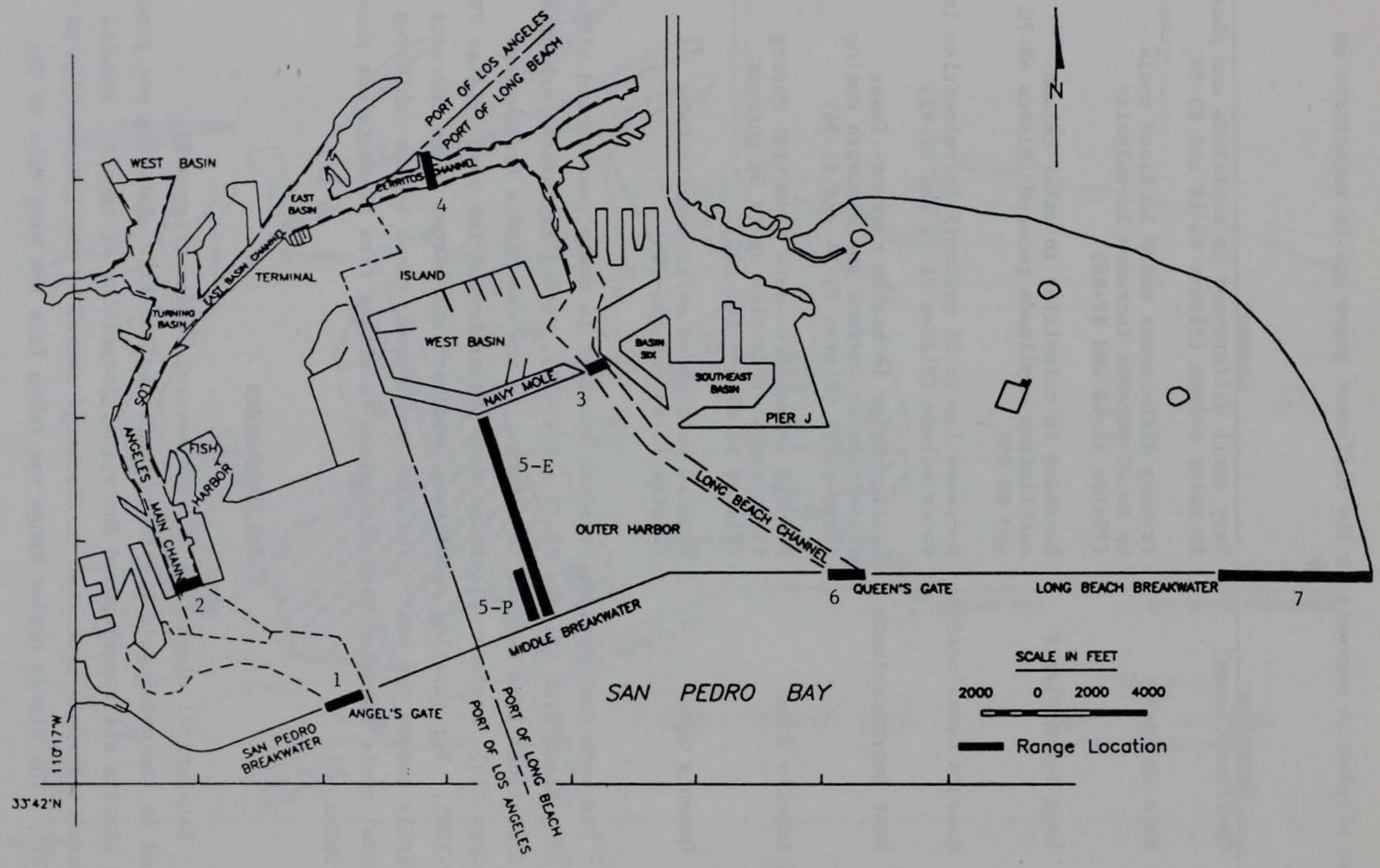

Figure 26. Range locations for plan impact analysis

Middle Breakwater for existing conditions (Range 5E). With plan conditions, this range was taken from the PACTEX landfill to the Middle Breakwater (Range 5P). Plates 107 and 111 display results from this range indicating similar discharge cycles with a 2- to 3-hr phase lag.

56. In additon to comparing time series of discharge, the total discharge was integrated over a specific period during the simulation to estimate changes in tidal prism of the harbors. Ranges 1, 6, and 7, located across Angel's Gate, Queen's Gate, and the East Entrance, respectively, were used for the tidal prism computation since they control flow into and out of the harbors. Range 7 extends from the easternmost tip of the Long Beach Breakwater to the shore south of Anaheim Bay. Because of the rectilinear nature of the grid, it was convenient to select Range 7 in this manner. The total water surface area bounded by these three ranges is approximately 660×10^6 sq ft. The total landfill area associated with Scheme B, Phase 1, within the harbor complex is 67×10^6 sq ft. Therefore, a 10.1-percent reduction in available water surface area is expected to cause a corresponding loss of tidal prism.

57. A period of 2 lunar days was chosen to calculate total and net range discharge (hours 5282 to 5331.6 in the 7-11 August period and 5571 to 5620.6 in the 19-23 August period). Since the tidal range is fluctuating over the entire period and the flows are influenced by wind, the total discharge into the system will not equal total discharge out of the system. The approach adopted is to sum results over each range and average inflow and outflow for the two tidal cycles. Table 2 gives total flood and ebb volumes for both simulation periods and prism computations. Percent reductions for both periods are similar and compare well with the expected reduction.

Circulation

58. To aid in comparing plan with existing conditions, plate figures for circulation during near peak flood and ebb and slack water for existing conditions are presented along with patterns for plan conditions to permit easy visual inspection of plan impact (Plates 113-124). Velocity vectors are plotted at every third grid cell. Of course, the first conclusion reached is that the new landfill eliminates the gyre circulation in the Outer Harbor and peak flood and ebb velocities in the outer breakwater entrances are reduced. Specific comments for the three snapshot periods are:

a. Peak flood. Changes in circulation patterns are confined to the Outer and Inner Harbor areas. For the specific point in the calibration period at which the peak flood snapshot was taken, flow direction was changed by the plan from westerly to easterly. A stronger clockwise circulation within the Navy Mole was noted for the middepth and bottom layers with the plan. Flow directions within new slips are reversed in the upper and lower layers.

b. Peak ebb. Changes in circulation patterns are again confined to the same areas as for peak flood.

c. Slack water. Plan condition results show the absence of the large gyre observed for existing conditions.

59. In order to determine the effect of the plan on net circulation in the Inner Harbor areas (Los Angeles Main Channel, East Basin Channel, Cerritos Channel, and Back Channel), the discharges across Ranges 2, 3, and 4 (Figure 26) were integrated over two lunar cycles for existing and plan conditions, and net flow volumes across the ranges were computed. The direction or sign of the discharges was duly taken into account in these calculations. The resulting net flow volumes are shown in Table 3 for calibration and verification periods. Ranges 2 and 3 are located across the entrance to Los Angeles Main Channel and the Navy Basin, respectively, whereas Range 4 is located across Cerritos Channel. The following sign conventions are used for net flow volumes (Table 3) and net flows. At both Ranges 2 and 3, positive and negative signs respectively indicate that net flow across the ranges is to the north and south. At Range 4, positive and negative signs denote that net flow across the range is to the east and west, respectively.

60. Considering existing conditions, it is seen that for both calibration and verification, the net flow is negative at Ranges 2 and 4, and positive at Range 3. This means the net flow is directed towards the south at Range 2, towards the north at Range 3, and towards the west at Range 4, implying a net counterclockwise circulation (i.e., from Long Beach to Los Angeles) in the Inner Harbor areas. This agrees with the results of previous WES studies, as mentioned in Part II. Similarly, it can be deduced from Table 3 that for the plan, the net circulation is clockwise during the calibration period and has a strong tendency towards the clockwise direction during the verification period.

61. In summary, with the introduction of Scheme B, Phase 1, tidal elevations remain unchanged; however, current velocities through the harbor entrances are reduced along with the tidal prism. There were some changes in the harbor circulation, but these changes were primarily confined to the Outer

Harbor and Inner Harbor areas. Results indicate the plan has a tendency to cause a reversal in the net flow through the Inner Harbor.

PART VII: HYDRODYNAMIC SIMULATIONS FOR WATER QUALITY MODELING

62. Several hydrodynamic simulations were made in support of the water quality modeling effort. These included: (a) establishing the length of time required to reach a dynamic steady state, (b) repeating a steady-state tidal cycle for several days and tracking dye tracer movements within the Outer and Inner Harbors, and (c) simulating conditions for the month of August 1987 for both existing and plan conditions.

63. As mentioned previously, the fundamental interfacing problem consists of processing hydrodynamic output so that advection and diffusion are accurately depicted in the WQM. The first step in developing interface procedures was to provide sample HM output from an uncalibrated model for checking WQM representation of cell volumes, flow among cells, discretization, and mass conservation. These and all tests described in this section are reported in a separate report (Hall 1990) on the WQM effort.

64. After the HM was calibrated and verified, the next step in the interface development was to assure that the transport properties of the HM were maintained in the WQM. The HM served as a standard for evaluating and adjusting the transport properties of the WQM. Results from HM simulations of a passive tracer in the Outer Harbor were used to initially adjust the WQM representation of the study area. These simulations were performed by forcing the HM with a 24-hr sinusoidal tide for 5 days. Examination of the results showed a dynamic steady-state condition in the harbor complex was reached in 2 days, i.e., velocities during the third day were reproduced in the fourth day. The simulation was restarted, and a passive tracer patch was introduced in the surface layer of several cells in the Outer Harbor and tracked for 3 days. Results show the tracer diffuses to the bottom and disperses throughout the Outer Harbor during the test period.

65. Hydrodynamic information for calibration and verification of the WQM was provided by simulating most of the month of August 1987. Appropriate tidal elevation and wind data were selected from the field measurements to force the HM for the simulations. Several overlapping HM runs, each approximately 5 days in duration, were made, and the results were concatenated to form a continuous output file of HM results averaged over 1-hr intervals. Similar information was produced for both existing conditions and for the Scheme B, Phase 1 demonstration test. This information was used as input to run the WQM simulations from 2300 hr on 1 August to 0600 hr on 28 August 1987.

PART VIII: SUMMARY AND CONCLUSIONS

66. Based on the results of the 3-D numerical model tidal circulation study of the LA/LB Harbors and plan demonstration, it is concluded that:

a. Significant subtidal oscillations are present in the observed data. The model did a good job in representing the magnitude of these oscillations (up to 0.6 ft in elevation and 0.6 ft/sec in velocity).

b. The 3-D model was successively calibrated and verified to represent observed conditions in the LA/LB Harbor complex.

c. The landfill of the plan did not affect the filling of the harbors since tidal ranges were maintained and no discernible differences in phase were noted.

d. Discharge into the system was reduced by an amount equivalent to the reduced harbor surface area (about 10 percent) implying no change in the net tidal flushing per unit volume between existing conditions and the plan.

e. The plan caused only small changes in the flow distribution throughout the harbor complex.

f. Velocity magnitude and direction were changed at specific locations. The greatest change in magnitude occurred at the entrances of the harbors. Peak flood and ebb velocities at Angel's and Queen's Gates were reduced up to 50 and 40 percent, respectively, for a large spring tide condition. The decrease in velocity was due to increased channel depths and reduction of harbor surface area served by these channels. While percentage changes were large, it should be noted that velocity magnitudes throughout the harbor are small (less than 1 ft/sec). Even for a large spring tide (tide ranges of almost 9 ft), maximum velocities in Angel's gate were less than 1.5 ft/sec.

g. Net circulation in the Inner Harbor showed a tendency to reverse under plan conditions. The net circulation for existing conditions is from east to west (i.e. from Long Beach to Los Angeles Harbor), while under plan conditons the net flow was from west to east toward Long Beach.

h. Circulation vector plots provided information on overall flow patterns in the harbors. Existing condition patterns were dominated by large horizontal eddies within the Outer Harbor. Introduction of the plan landfill eliminated these eddies. The plan also caused stronger gradients in velocity profiles. Often upper and lower layers were characterized by flows in opposite directions, especially in the new slips.

i. Production simulations were made in support of the water quality modeling effort. The results of this effort are described in a companion report.

REFERENCES

Butler, H. Lee. 1978a (Jun). "Numerical Simulation of Tidal Hydrodynamics; Great Egg Harbor and Corson Inlets, New Jersey," Technical Report H-78-11, US Army Engineer Waterways Experiment Station, Vicksburg, MS.

_____. 1978b (Aug). "Coastal Flood Simulation in Stretched Coordinates," Proceedings, 16th International Conference on Coastal Engineering, American Society of Civil Engineers, New York, pp 1030-1048.

_____. 1978c (Dec). "Numerical Simulation of the Coos Bay-South Slough Complex," Technical Report H-78-22, US Army Engineer Waterways Experiment Station, Vicksburg, MS.

_____. 1980. "Evolution of a Numerical Model for Simulating Long-Period Wave Behavior in Ocean Estuarine Systems," Estuarine and Wetland Processes: with Emphasis on Modeling, Marine Science, Vol 11, Plenum Press, New York.

Butler, H. L., and Sheng, Y. P. 1982 (Feb). "ADI Procedures for Solving the Shallow Water Equations in Transformed Coordinates, "Proceedings of the 1982 Army Numerical Analysis and Computers Conference, US Army Research Office, Research Triangle Park, NC.

Flick, Reinhard E., and Cayan, Daniel R. 1984. "Extreme Sea Levels in the Coast of California," Proceedings of the Nineteenth Coastal Engineering Conference, American Society of Civil Engineers, Houston, TX, Vol I, pp 886-898.

Garrat, J. R. 1977. "Review of Drag Coefficients over Oceans and Continents," Monthly Weather Review 105, pp 915-929.

Hall, R. W. 1990. "Los Angeles and Long Beach Harbors Model Enhancement Program; Numerical Water Quality Model Study of Harbor Enhancements," Technical Report EL-90-2, US Army Engineer Waterways Experiment Station, Vicksburg, MS.

Meadows, Guy A. 1987 (Sep). "A Remote Sensing Experiment in Los Angeles Harbor to Determine Tidally Induced Advective Effects in the Harbor Basin," Final Report, Coastal Dynamics Inc., Ann Arbor, MI.

McAnally, W. H., Jr. 1975 (Sep). "Los Angeles and Long Beach Harbors Model Study; Report 5: Tidal Verification and Base Circulation Tests," Technical Report H-75-4, US Army Engineer Waterways Experiment Station, Vicksburg, MS.

McGehee, D. W., McKinney, J. P., and Dickey, M. D. 1989. "Los Angeles and Long Beach Harbors Model Enhancement Program; Tidal Circulation Prototype Data Collection Effort for the Los Angeles/Long Beach Harbors Model Enhancement Program," Technical Report CERC-89-17, US Army Engineer Waterways Experiment Station, Vicksburg, MS.

Outlaw, D. G., and Raney, D. C. 1979 (May). "Numerical Analysis of Tidal Circulation for Long Beach Outer Harbor Proposed Landfill," Miscellaneous Paper H-79-5, US Army Engineer Waterways Experiment Station, Vicksburg, MS.

Pickett, Ellis B., et al. 1975 (Jun). "Los Angeles and Long Beach Harbors Model Study; Report 1, Prototype Data Acquisition and Observation," Technical Report H-75-4, US Army Engineer Waterways Experiment Station, Vicksburg, MS.

Raney, D. C. 1976a (Sep). "Numerical Analysis of Tidal Circulation for Long Beach Harbor; Report 1: Existing Conditions and Alternate Plans for Pier J

Completion and Tanker Terminal Study," Miscellaneous Paper H-76-4, US Army Engineer Waterways Experiment Station, Vicksburg, MS.

_____. 1976b (Sep). "Numerical Analysis of Tidal Circulation for Long Beach Harbor; Report 3: Existing Conditions and Alternate Plans for Pier J Completion and Tanker Terminal Study with -82 Ft Channel," Miscellaneous Paper H-76-4, US Army Engineer Waterways Experiment Station, Vicksburg, MS.

Schmalz, R. A., Jr. 1983 (Sep). "The Development of a Numerical Solution to the Transport Equation; Report 1: Methodology, Report 2: Computational Procedures, Report 3: Test Results," Miscellaneous Paper CERC-83-2, US Army Engineer Waterways Experiment Station, Vicksburg, MS.

Seabergh, W. C. 1985 (Jul). "Los Angeles and Long Beach Harbors Model Study, Deep-Draft Dry Bulk Export Terminal, Alternative No. 6: Resonant Response and Tidal Circulation Studies," Miscellaneous Paper CERC-85-8, US Army Engineer Waterways Experiment Station, Vicksburg, MS.

Seabergh, W. C., and Outlaw, D. G. 1984 (Jun). "Los Angeles and Long Beach Harbors Model Study; Numerical Analysis of Tidal Circulation for the 2020 Master Plan," Miscellaneous Paper CERC-84-5, US Army Engineer Waterways Experiment Station, Vicksburg, MS.

Sheng, Y. P. 1983 (Sep). "Mathematical Modeling of Three-Dimensional Coastal Currents and Sediment Dispersion: Model Development and Application," Technical Report CERC-83-2, US Army Engineer Waterways Experiment Station, Vicksburg, MS.

Thompson, Joe F. 1987a. "Program EAGLE - Numerical Grid Generation System User's Manual, Vol 2: Surface Generation System, USAF Armament Laboratory, Eglin Air Force Base, FL.

_____. 1987b. "Program EAGLE - Numerical Grid Generation System User's Manual, Vol 3: Grid Generation System, USAF Armament Laboratory, Eglin Air Force Base, FL.

Thompson, Joe F., Warsi, Z. U. A., and Mastin, C. Wayne. 1984. Numerical Grid Generation: Foundations and Applications, North-Holland, New York.

Wilson, B. W., et al. 1968 (Jul). "Final Report; Wave and Surge-Action Study for Los Angeles-Long Beach Harbors," (in 2 vols), Science Engineering Associates, San Marino, CA.

Table 1

Prototype Velocity Gage Locations

Gage Number	Location Water Depth, ft, MLLW	Meter Location	Meter Depth, ft, MLLW
CM1	Cerritos Channel (30)	Surface	5
		Bottom	24
CM2	Main Channel (35)	Surface	10
		Middepth	17
		Bottom	29
CM3	Long Beach-Pier F (60)	Surface	7
		Middepth	32
		Bottom	54
CM4	Outer Harbor (30)	Bottom	24
CM6	Queen's Gate-Interior (65)	Surface	10
		Bottom	50
CM7	East Entrance-South (46)	Surface	14
		Bottom	40

Table 2

Total Flood and Ebb Volumes (10^6 cu ft) During Two Lunar Cycles

	Calibration				Verification			
	Flood		Ebb		Flood		Ebb	
Range No.	Ex*	Plan	Ex	Plan	Ex	Plan	Ex	Plan
1	5830	5280	5210	3930	5190	4530	3330	2410
6	3570	3580	3880	3750	2320	2380	3080	2880
7	5340	4110	5490	5800	2690	2170	4620	4720
Total	14740	12970	14580	13480	10200	9080	11030	10010
Average	Ex 14660		Plan 13225		Ex 10615		Plan 9545	
Difference	1435				1070			
Percent Change	-9.8				-10.1			

* Ex = existing conditions

Table 3

Net Flow Volumes (10^6 cu ft) During Two Lunar Cycles

Range No.	Calibration		Verification	
	Ex*	Plan	Ex	Plan
2	-109	56	-138	26
3	179	-11	179	21
4	-166	22	-157	5

* Ex = existing conditions

PLATES 1-124

Plates are positioned for ease in comparison of velocity magnitude and direction plots and existing and plan conditions.

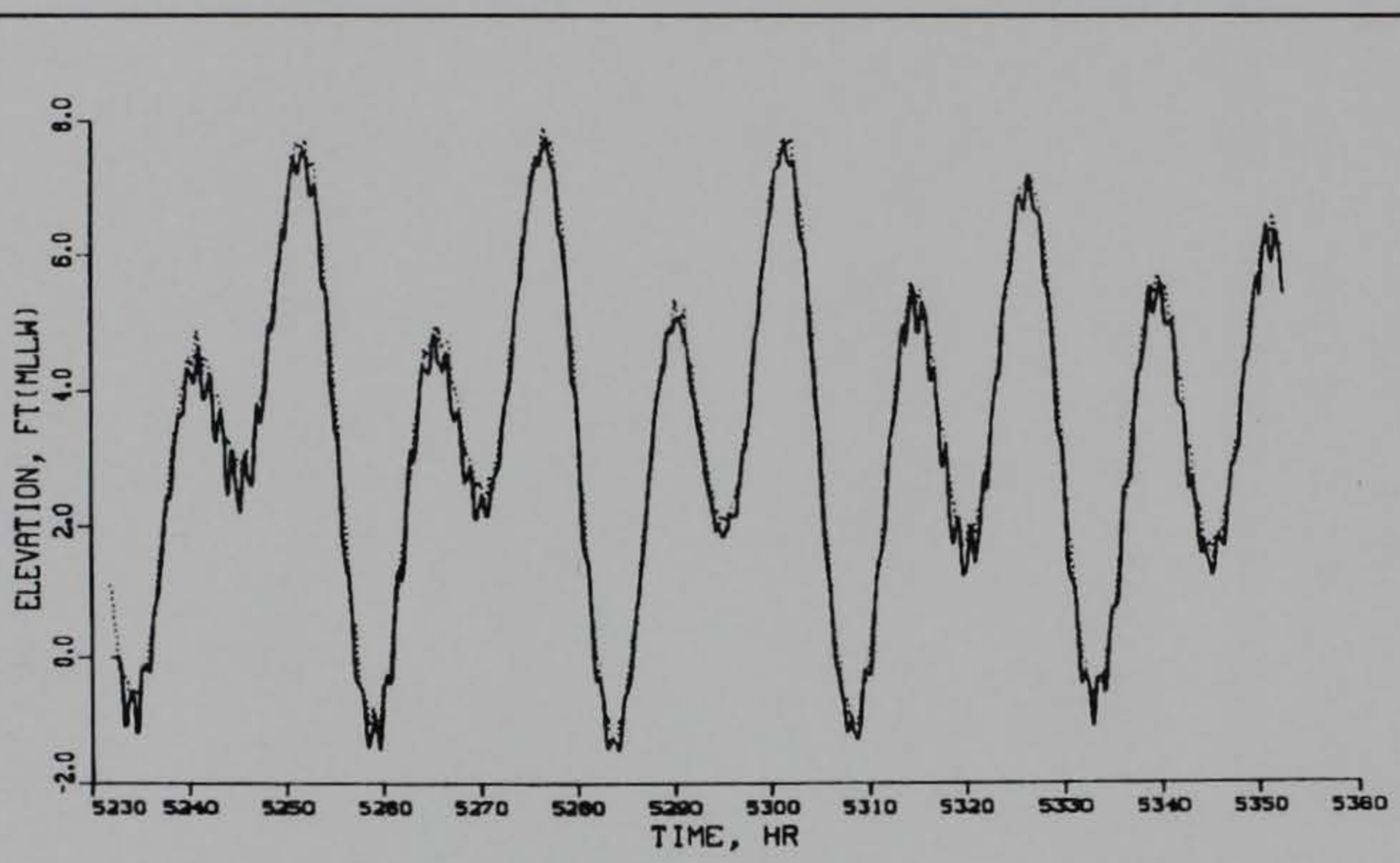

TIDE GAGE TG 3

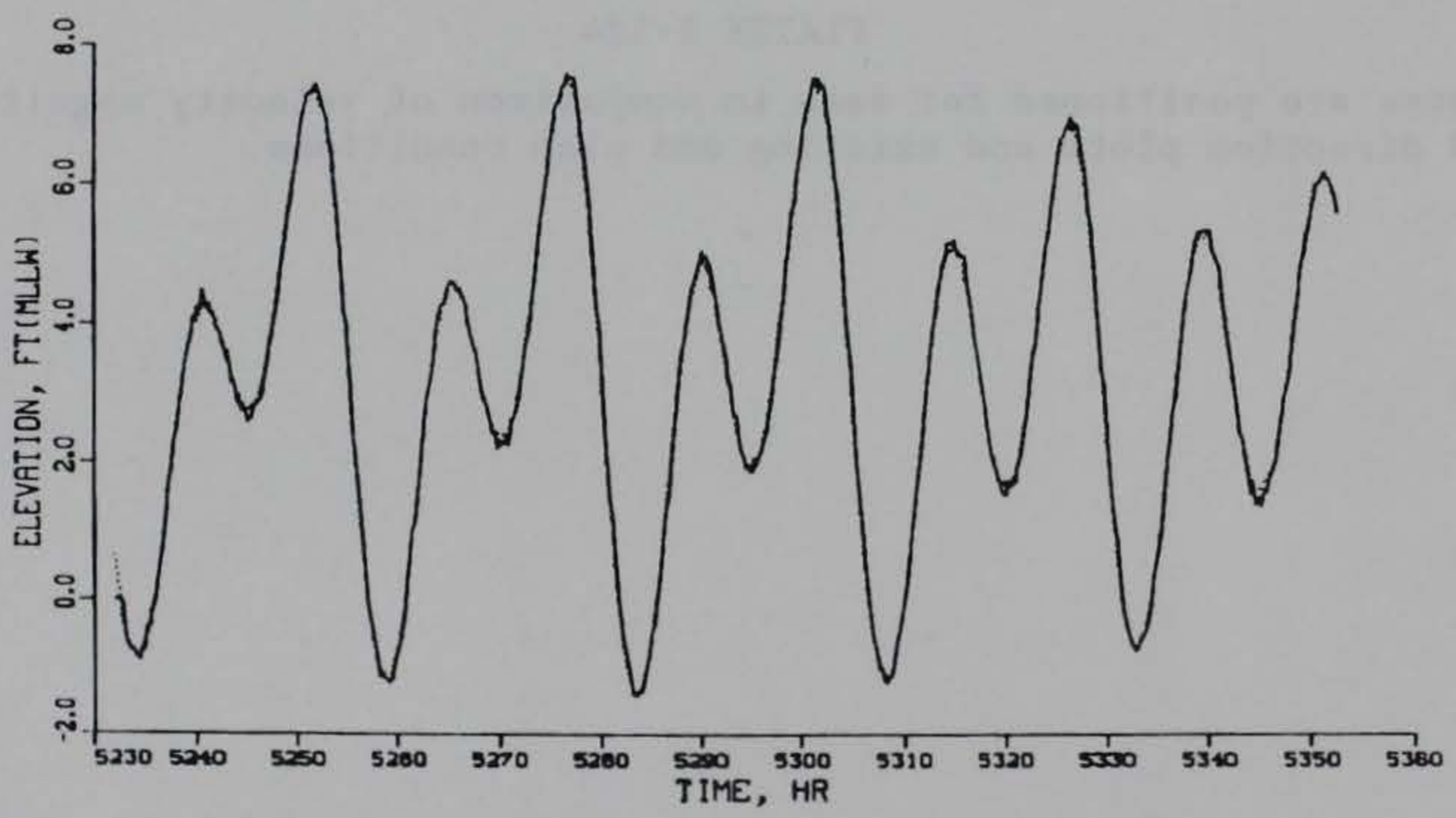

TIDE GAGE TG 7

TIDAL ELEVATION **CALIBRATION PERIOD**

COMPUTED (SOLID) VS OBSERVED (DOTTED)

PLATE 1

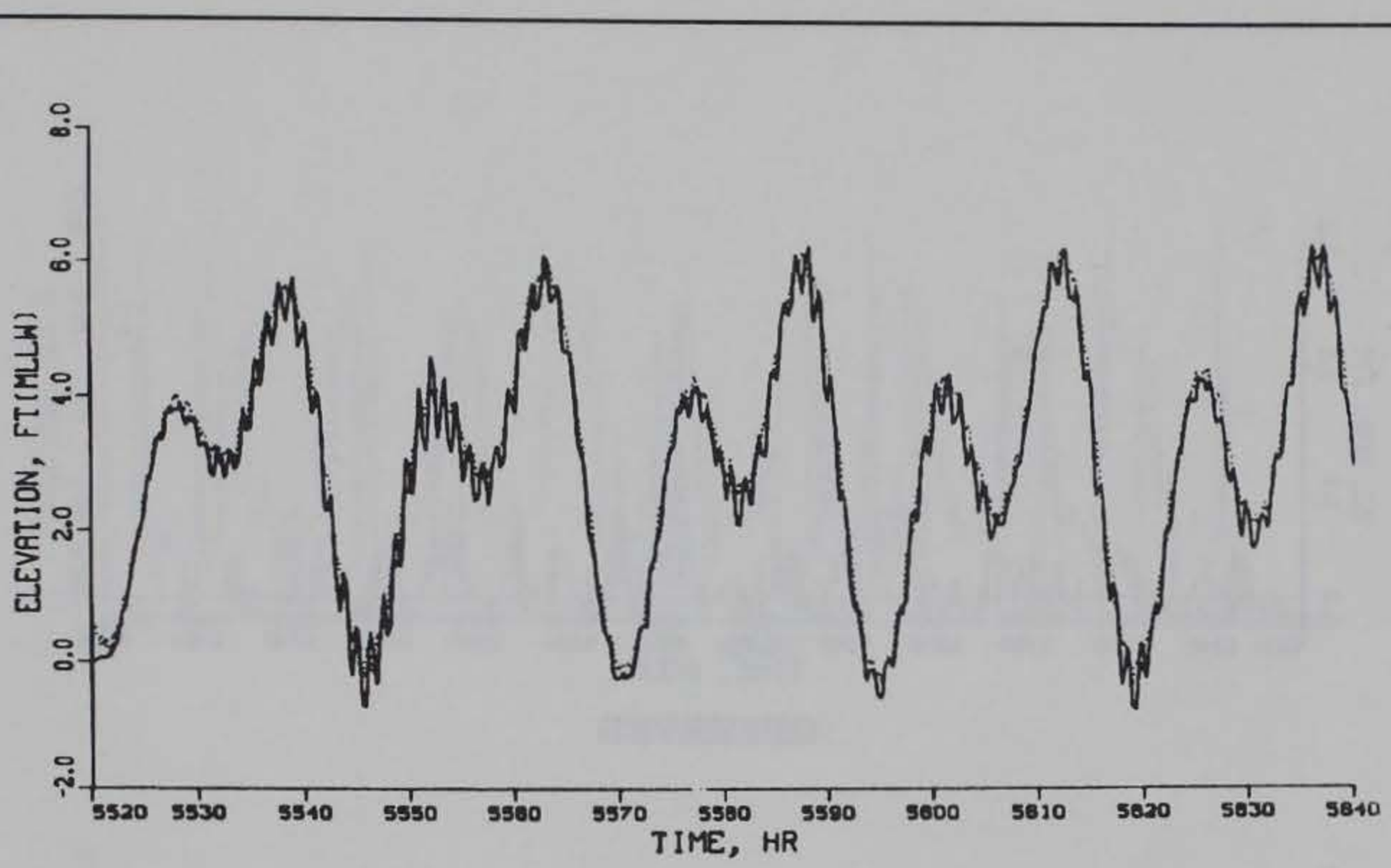

TIDE GAGE TG 3

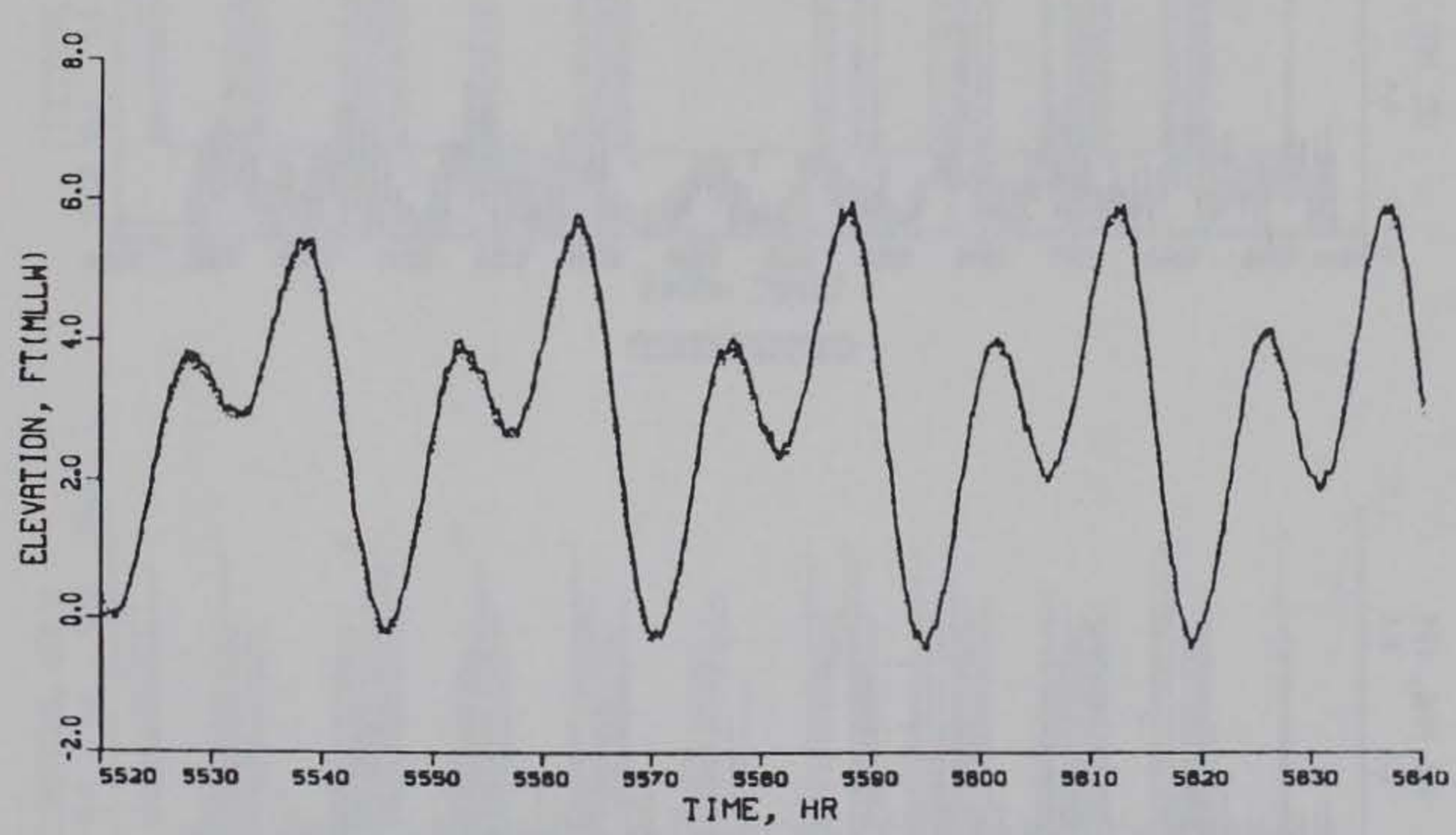

TIDE GAGE TG 7

TIDAL EVEVATION VERIFICATION PERIOD

COMPUTED (SOLID) VS OBSERVED (DOTTED)

PLATE 2

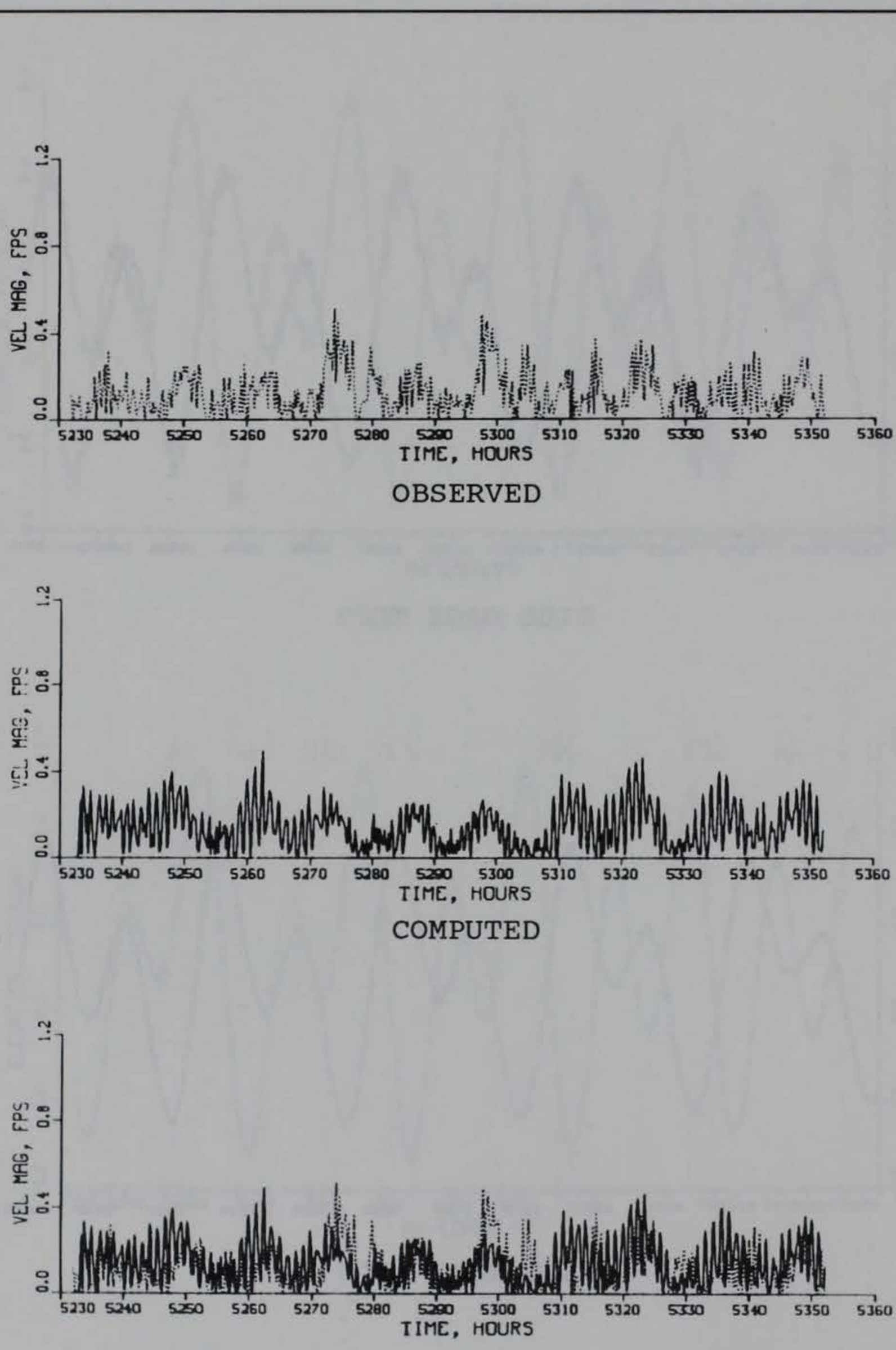

TIDAL VELOCITY

MAGNITUDE

CALIBRATION PERIOD

GAGE CM1

SURFACE

PLATE 3

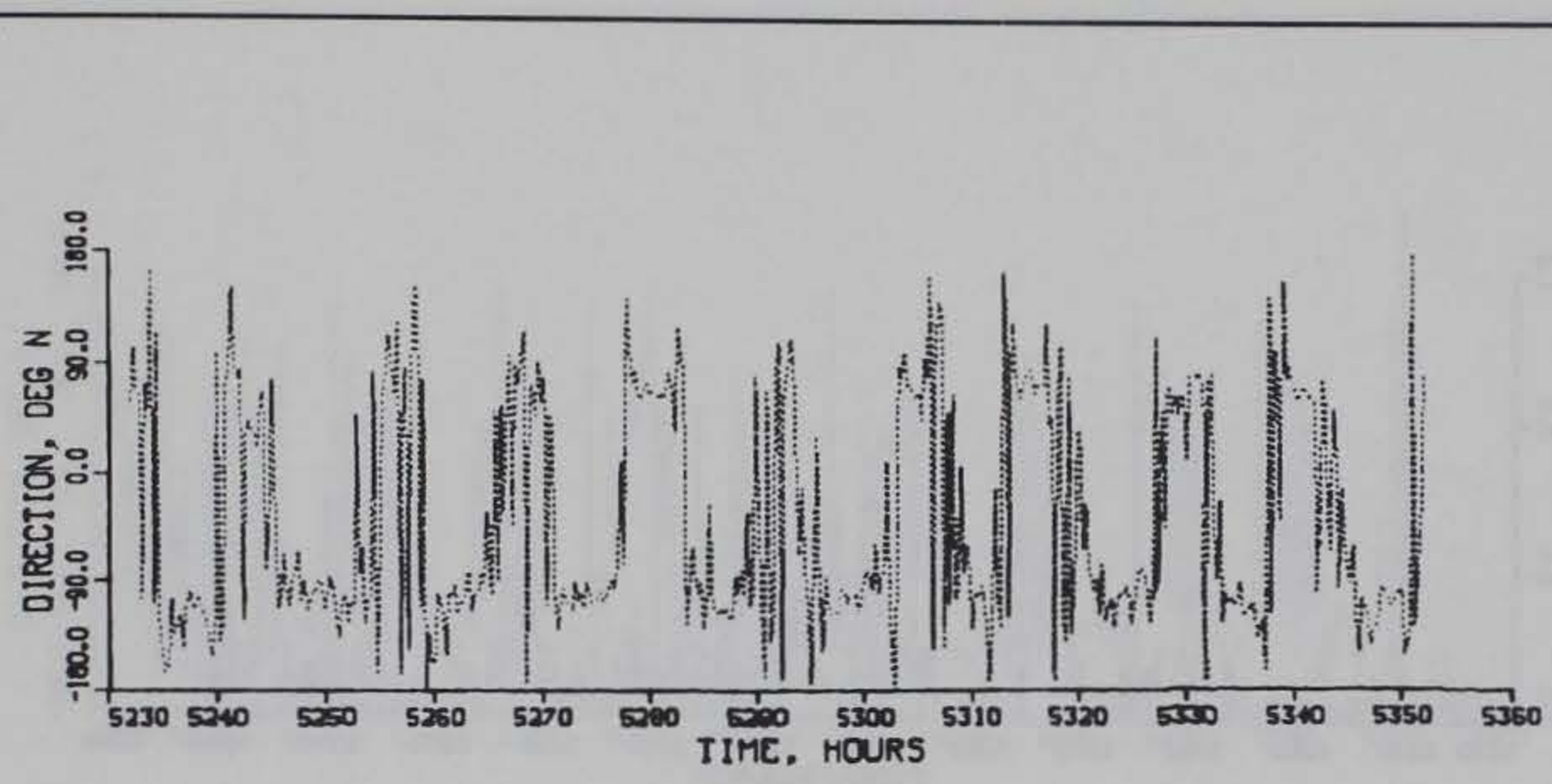

OBSERVED

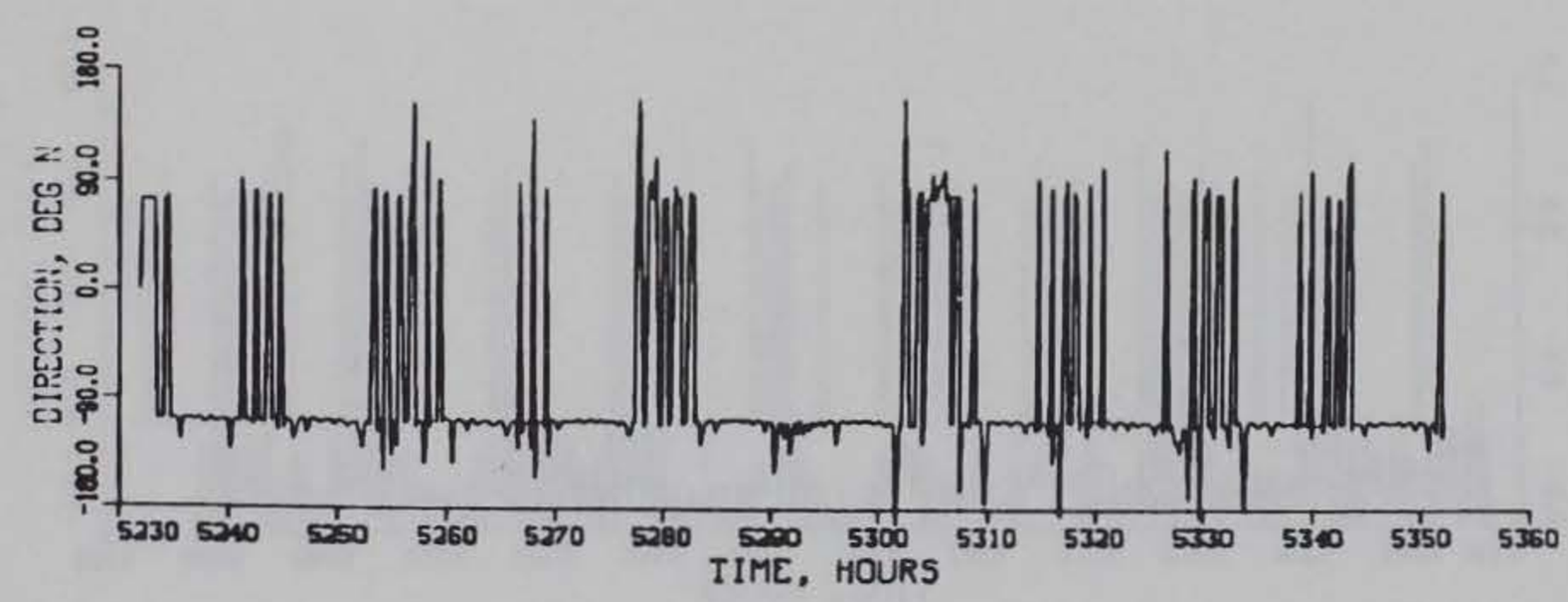

COMPUTED

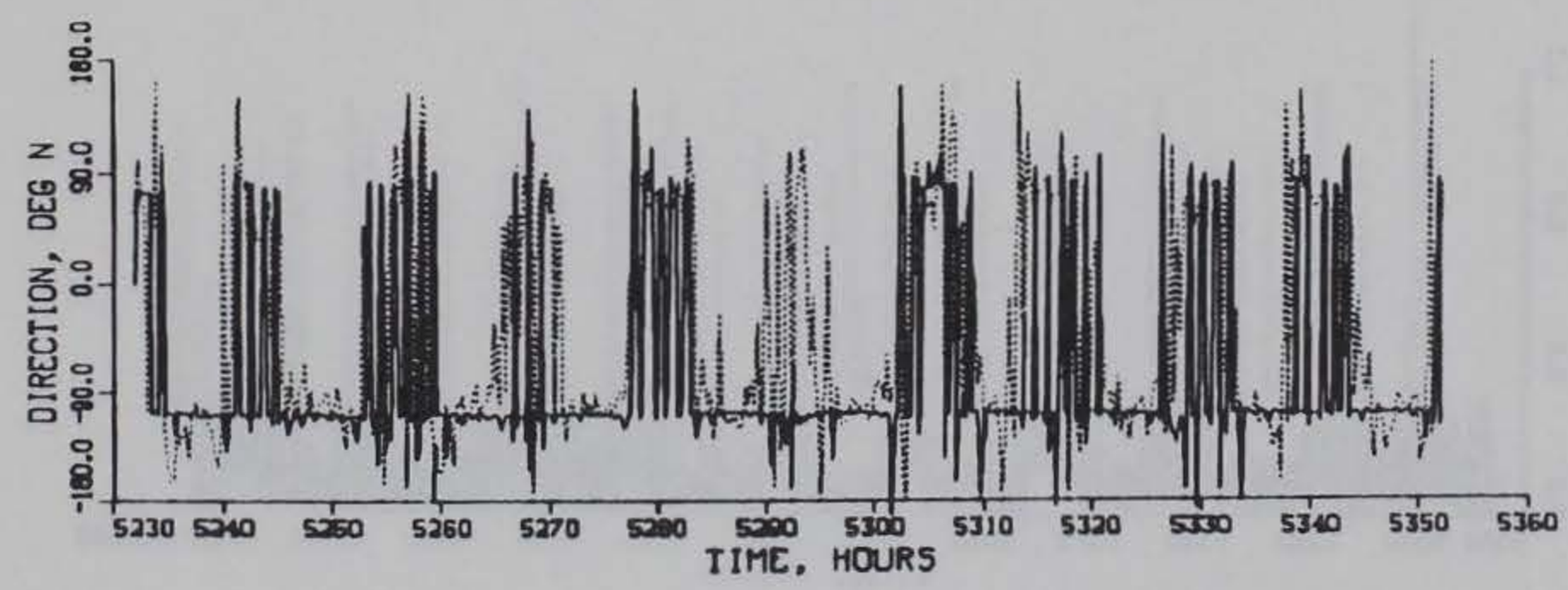

COMPUTED (SOLID) VS OBSERVED (DOTTED)

TIDAL VELOCITY

DIRECTION

CALIBRATION PERIOD

GAGE CM1

SURFACE

PLATE 4

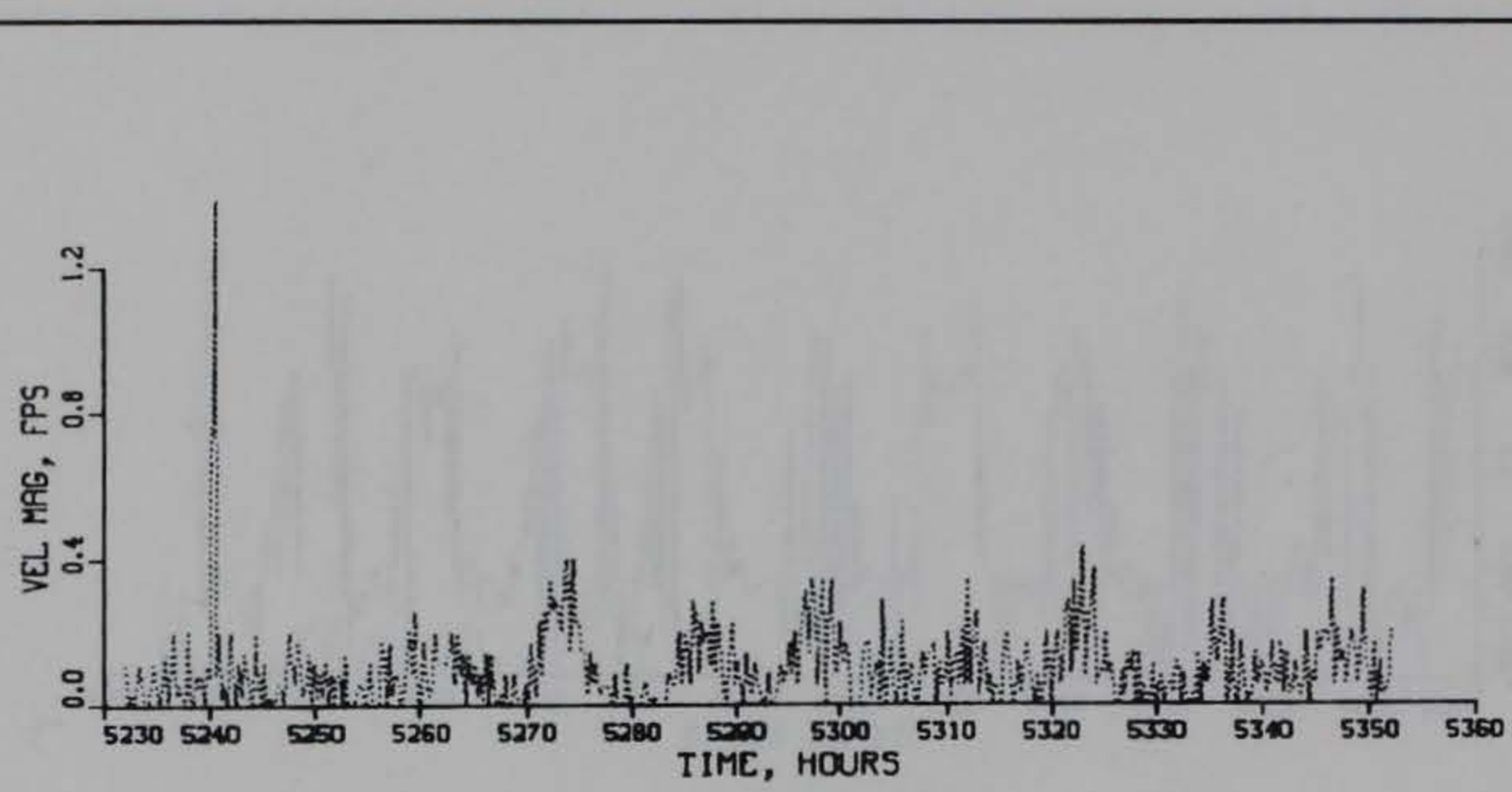

OBSERVED

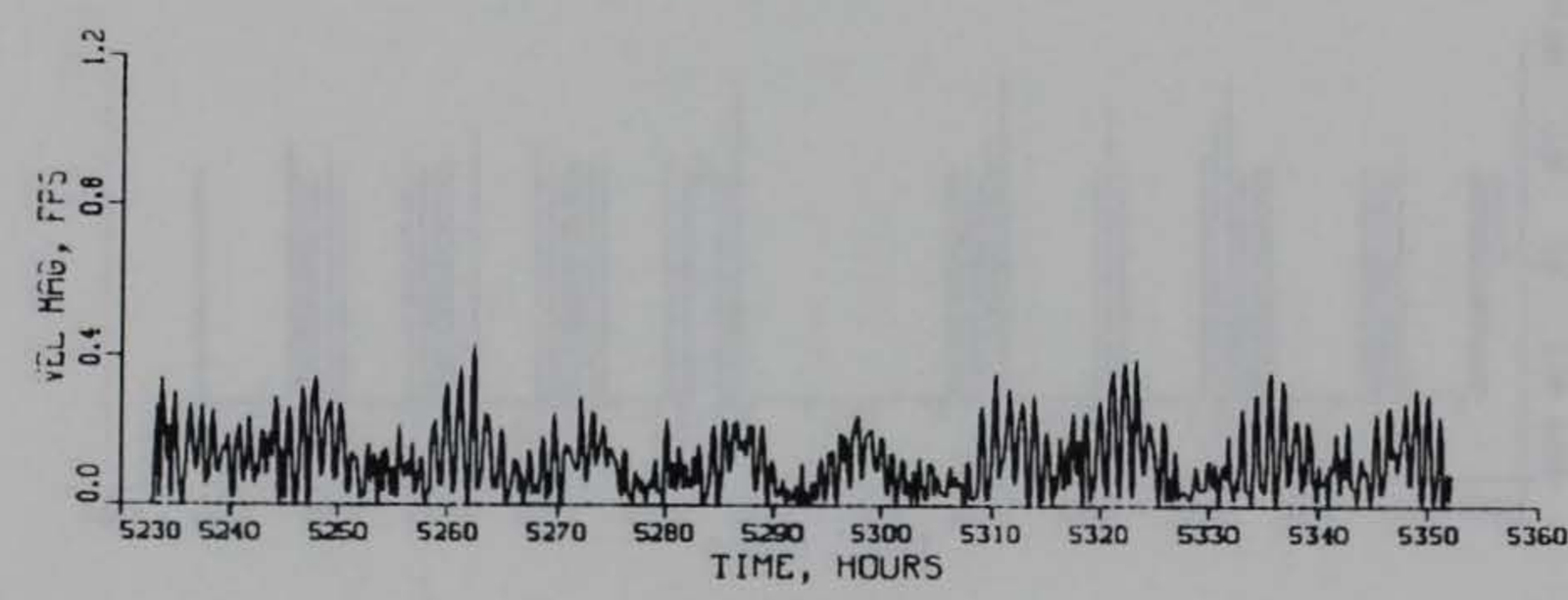

COMPUTED

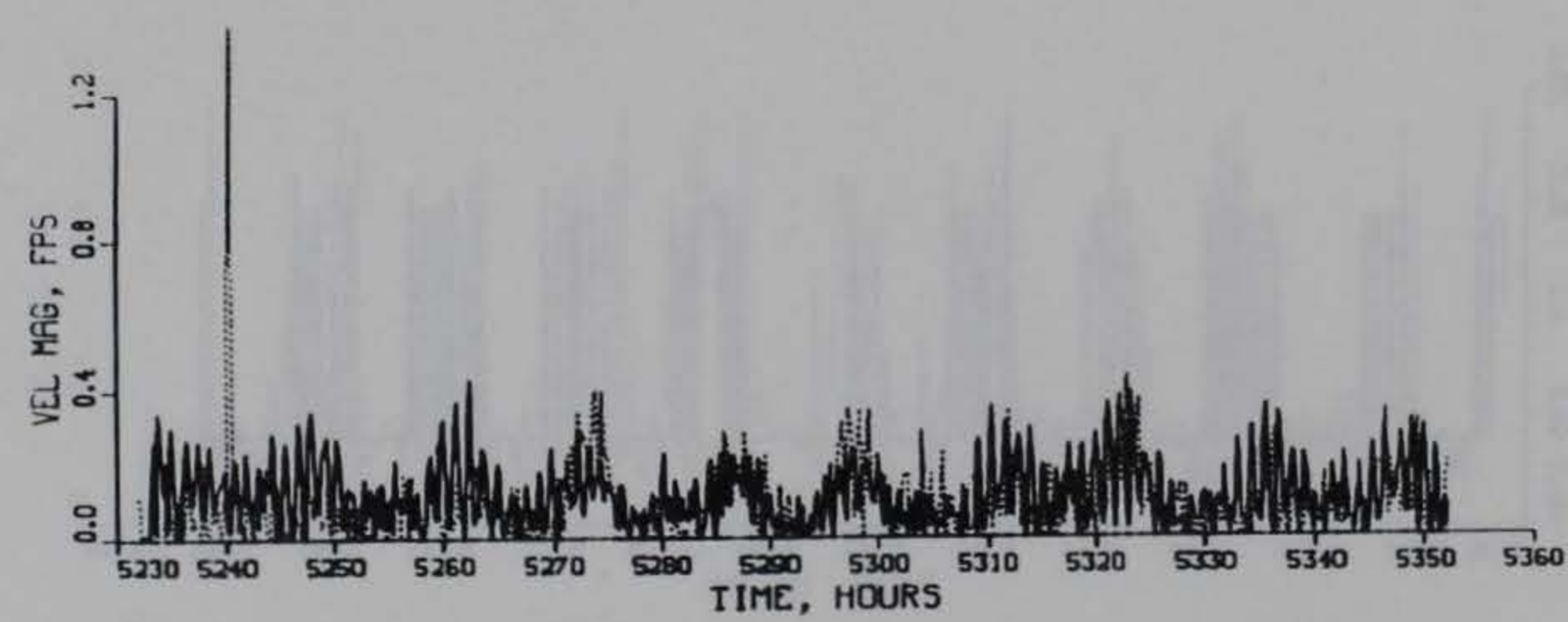

COMPUTED (SOLID) VS (DOTTED) OBSERVED

TIDAL VELOCITY

MAGNITUDE

CALIBRATION PERIOD

GAGE CM1

BOTTOM

PLATE 5

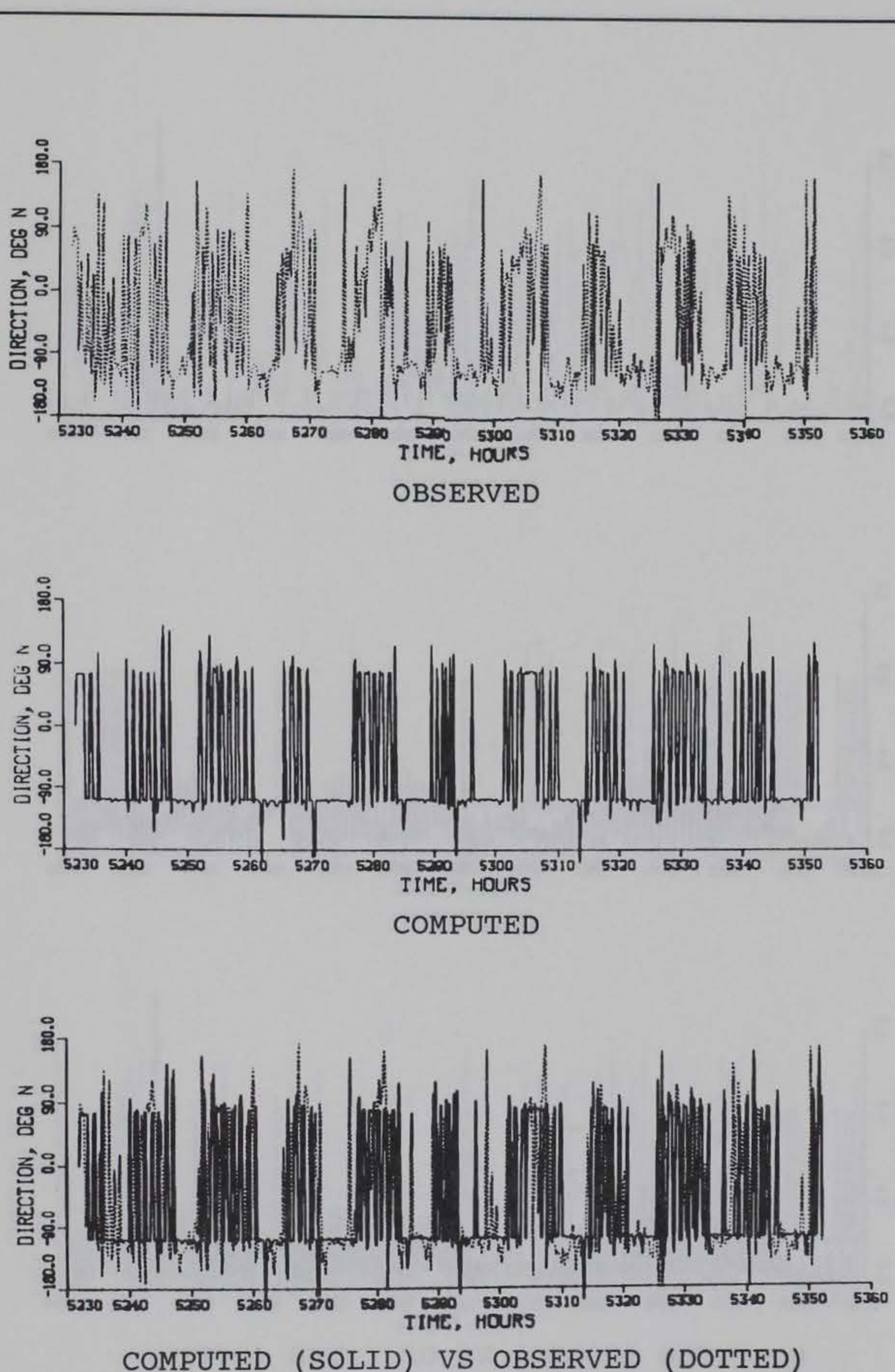

OBSERVED

COMPUTED

COMPUTED (SOLID) VS OBSERVED (DOTTED)

TIDAL VELOCITY

DIRECTION

CALIBRATION PERIOD

GAGE CM1

BOTTOM

PLATE 6

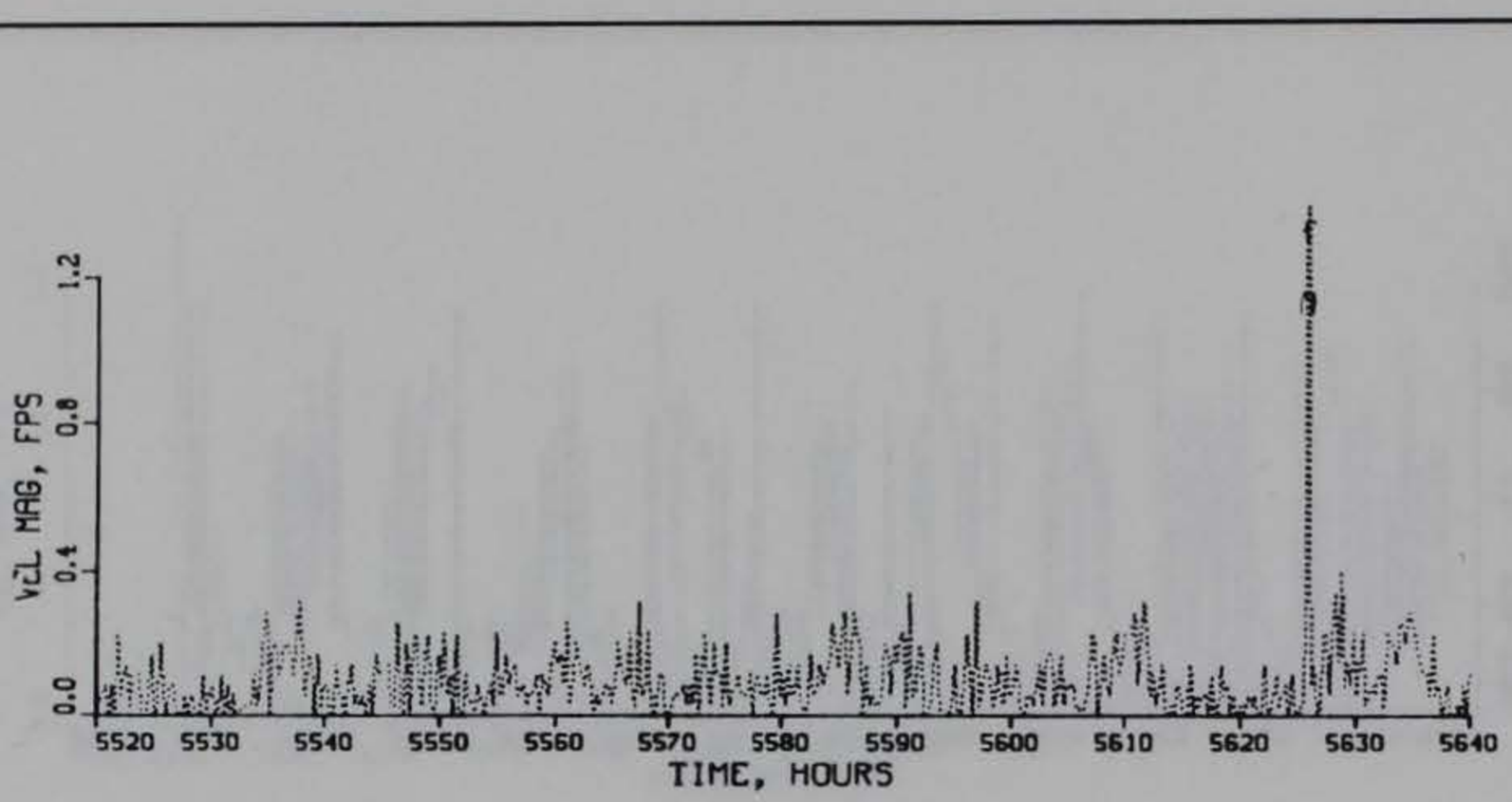

OBSERVED

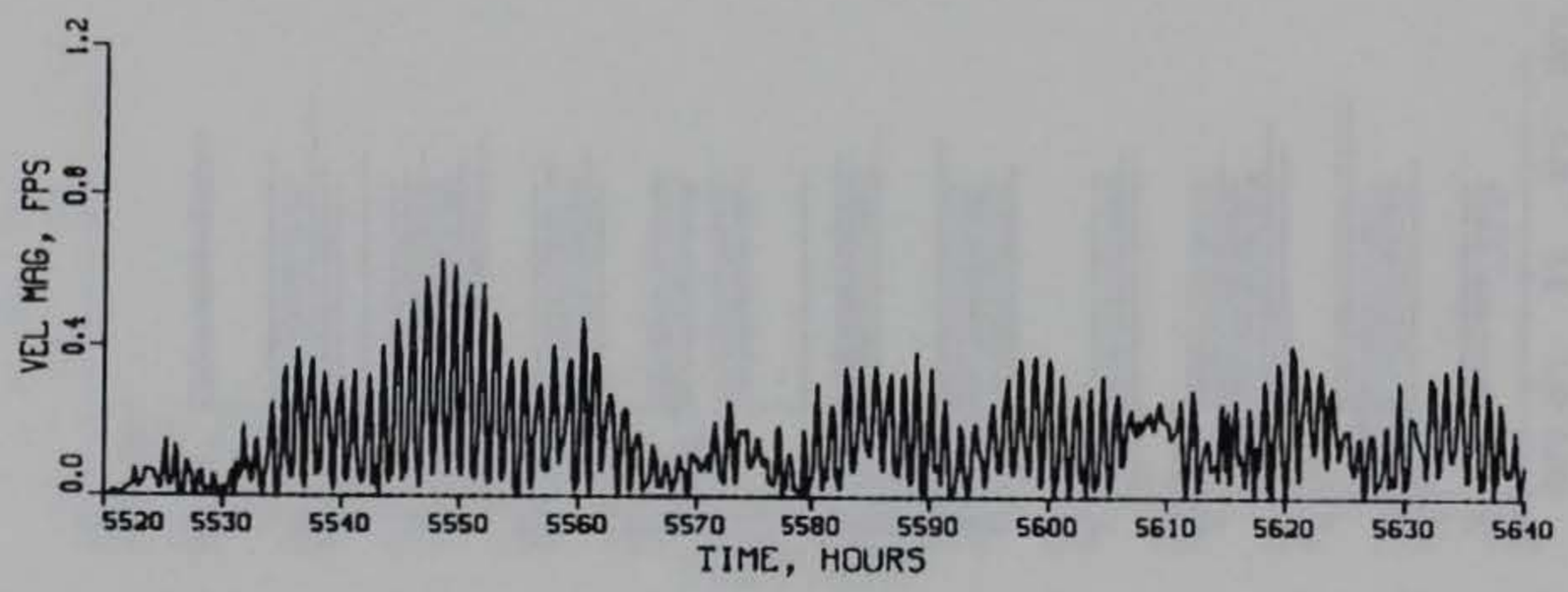

COMPUTED

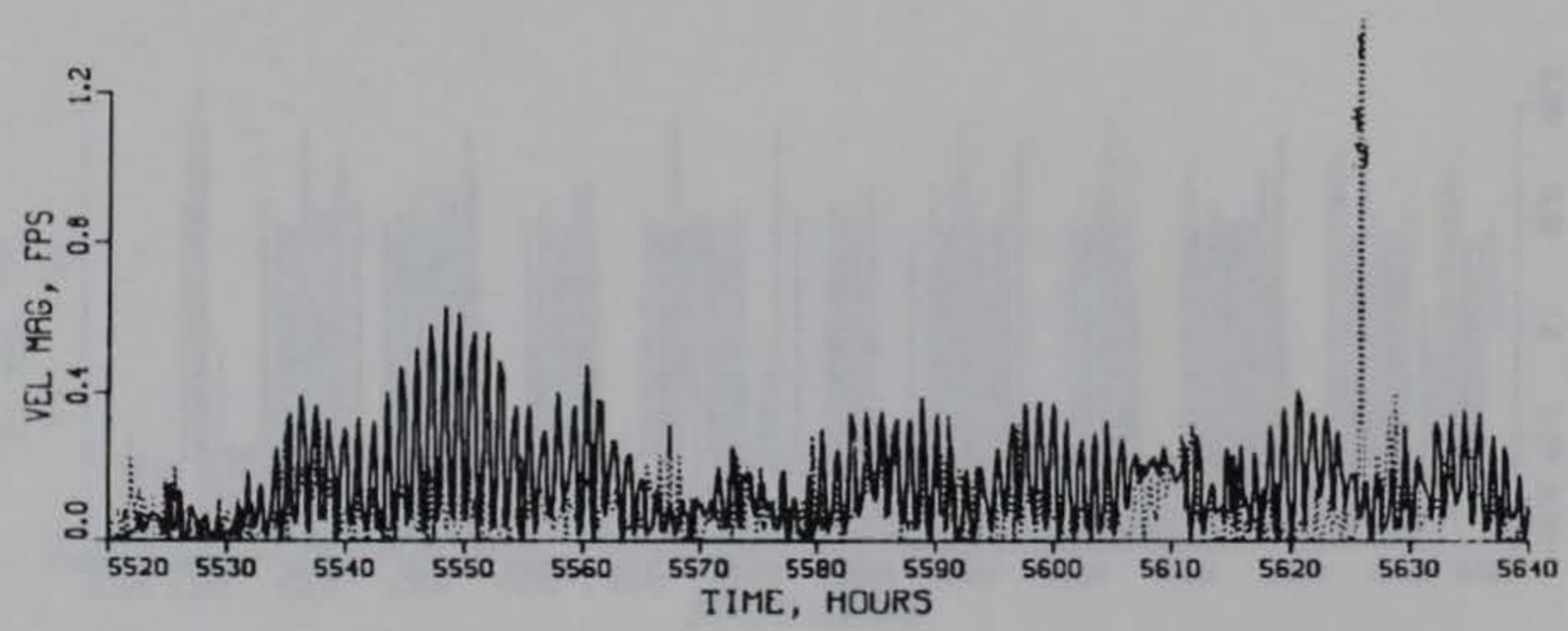

COMPUTED (SOLID) VS OBSERVED (DOTTED)

TIDAL VELOCITY

MAGNITUDE

VERIFICATION PERIOD

GAGE CM1

SURFACE

PLATE 7

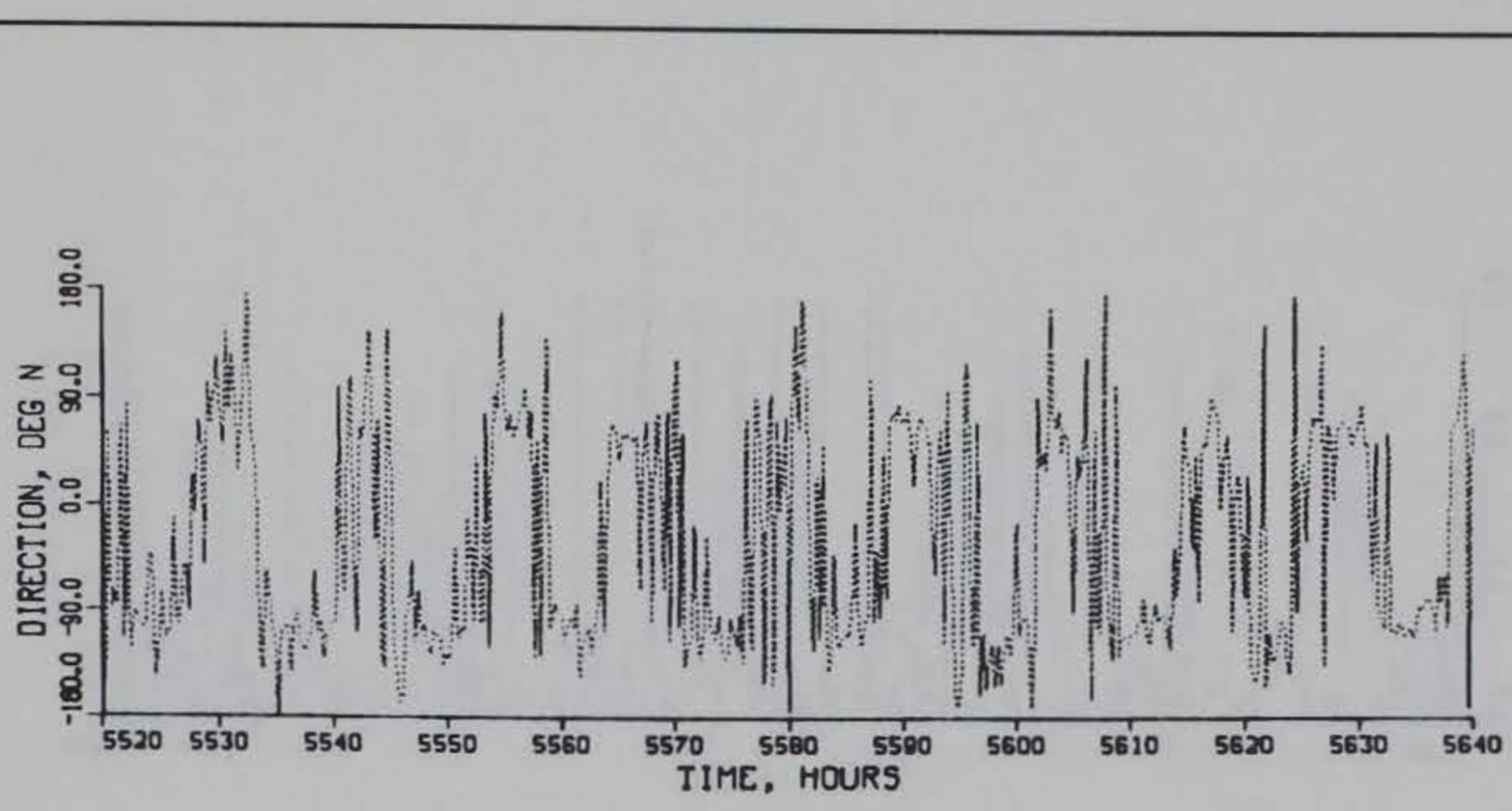

OBSERVED

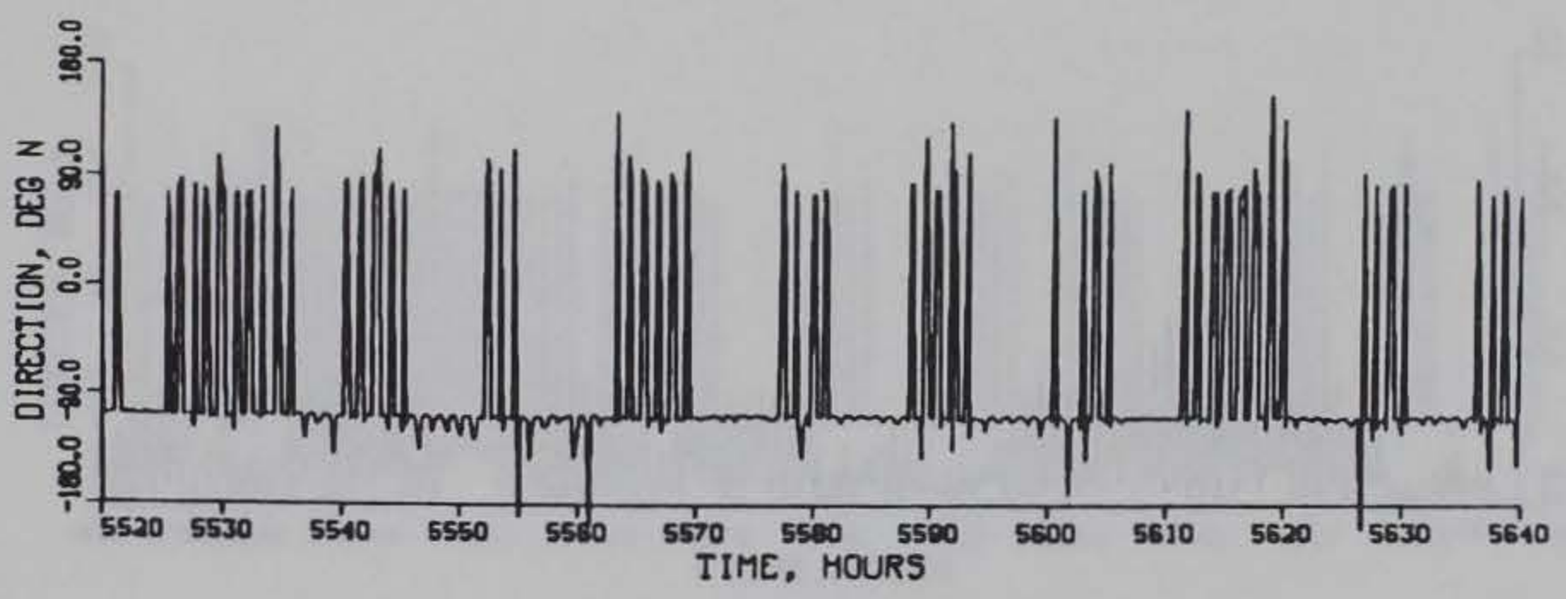

COMPUTED

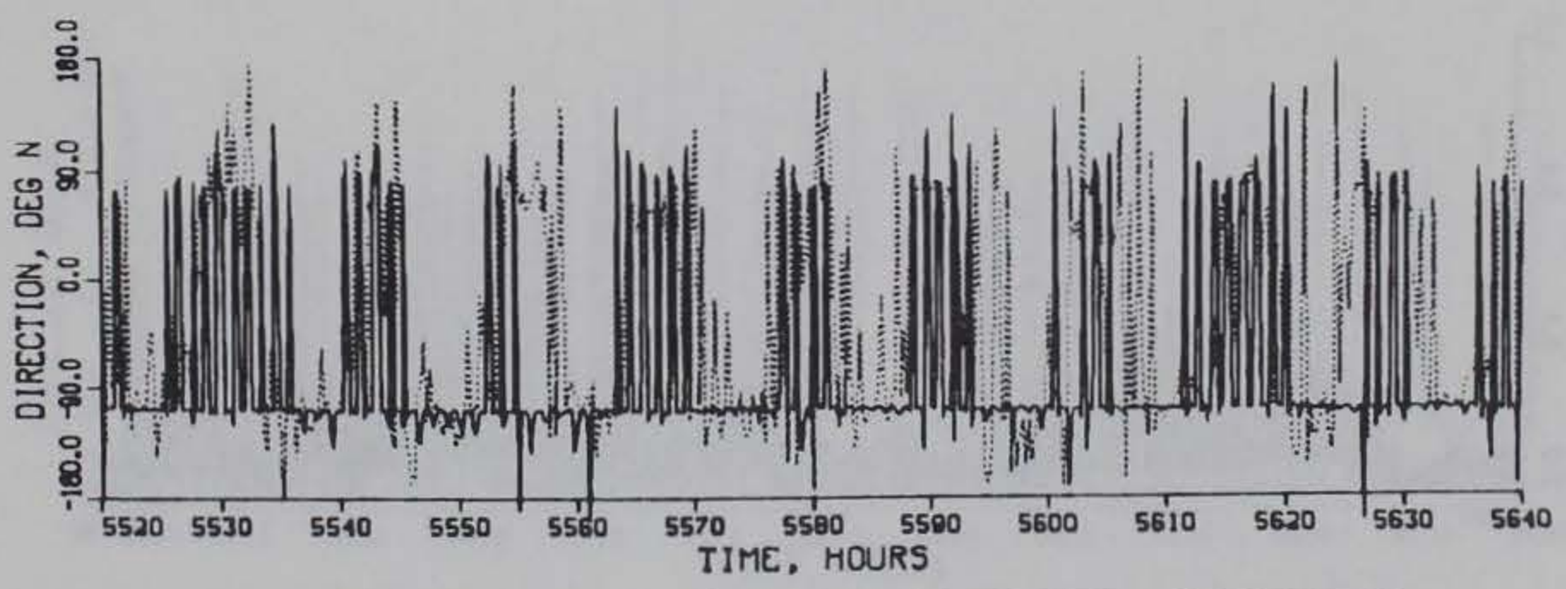

COMPUTED (SOLID) VS OBSERVED (DOTTED)

TIDAL VELOCITY

DIRECTION

VERIFICATION PERIOD

GAGE CM1

SURFACE

PLATE 8

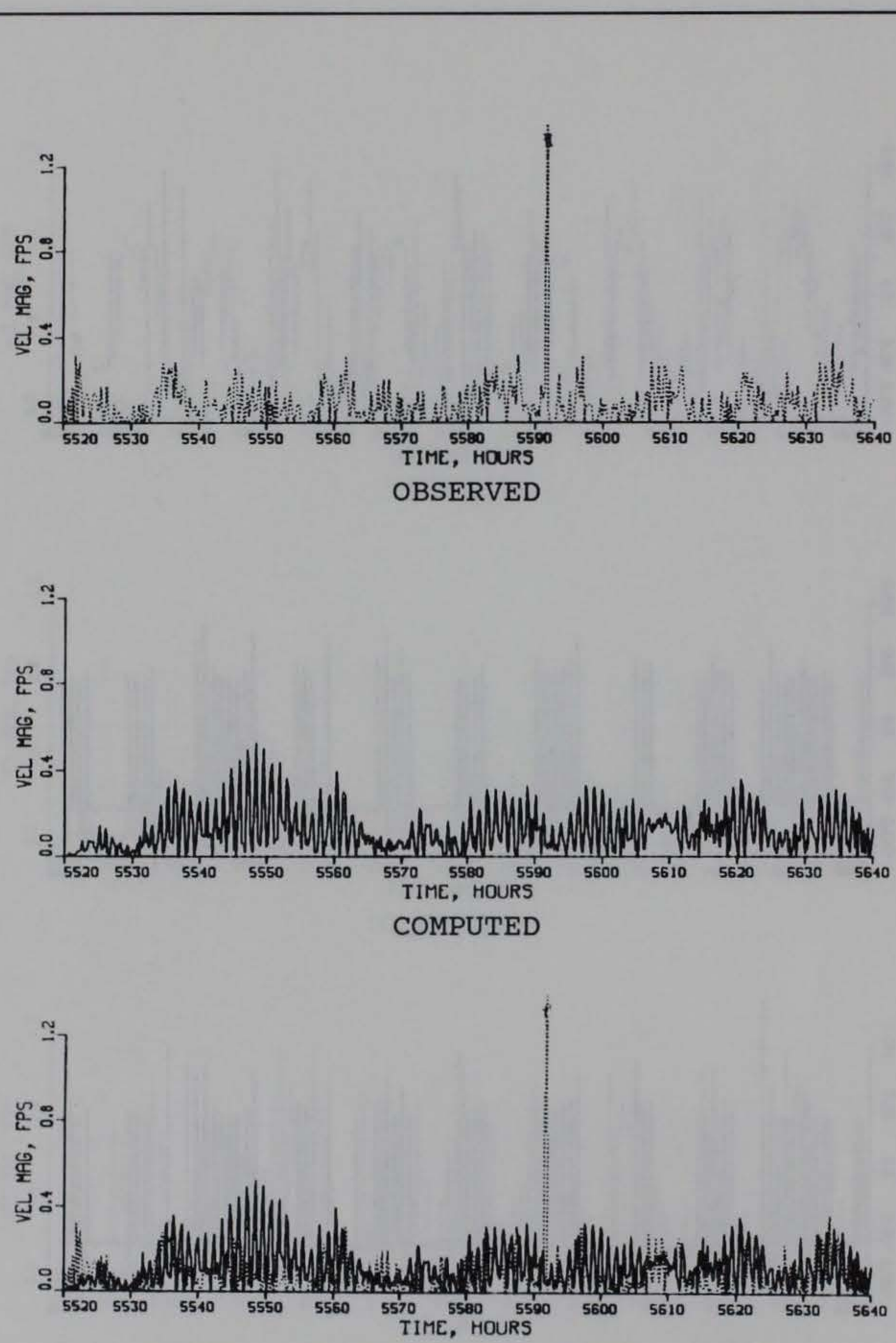

TIDAL VELOCITY

MAGNITUDE

VERIFICATION PERIOD

GAGE CM1

BOTTOM

PLATE 9

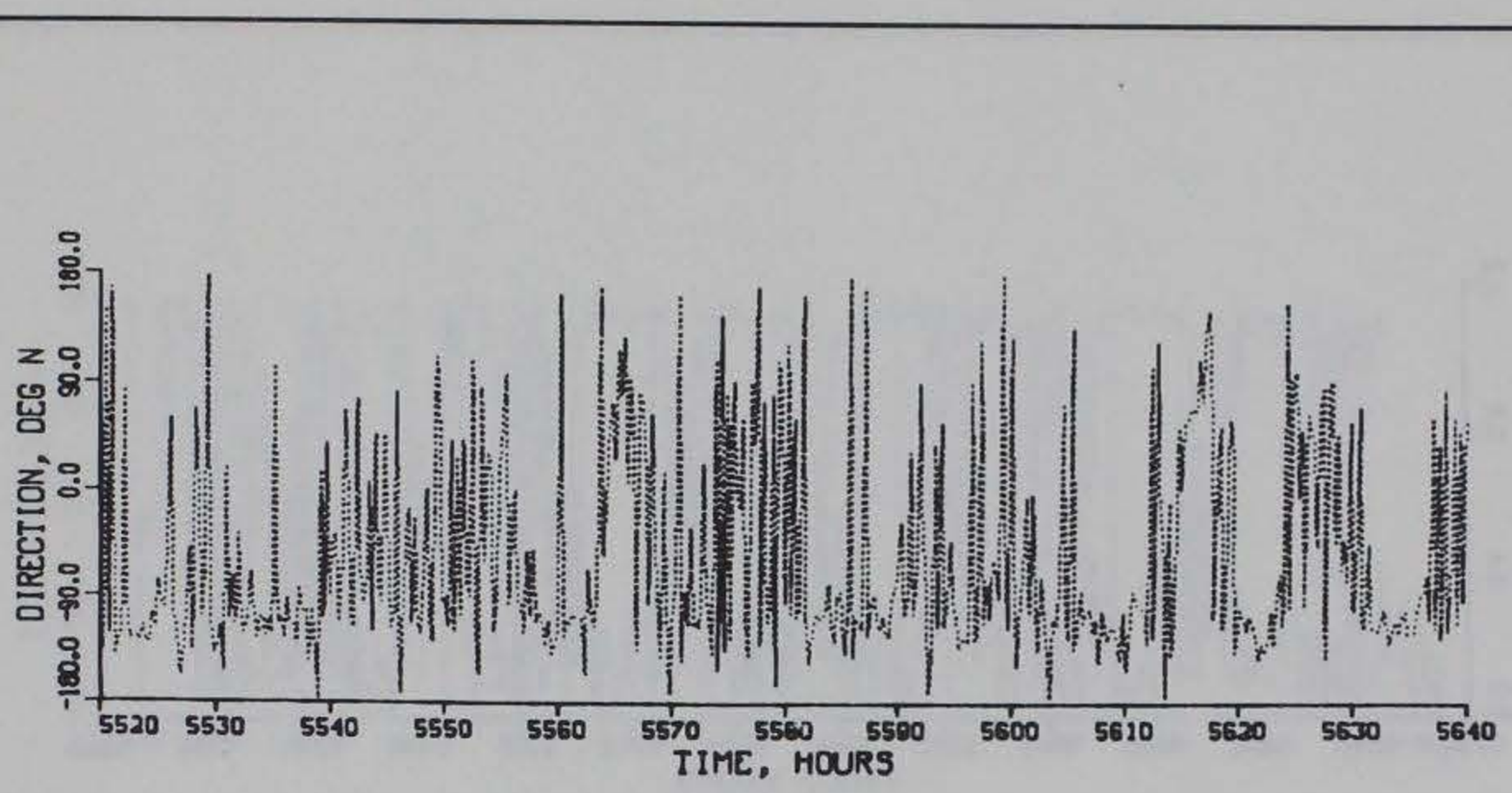

OBSERVED

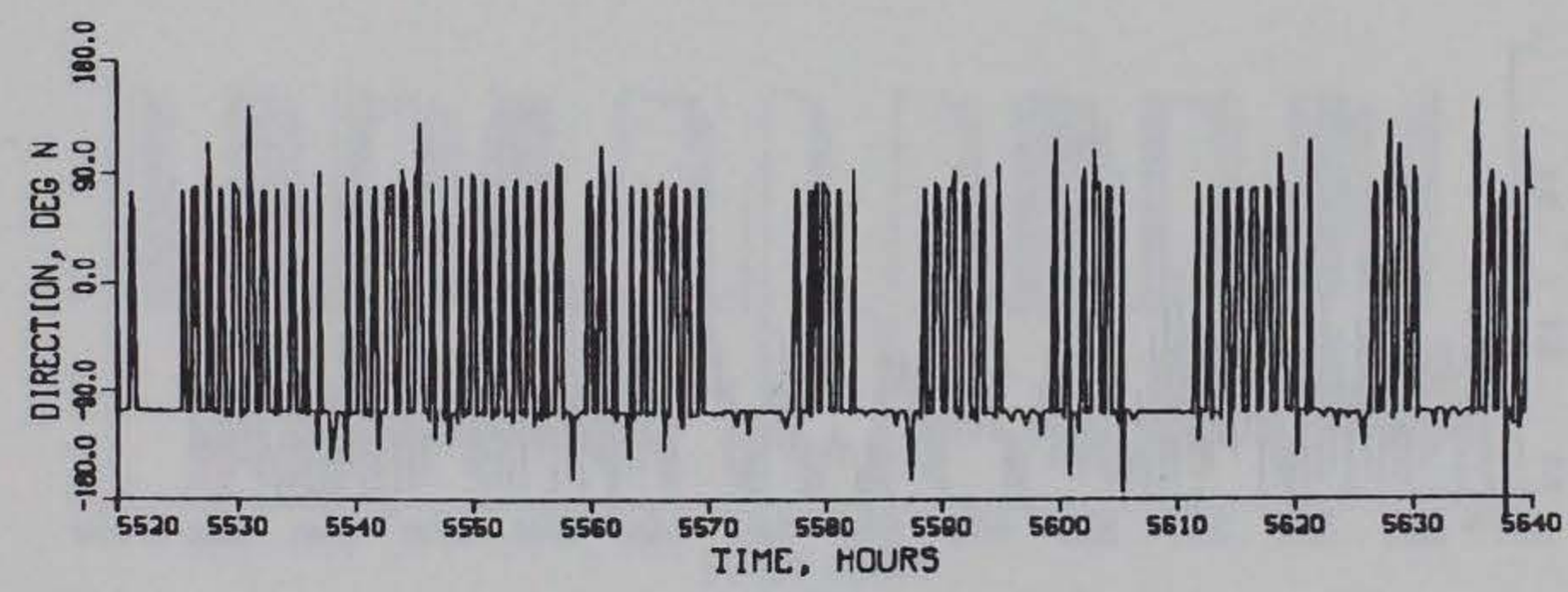

COMPUTED

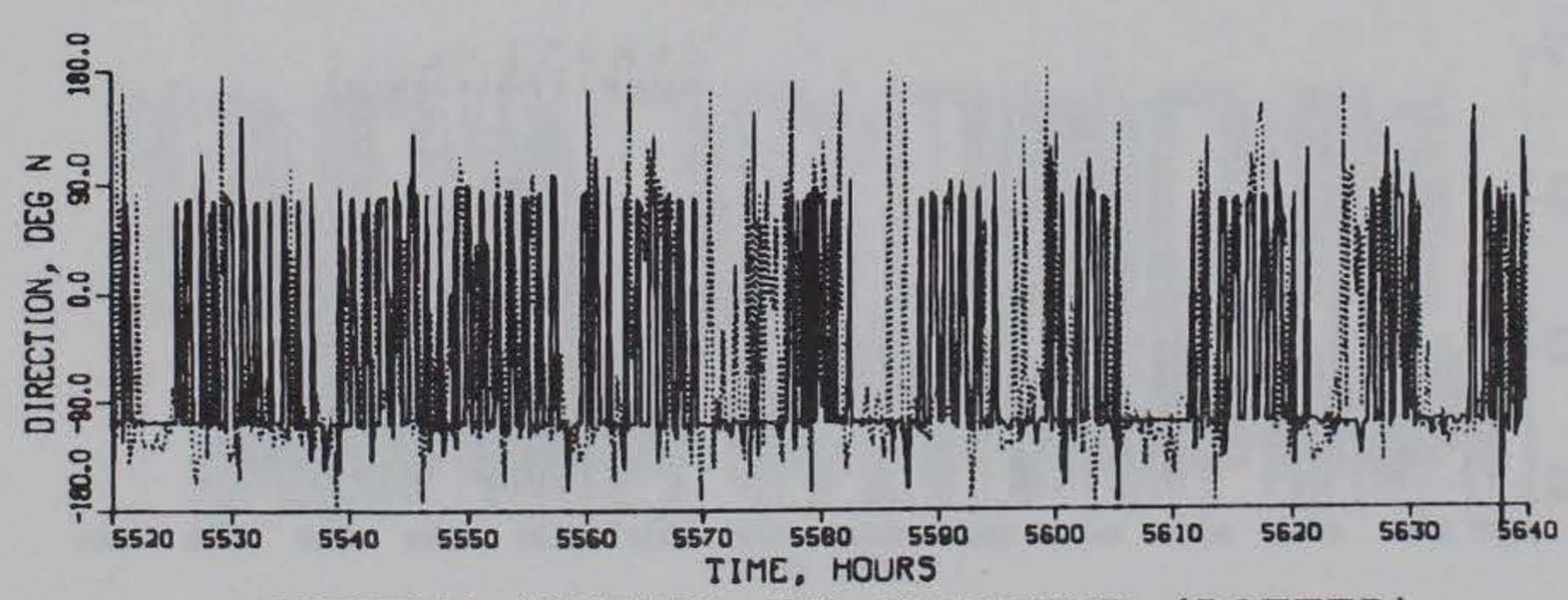

COMPUTED (SOLID) VS OBSERVED (DOTTED)

TIDAL VELOCITY **VERIFICATION PERIOD**

DIRECTION

GAGE CM1

BOTTOM

PLATE 10

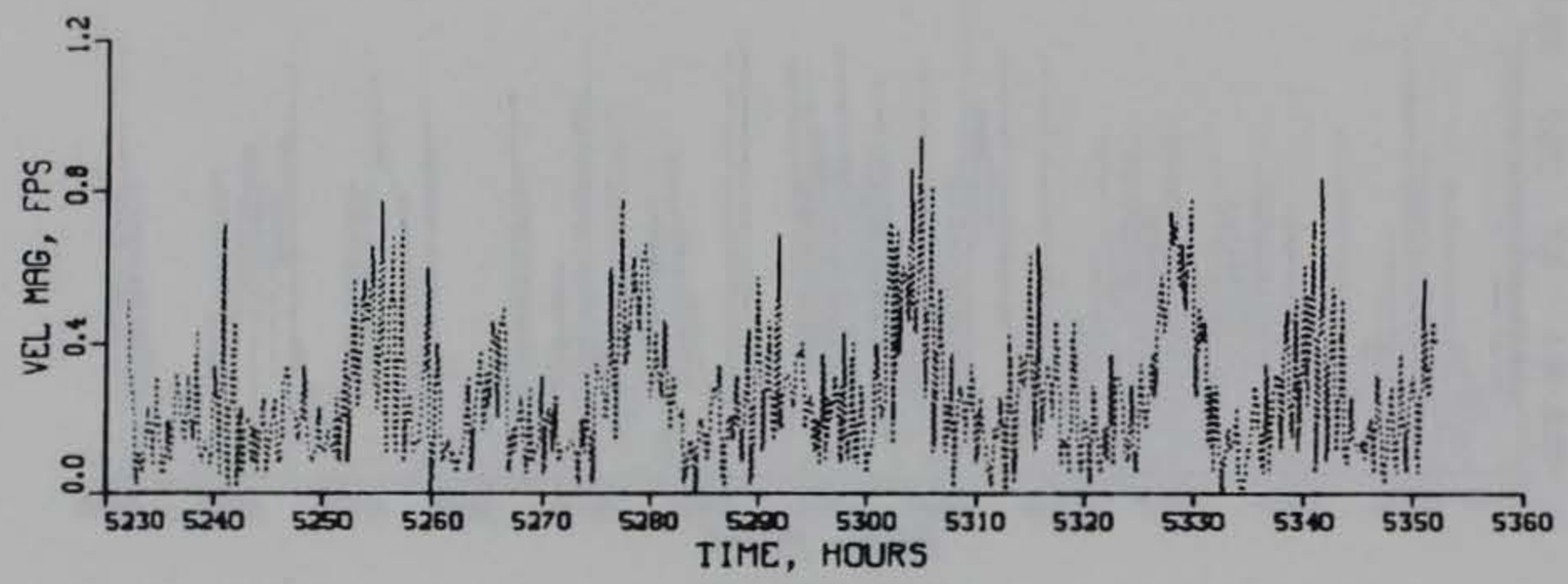

OBSERVED

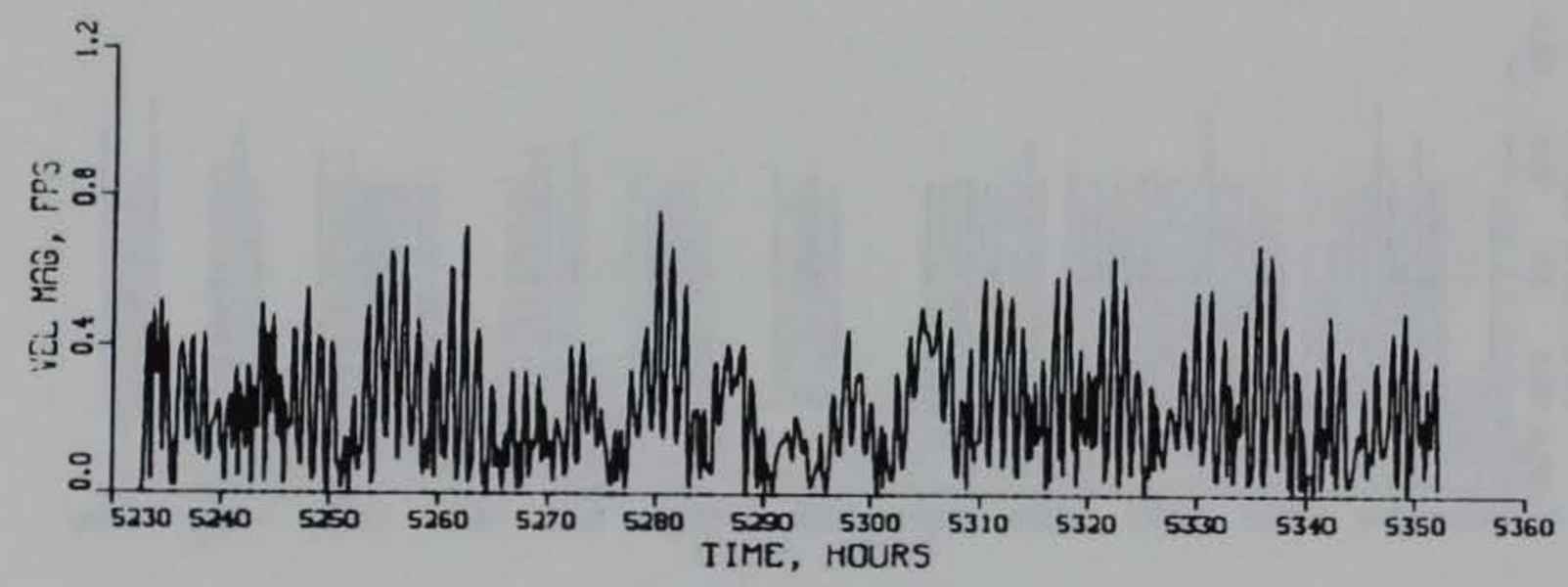

COMPUTED

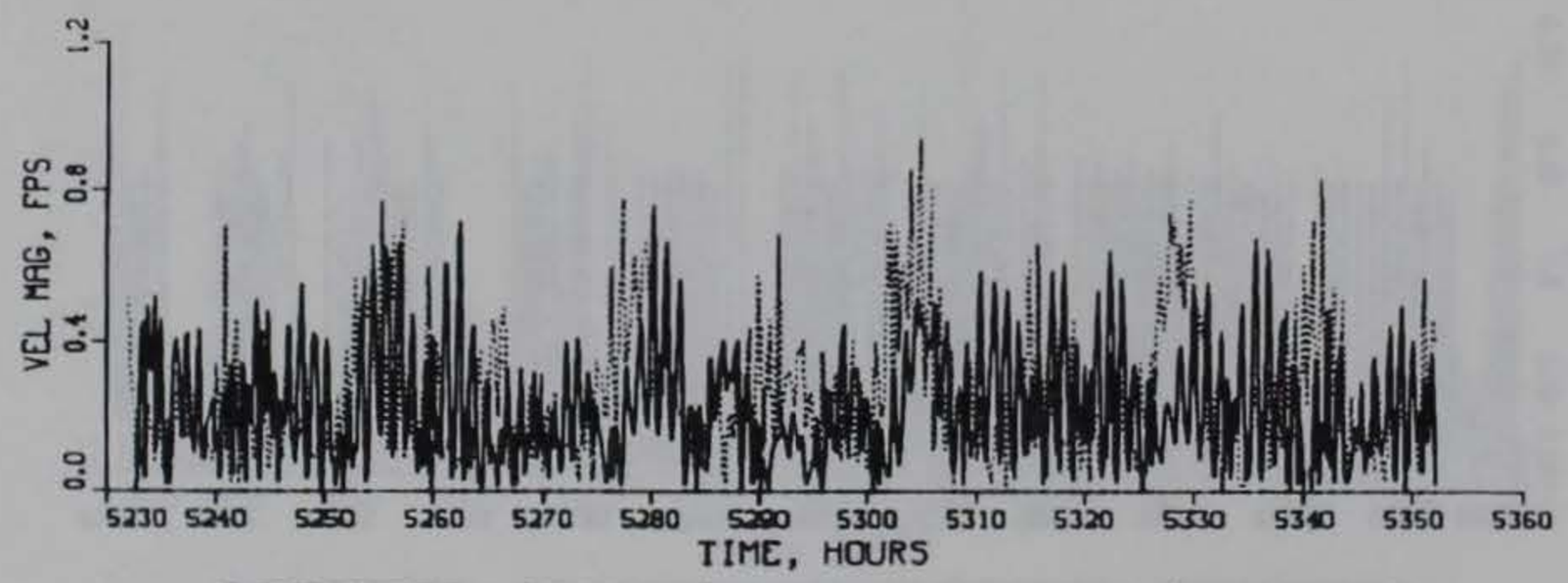

COMPUTED (SOLID) VS OBSERVED (DOTTED)

TIDAL VELOCITY

MAGNITUDE

CALIBRATION PERIOD

GAGE CM2

SURFACE

PLATE 11

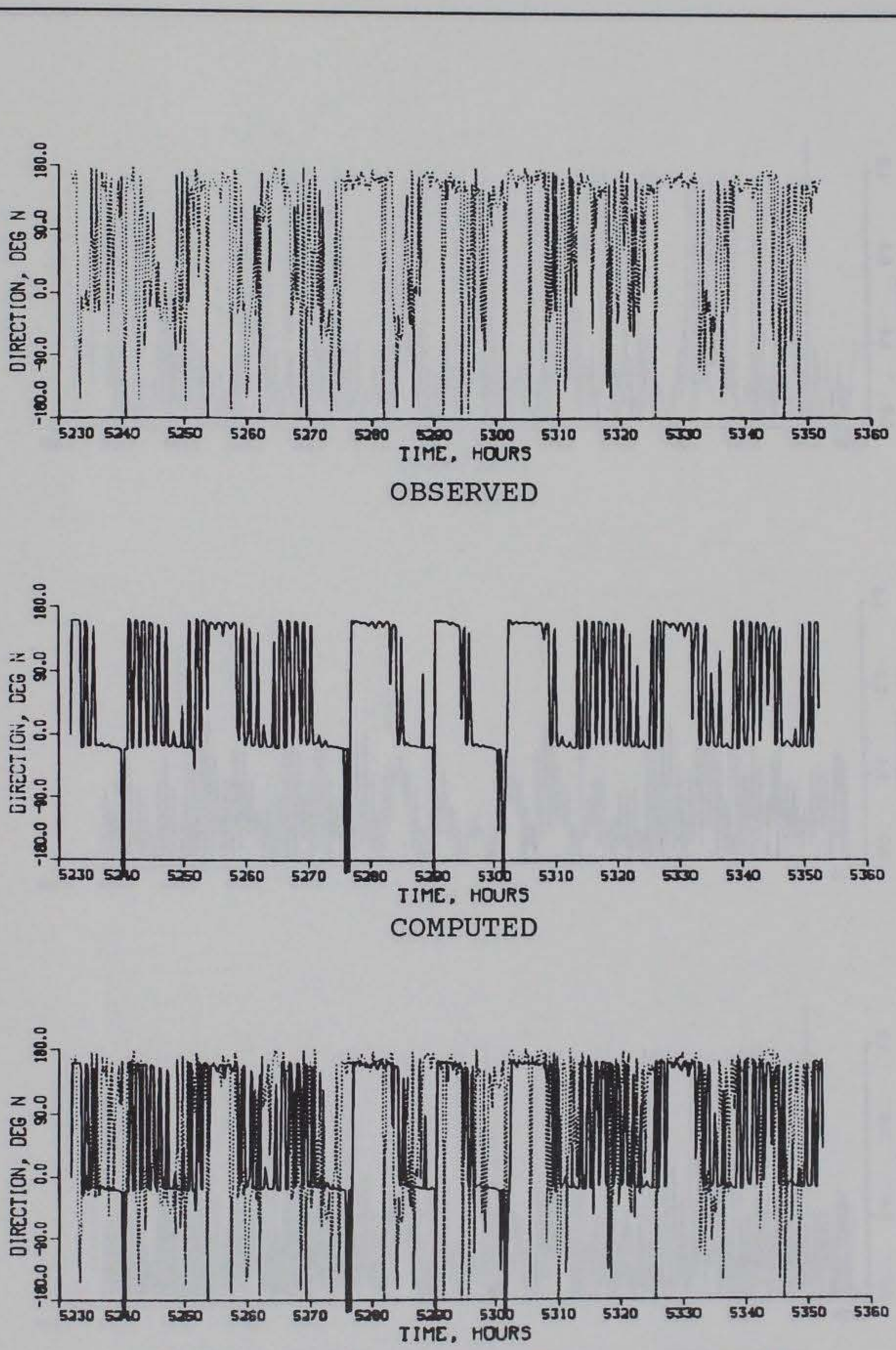

OBSERVED

COMPUTED

COMPUTED (SOLID) VS OBSERVED (DOTTED)

TIDAL VELOCITY

DIRECTION

CALIBRATION PERIOD

GAGE CM2

SURFACE

PLATE 12

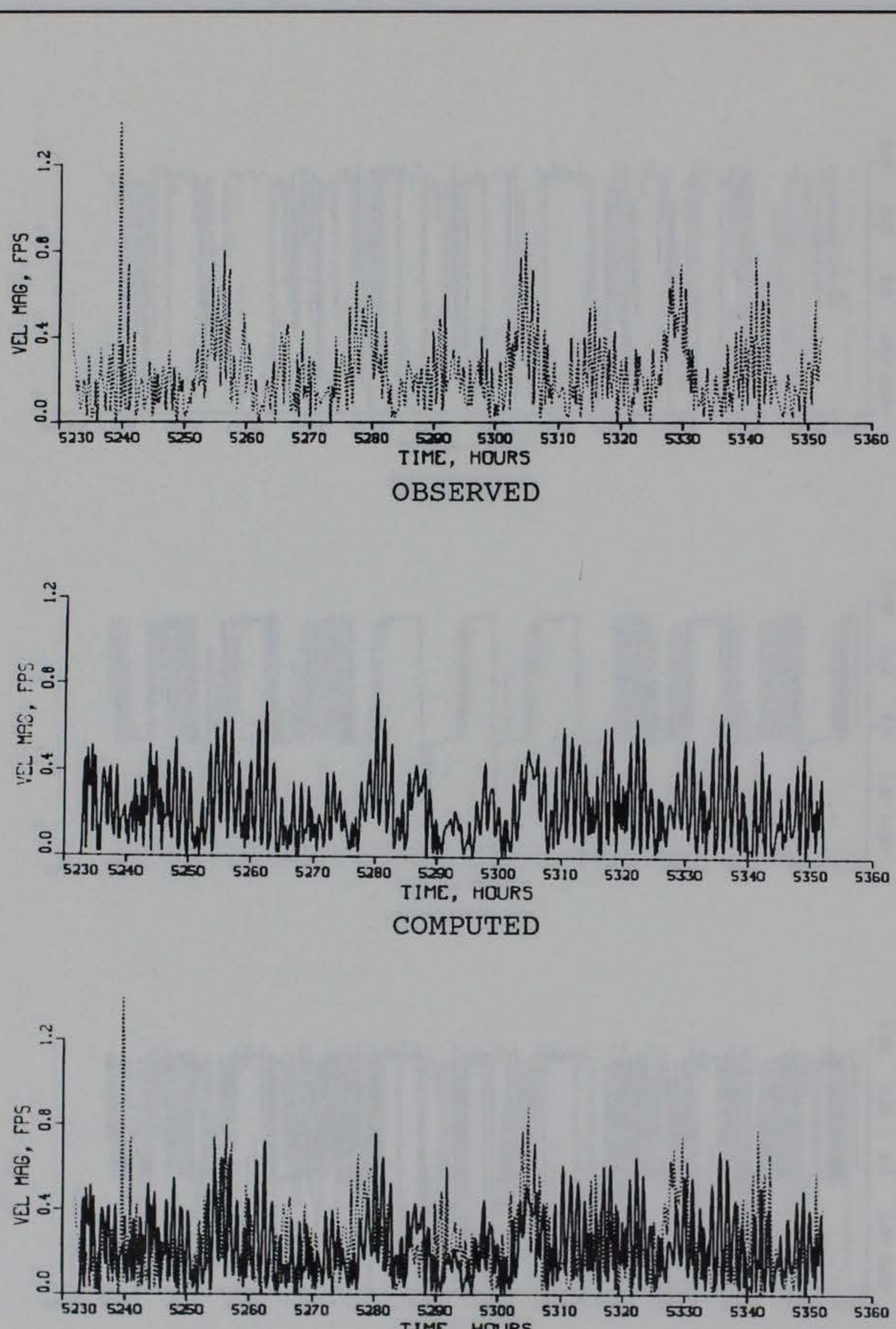

OBSERVED

COMPUTED

COMPUTED (SOLID) VS OBSERVED (DOTTED)

TIDAL VELOCITY

MAGNITUDE

CALIBRATION PERIOD

GAGE CM2

MID-DEPTH

PLATE 13

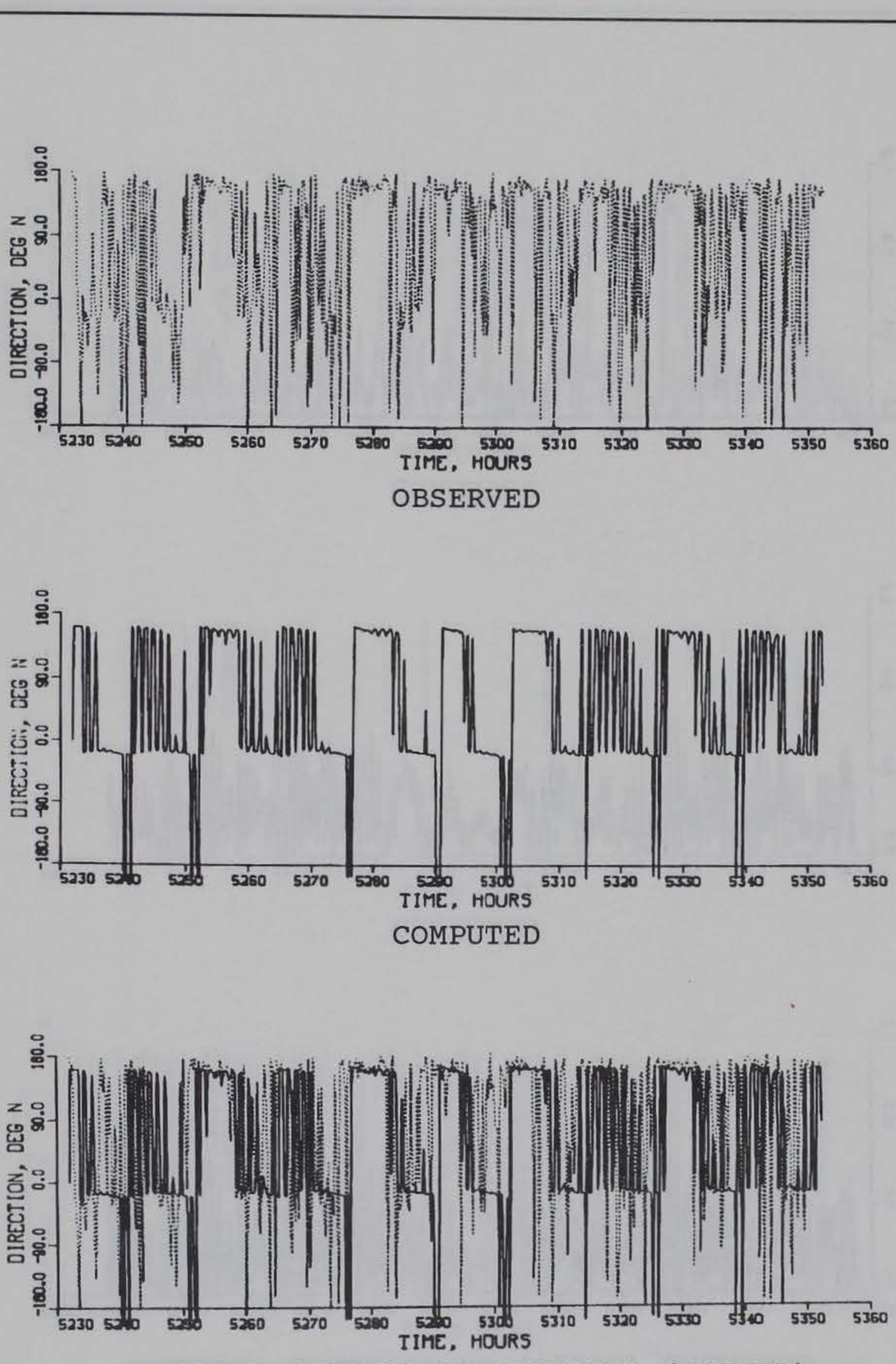

OBSERVED

COMPUTED

COMPUTED (SOLID) VS OBSERVED (DOTTED)

TIDAL VELOCITY

DIRECTION

CALIBRATION PERIOD

GAGE CM2

MID-DEPTH

PLATE 14

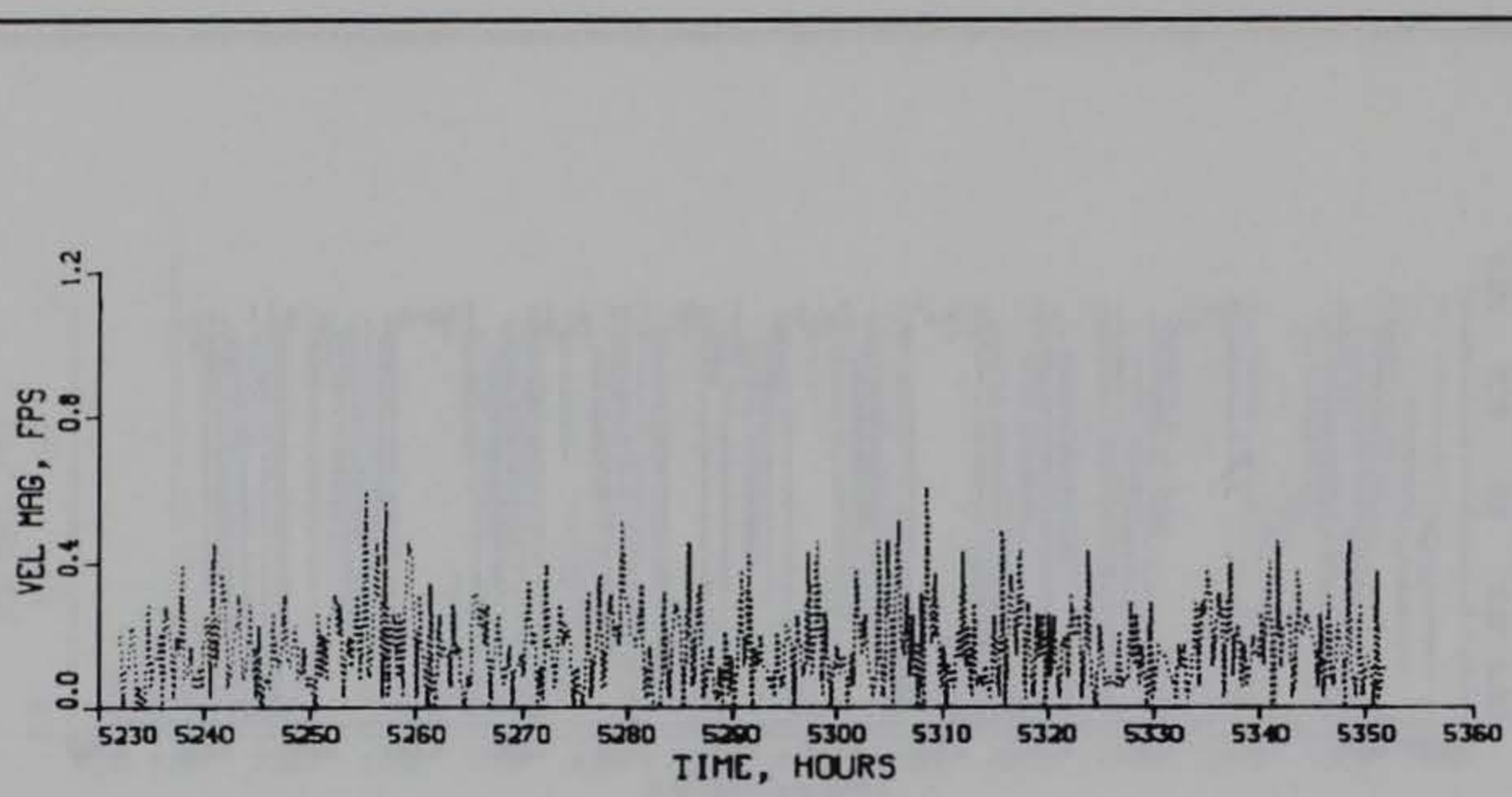

OBSERVED

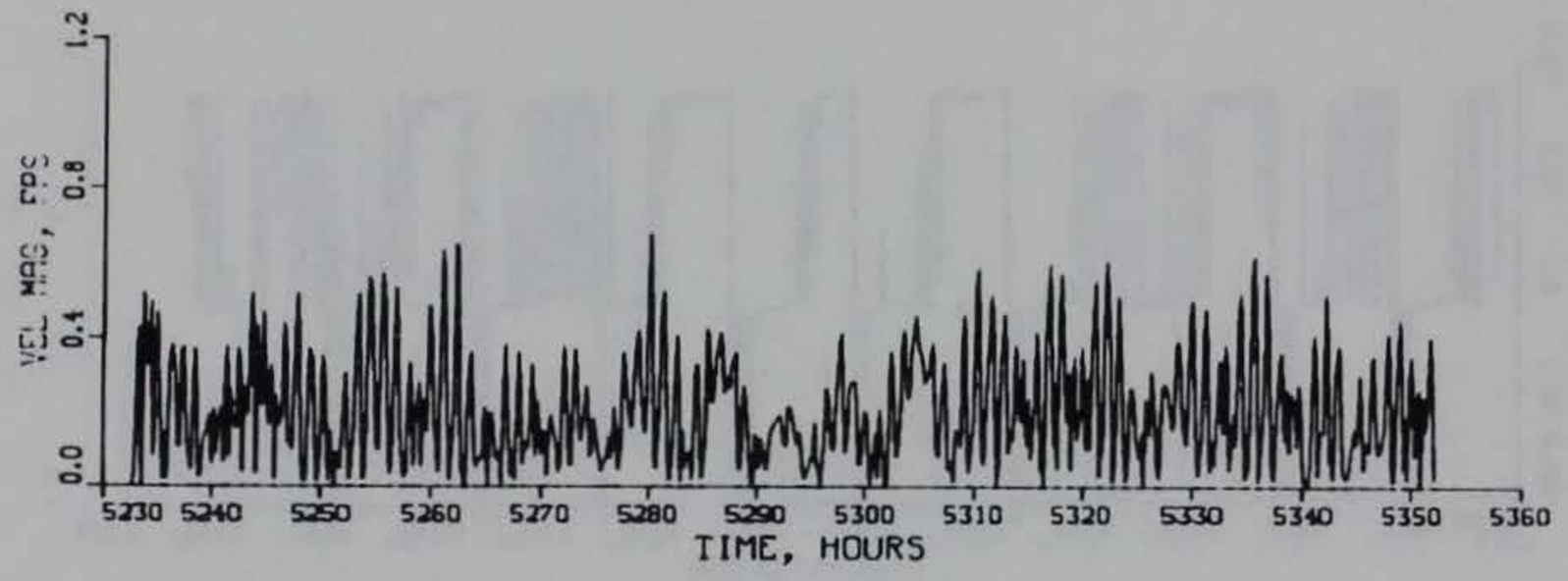

COMPUTED

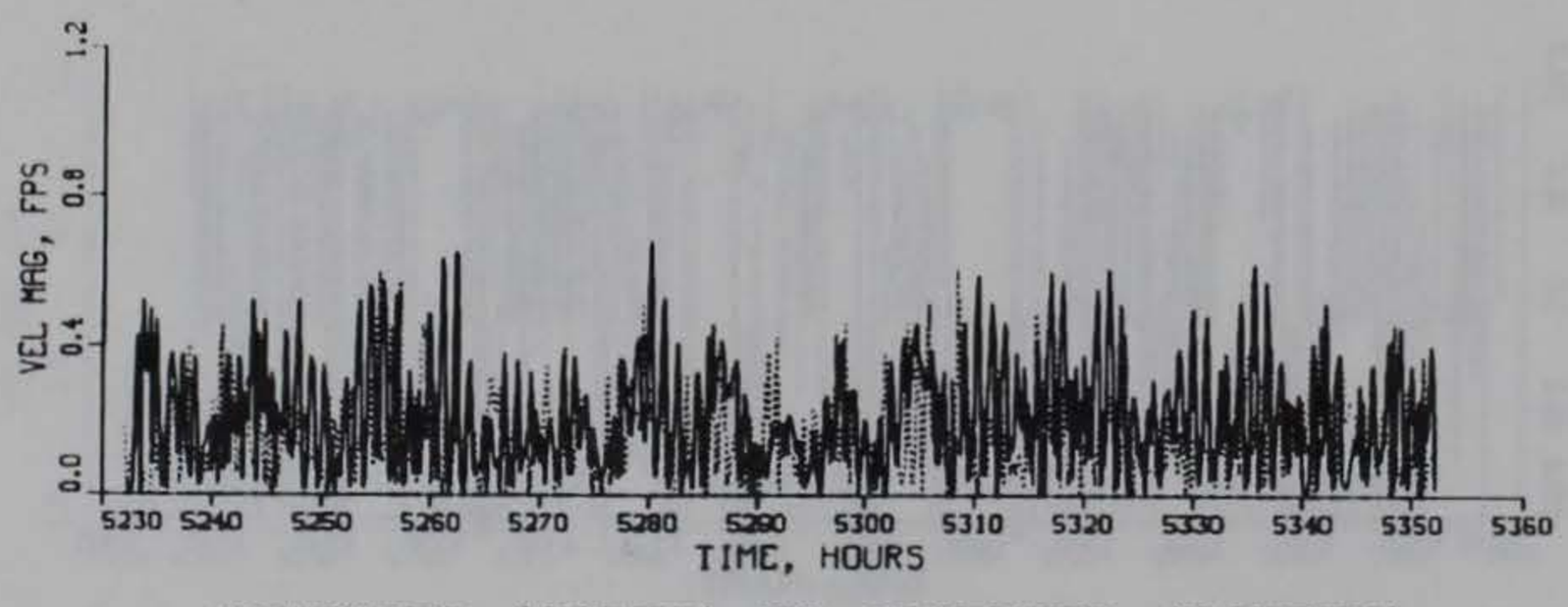

COMPUTED (SOLID) VS OBSERVED (DOTTED)

TIDAL VELOCITY

MAGNITUDE

CALIBRATION PERIOD

GAGE CM2

BOTTOM

PLATE 15

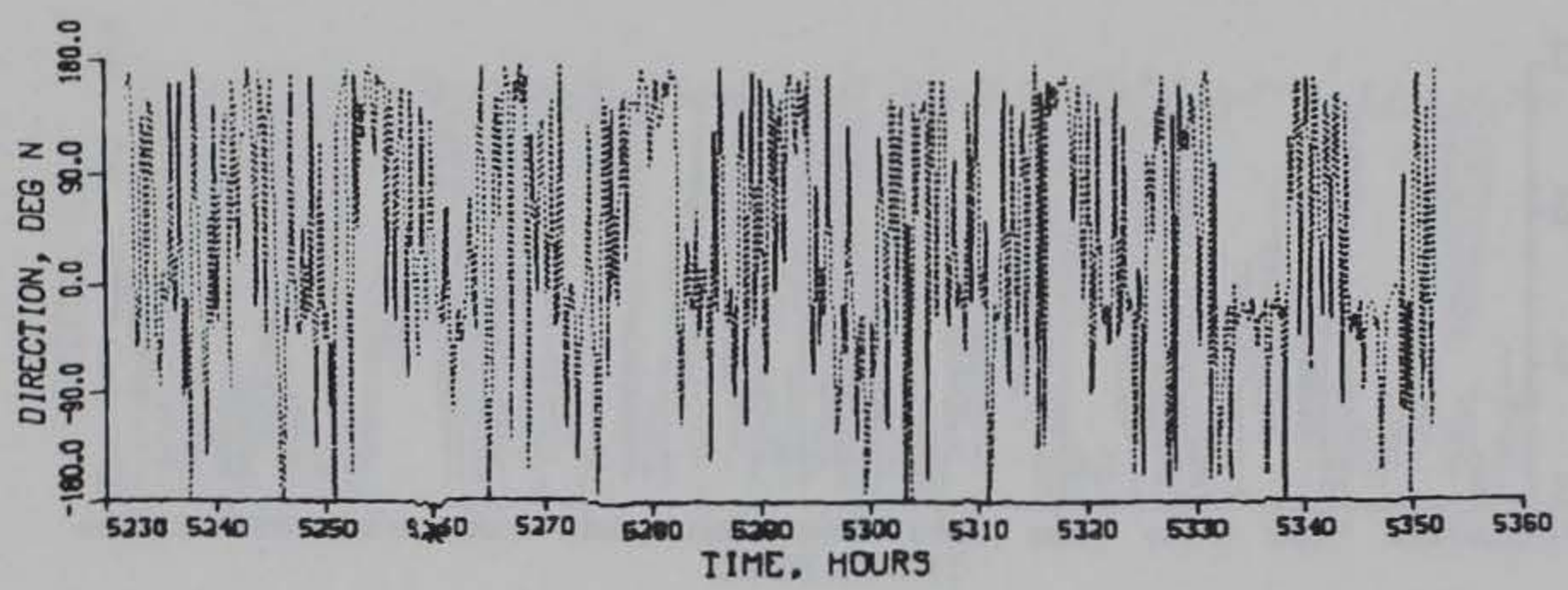

OBSERVED

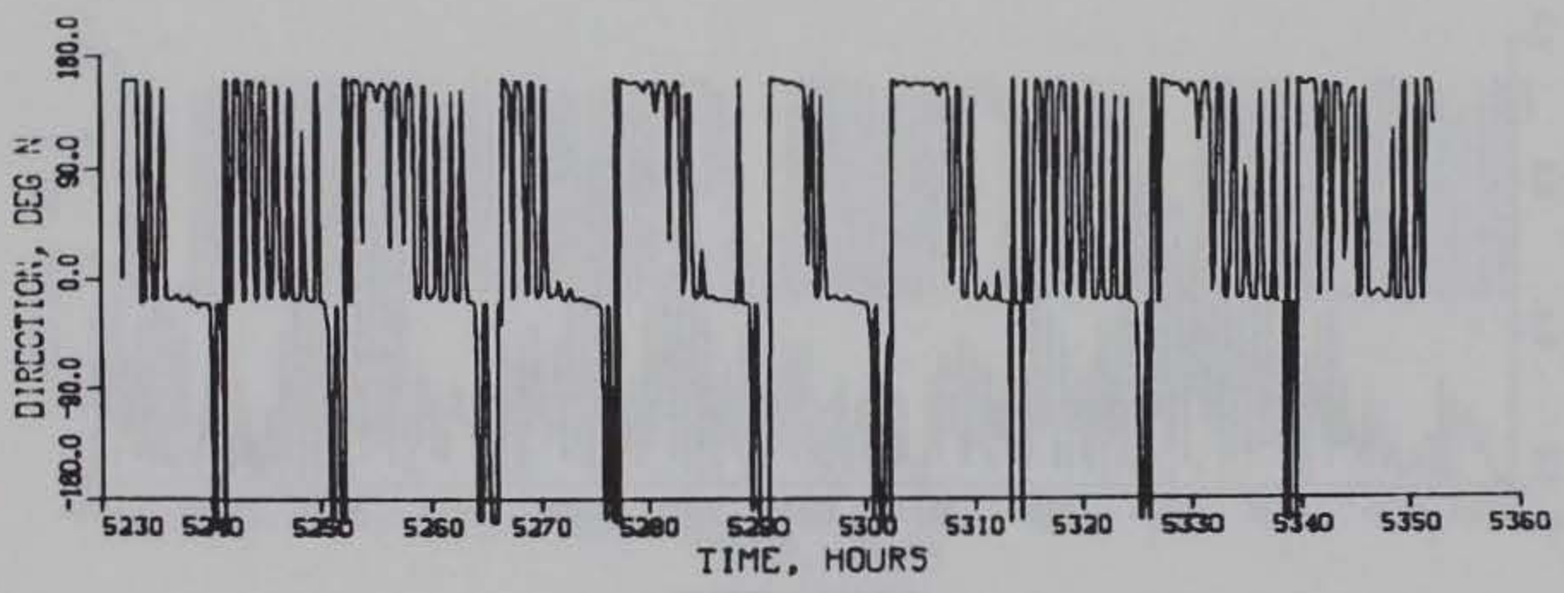

COMPUTED

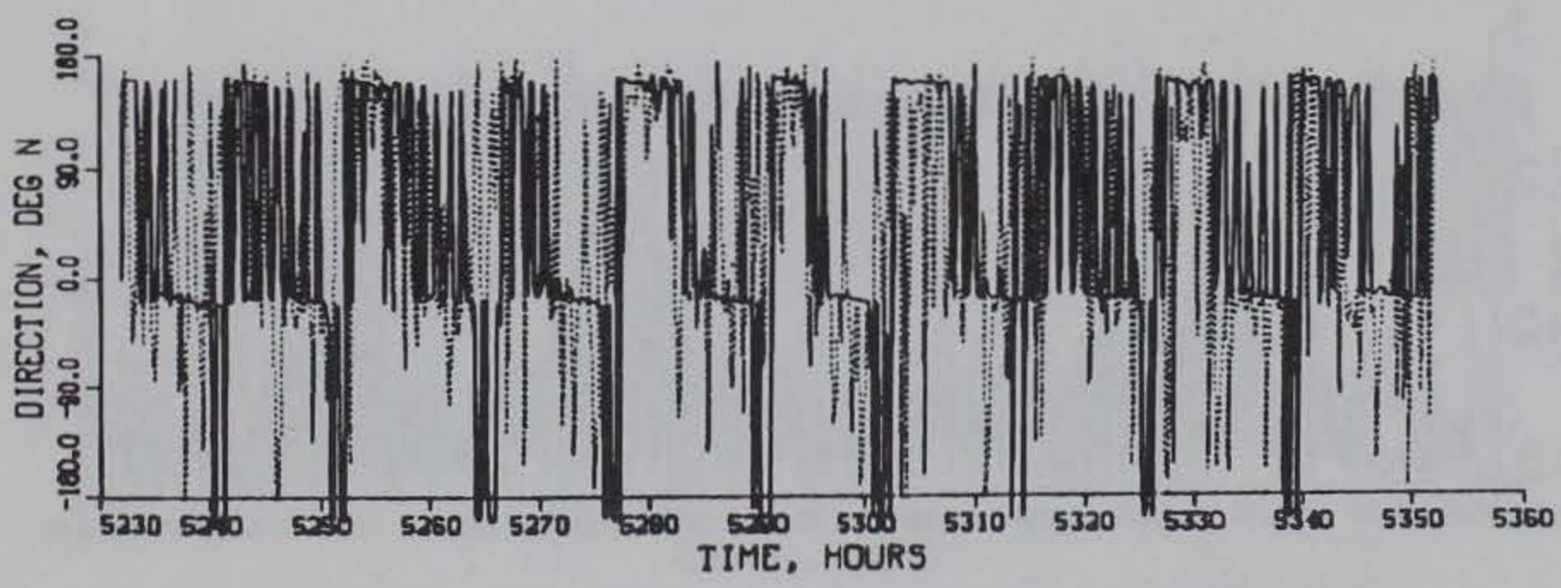

COMPUTED (SOLID) VS OBSERVED (DOTTED)

TIDAL VELOCITY

DIRECTION

CALIBRATION PERIOD

GAGE CM2

BOTTOM

PLATE 16

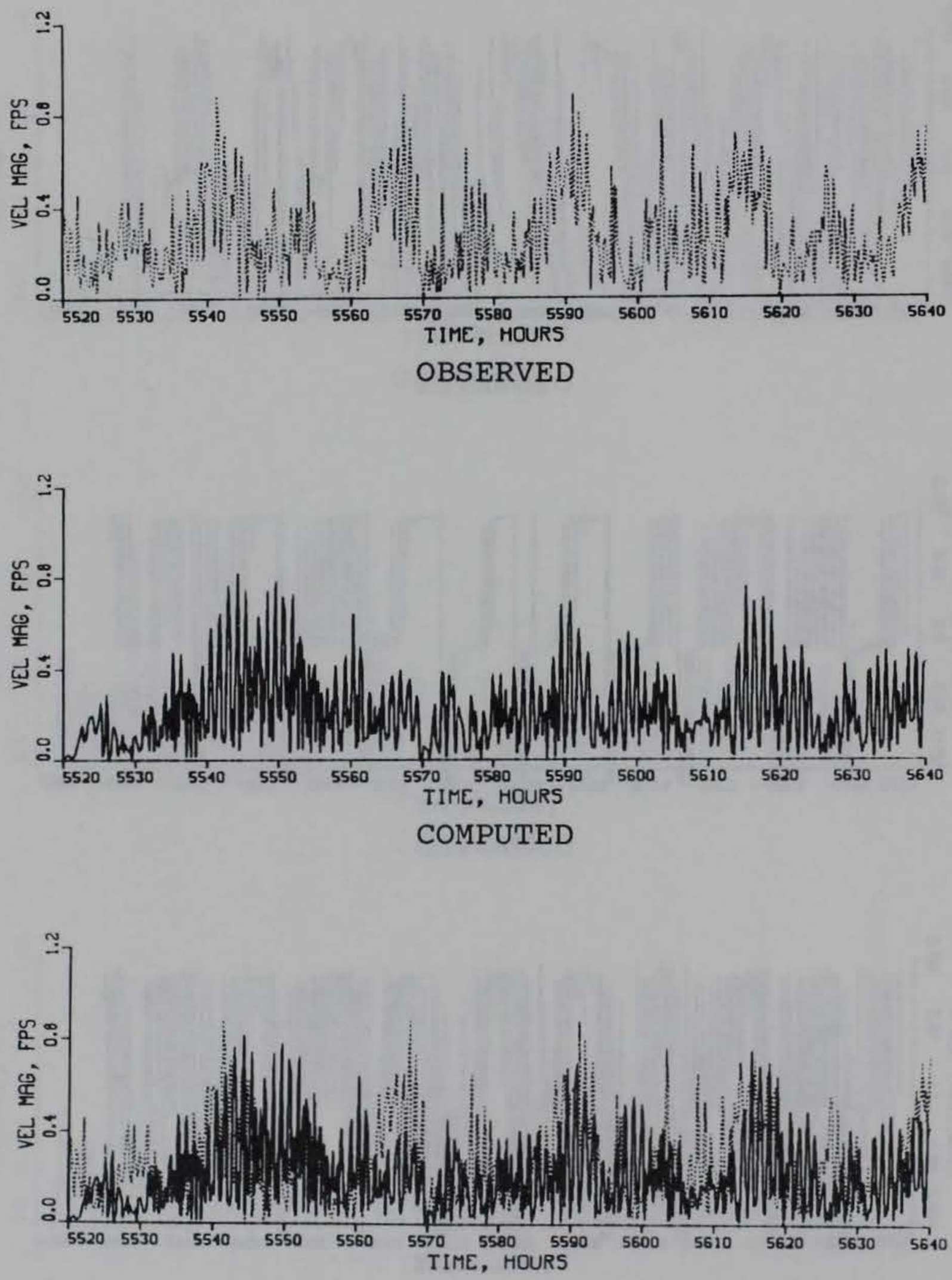

OBSERVED

COMPUTED

COMPUTED (SOLID) VS OBSERVED (DOTTED)

TIDAL VELOCITY **VERIFICATION PERIOD**

MAGNITUDE

GAGE CM2

SURFACE

PLATE 17

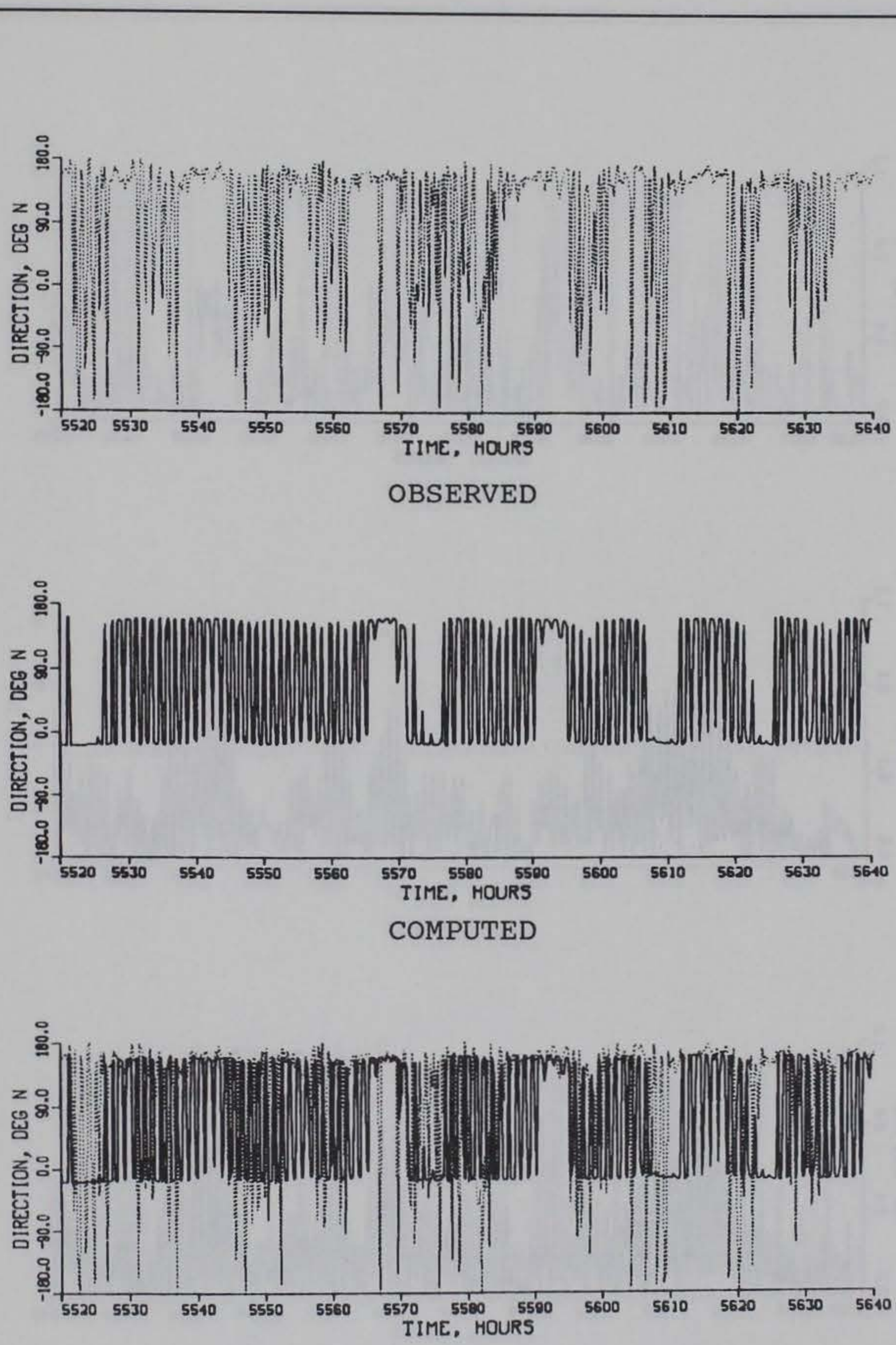

OBSERVED

COMPUTED

COMPUTED (SOLID) VS OBSERVED (DOTTED)

TIDAL VELOCITY

DIRECTION

VERIFICATION PERIOD

GAGE CM2

SURFACE

PLATE 18

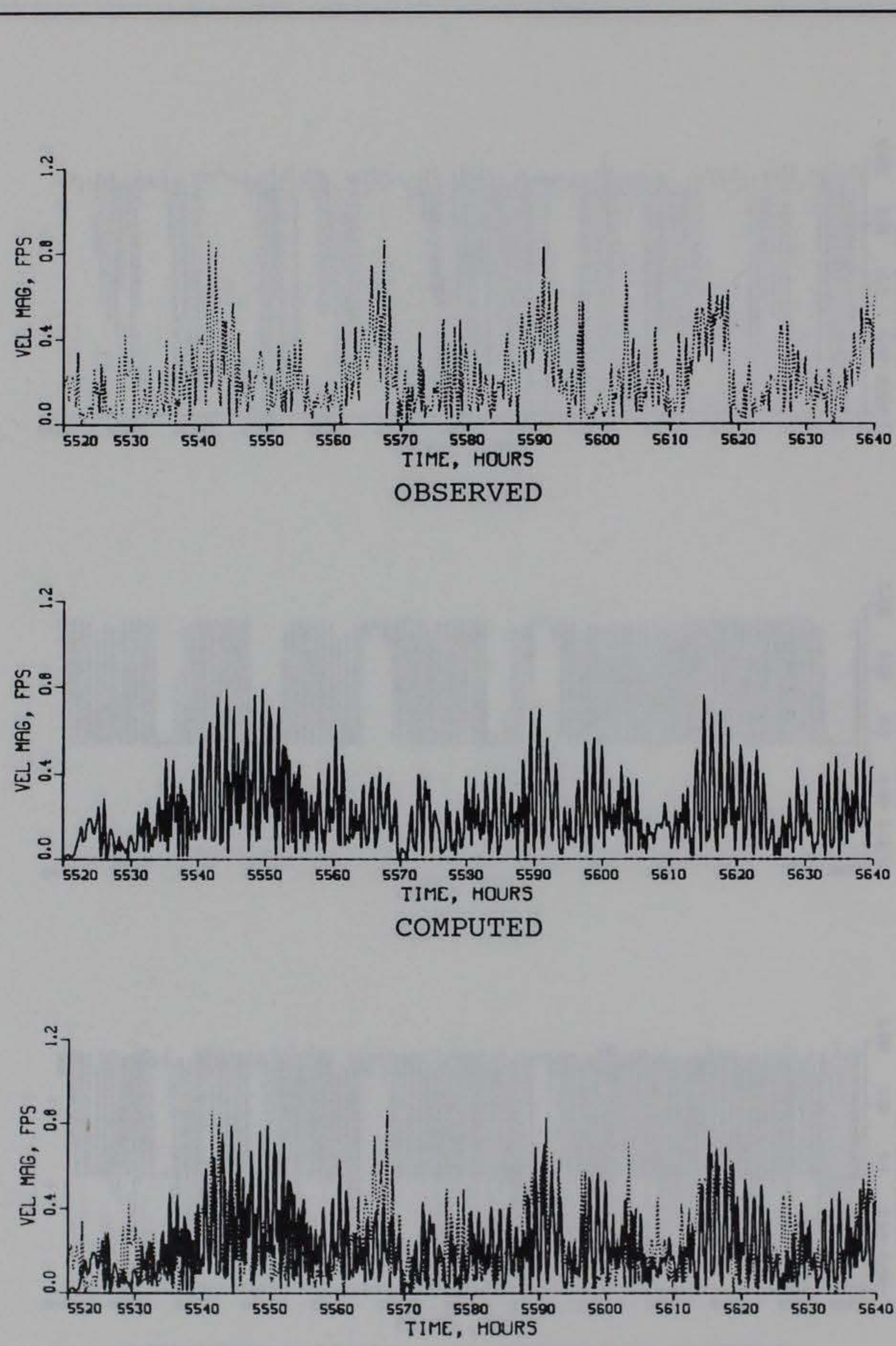

TIDAL VELOCITY

MAGNITUDE

VERIFICATION PERIOD

GAGE CM2

MID-DEPTH

PLATE 19

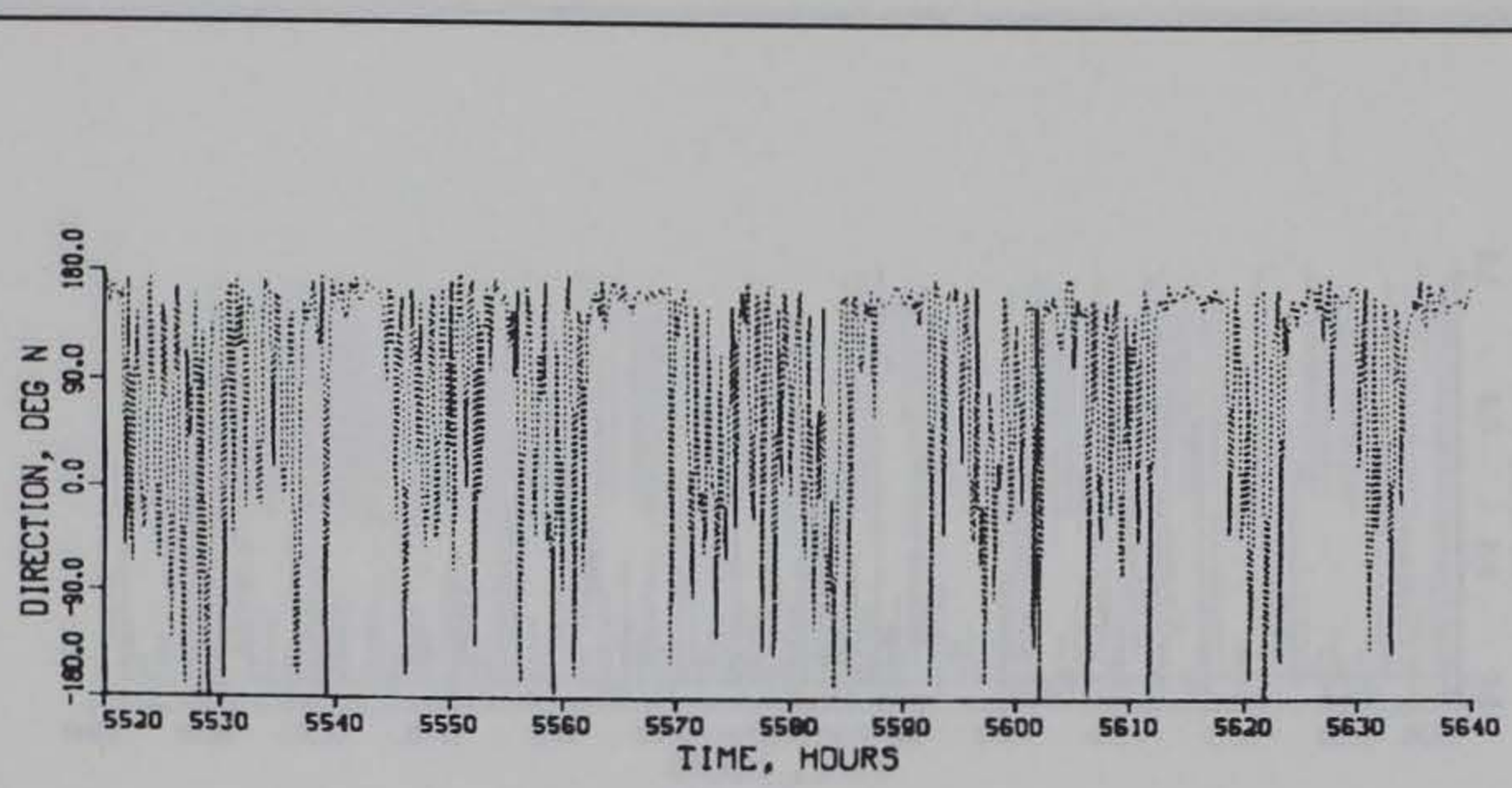

OBSERVED

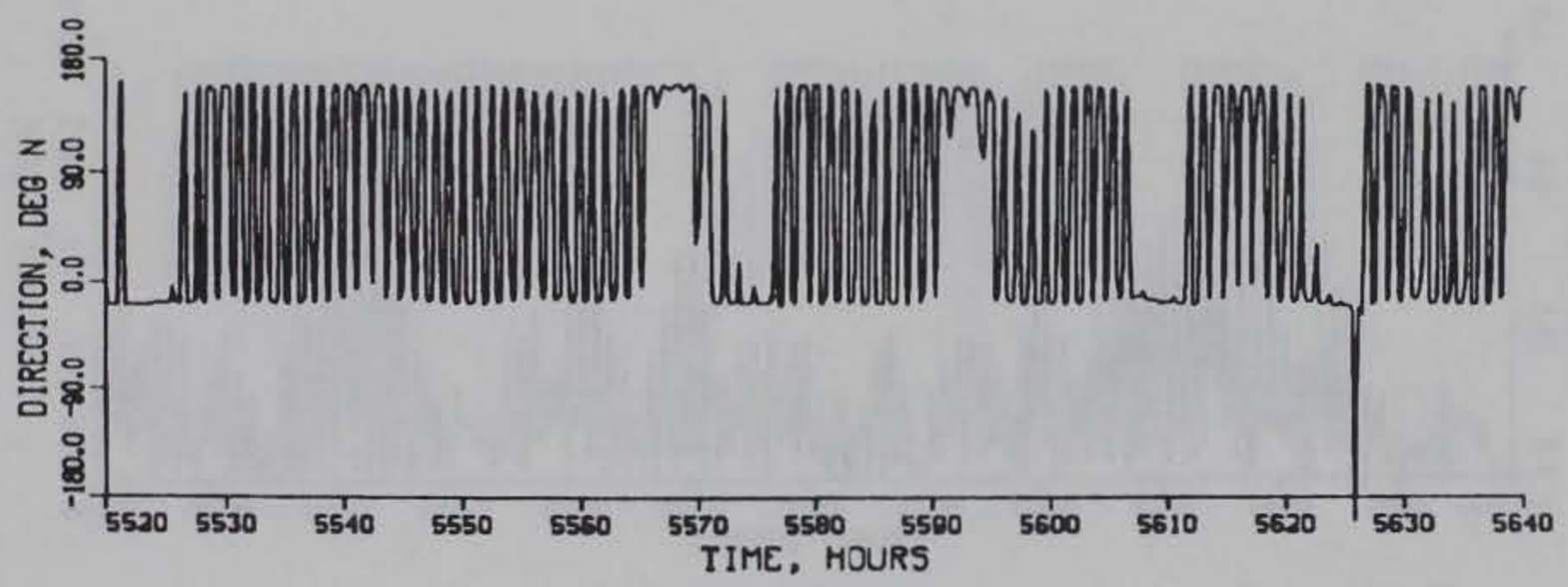

COMPUTED

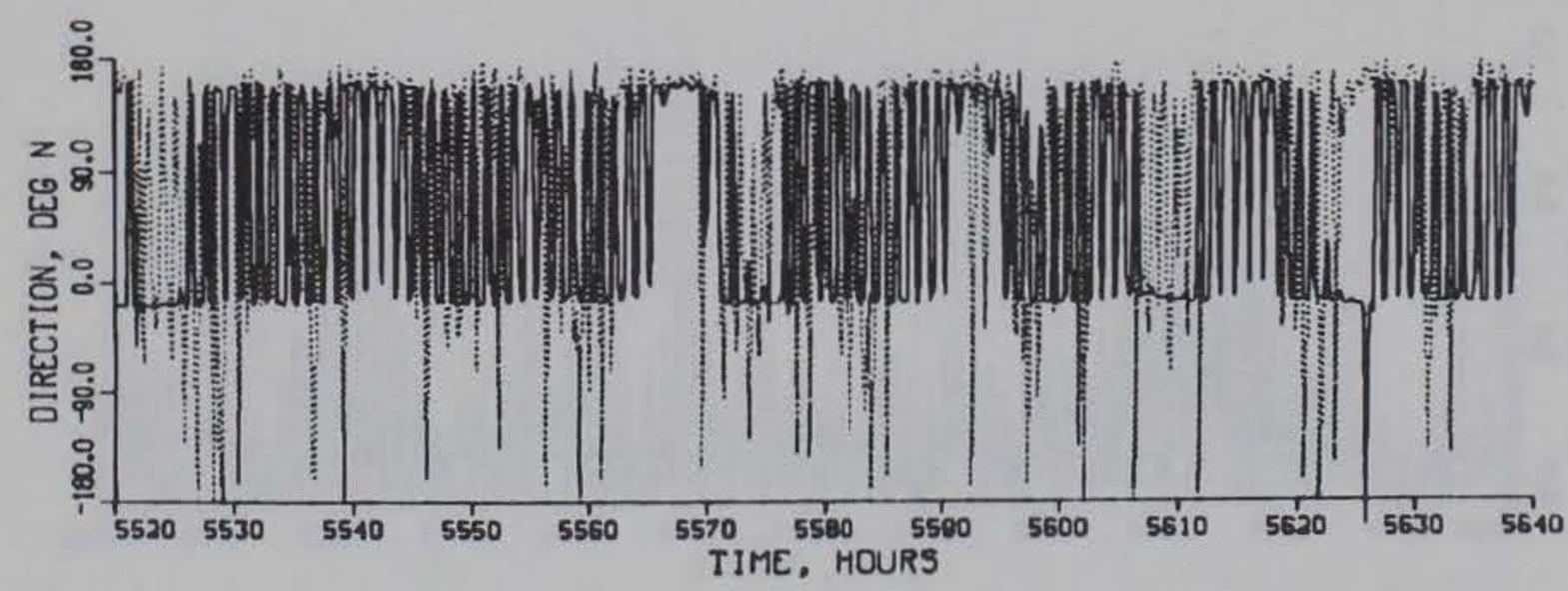

COMPUTED (SOLID) VS OBSERVED (DOTTED)

TIDAL VELOCITY **VERIFICATION PERIOD**

DIRECTION

GAGE CM2

MID-DEPTH

PLATE 20

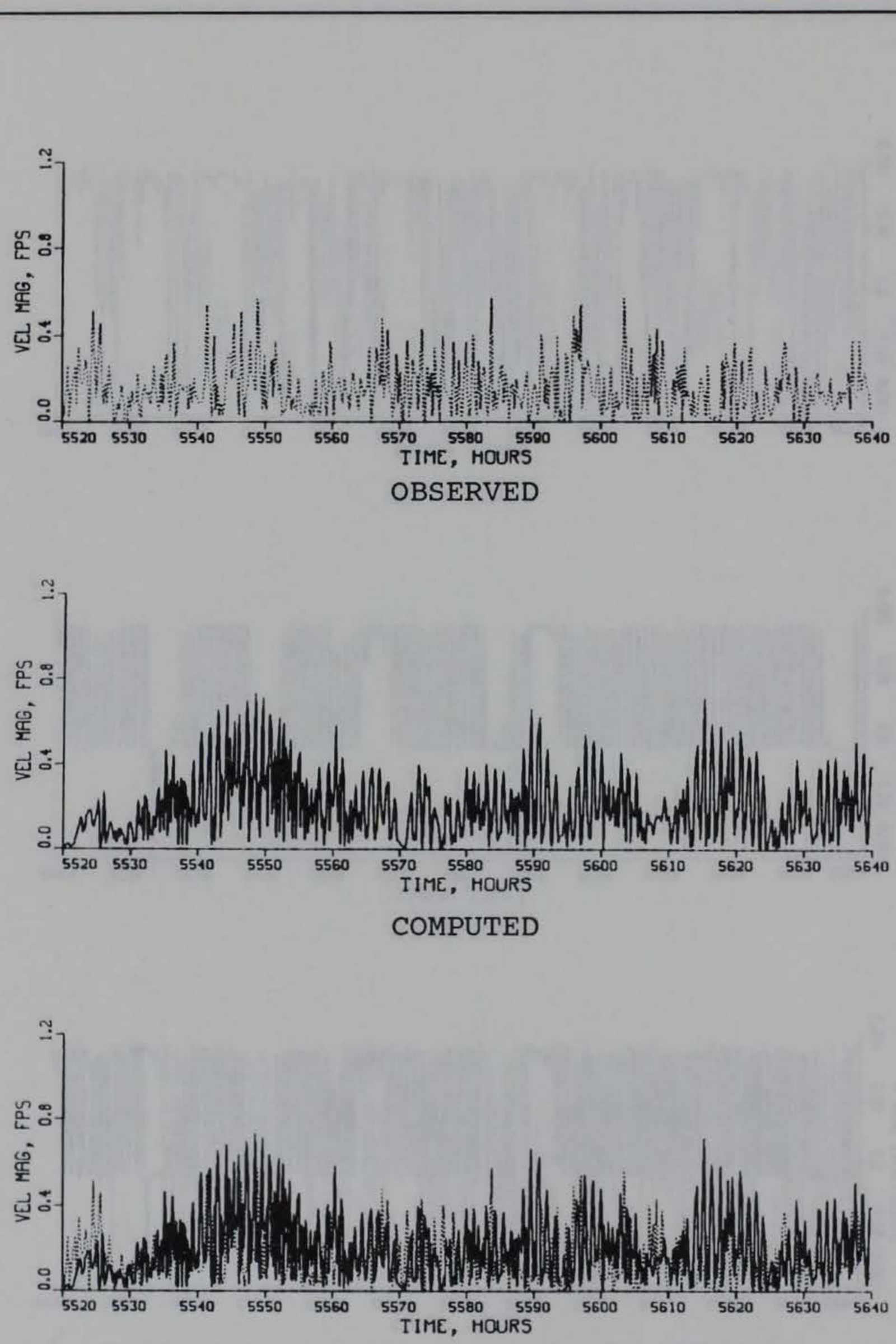

TIDAL VELOCITY

MAGNITUDE

VERIFICATION PERIOD

GAGE CM2

BOTTOM

PLATE 21

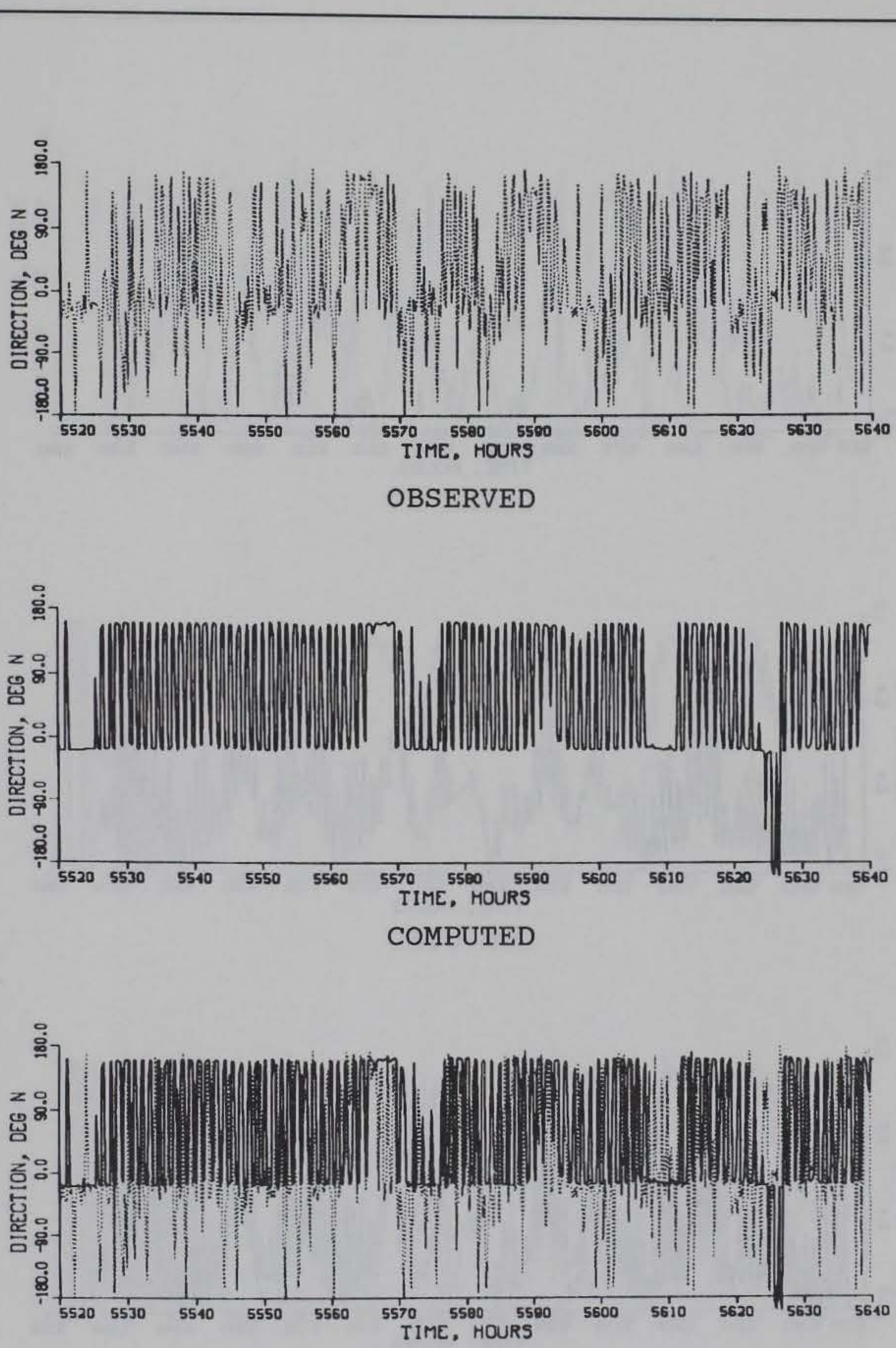

OBSERVED

COMPUTED

COMPUTED (SOLID) VS OBSERVED (DOTTED)

TIDAL VELOCITY

DIRECTION

VERIFICATION PERIOD

GAGE CM2

BOTTOM

PLATE 22

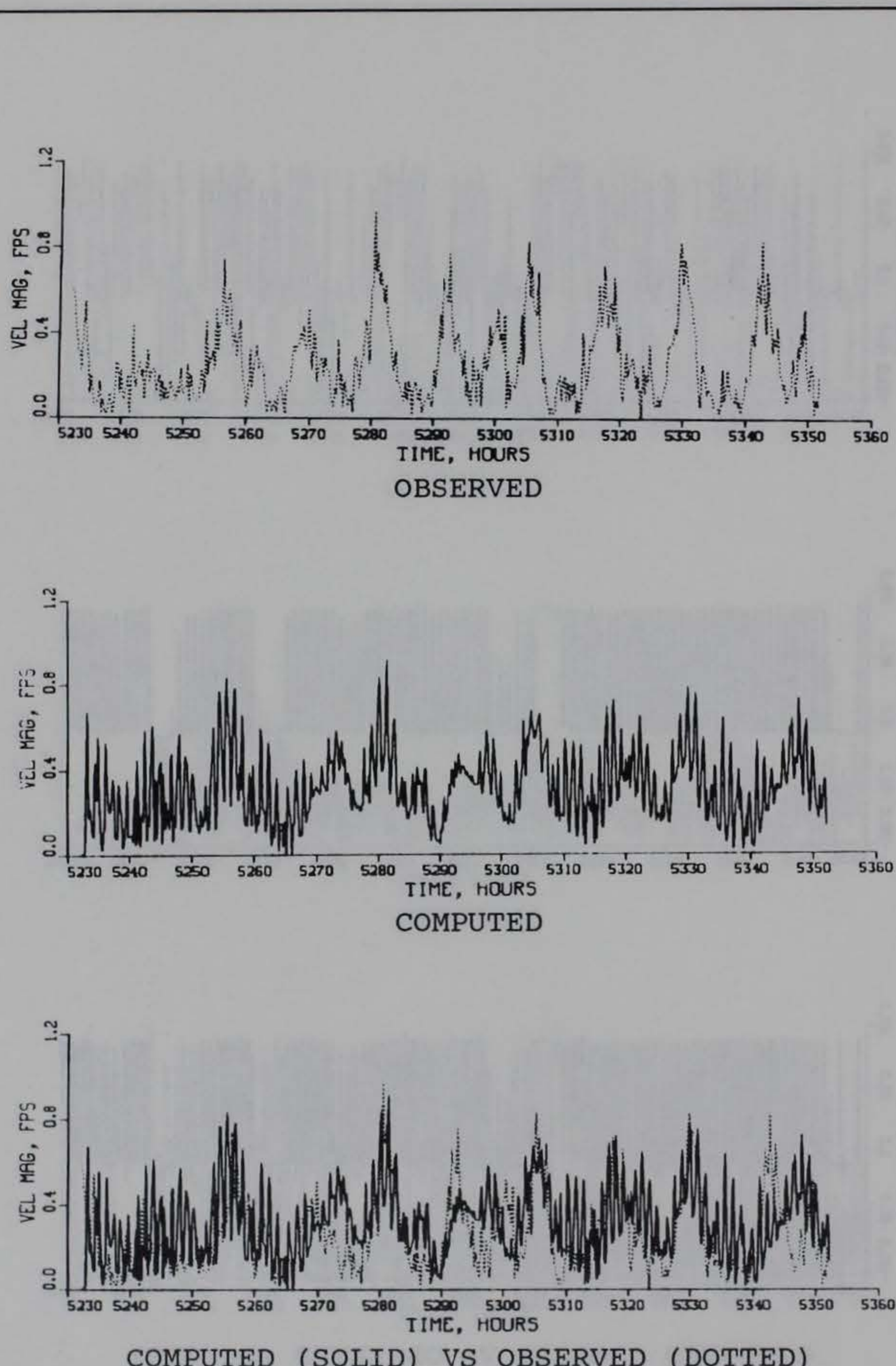

TIDAL VELOCITY

MAGNITUDE

CALIBRATION PERIOD

GAGE CM3

SURFACE

PLATE 23

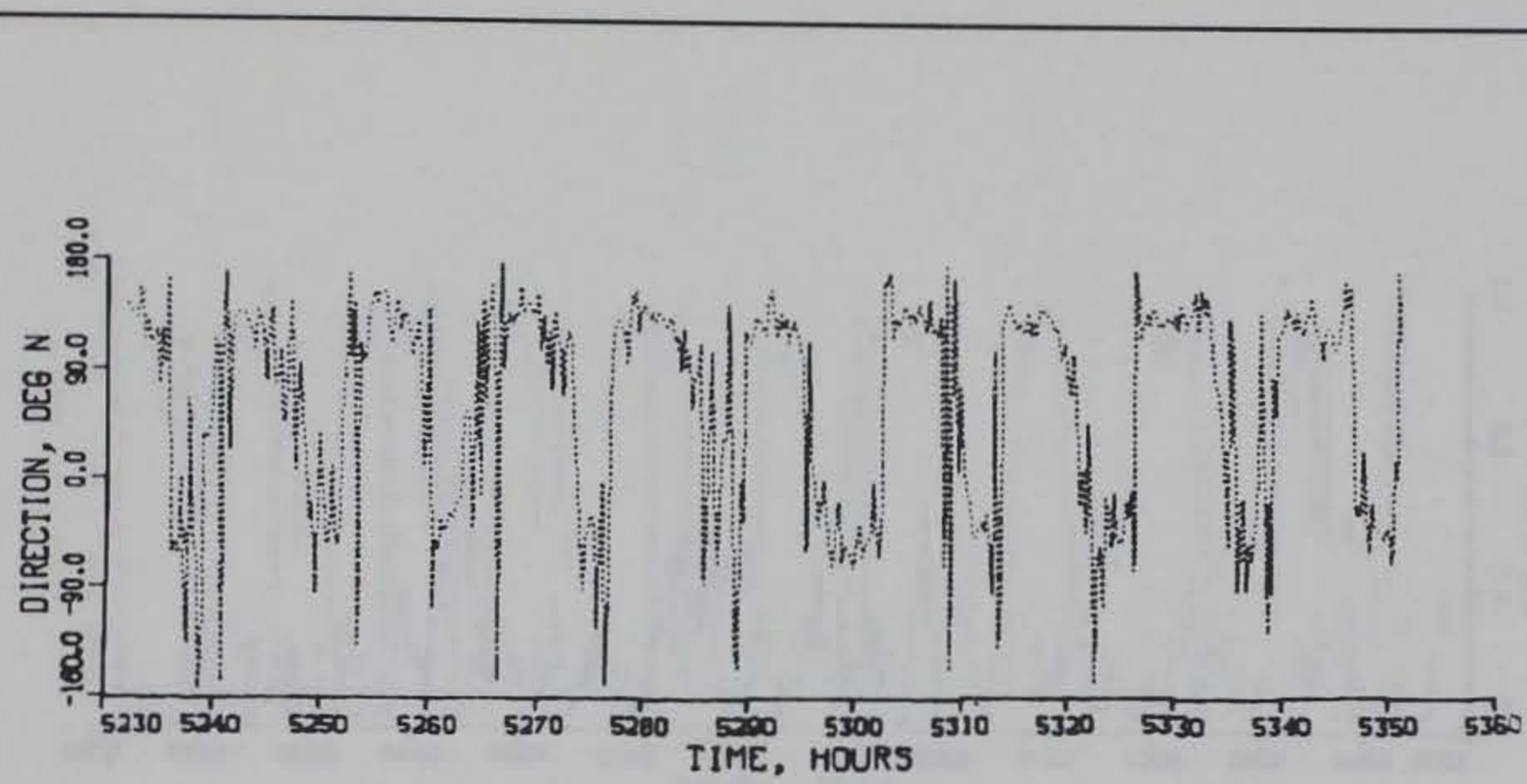

OBSERVED

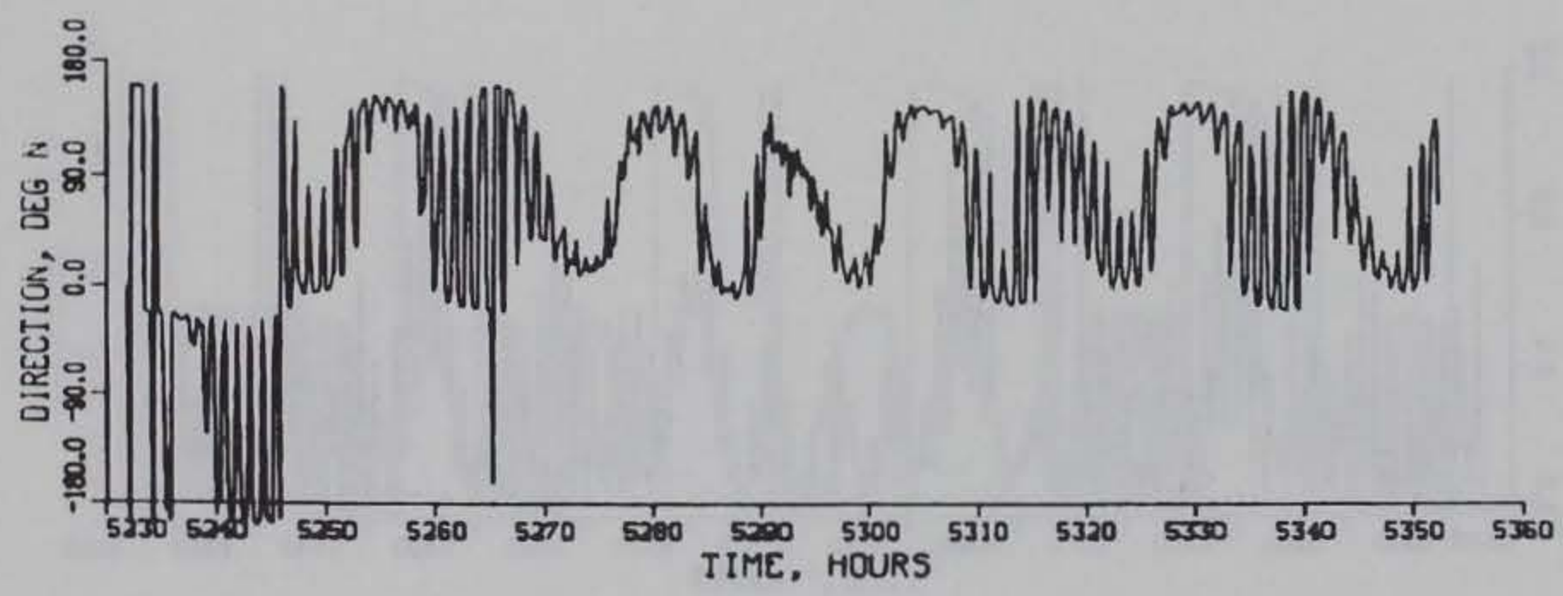

COMPUTED

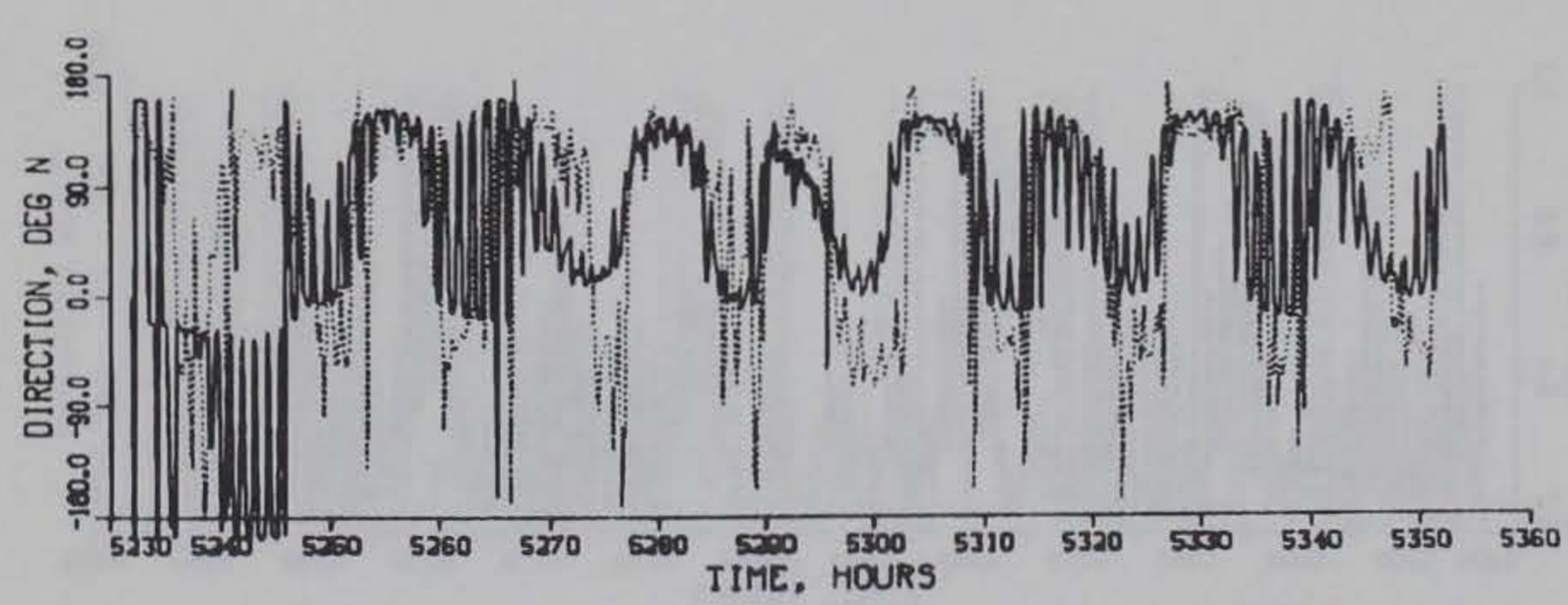

COMPUTED (SOLID) VS OBSERVED (DOTTED)

TIDAL VELOCITY

DIRECTION

CALIBRATION PERIOD

GAGE CM3

SURFACE

PLATE 24

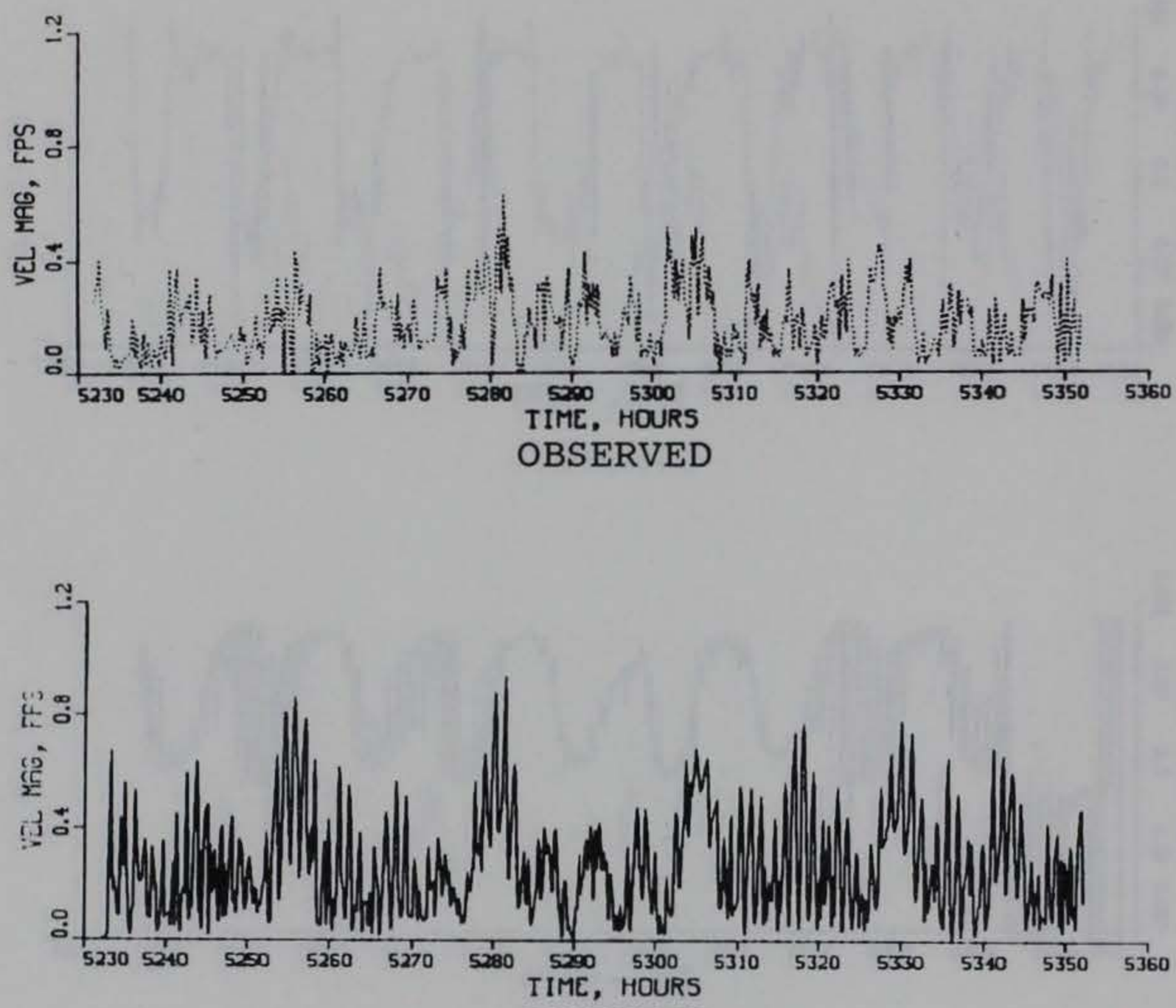

OBSERVED

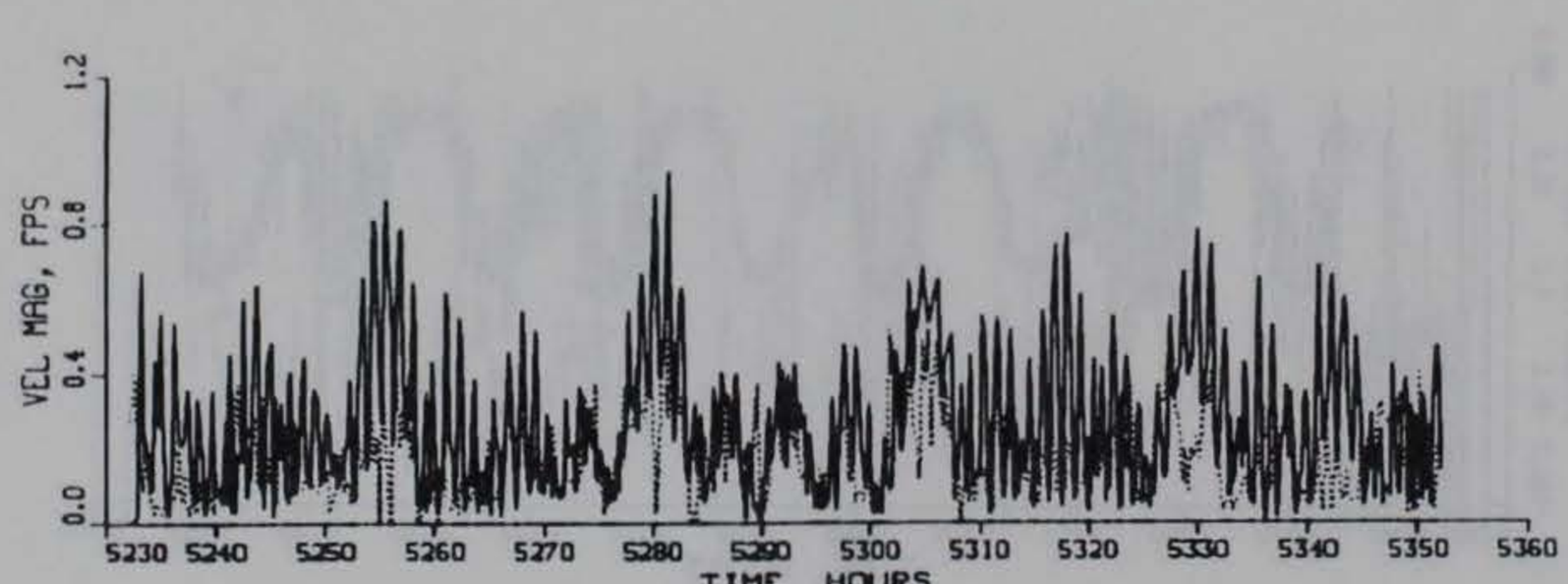

COMPUTED

COMPUTED (SOLID) VS OBSERVED (DOTTED)

TIDAL VELOCITY

MAGNITUDE

CALIBRATION PERIOD

GAGE CM3

MID-DEPTH

PLATE 25

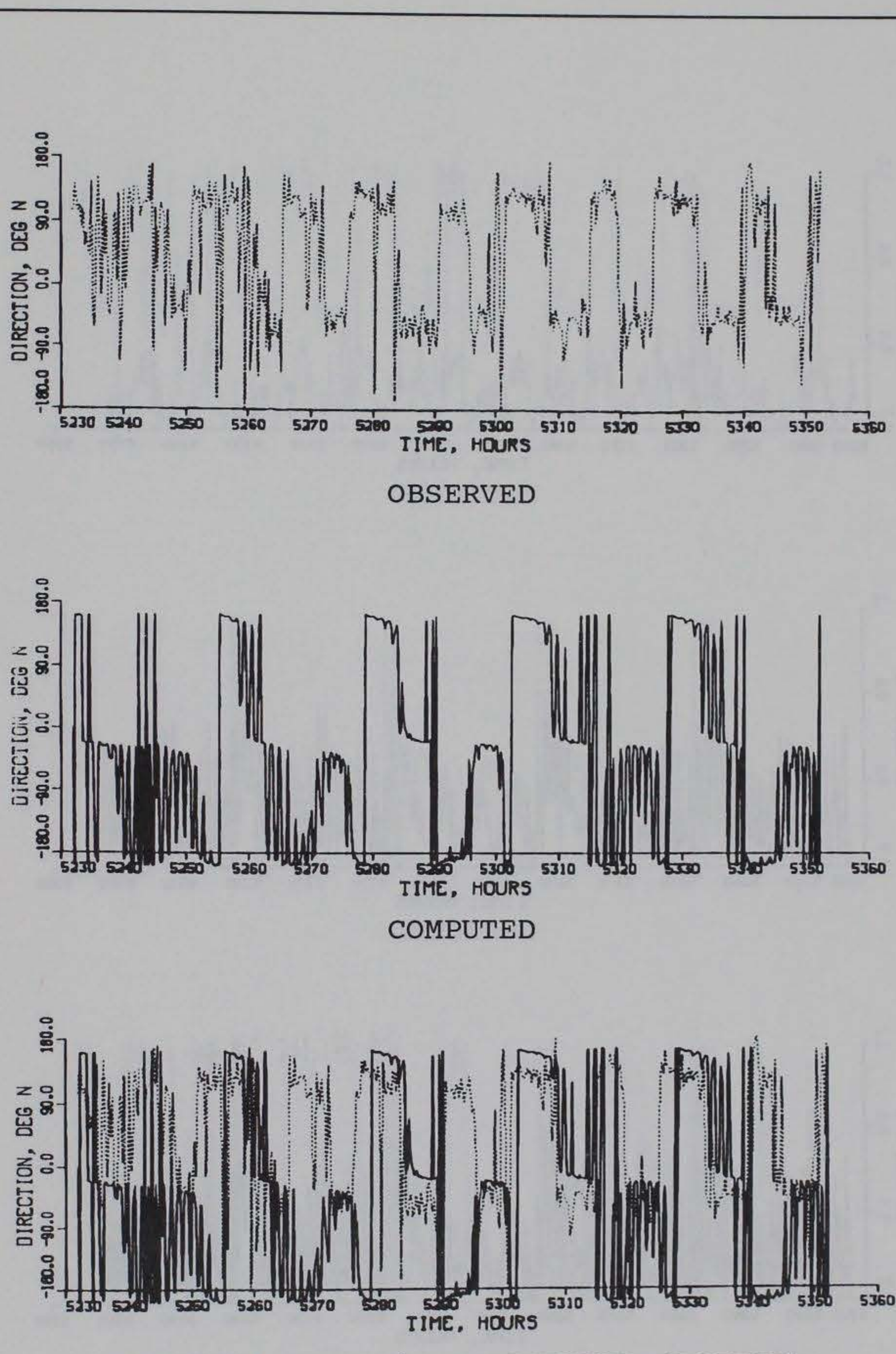

COMPUTED (SOLID) VS OBSERVED (DOTTED)

TIDAL VELOCITY

DIRECTION

CALIBRATION PERIOD

GAGE CM3

MID-DEPTH

PLATE 26

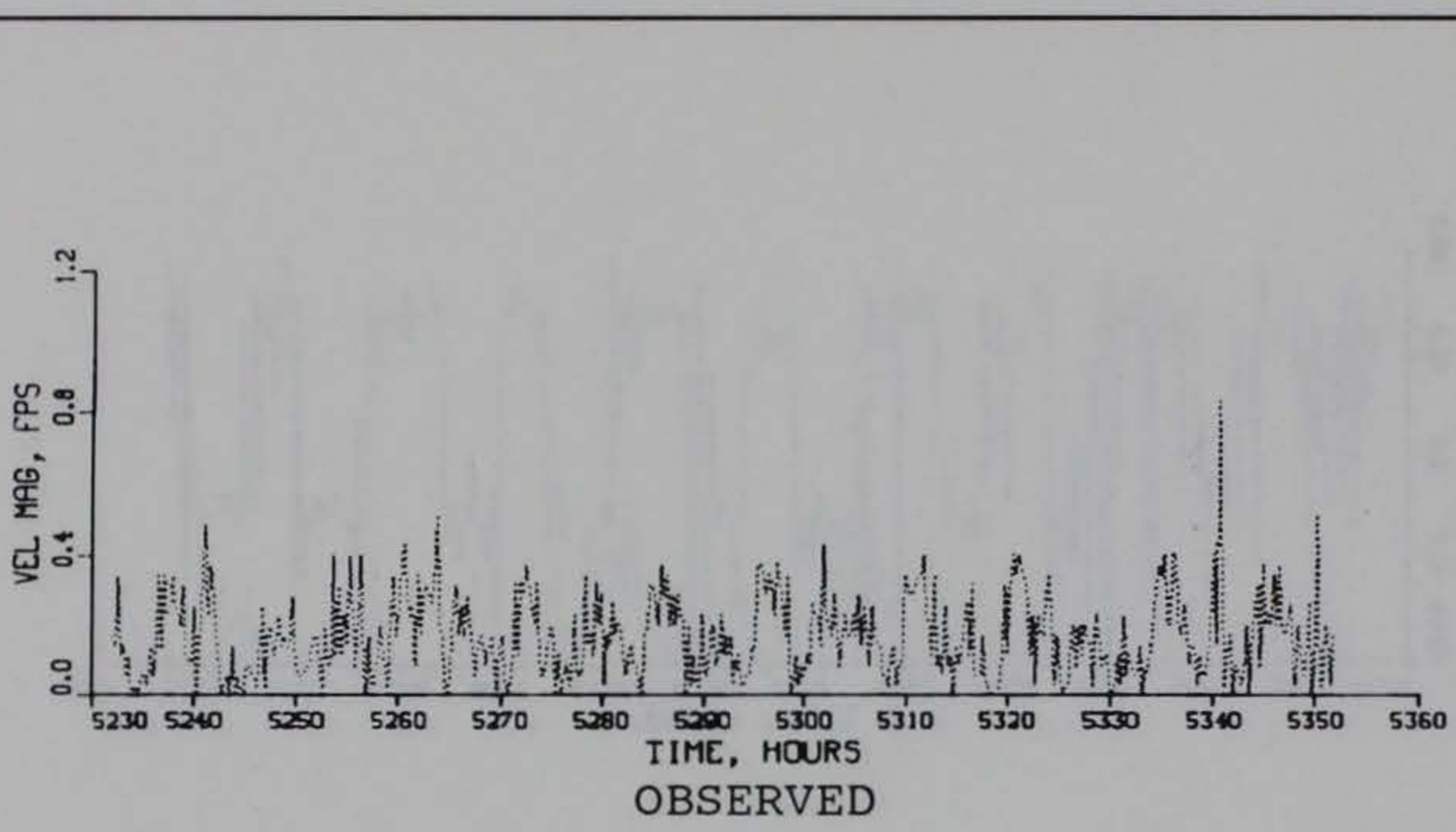

OBSERVED

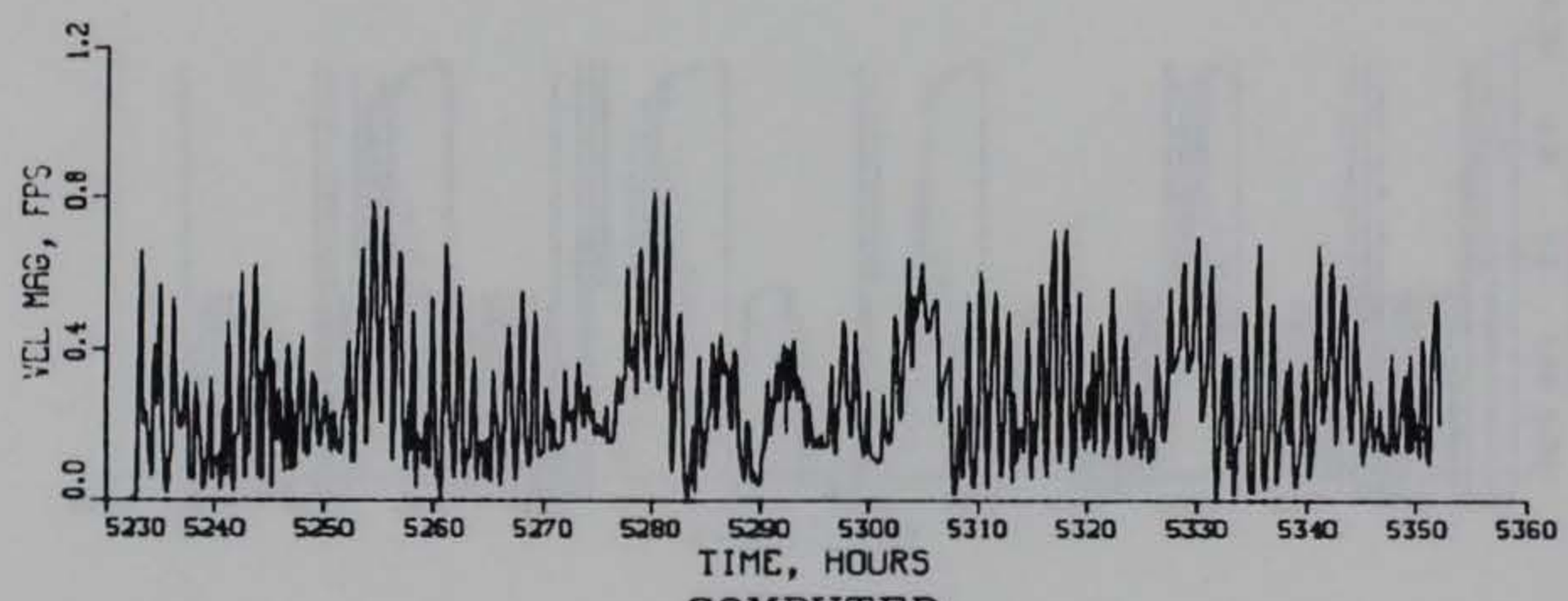

COMPUTED

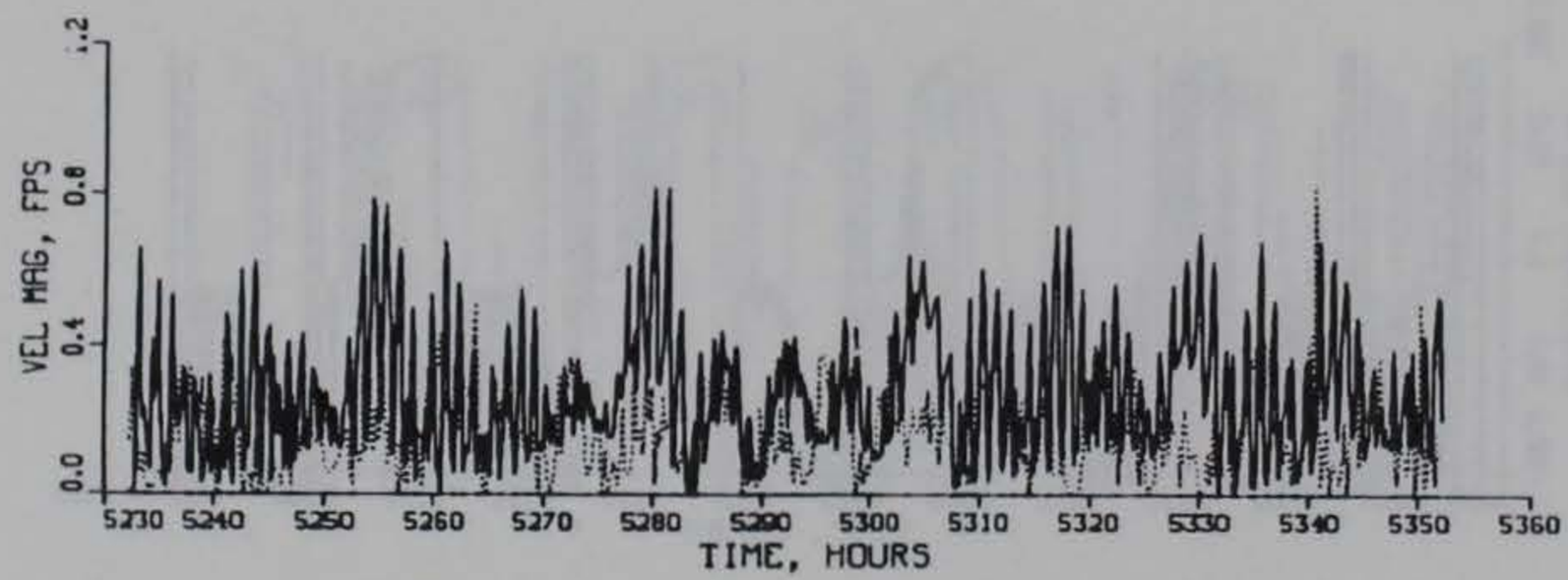

COMPUTED (SOLID) VS OBSERVED (DOTTED)

TIDAL VELOCITY

MAGNITUDE

CALIBRATION PERIOD

GAGE CM3

BOTTOM

PLATE 27

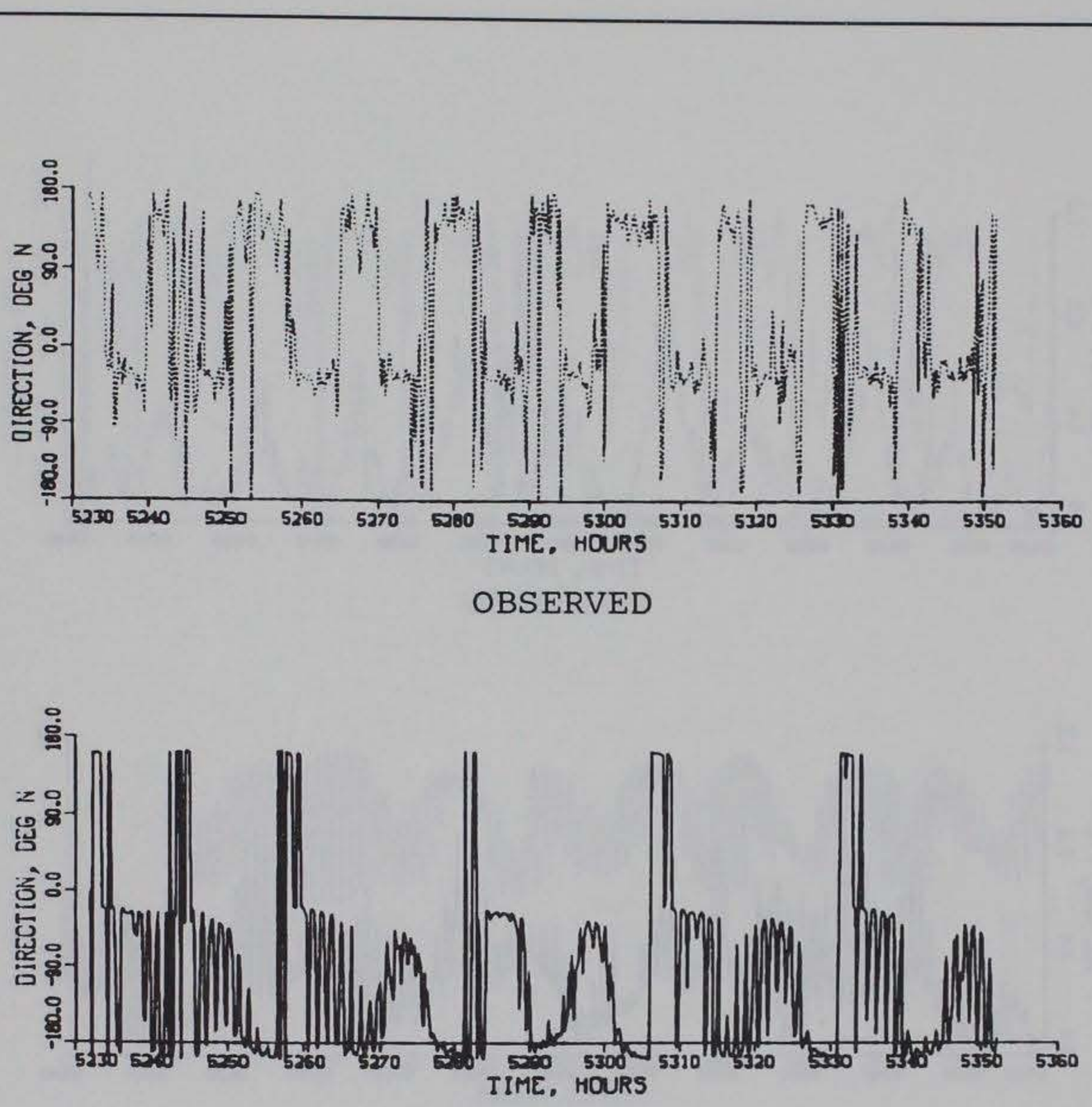

OBSERVED

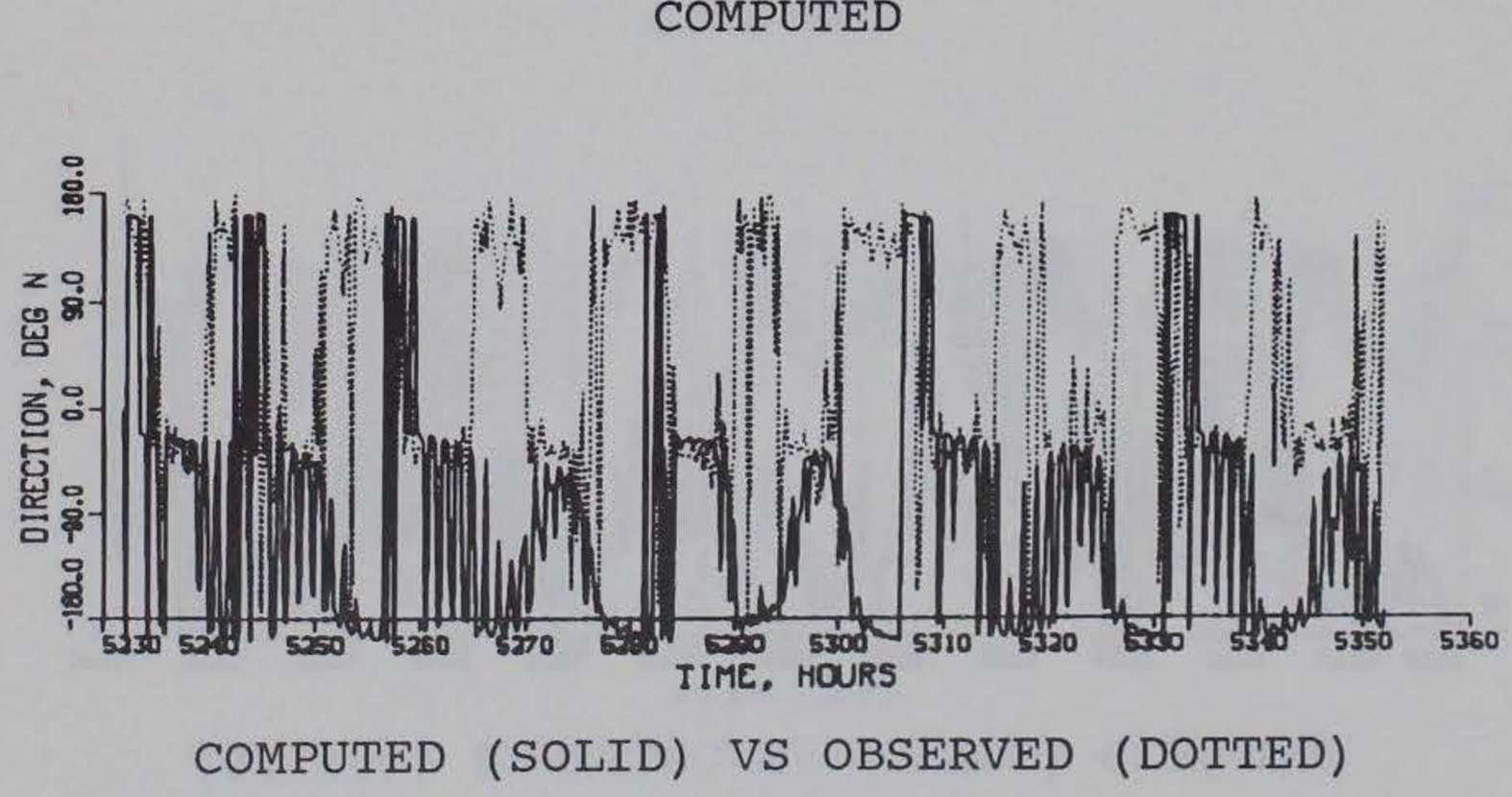

COMPUTED

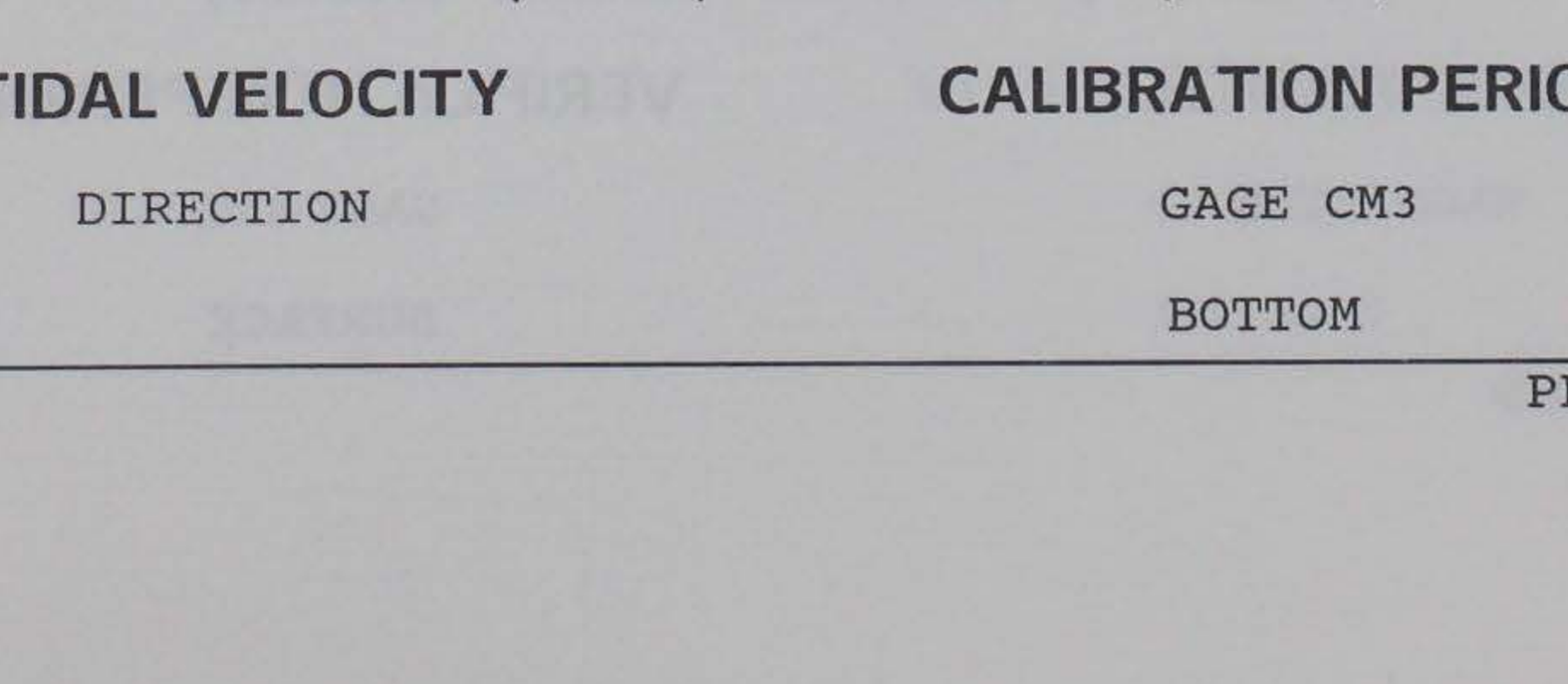

COMPUTED (SOLID) VS OBSERVED (DOTTED)

TIDAL VELOCITY

DIRECTION

CALIBRATION PERIOD

GAGE CM3

BOTTOM

PLATE 28

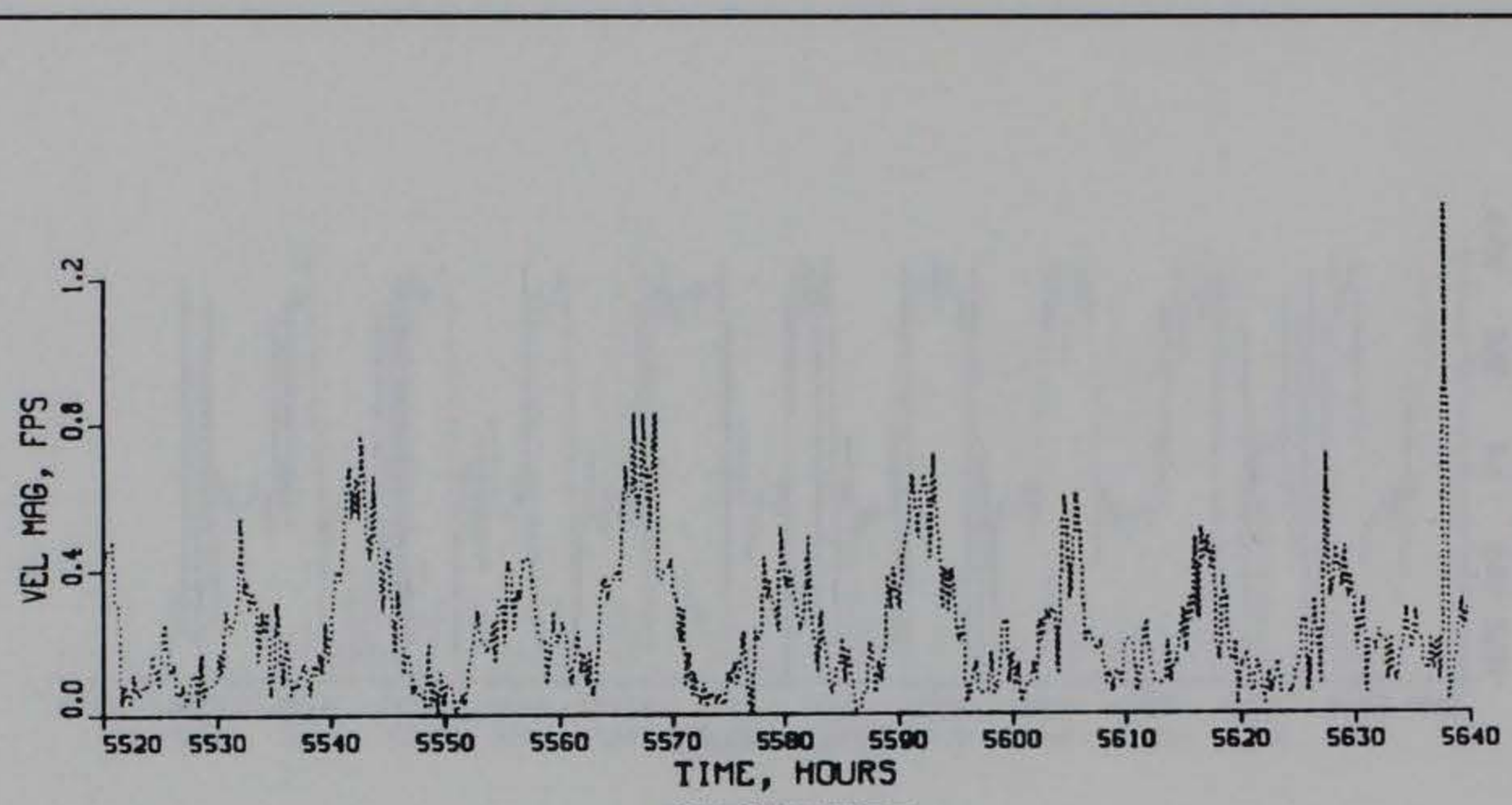

OBSERVED

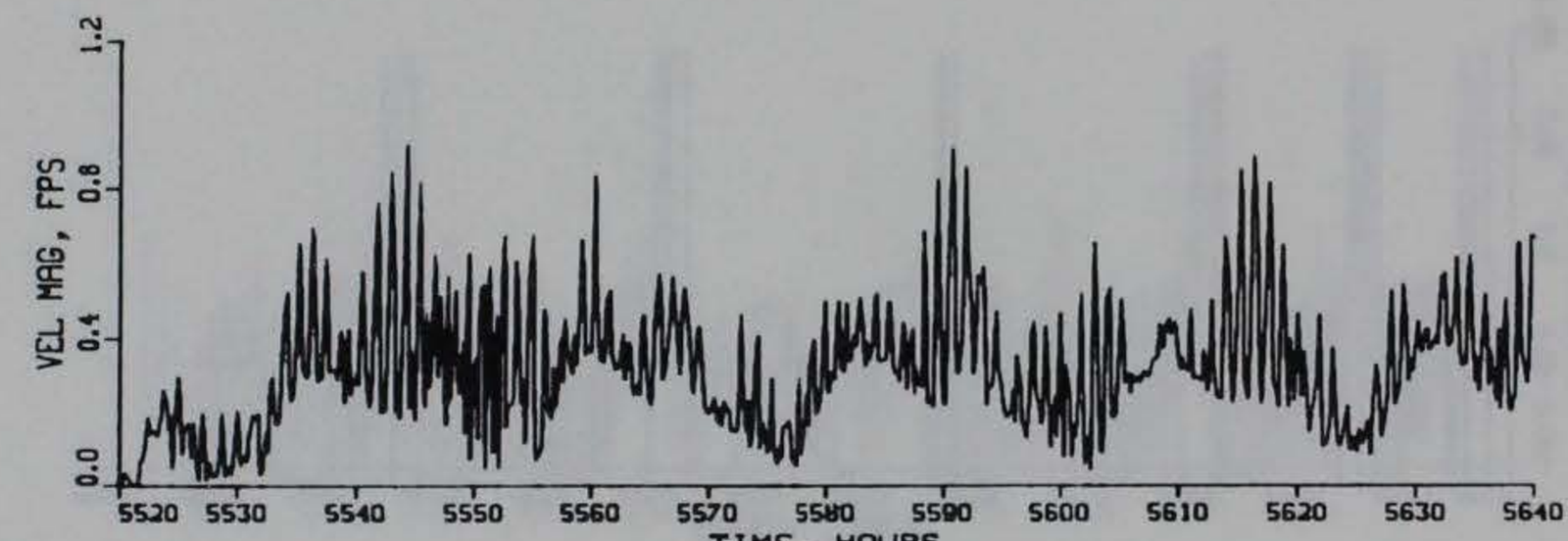

COMPUTED

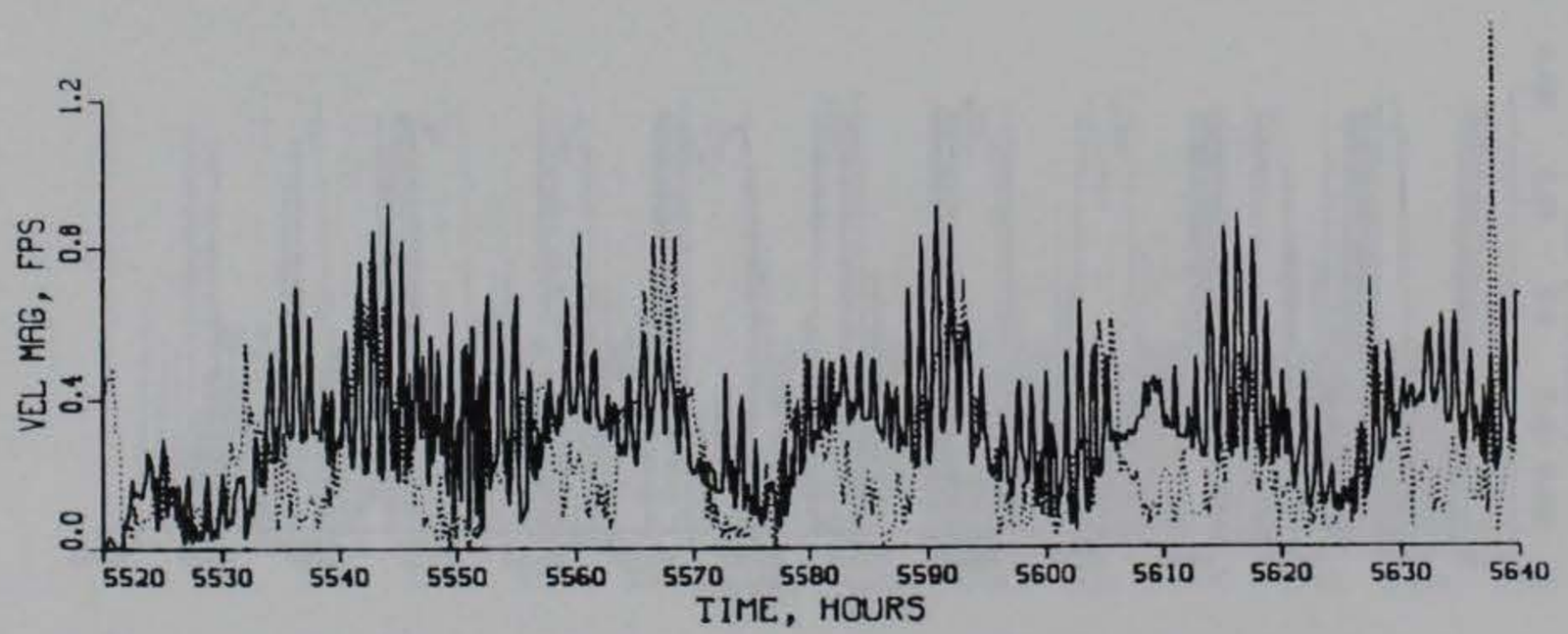

COMPUTED (SOLID) VS OBSERVED (DOTTED)

TIDAL VELOCITY **VERIFICATION PERIOD**

MAGNITUDE

GAGE CM3

SURFACE

PLATE 29

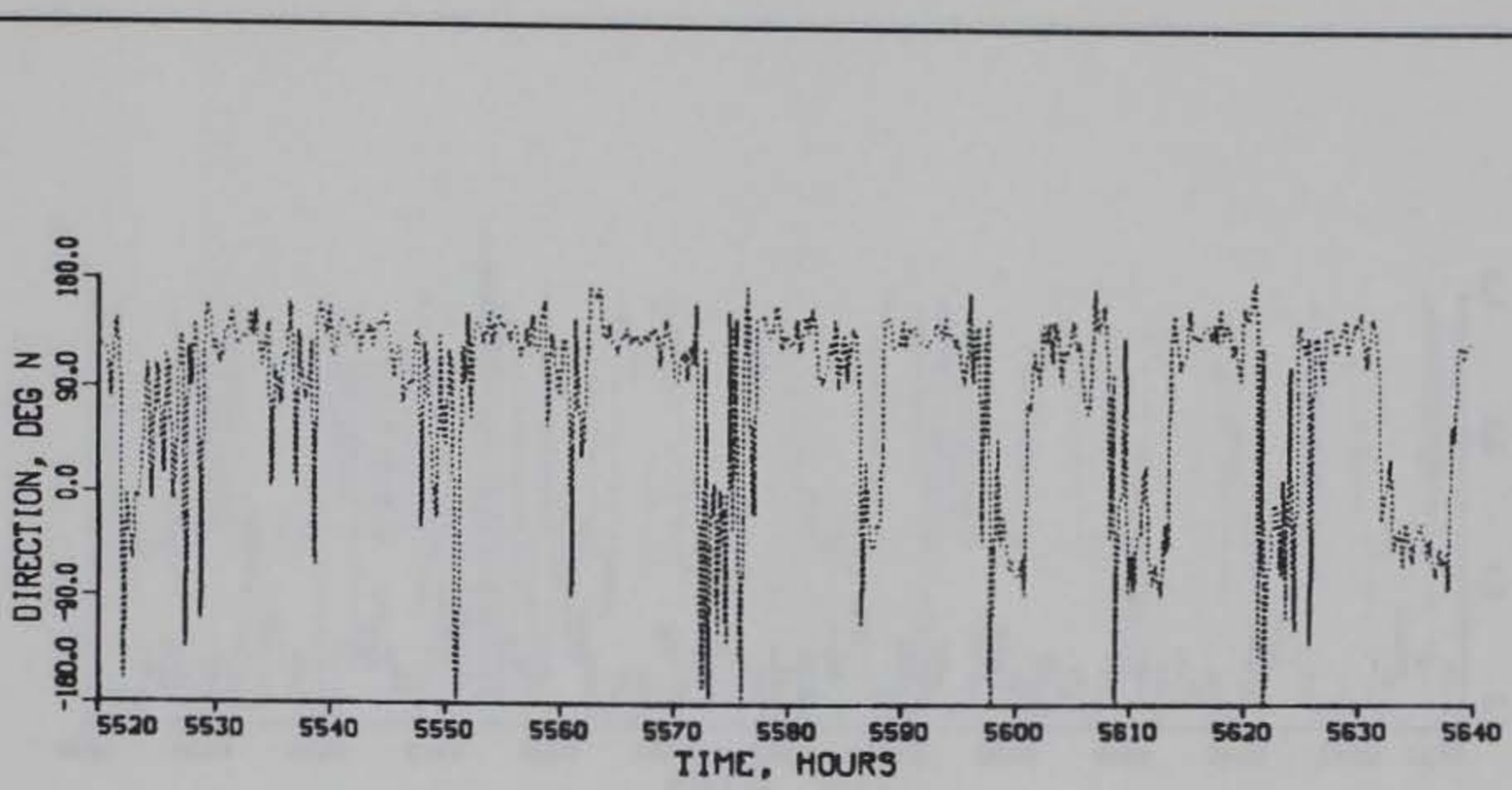

OBSERVED

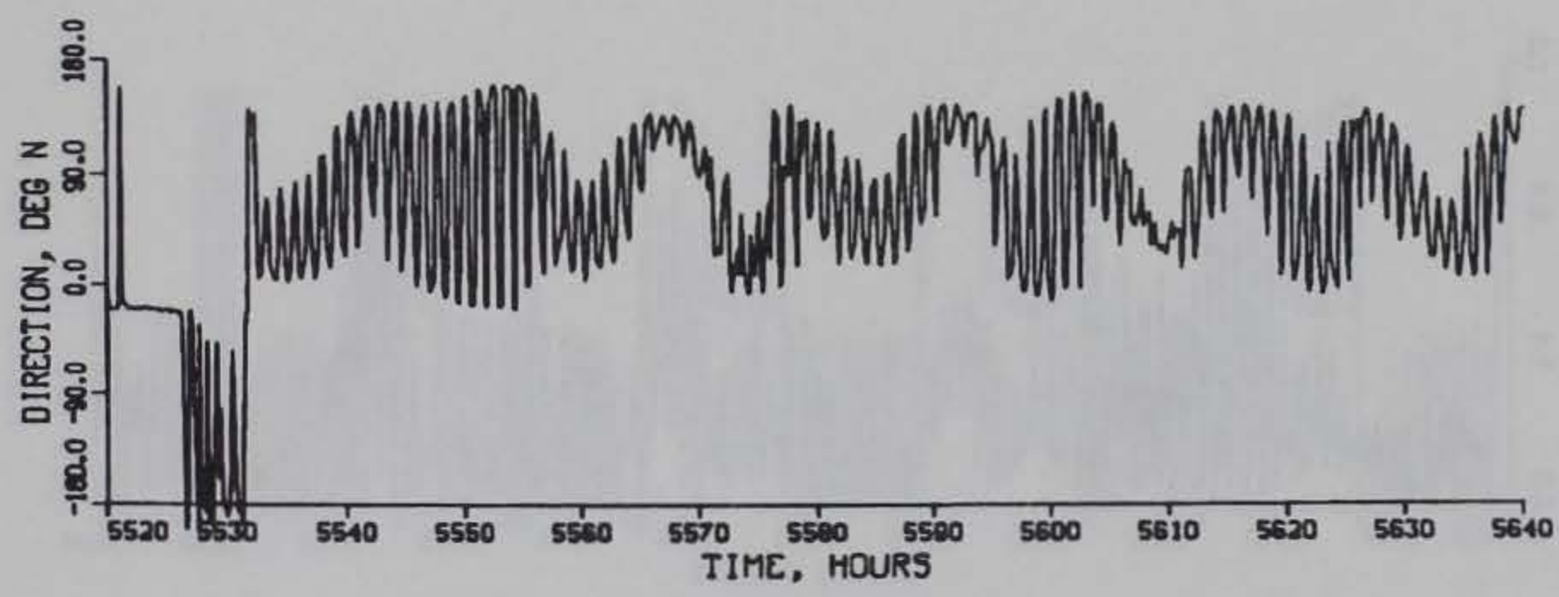

COMPUTED

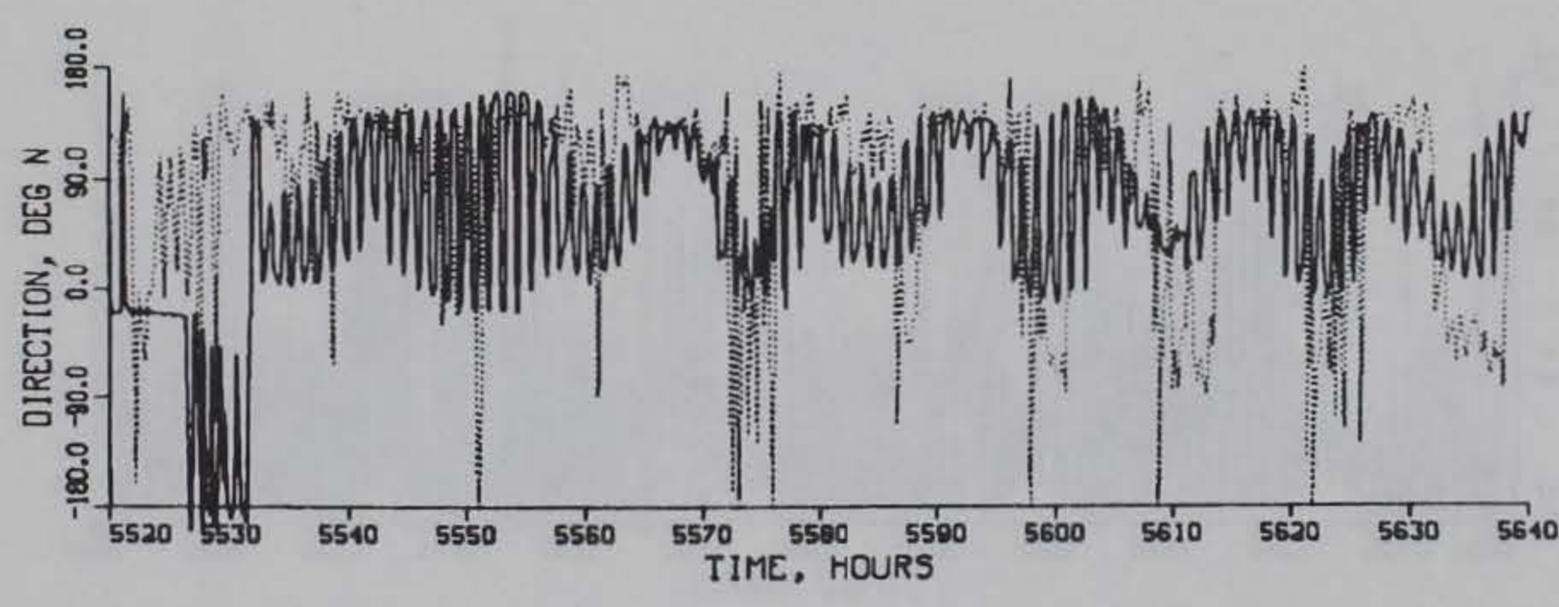

COMPUTED (SOLID) VS OBSERVED (DOTTED)

TIDAL VELOCITY

DIRECTION

VERIFICATION PERIOD

GAGE CM3

SURFACE

PLATE 30

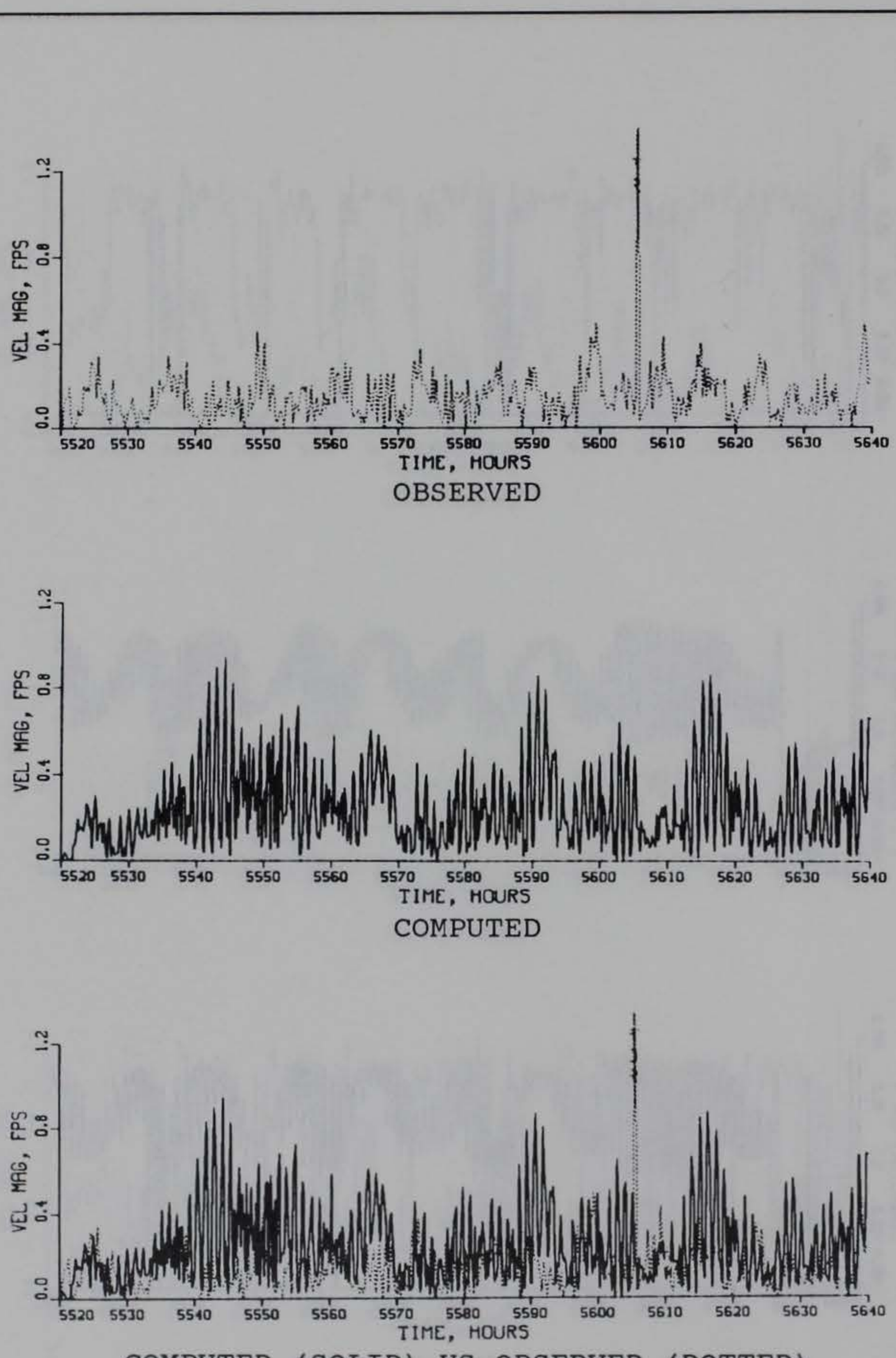

TIDAL VELOCITY

MAGNITUDE

VERIFICATION PERIOD

GAGE CM3

MID-DEPTH

PLATE 31

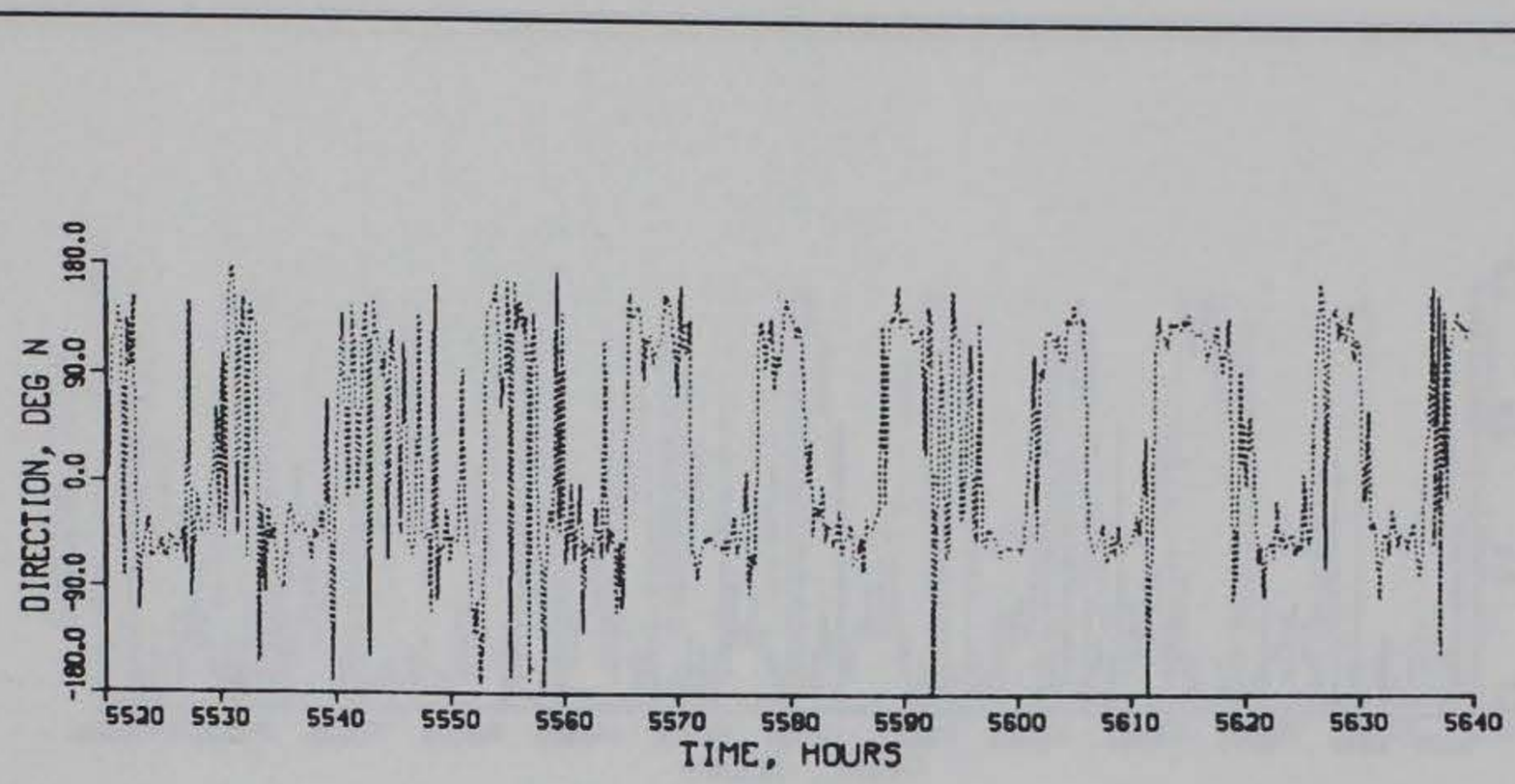

OBSERVED

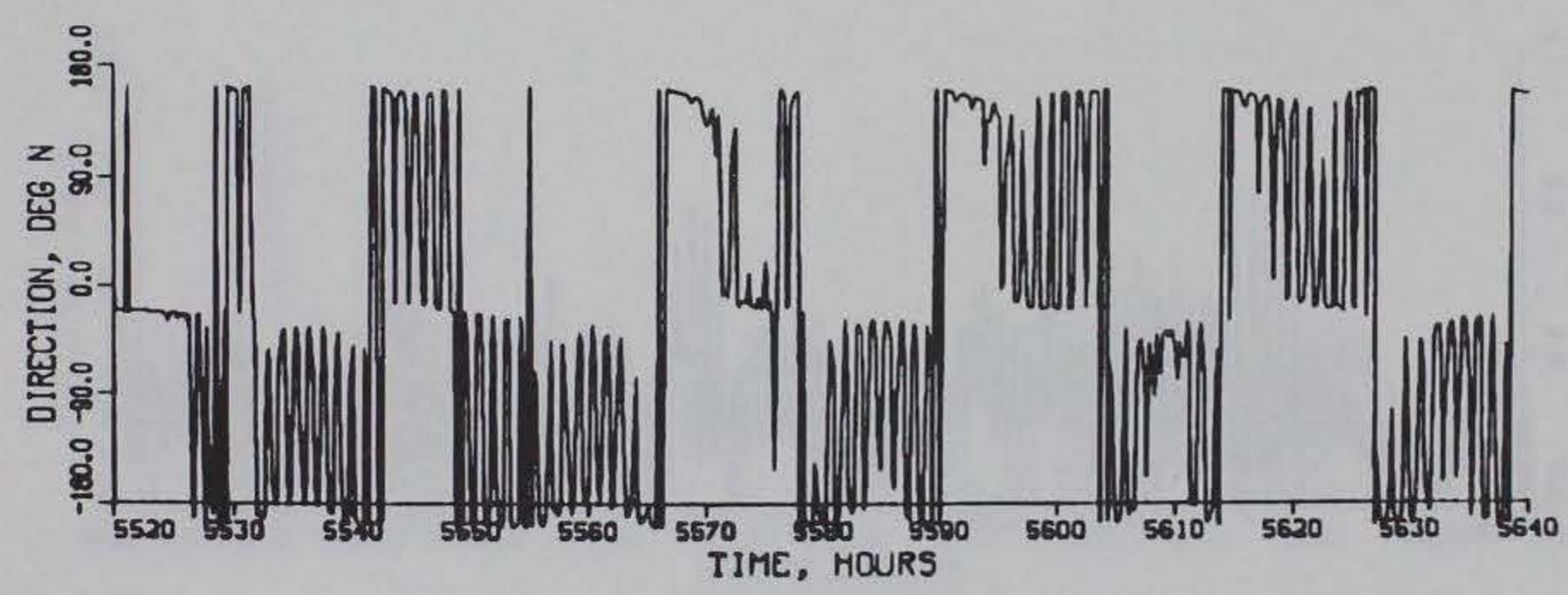

COMPUTED

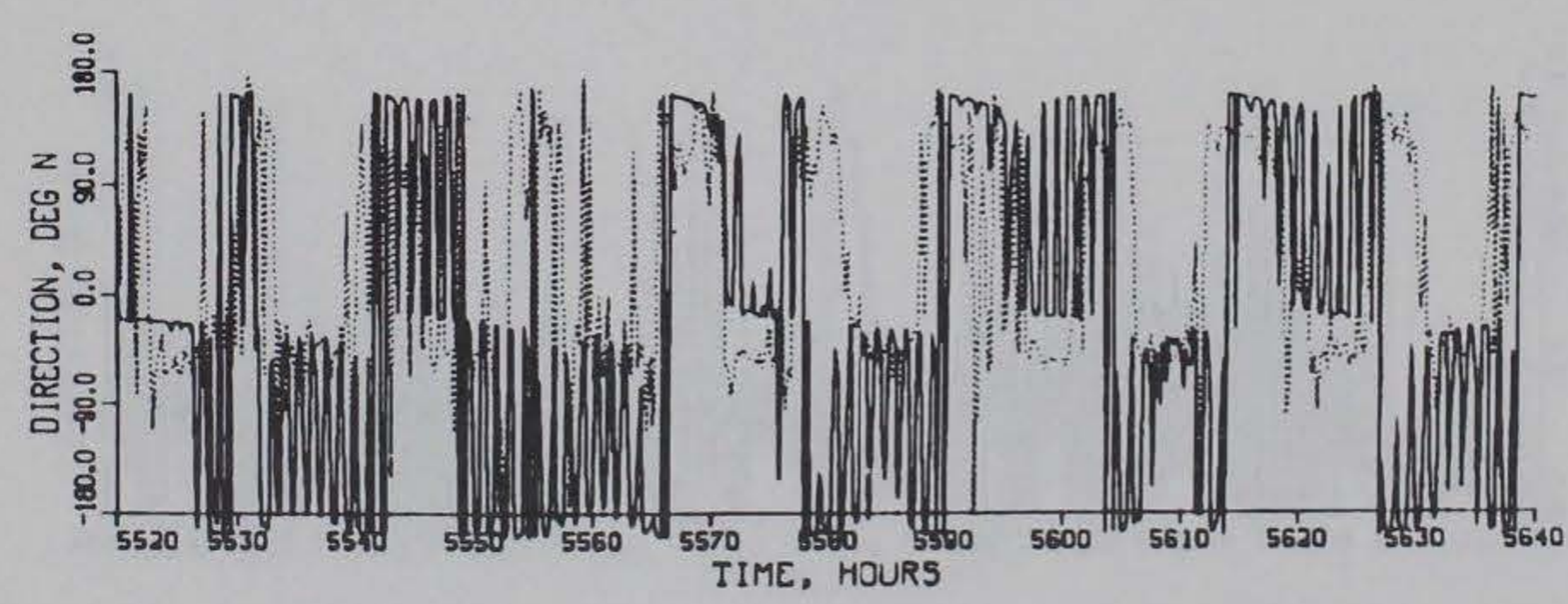

COMPUTED (SOLID) VS OBSERVED (DOTTED)

TIDAL VELOCITY **VERIFICATION PERIOD**

DIRECTION

GAGE CM3

MID-DEPTH

PLATE 32

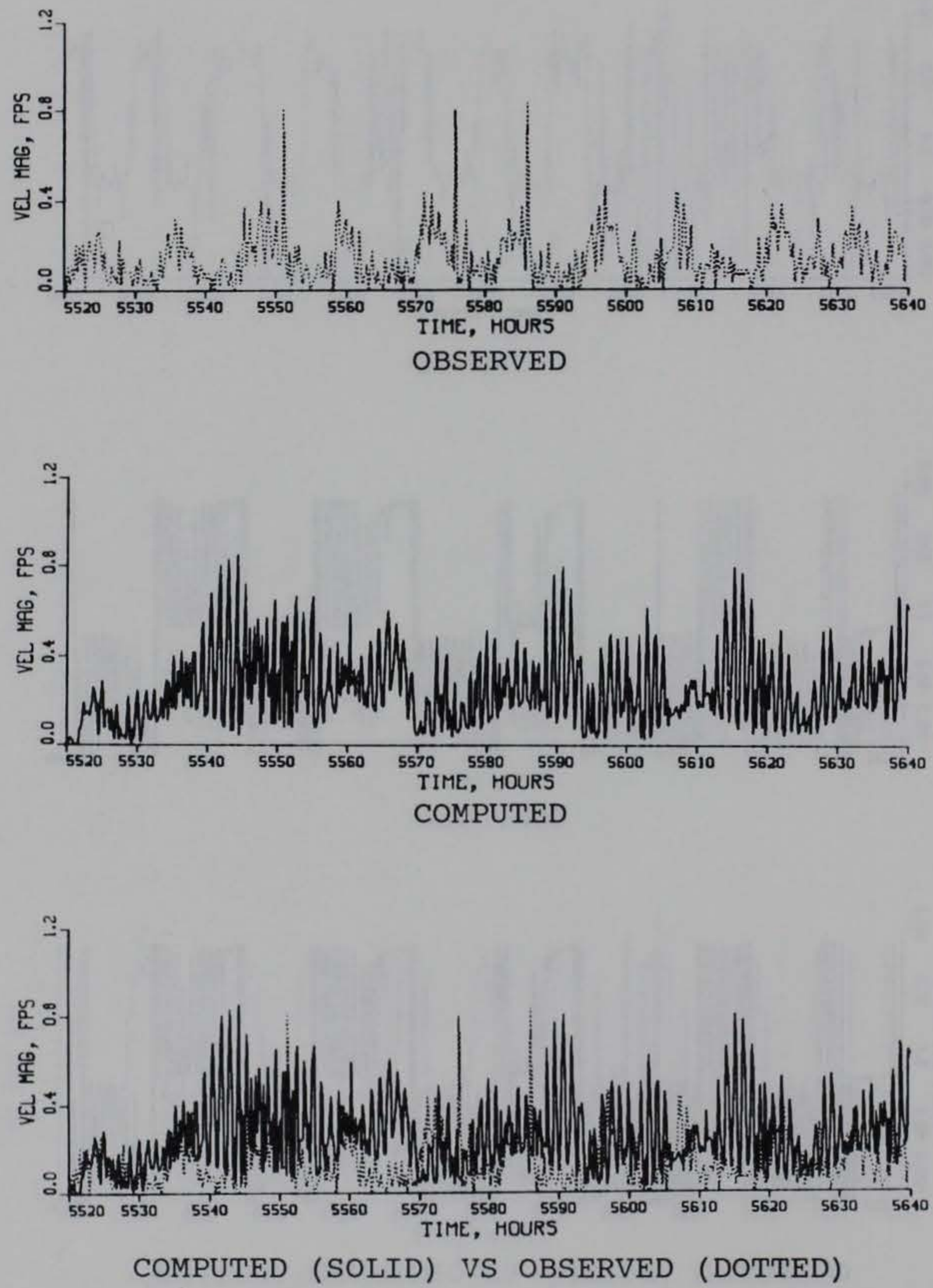

TIDAL VELOCITY

MAGNITUDE

VERIFICATION PERIOD

GAGE CM3

BOTTOM

PLATE 33

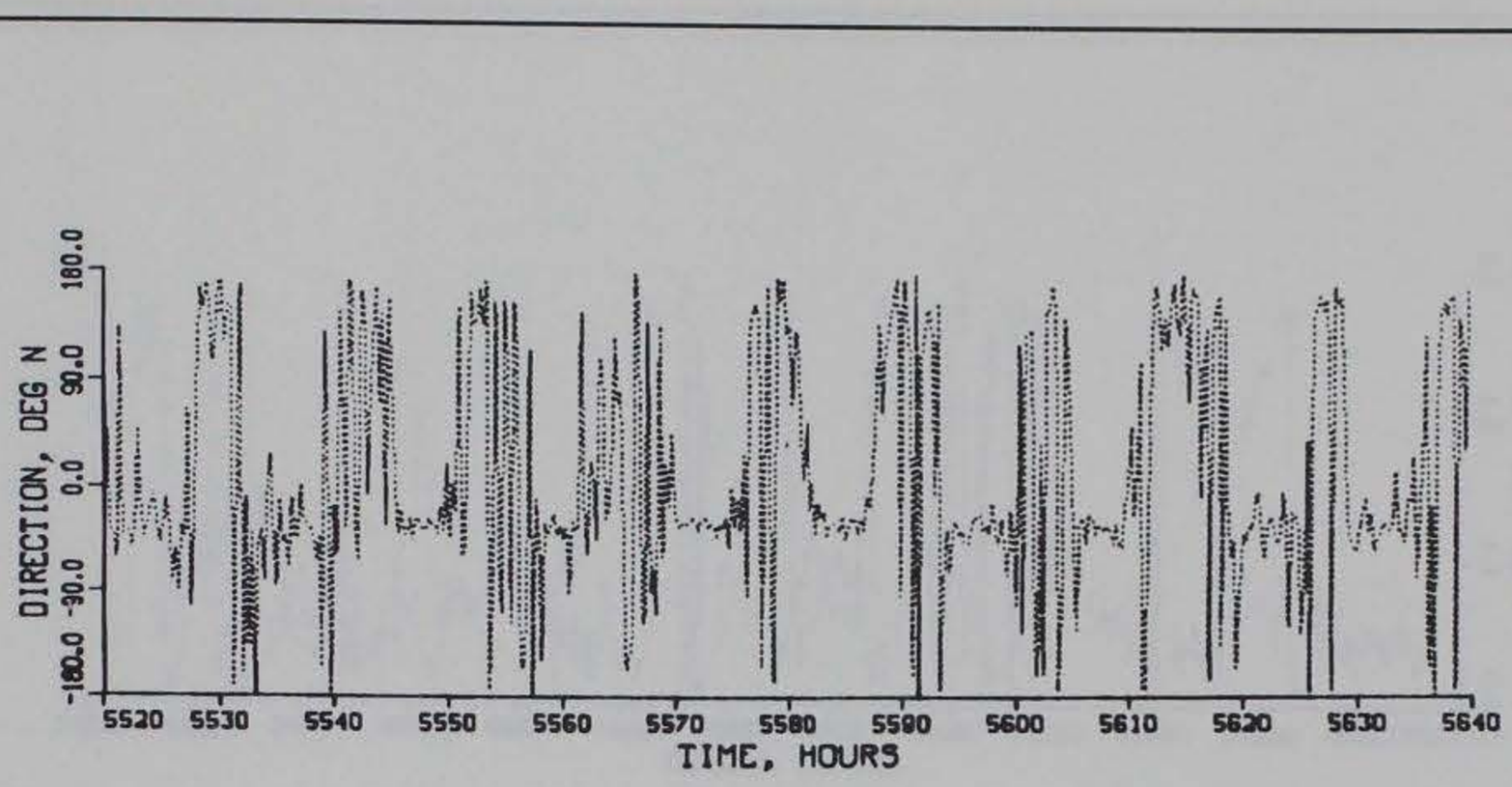

OBSERVED

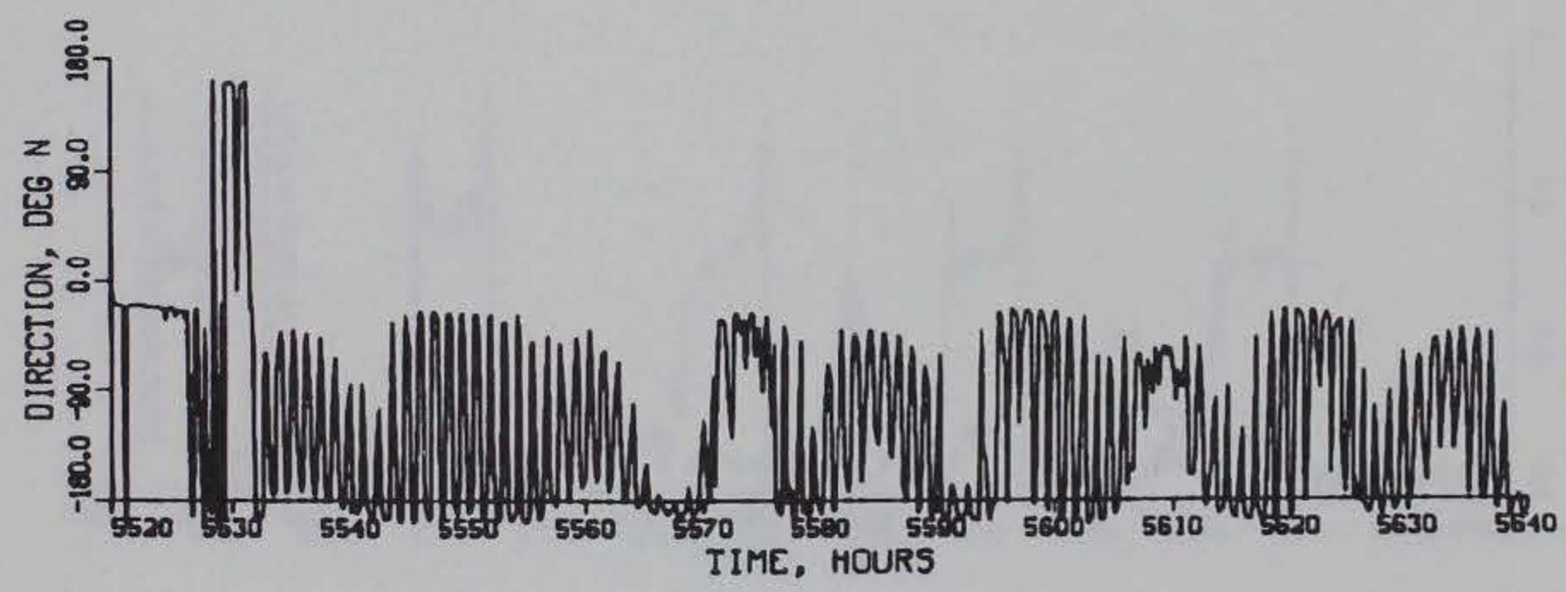

COMPUTED

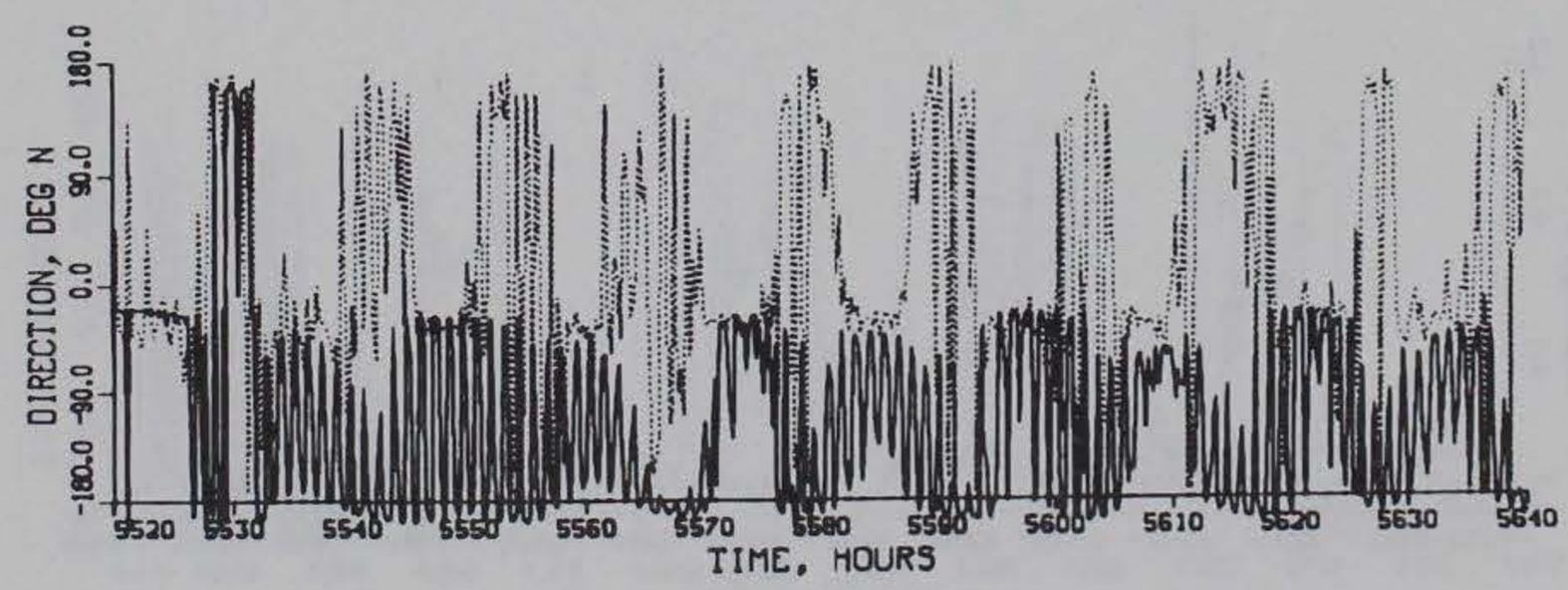

COMPUTED (SOLID) VS OBSERVED (DOTTED)

TIDAL VELOCITY

DIRECTION

VERIFICATION PERIOD

GAGE CM3

BOTTOM

PLATE 34

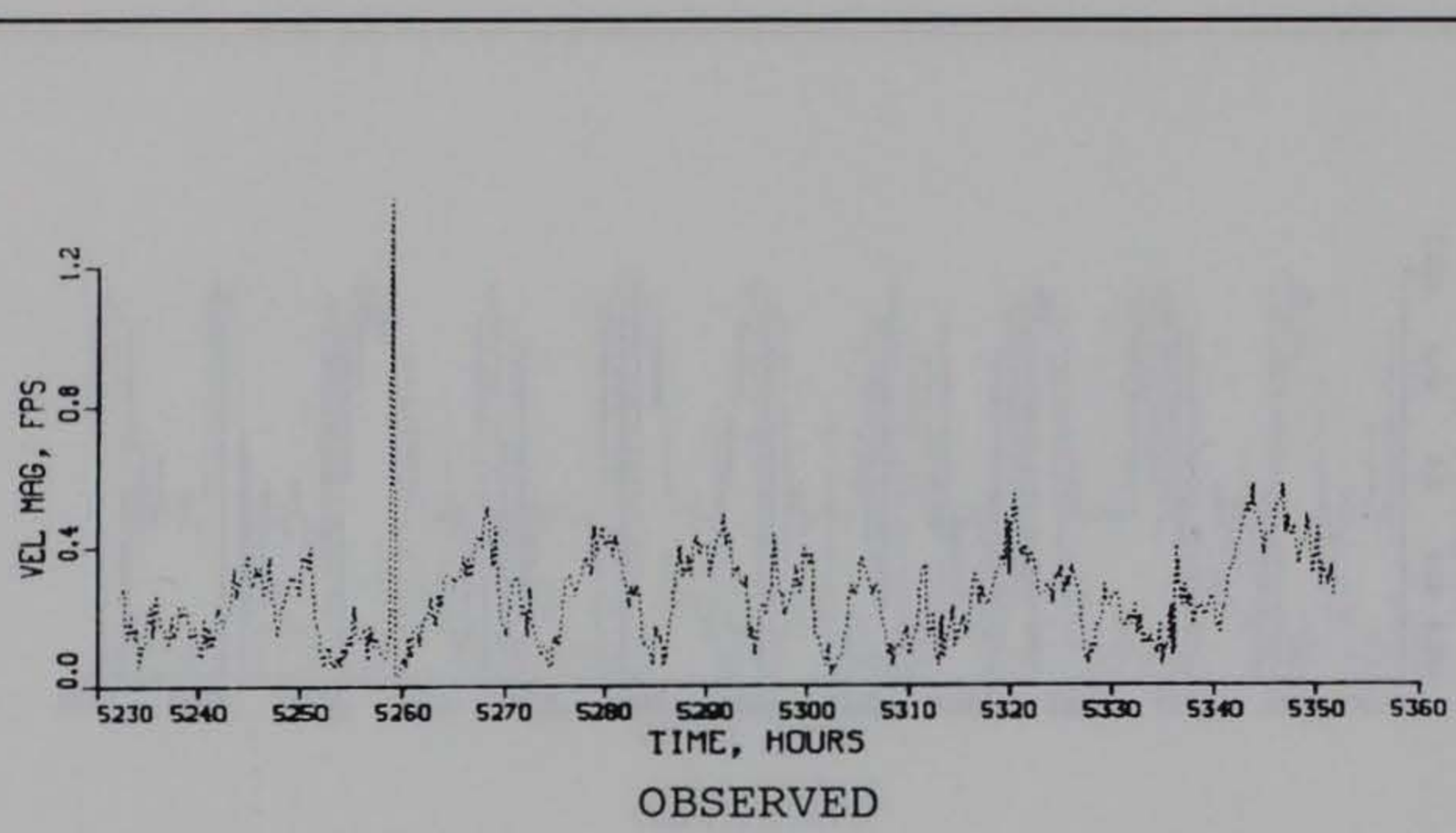

OBSERVED

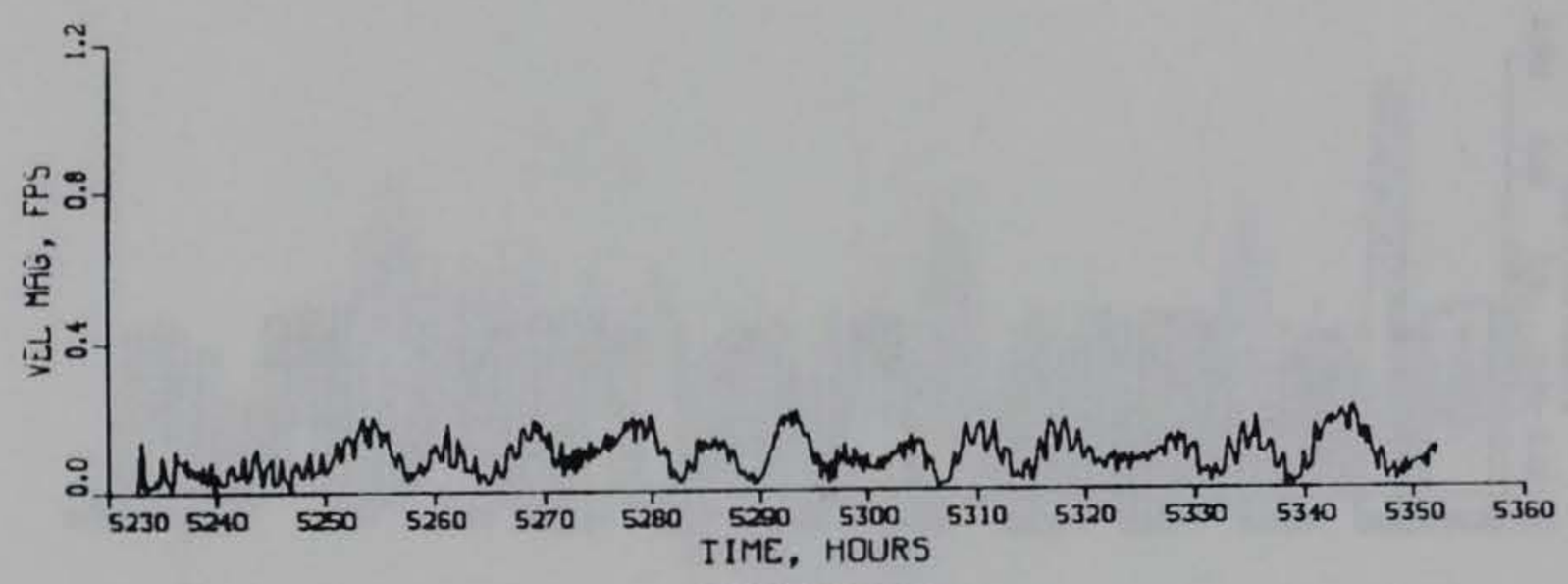

COMPUTED

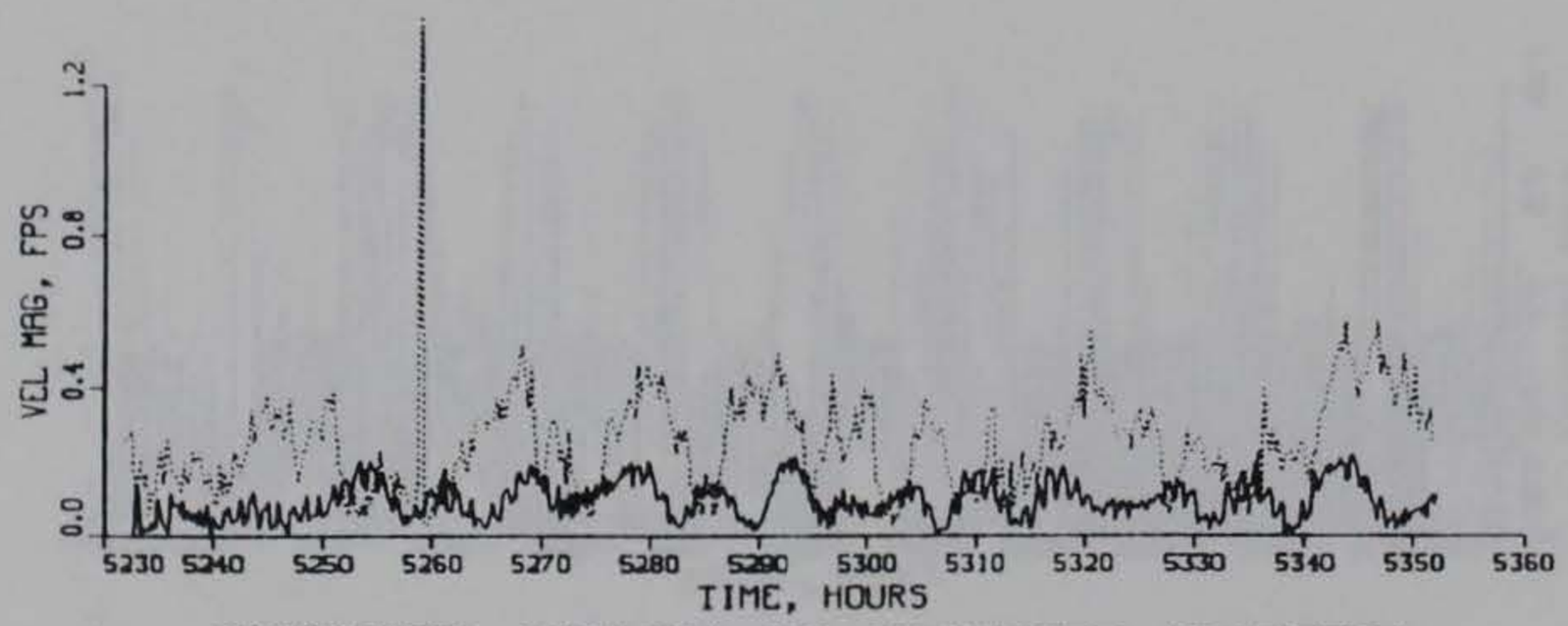

COMPUTED (SOLID) VS OBSERVED (DOTTED)

TIDAL VELOCITY

MAGNITUDE

CALIBRATION PERIOD

GAGE CM4

BOTTOM

PLATE 35

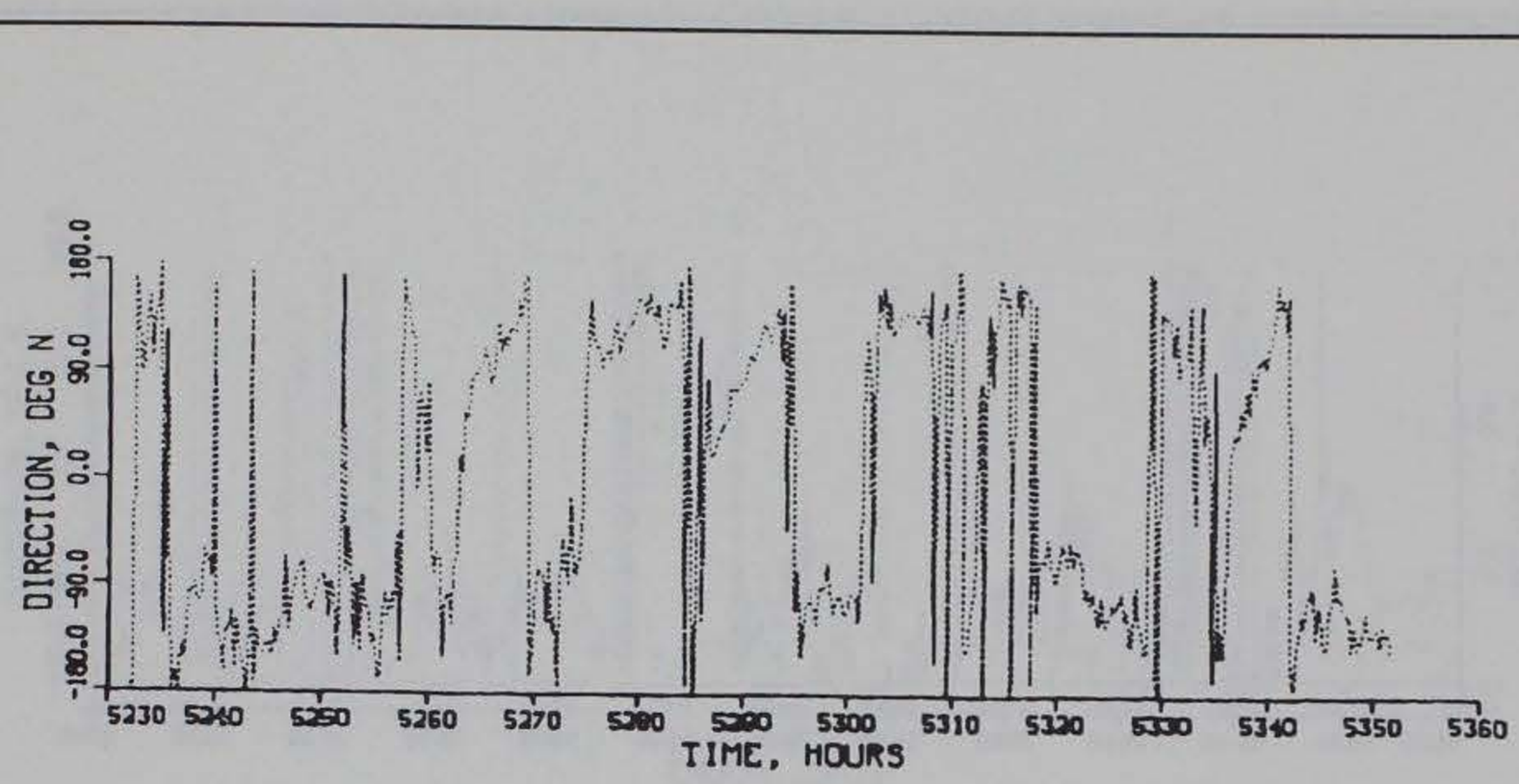

OBSERVED

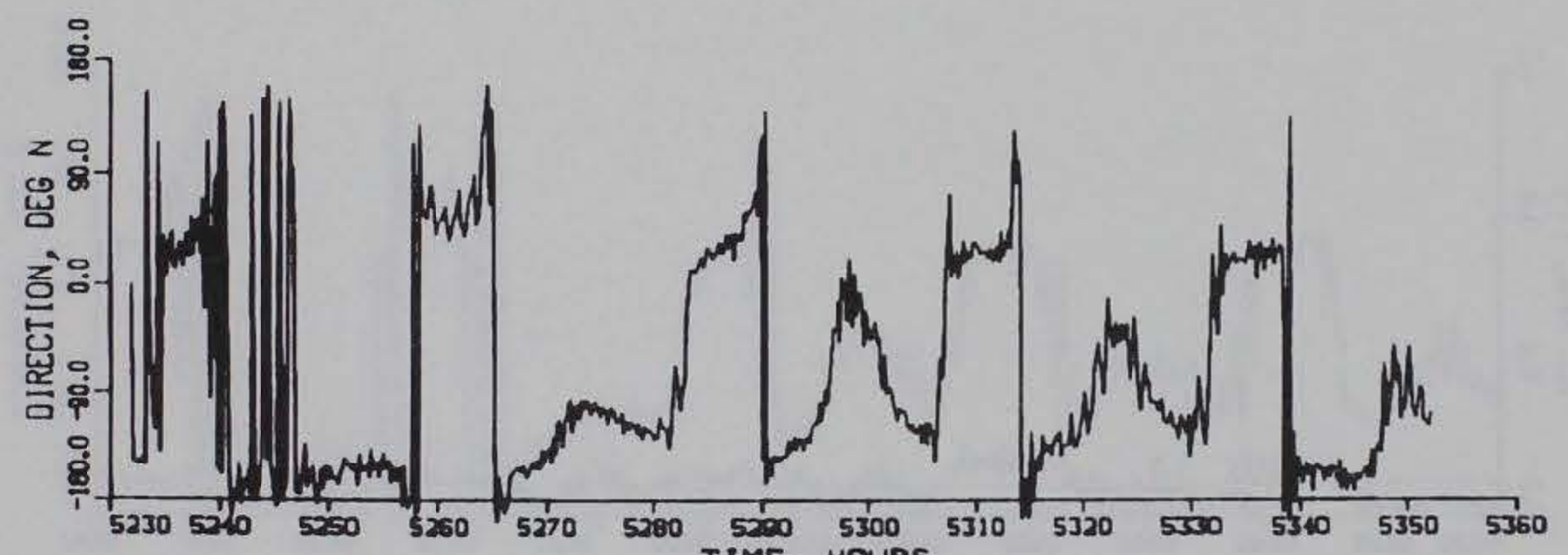

COMPUTED

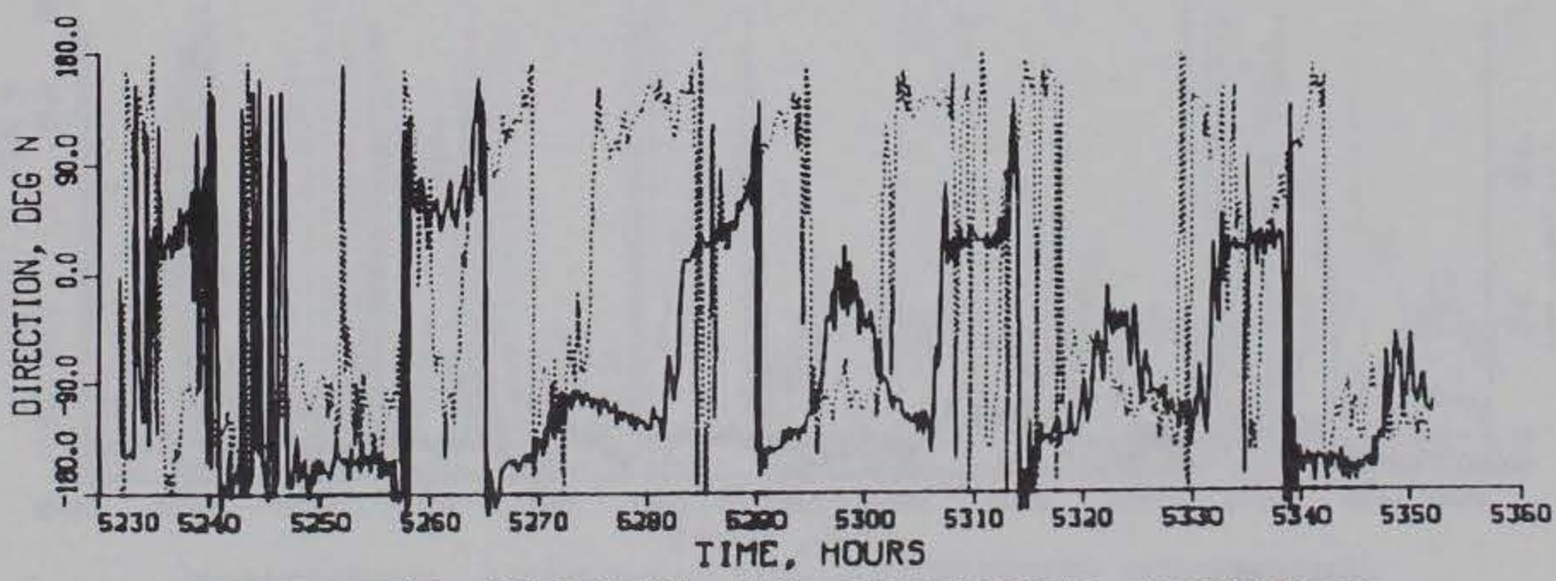

COMPUTED (SOLID) VS OBSERVED (DOTTED)

TIDAL VELOCITY

DIRECTION

CALIBRATION PERIOD

GAGE CM4

BOTTOM

PLATE 36

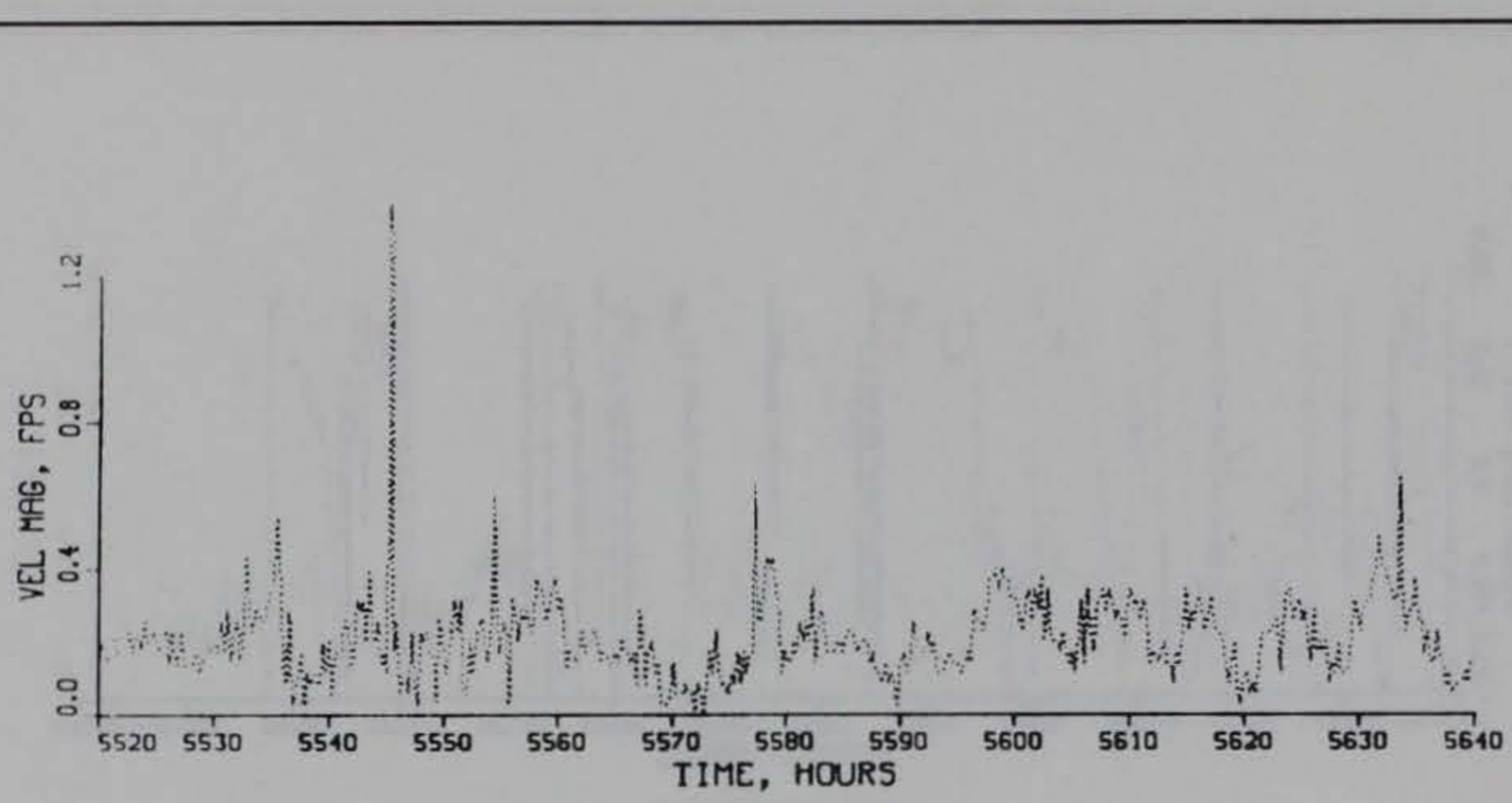

OBSERVED

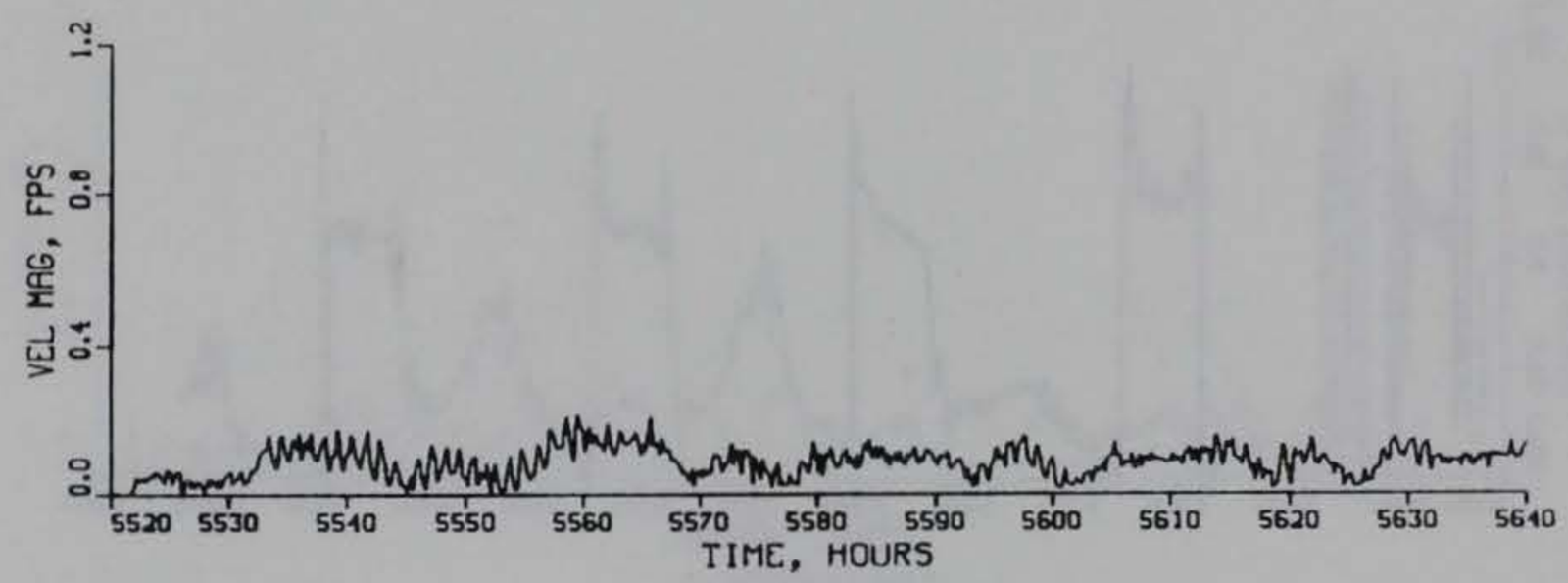

COMPUTED

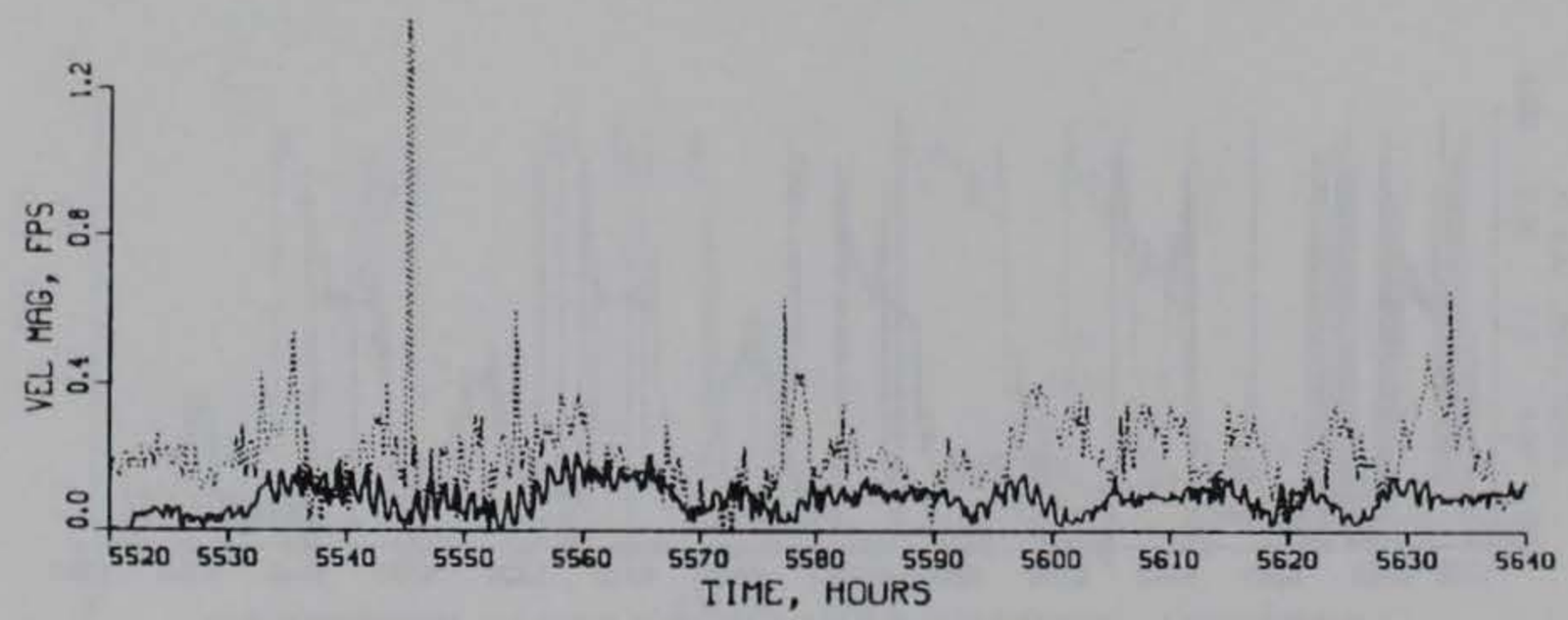

COMPUTED (SOLID) VS OBSERVED (DOTTED)

TIDAL VELOCITY

MAGNITUDE

VERIFICATION PERIOD

GAGE CM4

BOTTOM

PLATE 37

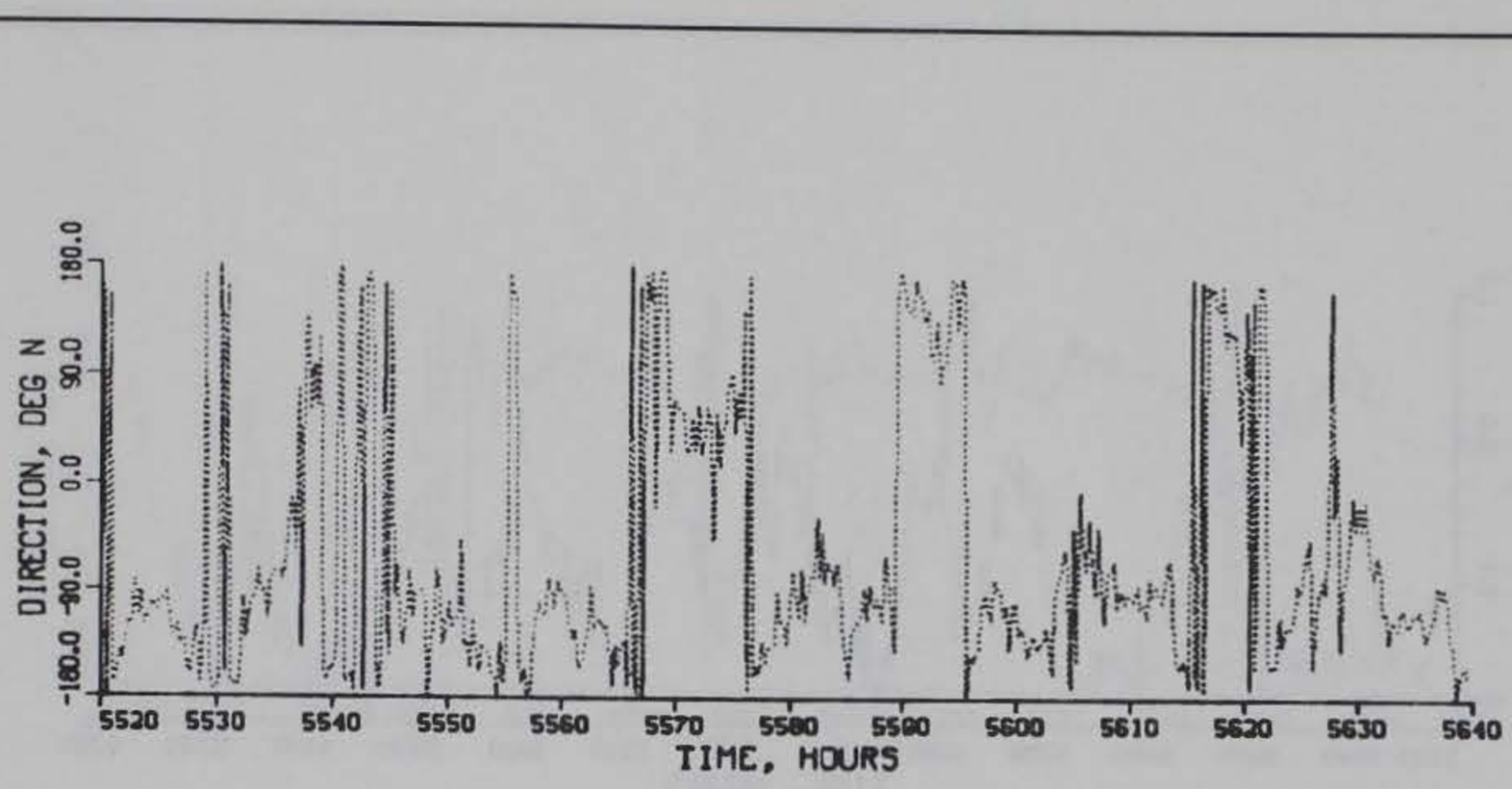

OBSERVED

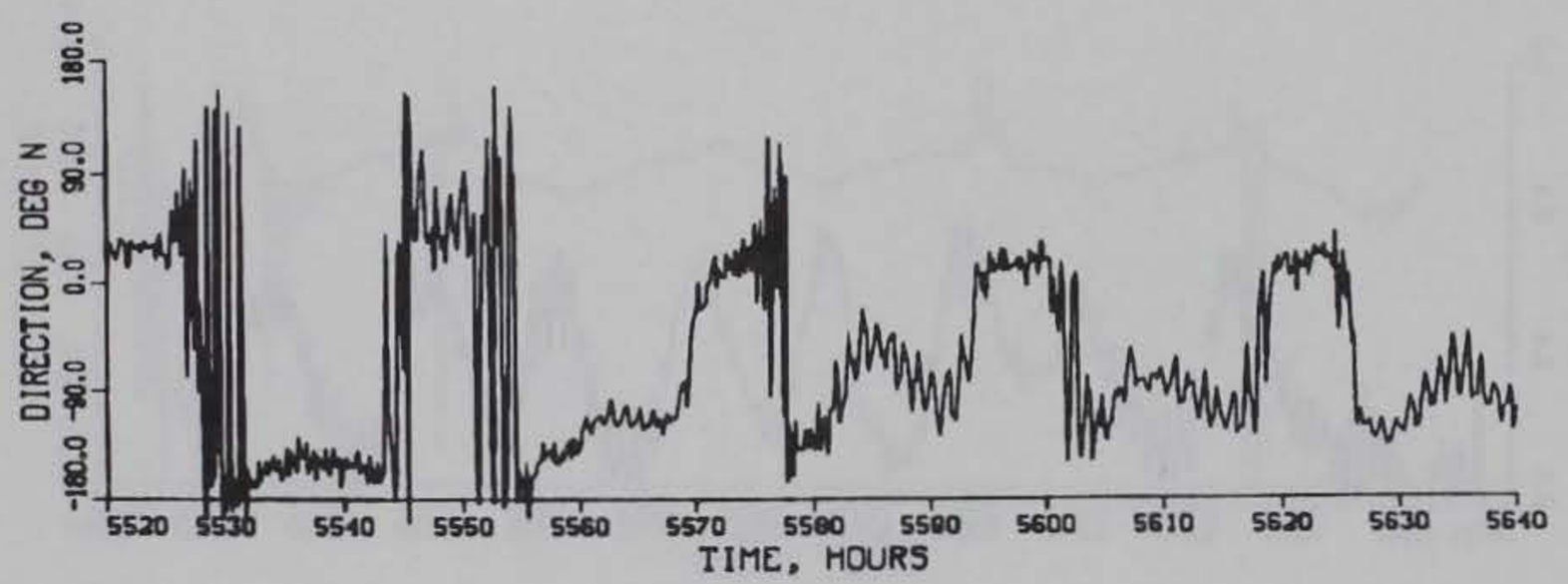

COMPUTED

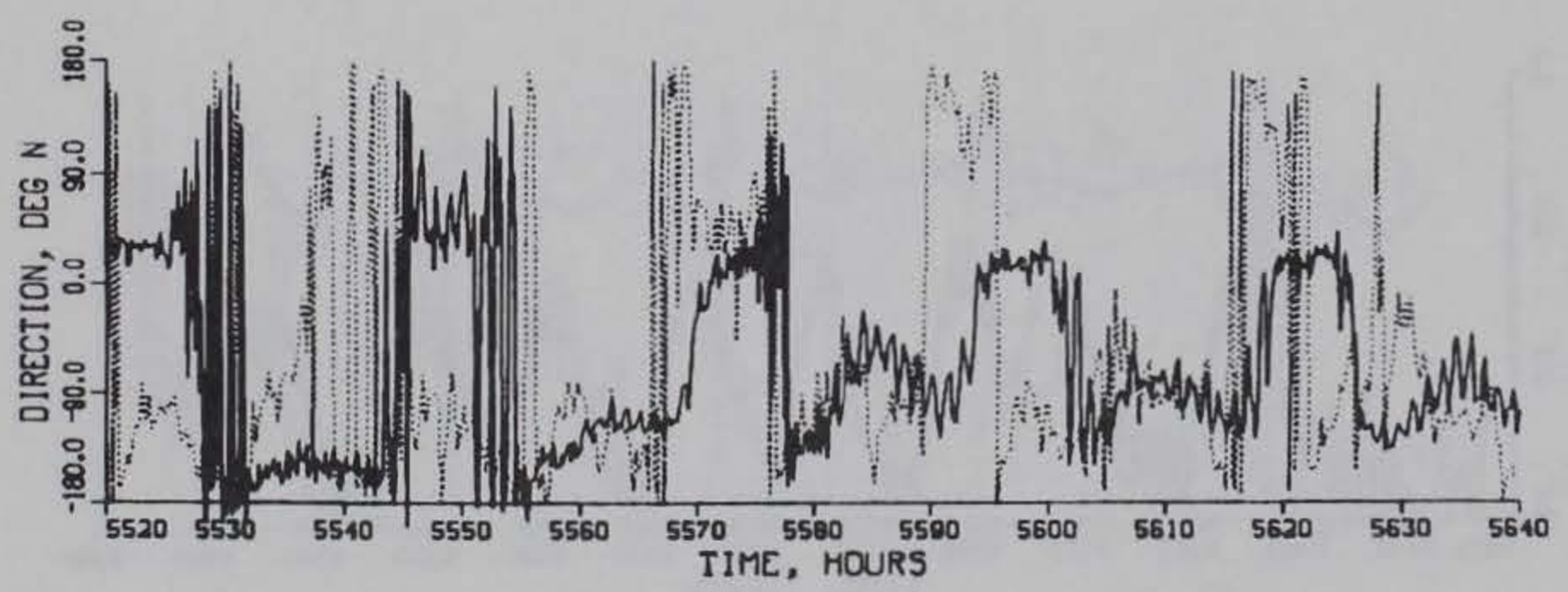

COMPUTED (SOLID) VS OBSERVED (DOTTED)

TIDAL VELOCITY

DIRECTION

VERIFICATION PERIOD

GAGE CM4

BOTTOM

PLATE 38

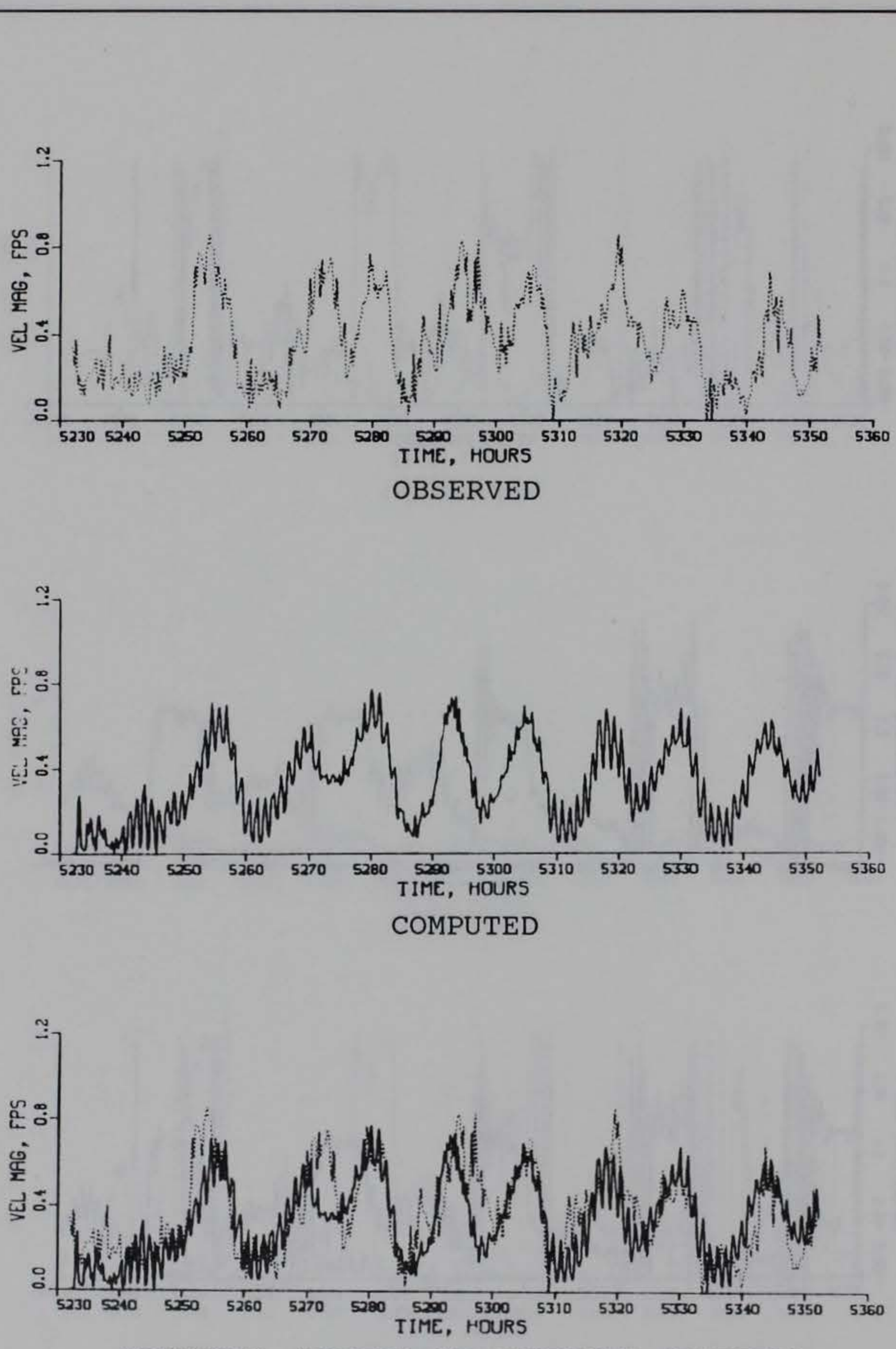

TIDAL VELOCITY

MAGNITUDE

CALIBRATION PERIOD

GAGE CM6

SURFACE

PLATE 39

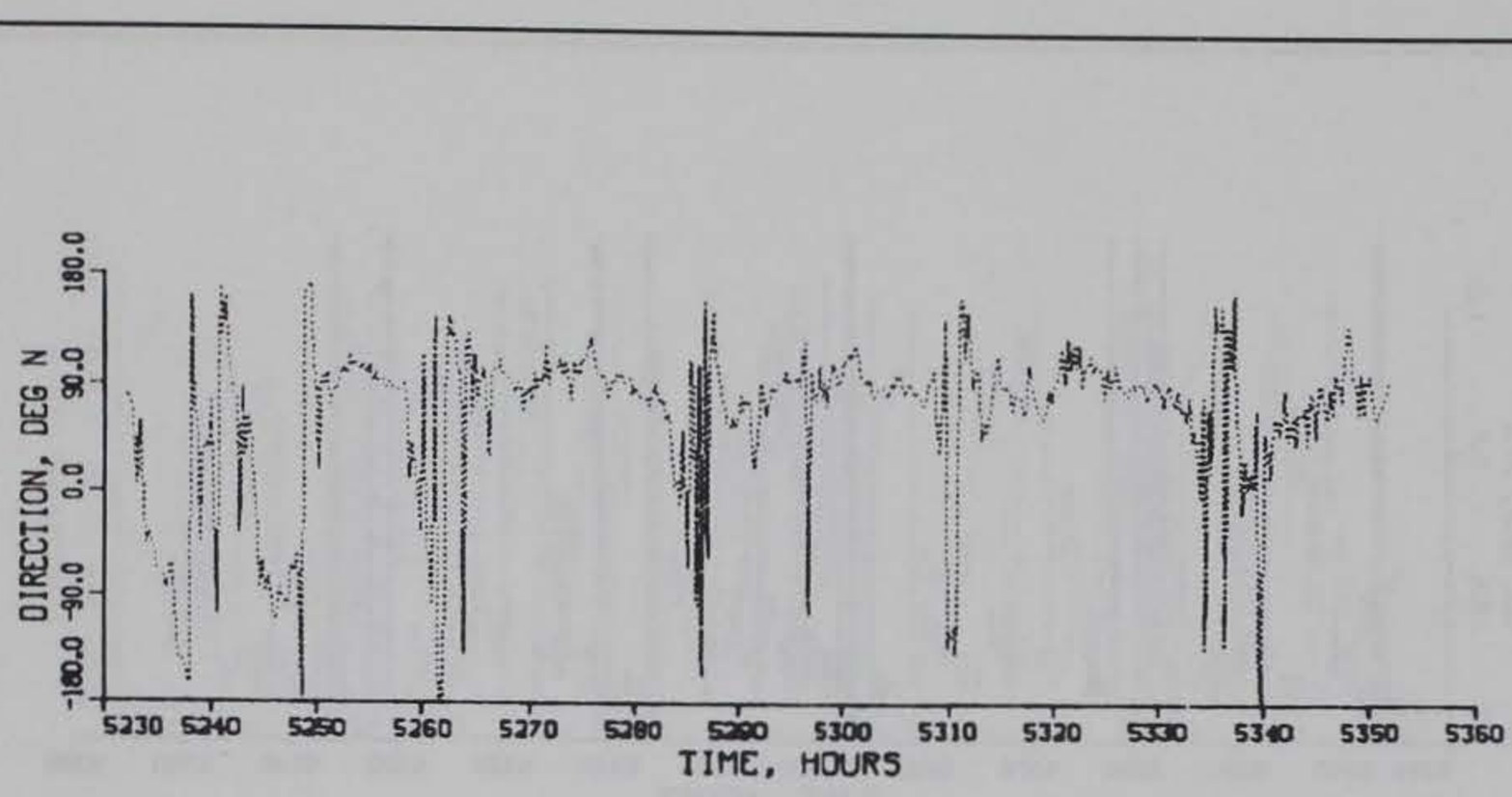

OBSERVED

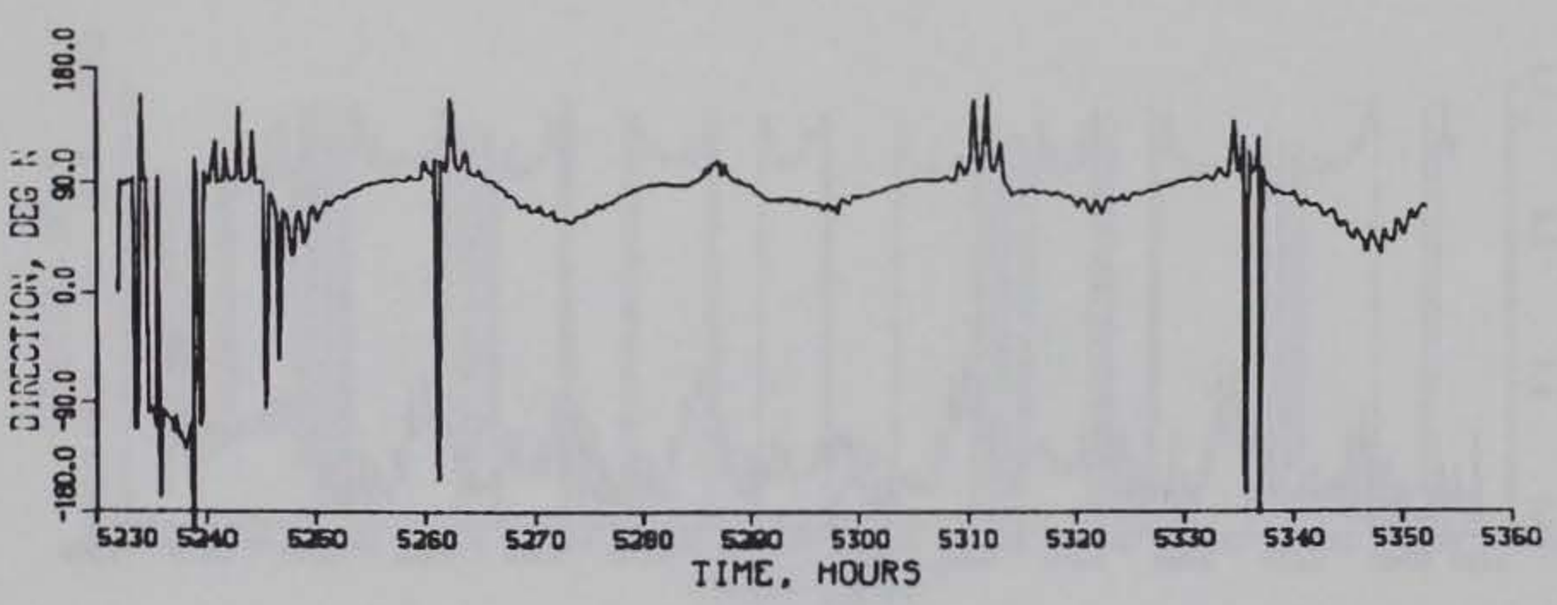

COMPUTED

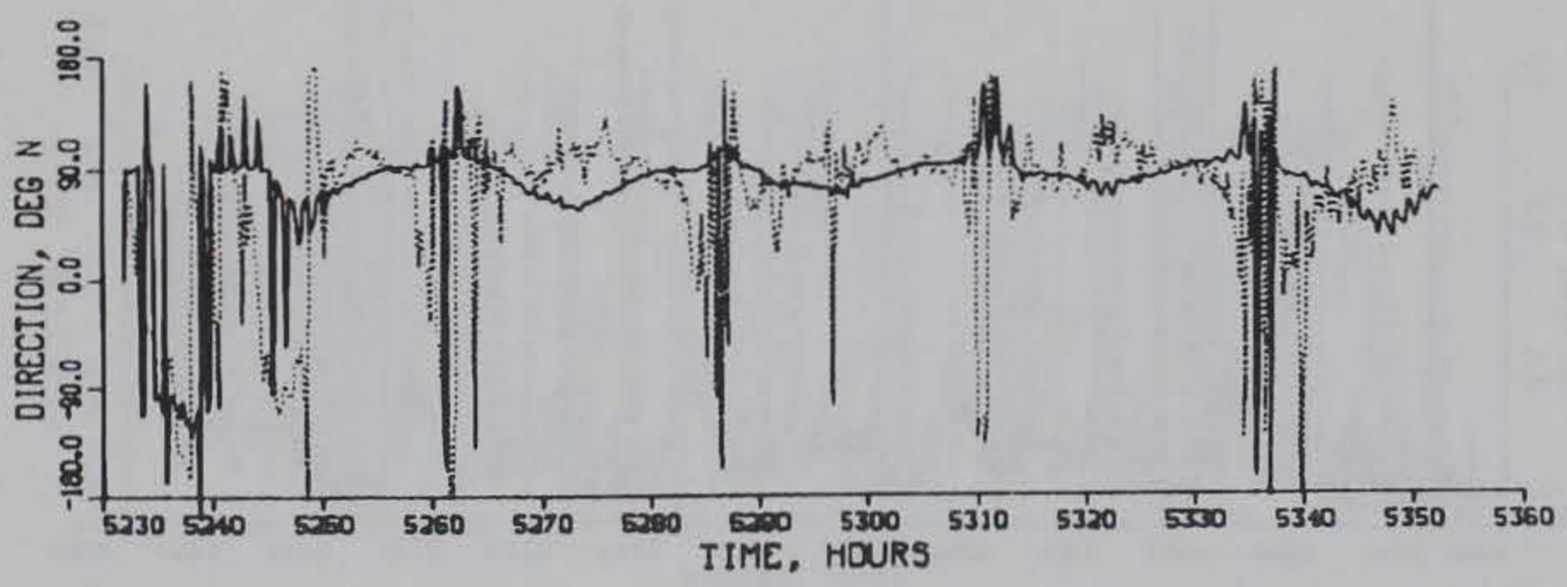

COMPUTED (SOLID) VS OBSERVED (DOTTED)

TIDAL VELOCITY

DIRECTION

CALIBRATION PERIOD

GAGE CM6

SURFACE

PLATE 40

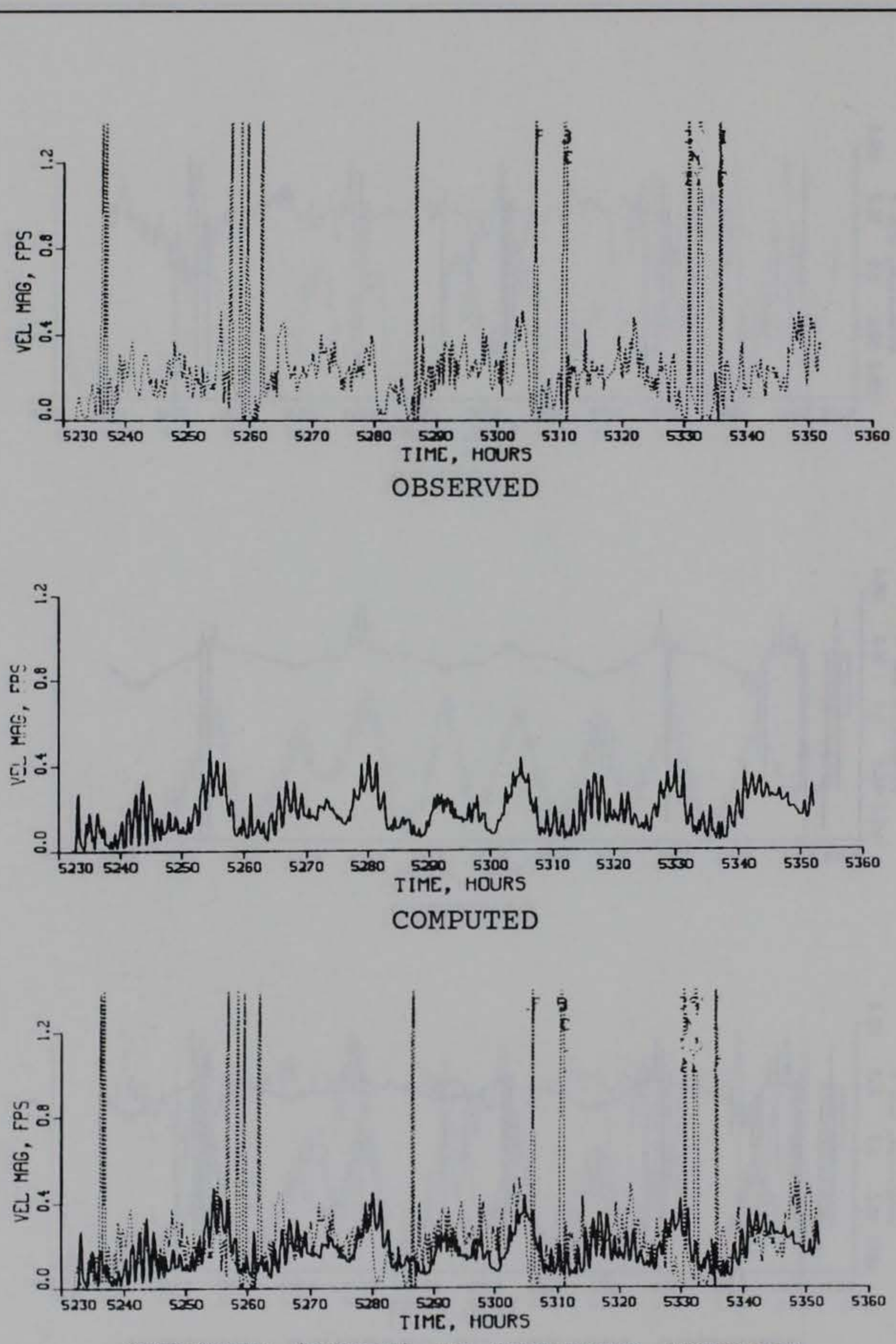

OBSERVED

COMPUTED

COMPUTED (SOLID) VS OBSERVED (DOTTED)

TIDAL VELOCITY

MAGNITUDE

CALIBRATION PERIOD

GAGE CM6

BOTTOM

PLATE 41

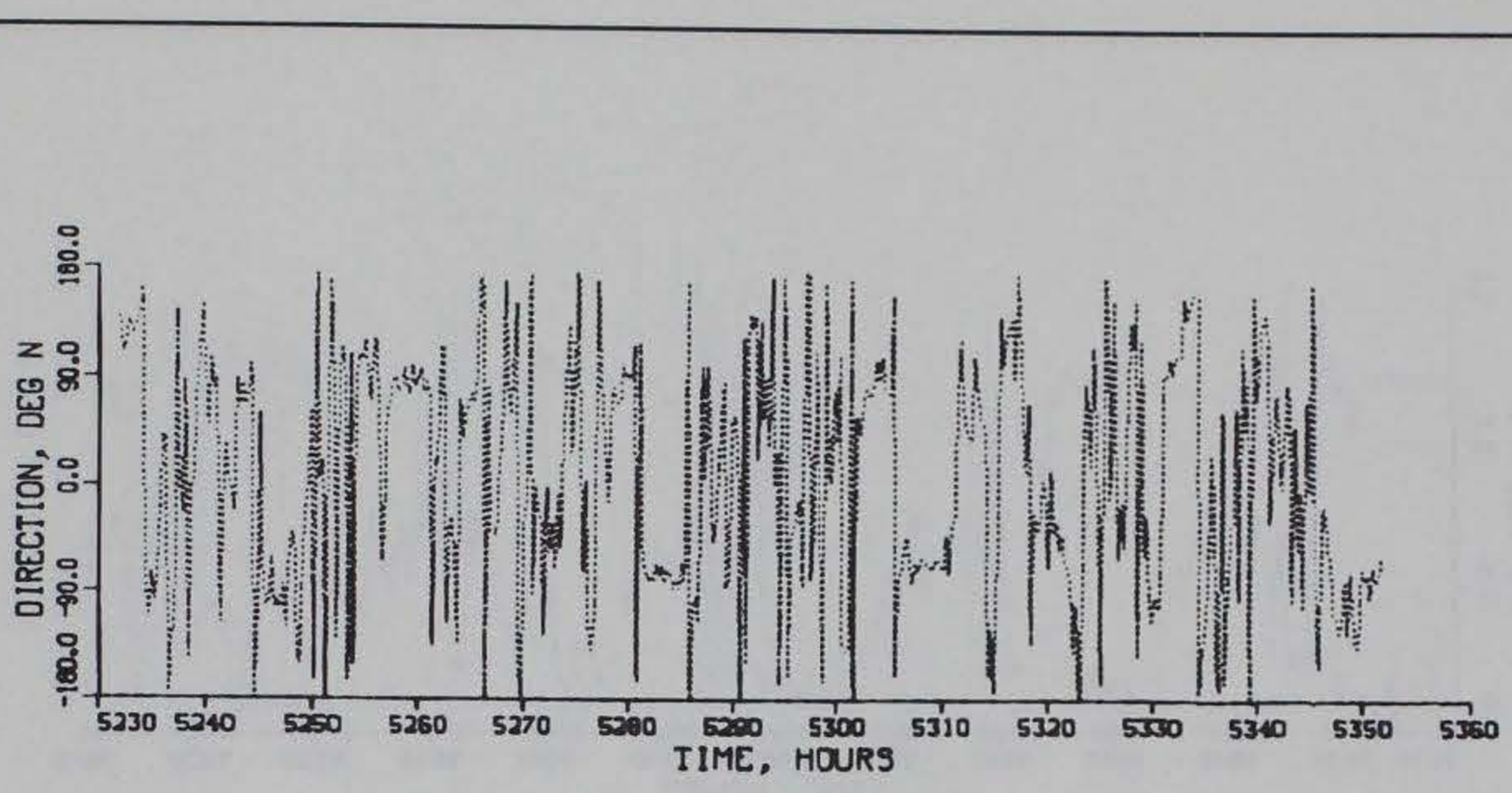

OBSERVED

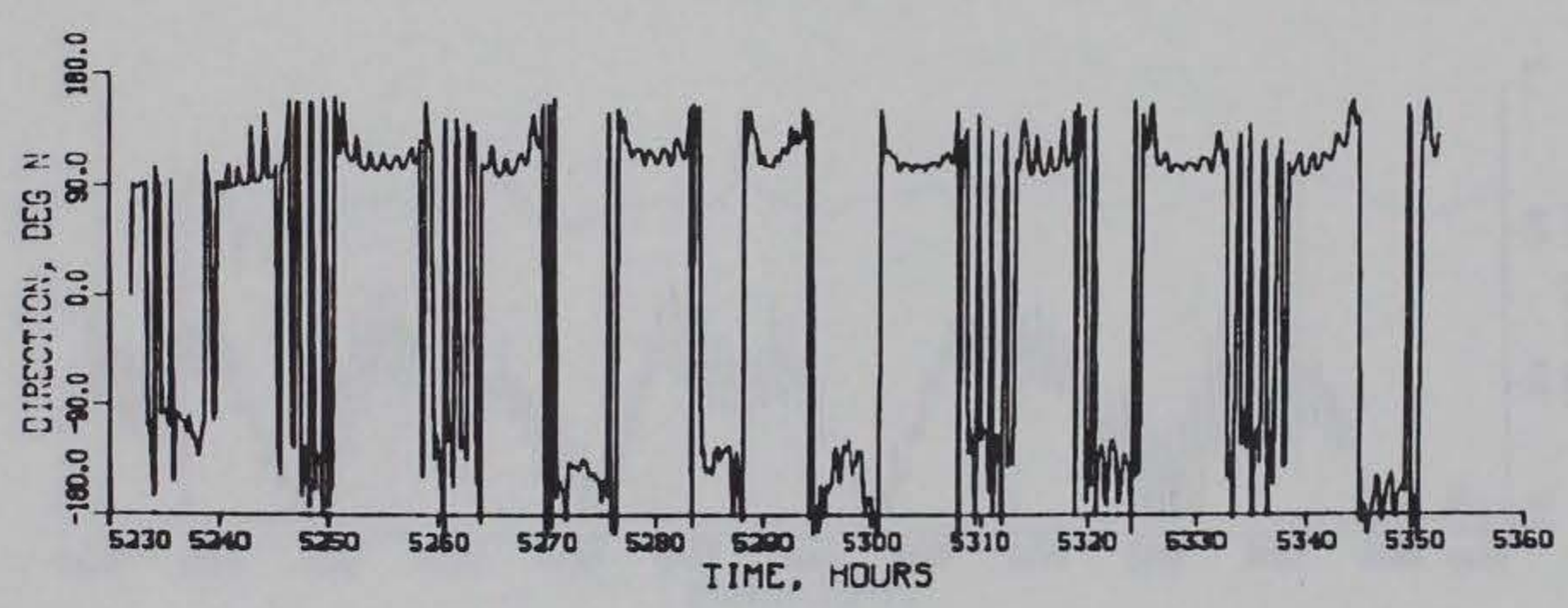

COMPUTED

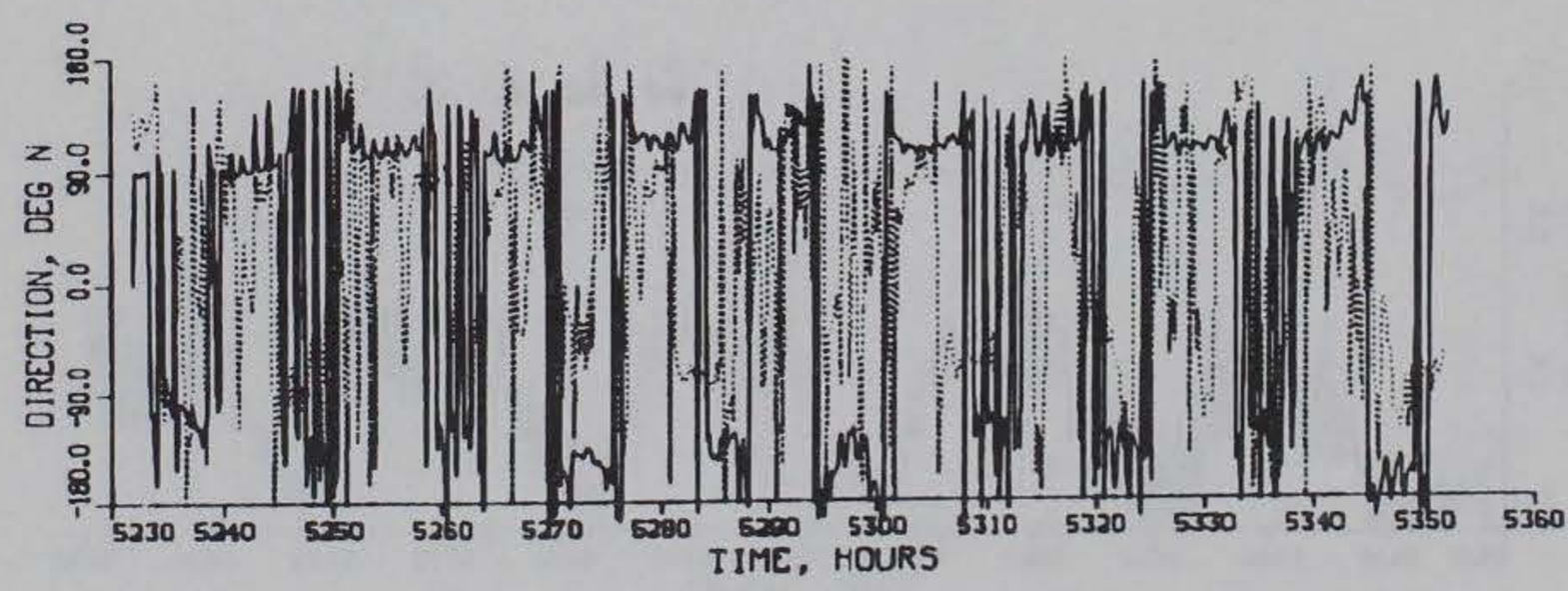

COMPUTED (SOLID) VS OBSERVED (DOTTED)

TIDAL VELOCITY

DIRECTION

CALIBRATION PERIOD

GAGE CM6

BOTTOM

PLATE 42

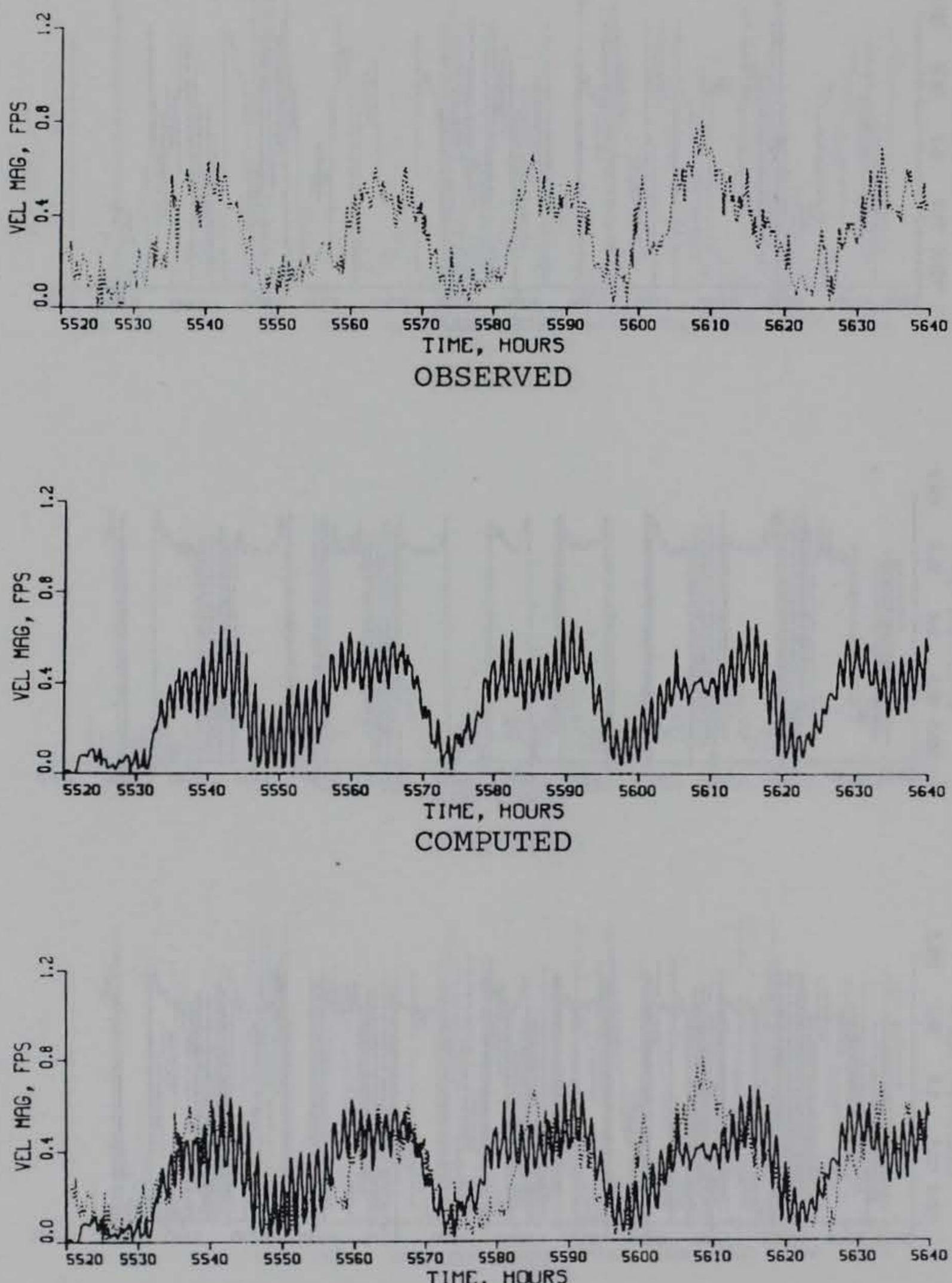

TIDAL VELOCITY

MAGNITUDE

VERIFICATION PERIOD

GAGE CM6

SURFACE

PLATE 43

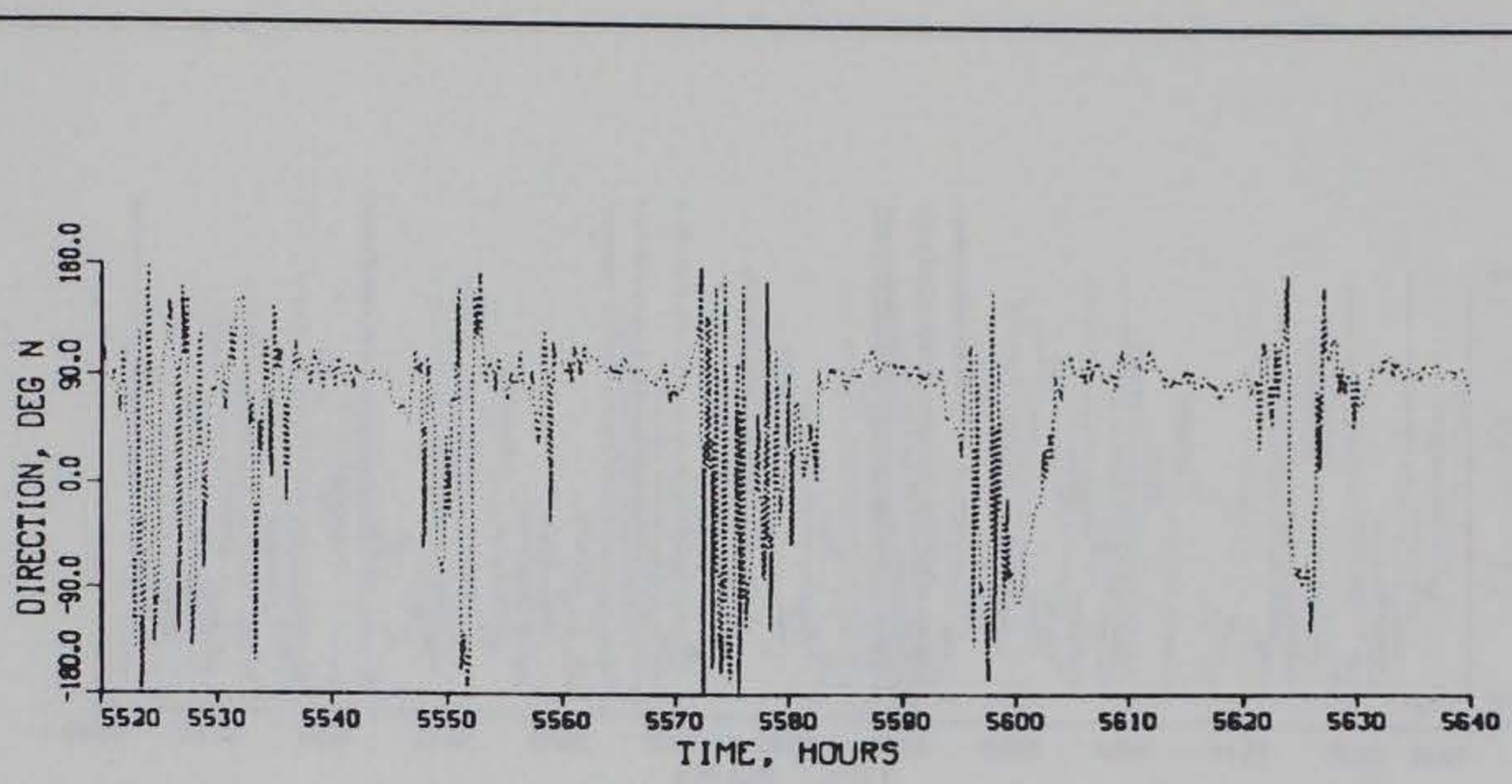

OBSERVED

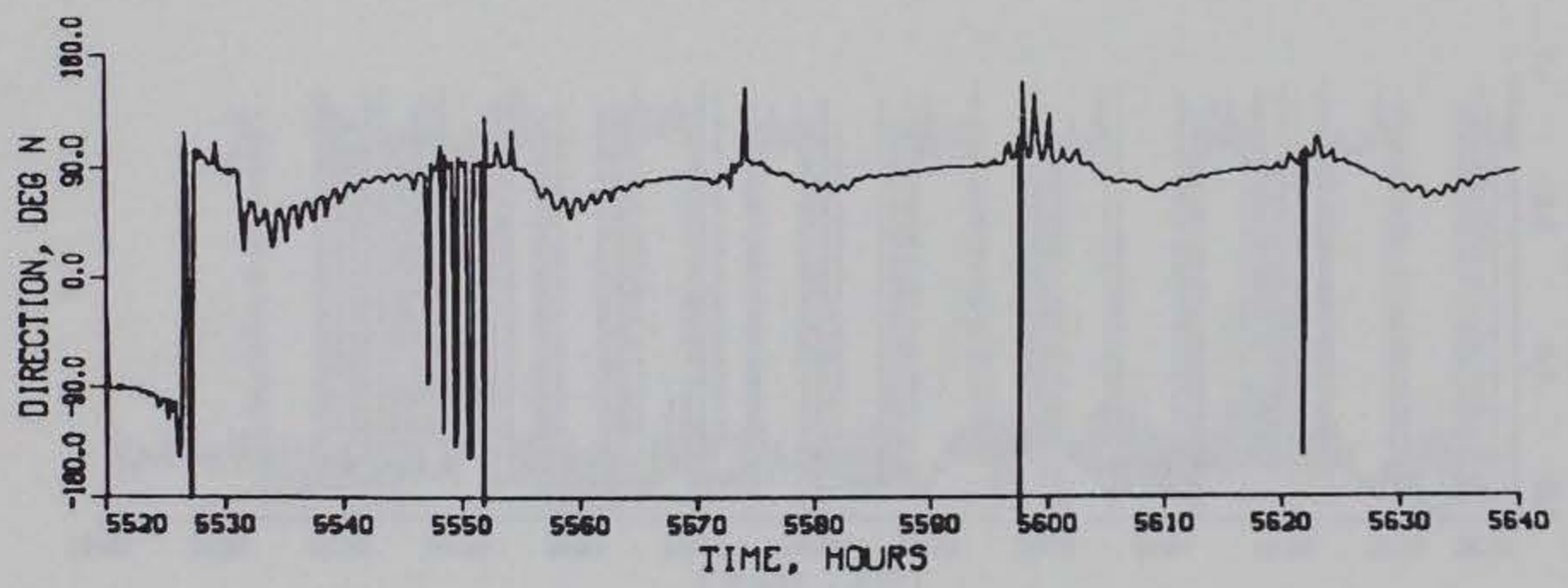

COMPUTED

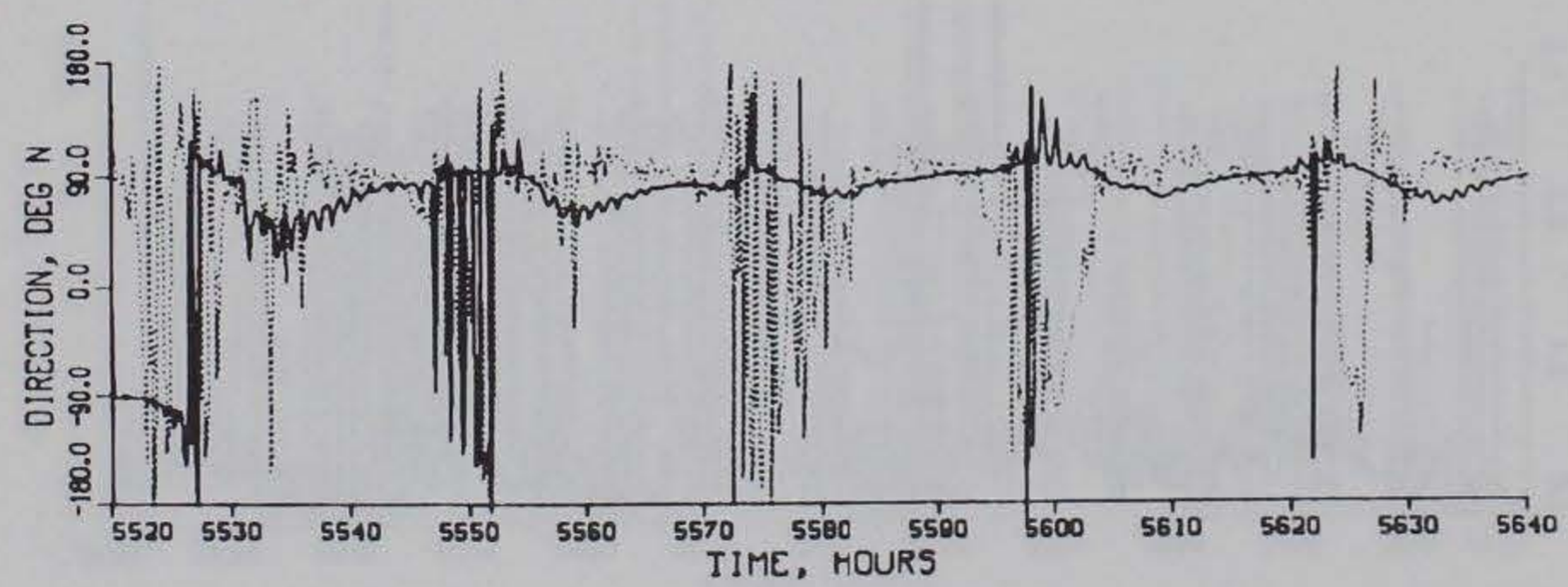

COMPUTED (SOLID) VS OBSERVED (DOTTED)

TIDAL VELOCITY

DIRECTION

VERIFICATION PERIOD

GAGE CM6

SURFACE

PLATE 44

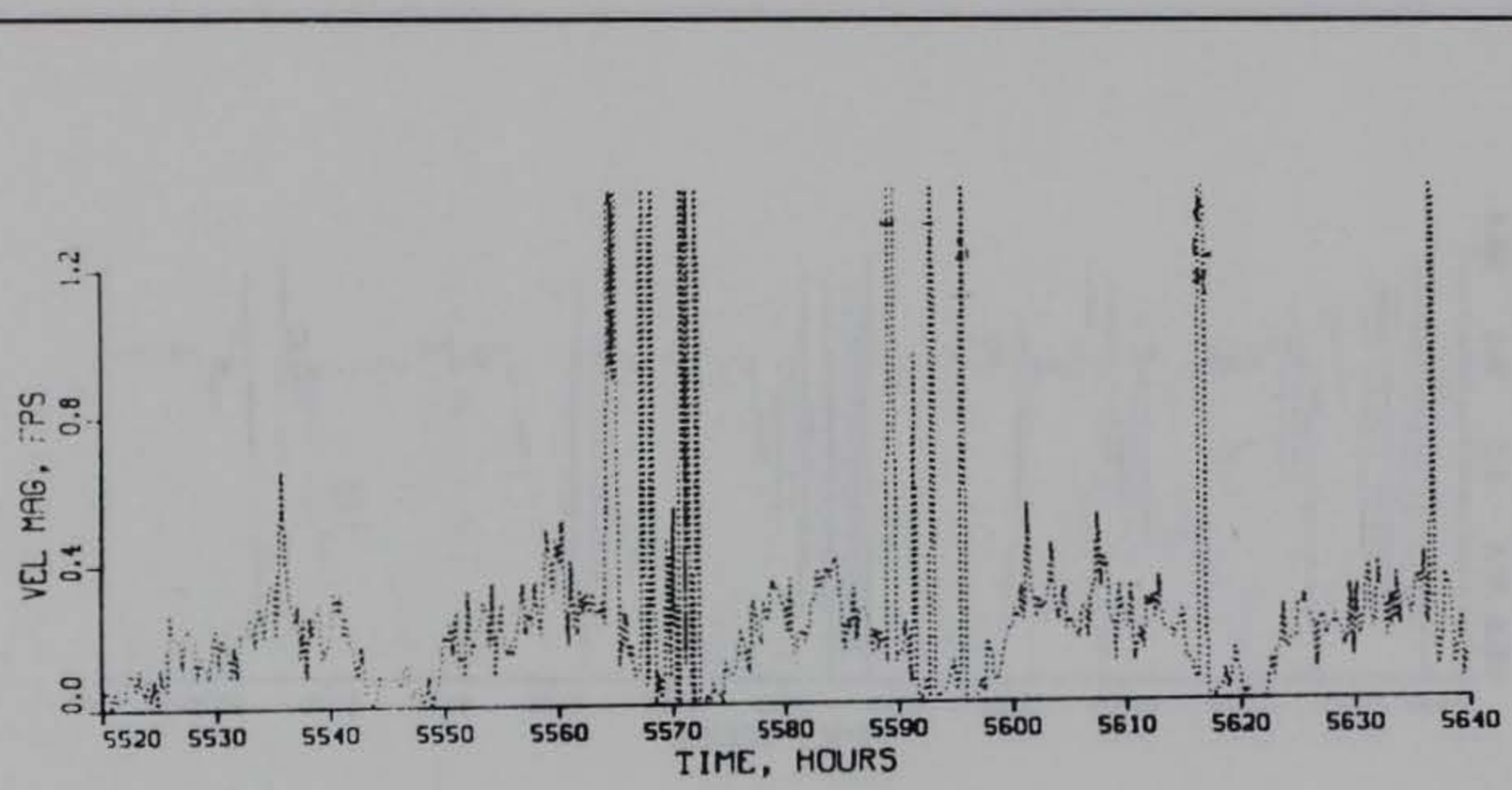

OBSERVED

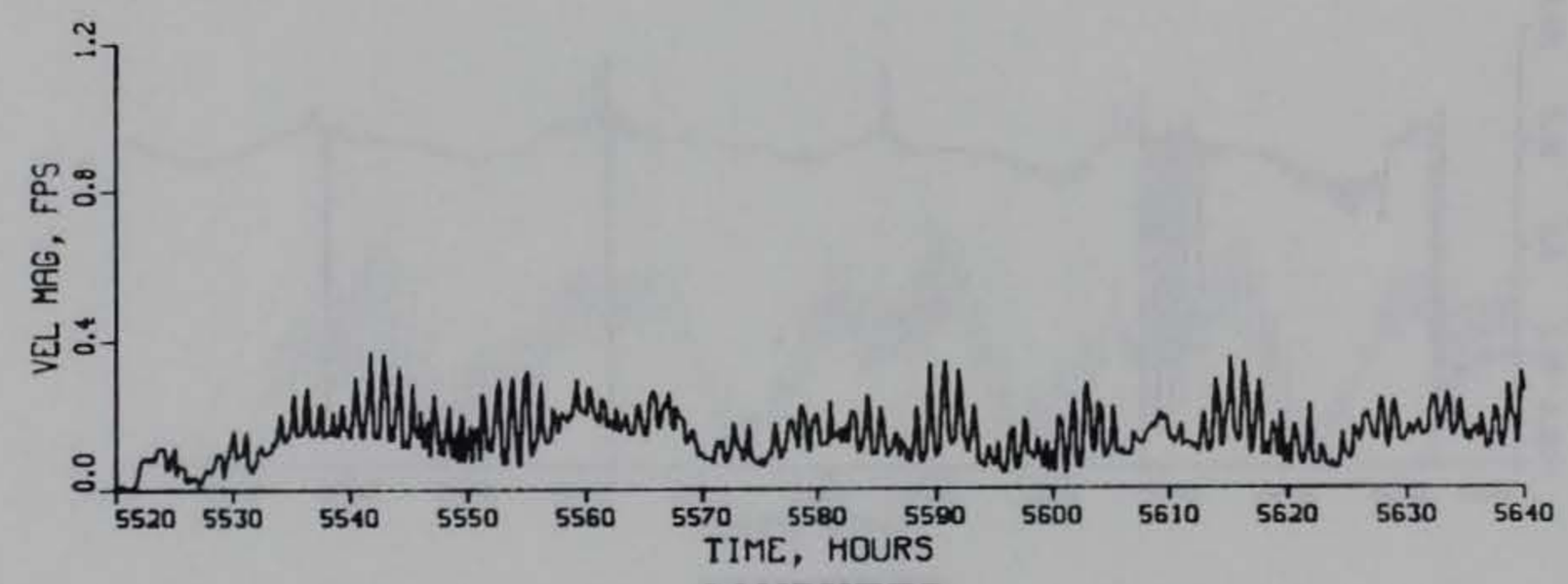

COMPUTED

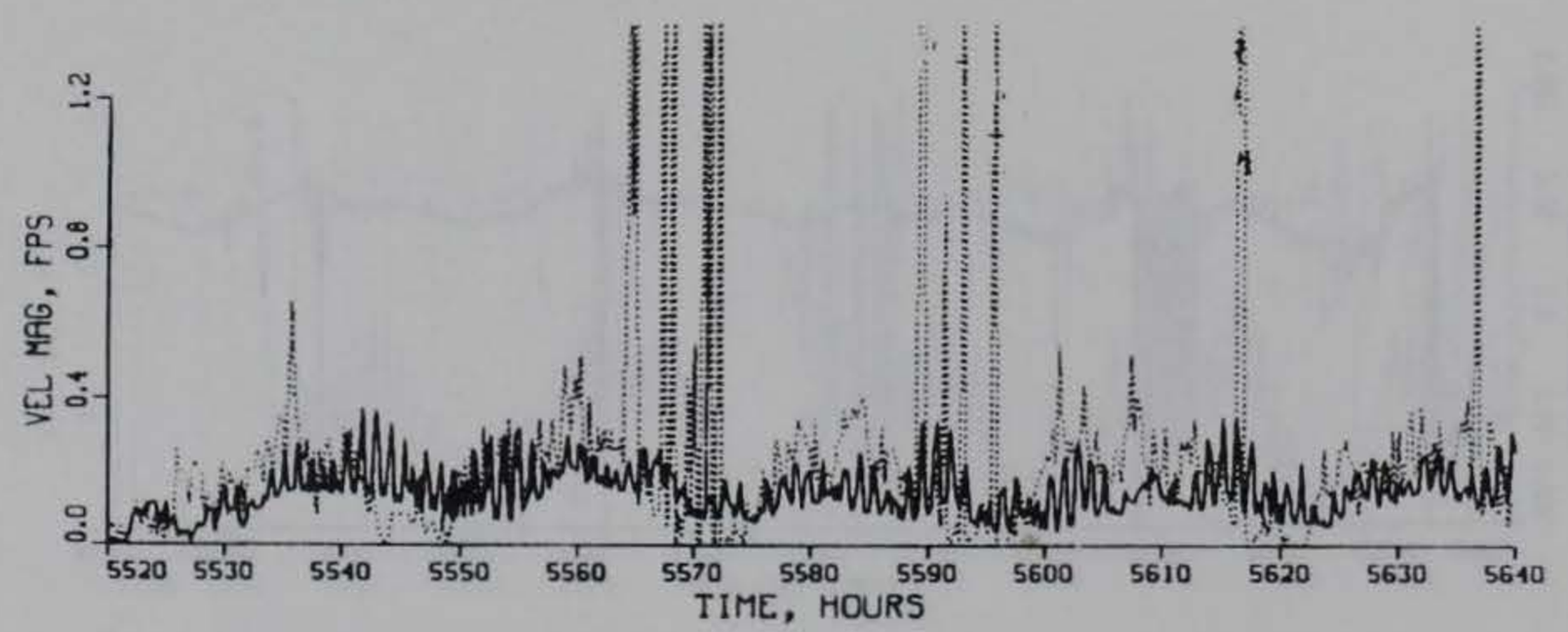

COMPUTED (SOLID) VS OBSERVED (DOTTED)

TIDAL VELOCITY

MAGNITUDE

VERIFICATION PERIOD

GAGE CM6

BOTTOM

PLATE 45

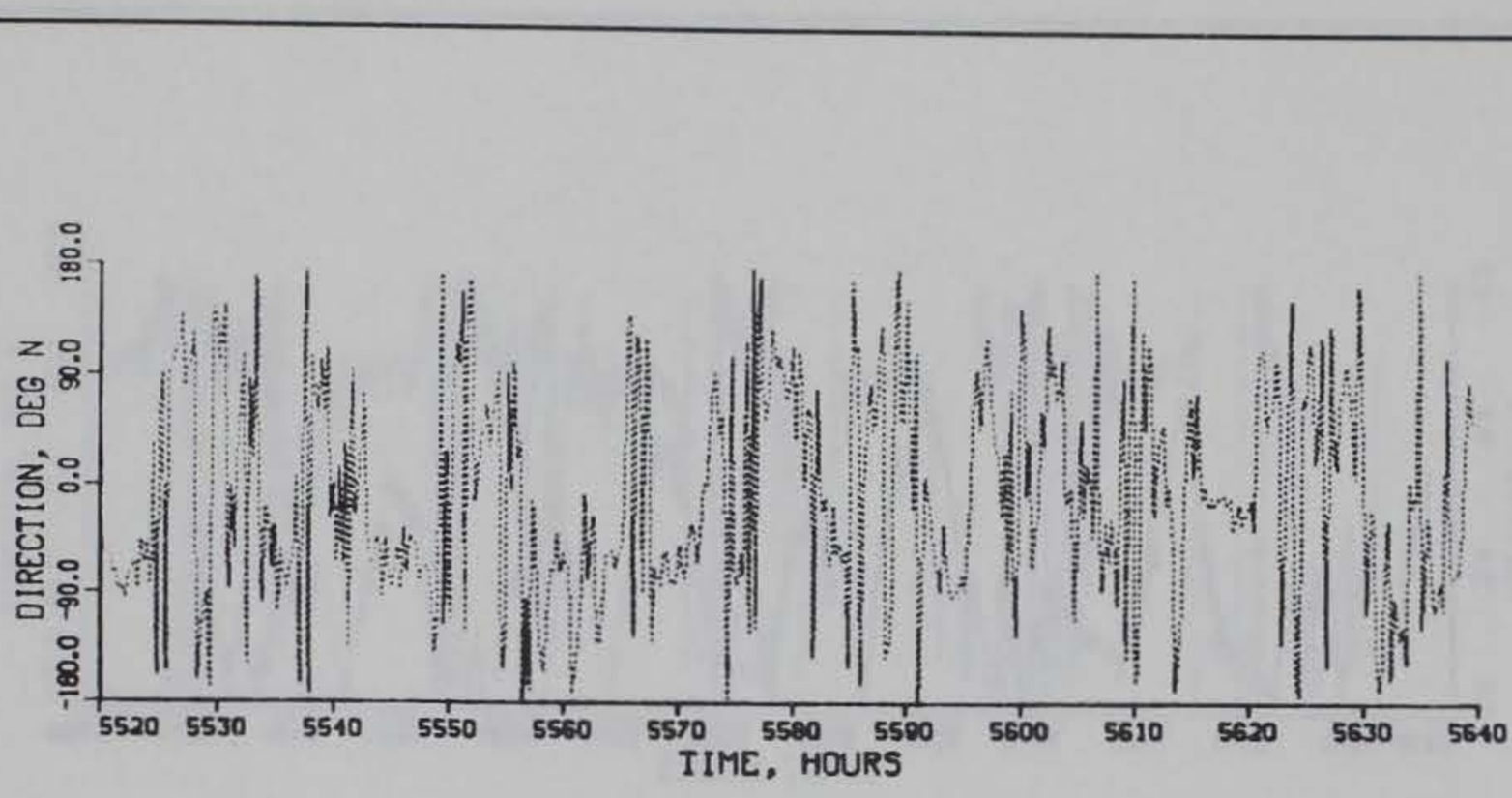

OBSERVED

COMPUTED

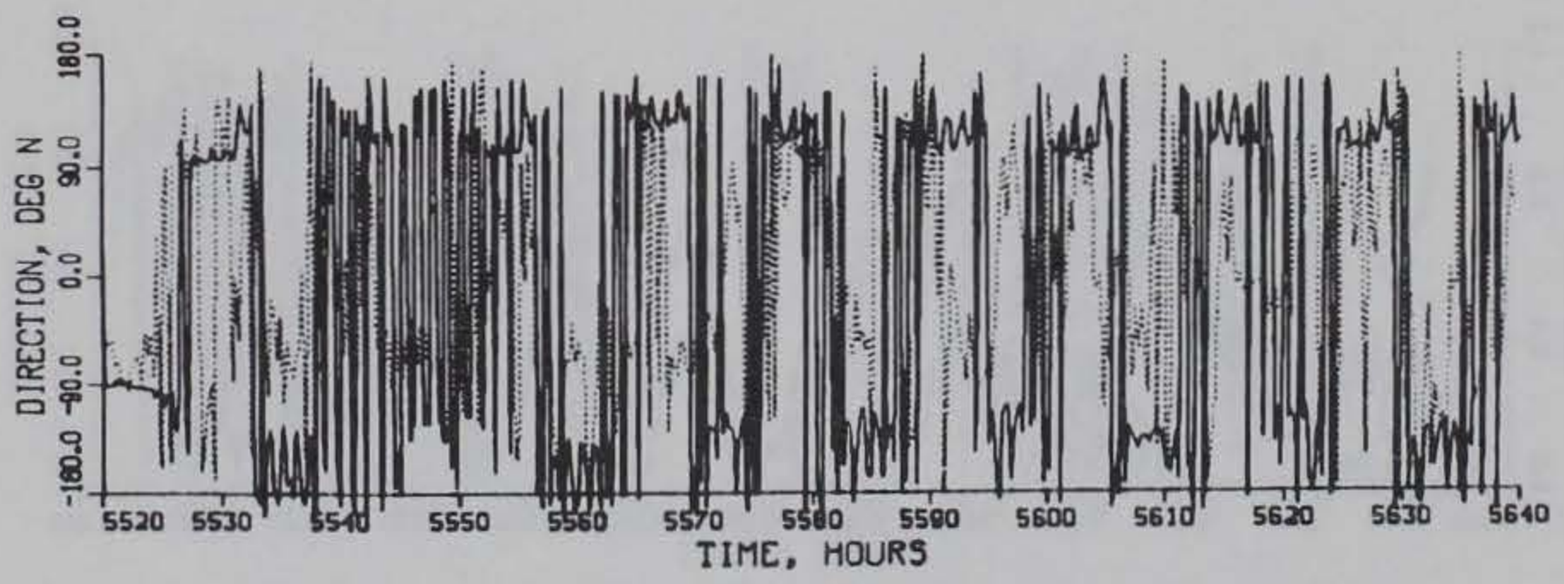

COMPUTED (SOLID) VS OBSERVED (DOTTED)

TIDAL VELOCITY

DIRECTION

VERIFICATION PERIOD

GAGE CM6

BOTTOM

PLATE 46

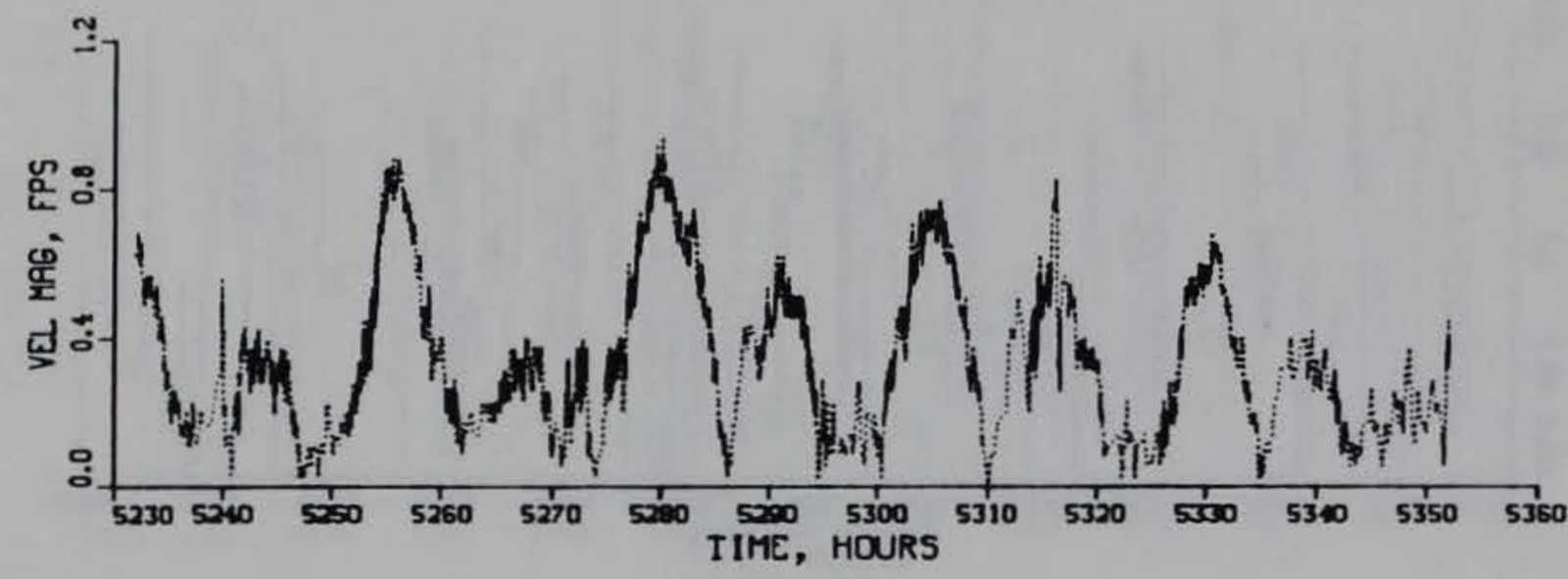

OBSERVED

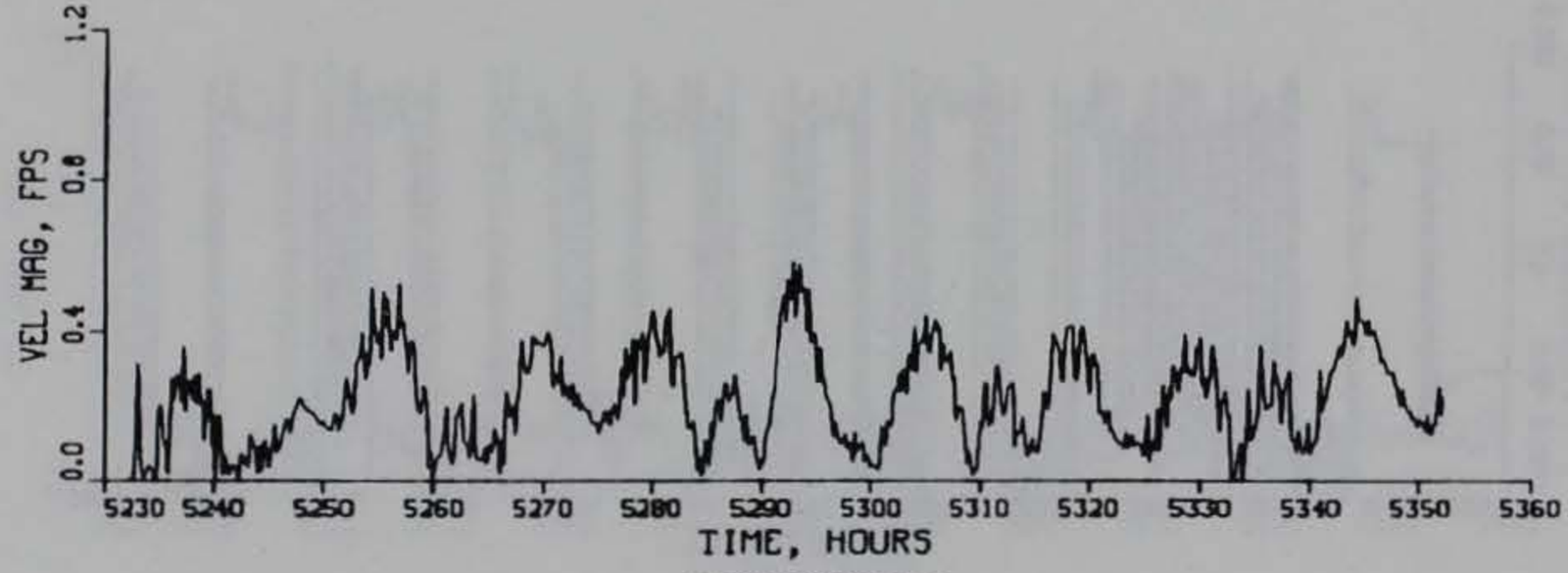

COMPUTED

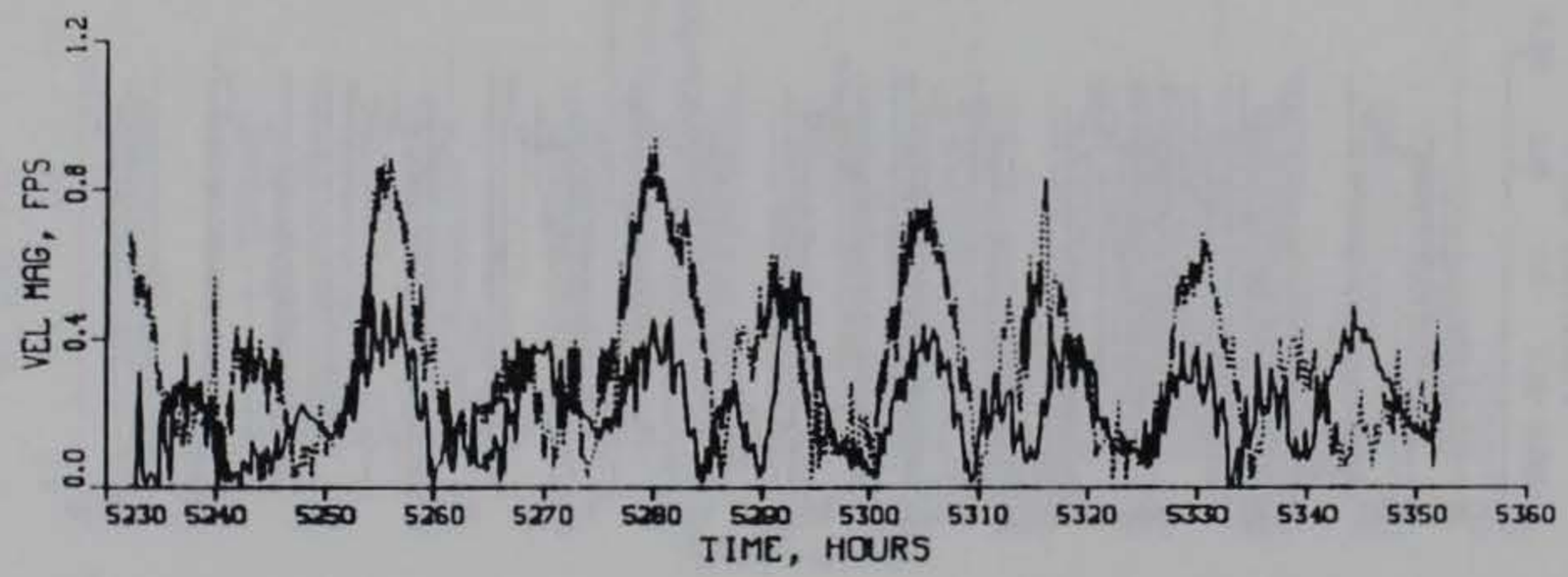

COMPUTED (SOLID) VS OBSERVED (DOTTED)

TIDAL VELOCITY

MAGNITUDE

CALIBRATION PERIOD

GAGE CM7

SURFACE

PLATE 47

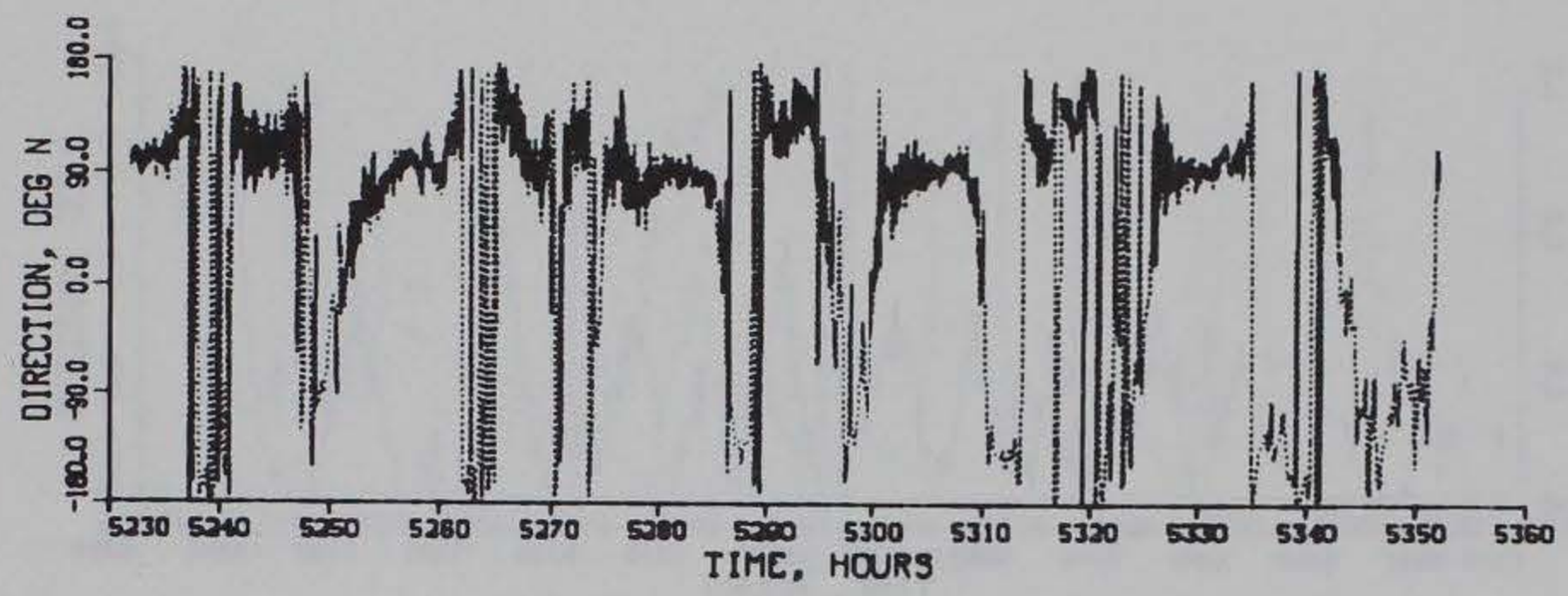

OBSERVED

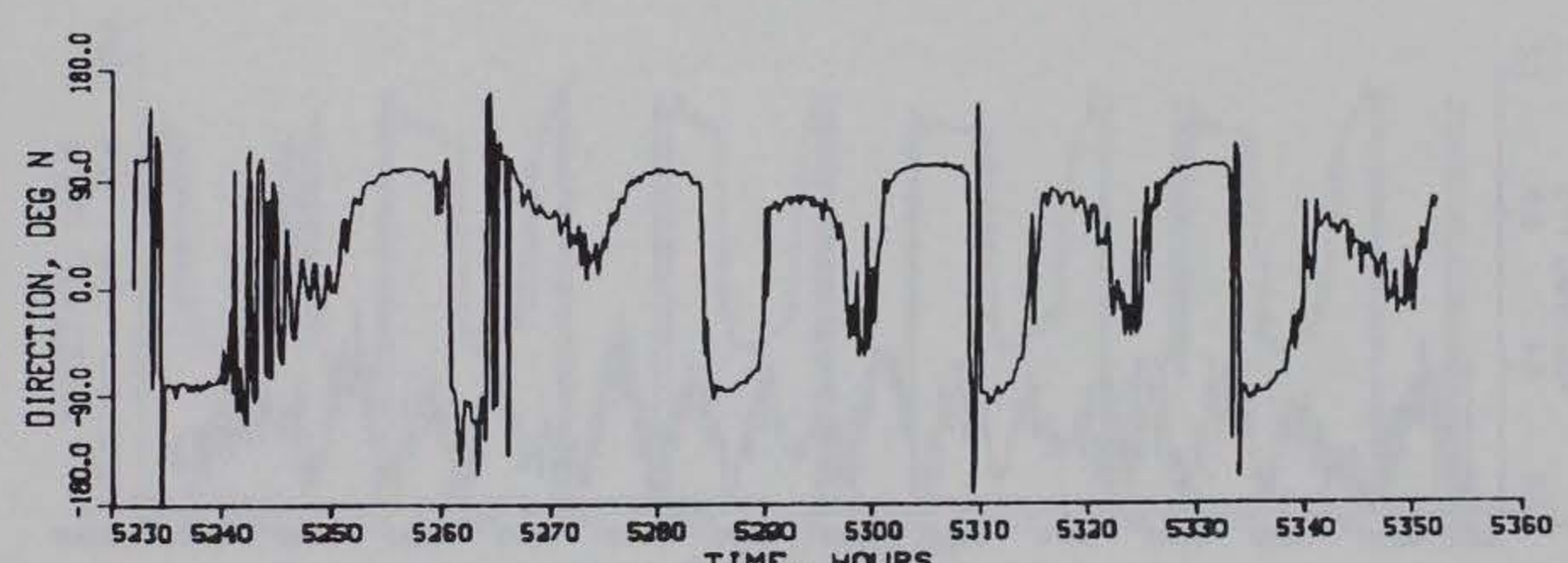

COMPUTED

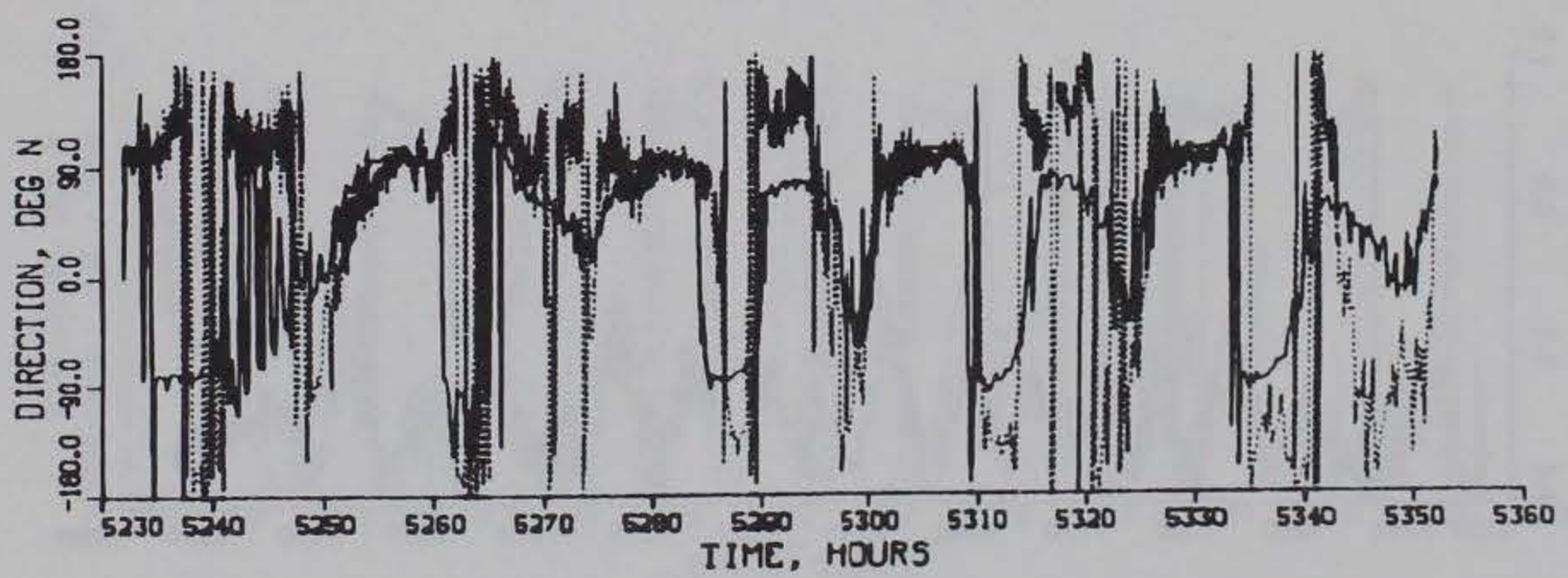

COMPUTED (SOLID) VS OBSERVED (DOTTED)

TIDAL VELOCITY

DIRECTION

CALIBRATION PERIOD

GAGE CM7

SURFACE

PLATE 48

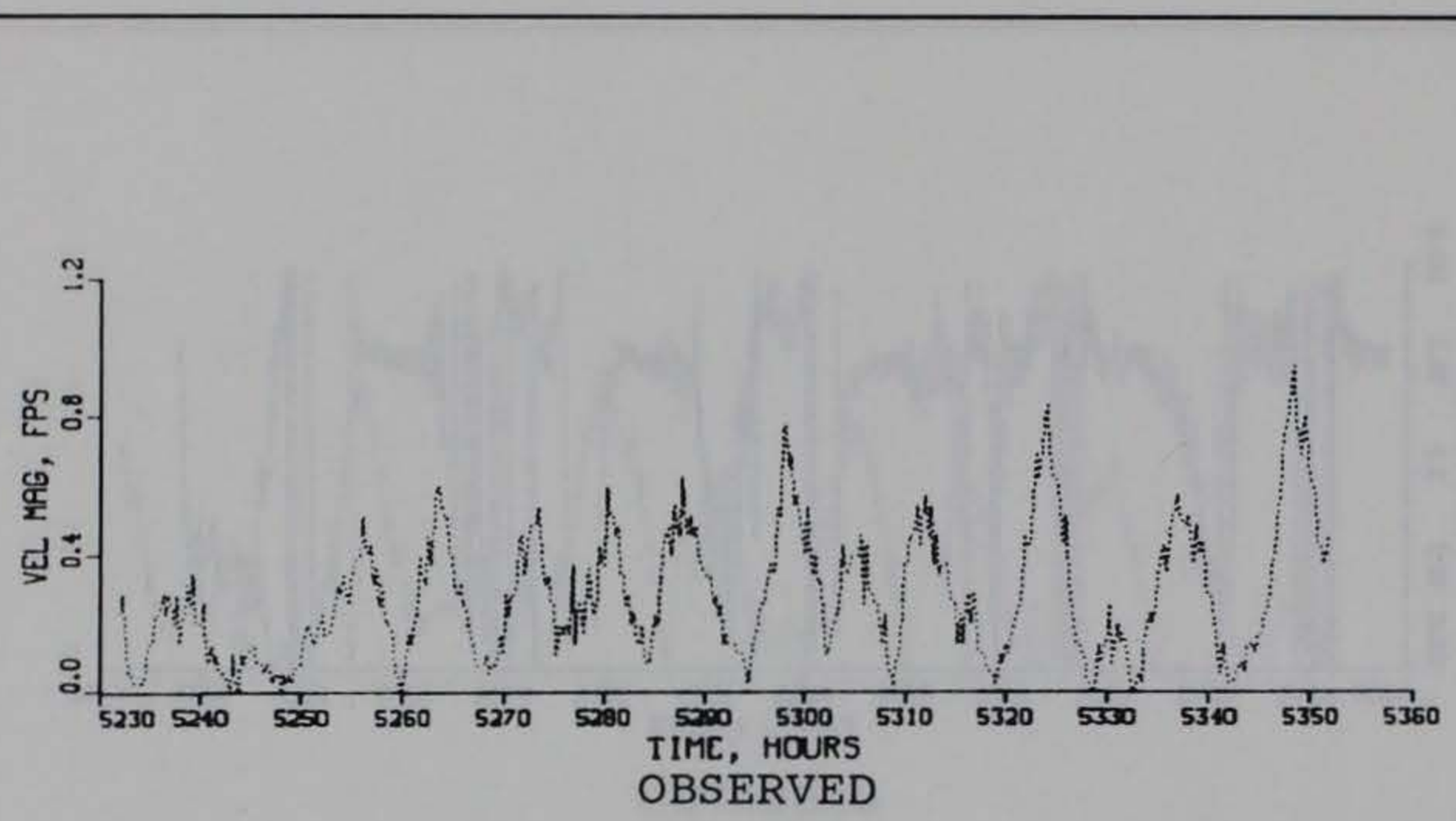

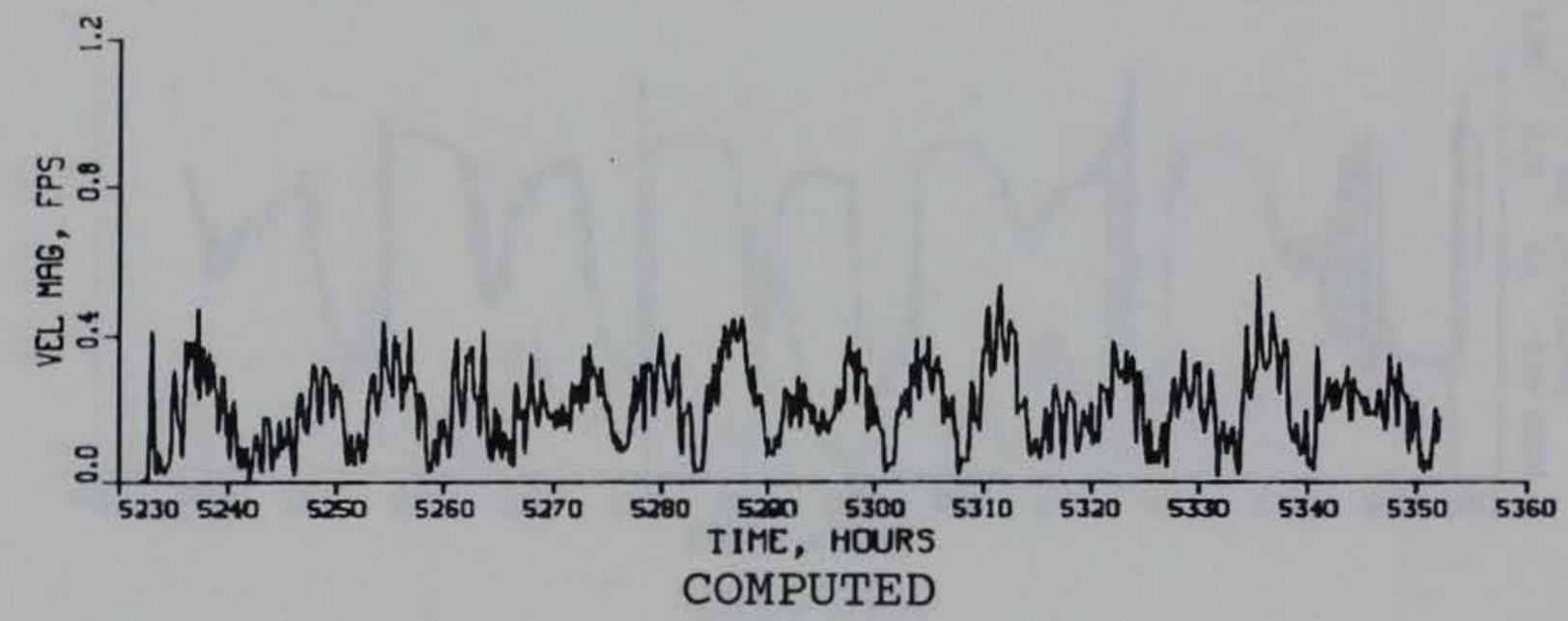

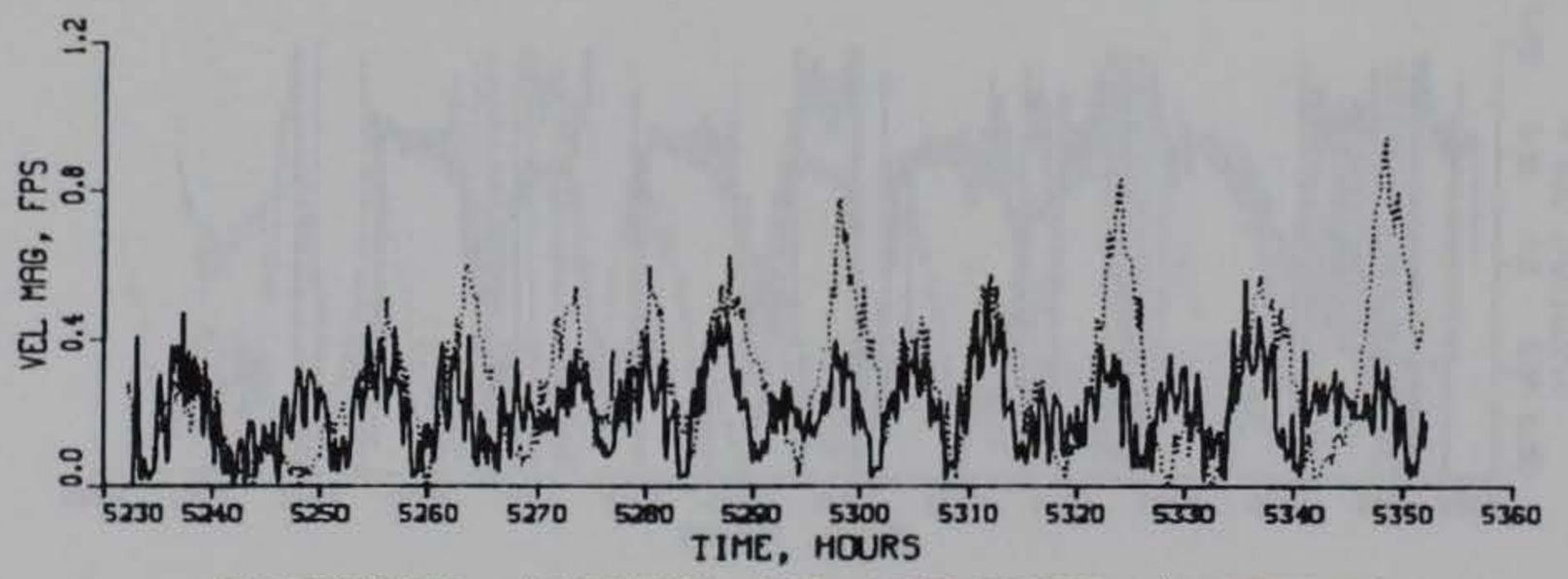

COMPUTED (SOLID) VS OBSERVED (DOTTED)

TIDAL VELOCITY

MAGNITUDE

CALIBRATION PERIOD

GAGE CM7

BOTTOM

PLATE 49

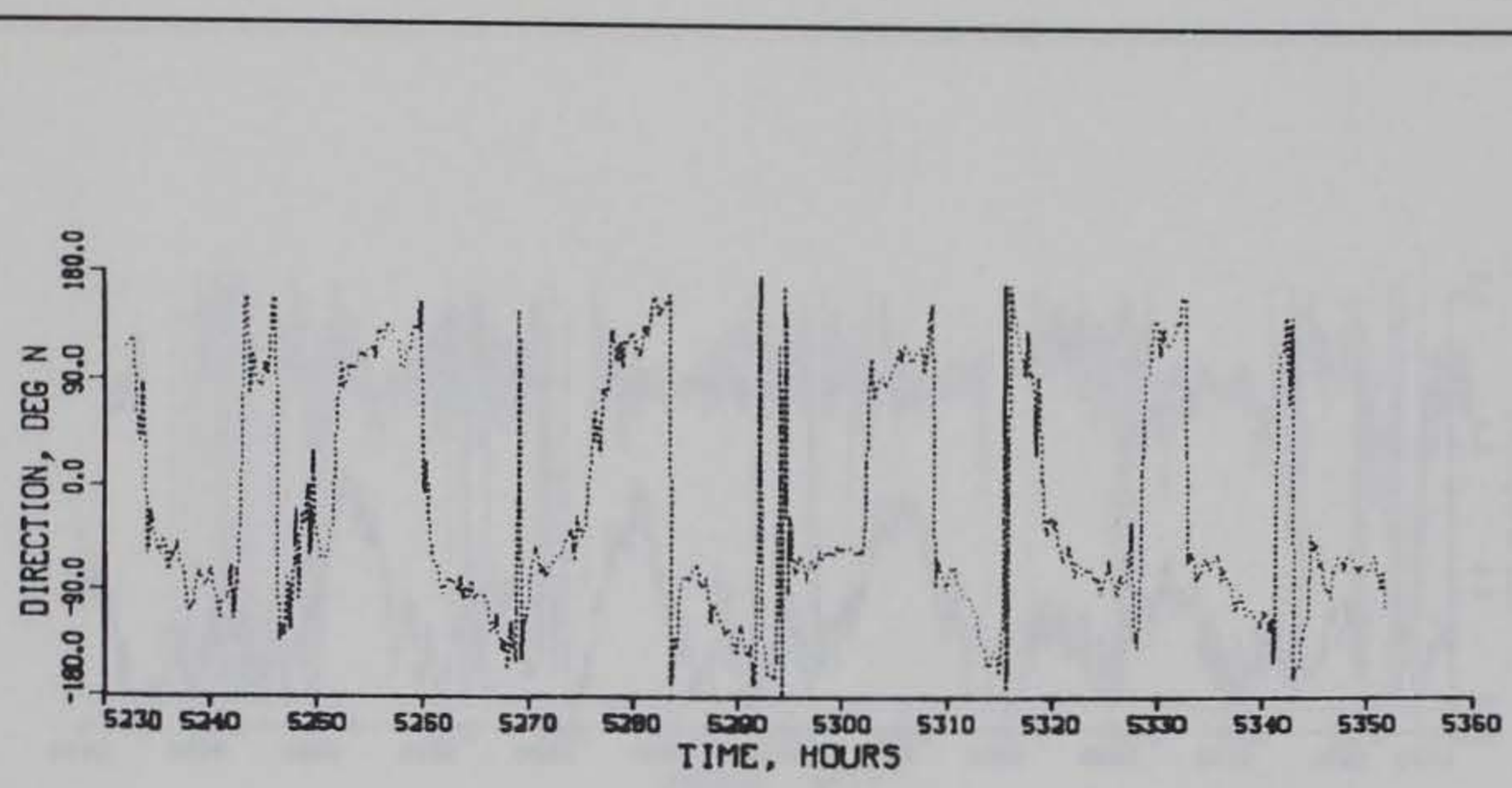

OBSERVED

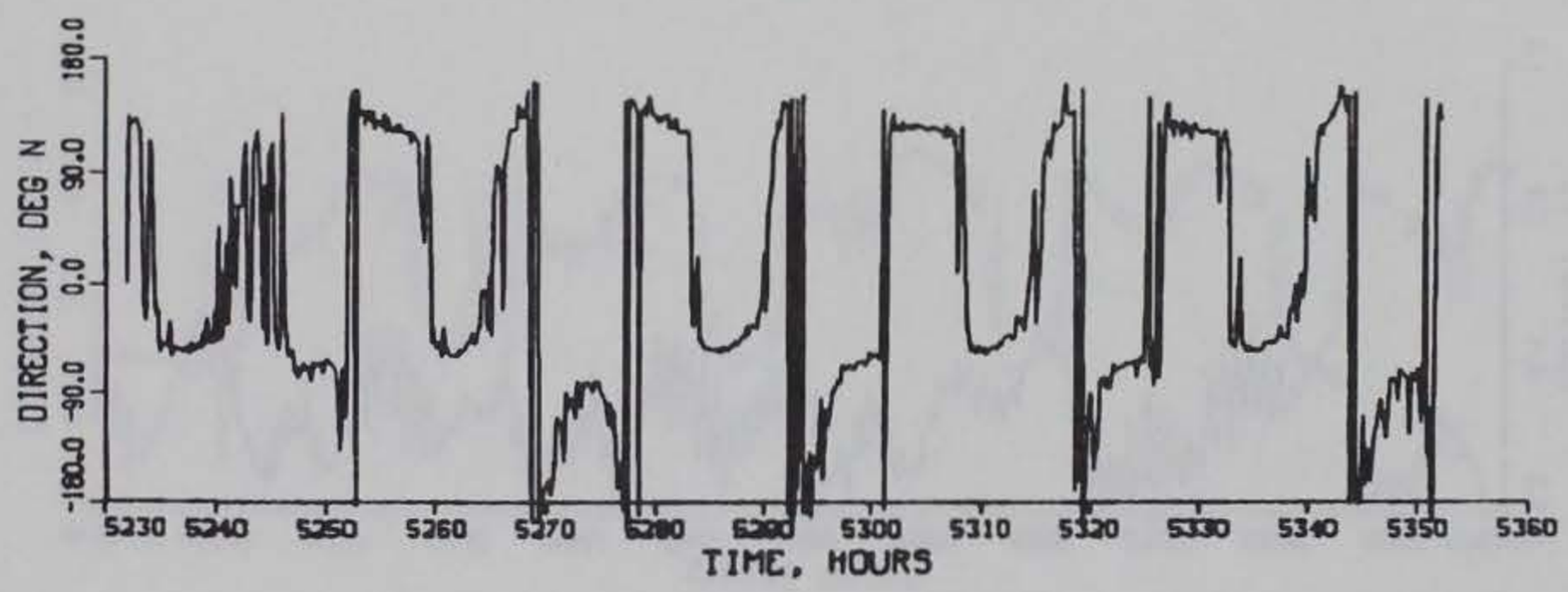

COMPUTED

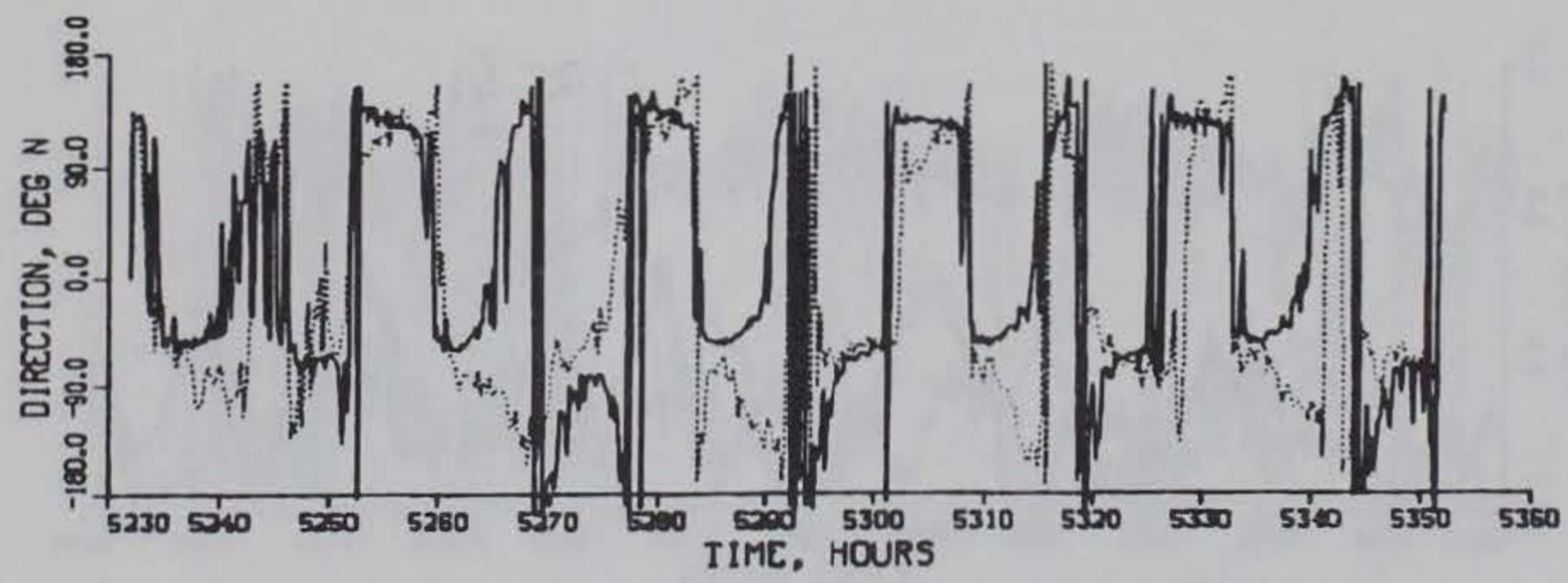

COMPUTED (SOLID) VS OBSERVED (DOTTED)

TIDAL VELOCITY

DIRECTION

CALIBRATION PERIOD

GAGE CM7

BOTTOM

PLATE 50

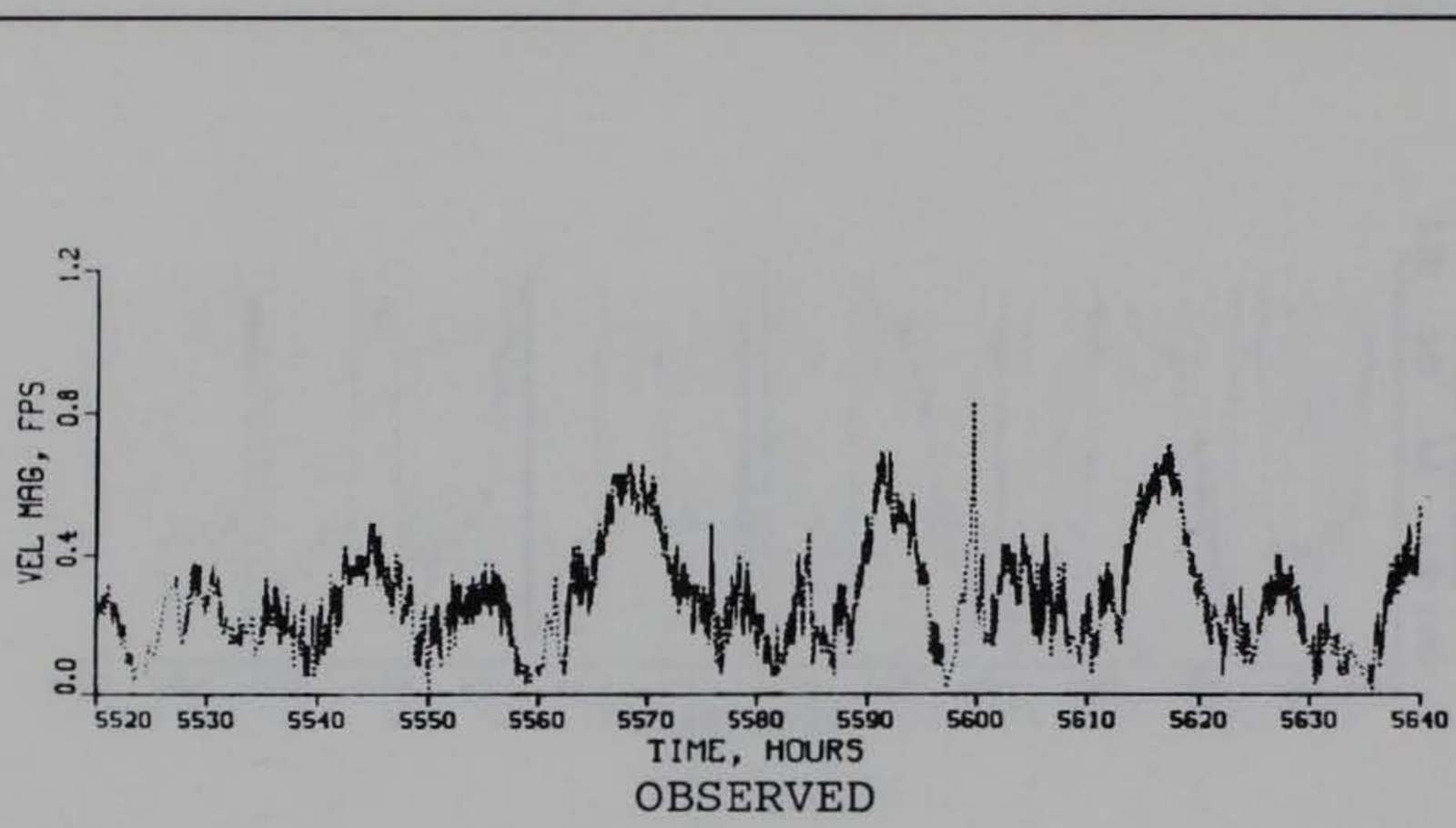

OBSERVED

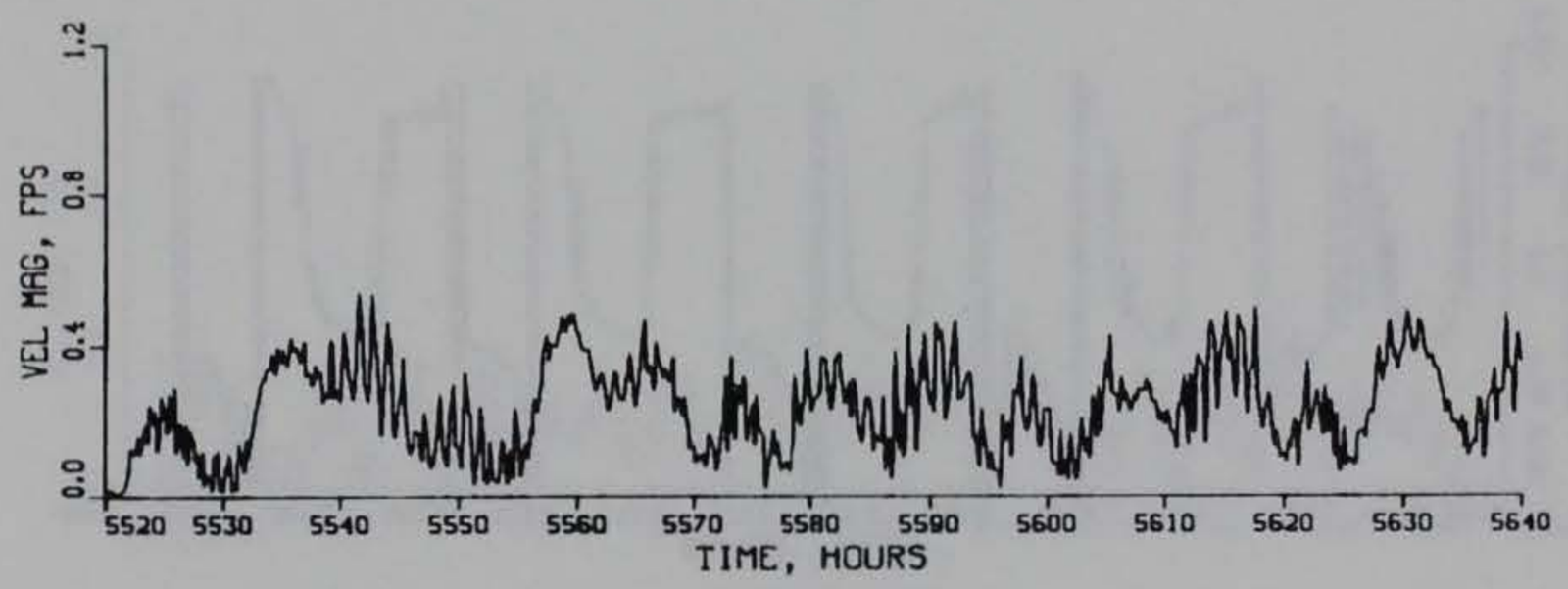

COMPUTED

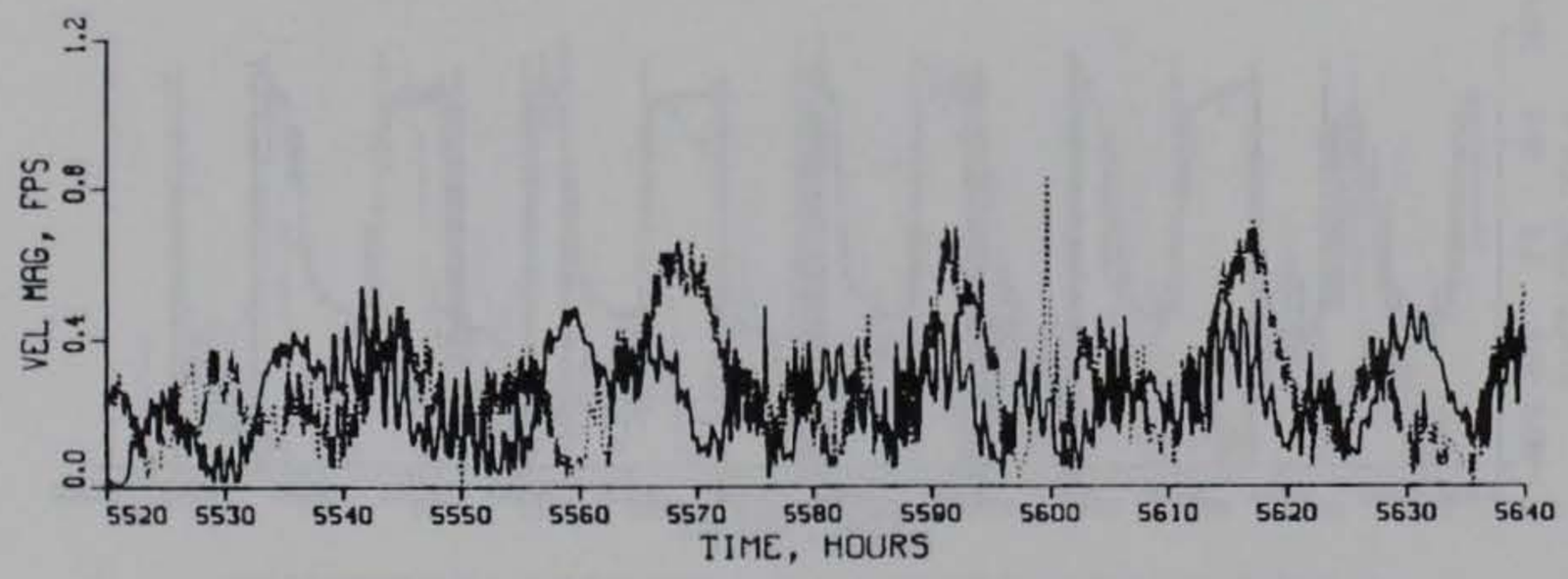

COMPUTED (SOLID) VS OBSERVED (DOTTED)

TIDAL VELOCITY

MAGNITUDE

VERIFICATION PERIOD

GAGE CM7

SURFACE

PLATE 51

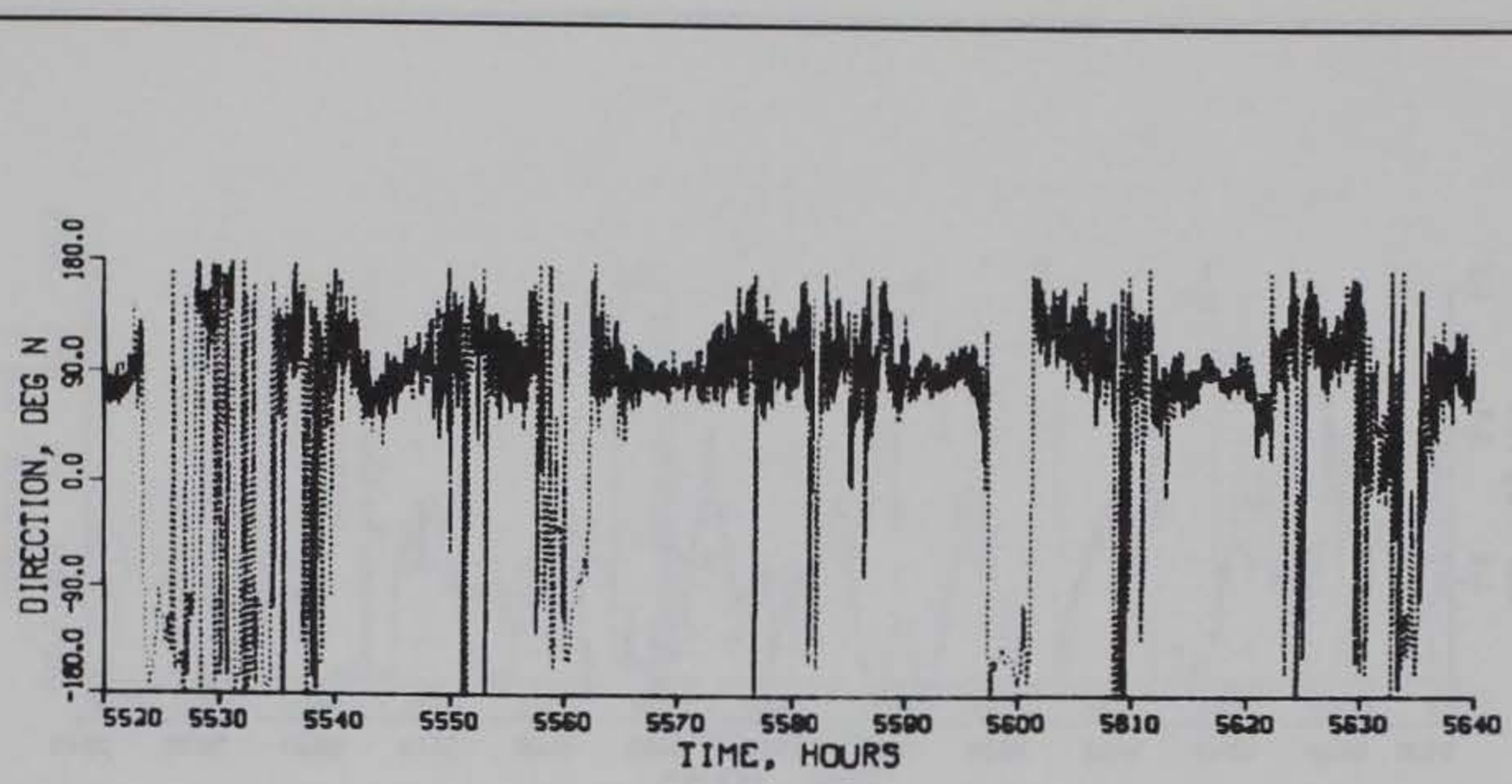

OBSERVED

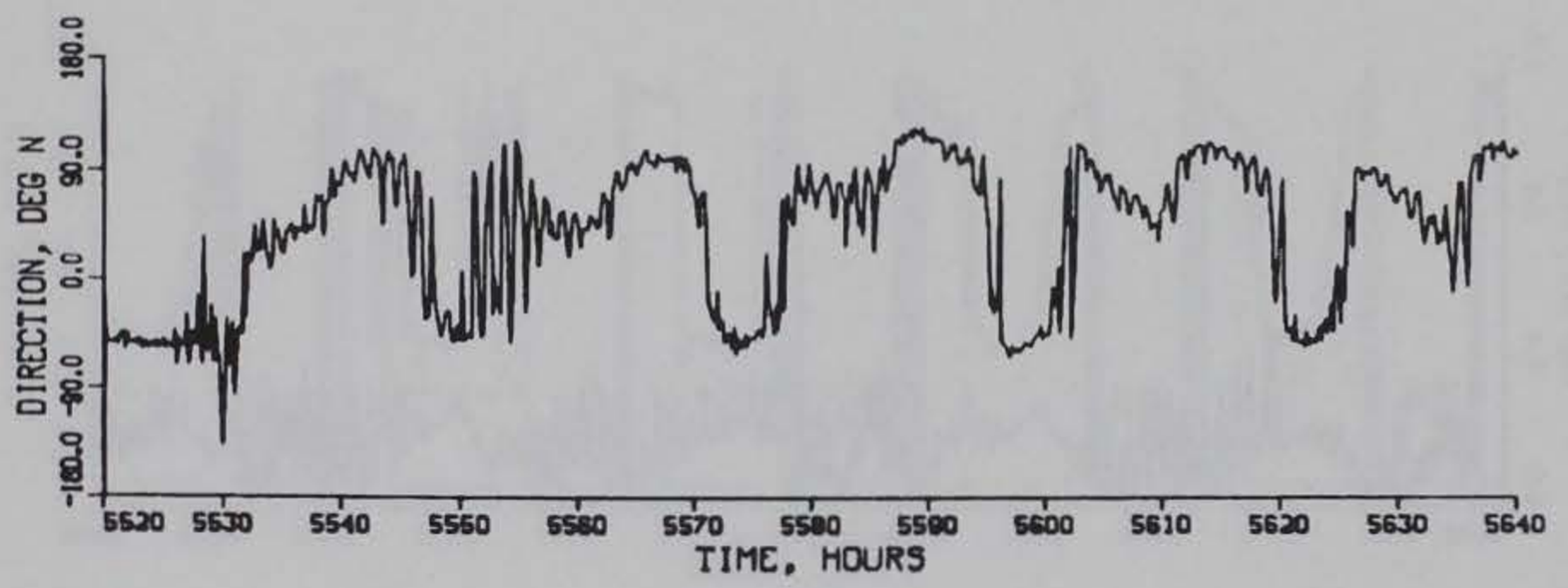

COMPUTED

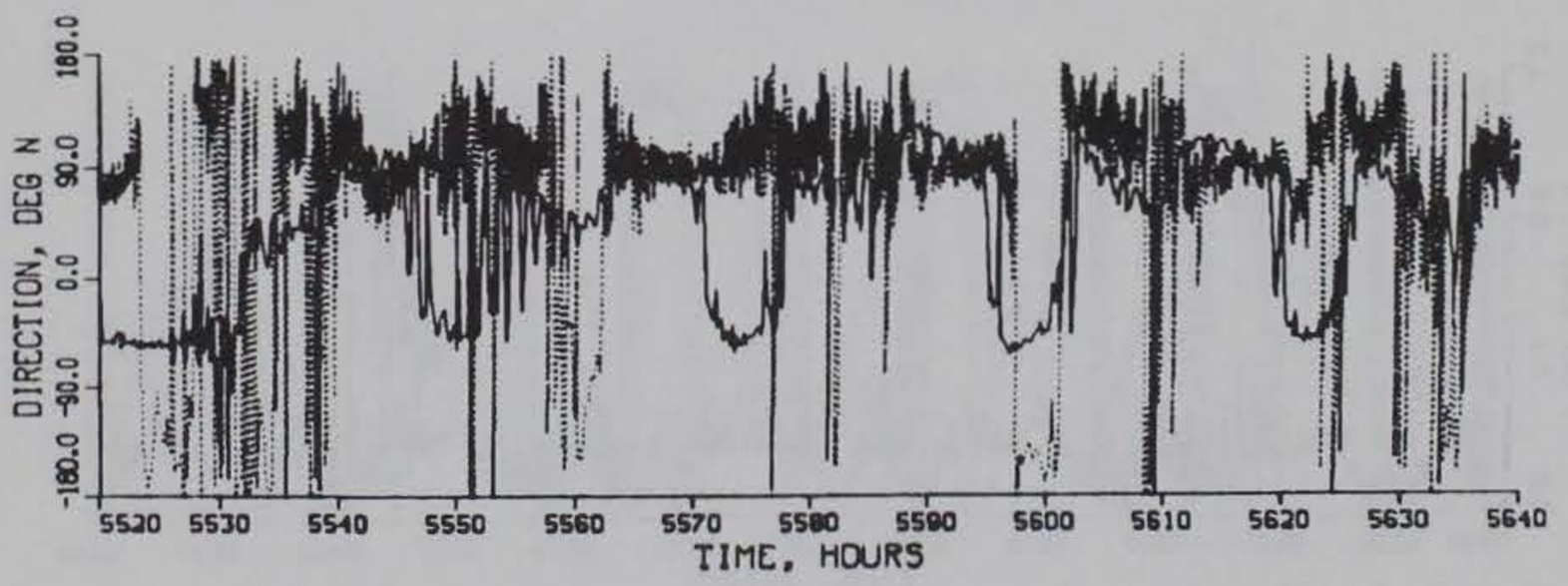

COMPUTED (SOLID) VS OBSERVED (DOTTED)

TIDAL VELOCITY

VERIFICATION PERIOD

DIRECTION

GAGE CM7

SURFACE

PLATE 52

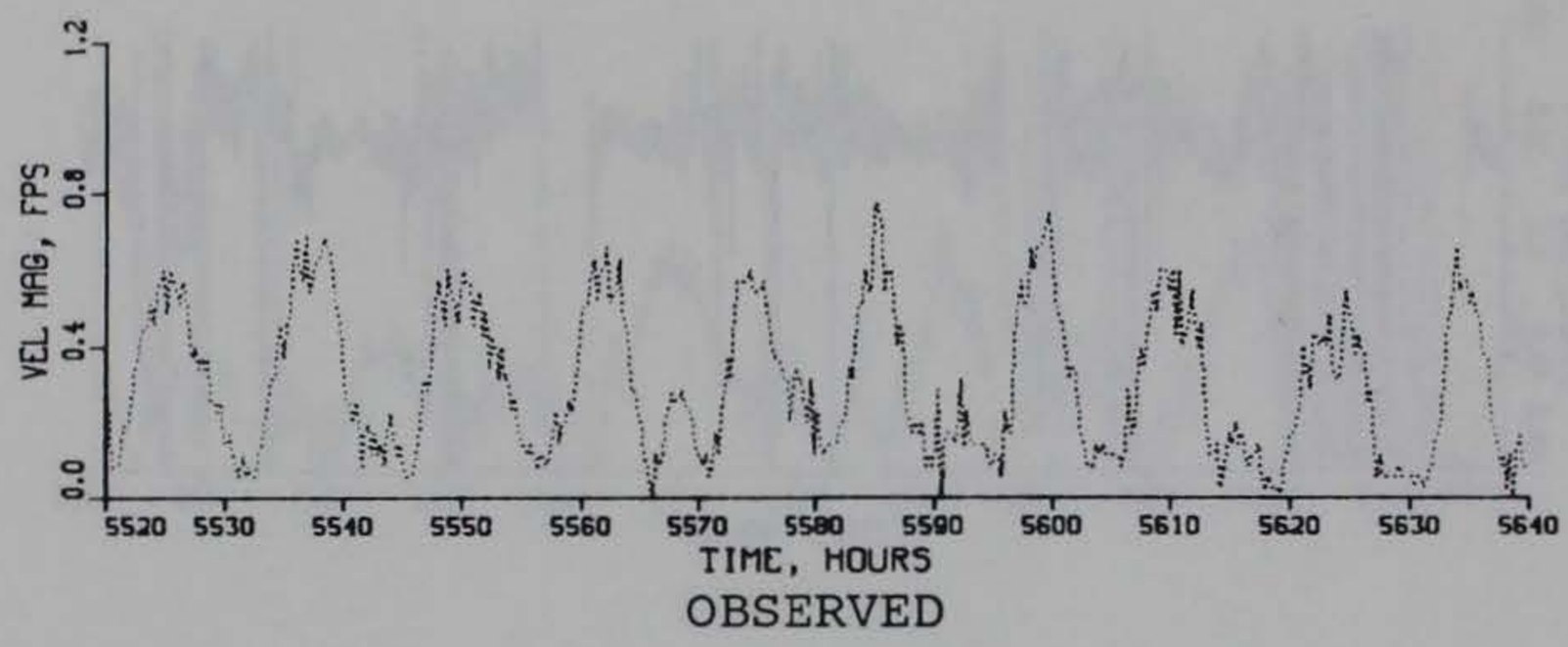

OBSERVED

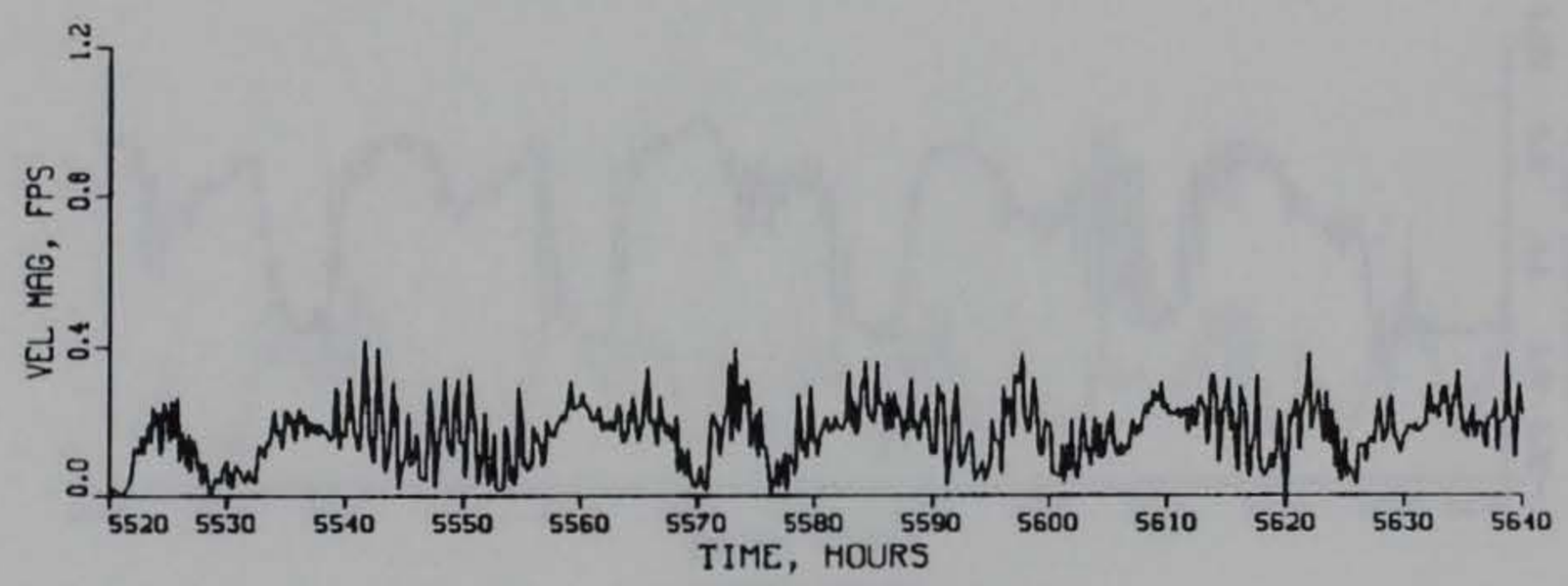

COMPUTED

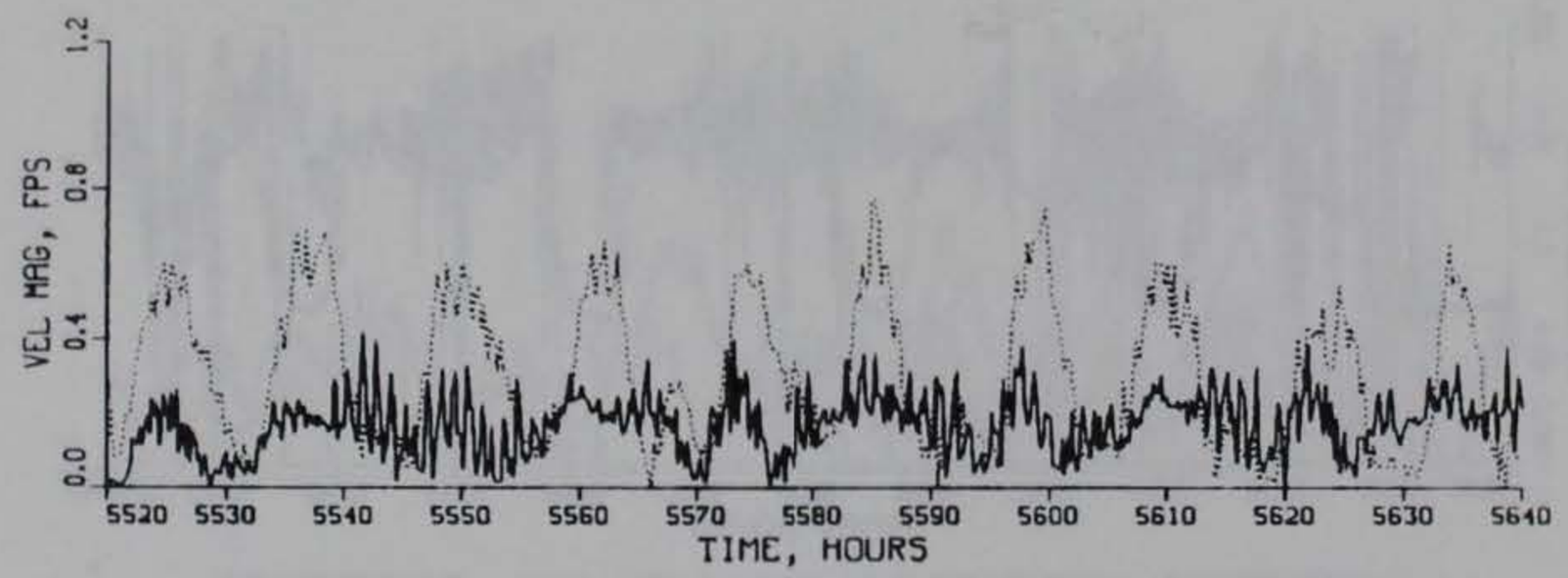

COMPUTED (SOLID) VS OBSERVED (DOTTED)

TIDAL VELOCITY

MAGNITUDE

VERIFICATION PERIOD

GAGE CM7

BOTTOM

PLATE 53

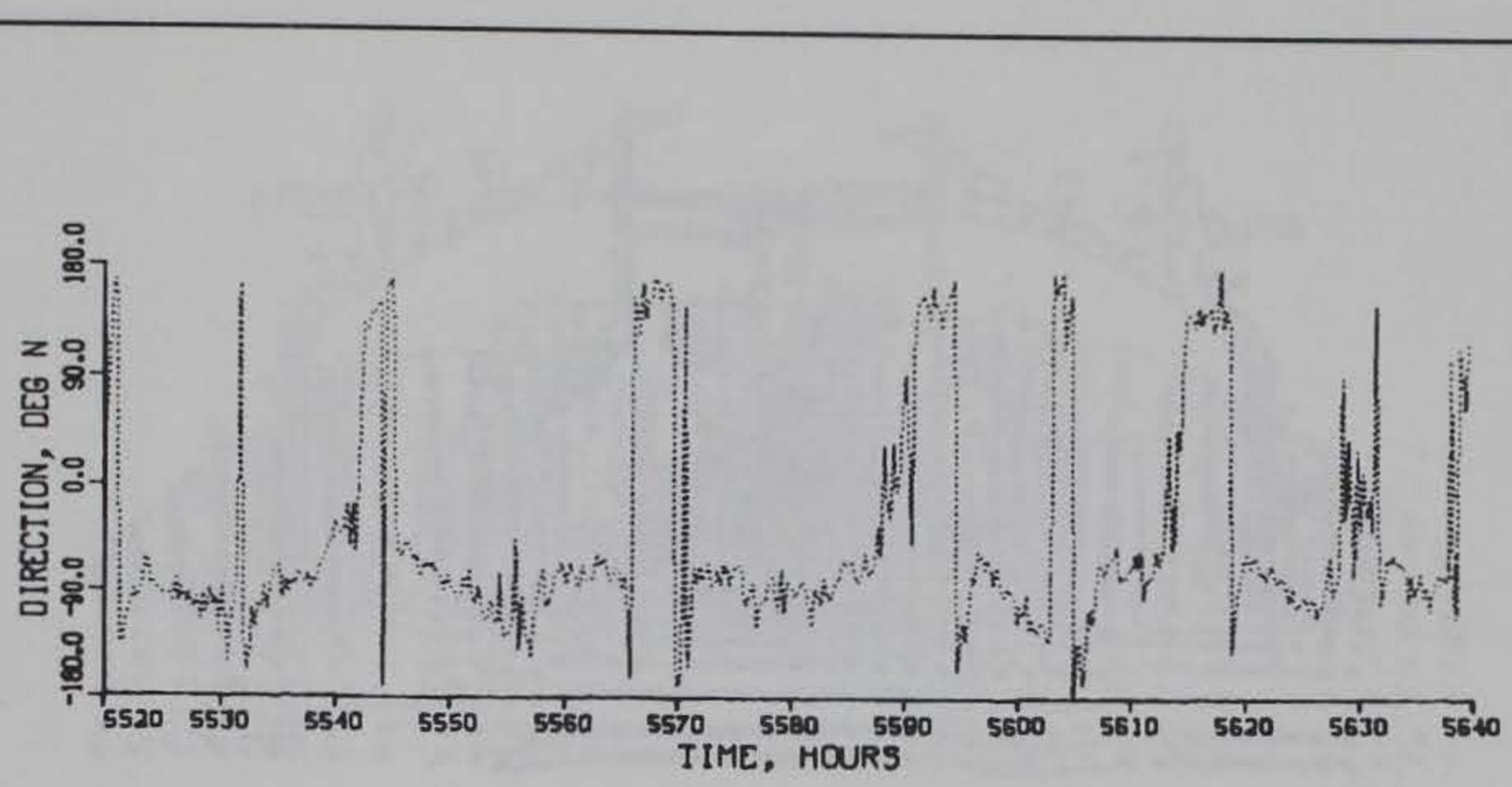

OBSERVED

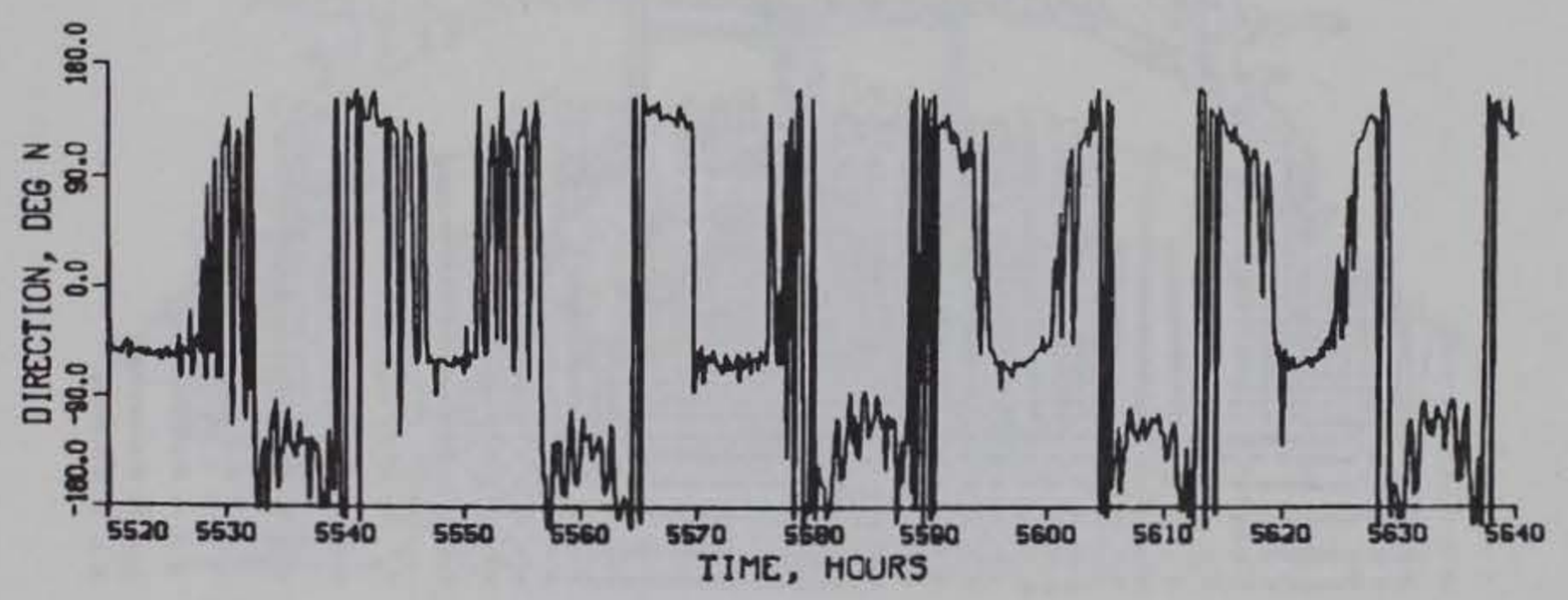

COMPUTED

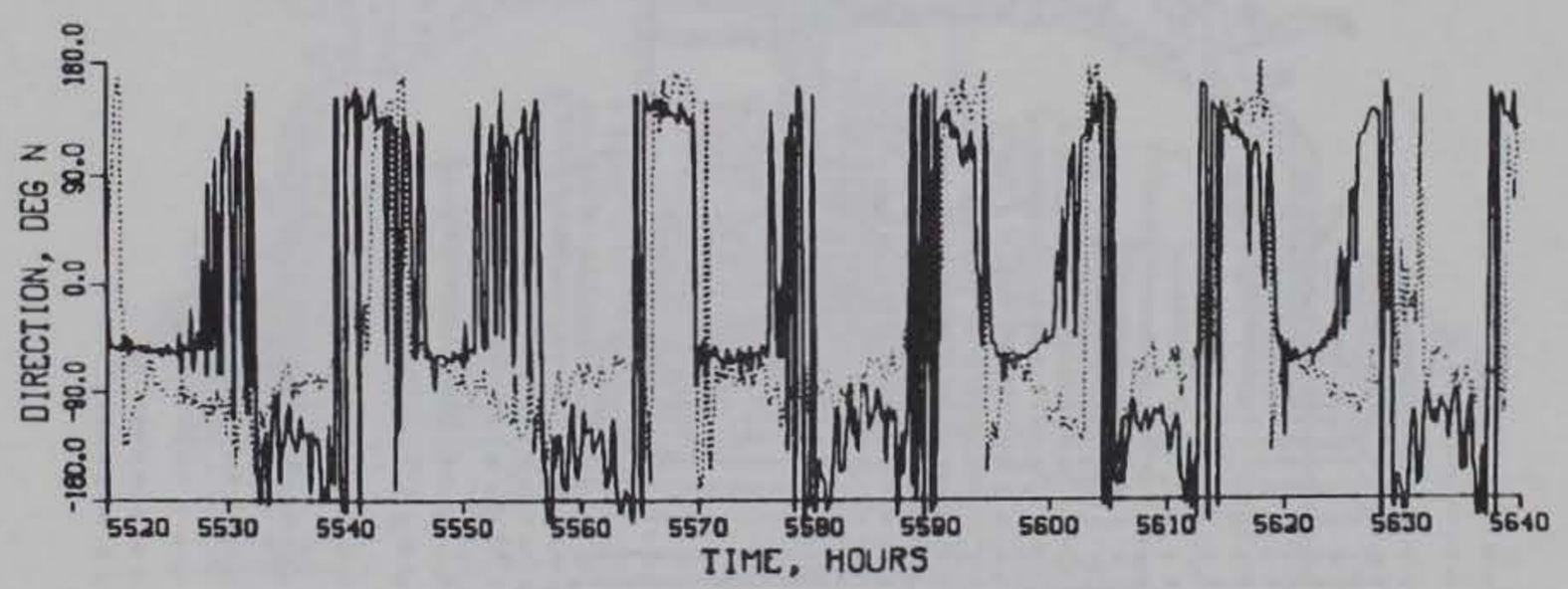

COMPUTED (SOLID) VS OBSERVED (DOTTED)

TIDAL VELOCITY

DIRECTION

VERIFICATION PERIOD

GAGE CM7

BOTTOM

PLATE 54

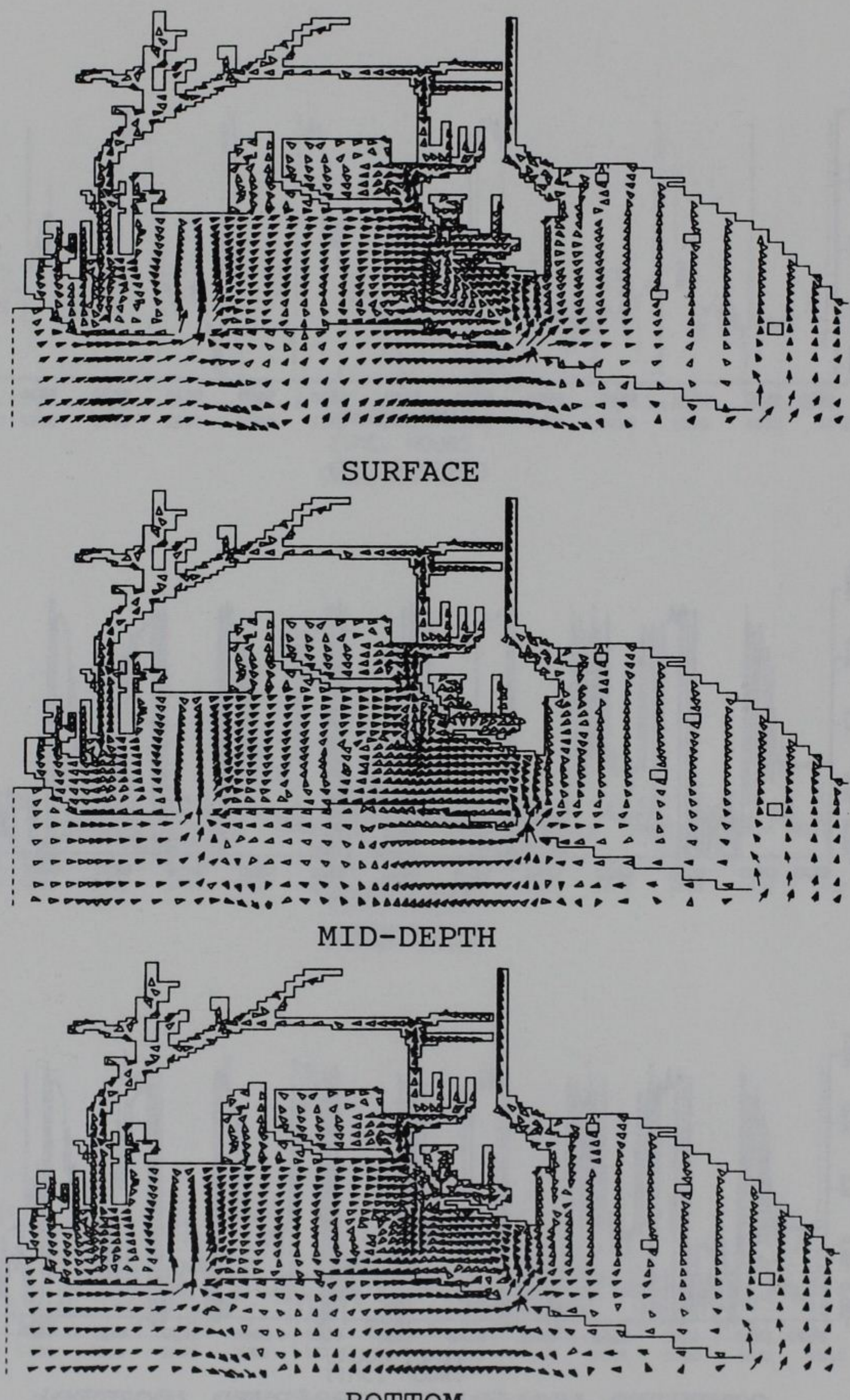

SURFACE

MID-DEPTH

BOTTOM

CIRCULATION PATTERNS

⟶ 1 FT/SEC

CALIBRATION PERIOD

PEAK FLOOD

PLATE 55

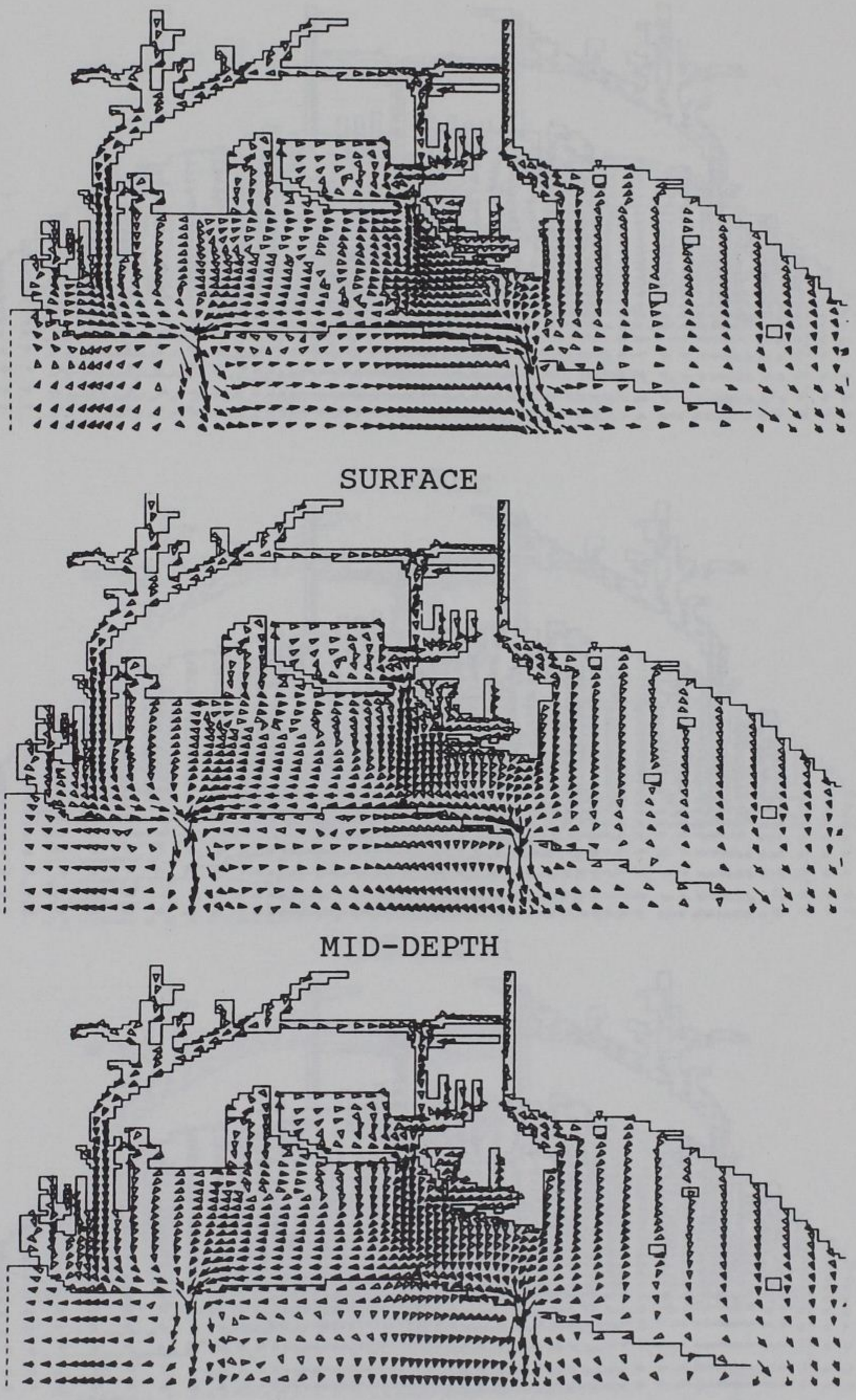

SURFACE

MID-DEPTH

BOTTOM

CIRCULATION PATTERNS

⟶ 1 FT/SEC

CALIBRATION PERIOD

PEAK EBB

PLATE 56

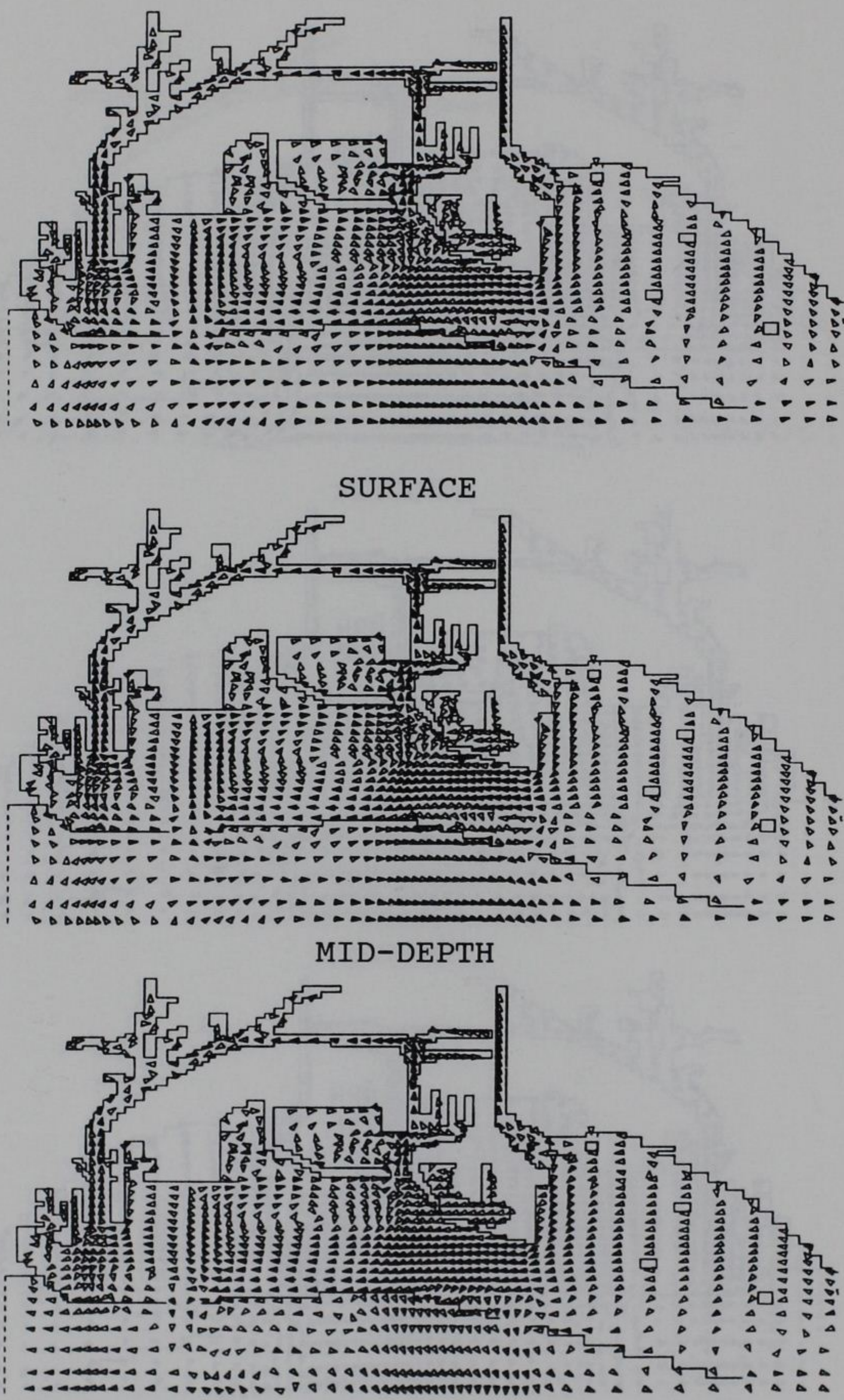

SURFACE

MID-DEPTH

BOTTOM

CIRCULATION PATTERNS

CALIBRATION PERIOD

⟶ 1 FT/SEC

SLACK WATER

PLATE 57

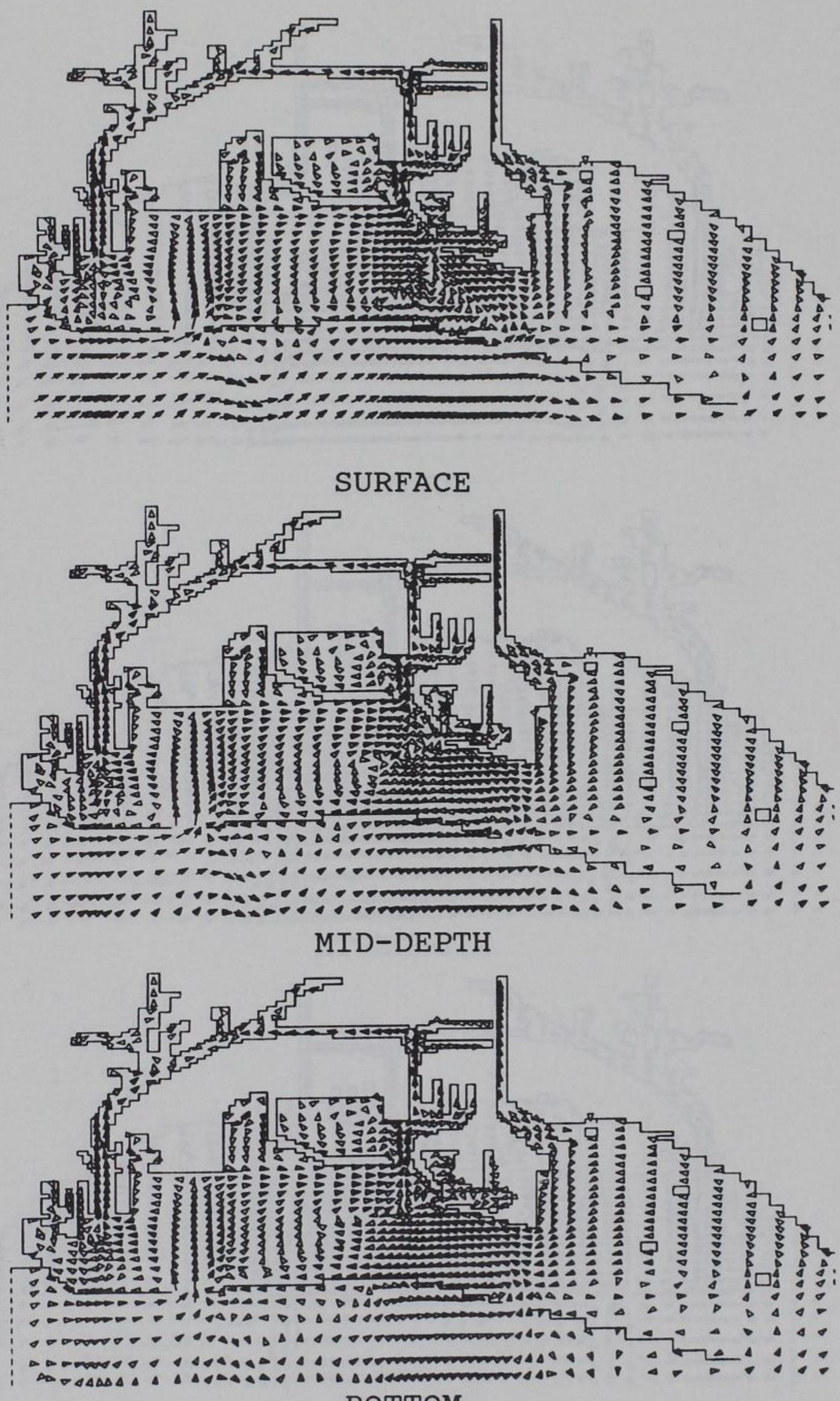

SURFACE

MID-DEPTH

BOTTOM

CIRCULATION PATTERNS **VERIFICATION PERIOD**

⟶ 1 FT/SEC PEAK FLOOD

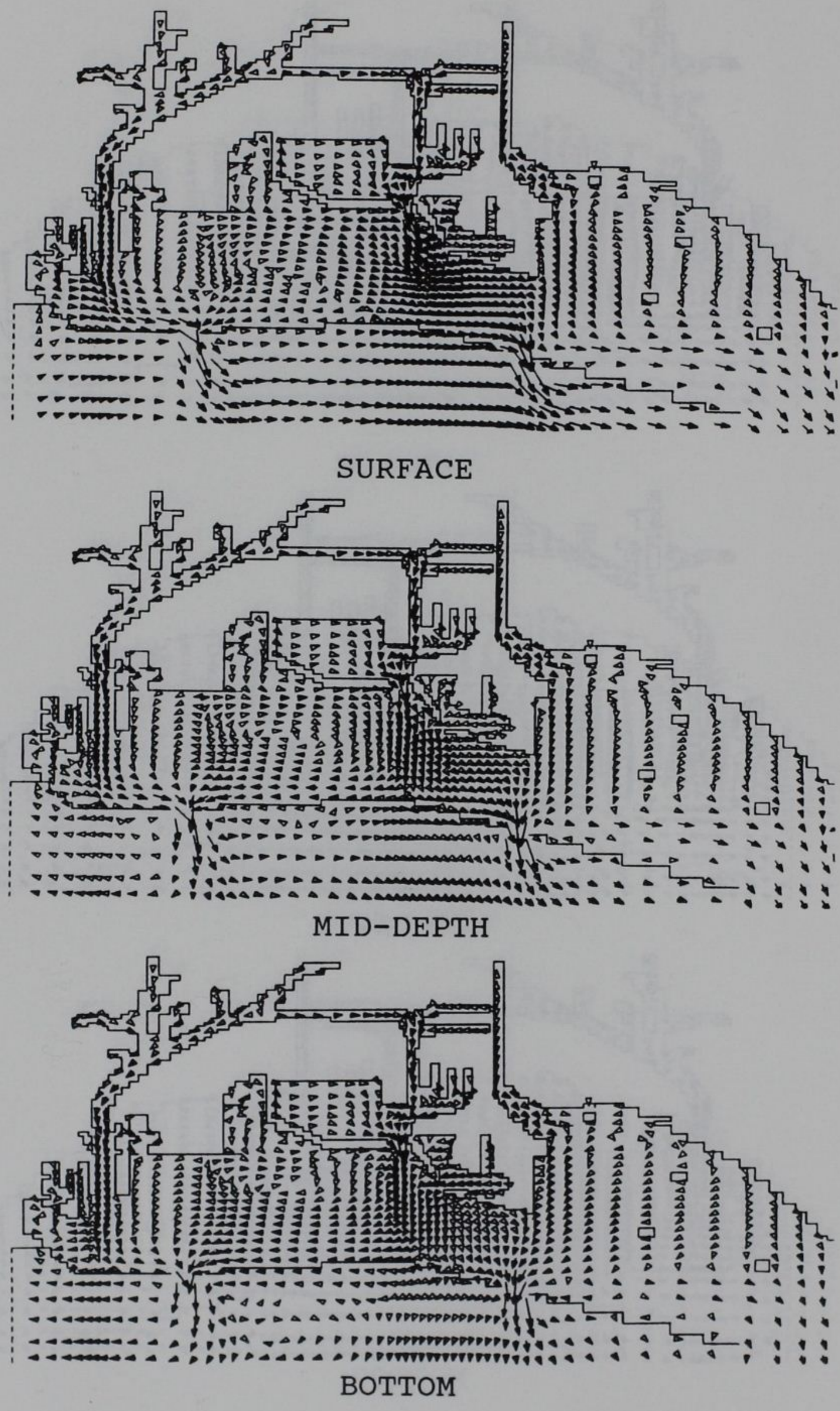

SURFACE

MID-DEPTH

BOTTOM

CIRCULATION PATTERNS

⟶ 1 FT/SEC

VERIFICATION PERIOD

PEAK EBB

PLATE 59

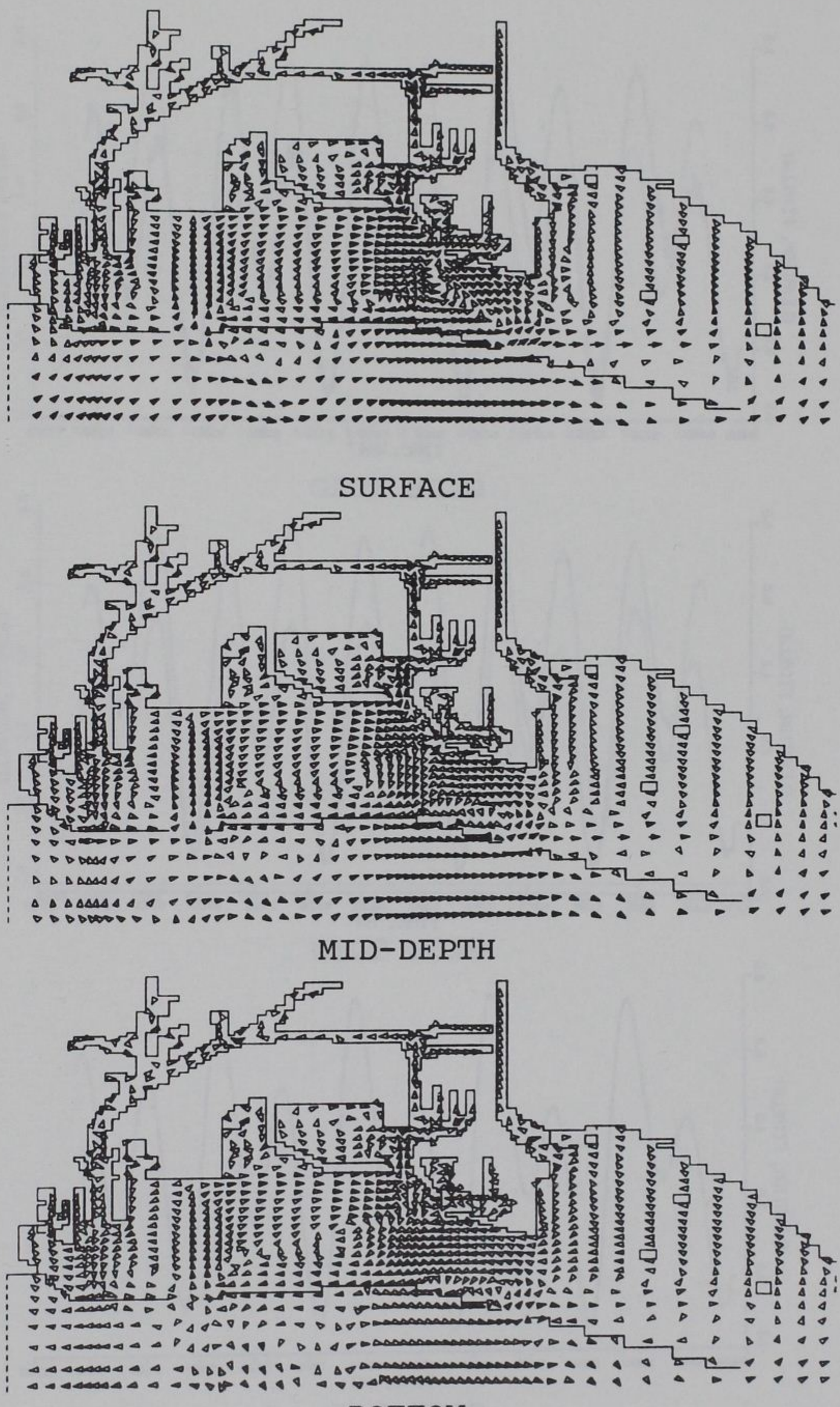

CIRCULATION PATTERNS

⟶ 1 FT/SEC

VERIFICATION PERIOD

SLACK WATER

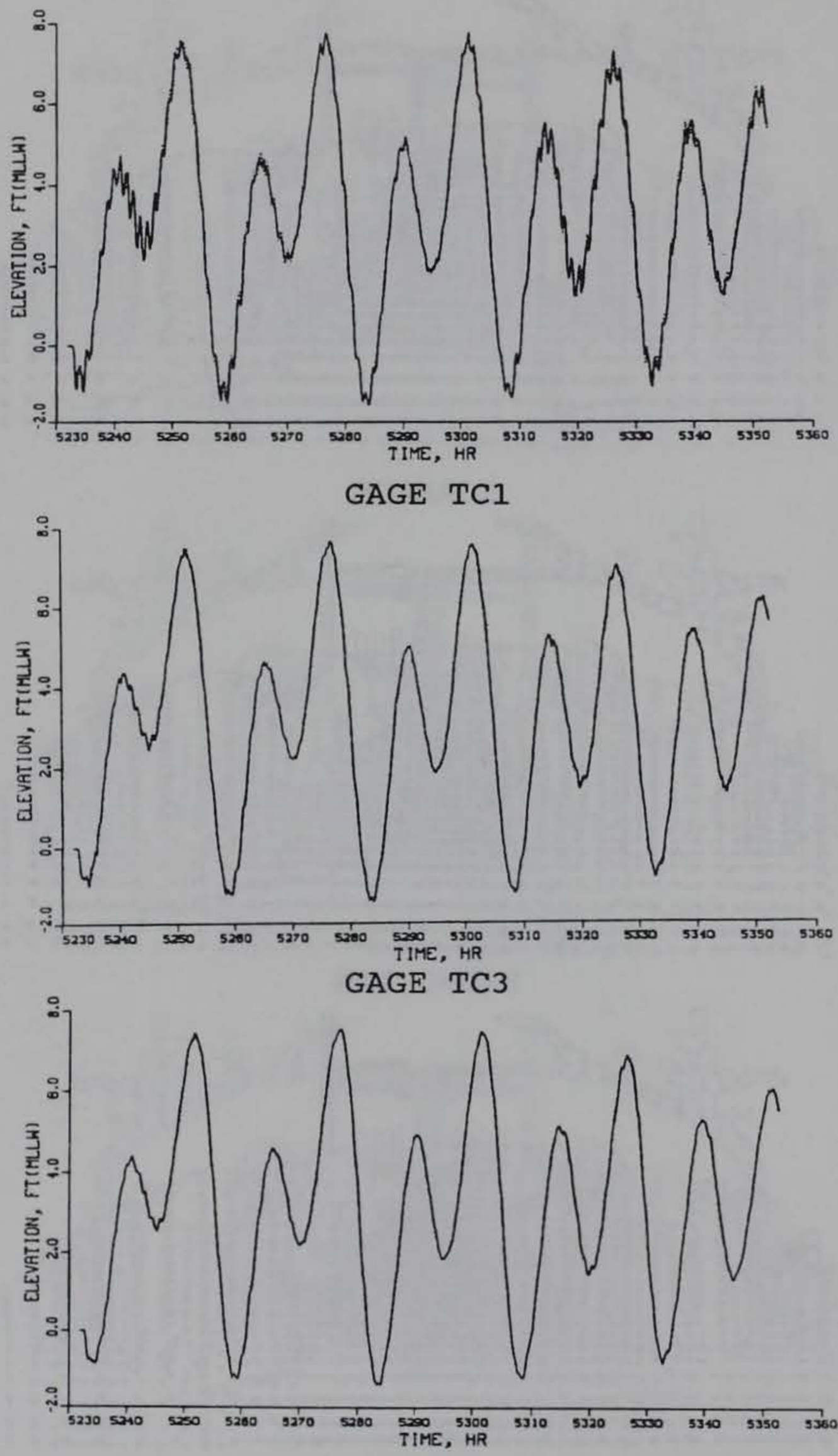

GAGE TC1

GAGE TC3

GAGE TC5

TIDAL ELEVATIONS **CALIBRATION PERIOD**

PLAN (SOLID) VS EXISTING (DOTTED) CONDITIONS

PLATE 61

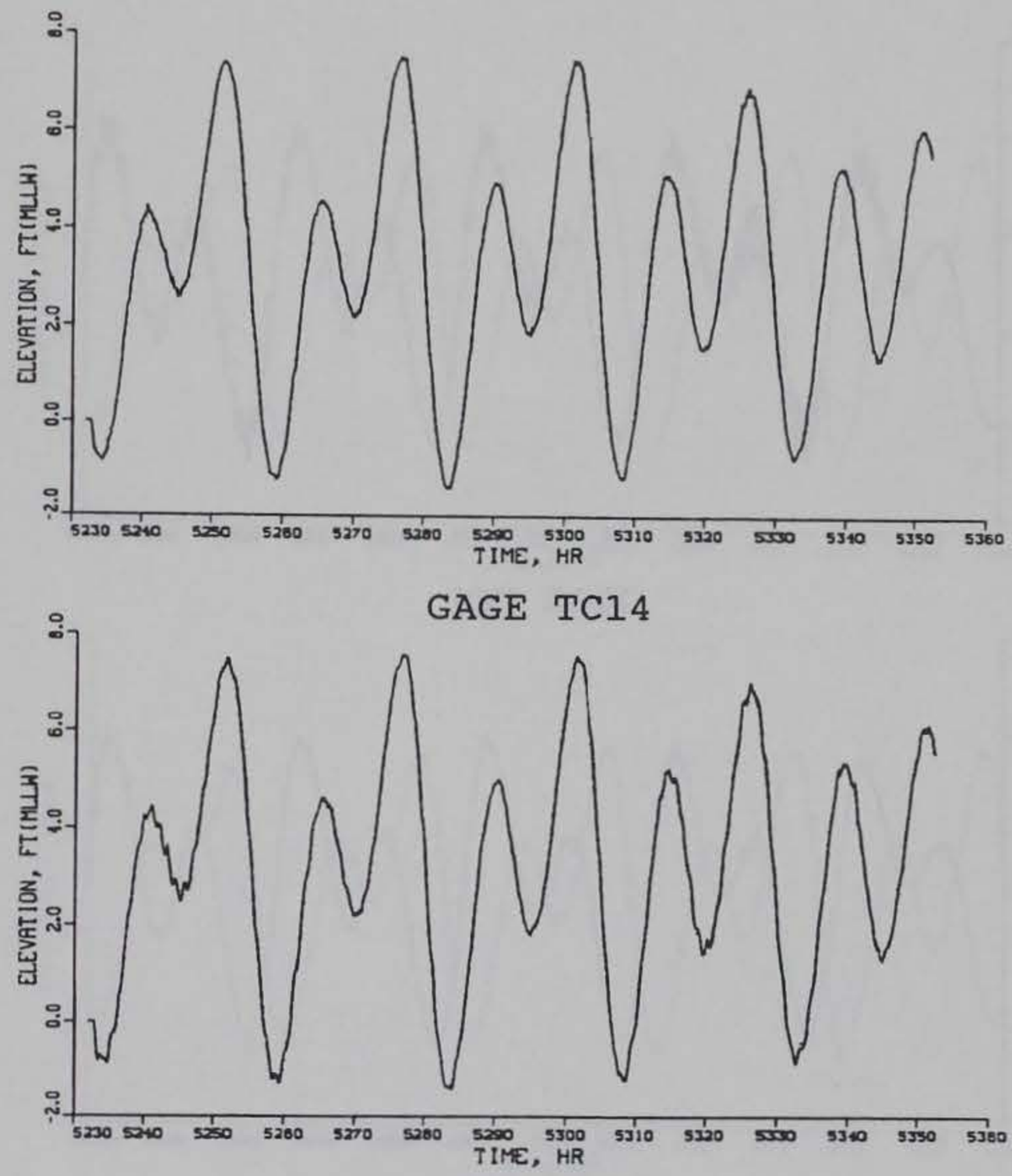

GAGE TC14

GAGE TC17

TIDAL ELEVATIONS CALIBRATION PERIOD

PLAN (SOLID) VS EXISTING (DOTTED) CONDITIONS

PLATE 62

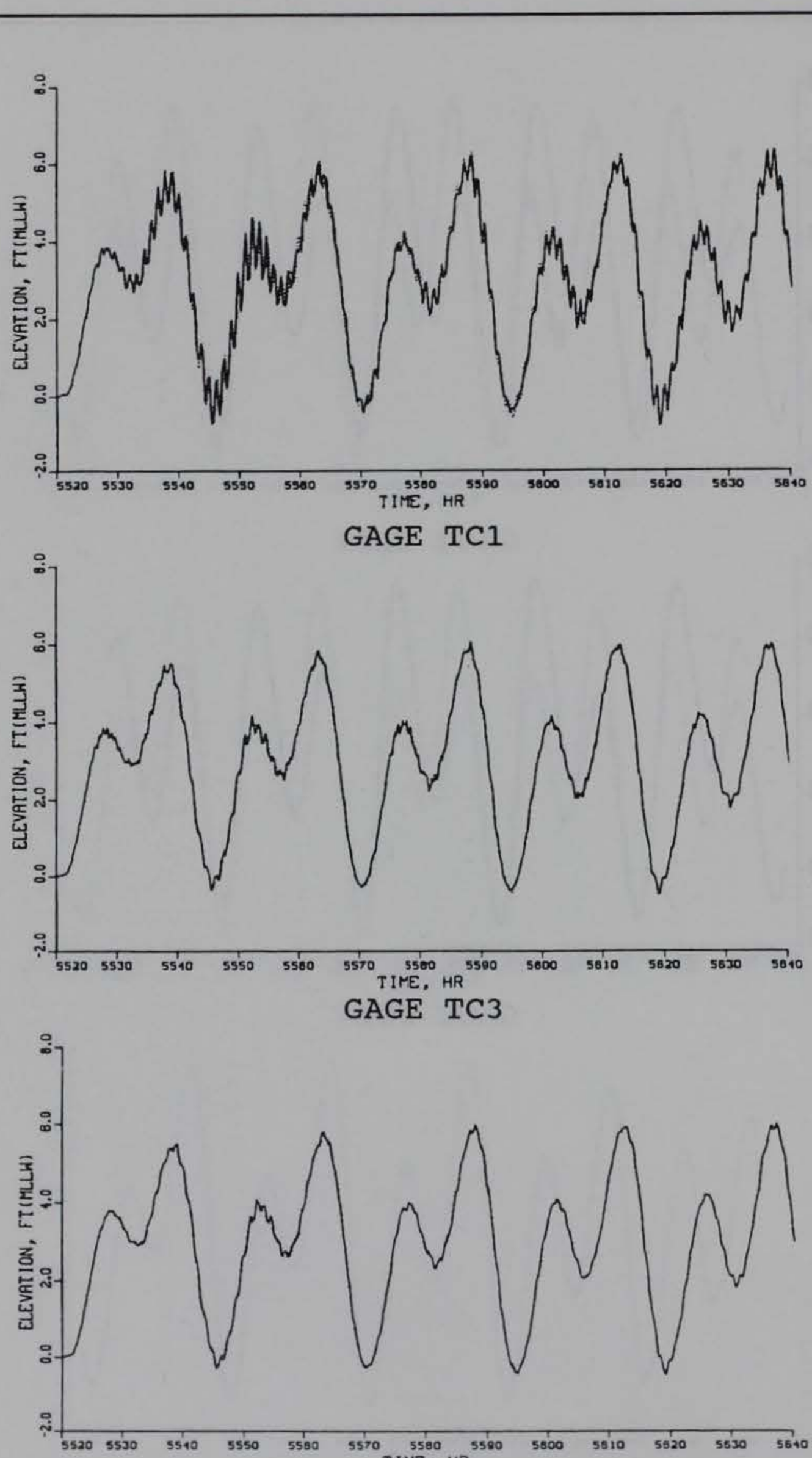

TIDAL ELEVATIONS VERIFICATION PERIOD

PLAN (SOLID) VS EXISTING (DOTTED) CONDITIONS

PLATE 63

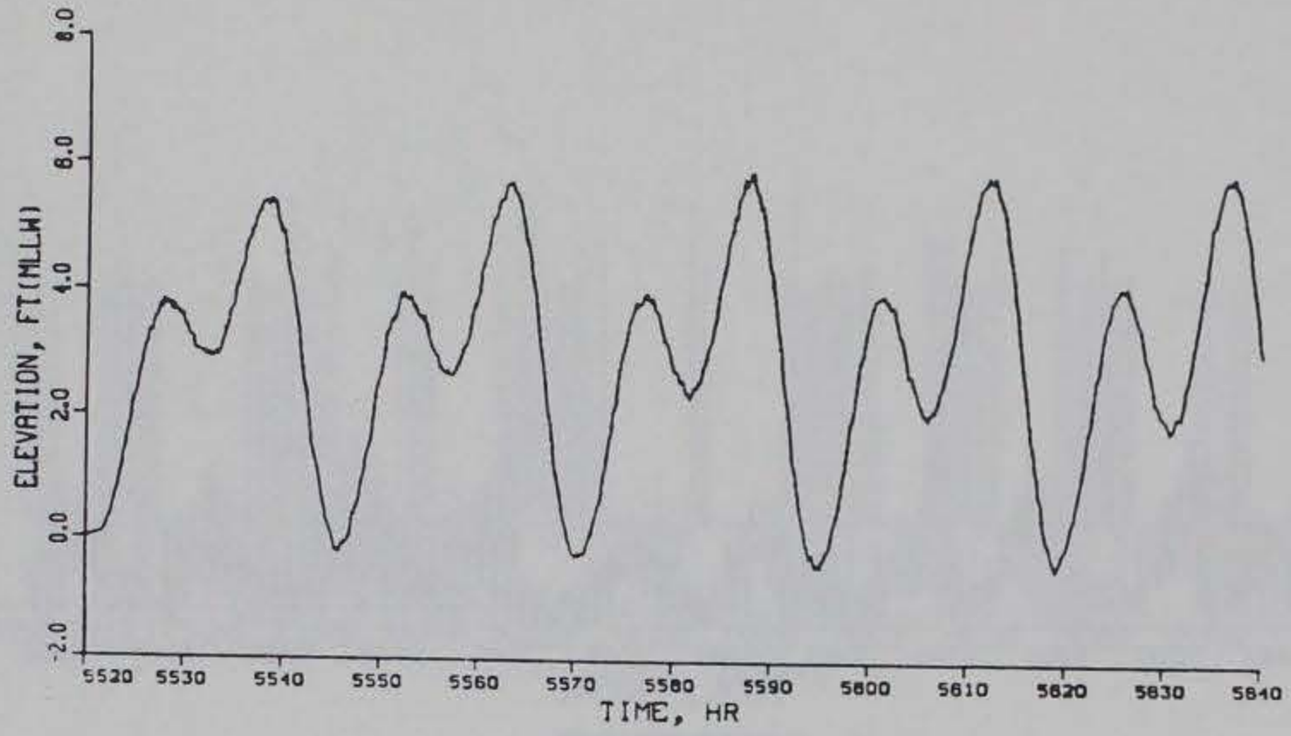

GAGE TC14

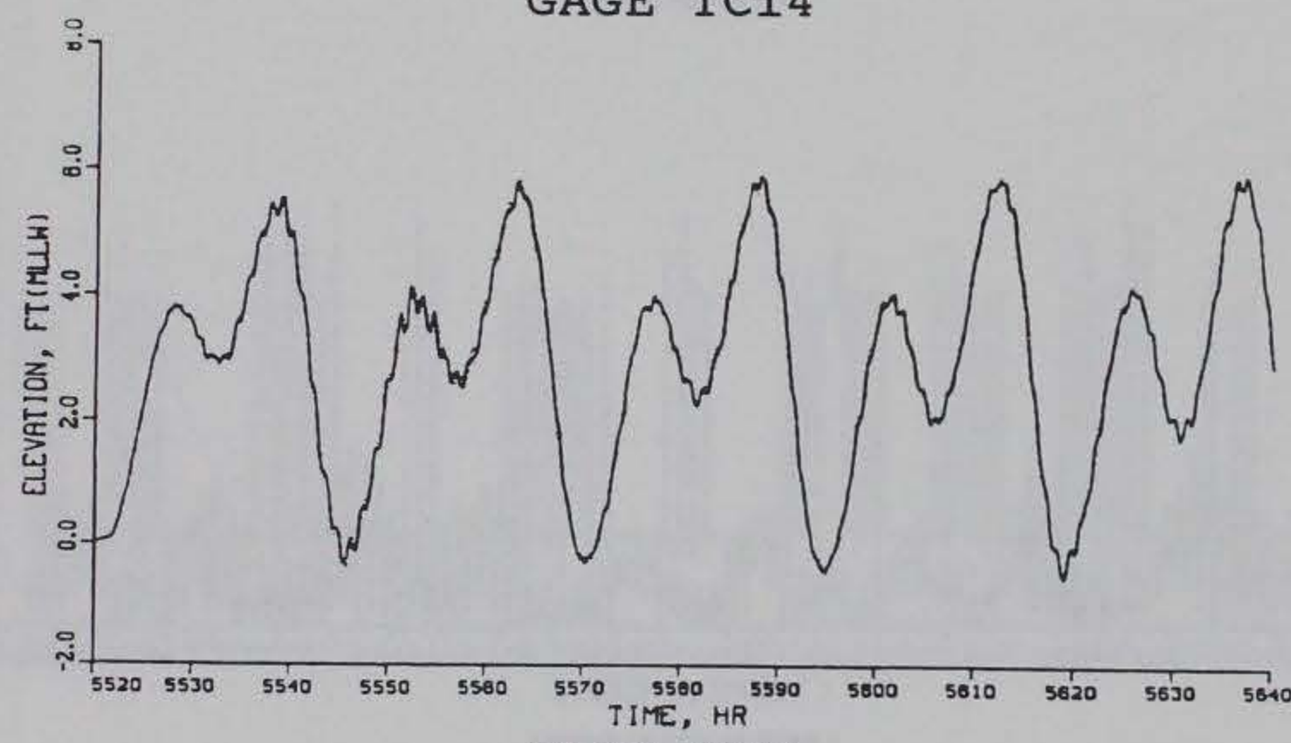

GAGE TC17

TIDAL ELEVATIONS **VERIFICATION PERIOD**

PLAN (SOLID) VS EXISTING (DOTTED) CONDITIONS

PLATE 64

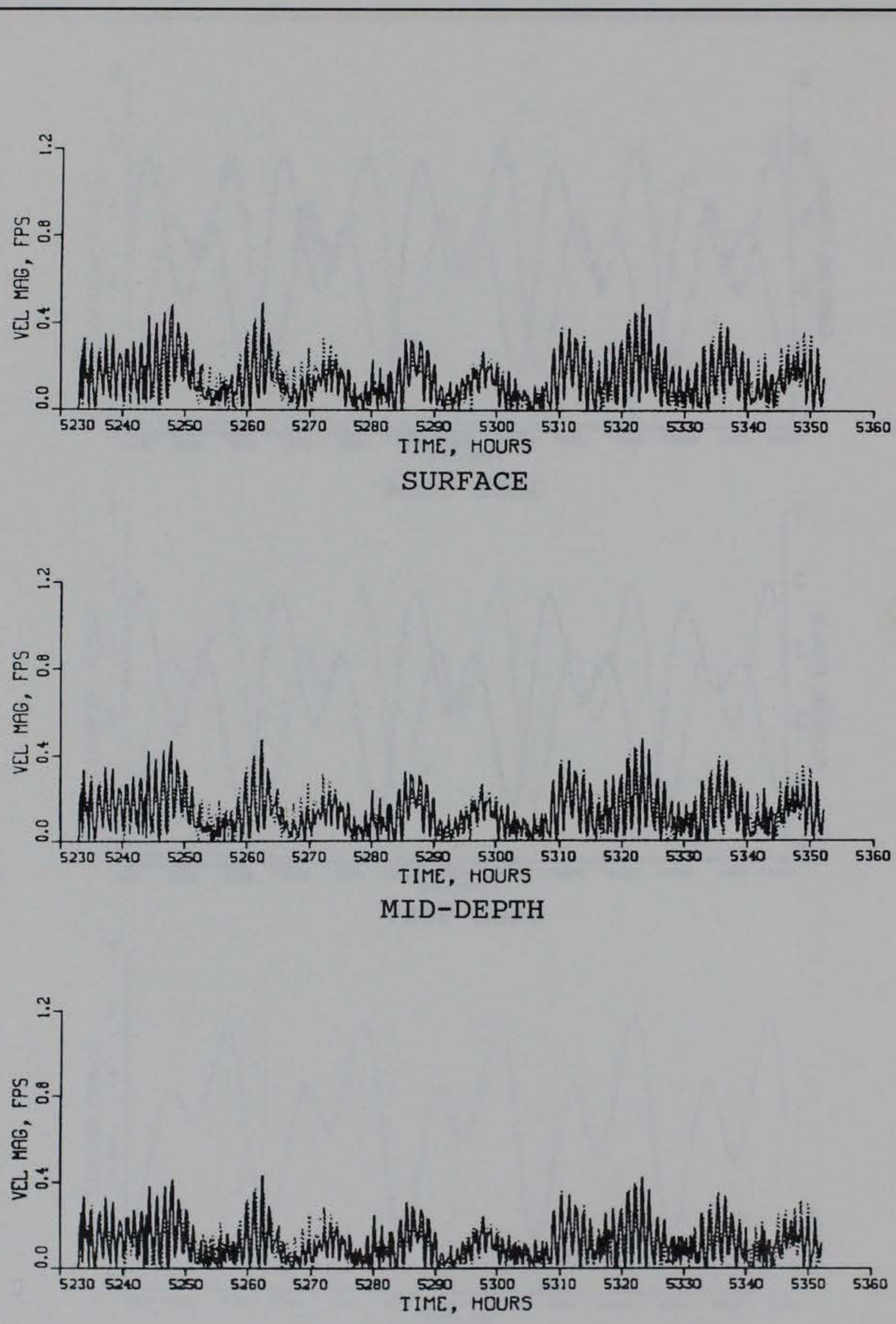

TIDAL VELOCITY **CALIBRATION PERIOD**

MAGNITUDE GAGE C1

PLAN (SOLID) VS EXISTING (DOTTED) CONDITIONS

PLATE 65

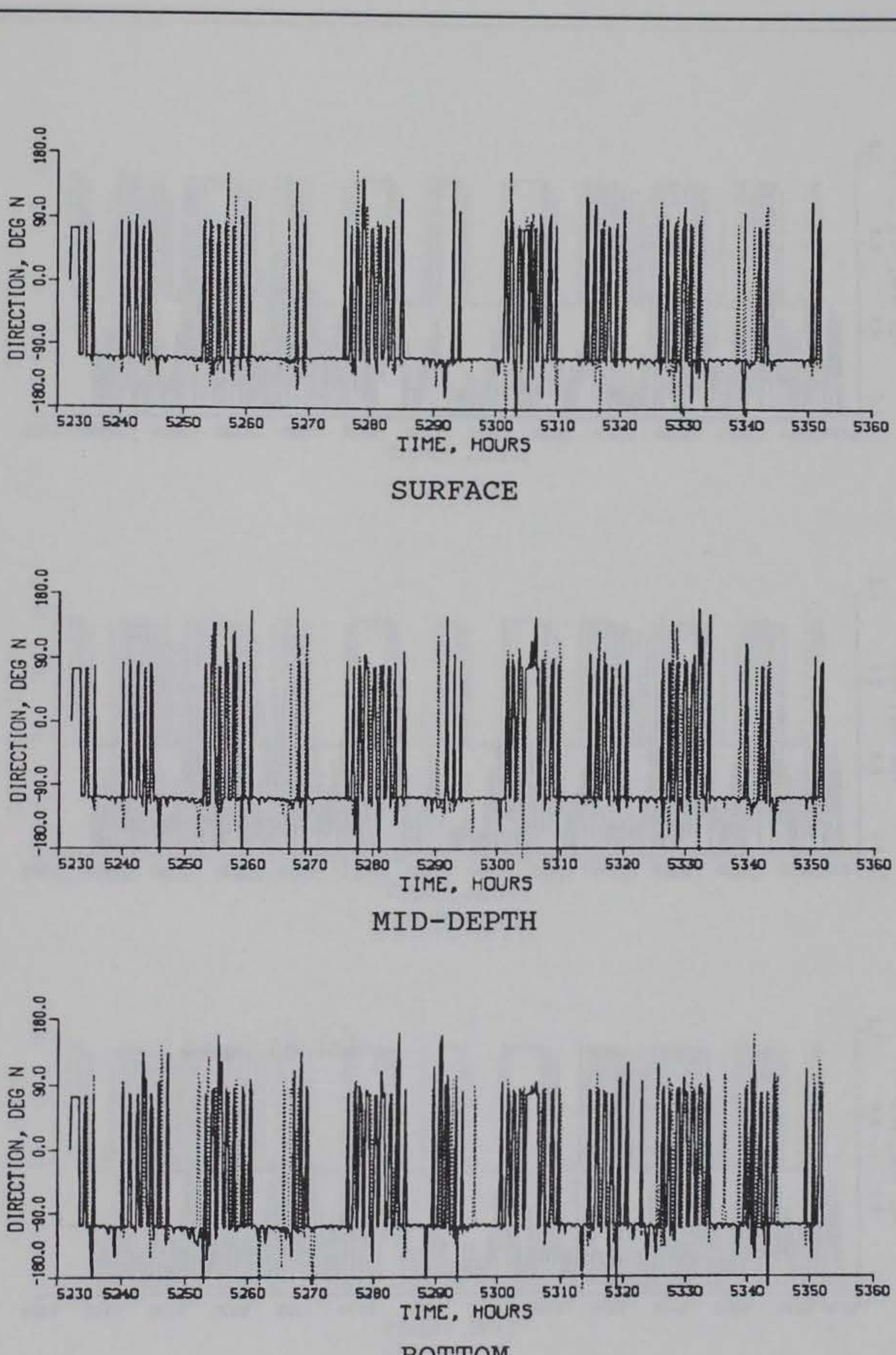

TIDAL VELOCITY

CALIBRATION PERIOD

DIRECTION

GAGE C1

PLAN (SOLID) VS EXISTING (DOTTED) CONDITIONS

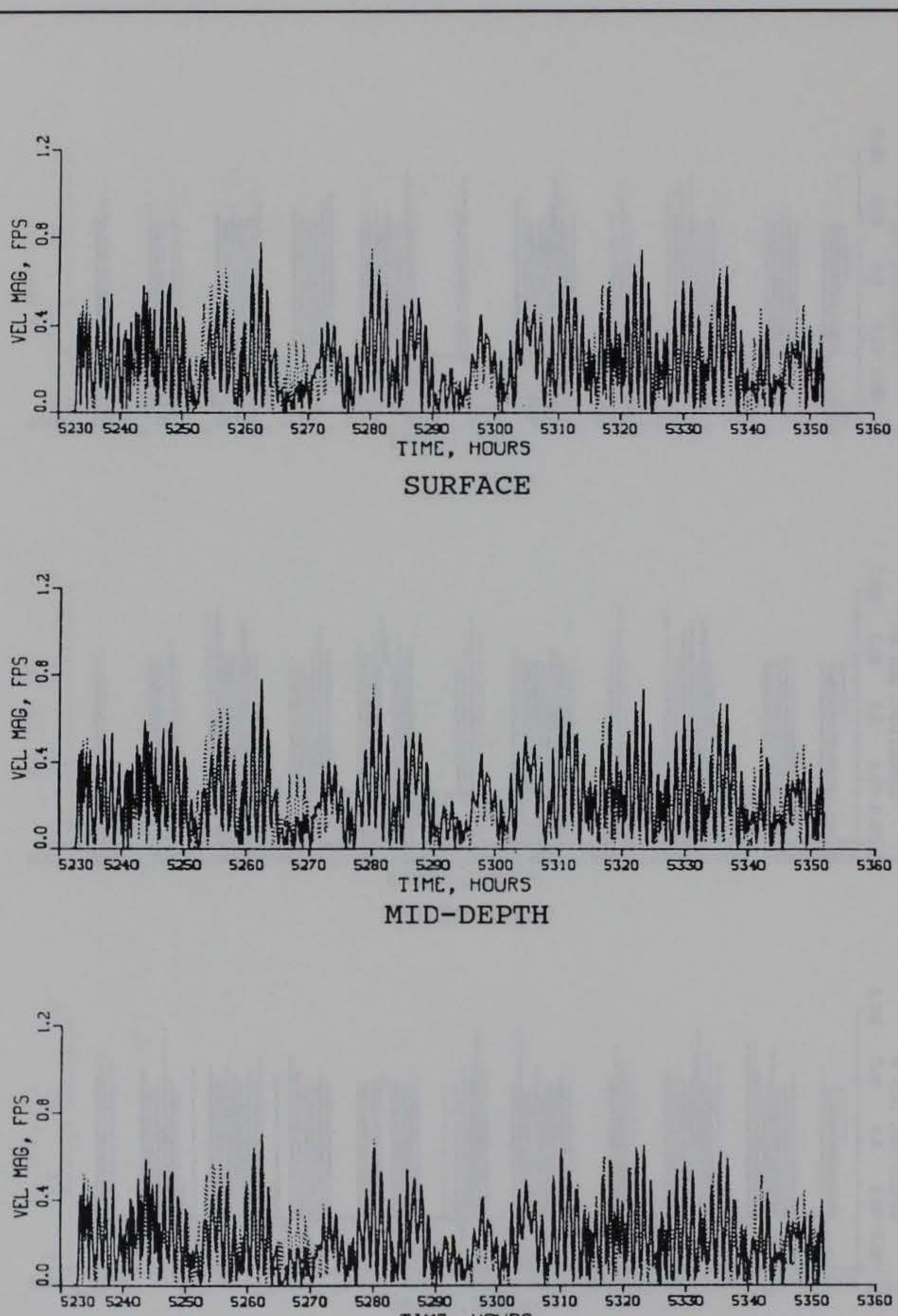

TIDAL VELOCITY **CALIBRATION PERIOD**

MAGNITUDE GAGE C2

PLAN (SOLID) VS EXISTING (DOTTED) CONDITIONS

PLATE 67

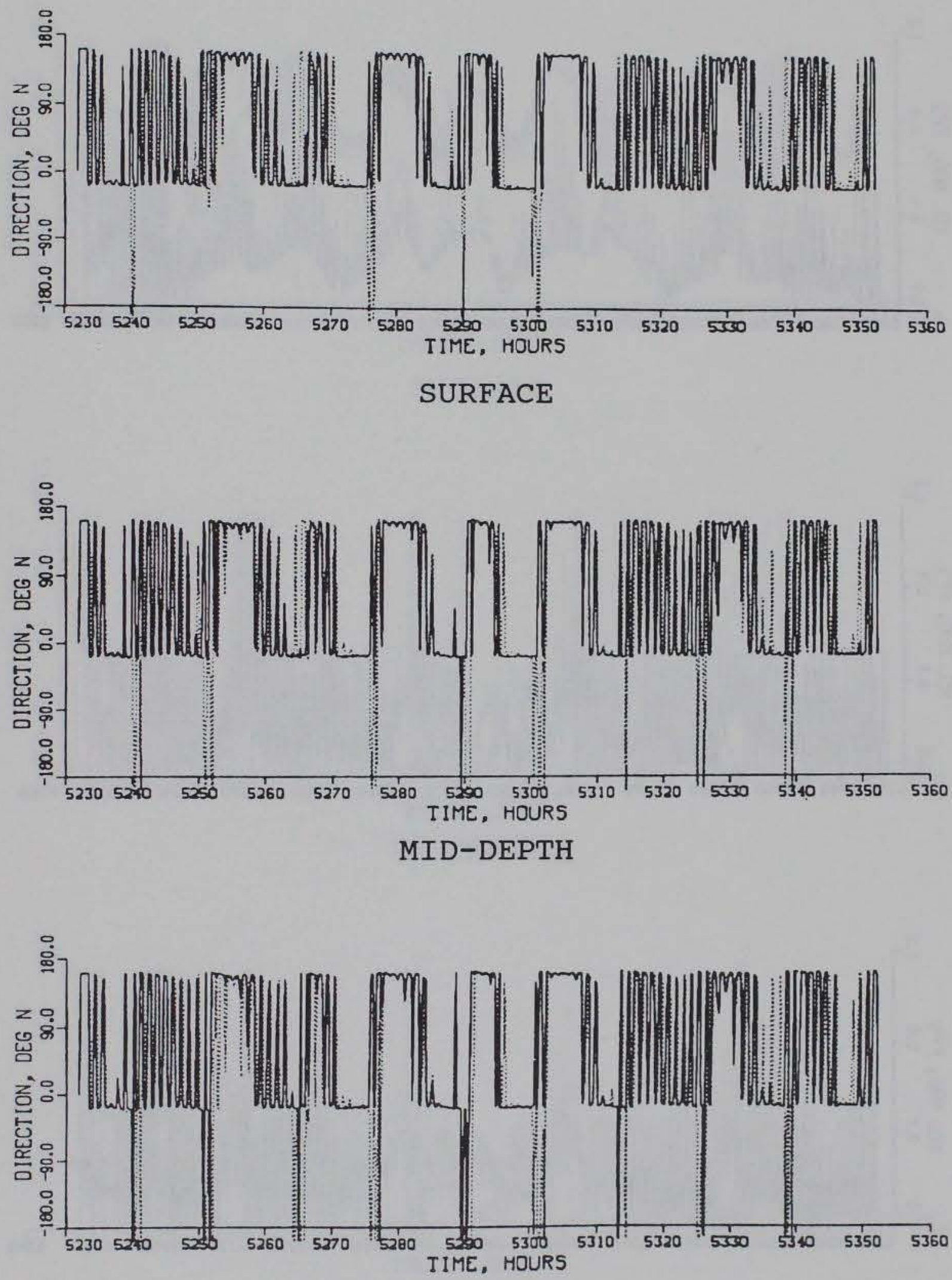

SURFACE

MID-DEPTH

BOTTOM

TIDAL VELOCITY — CALIBRATION PERIOD

DIRECTION — GAGE C2

PLAN (SOLID) VS EXISTING (DOTTED) CONDITIONS

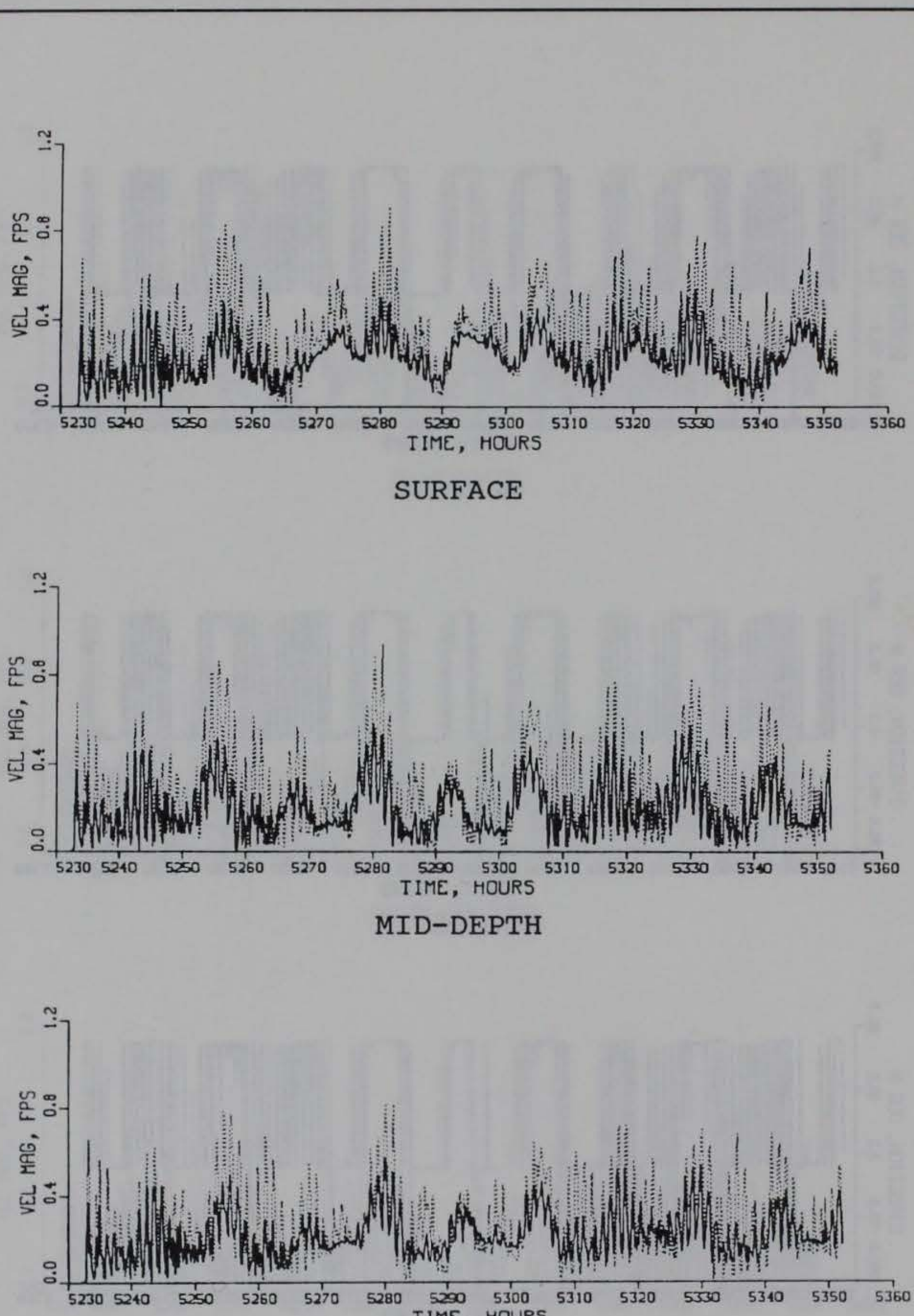

SURFACE

MID-DEPTH

BOTTOM

TIDAL VELOCITY **CALIBRATION PERIOD**

MAGNITUDE GAGE C3

PLAN (SOLID) VS EXISTING (DOTTED) CONDITIONS

PLATE 69

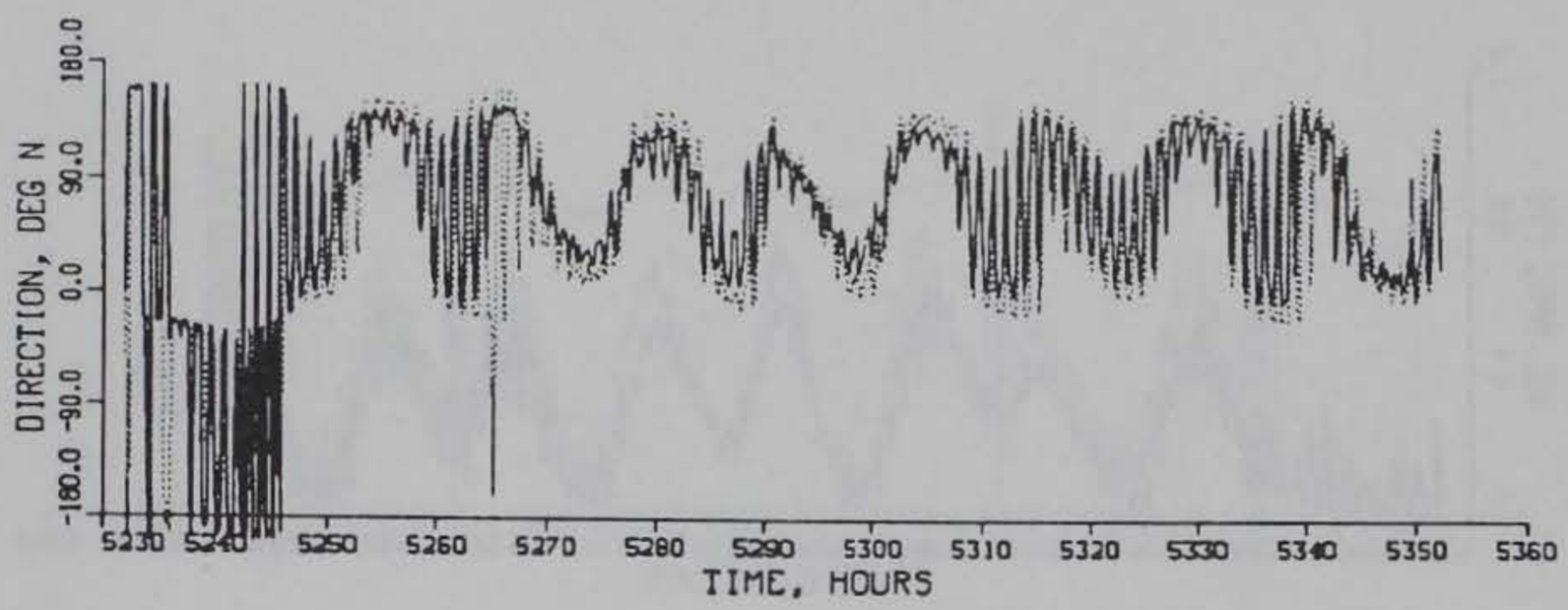

SURFACE

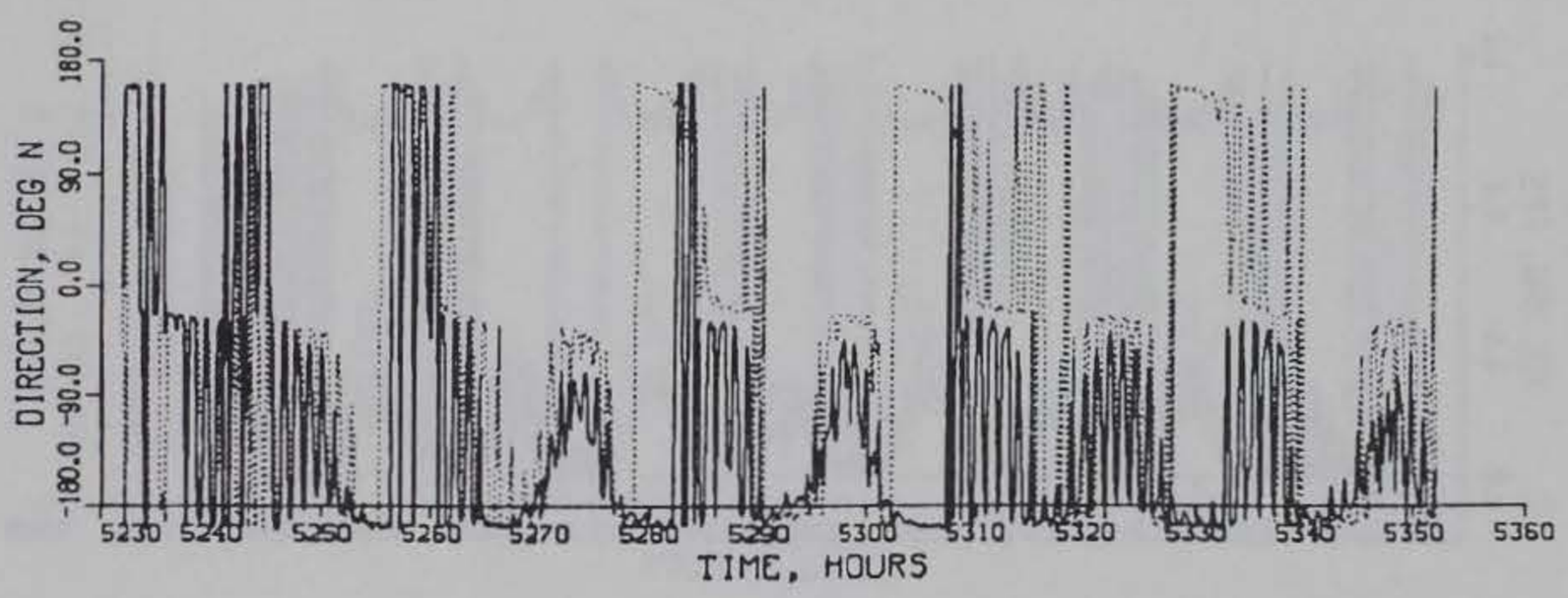

MID-DEPTH

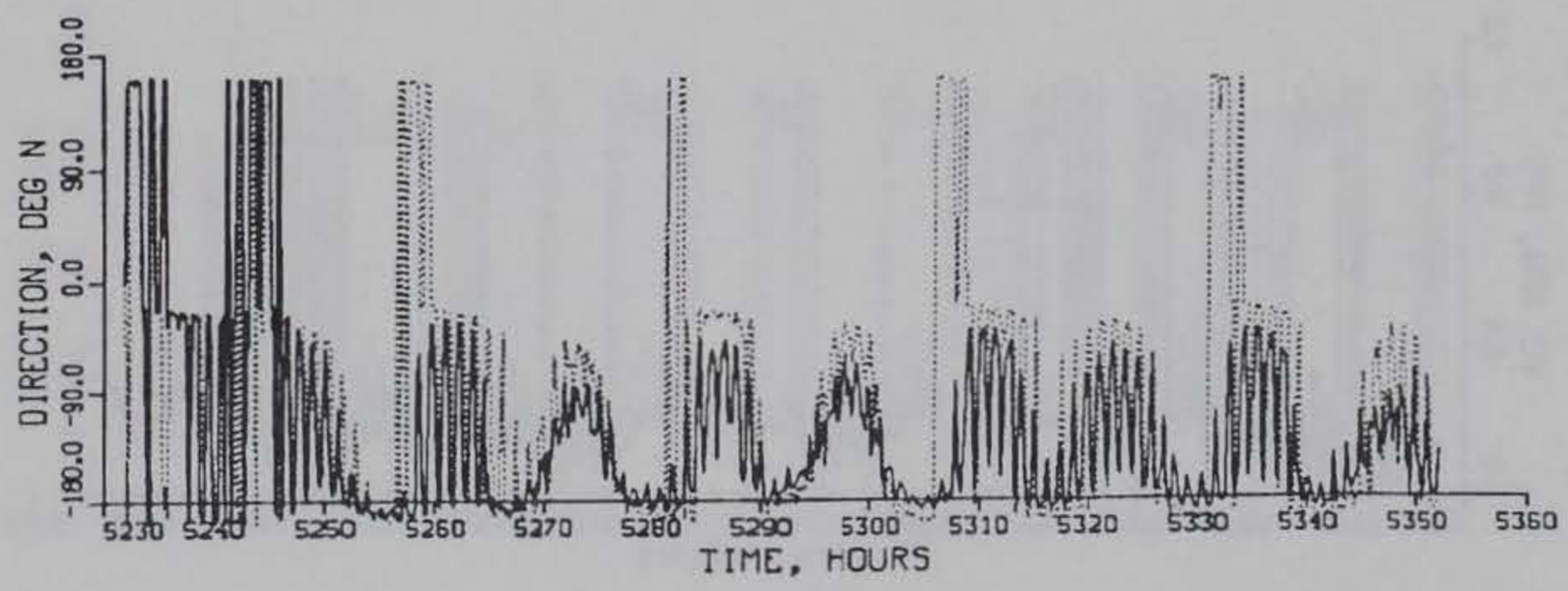

BOTTOM

TIDAL VELOCITY

CALIBRATION PERIOD

DIRECTION

GAGE C3

PLAN (SOLID) VS EXISTING (DOTTED) CONDITIONS

PLATE 70

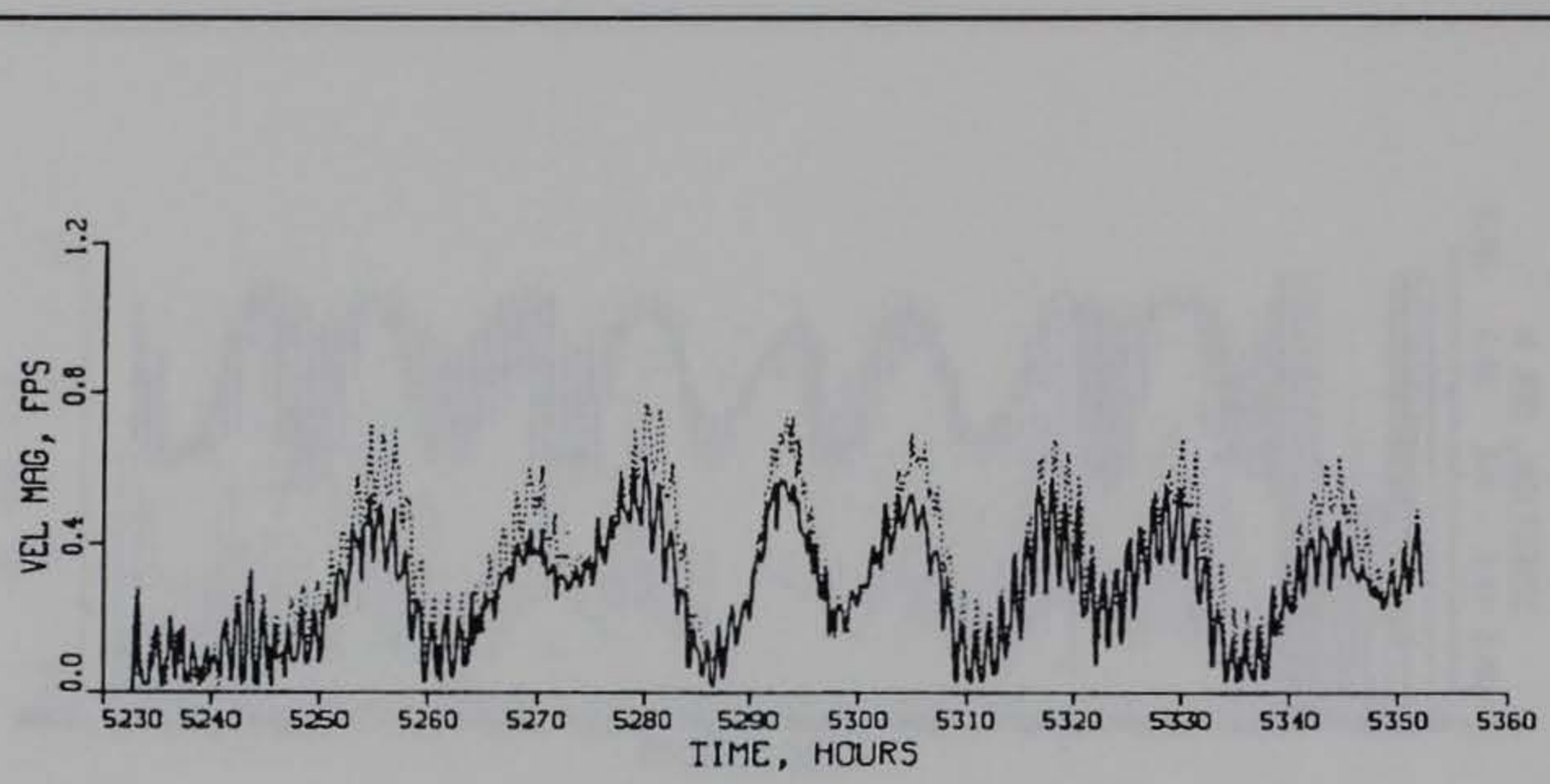

SURFACE

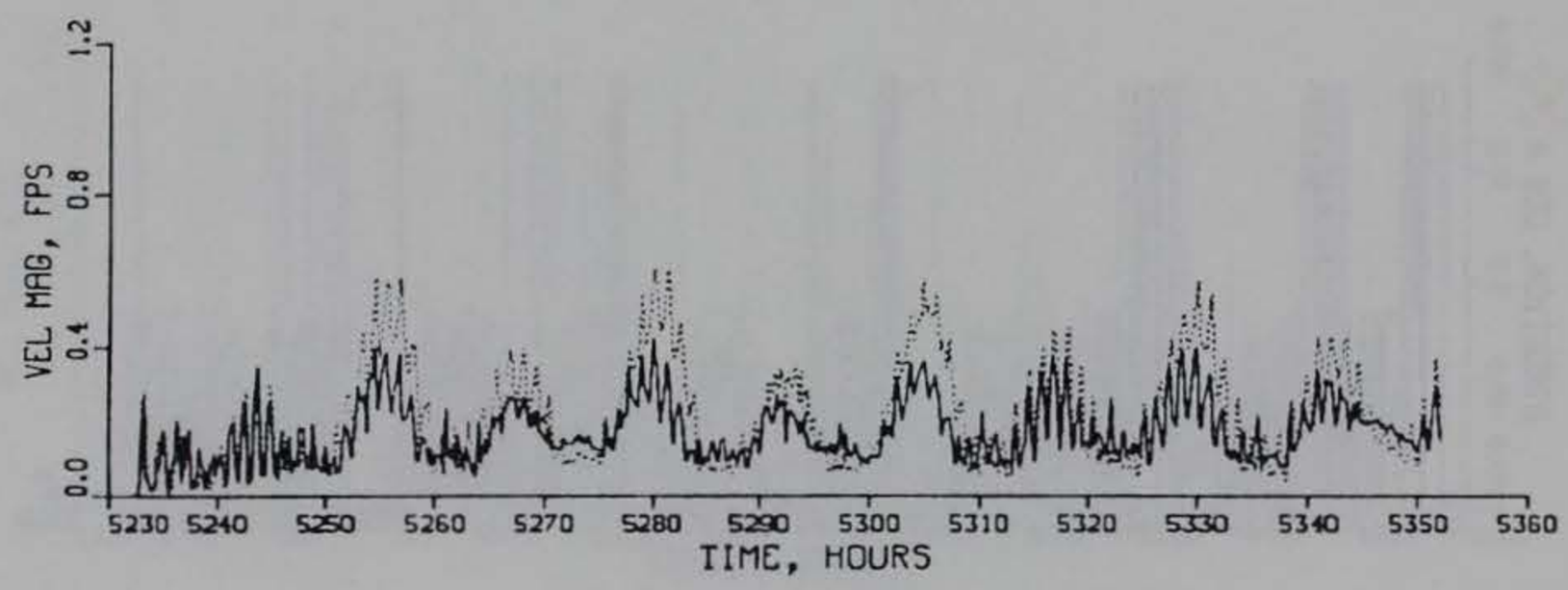

MID-DEPTH

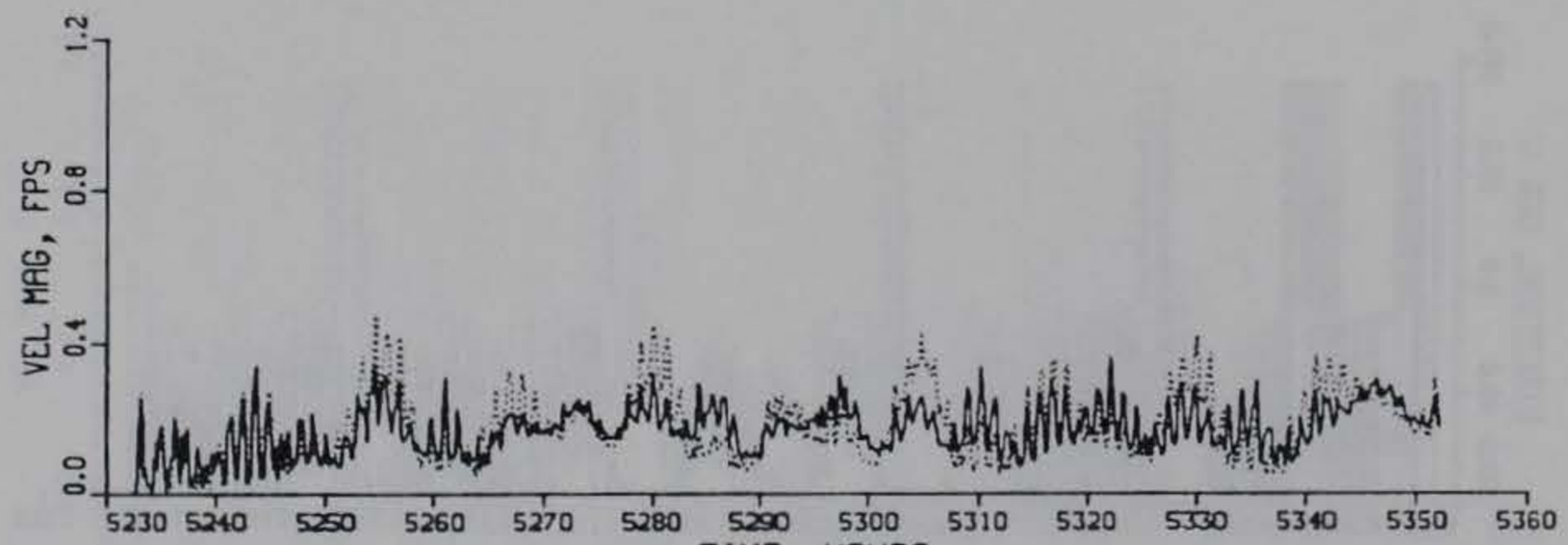

BOTTOM

TIDAL VELOCITY **CALIBRATION PERIOD**

MAGNITUDE GAGE C4

PLAN (SOLID) VS EXISTING (DOTTED) CONDITIONS

PLATE 71

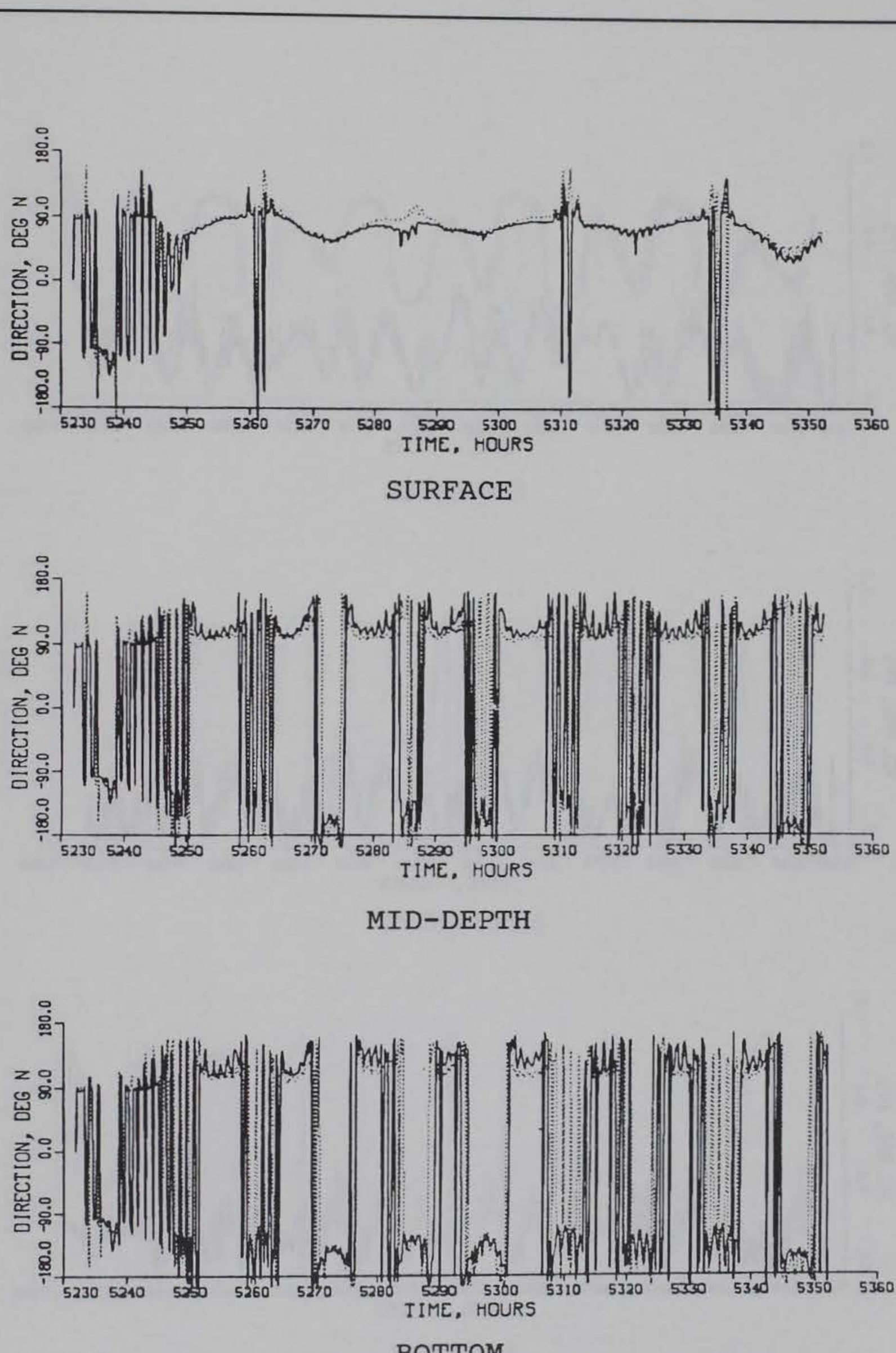

TIDAL VELOCITY **CALIBRATION PERIOD**

DIRECTION GAGE C4

PLAN (SOLID) VS EXISTING (DOTTED) CONDITIONS

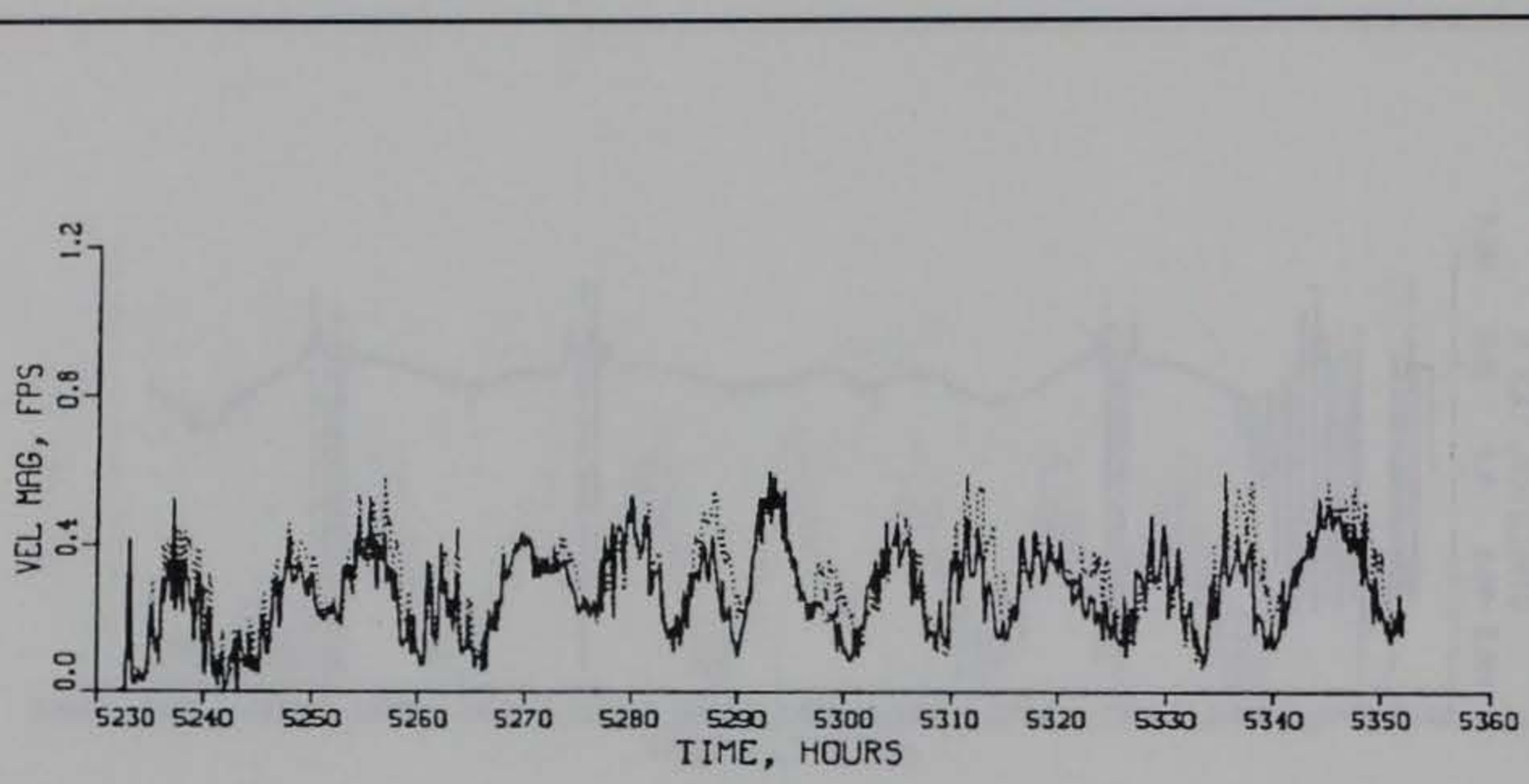

SURFACE

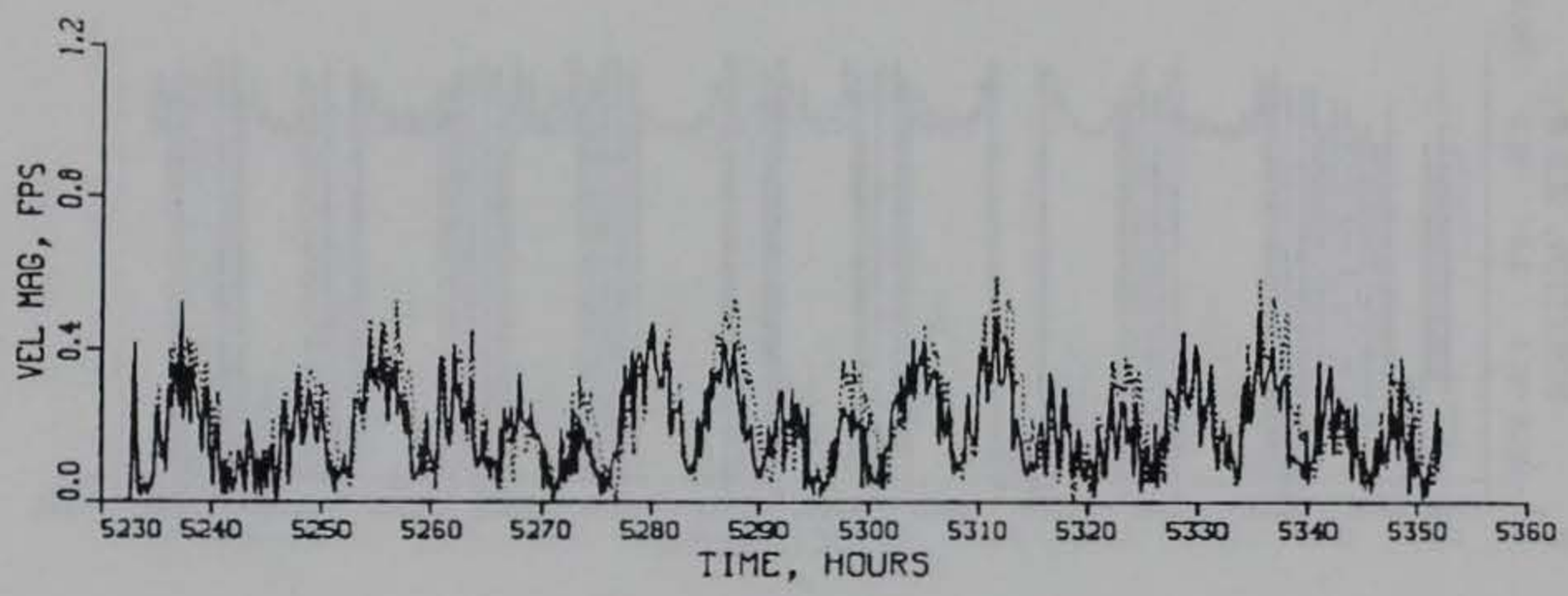

MID-DEPTH

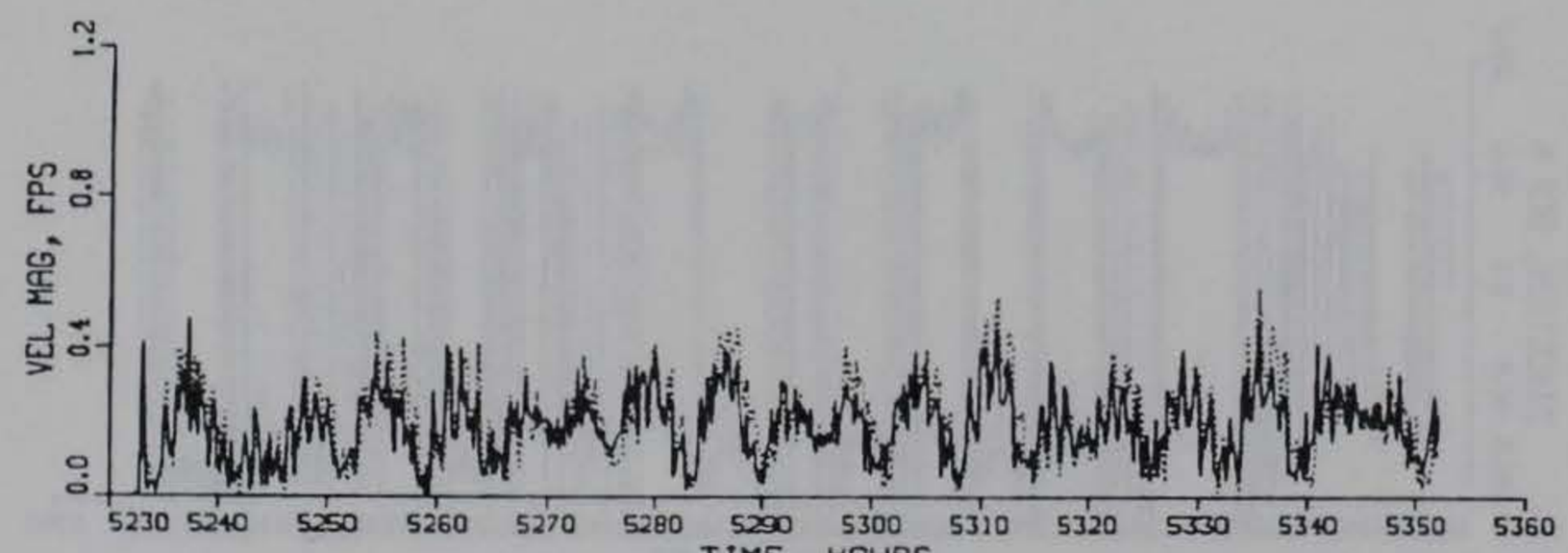

BOTTOM

TIDAL VELOCITY CALIBRATION PERIOD

MAGNITUDE GAGE C5

PLAN (SOLID) VS EXISTING (DOTTED) CONDITIONS

PLATE 73

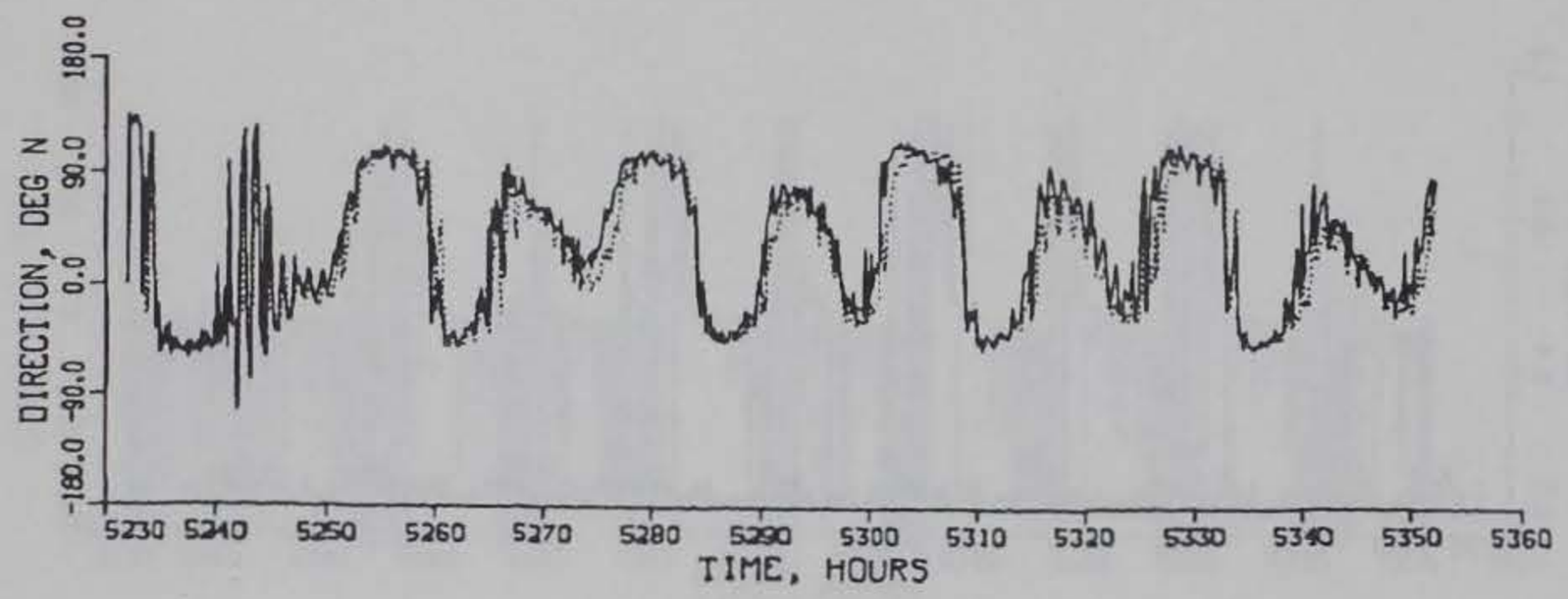

SURFACE

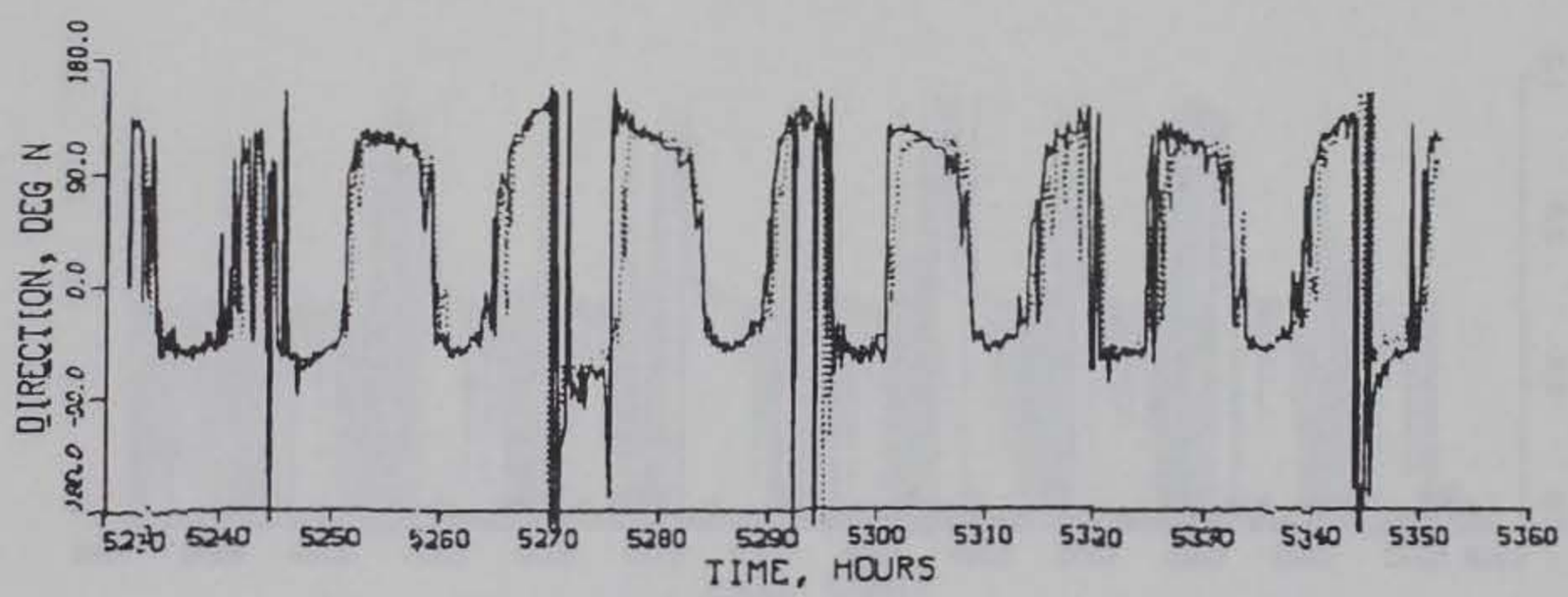

MID-DEPTH

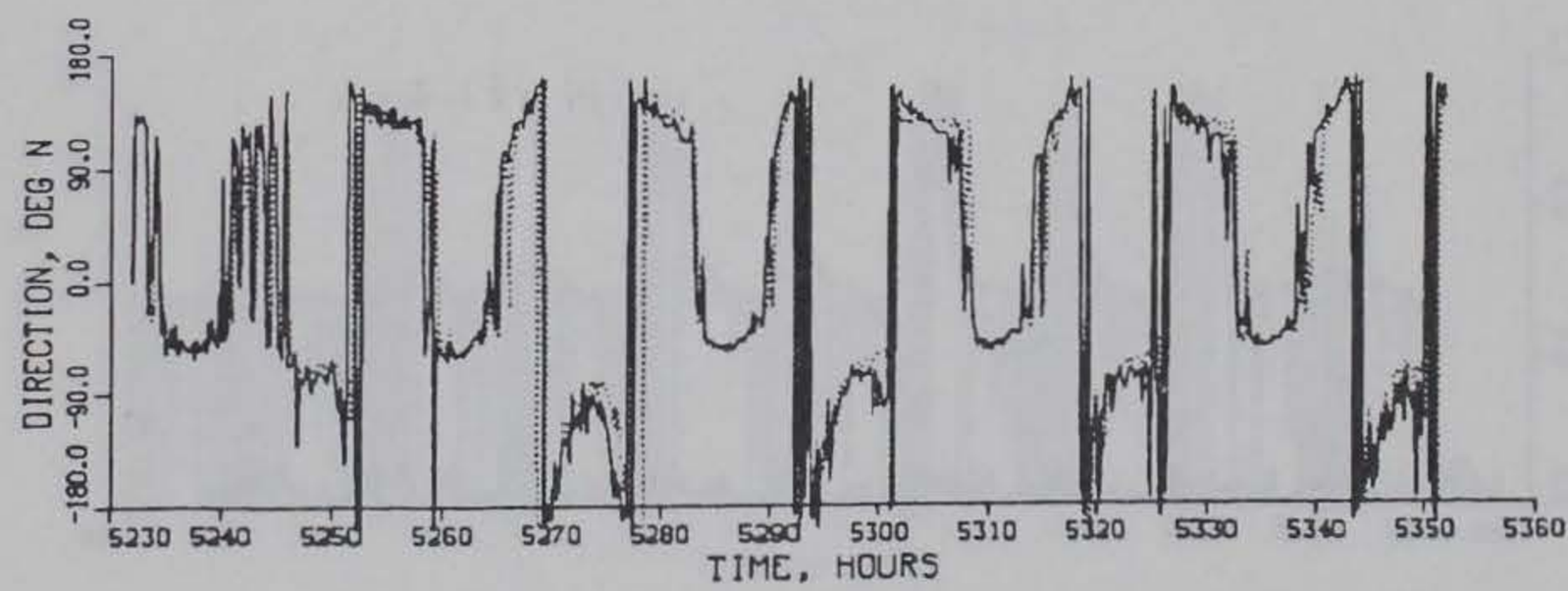

BOTTOM

TIDAL VELOCITY **CALIBRATION PERIOD**

DIRECTION GAGE C5

PLAN (SOLID) VS EXISTING (DOTTED) CONDITIONS

PLATE 74

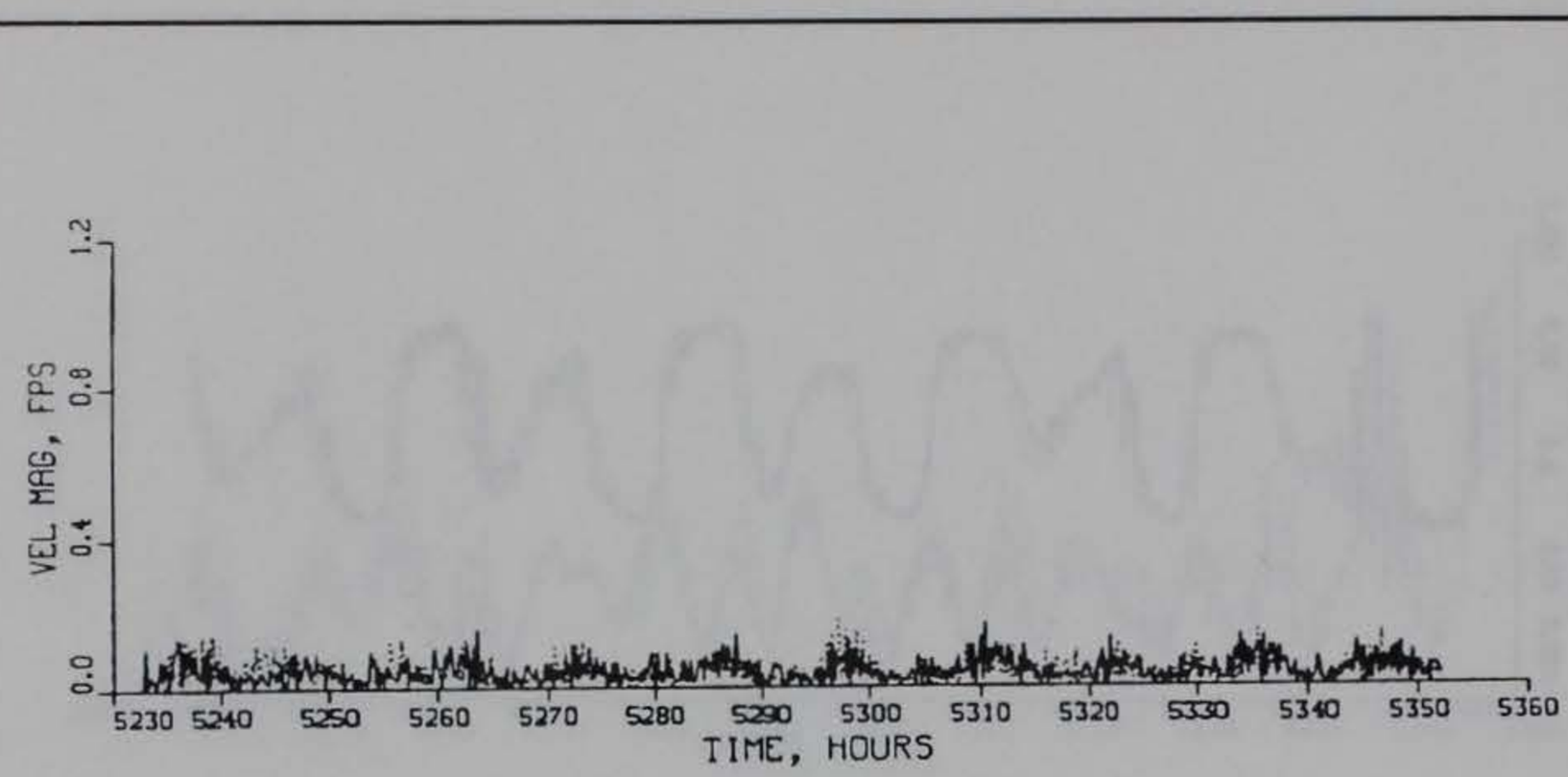

SURFACE

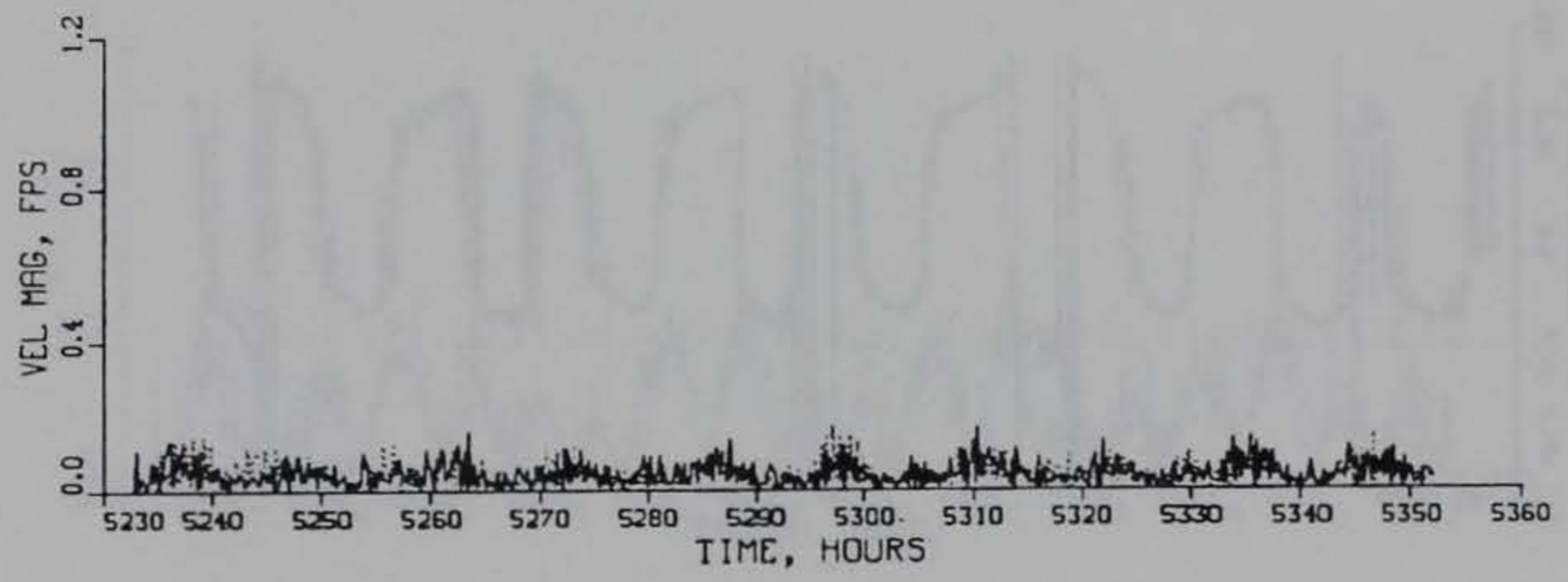

MID-DEPTH

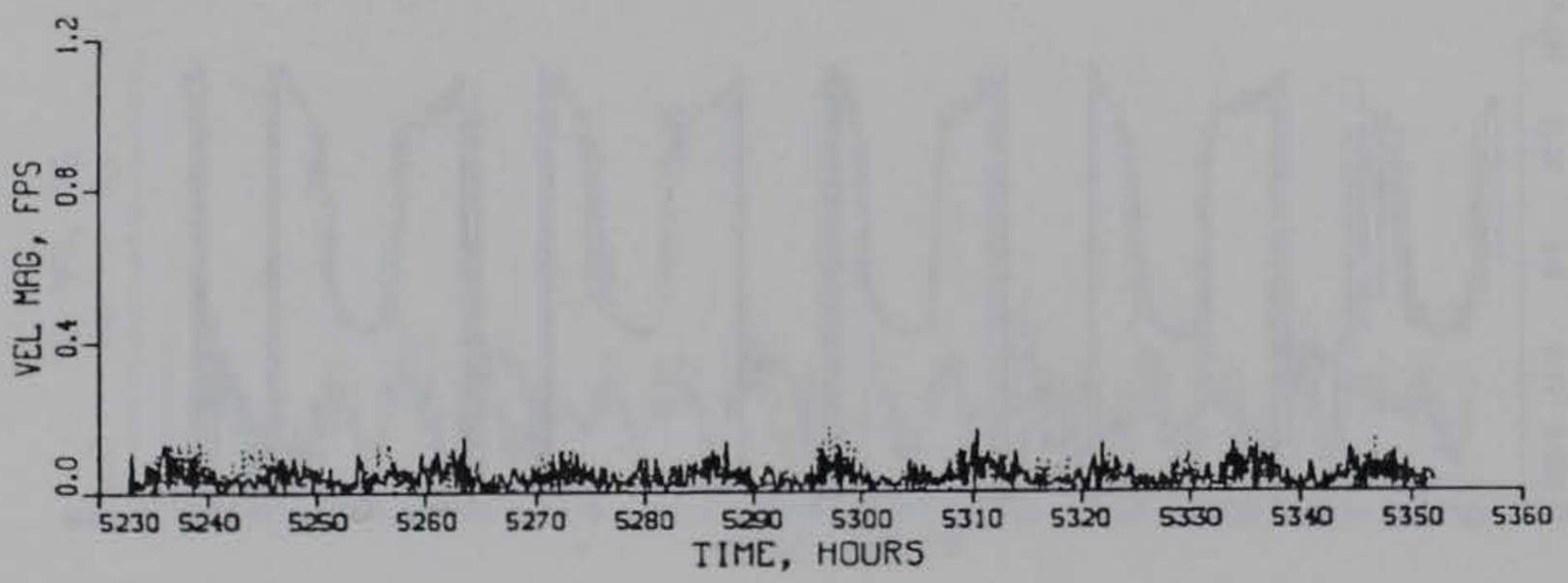

BOTTOM

TIDAL VELOCITY **CALIBRATION PERIOD**

MAGNITUDE GAGE C10

PLAN (SOLID) VS EXISTING (DOTTED) CONDITIONS

PLATE 75

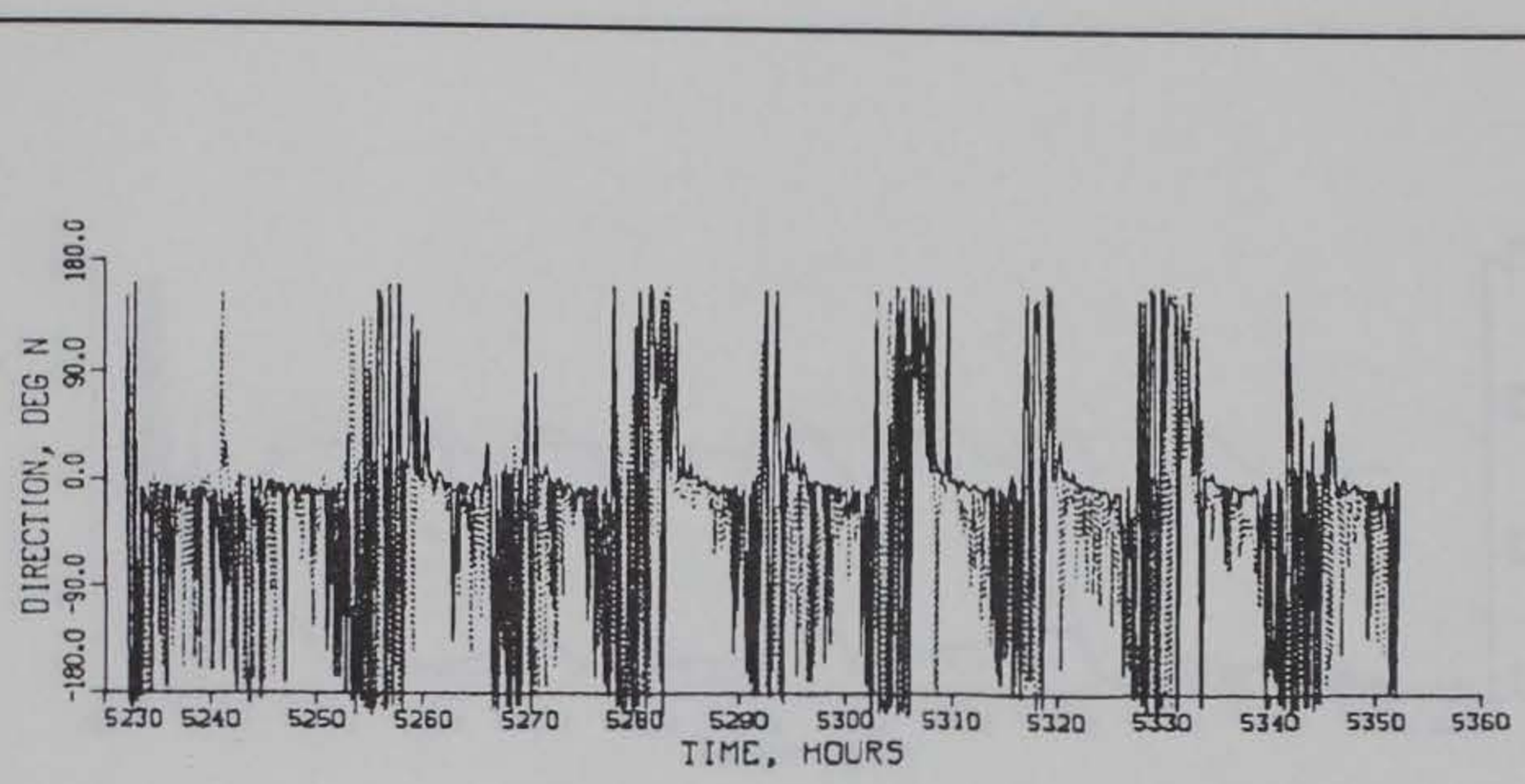

SURFACE

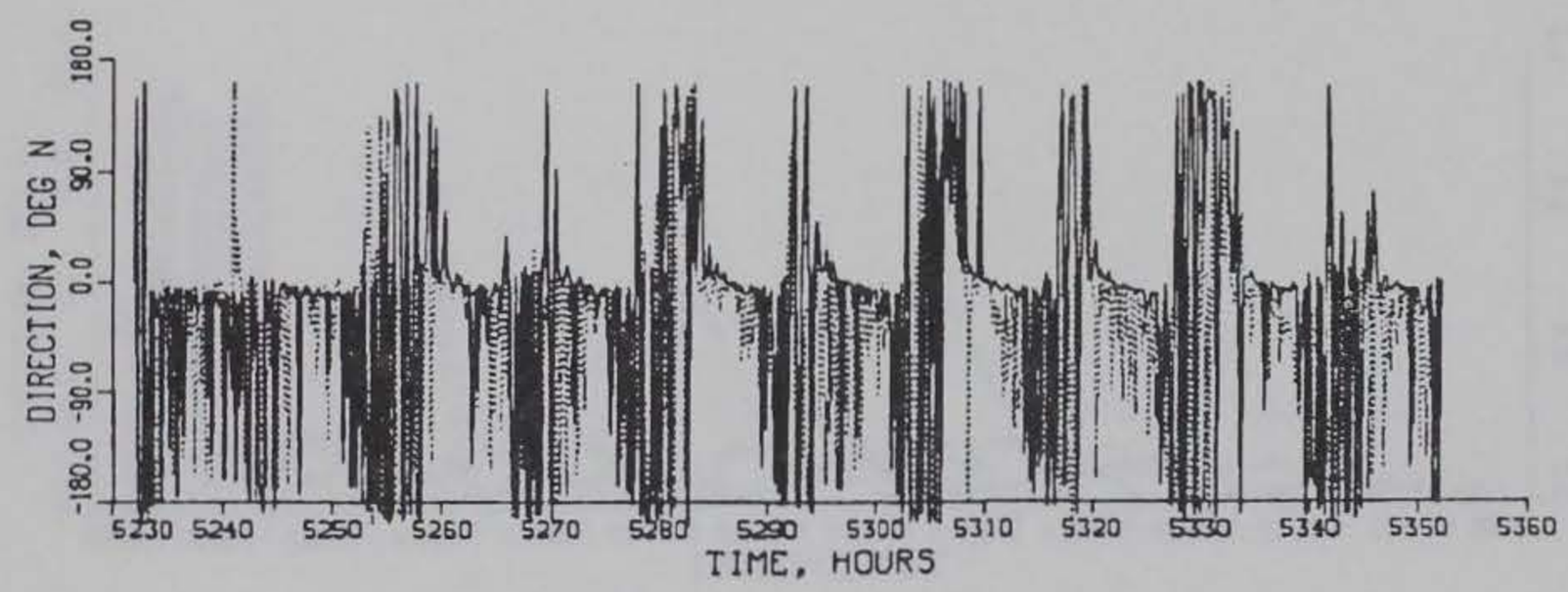

MID-DEPTH

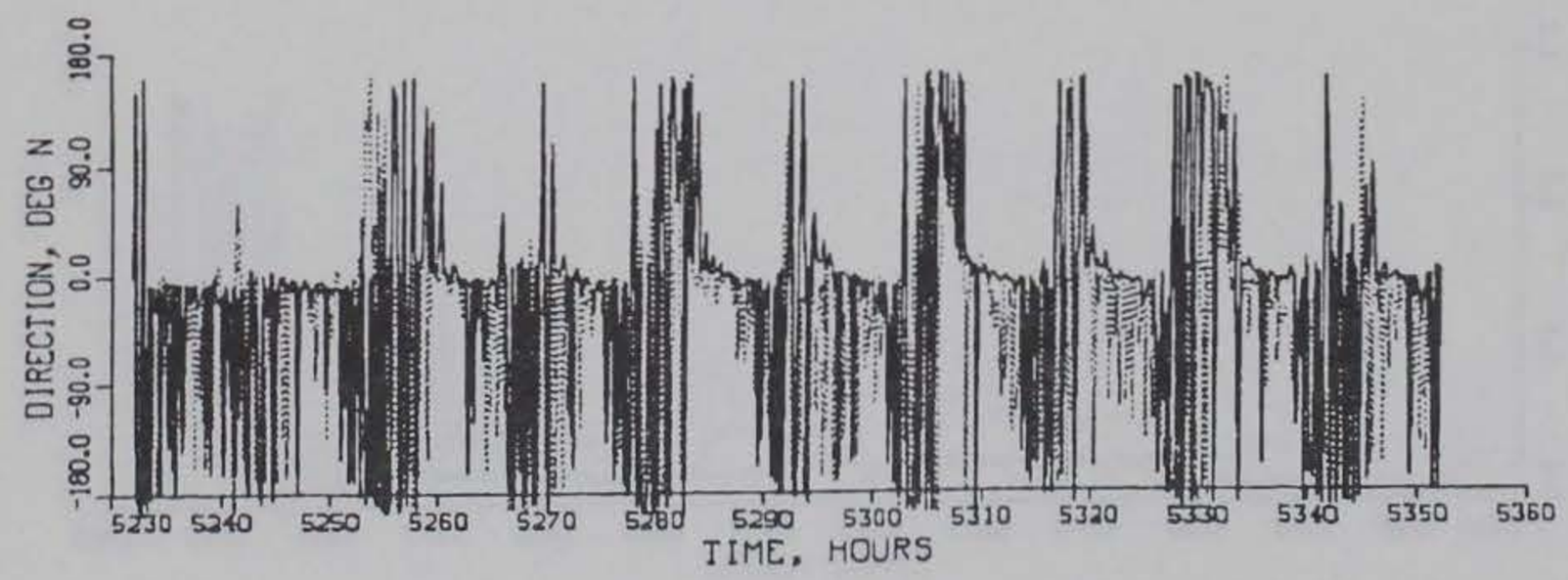

BOTTOM

TIDAL VELOCITY **CALIBRATION PERIOD**

DIRECTION GAGE C10

PLAN (SOLID) VS EXISTING (DOTTED) CONDITIONS

PLATE 76

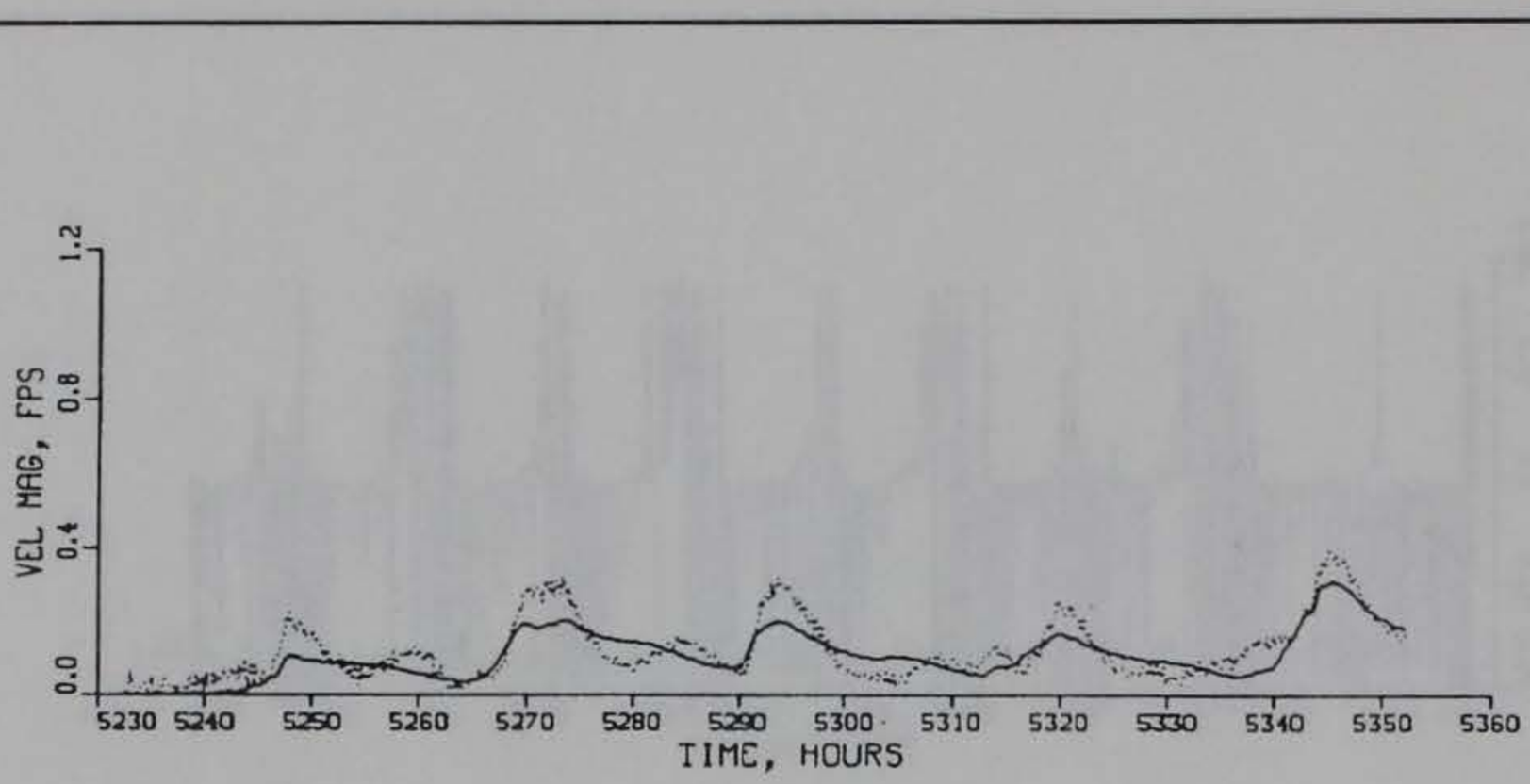

SURFACE

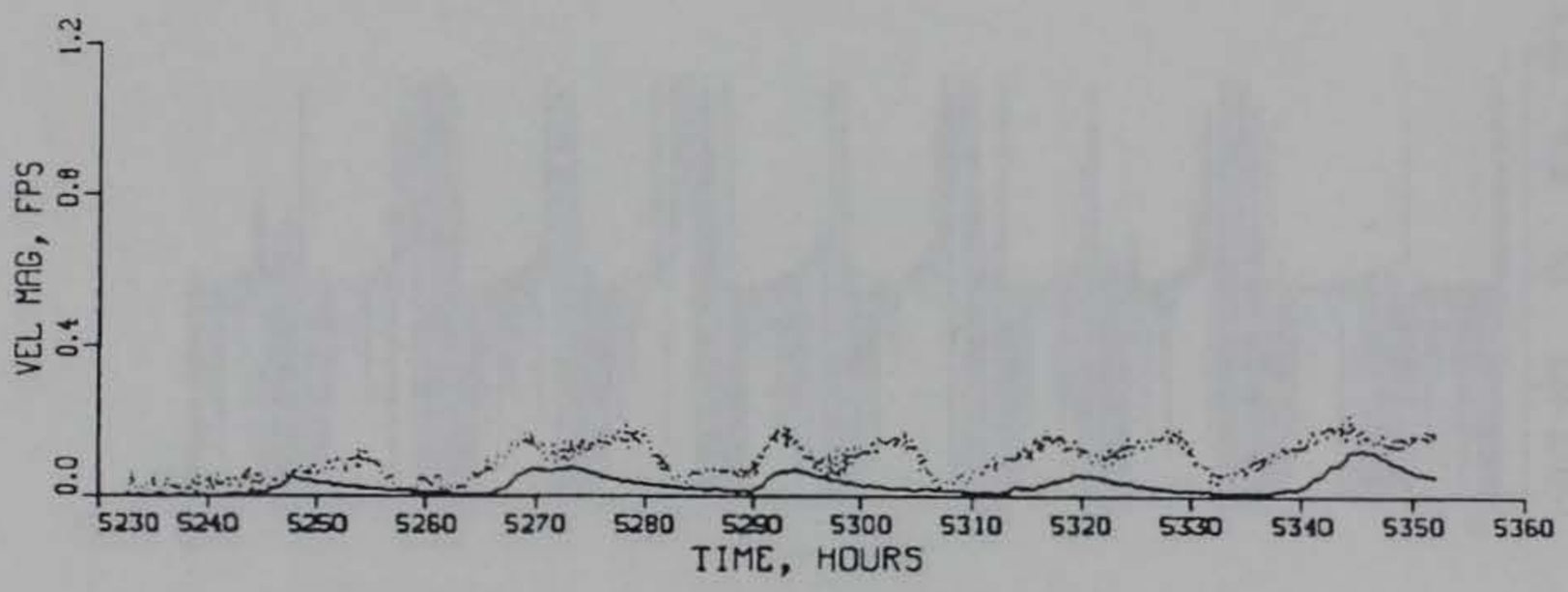

MID-DEPTH

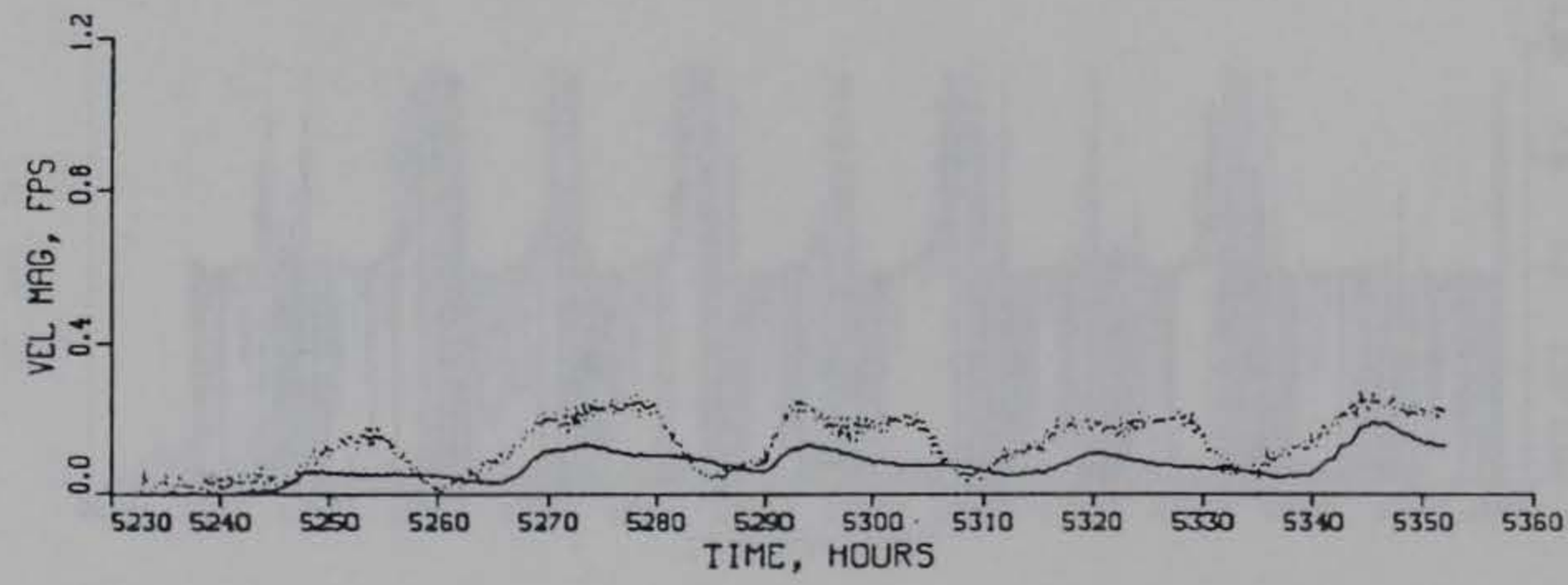

BOTTOM

TIDAL VELOCITY **CALIBRATION PERIOD**

MAGNITUDE GAGE C12

PLAN (SOLID) VS EXISTING (DOTTED) CONDITIONS

PLATE 77

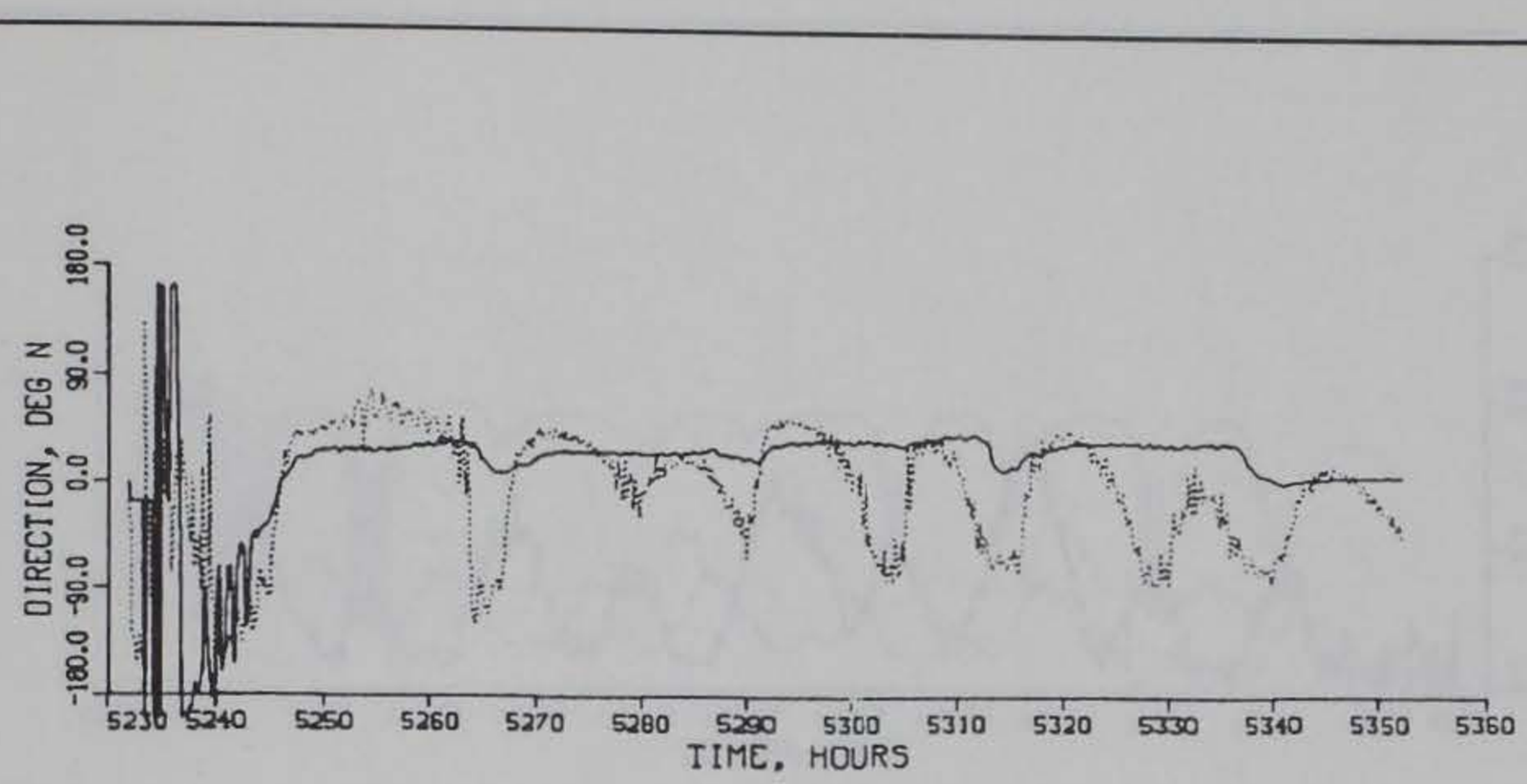

SURFACE

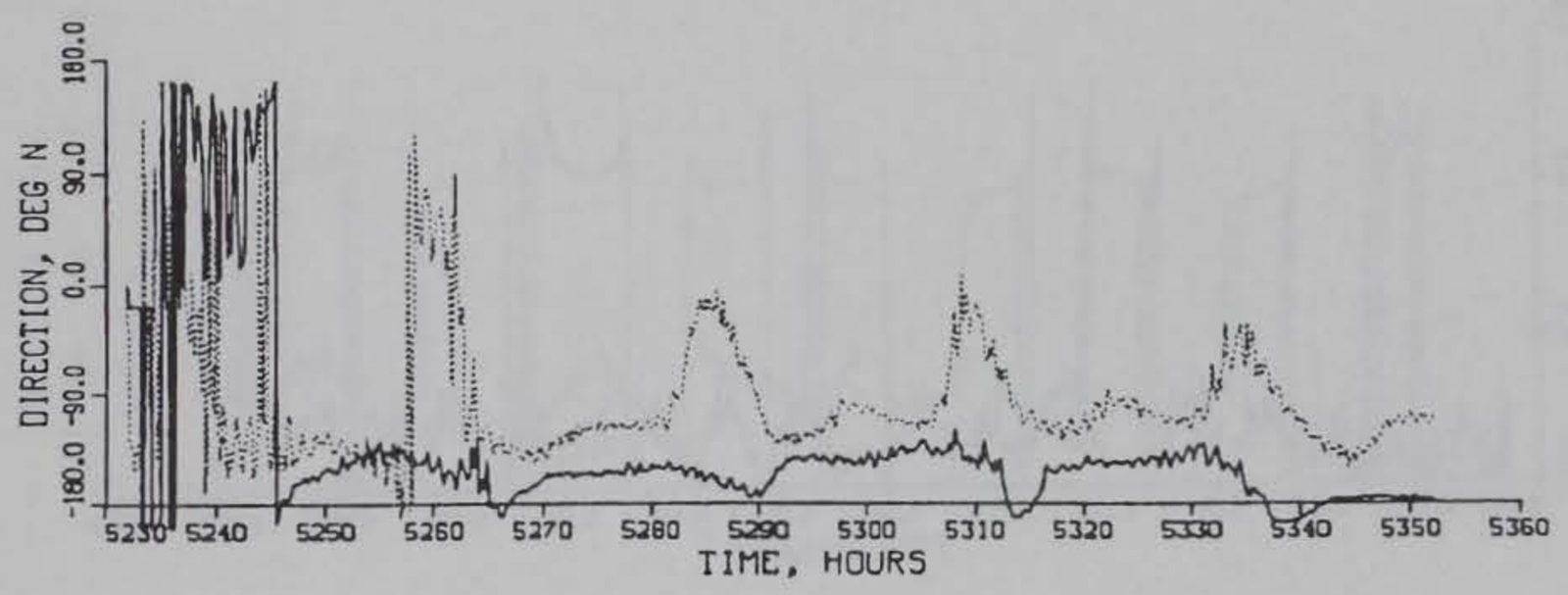

MID-DEPTH

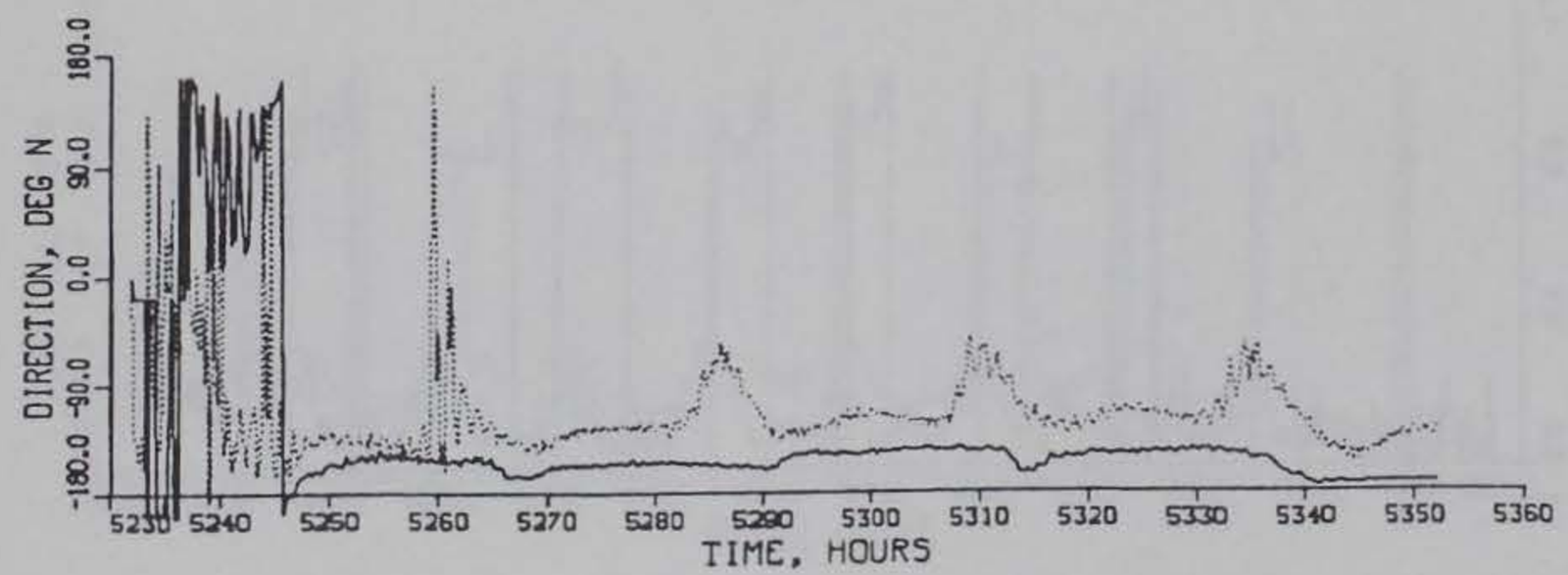

BOTTOM

TIDAL VELOCITY **CALIBRATION PERIOD**

DIRECTION GAGE C12

PLAN (SOLID) VS EXISTING (DOTTED) CONDITIONS

PLATE 78

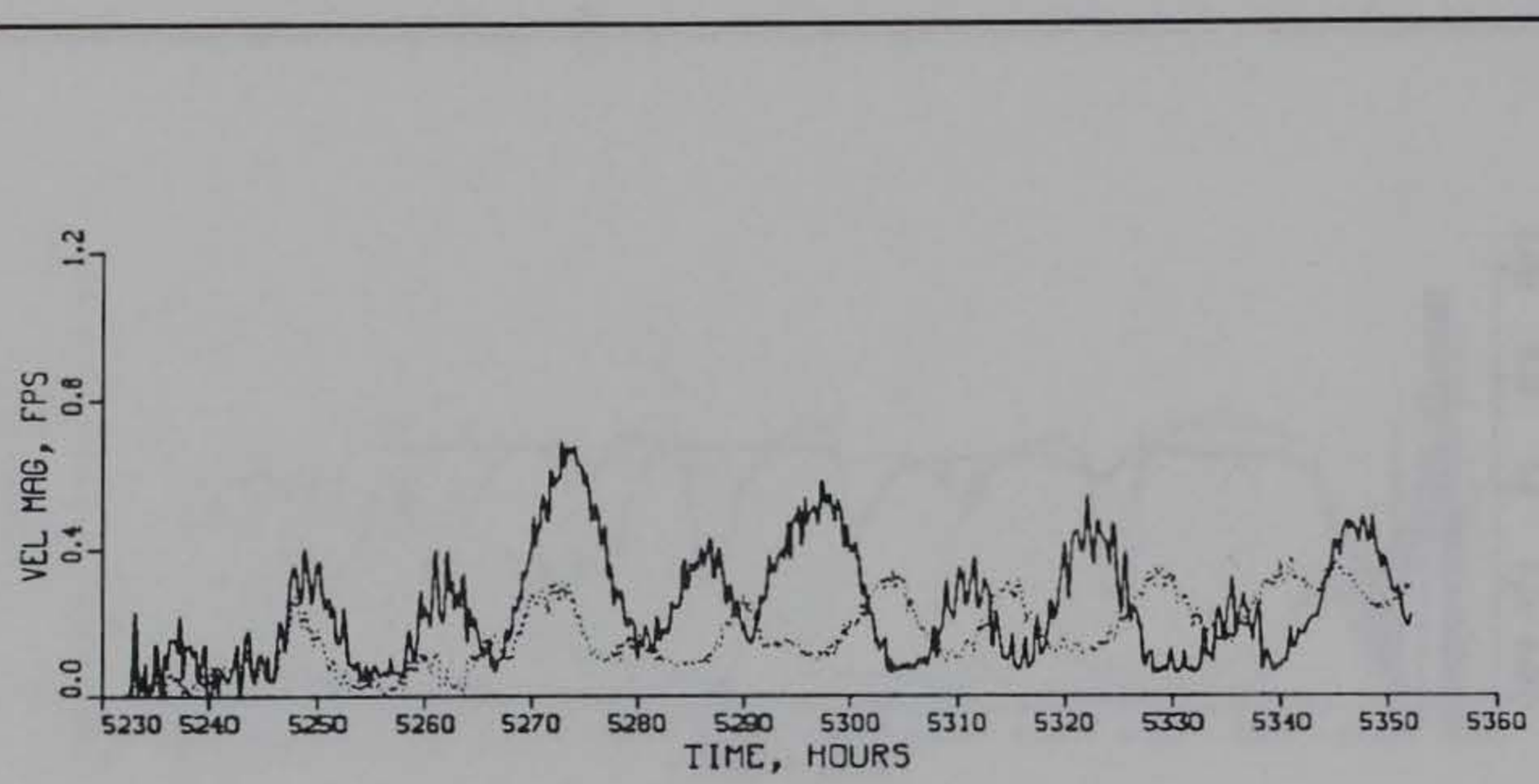

SURFACE

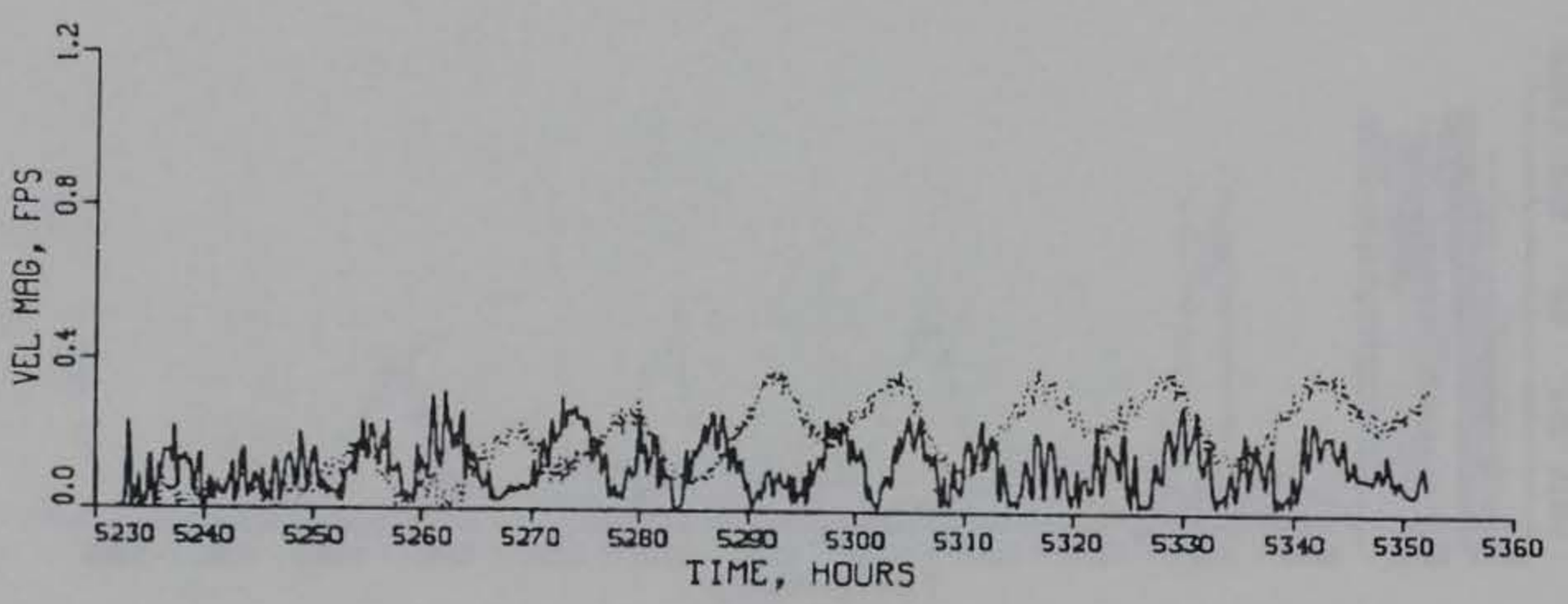

MID-DEPTH

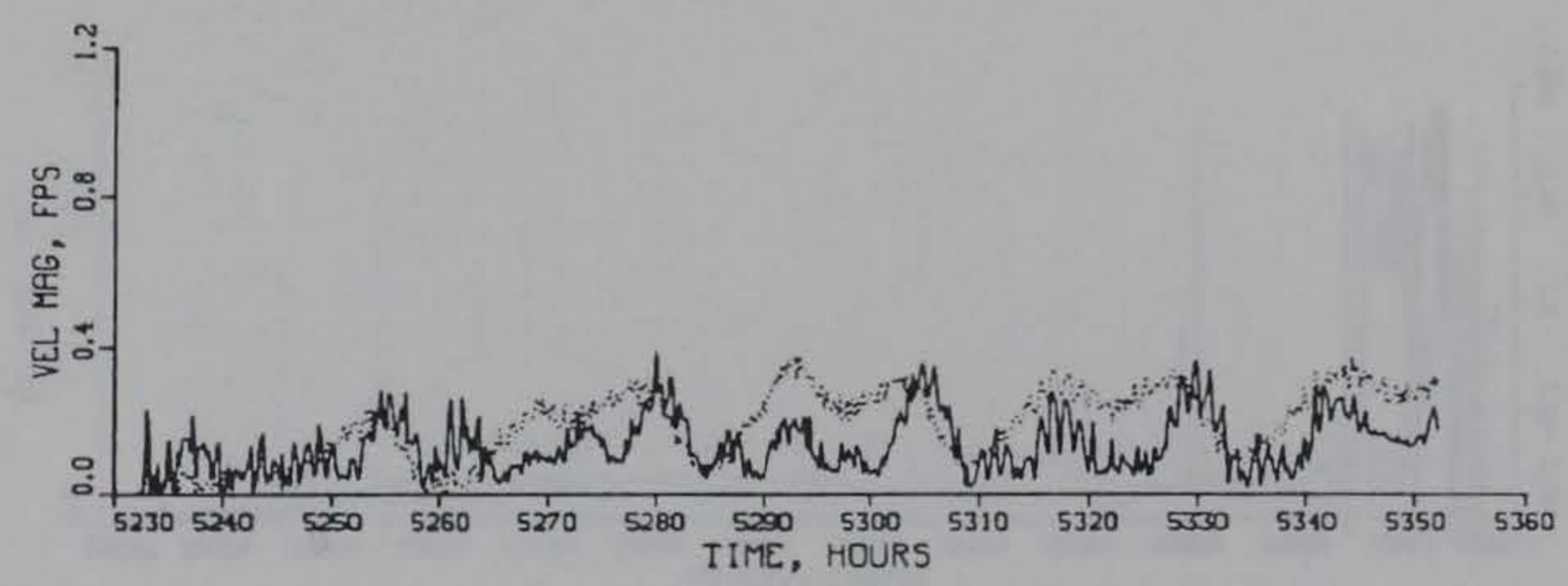

BOTTOM

TIDAL VELOCITY **CALIBRATION PERIOD**

MAGNITUDE GAGE C14

PLAN (SOLID) VS EXISTING (DOTTED) CONDITIONS

PLATE 79

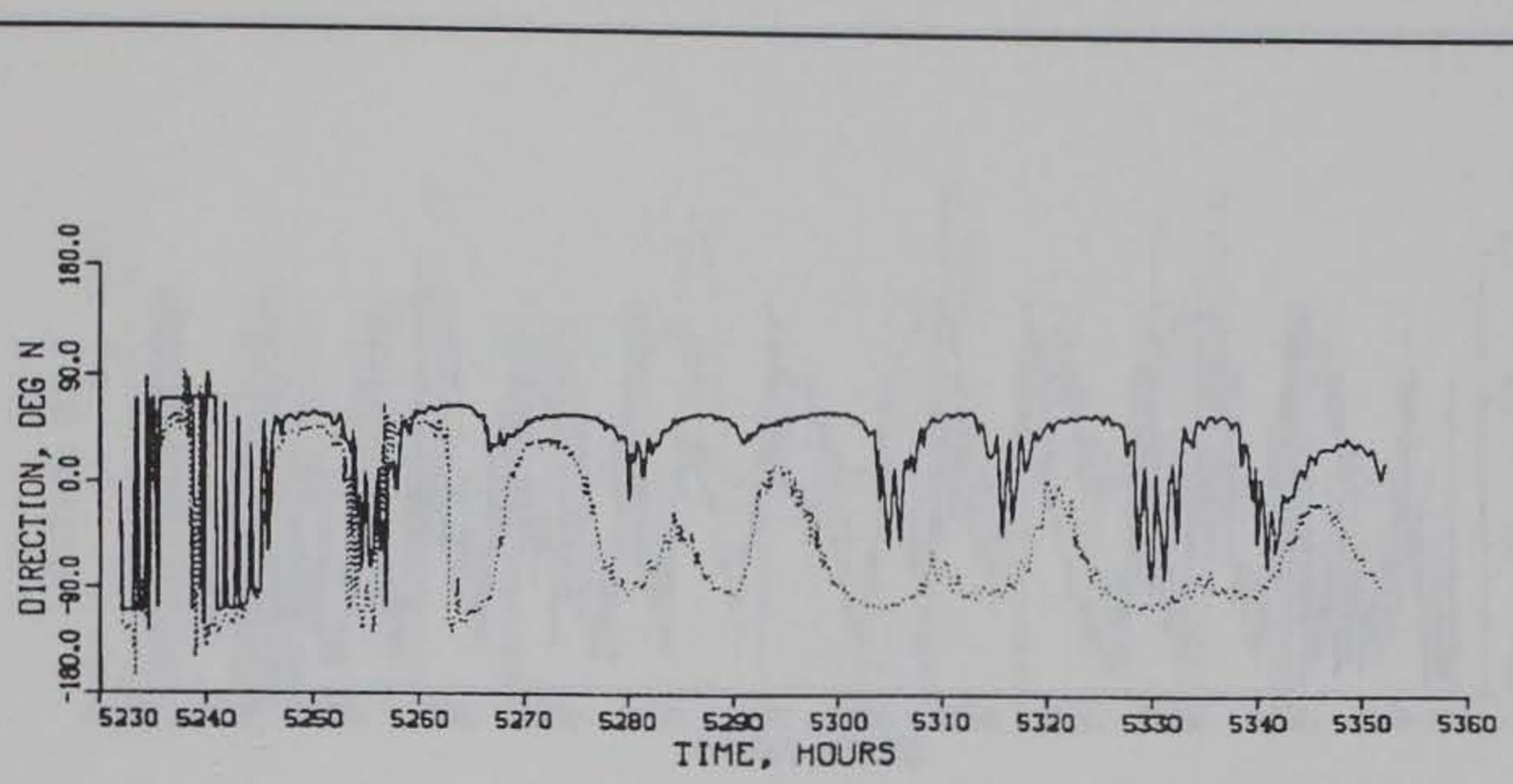

SURFACE

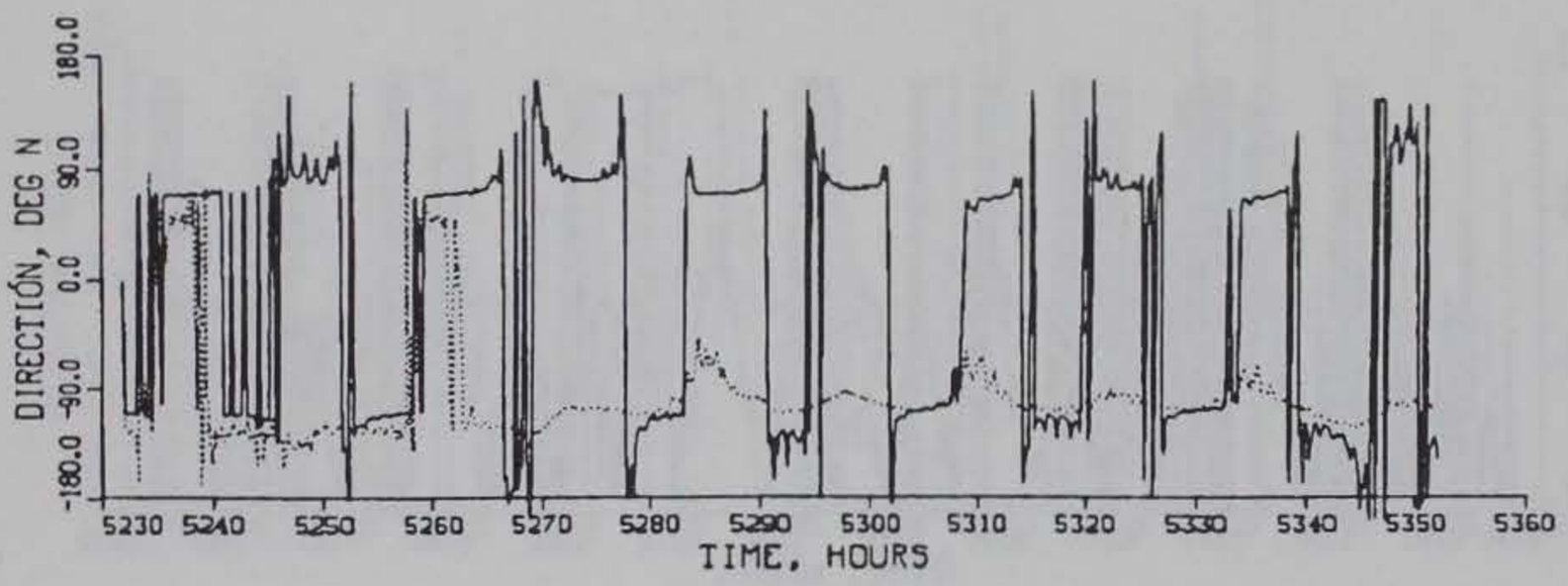

MID-DEPTH

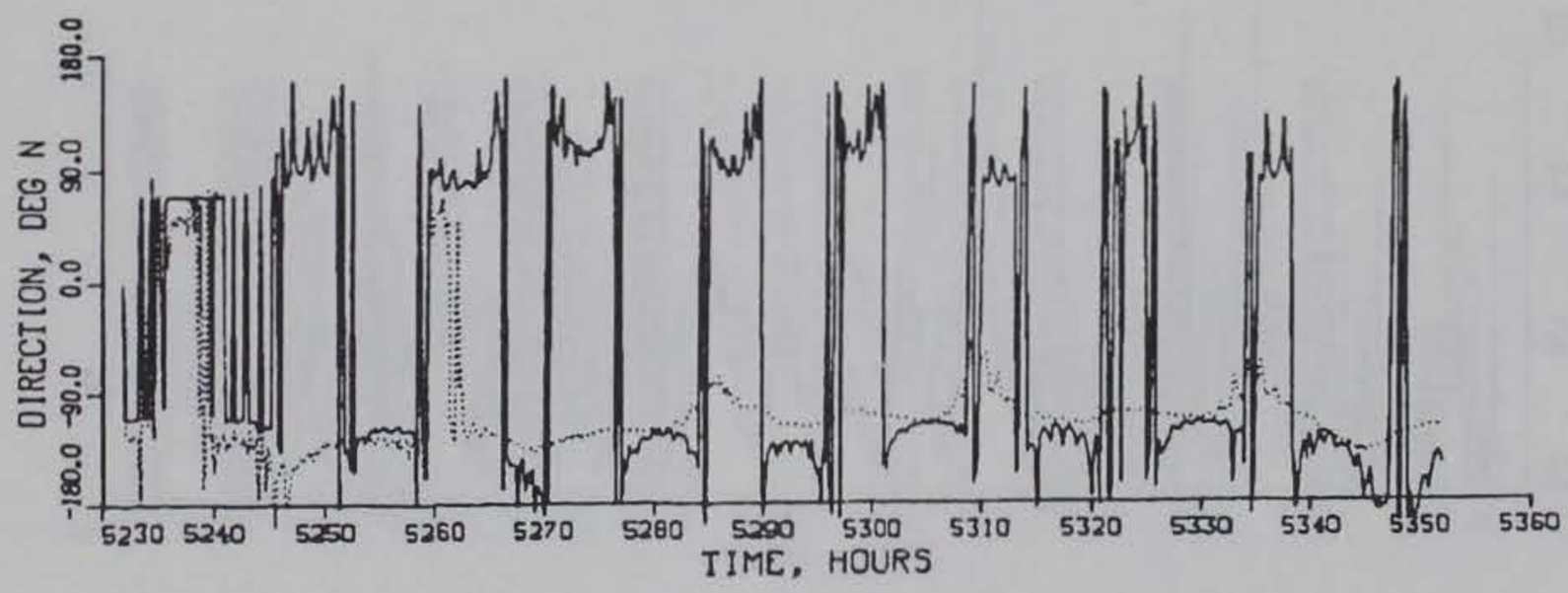

BOTTOM

TIDAL VELOCITY **CALIBRATION PERIOD**

DIRECTION GAGE C14

PLAN (SOLID) VS EXISTING (DOTTED) CONDITIONS

PLATE 80

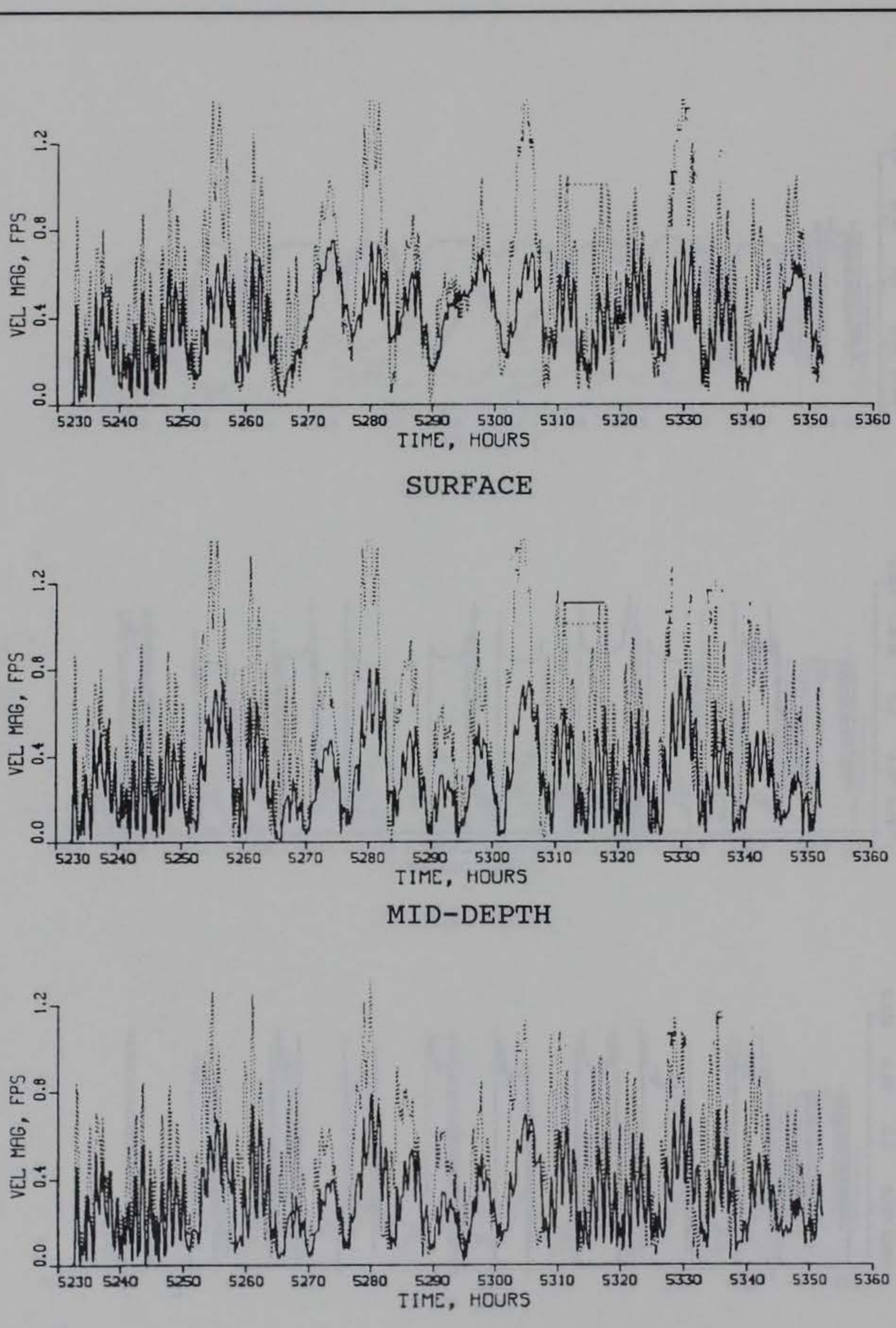

TIDAL VELOCITY **CALIBRATION PERIOD**

MAGNITUDE GAGE C18

PLAN (SOLID) VS EXISTING (DOTTED) CONDITIONS

PLATE 81

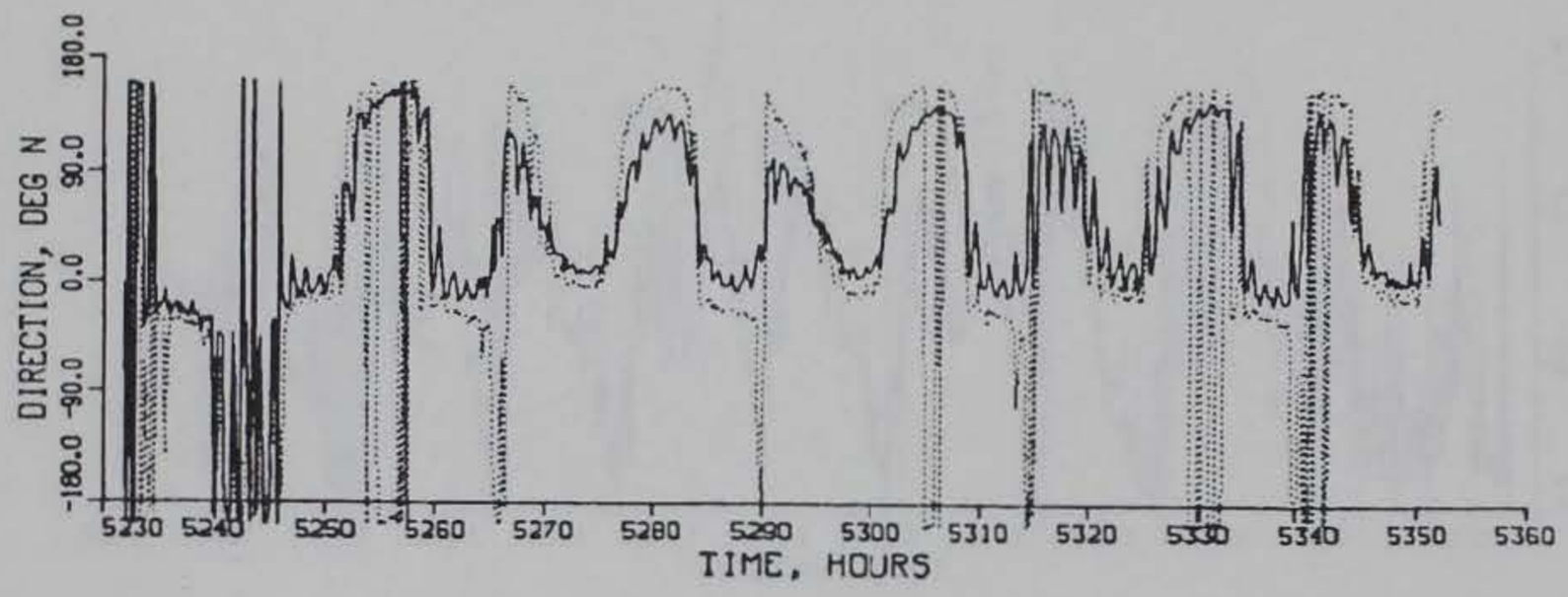

SURFACE

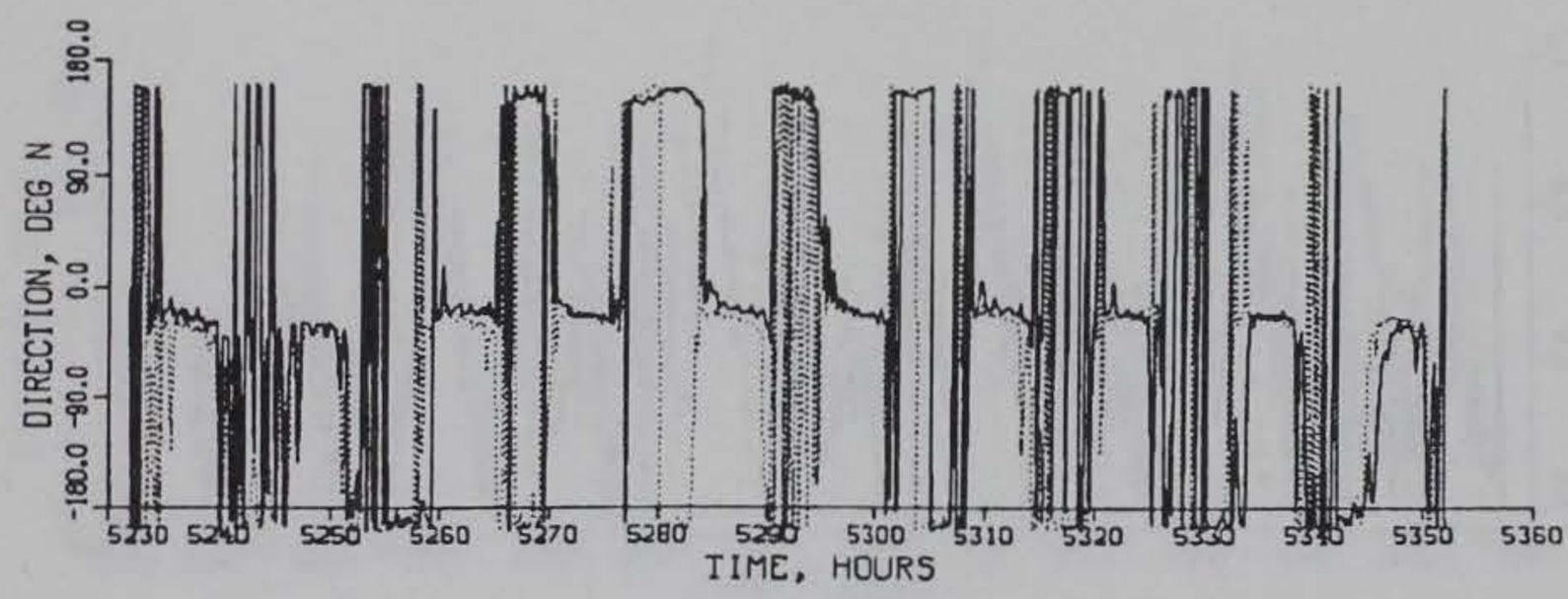

MID-DEPTH

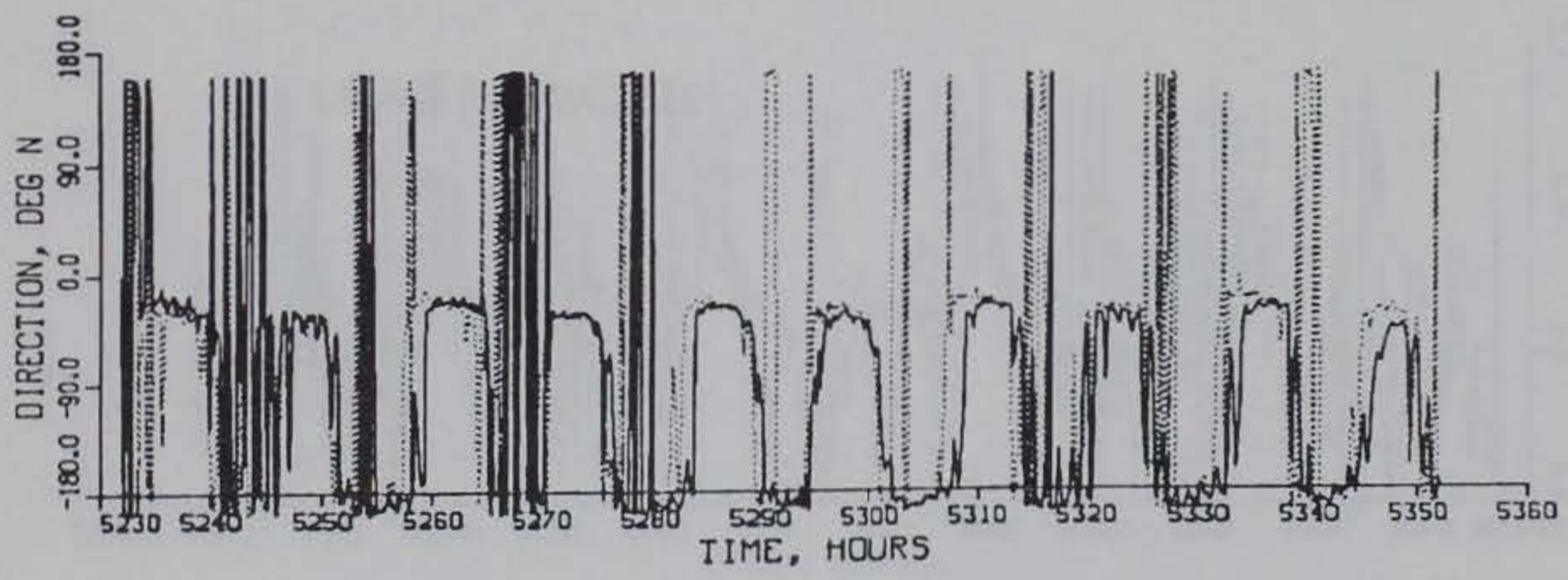

BOTTOM

TIDAL VELOCITY **CALIBRATION PERIOD**

DIRECTION GAGE C18

PLAN (SOLID) VS EXISTING (DOTTED) CONDITIONS

PLATE 82

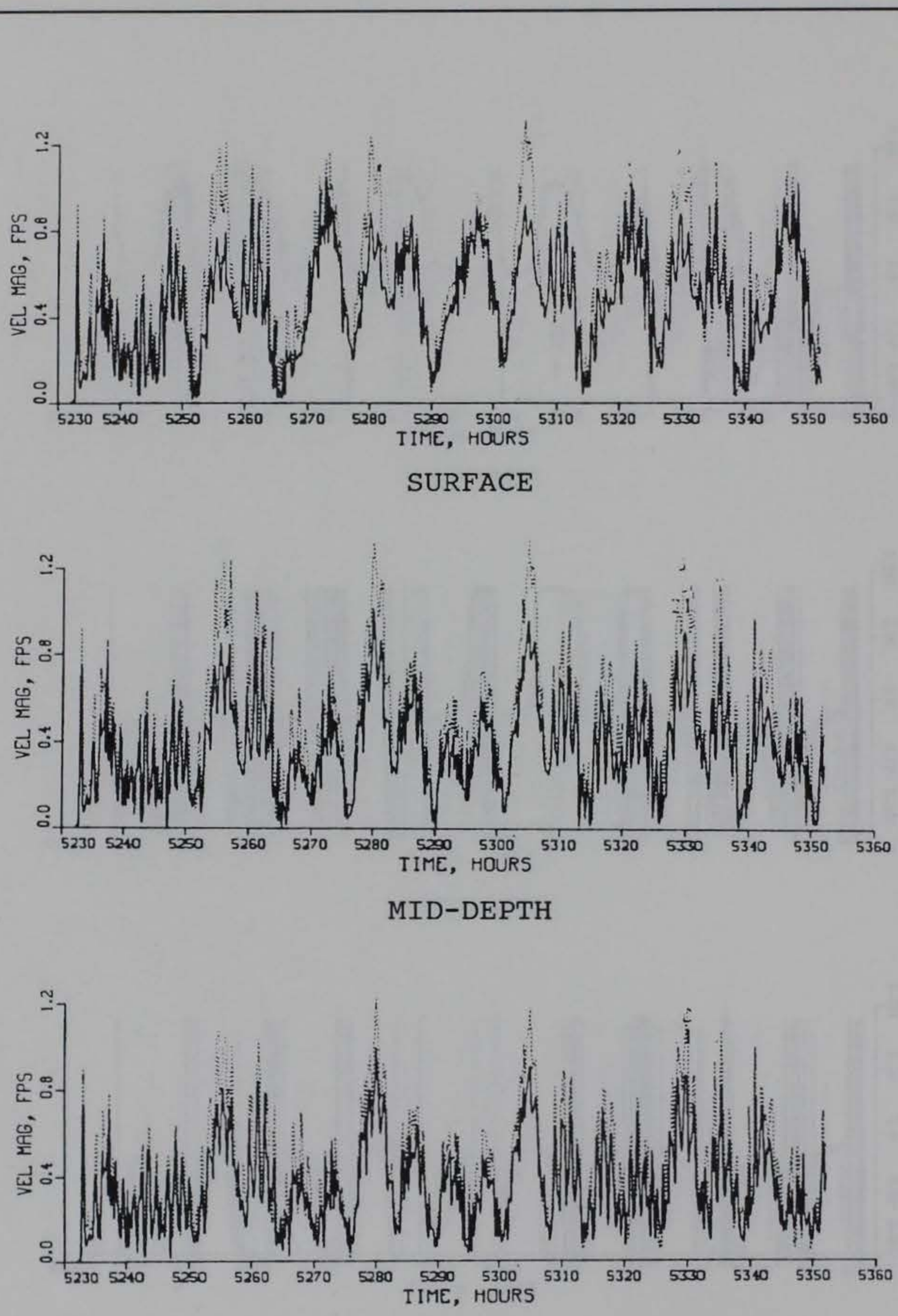

TIDAL VELOCITY **CALIBRATION PERIOD**

MAGNITUDE

GAGE C19

PLAN (SOLID) VS EXISTING (DOTTED) CONDITIONS

PLATE 83

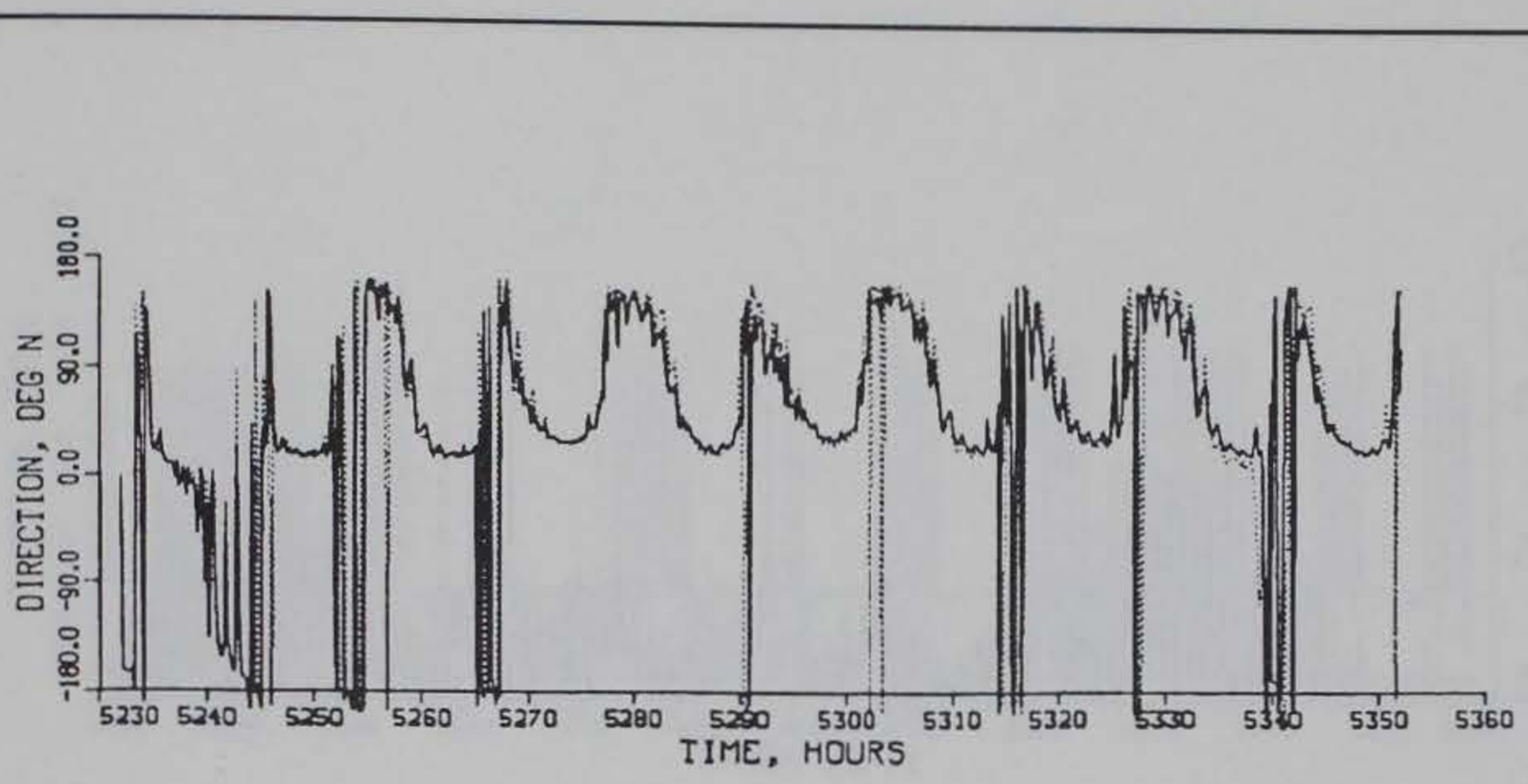

SURFACE

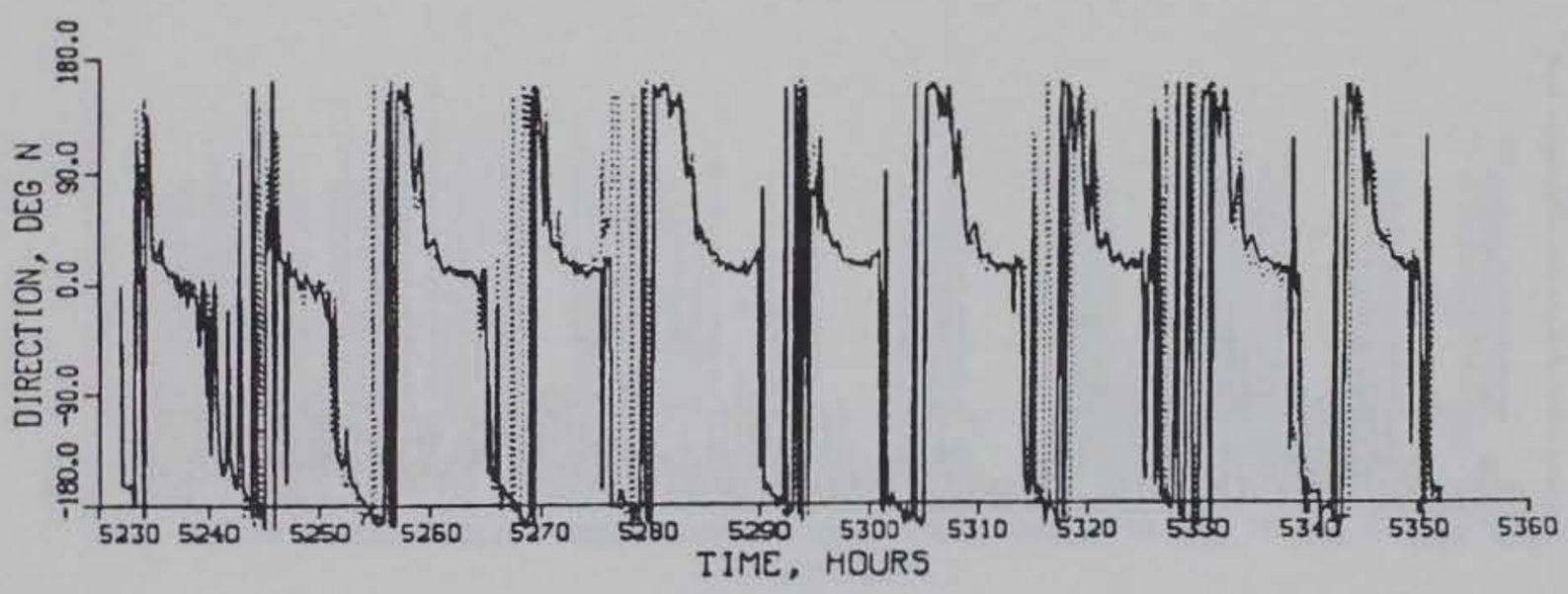

MID-DEPTH

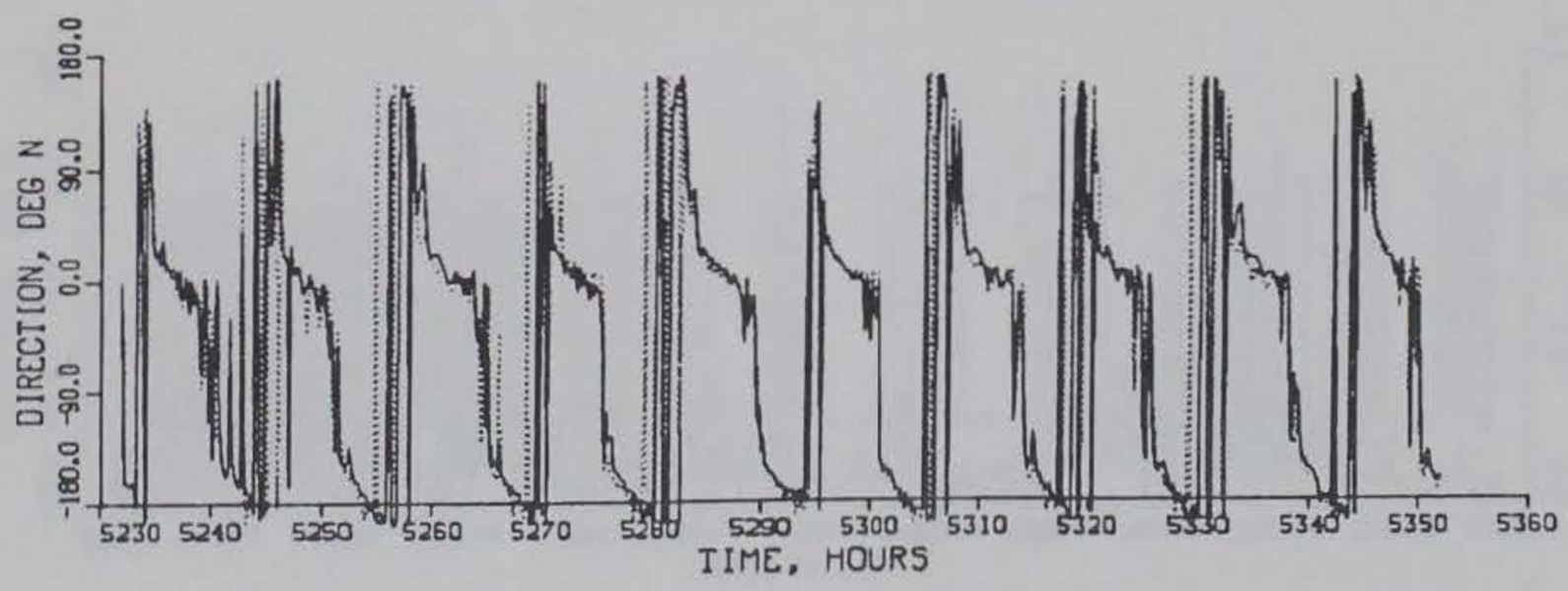

BOTTOM

TIDAL VELOCITY **CALIBRATION PERIOD**

DIRECTION GAGE C19

PLAN (SOLID) VS EXISTING (DOTTED) CONDITIONS

PLATE 84

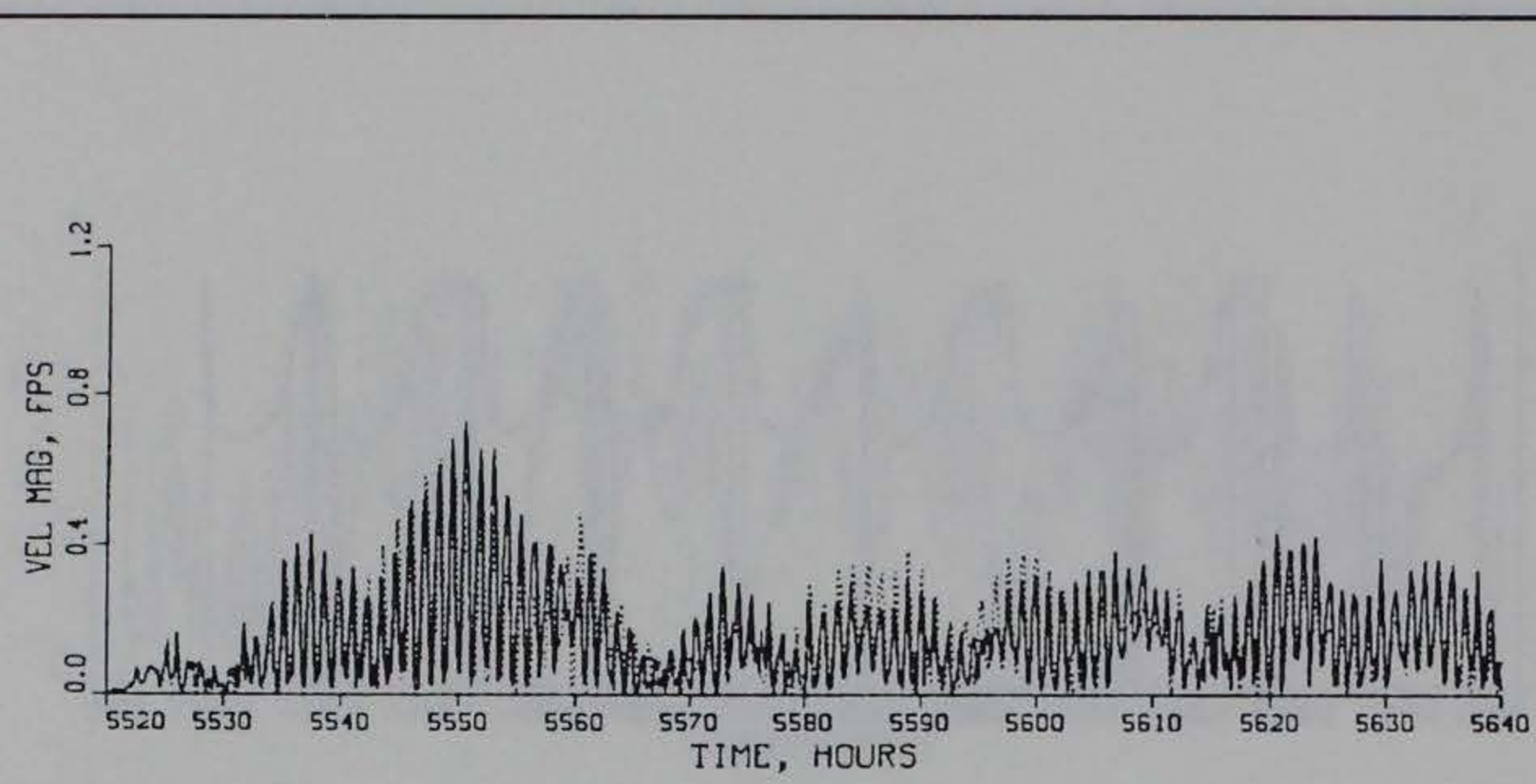

SURFACE

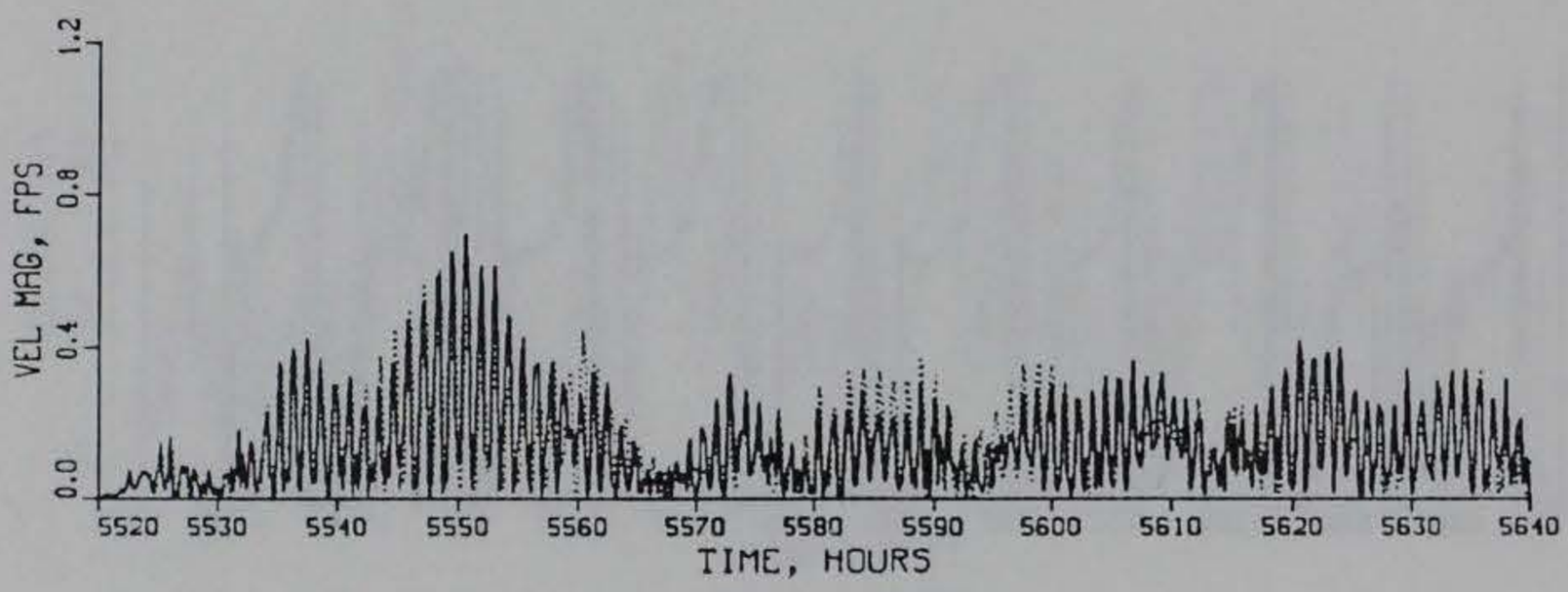

MID-DEPTH

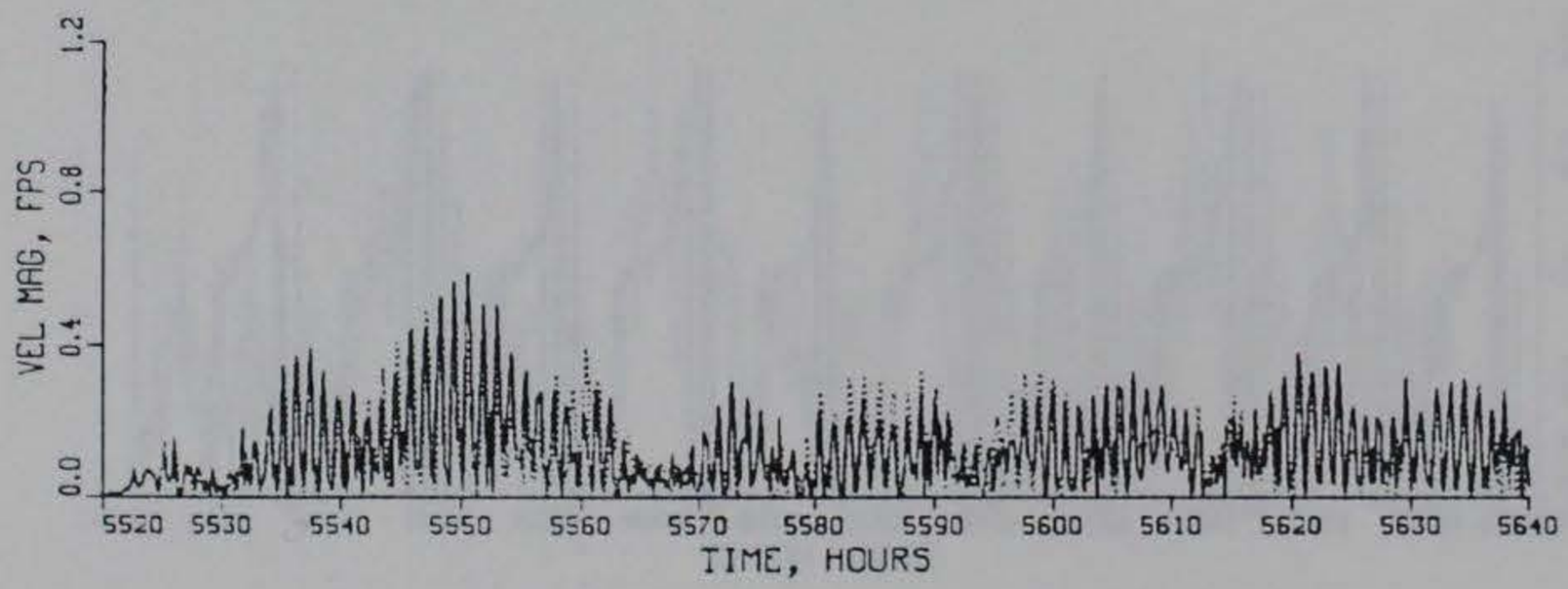

BOTTOM

TIDAL VELOCITY

VERIFICATION PERIOD

MAGNITUDE

GAGE C1

PLAN (SOLID) VS EXISTING (DOTTED) CONDITIONS

PLATE 85

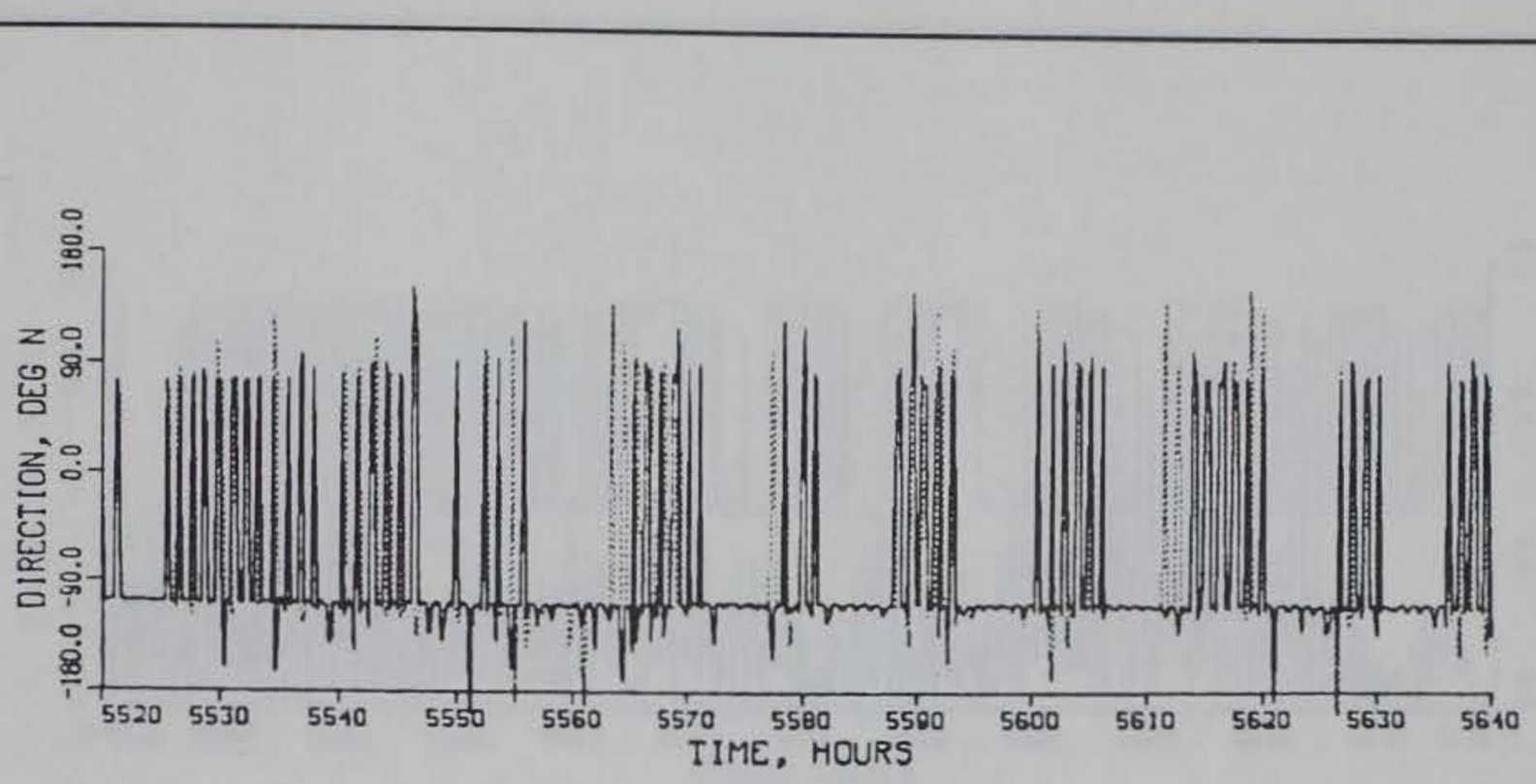

SURFACE

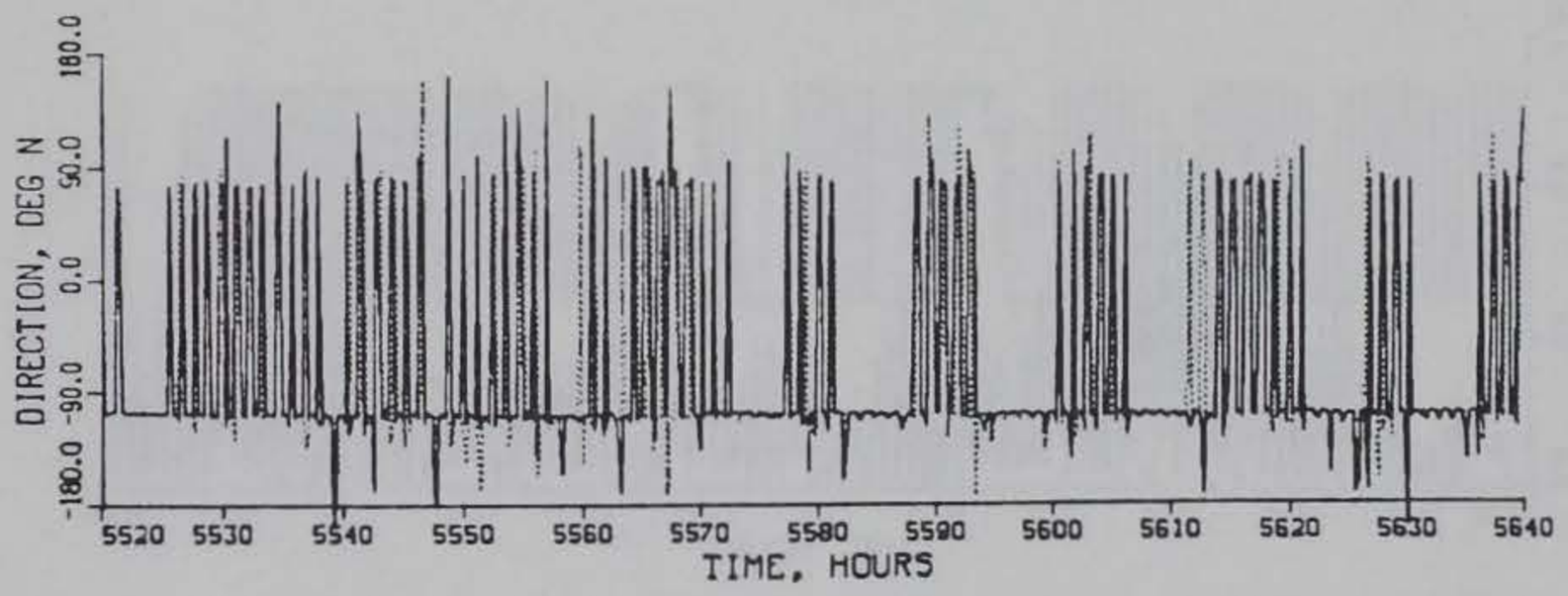

MID-DEPTH

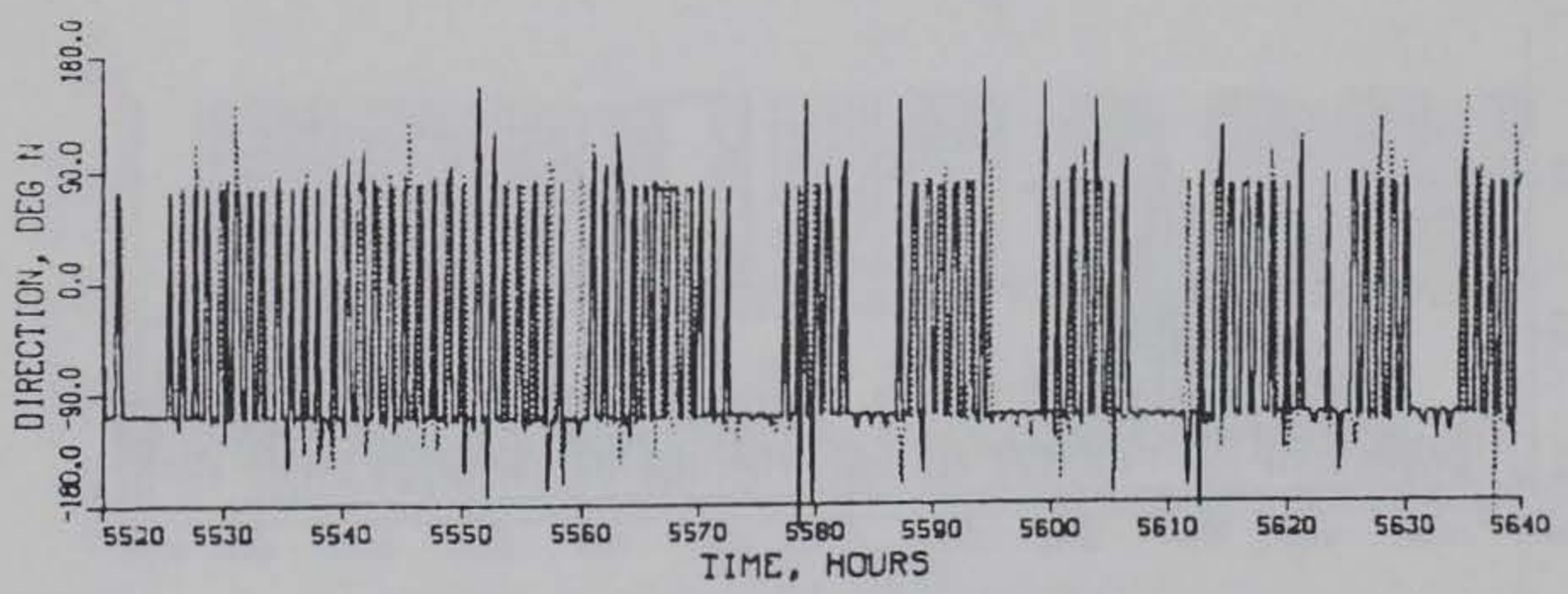

BOTTOM

TIDAL VELOCITY — VERIFICATION PERIOD

DIRECTION — GAGE C1

PLAN (SOLID) VS EXISTING (DOTTED) CONDITIONS

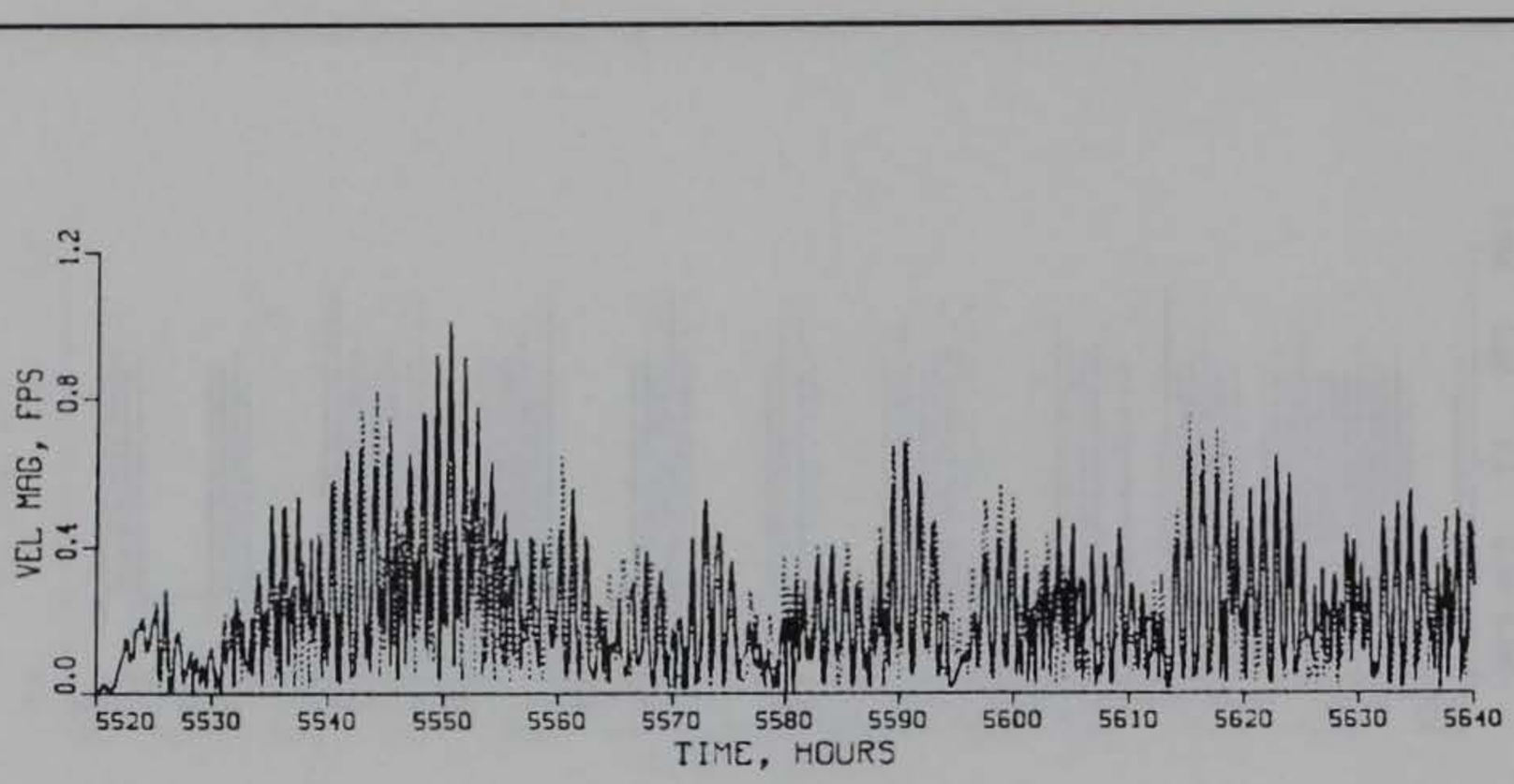

SURFACE

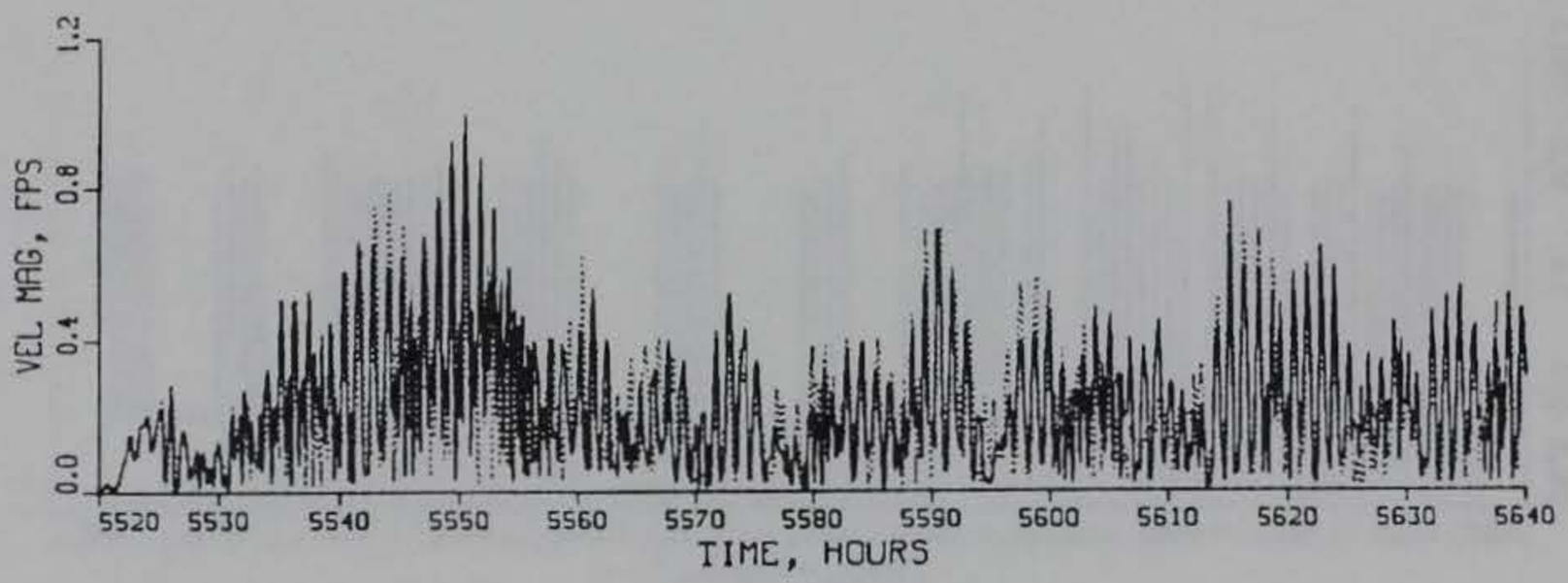

MID-DEPTH

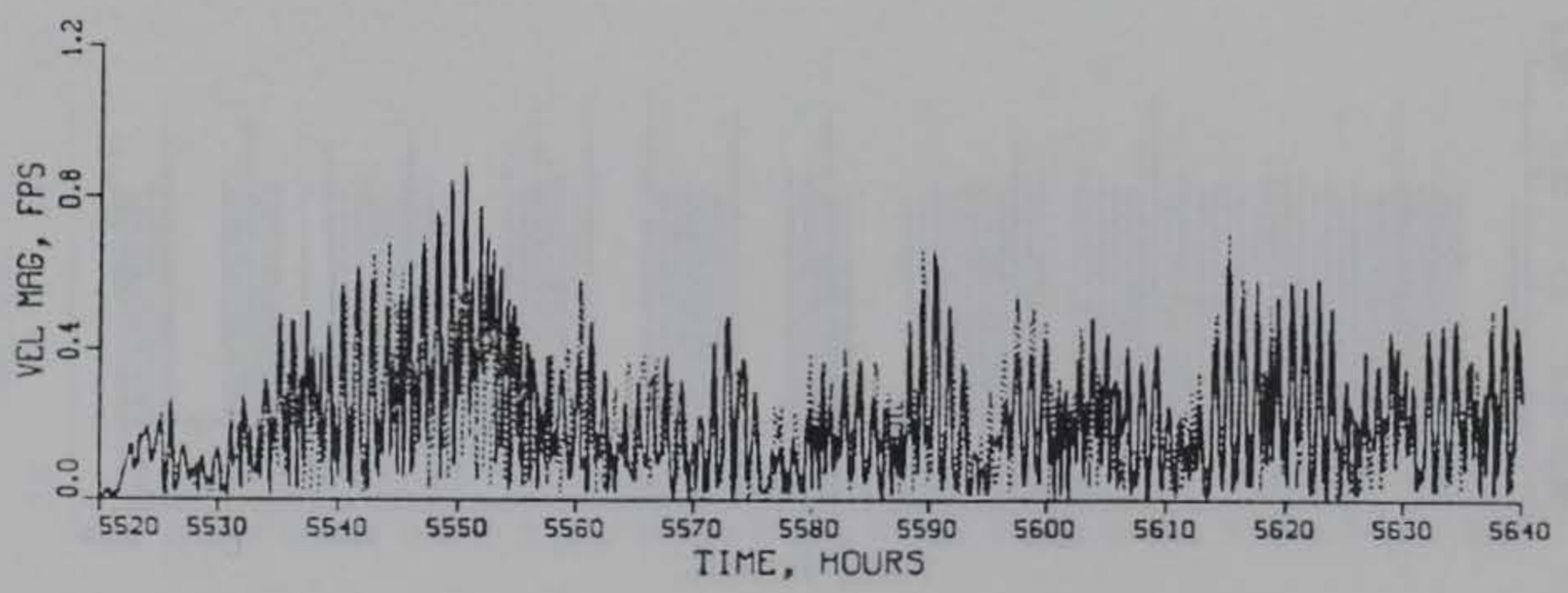

BOTTOM

TIDAL VELOCITY **VERIFICATION PERIOD**

MAGNITUDE GAGE C2

PLAN (SOLID) VS EXISTING (DOTTED) CONDITIONS

PLATE 87

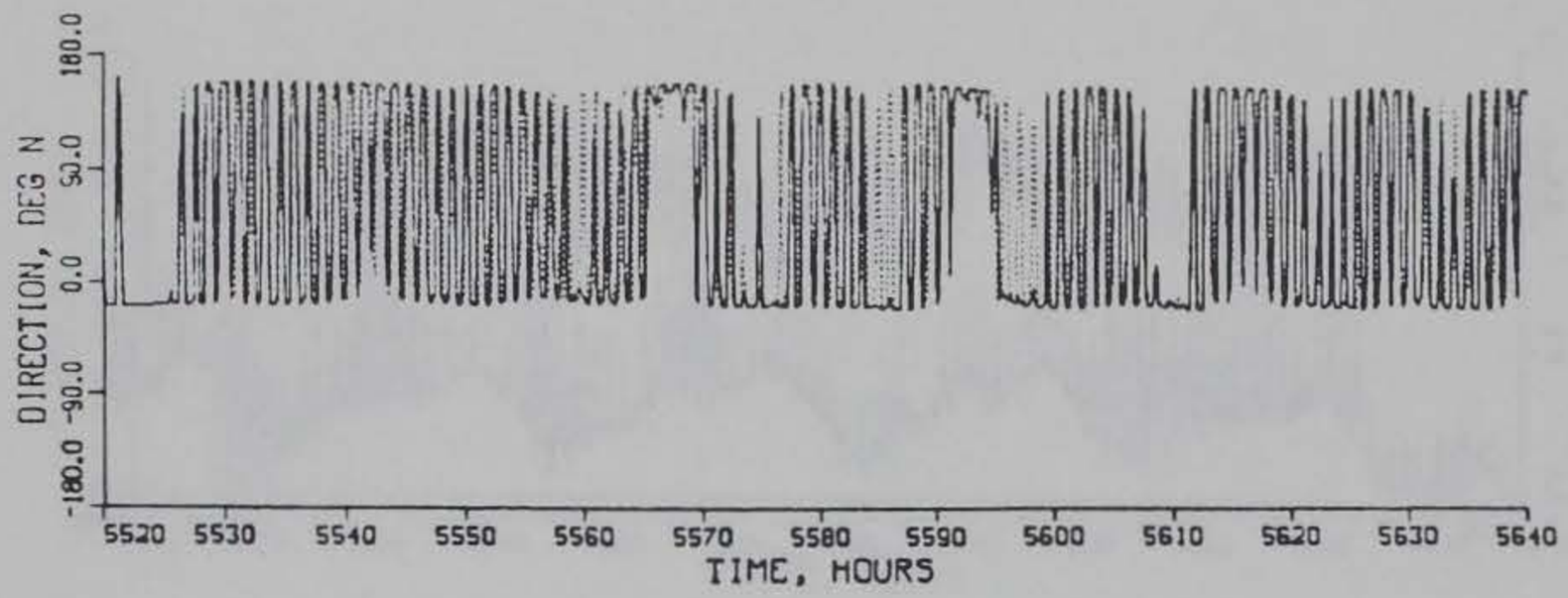

SURFACE

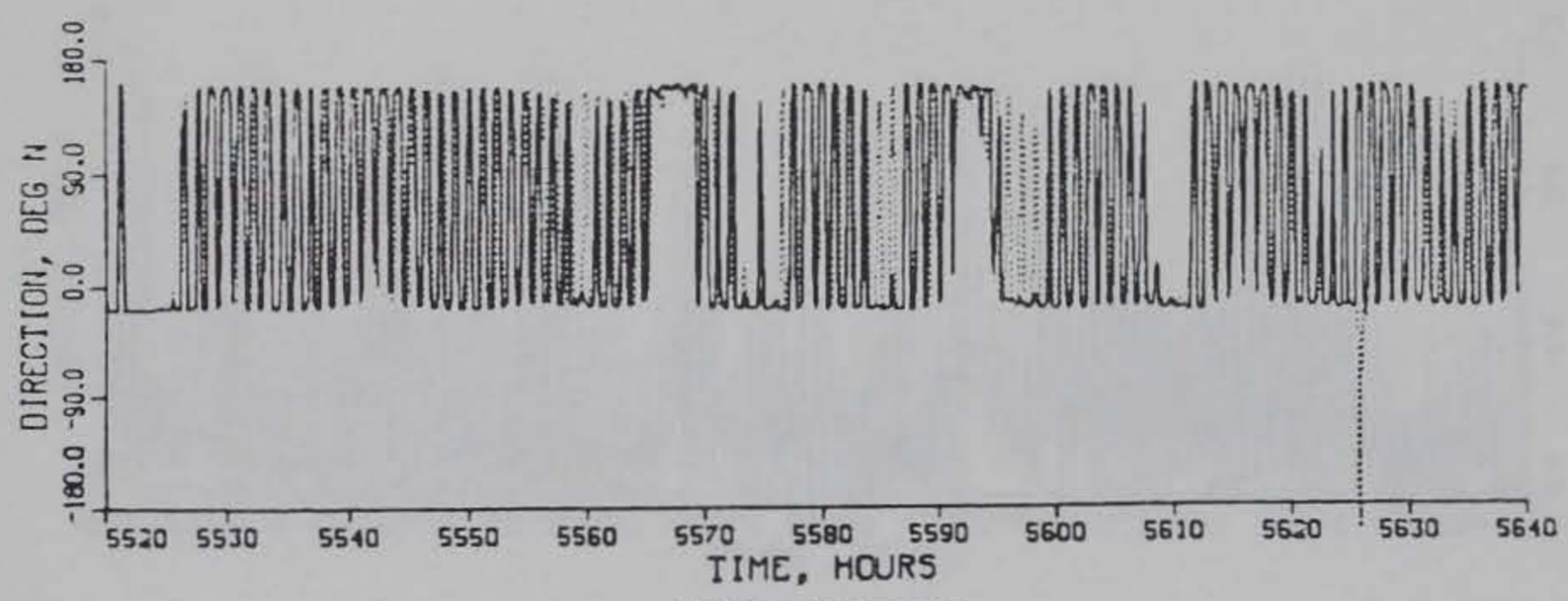

MID-DEPTH

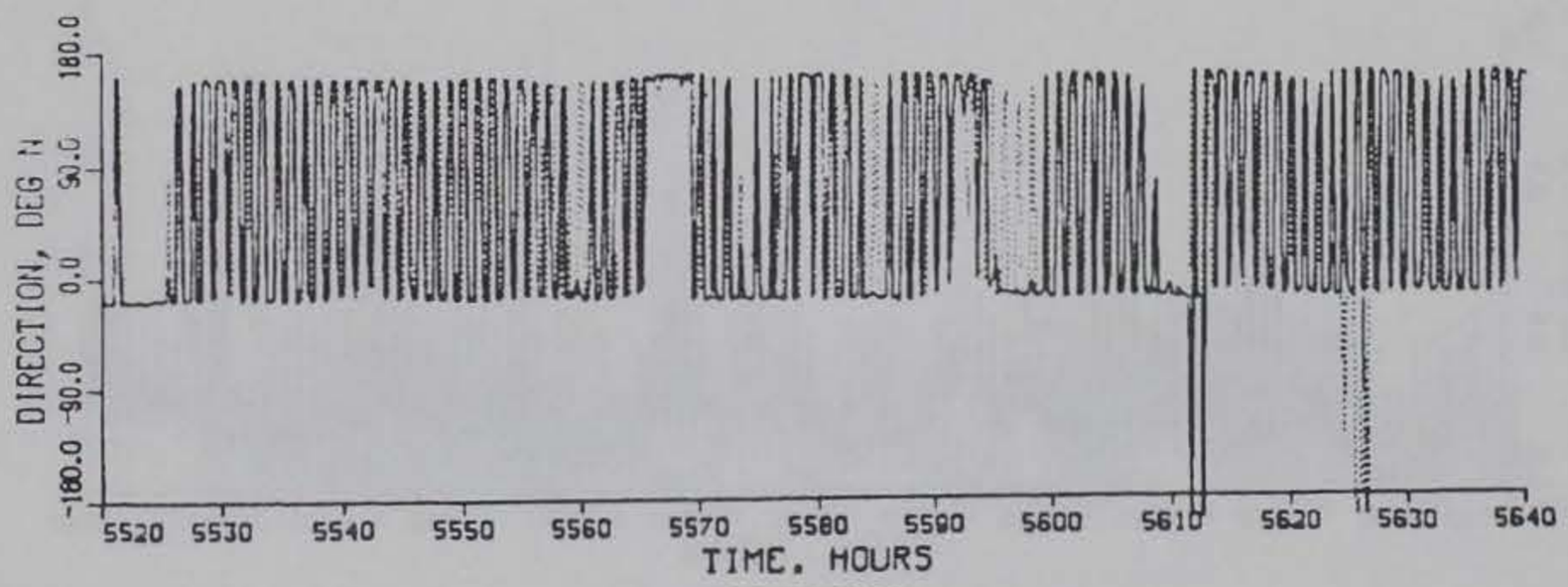

BOTTOM

TIDAL VELOCITY

VERIFICATION PERIOD

DIRECTION

GAGE C2

PLAN (SOLID) VS EXISTING (DOTTED) CONDITIONS

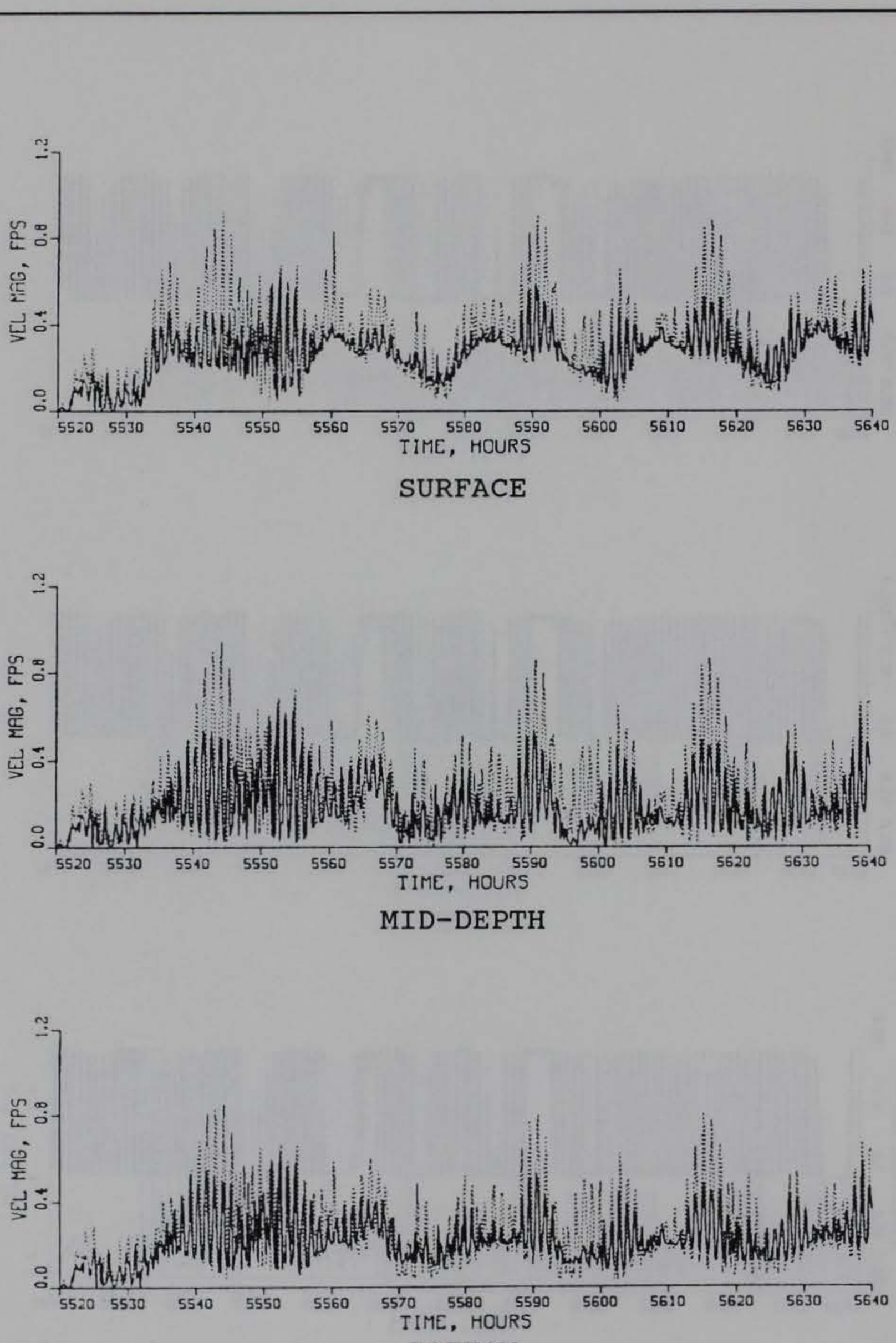

TIDAL VELOCITY VERIFICATION PERIOD

MAGNITUDE GAGE C3

PLAN (SOLID) VS EXISTING (DOTTED) CONDITIONS

PLATE 89

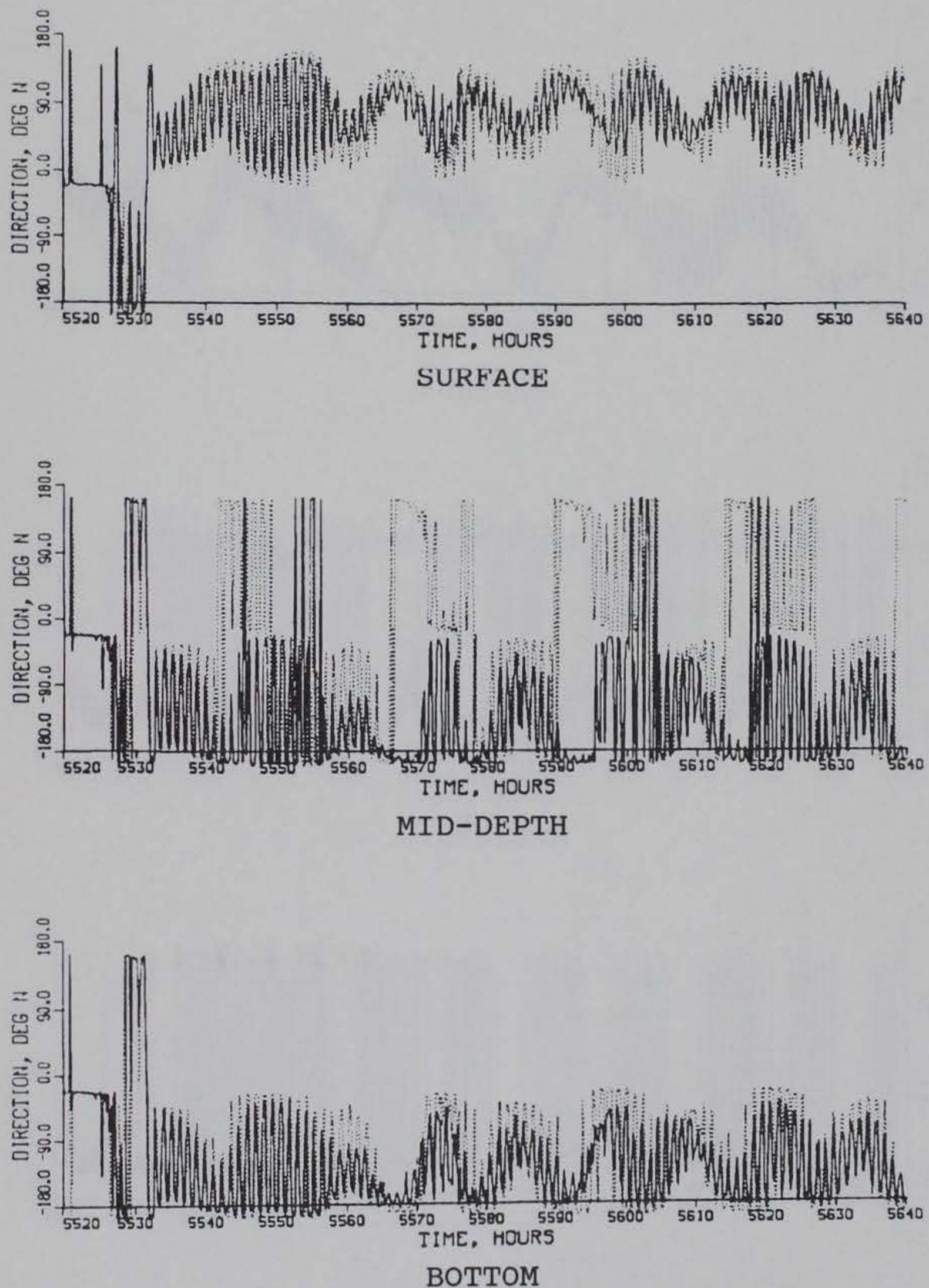

SURFACE

MID-DEPTH

BOTTOM

TIDAL VELOCITY

VERIFICATION PERIOD

DIRECTION

GAGE C3

PLAN (SOLID) VS EXISTING (DOTTED) CONDITIONS

PLATE 90

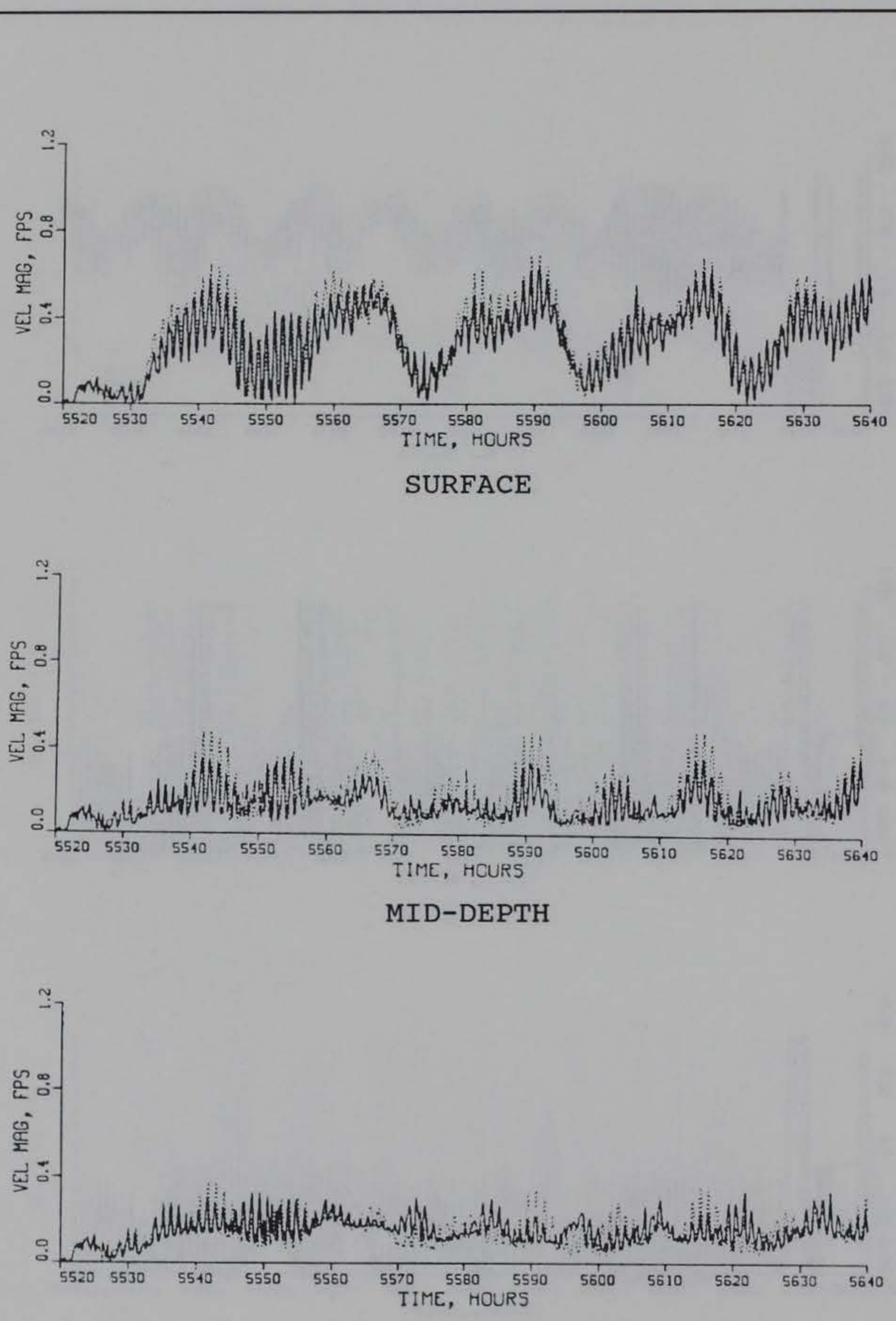

SURFACE

MID-DEPTH

BOTTOM

TIDAL VELOCITY VERIFICATION PERIOD

MAGNITUDE

GAGE C4

PLAN (SOLID) VS EXISTING (DOTTED) CONDITIONS

PLATE 91

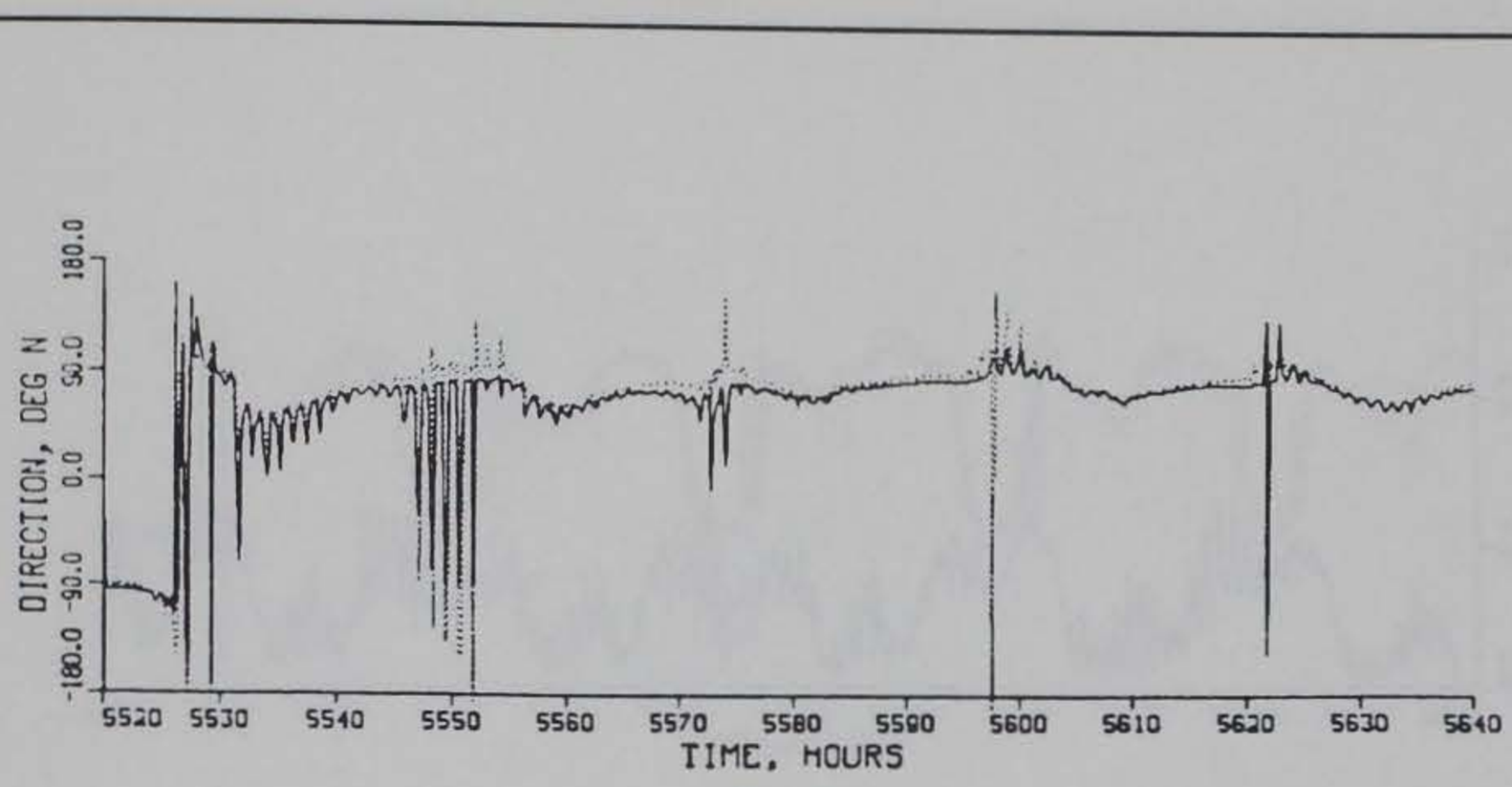

SURFACE

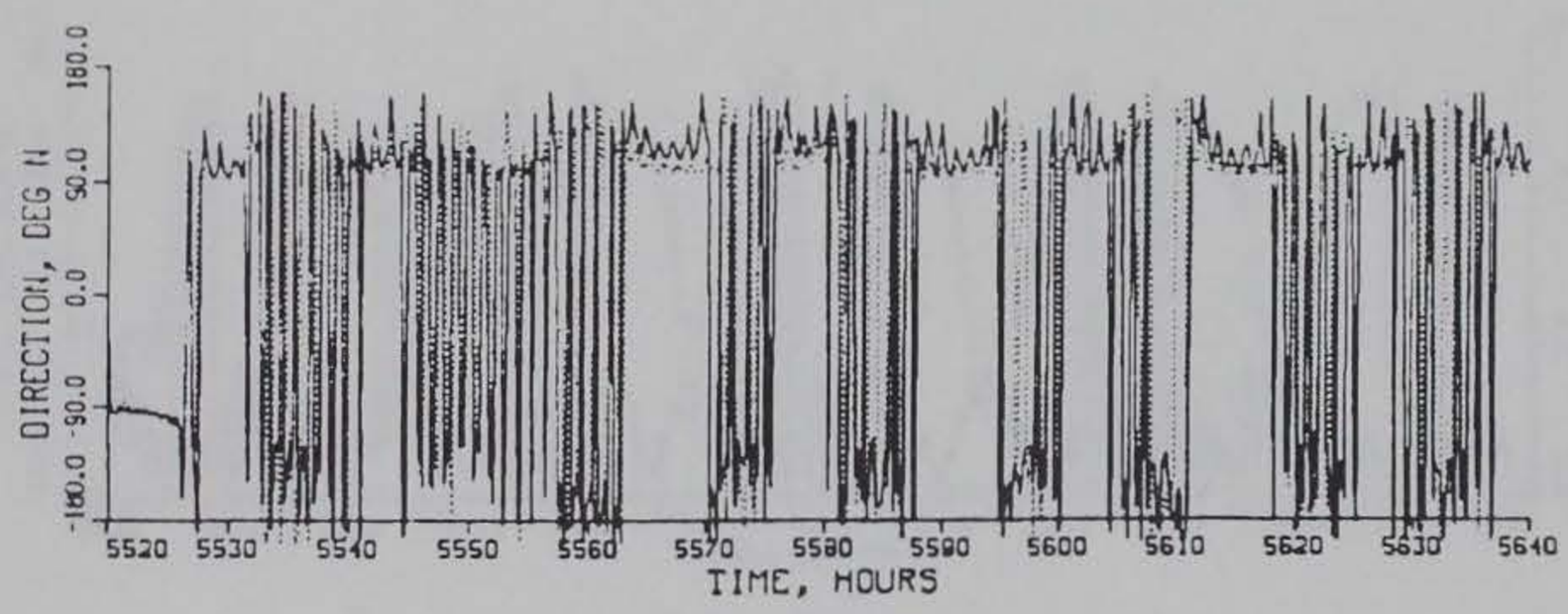

MID-DEPTH

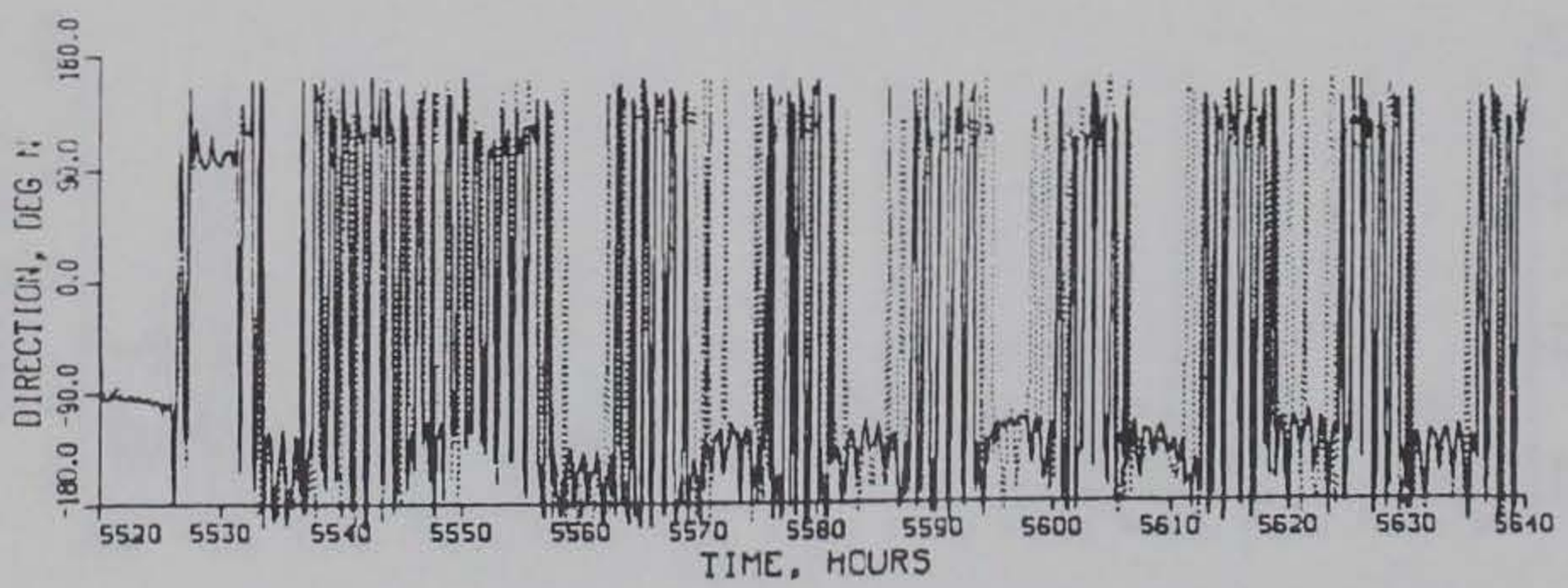

BOTTOM

TIDAL VELOCITY **VERIFICATION PERIOD**

DIRECTION GAGE C4

PLAN (SOLID) VS EXISTING (DOTTED) CONDITIONS

PLATE 92

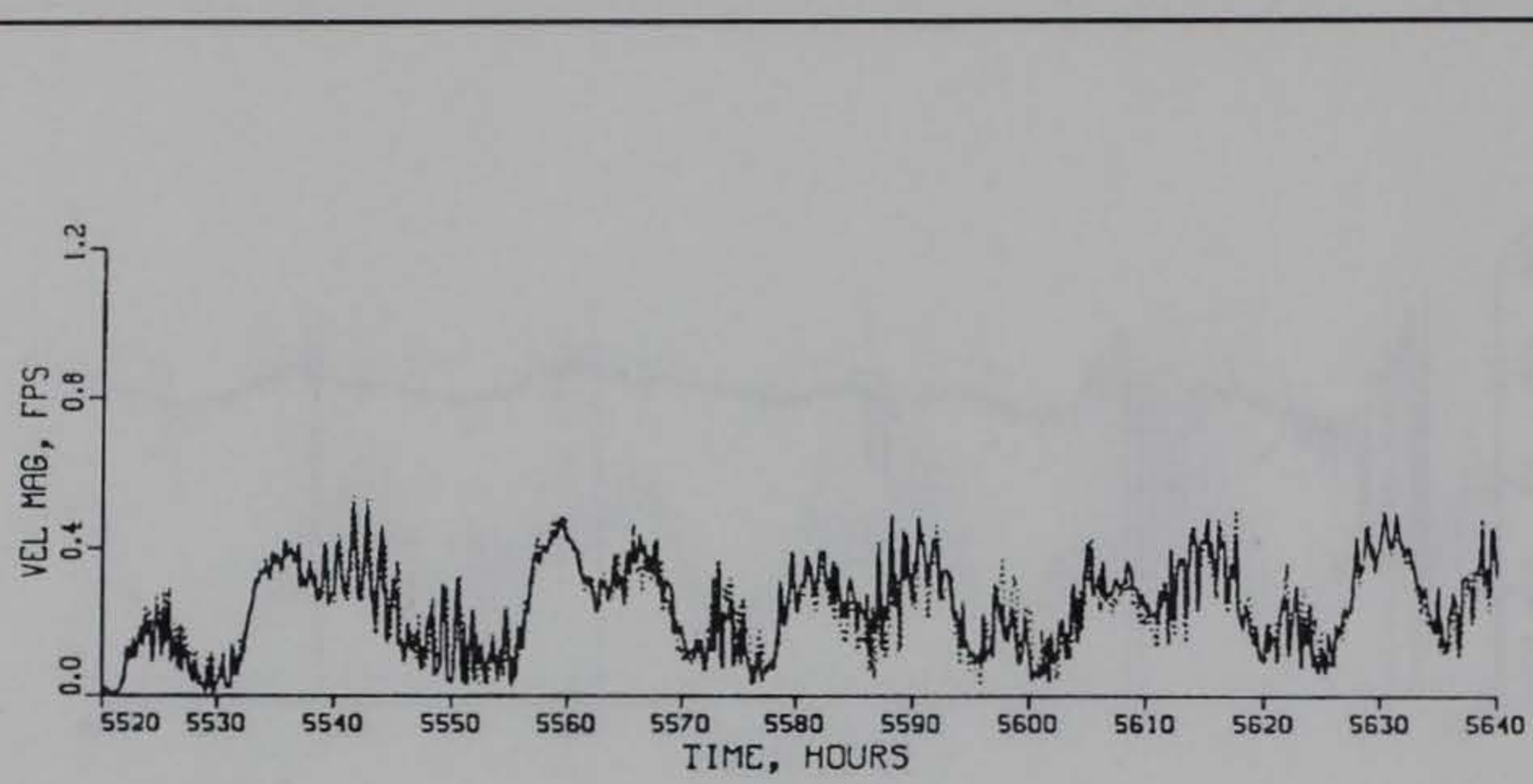

SURFACE

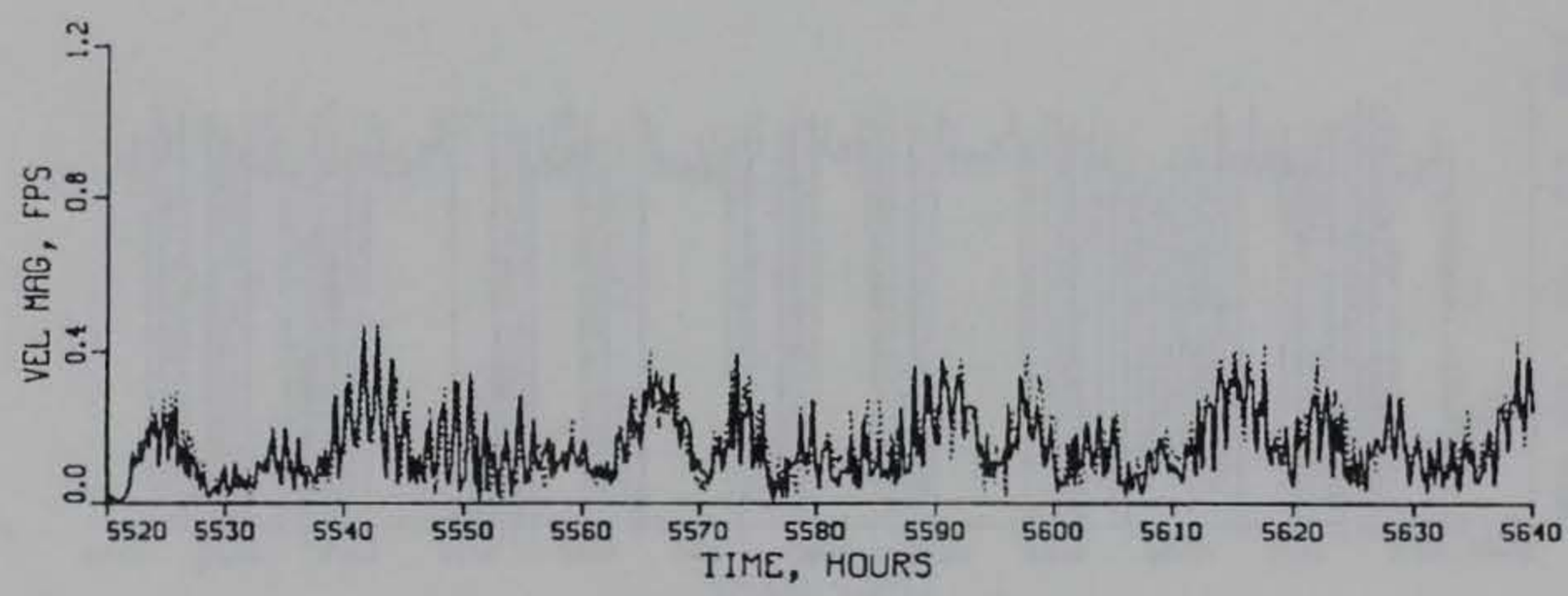

MID-DEPTH

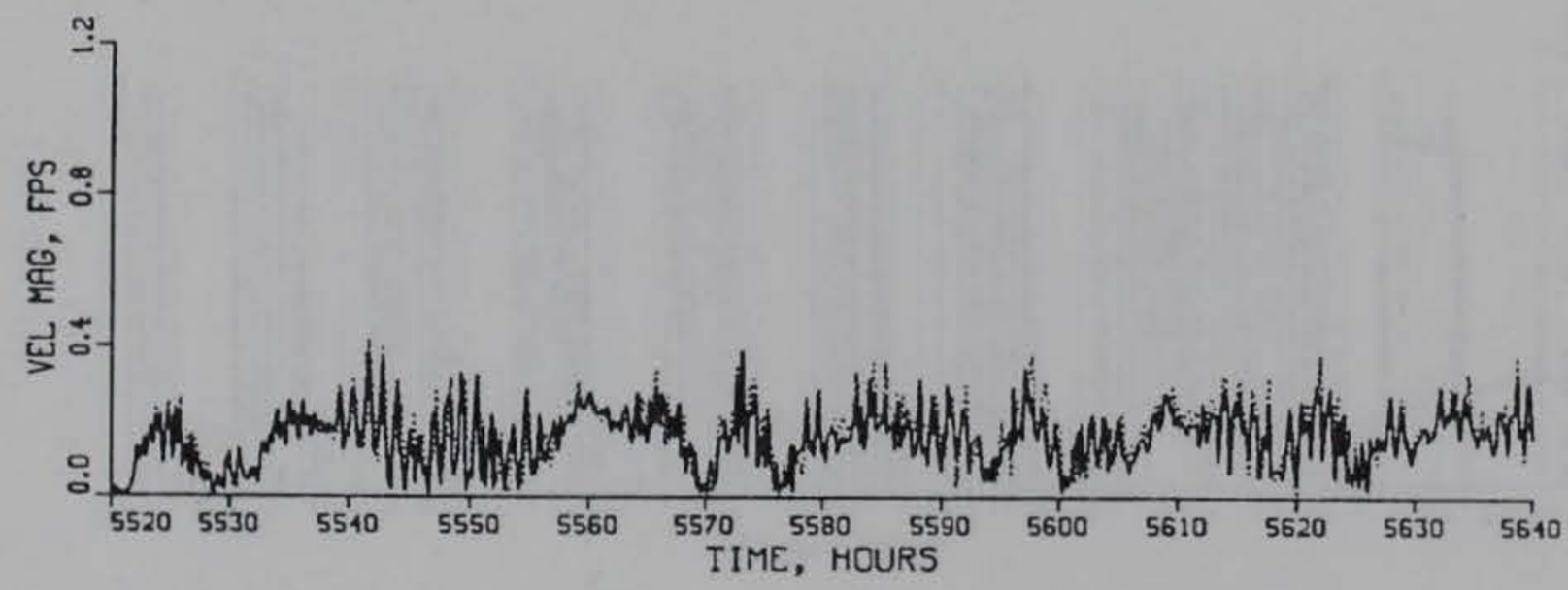

BOTTOM

TIDAL VELOCITY VERIFICATION PERIOD

MAGNITUDE

GAGE C5

PLAN (SOLID) VS EXISTING (DOTTED) CONDITIONS

PLATE 93

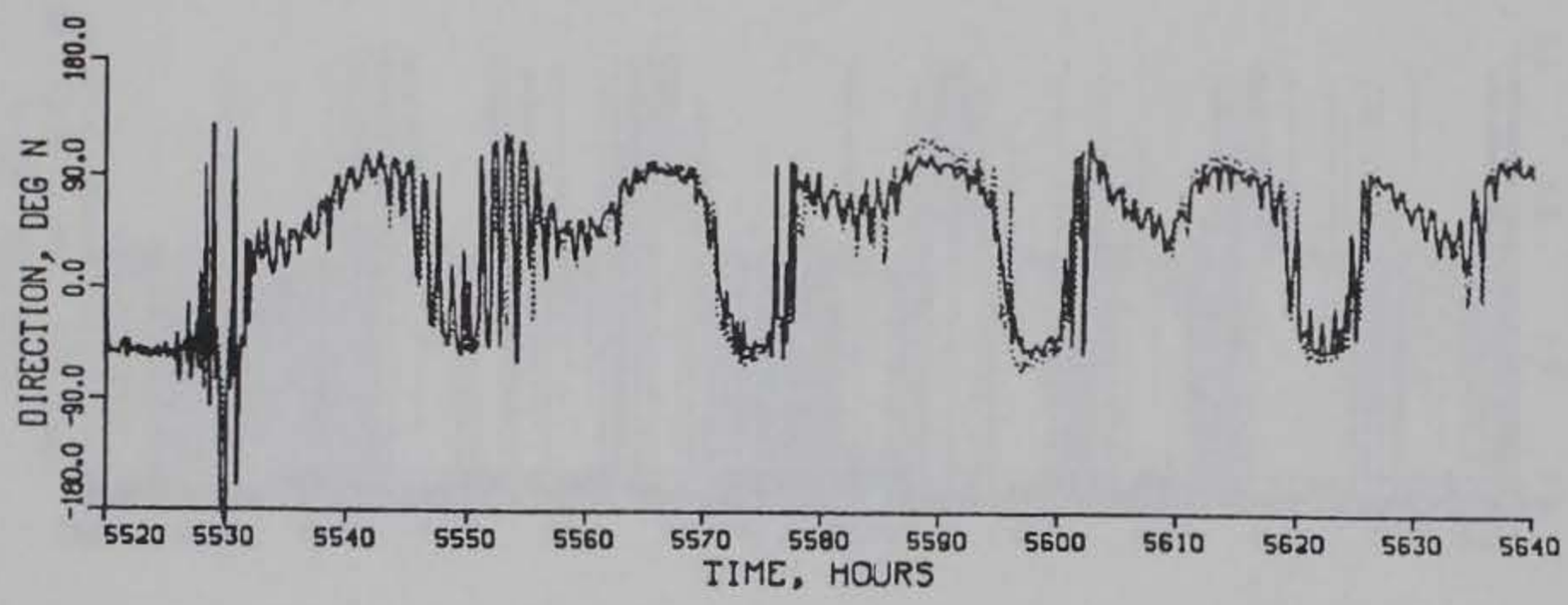

SURFACE

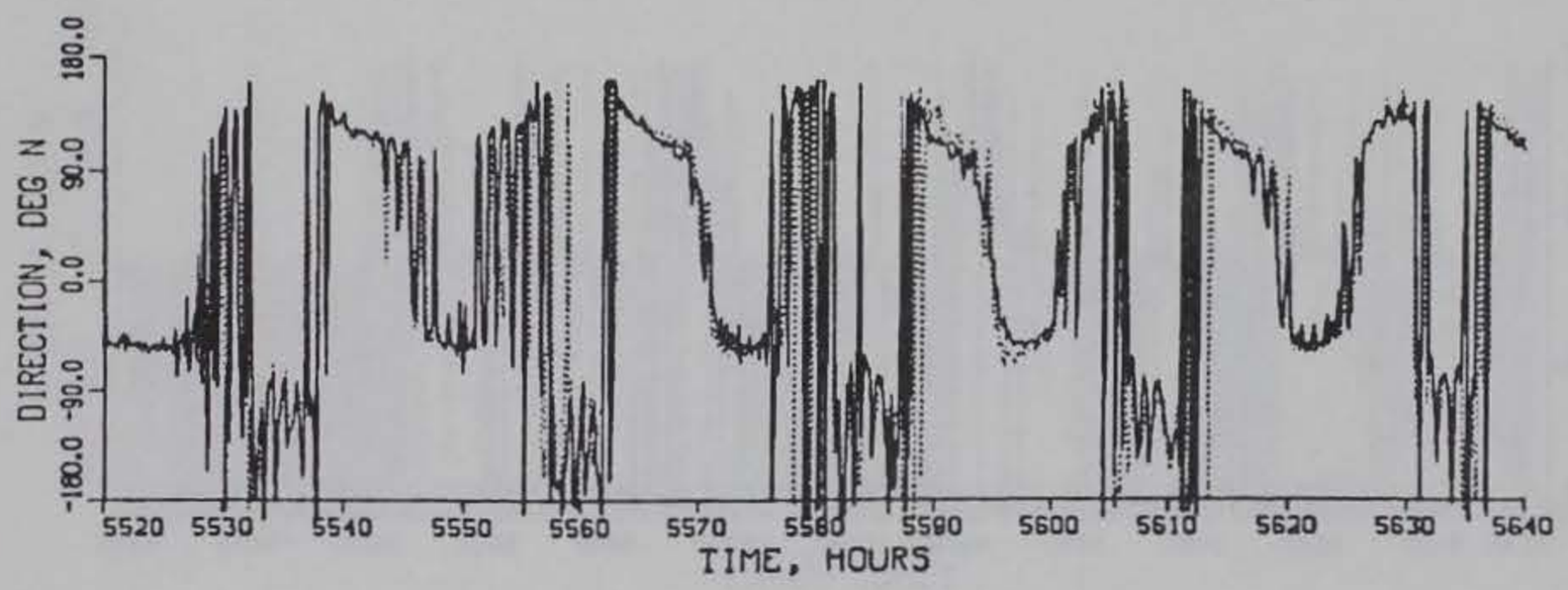

MID-DEPTH

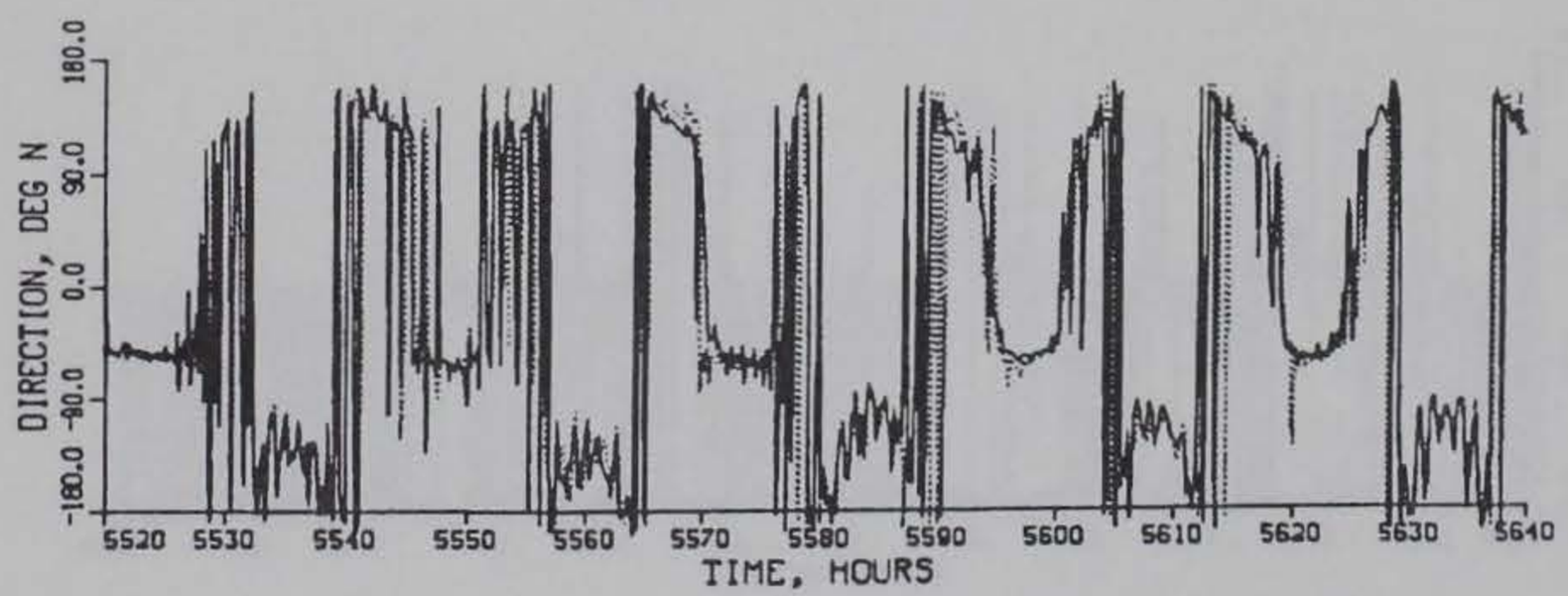

BOTTOM

TIDAL VELOCITY **VERIFICATION PERIOD**

DIRECTION GAGE C5

PLAN (SOLID) VS EXISTING (DOTTED) CONDITIONS

PLATE 94

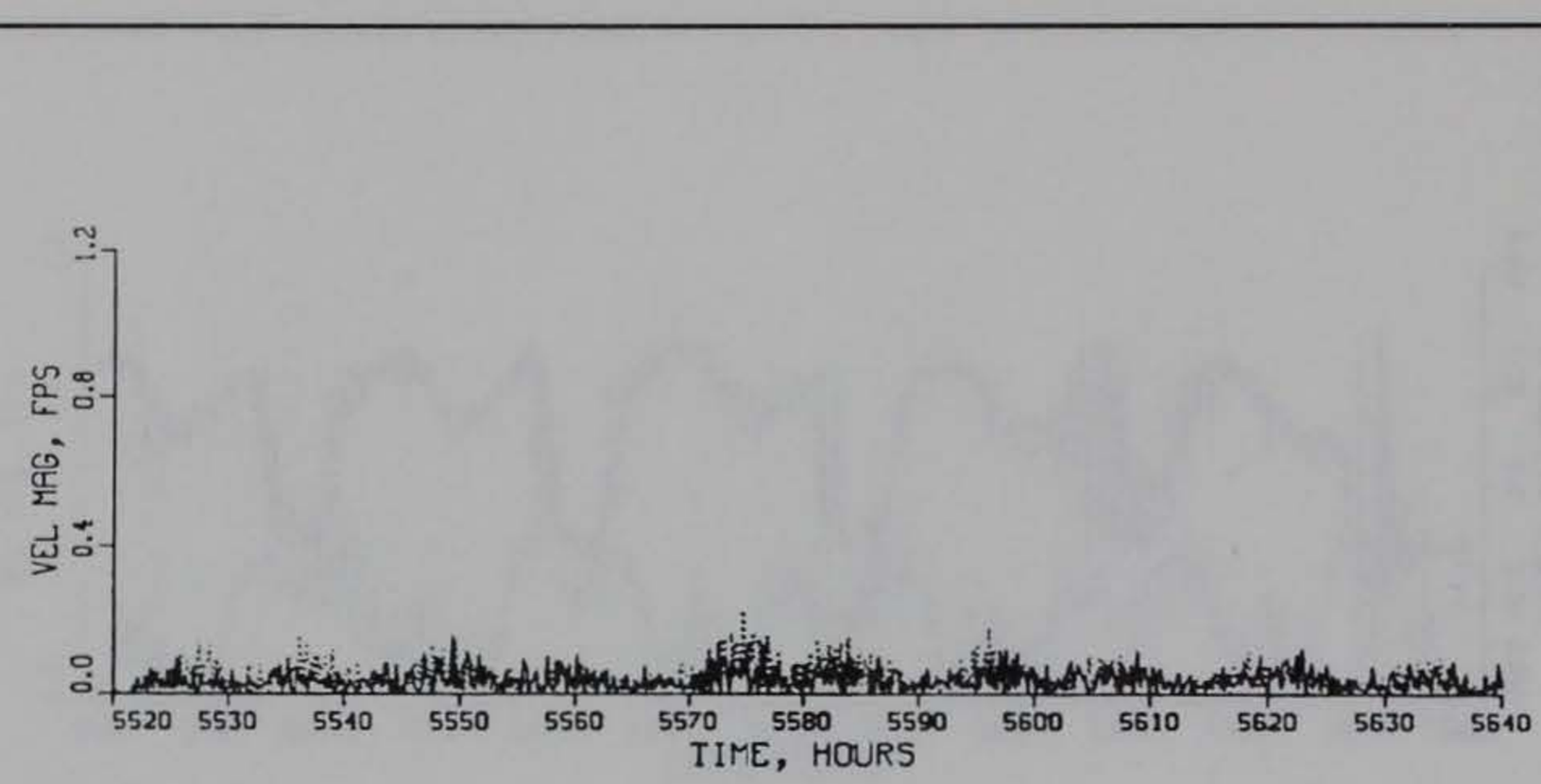

SURFACE

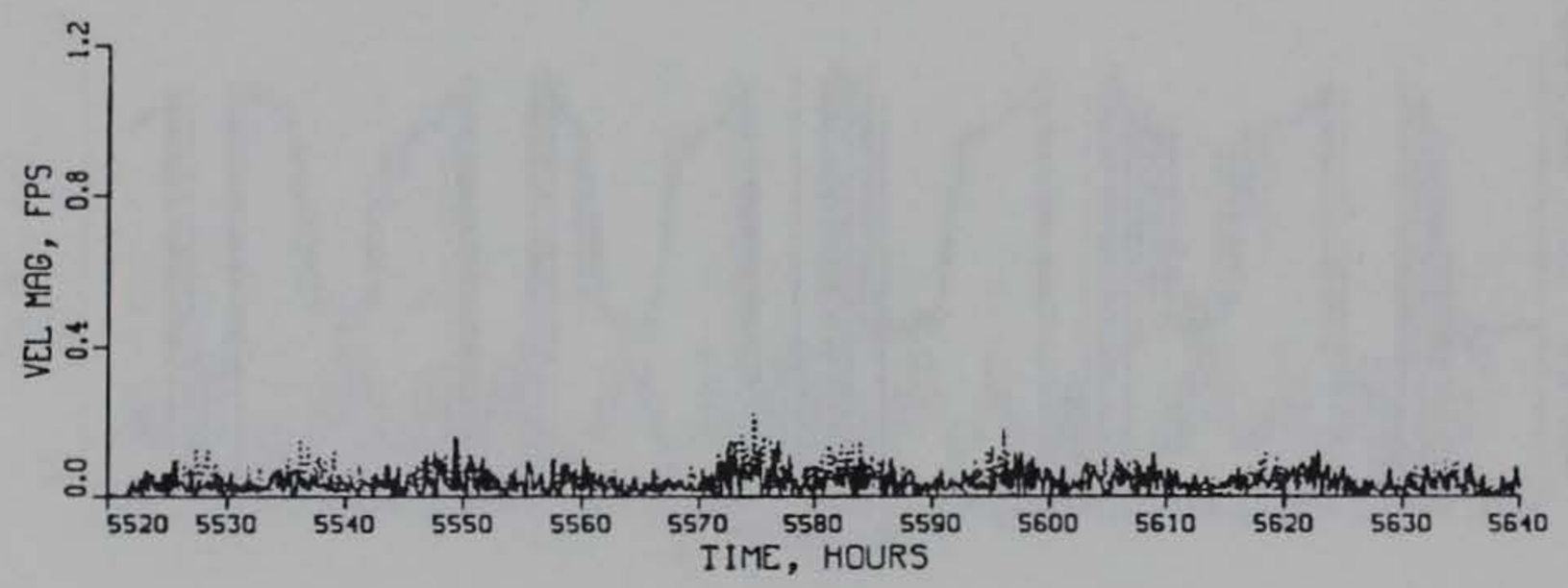

MID-DEPTH

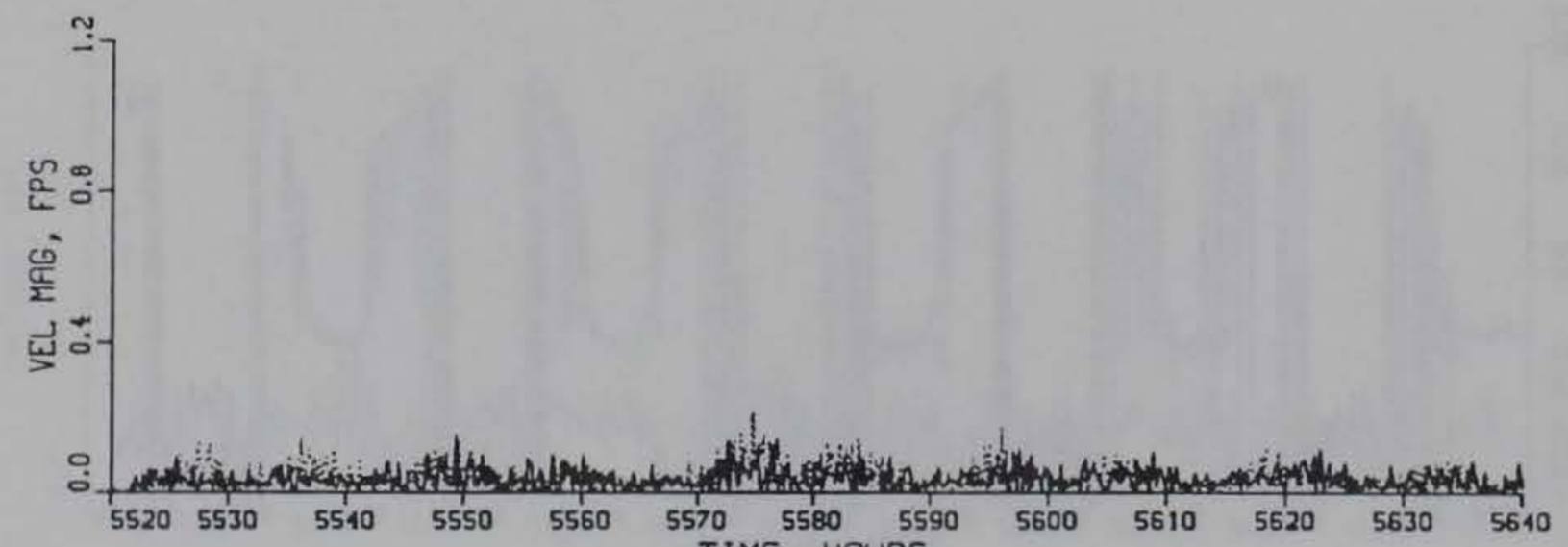

BOTTOM

TIDAL VELOCITY

VERIFICATION PERIOD

MAGNITUDE

GAGE C10

PLAN (SOLID) VS EXISTING (DOTTED) CONDITIONS

PLATE 95

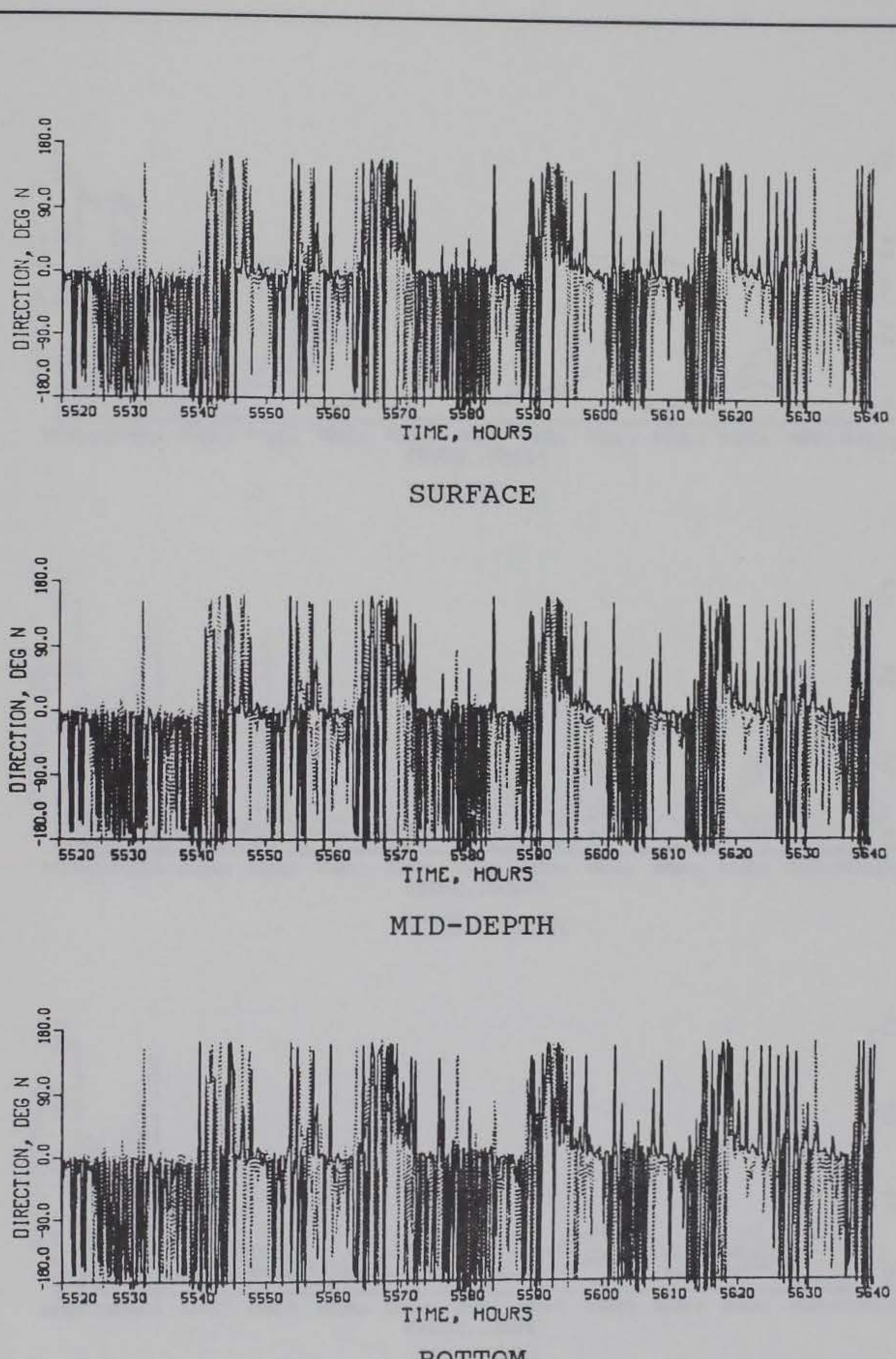

SURFACE

MID-DEPTH

BOTTOM

TIDAL VELOCITY **VERIFICATION PERIOD**

DIRECTION GAGE C10

PLAN (SOLID) VS EXISTING (DOTTED) CONDITIONS

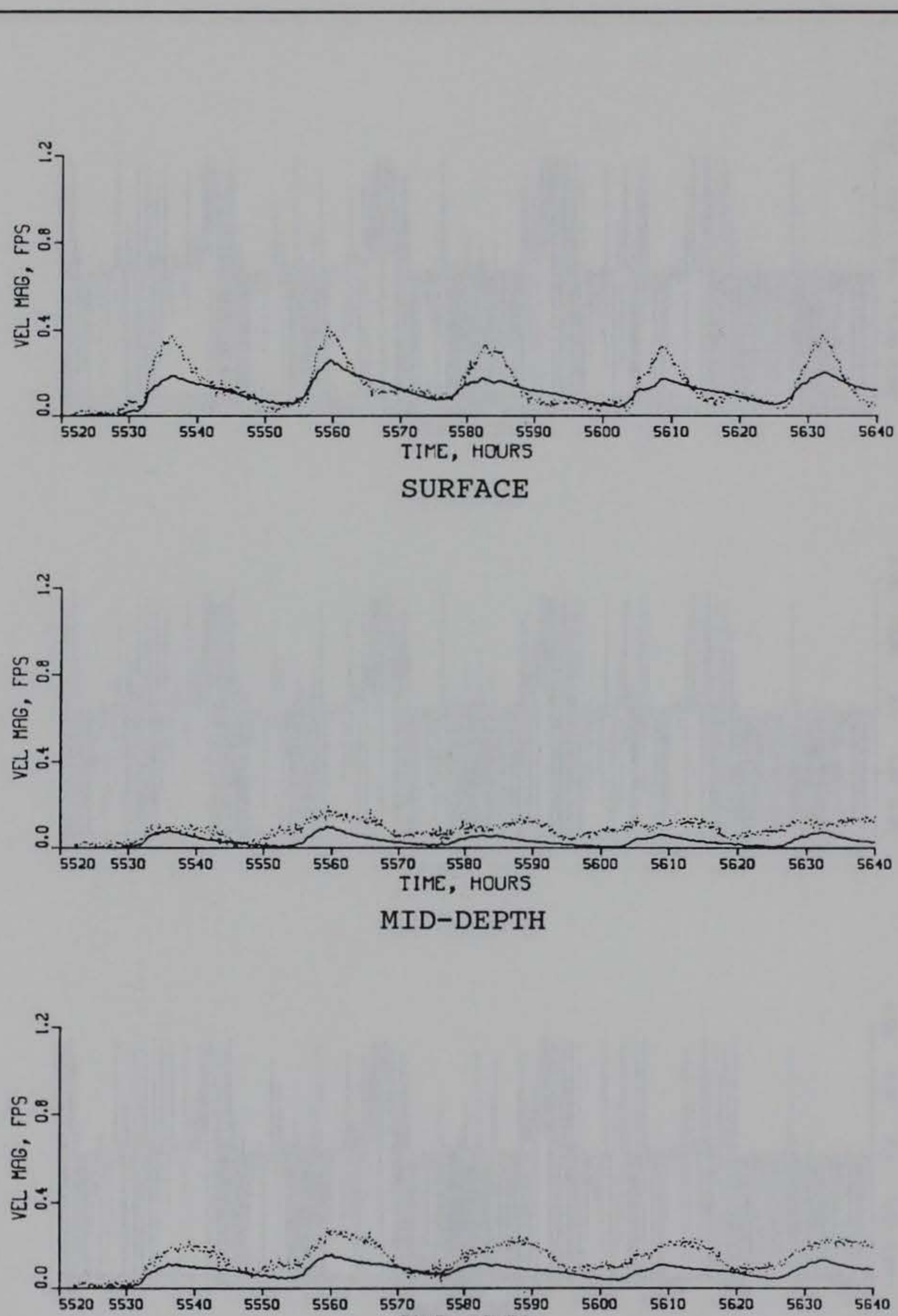

TIDAL VELOCITY VERIFICATION PERIOD

MAGNITUDE

GAGE C12

PLAN (SOLID) VS EXISTING (DOTTED) CONDITIONS

PLATE 97

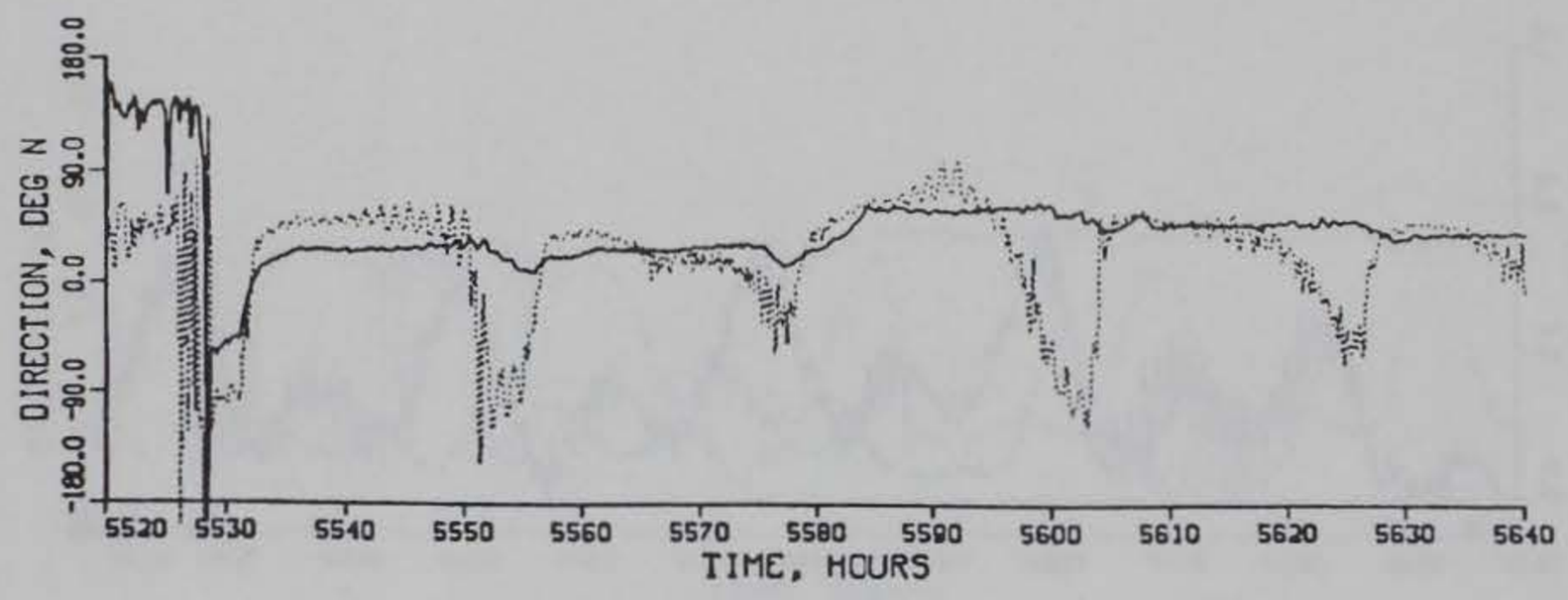

SURFACE

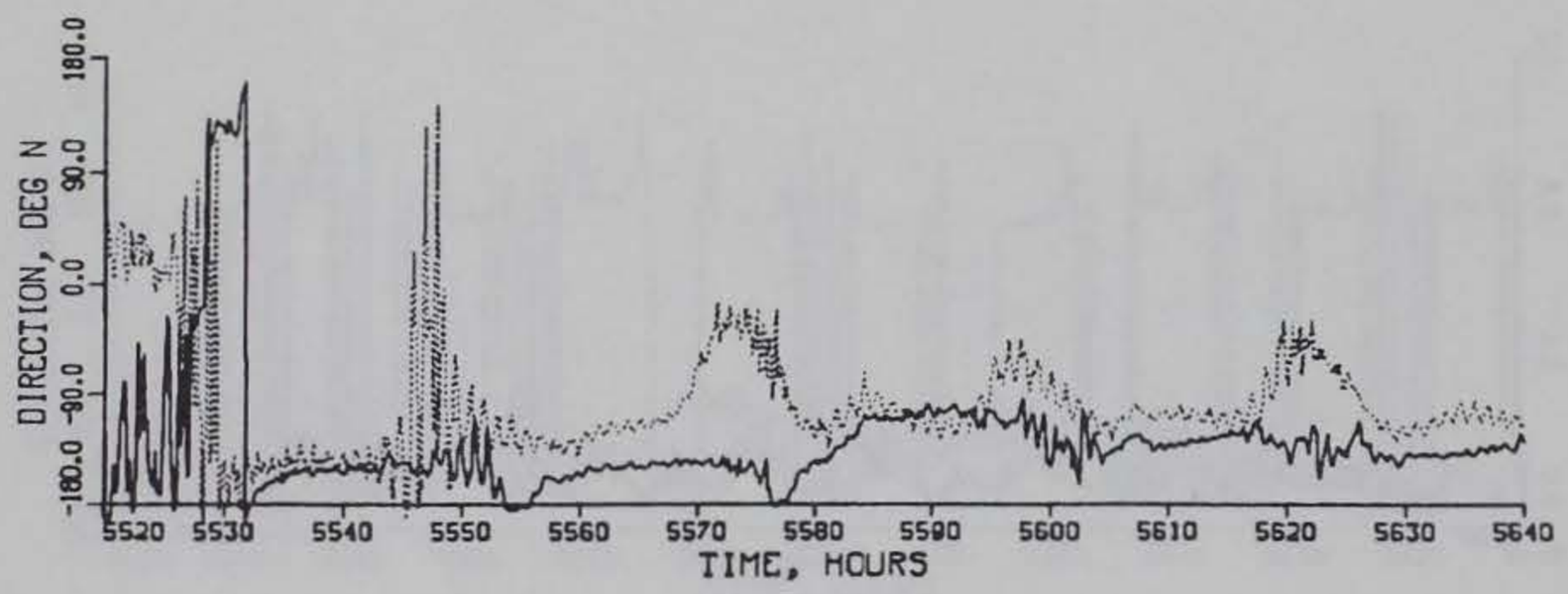

MID-DEPTH

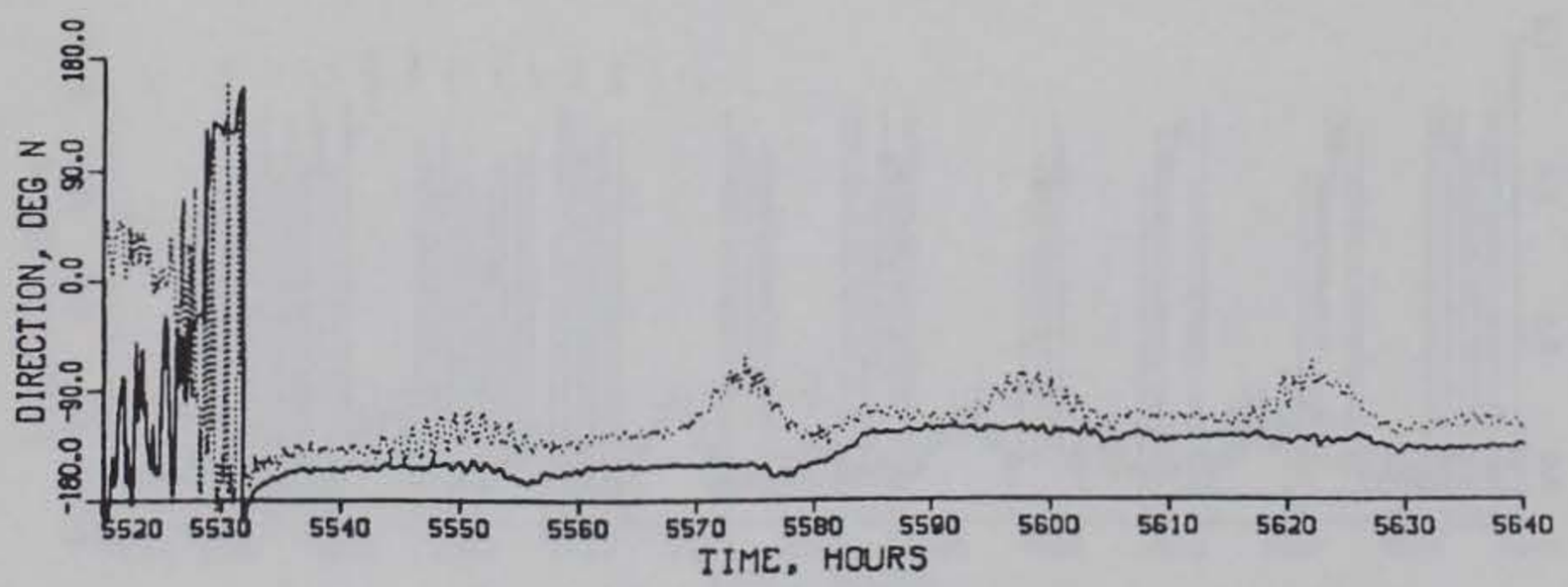

BOTTOM

TIDAL VELOCITY **VERIFICATION PERIOD**

DIRECTION GAGE C12

PLAN (SOLID) VS EXISTING (DOTTED) CONDITIONS

PLATE 98

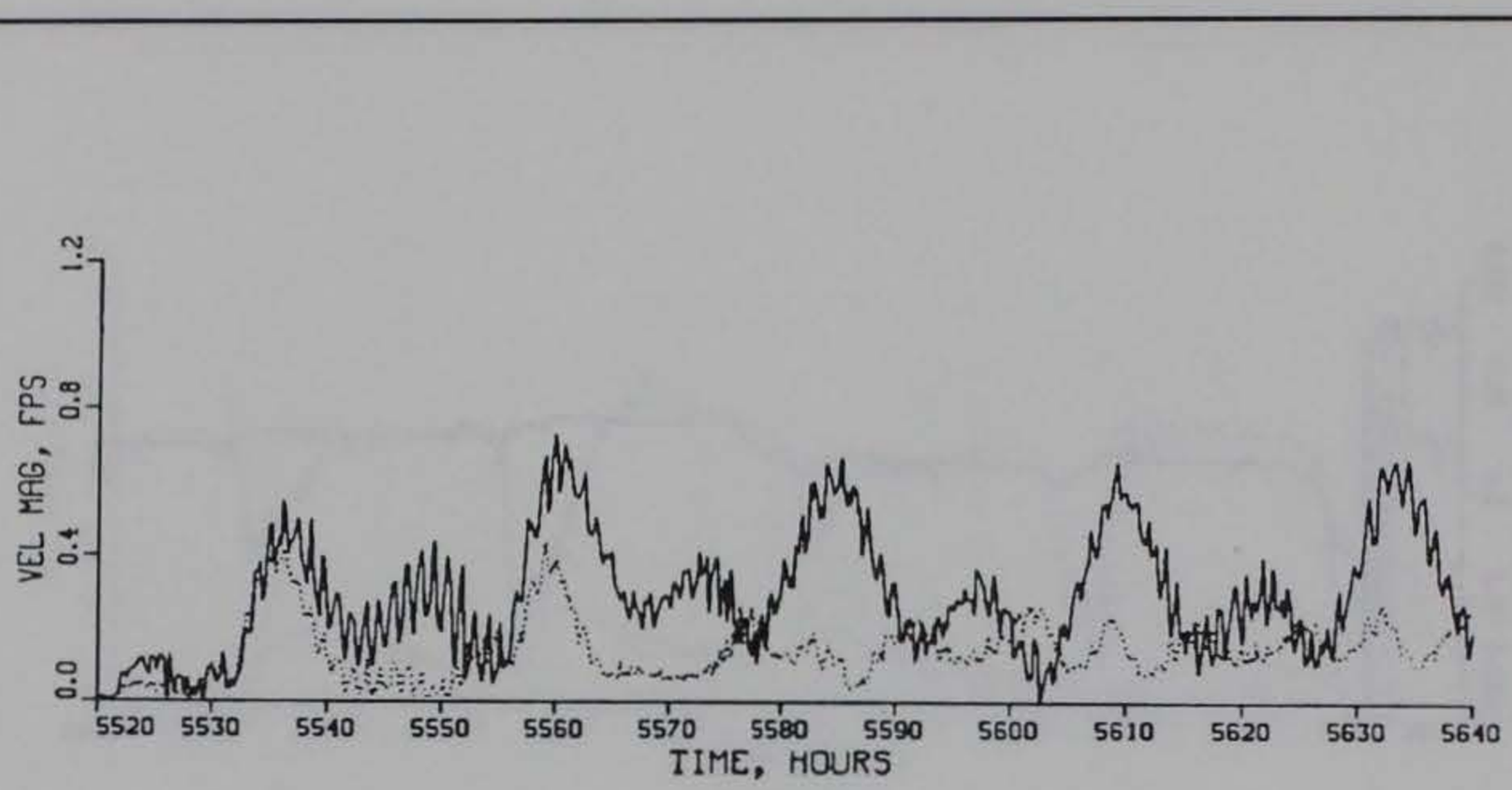

SURFACE

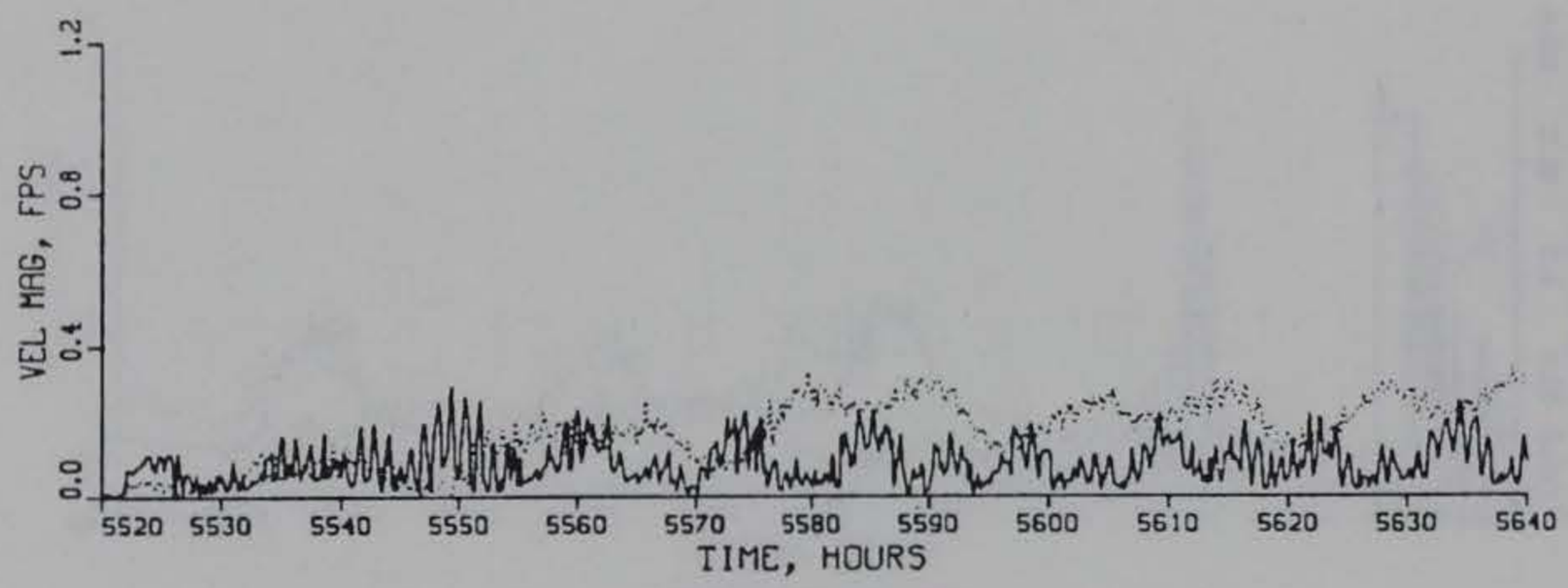

MID-DEPTH

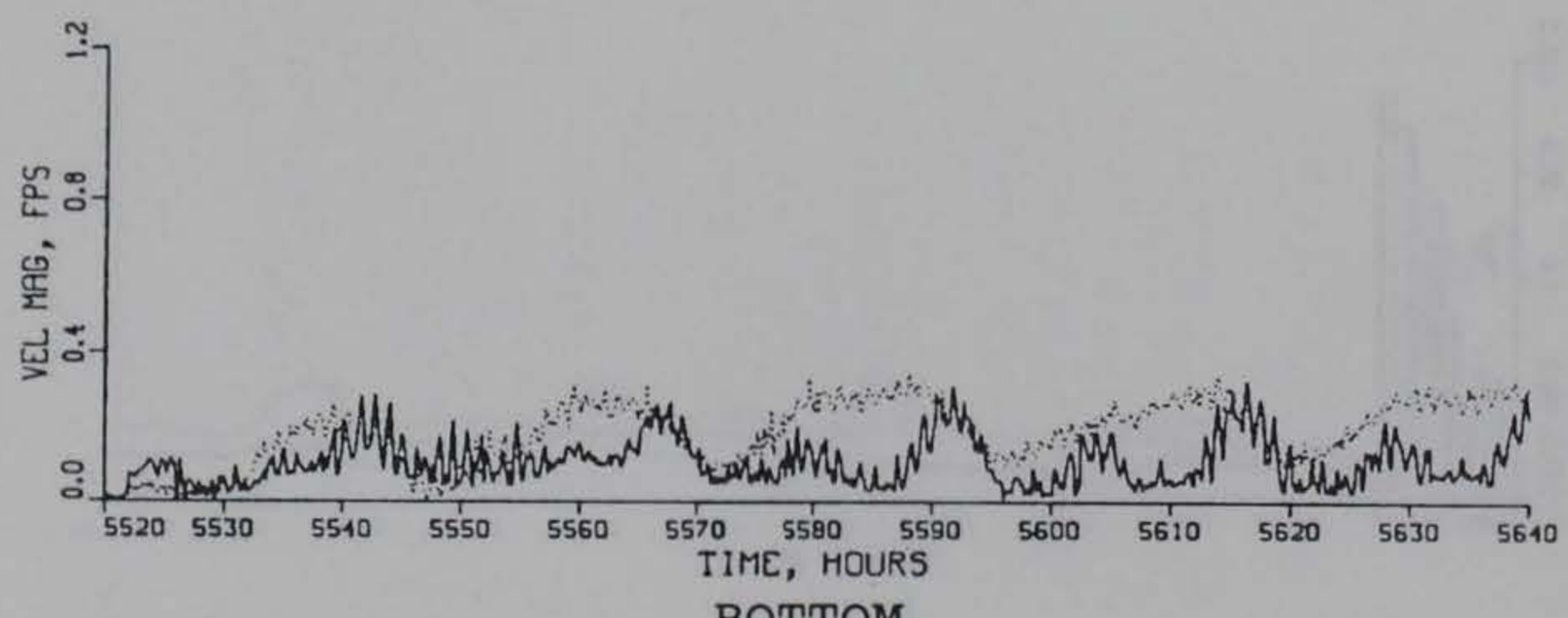

BOTTOM

TIDAL VELOCITY VERIFICATION PERIOD

MAGNITUDE GAGE C14

PLAN (SOLID) VS EXISTING (DOTTED) CONDITIONS

PLATE 99

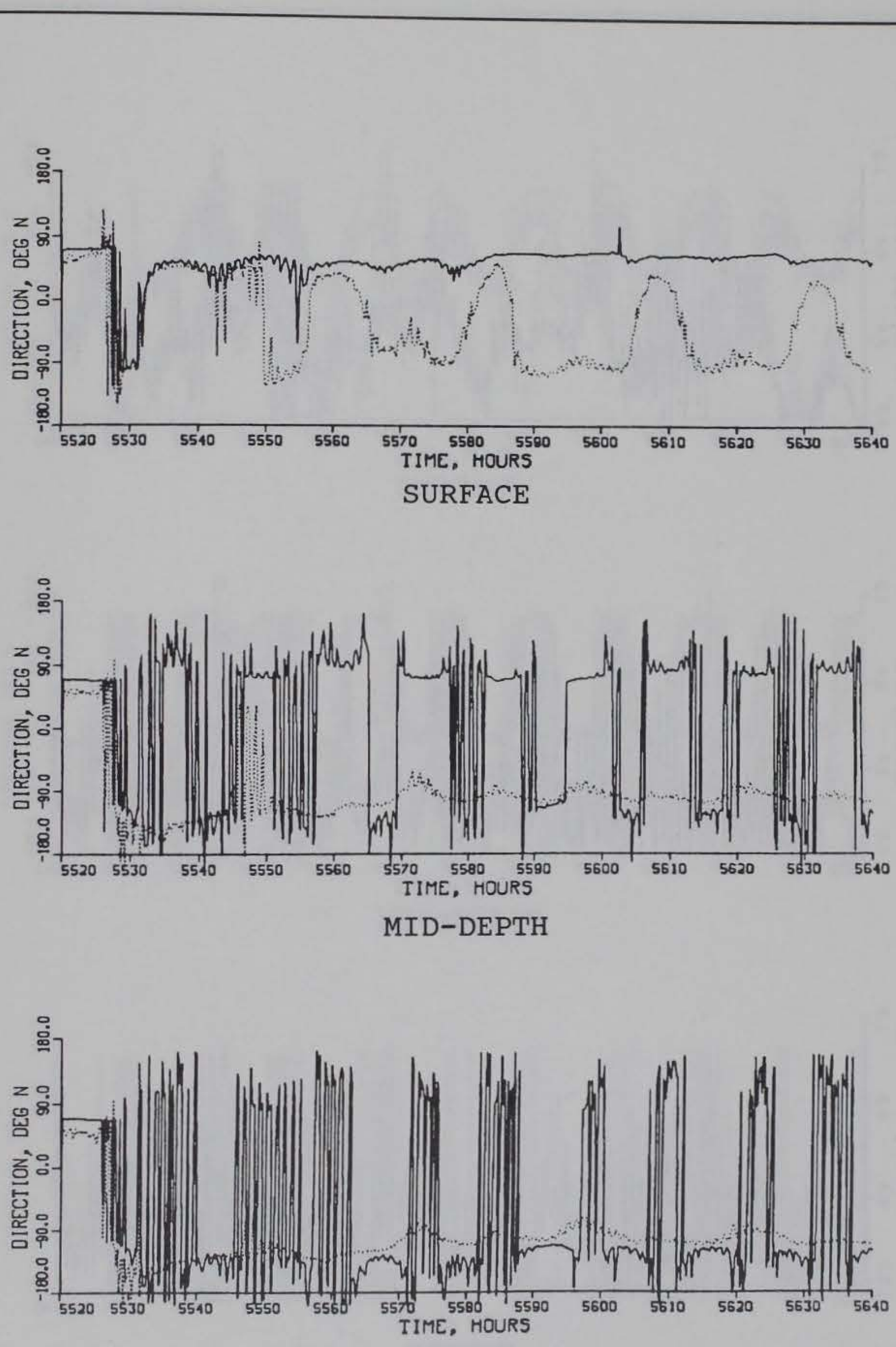

TIDAL VELOCITY VERIFICATION PERIOD

DIRECTION GAGE C14

PLAN (SOLID) VS EXISTING (DOTTED) CONDITIONS

PLATE 100

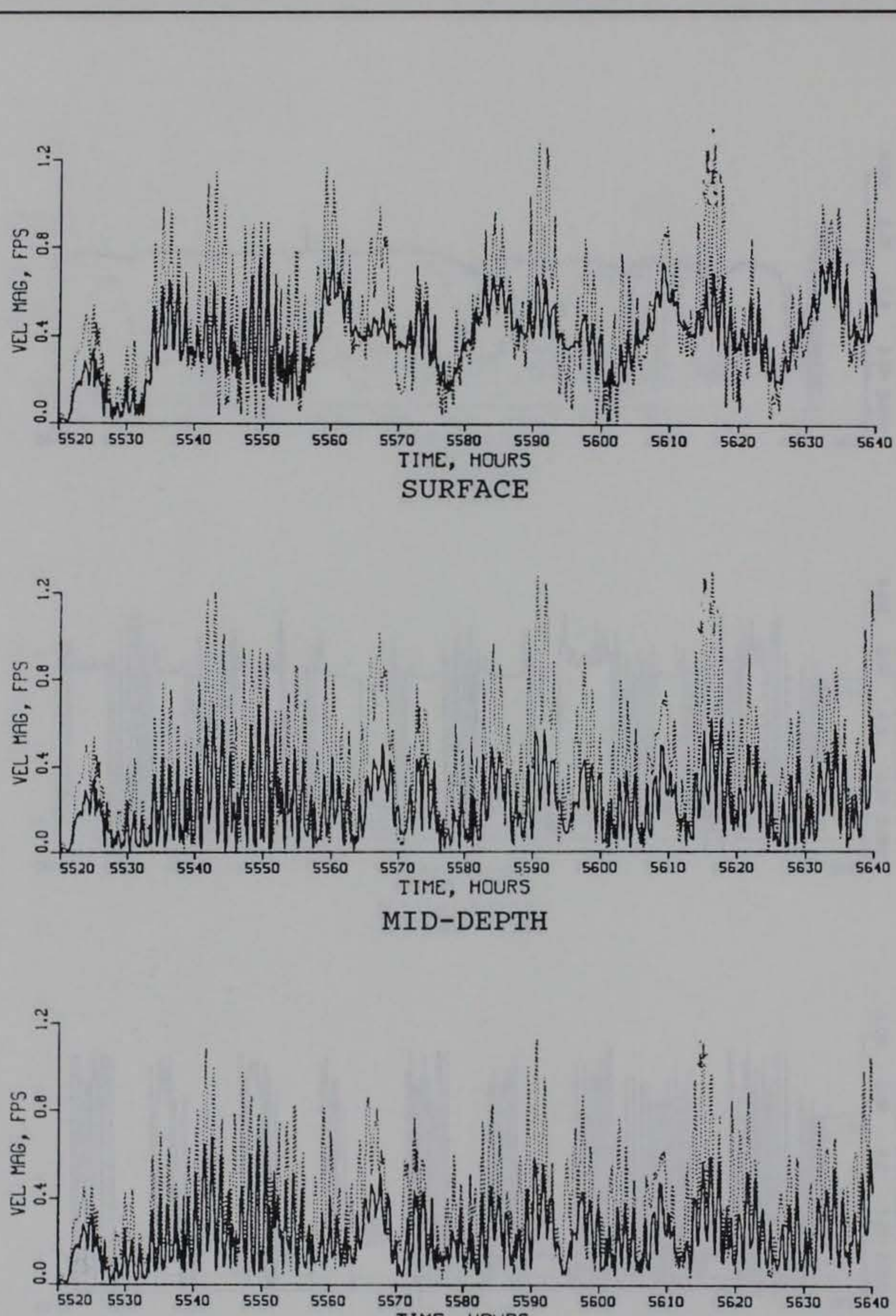

TIDAL VELOCITY VERIFICATION PERIOD

MAGNITUDE

GAGE C18

PLAN (SOLID) VS EXISTING (DOTTED) CONDITIONS

PLATE 101

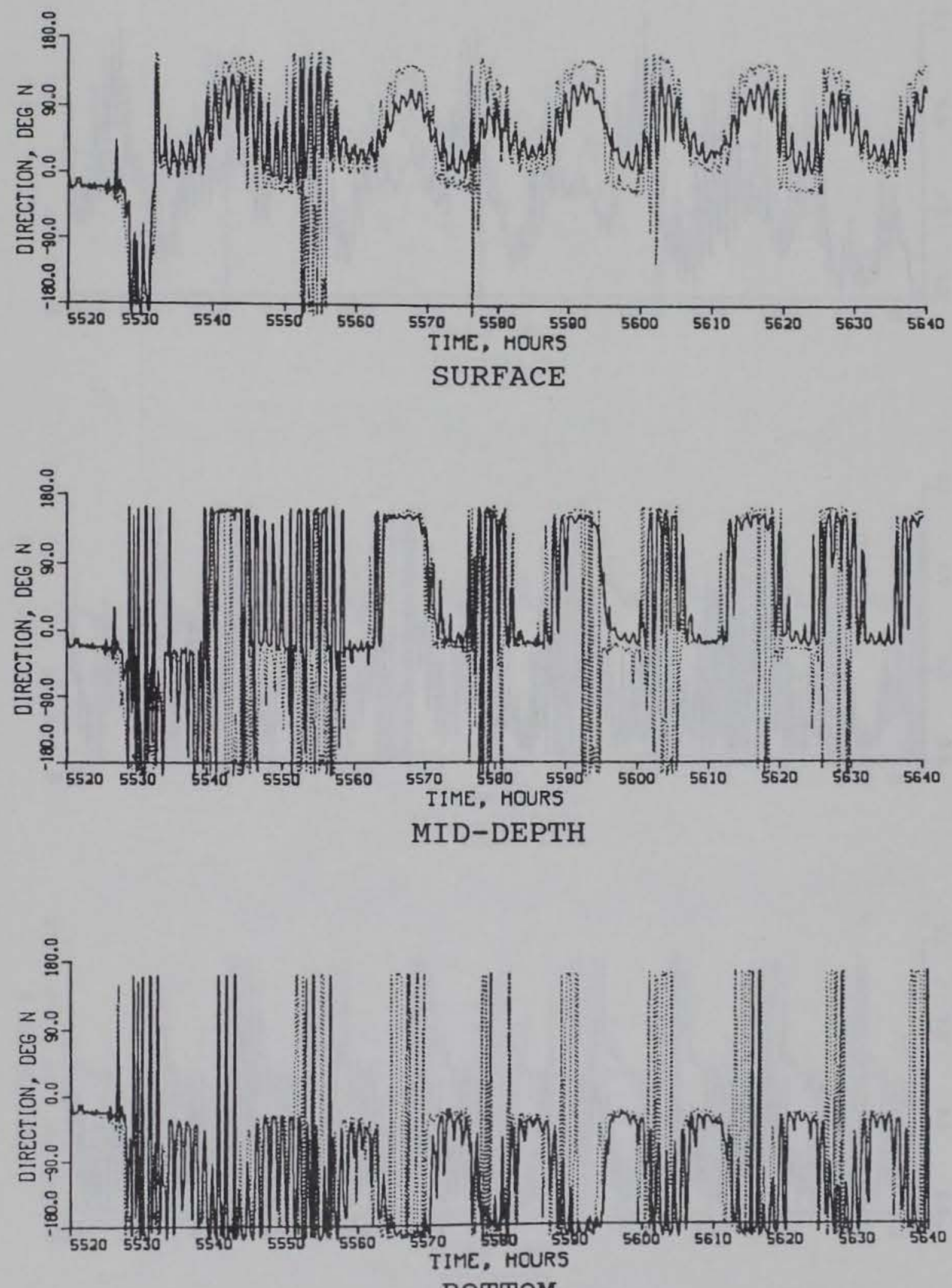

TIDAL VELOCITY **VERIFICATION PERIOD**

DIRECTION GAGE C18

PLAN (SOLID) VS EXISTING (DOTTED) CONDITIONS

PLATE 102

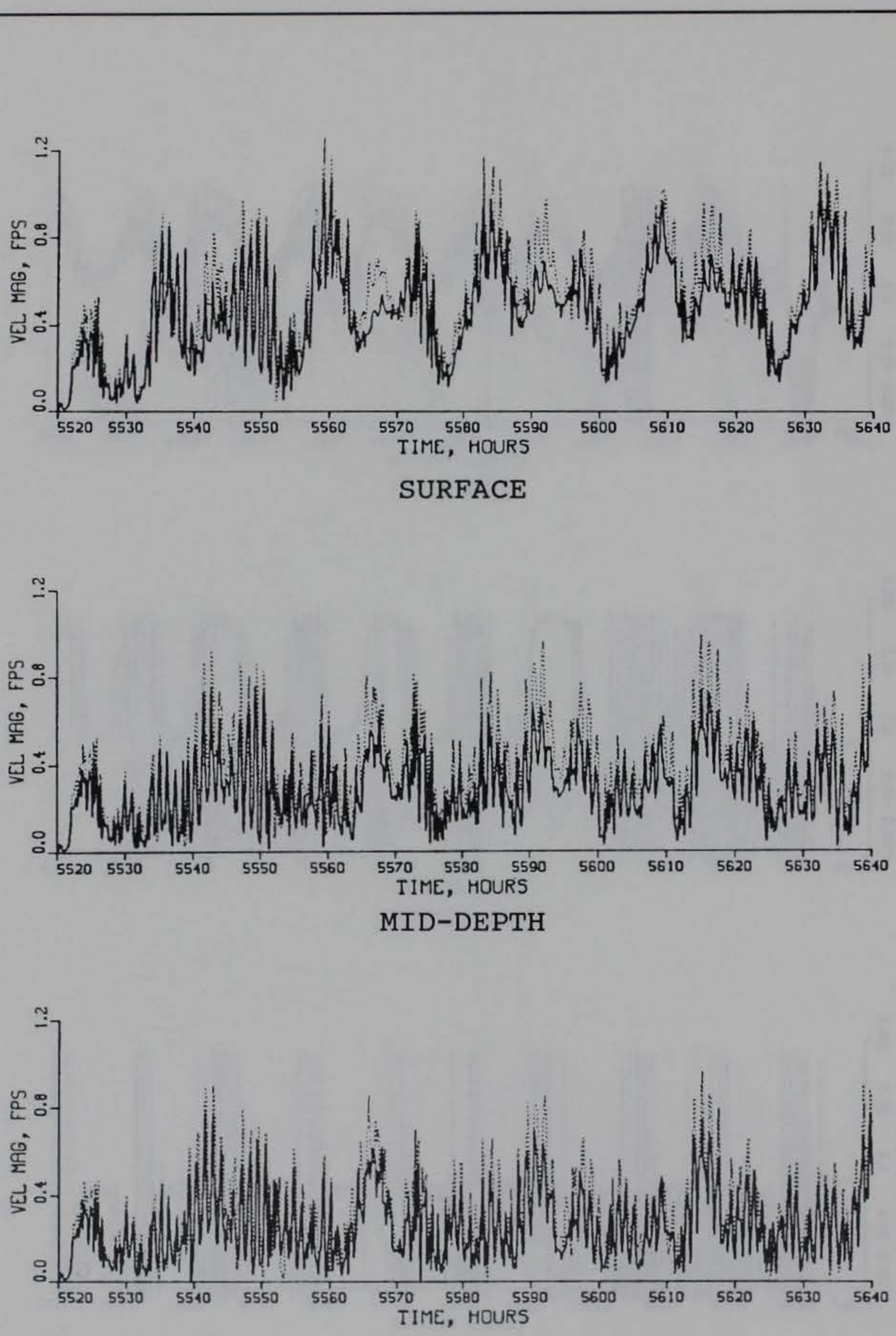

SURFACE

MID-DEPTH

BOTTOM

TIDAL VELOCITY VERIFICATION PERIOD

MAGNITUDE GAGE C19

PLAN (SOLID) VS EXISTING (DOTTED) CONDITIONS

PLATE 103

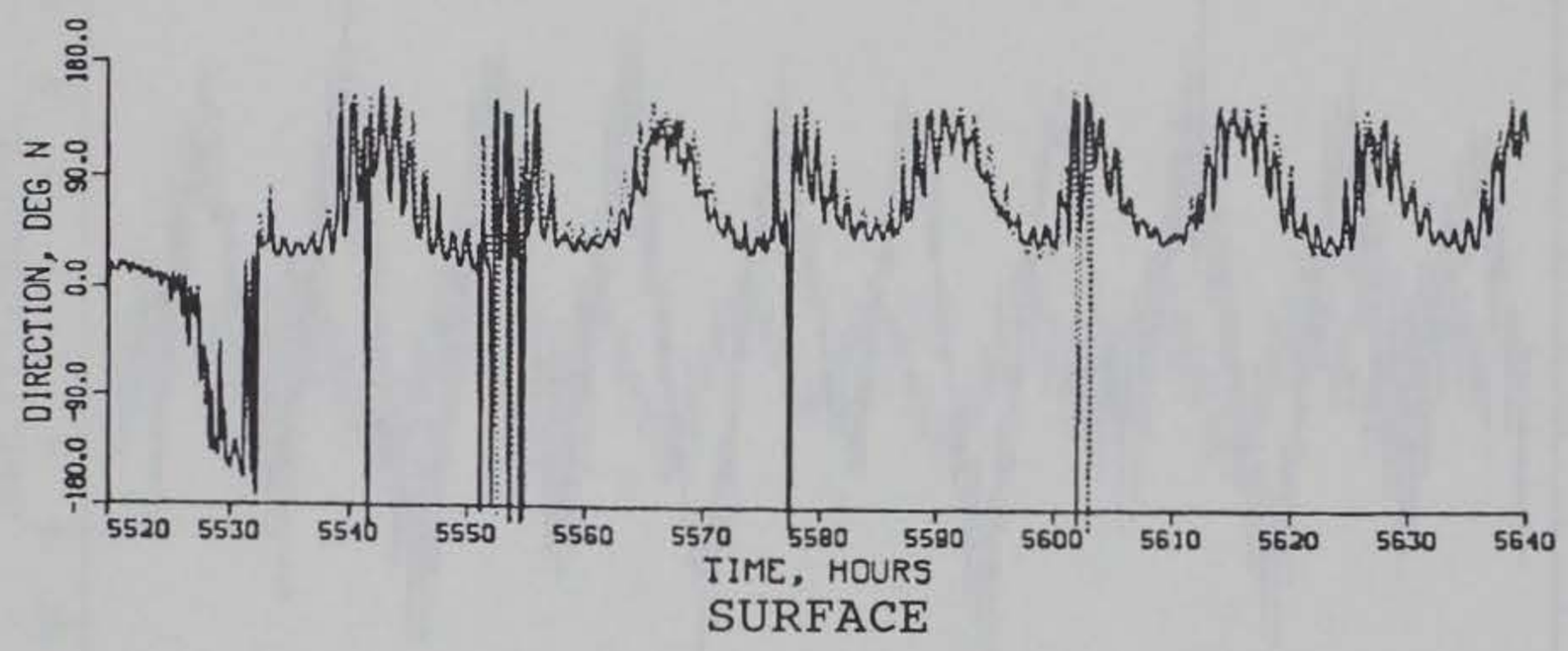

SURFACE

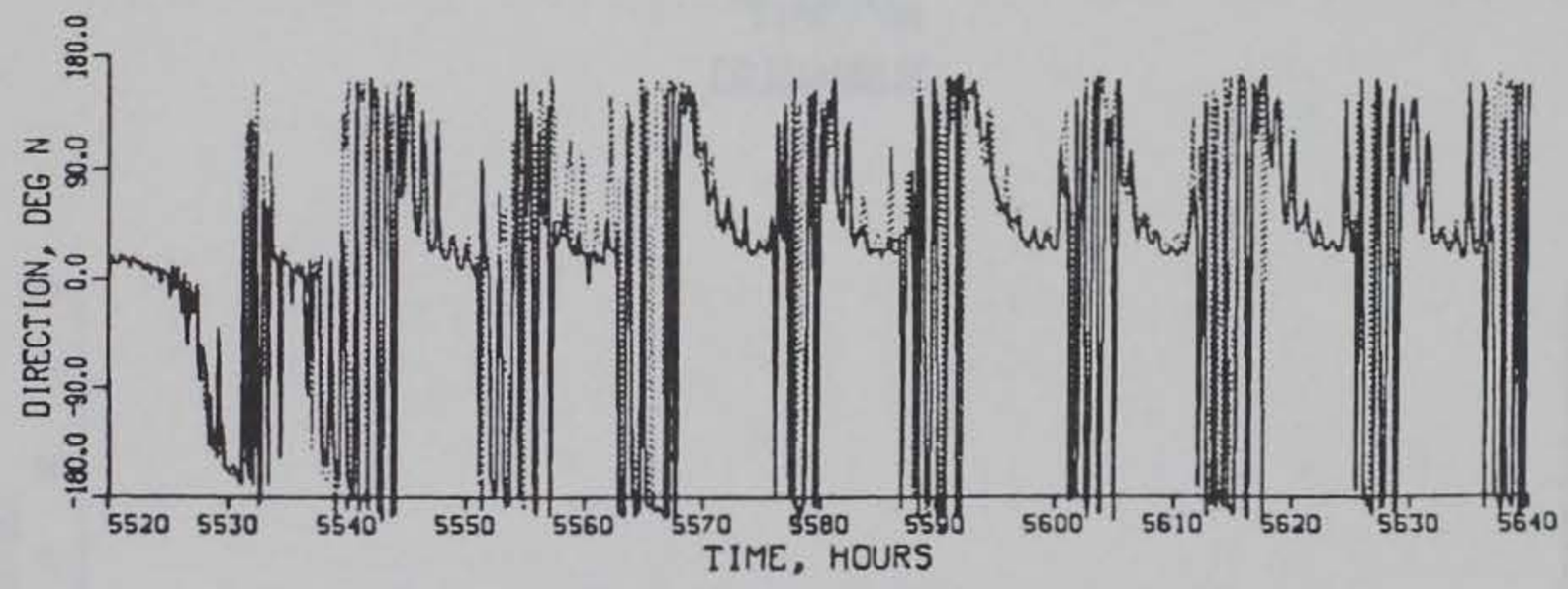

MID-DEPTH

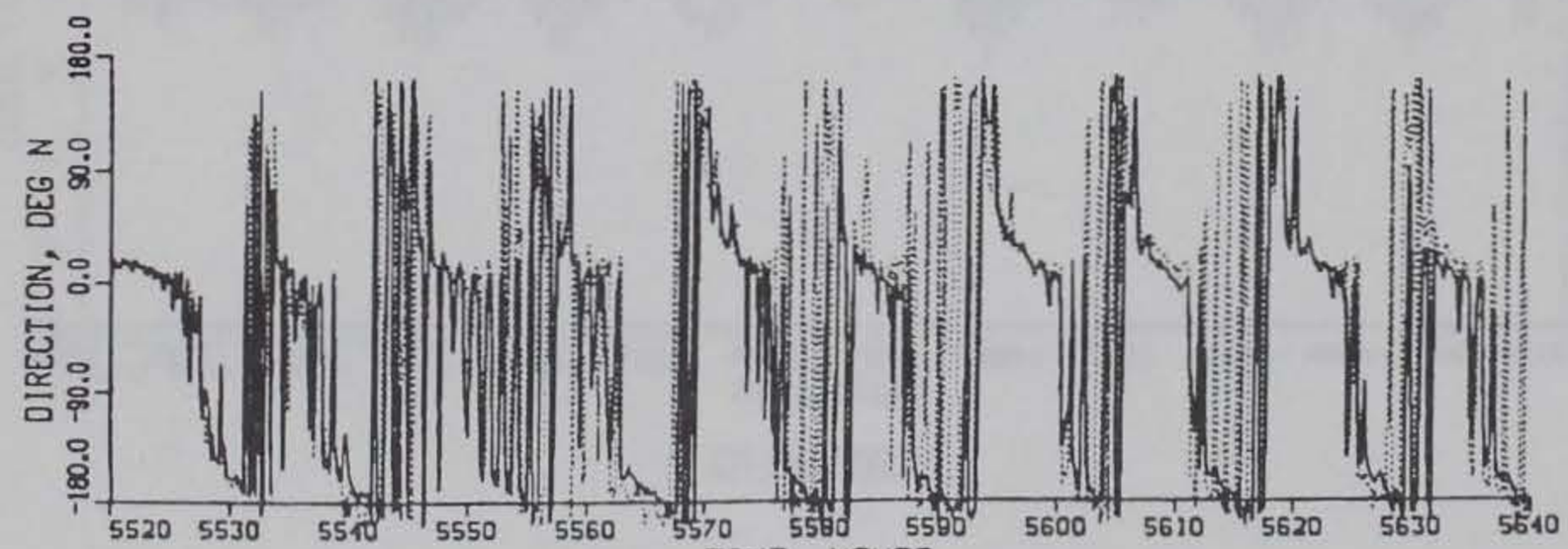

BOTTOM

TIDAL VELOCITY

VERIFICATION PERIOD

DIRECTION

GAGE C19

PLAN (SOLID) VS EXISTING (DOTTED) CONDITIONS

PLATE 104

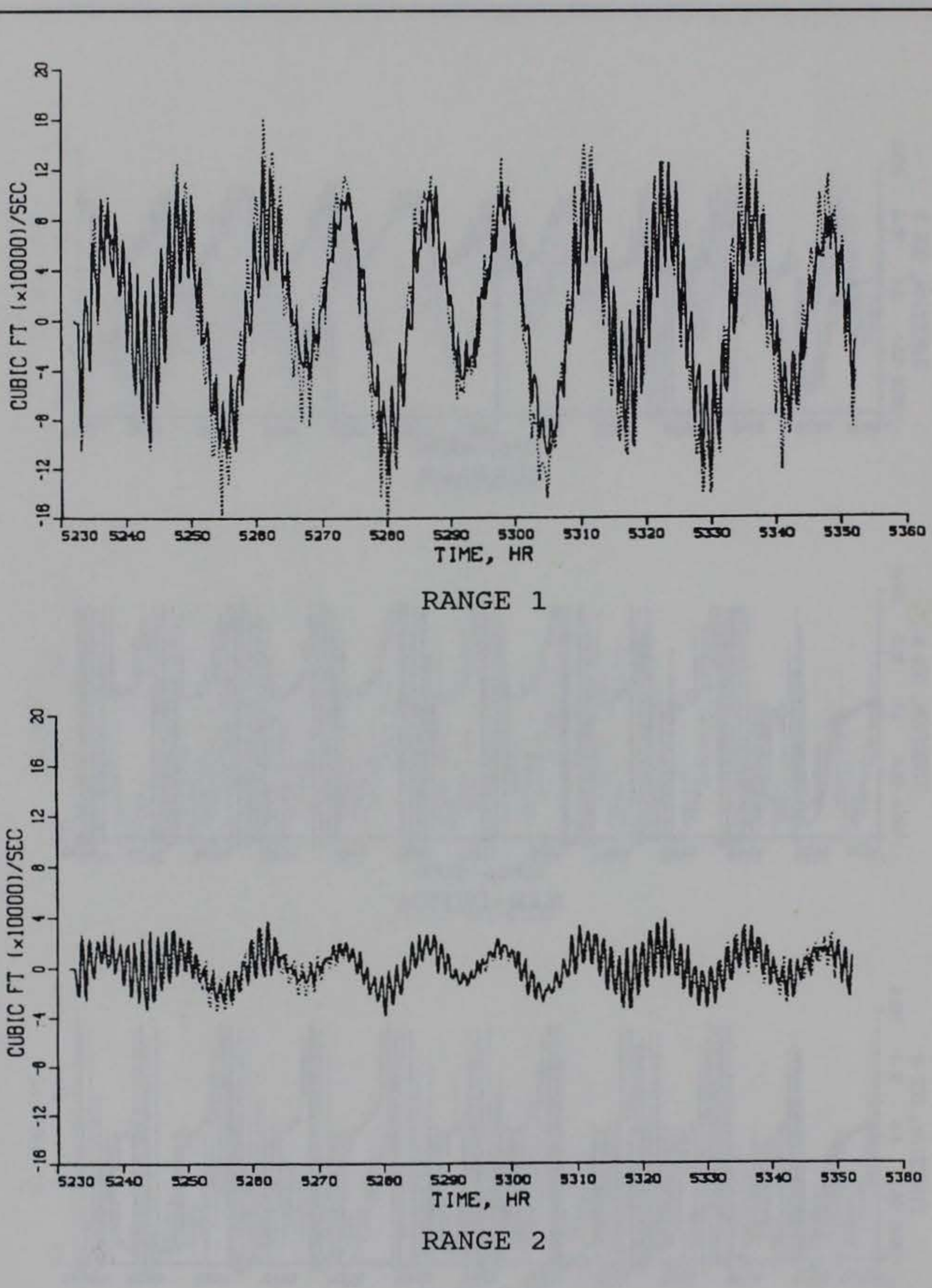

TIDAL DISCHARGE **CALIBRATION PERIOD**

PLAN (SOLID) VS EXISTING (DOTTED) CONDITIONS

PLATE 105

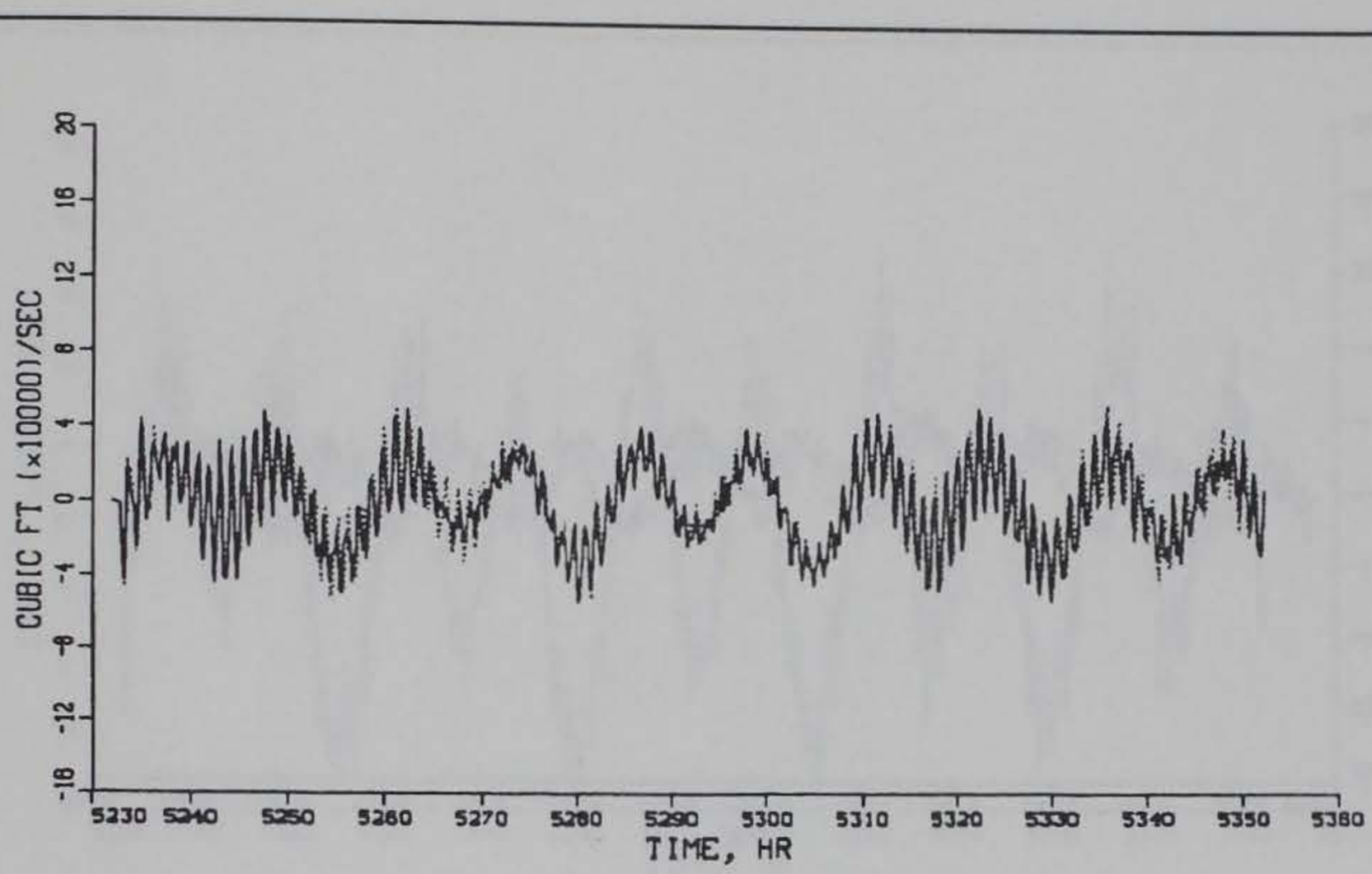

RANGE 3

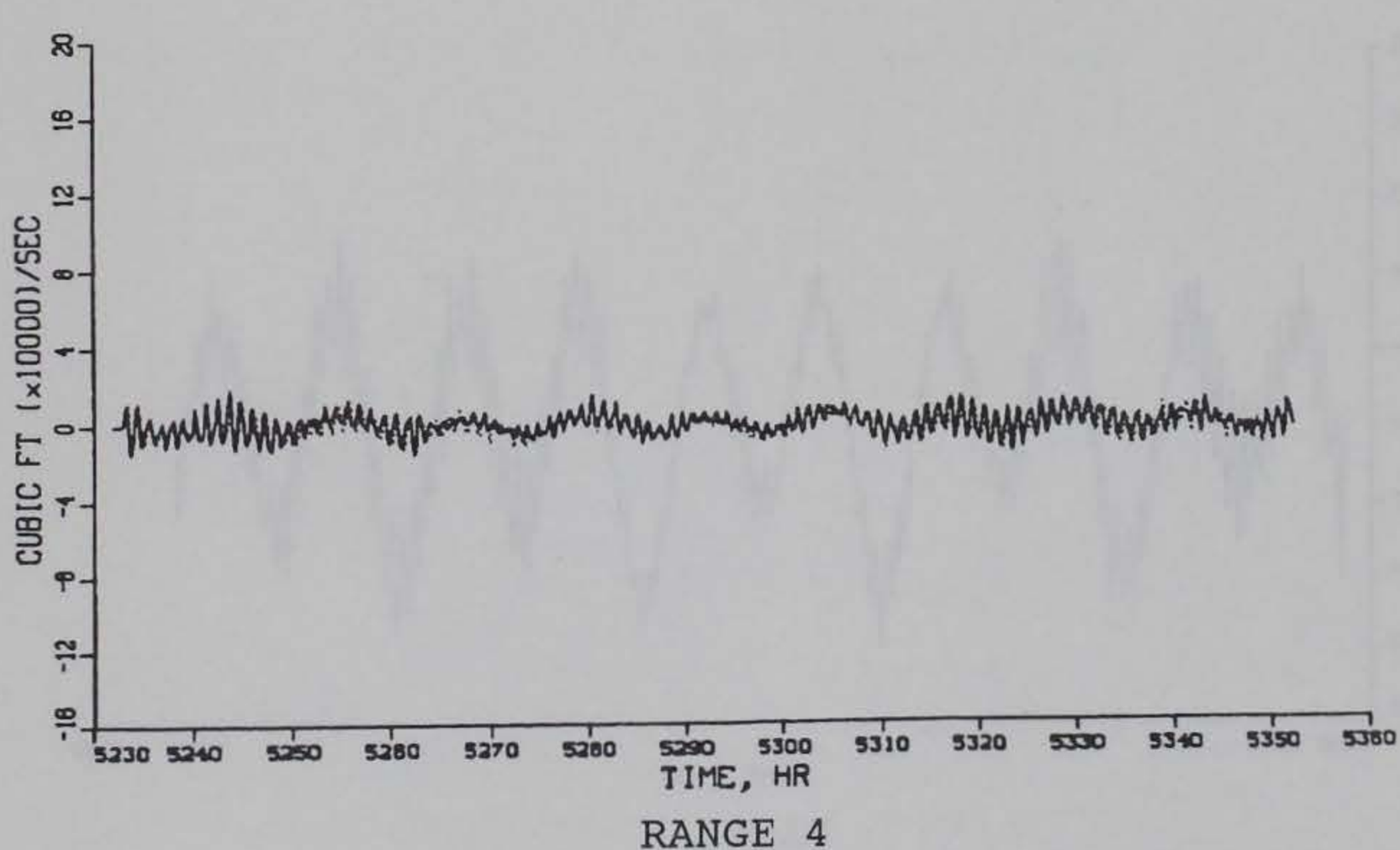

RANGE 4

TIDAL DISCHARGE CALIBRATION PERIOD

PLAN (SOLID) VS EXISTING (DOTTED) CONDITIONS

PLATE 106

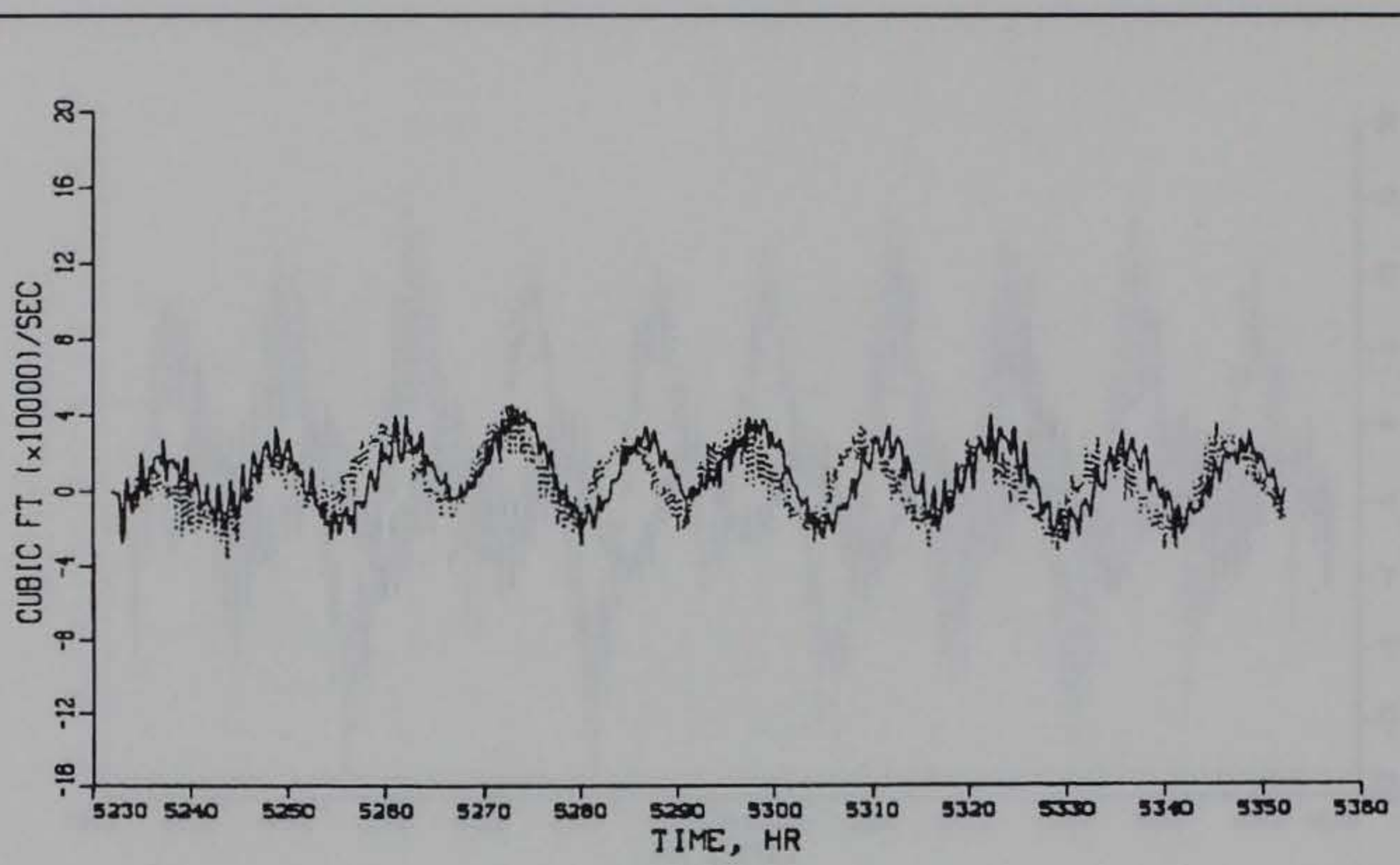

RANGE 5

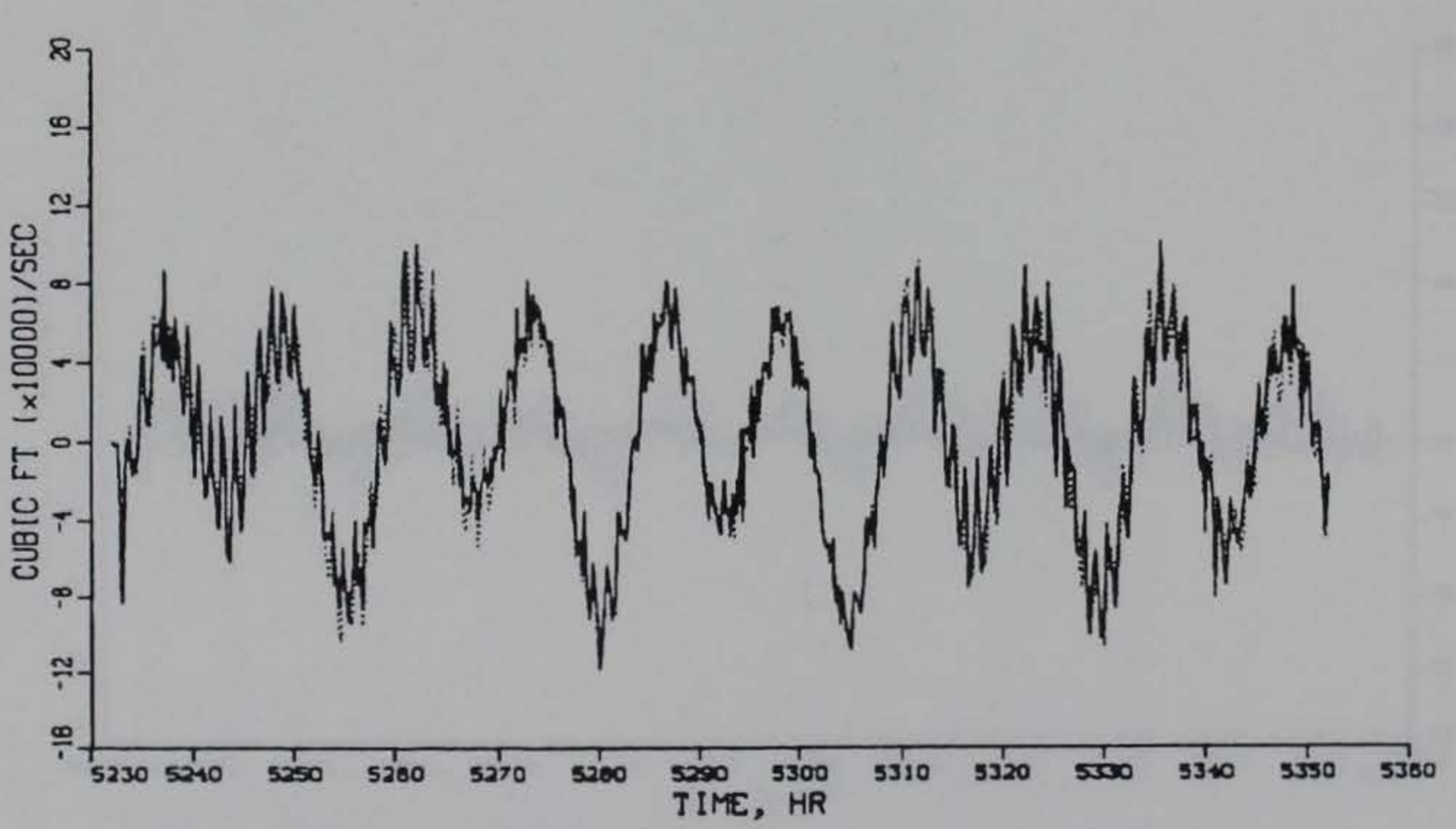

RANGE 6

TIDAL DISCHARGE CALIBRATION PERIOD

PLAN (SOLID) VS EXISTING (DOTTED) CONDITIONS

PLATE 107

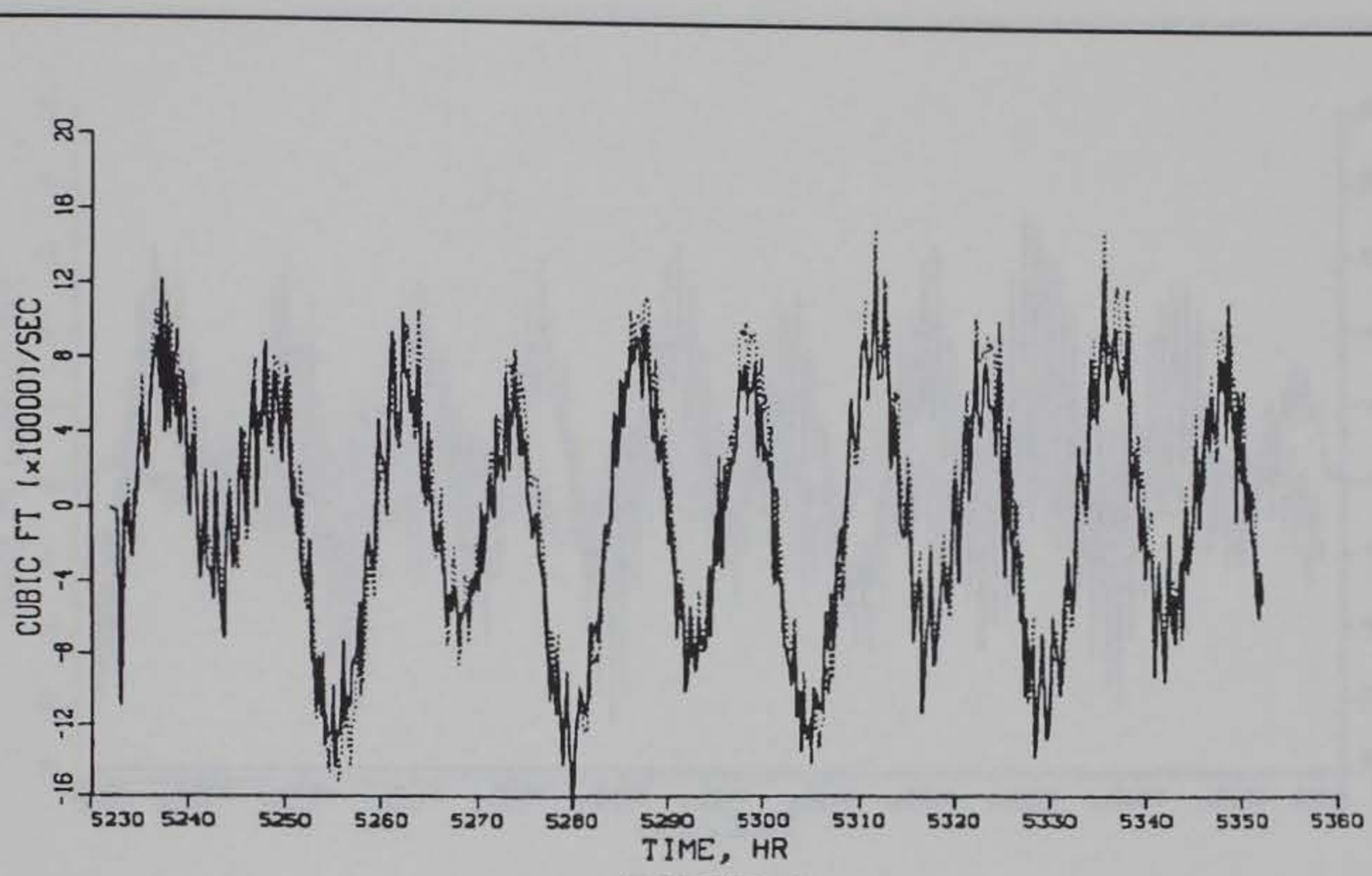

RANGE 7

TIDAL DISCHARGE CALIBRATION PERIOD

PLAN (SOLID) VS EXISTING (DOTTED) CONDITIONS

PLATE 108

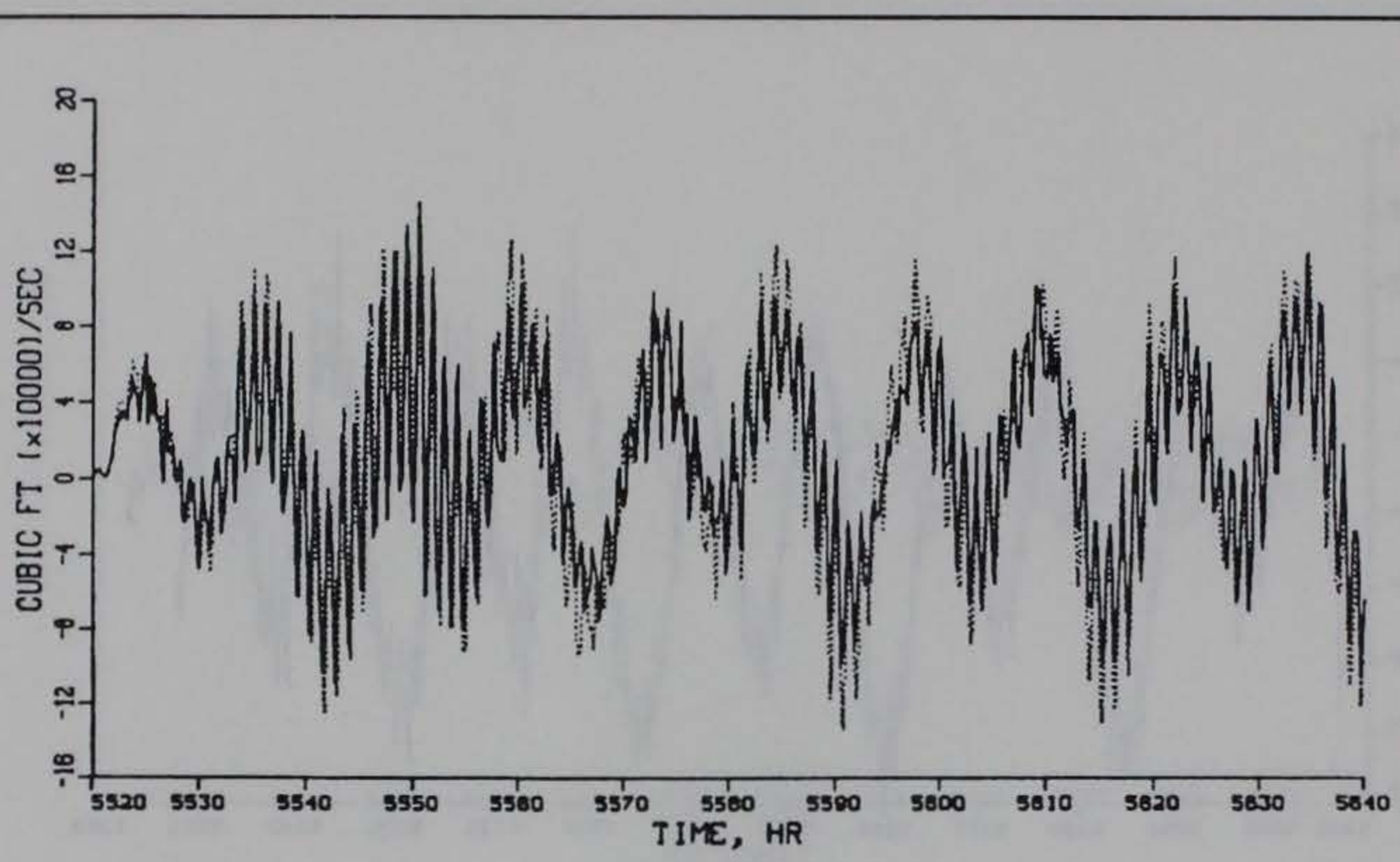

RANGE 1

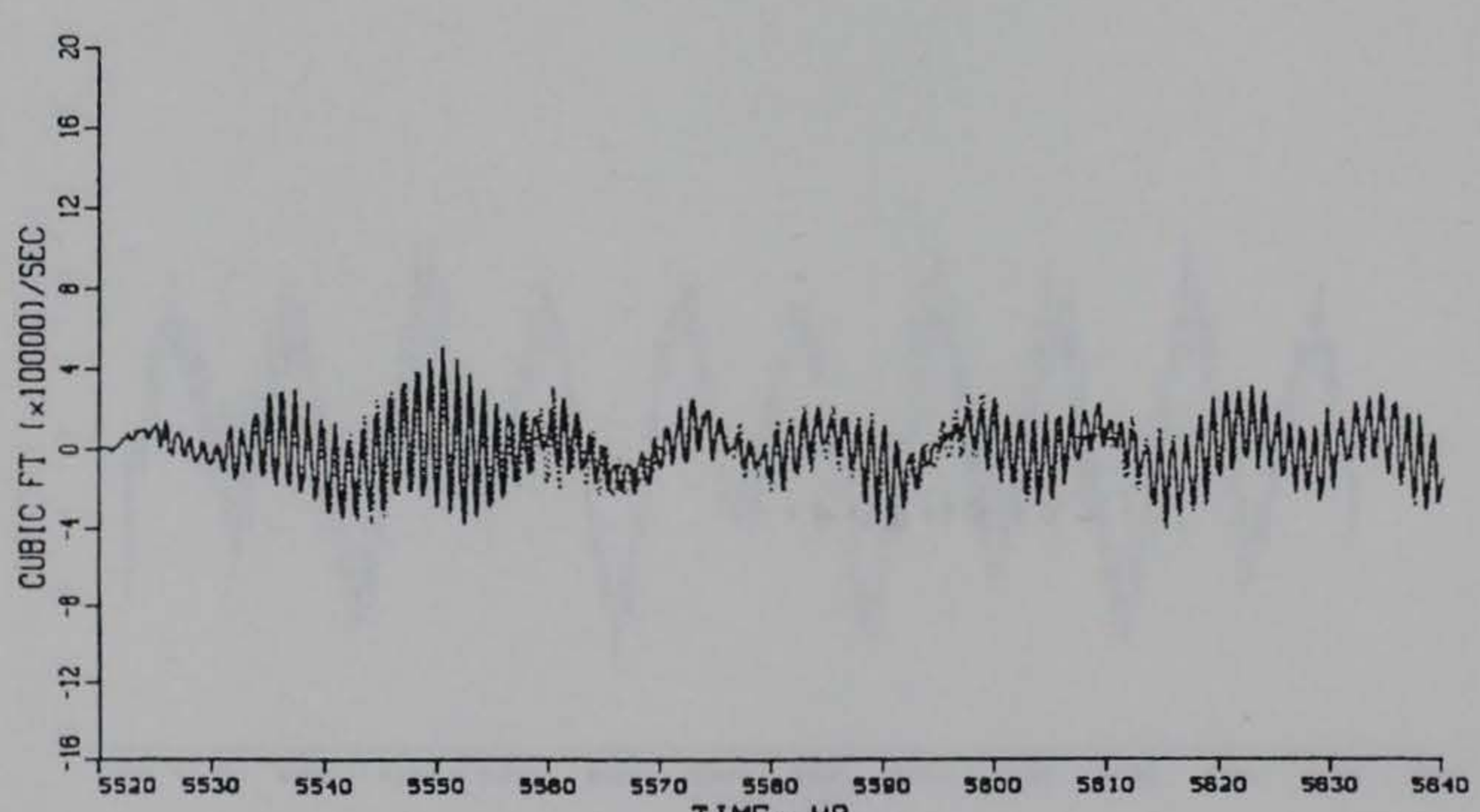

RANGE 2

TIDAL DISCHARGE VERIFICATION PERIOD

PLAN (SOLID) VS EXISTING (DOTTED) CONDITIONS

PLATE 109

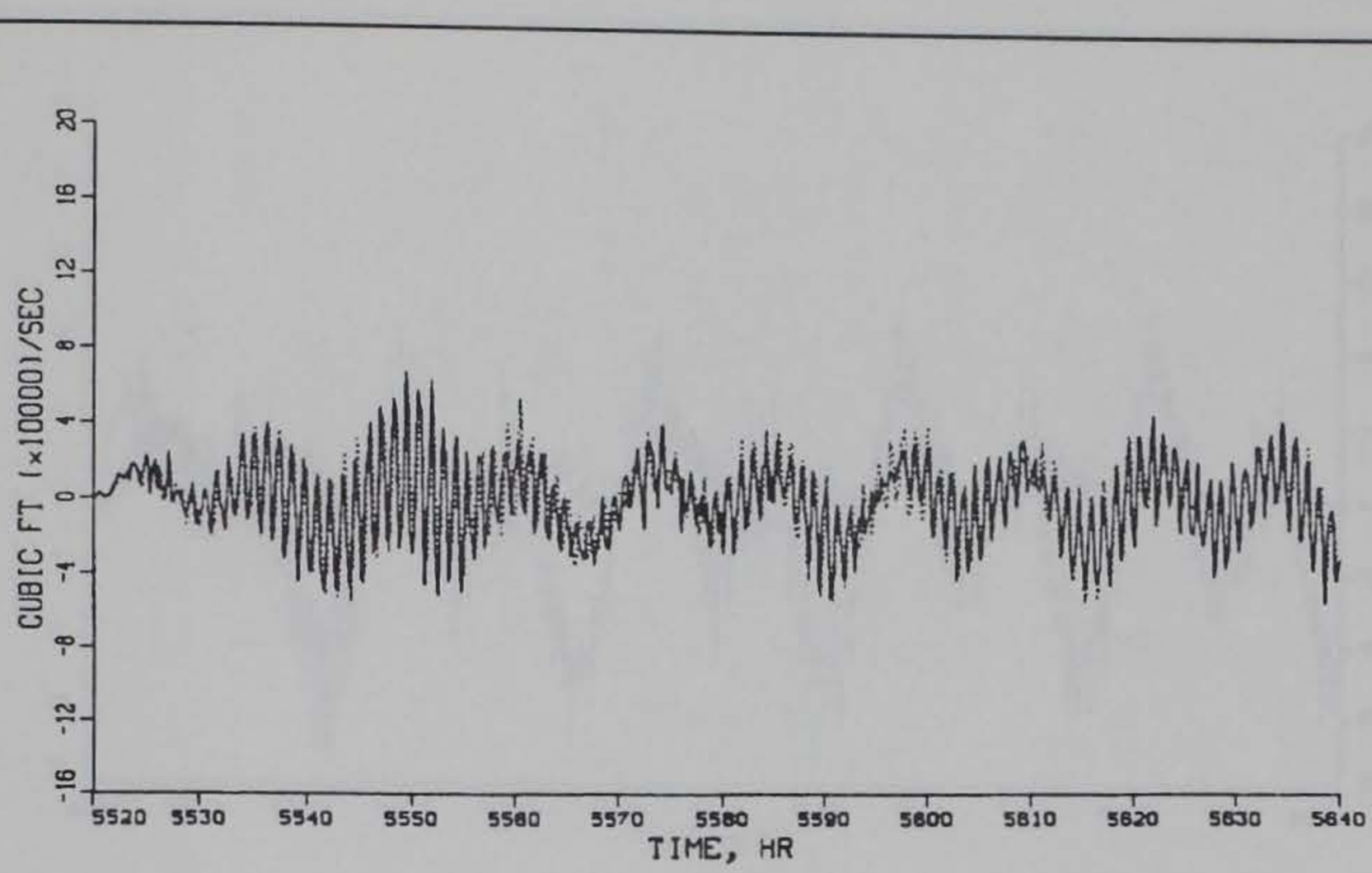

RANGE 3

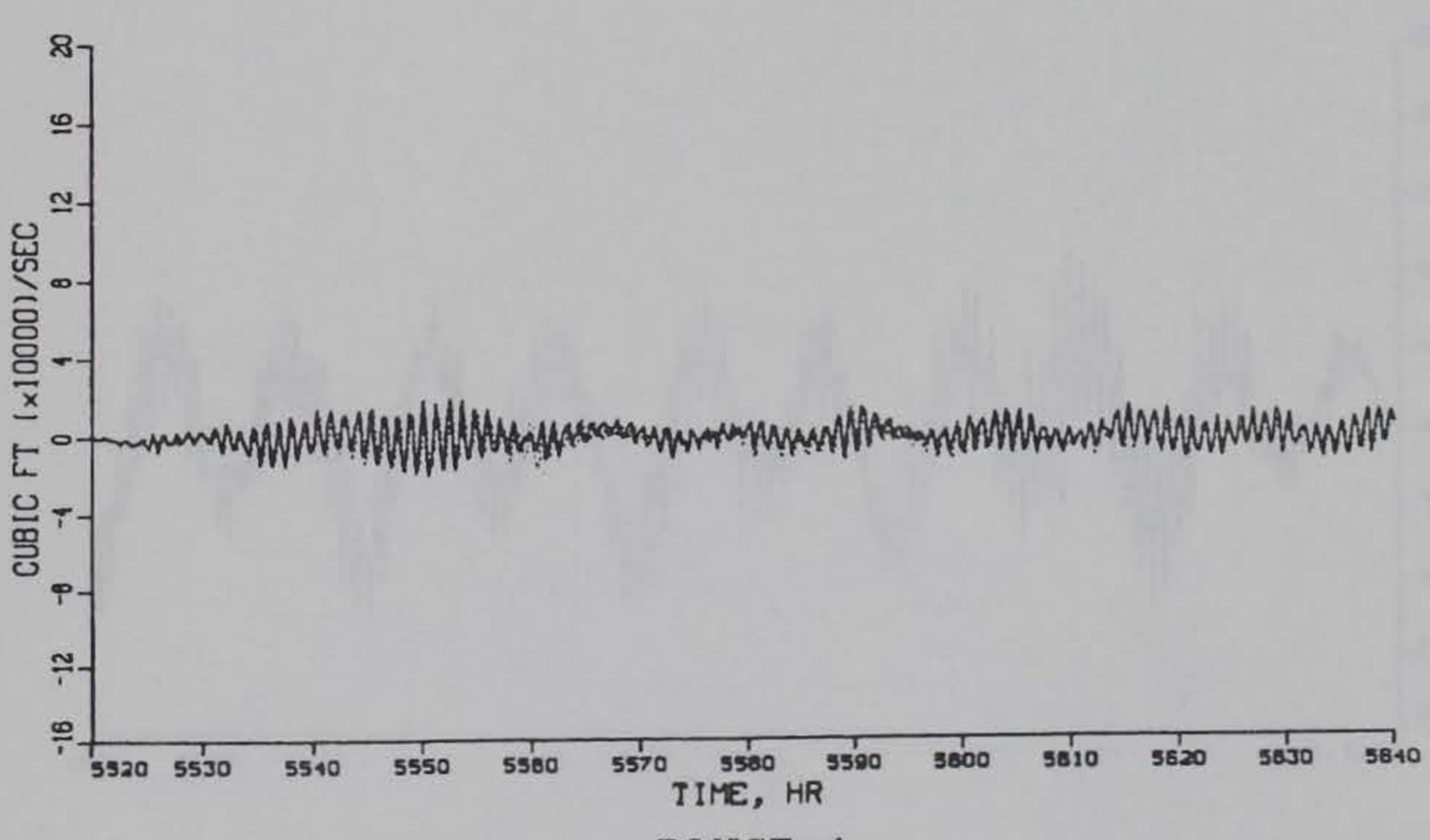

RANGE 4

TIDAL DISCHARGE VERIFICATION PERIOD

PLAN (SOLID) VS EXISTING (DOTTED) CONDITIONS

PLATE 110

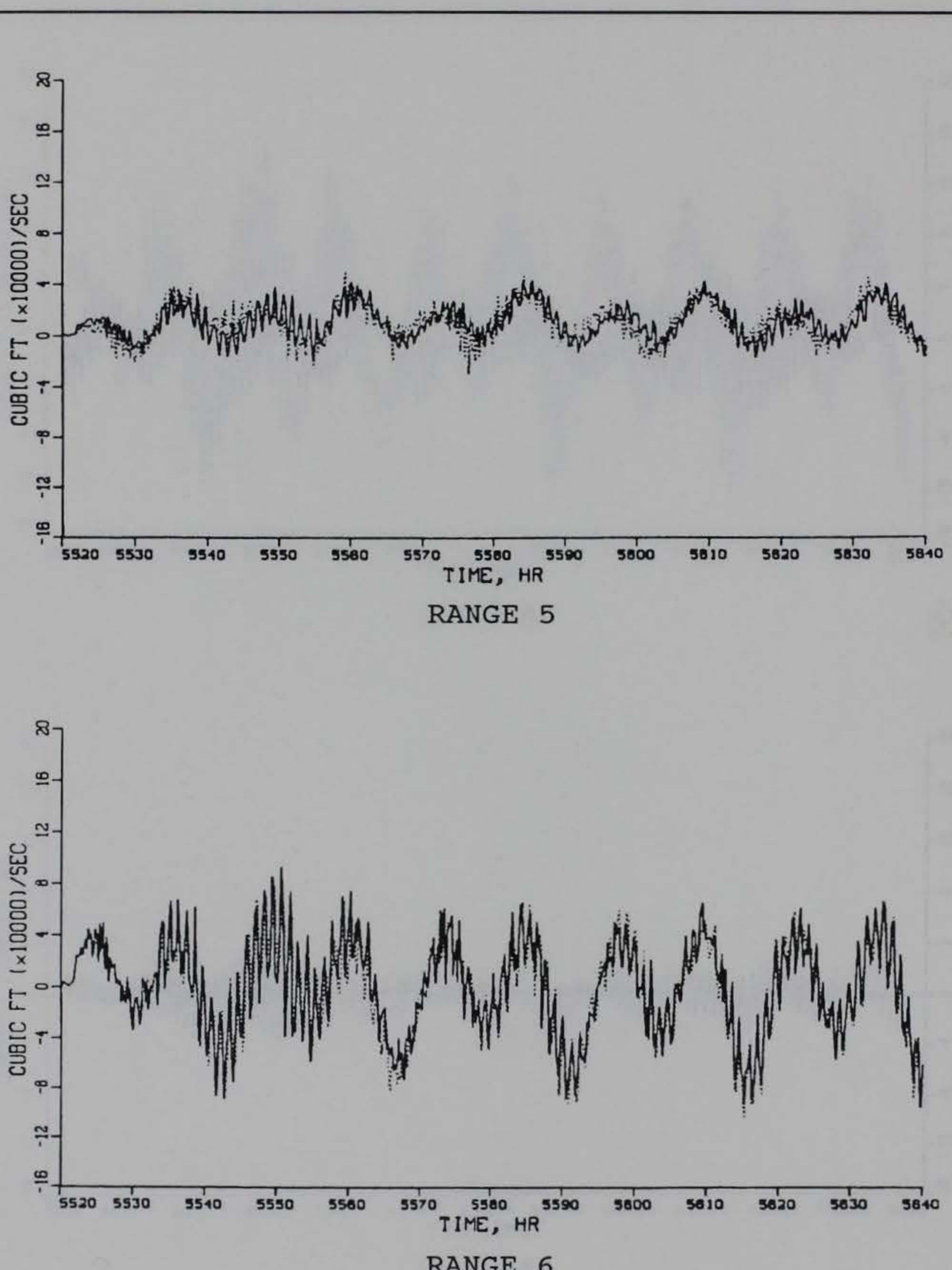

RANGE 5

RANGE 6

TIDAL DISCHARGE VERIFICATION PERIOD

PLAN (SOLID) VS EXISTING (DOTTED) CONDITIONS

PLATE 111

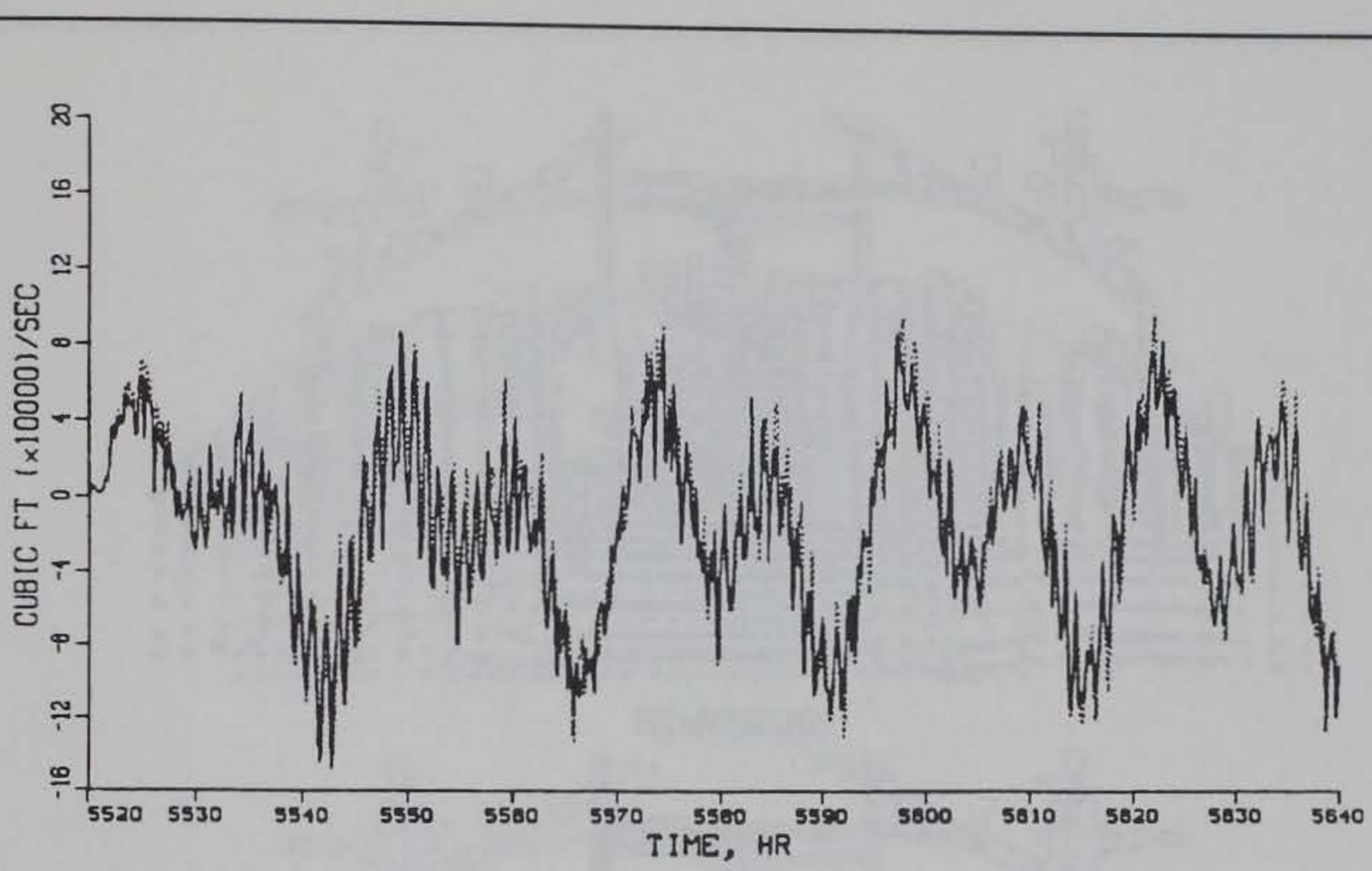

RANGE 7

TIDAL DISCHARGE VERIFICATION PERIOD

PLAN (SOLID) VS EXISTING (DOTTED) CONDITIONS

PLATE 112

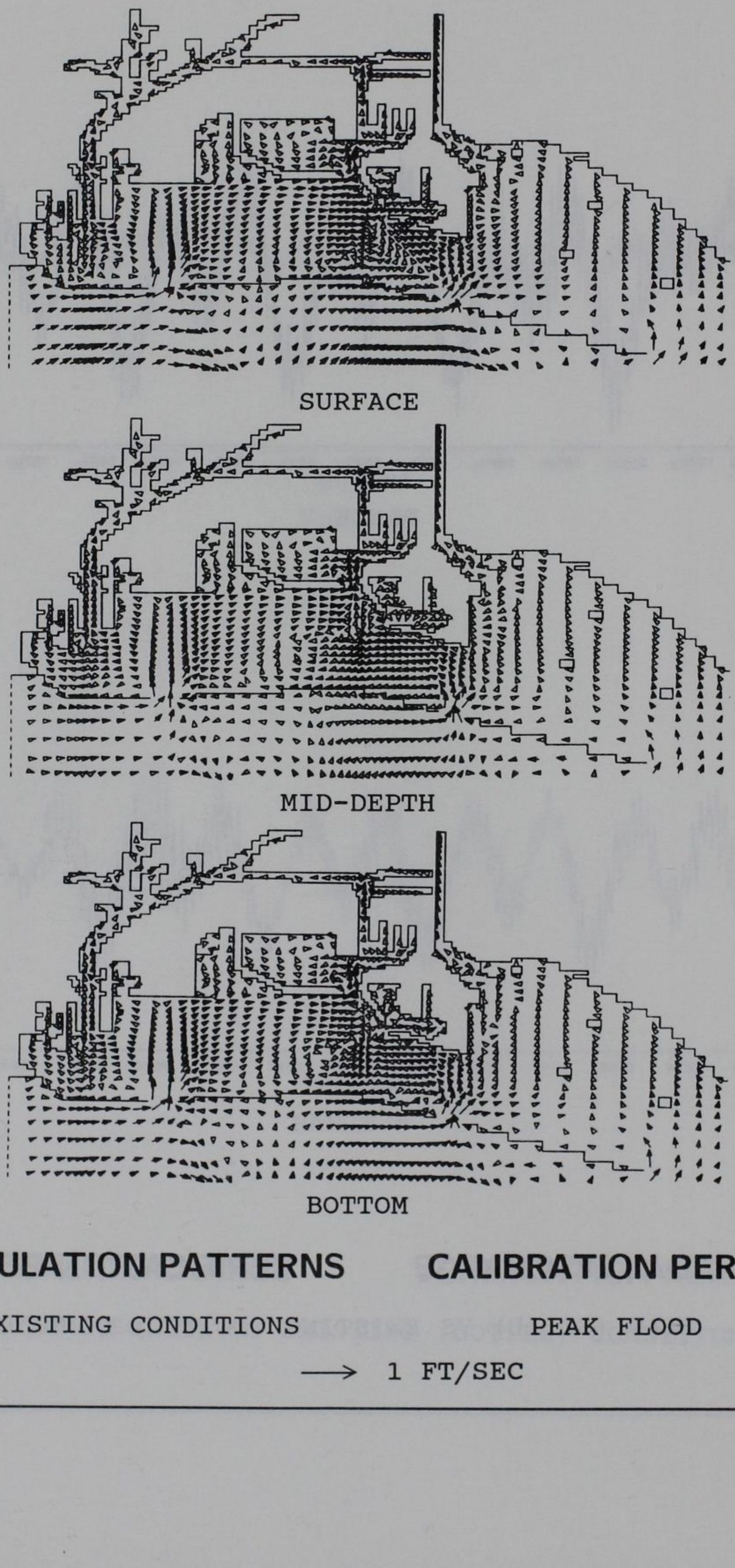

SURFACE

MID-DEPTH

BOTTOM

CIRCULATION PATTERNS **CALIBRATION PERIOD**

EXISTING CONDITIONS PEAK FLOOD

⟶ 1 FT/SEC

PLATE 113

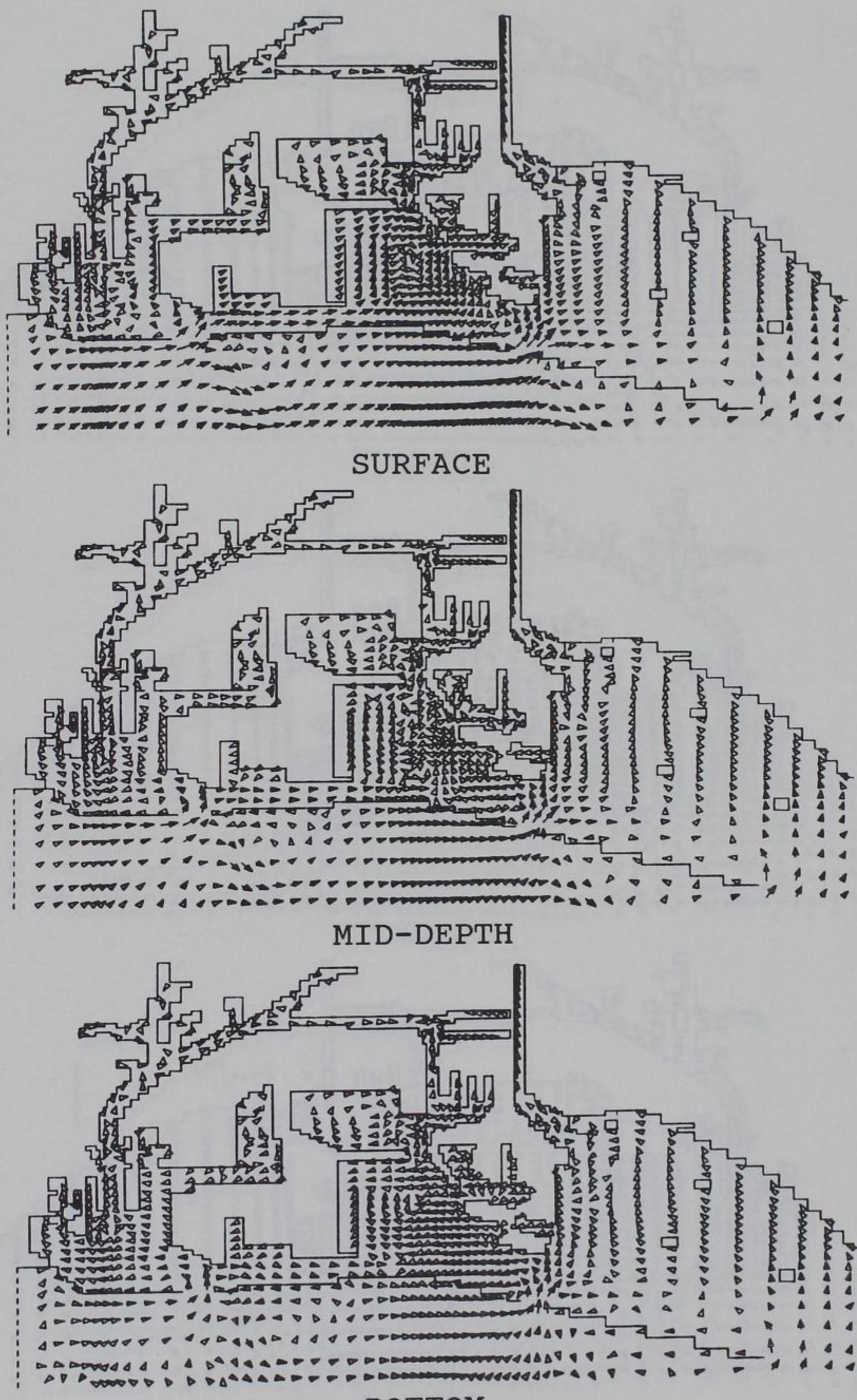

SURFACE

MID-DEPTH

BOTTOM

CIRCULATION PATTERNS

CALIBRATION PERIOD

PLAN CONDITIONS

PEAK FLOOD

⟶ 1 FT/SEC

PLATE 114

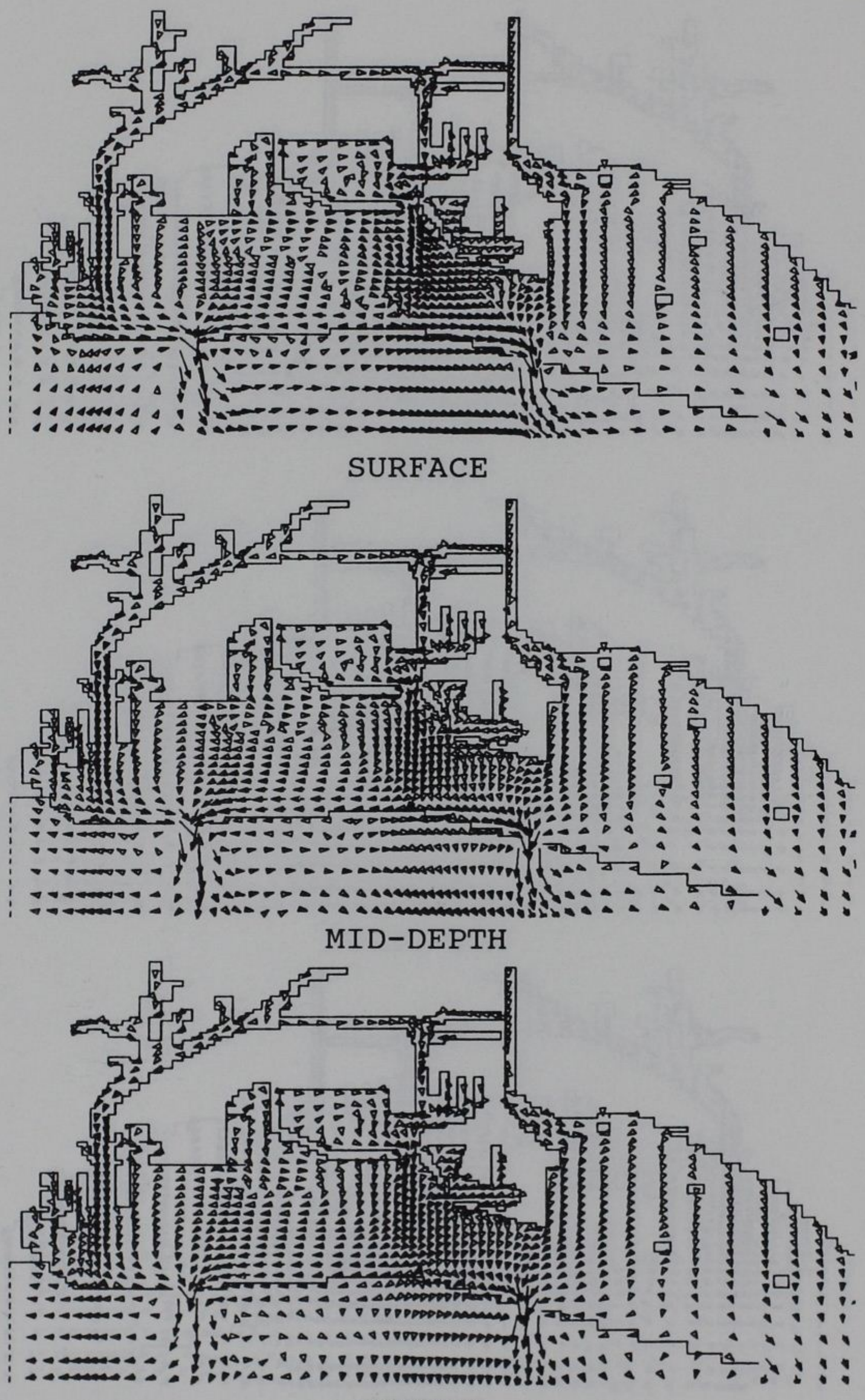

SURFACE

MID-DEPTH

BOTTOM

CIRCULATION PATTERNS CALIBRATION PERIOD

EXISTING CONDITIONS PEAK EBB

⟶ 1 FT/SEC

PLATE 115

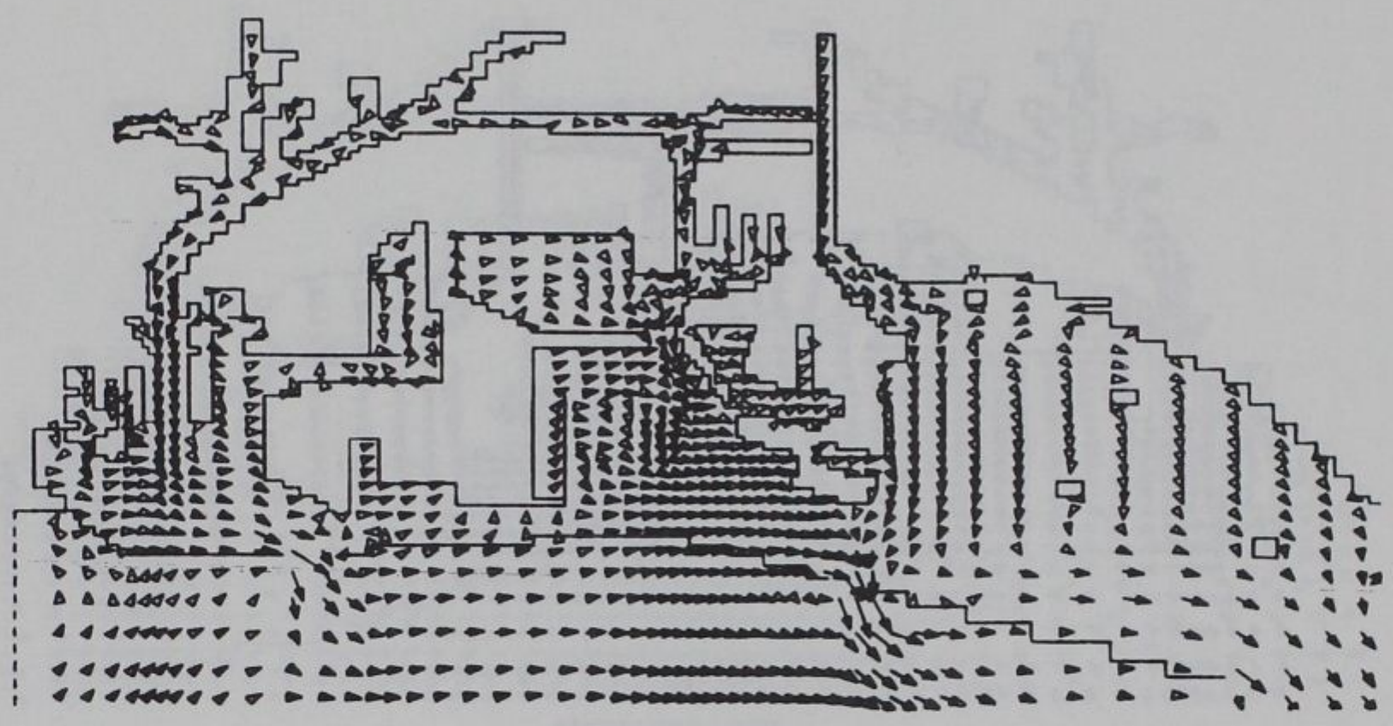

SURFACE

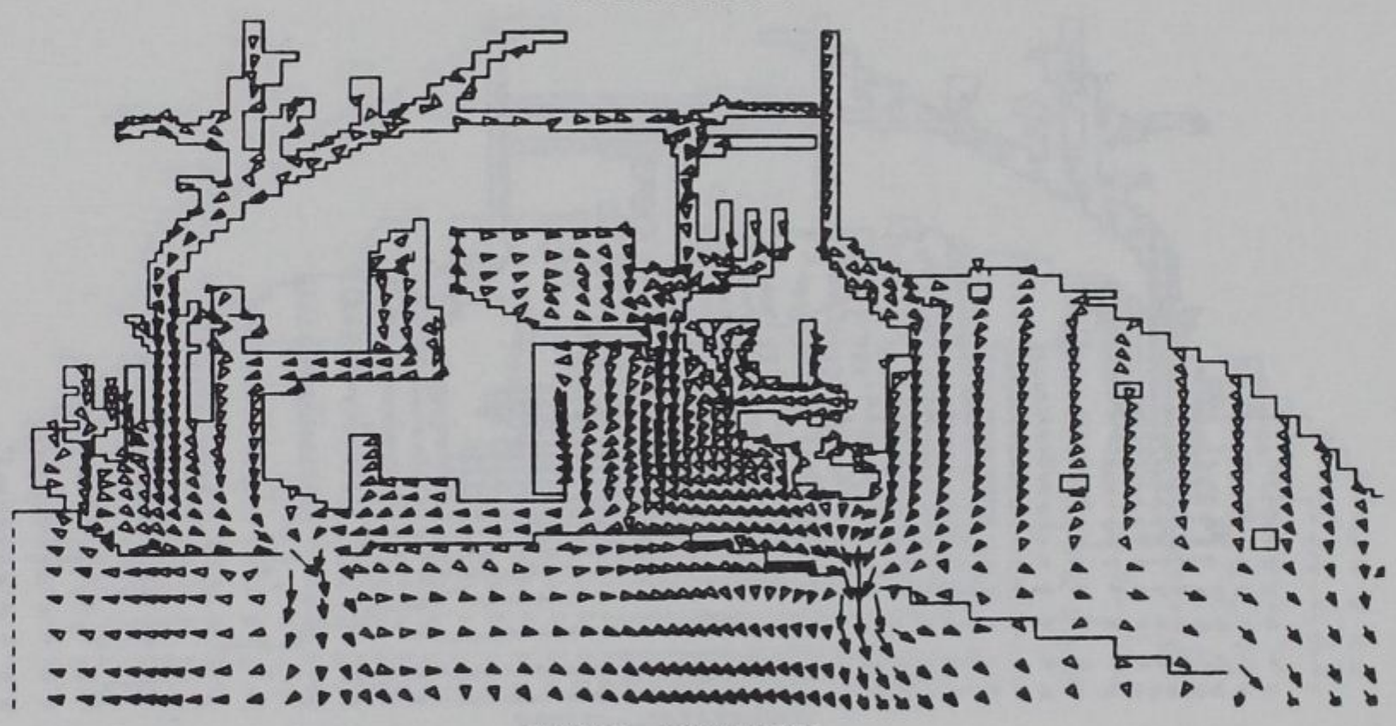

MID-DEPTH

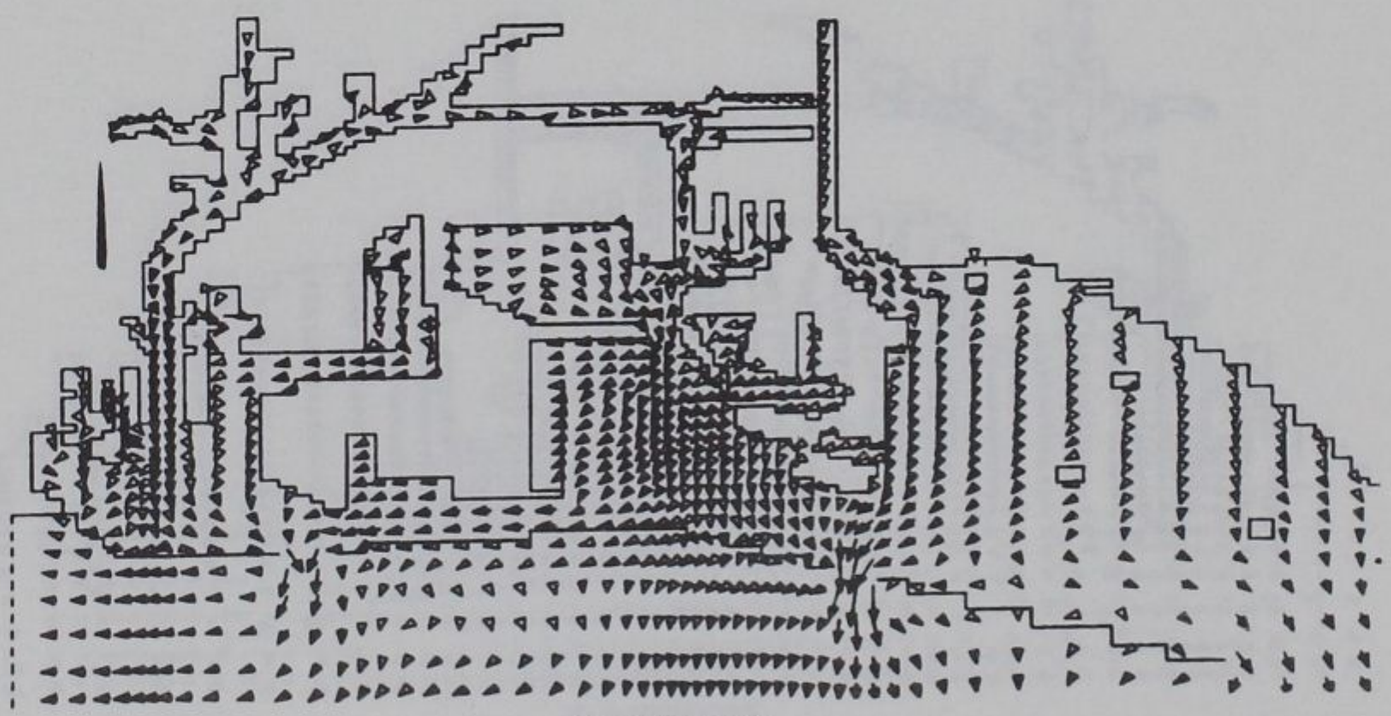

BOTTOM

CIRCULATION PATTERNS

CALIBRATION PERIOD

PLAN CONDITIONS

PEAK EBB

⟶ 1 FT/SEC

PLATE 116

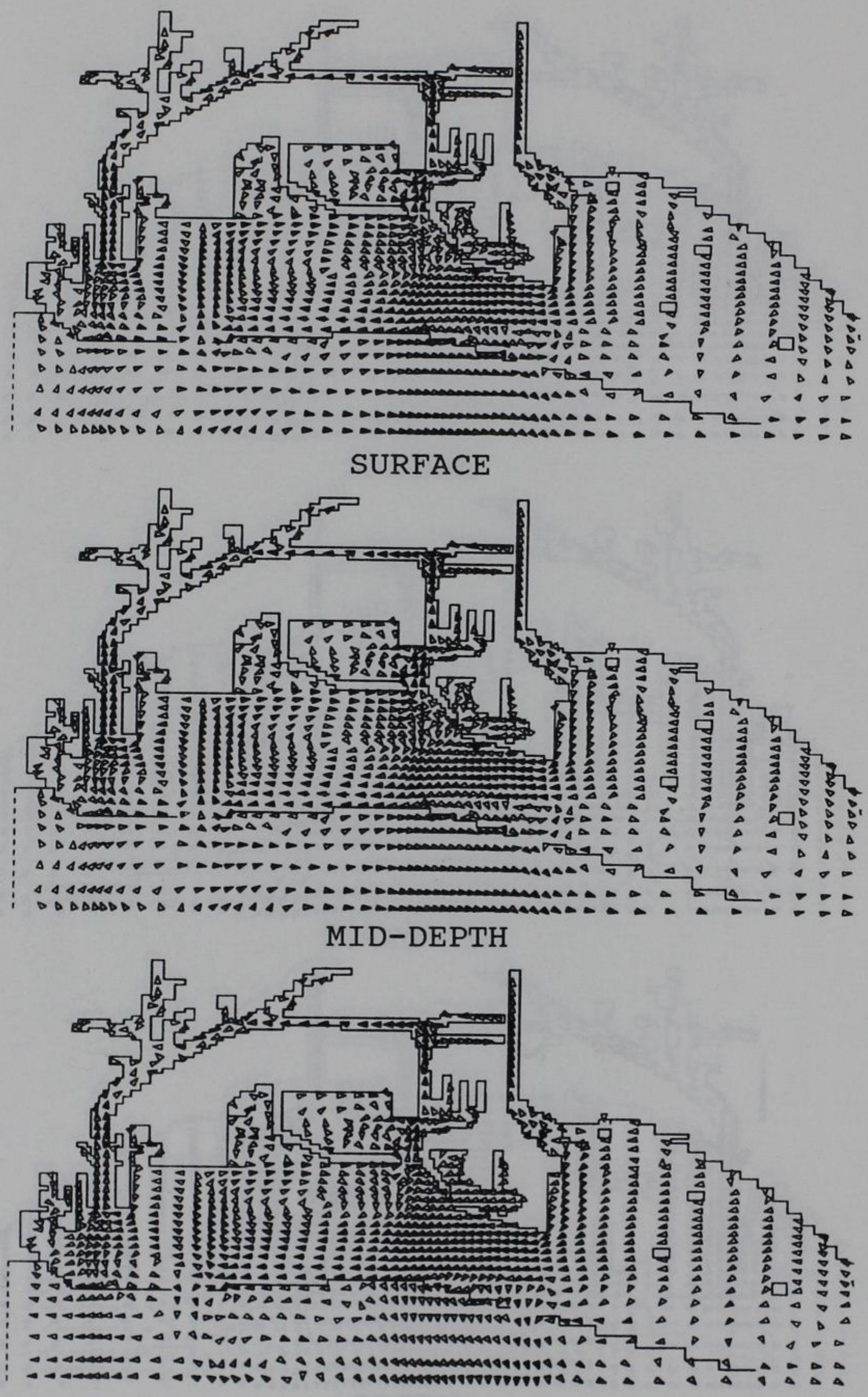

SURFACE

MID-DEPTH

BOTTOM

CIRCULATION PATTERNS

EXISTING CONDITIONS

CALIBRATION PERIOD

SLACK WATER

⟶ 1 FT/SEC

PLATE 117

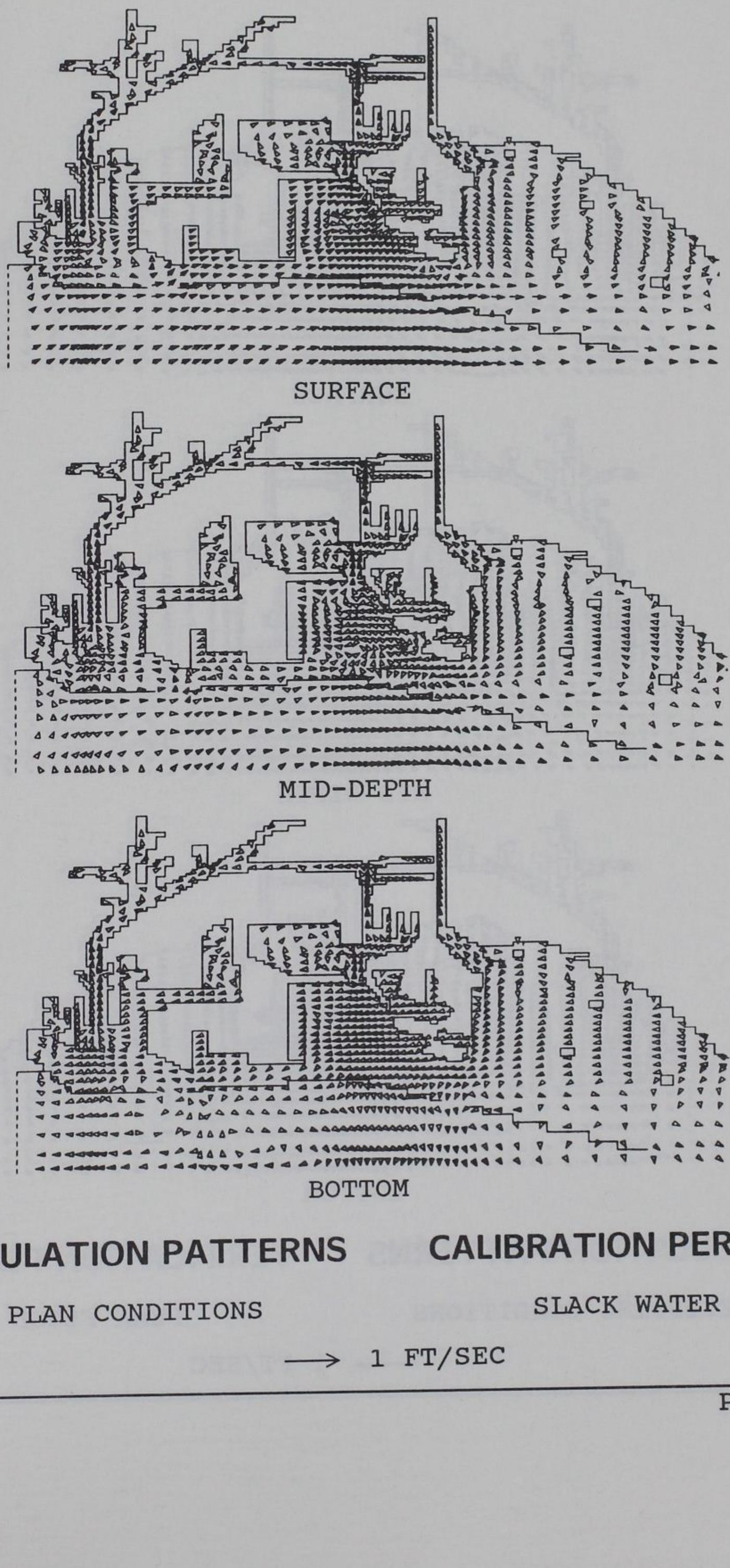

SURFACE

MID-DEPTH

BOTTOM

CIRCULATION PATTERNS

CALIBRATION PERIOD

PLAN CONDITIONS

SLACK WATER

⟶ 1 FT/SEC

PLATE 118

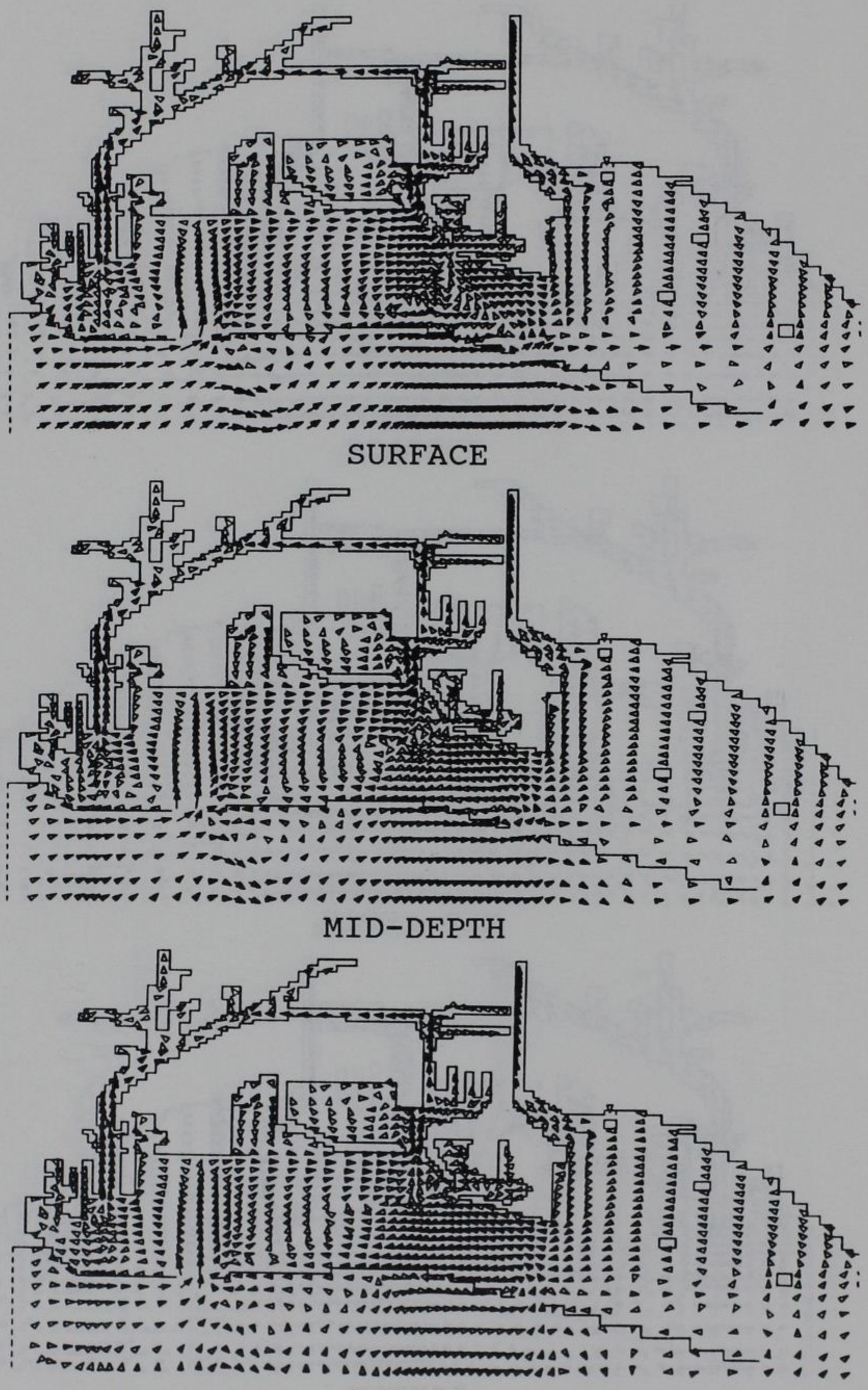

SURFACE

MID-DEPTH

BOTTOM

CIRCULATION PATTERNS

EXISTING CONDITIONS

VERIFICATION PERIOD

PEAK FLOOD

⟶ 1 FT/SEC

PLATE 119

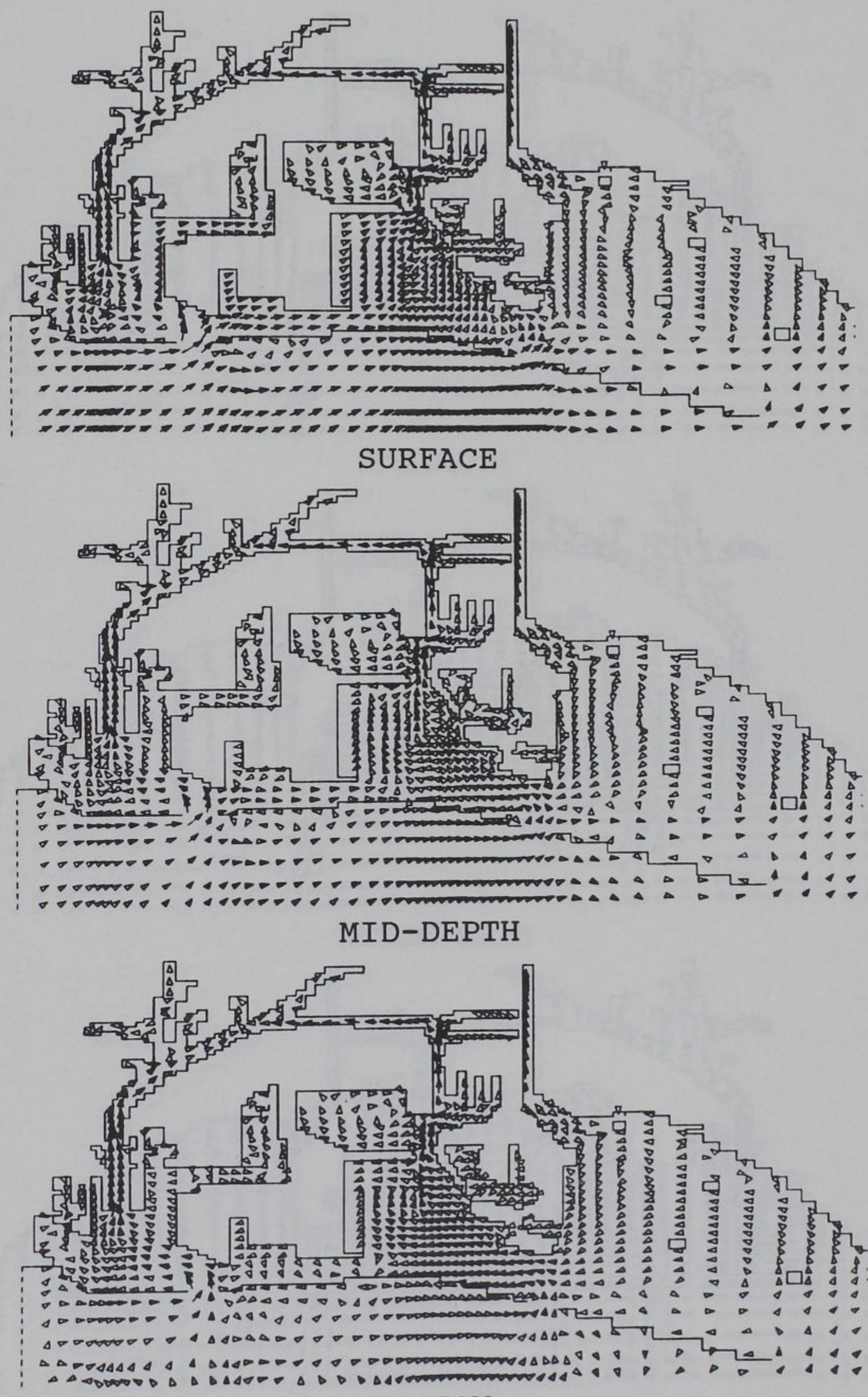

SURFACE

MID-DEPTH

BOTTOM

CIRCULATION PATTERNS

PLAN CONDITIONS

VERIFICATION PERIOD

PEAK FLOOD

⟶ 1 FT/SEC

PLATE 120

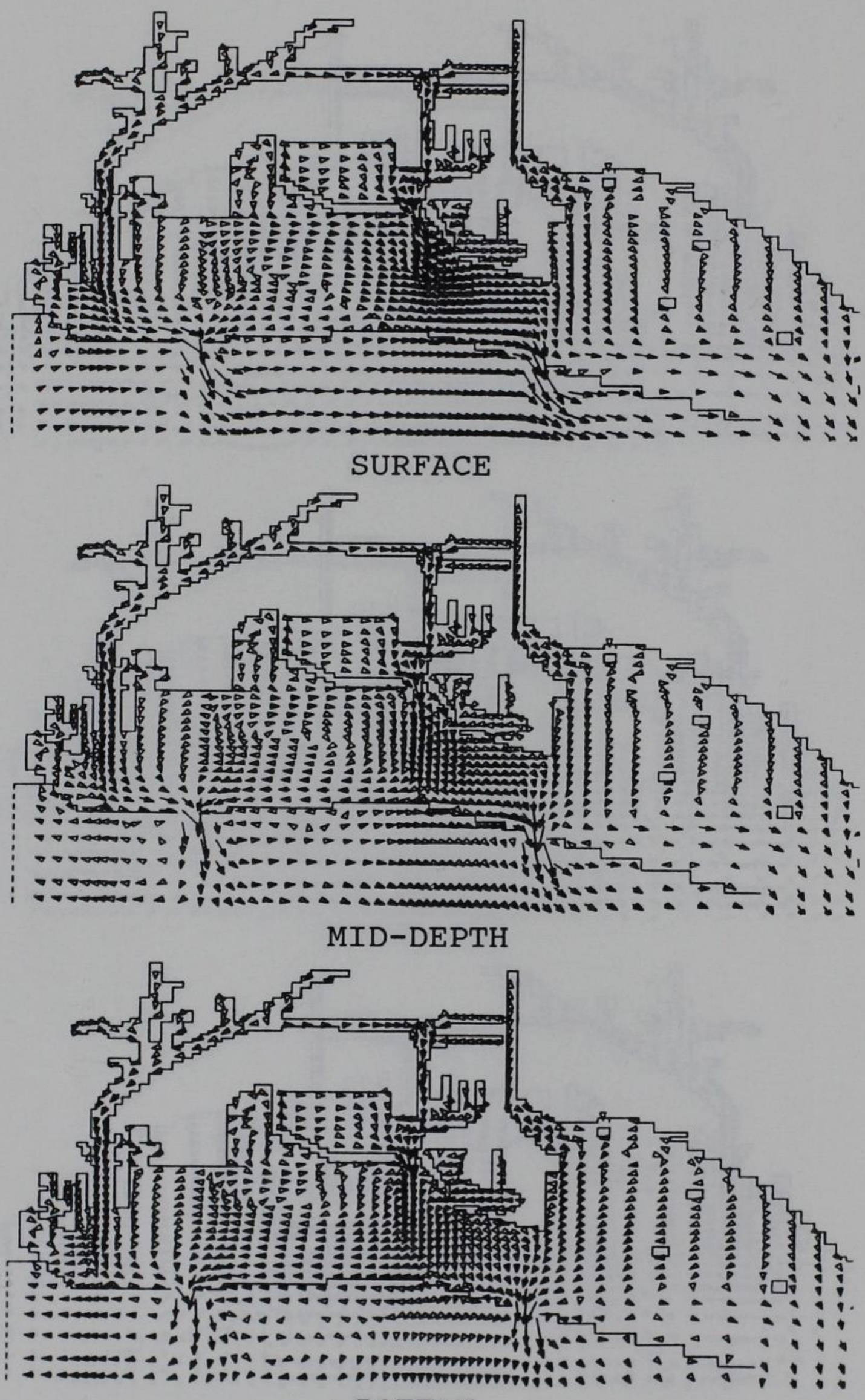

SURFACE

MID-DEPTH

BOTTOM

CIRCULATION PATTERNS VERIFICATION PERIOD

EXISTING CONDITIONS PEAK EBB

⟶ 1 FT/SEC

PLATE 121

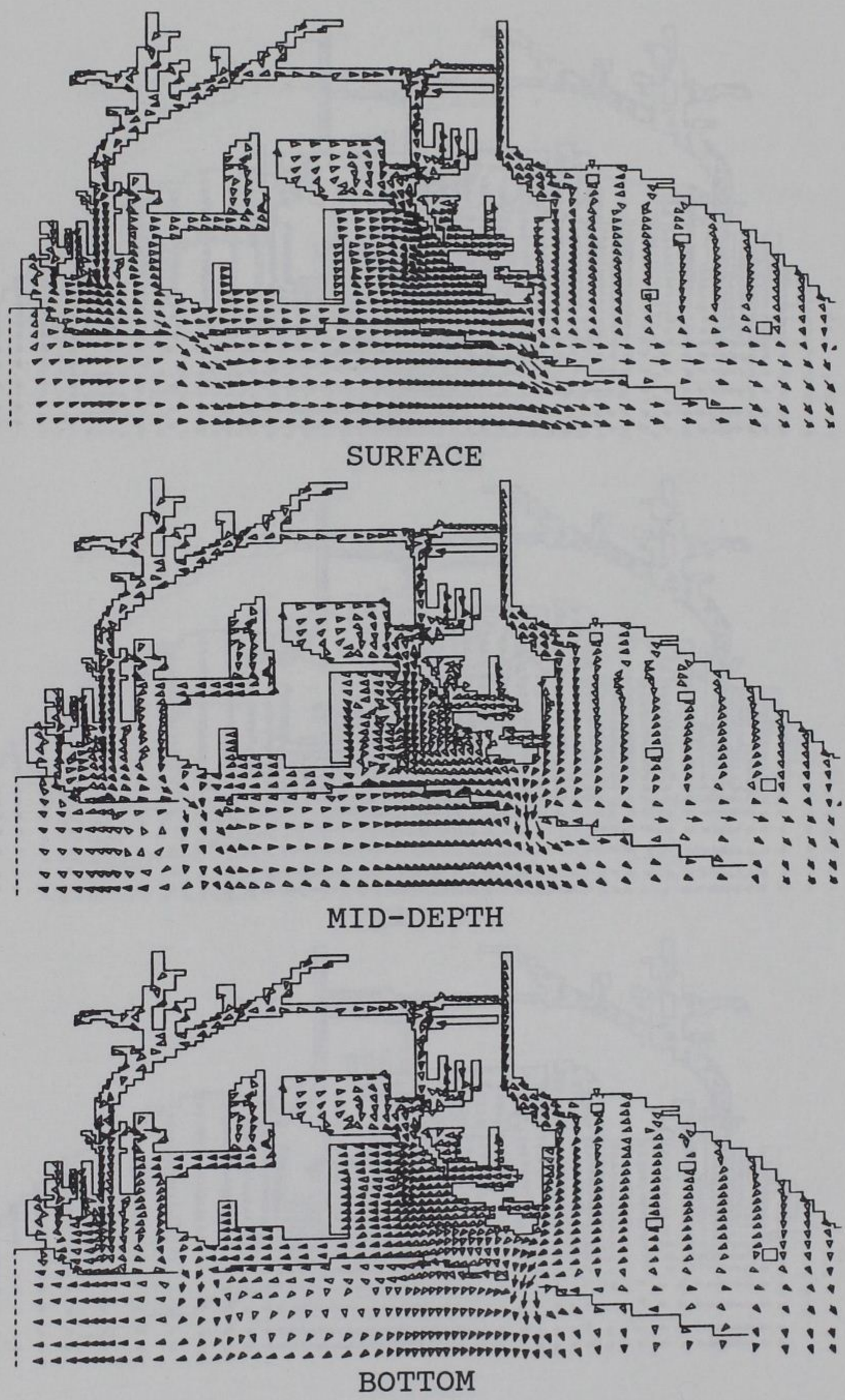

SURFACE

MID-DEPTH

BOTTOM

CIRCULATION PATTERNS

VERIFICATION PERIOD

PLAN CONDITIONS

PEAK EBB

⟶ 1 FT/SEC

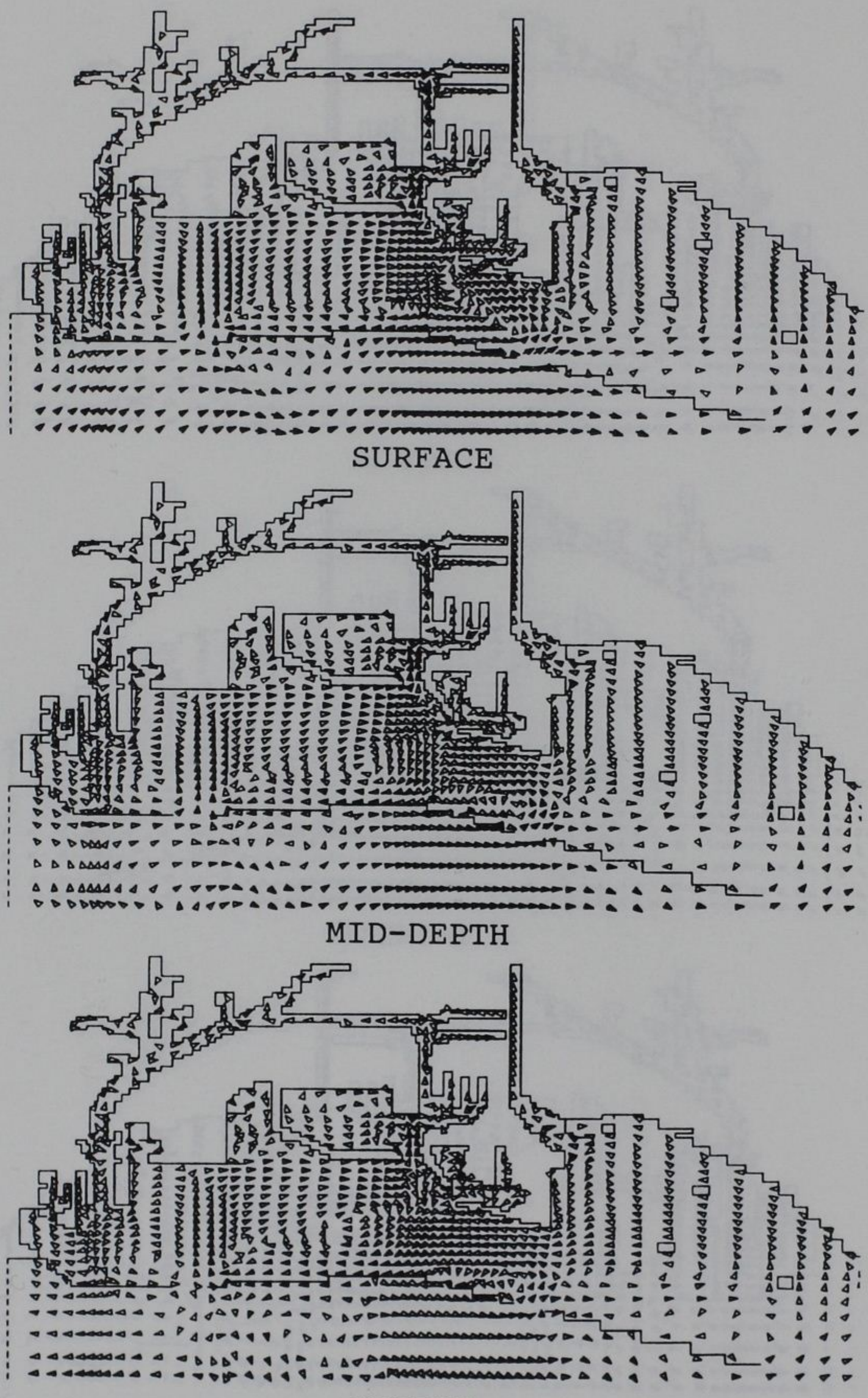

SURFACE

MID-DEPTH

BOTTOM

CIRCULATION PATTERNS

EXISTING CONDITIONS

VERIFICATION PERIOD

SLACK WATER

⟶ 1 FT/SEC

PLATE 123

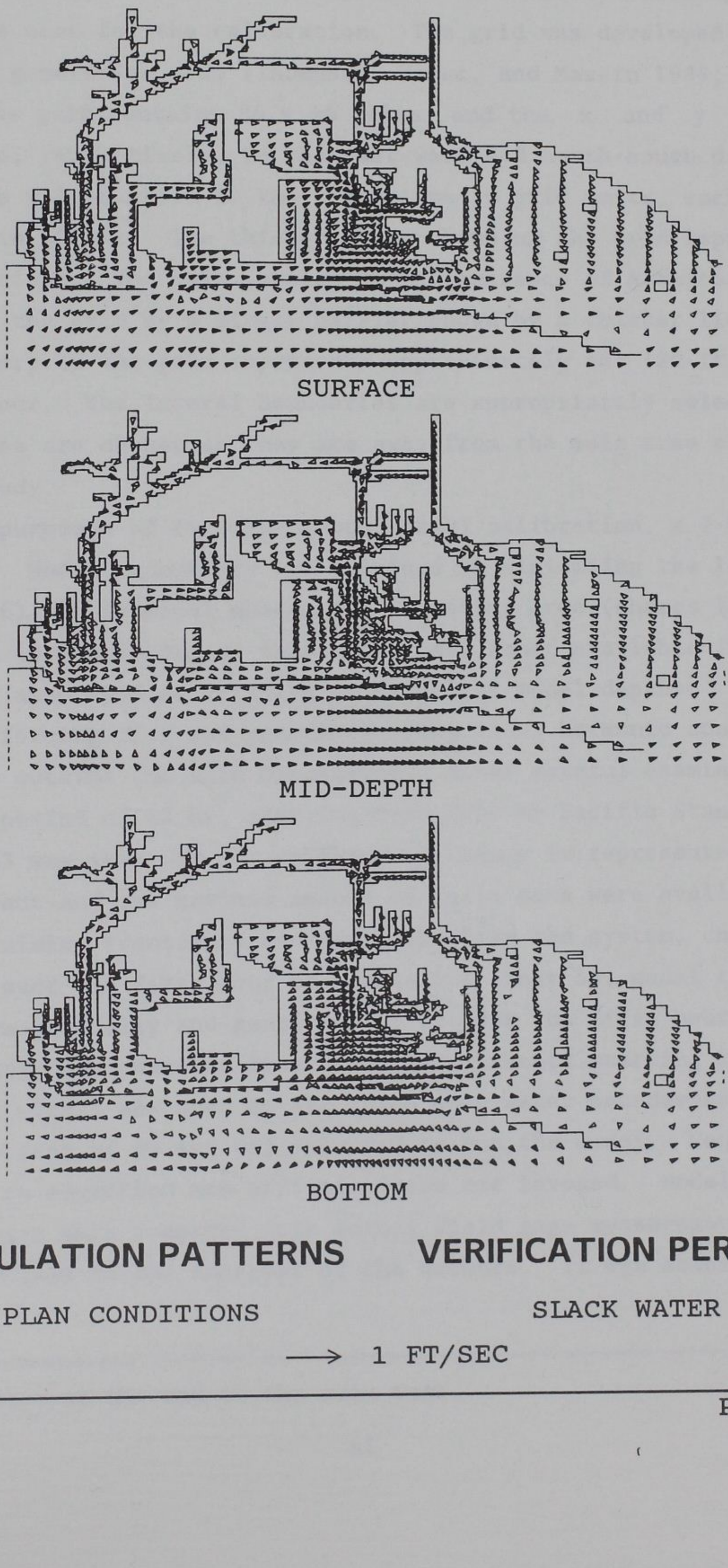

SURFACE

MID-DEPTH

BOTTOM

CIRCULATION PATTERNS VERIFICATION PERIOD

PLAN CONDITIONS SLACK WATER

⟶ 1 FT/SEC

APPENDIX A: MODEL CALIBRATION FOR A CURVILINEAR GRID

1. The hydrodynamic model was first calibrated in two dimensions, using National Ocean Service (NOS) 1983 field data. A boundary-fitted grid (Figure A1) was used for the calibration. The grid was developed using the EAGLE grid generation code (Thompson, Warsi, and Mastin 1984; Thompson 1987a, b*). The grid contains 86 x 46 cells, and the x and y coordinate axes correspond, respectively, to the east-west and north-south directions. Grid coordinate values shown in the figure are in grid units, each grid unit corresponding to 500 ft. The thicker lines shown on the grid represent harbor breakwater sections. The twin jetties at the entrance of Alamitos Bay are represented in the grid by a single barrier shown by a thicker line. The offshore boundary of the grid represents approximately the 120-ft mean lower low water contour. The lateral boundaries are appropriately selected. All three boundaries are chosen so they are away from the main area of interest to the present study.

2. For purposes of two-dimensional (2-D) calibration, a 2-D version of CH3D was used. Model bathymetry was obtained by digitizing the latest available (1986) NOS nautical charts for the study area (charts 18751, 18749, and 18746) and interpolating as necessary. All other available information on bathymetry was also used in arriving at the final model depths.

3. The forcing tide was generated using tidal harmonic constituents for the ocean area outside the main breakwater. After careful examination of the field data, a period of 48 hr, starting from 1200 hr Pacific Standard Time (PST) on 23 June 1983 was selected for calibration, since it represented a large spring tide event and the maximum amount of field data were available for this period. To minimize transients and avoid shock to the system, the tidal signal was feathered over the first hour of simulation (that is, model tides at the boundaries were gradually and gently built up over the first hour so that they matched the real tide computed from tidal constituents starting 1300 hr PST). The same tidal signal was used at all three open-water boundaries to force the model. A time step of 60 sec was selected to run the model. Nonlinear terms corresponding to advection and diffusion were not invoked. Model results for surface elevation were compared with actual field gage measurements at tide gages T660 and T680 in the interior of the harbors. It was observed from the

---

* See References at the end of the main text.

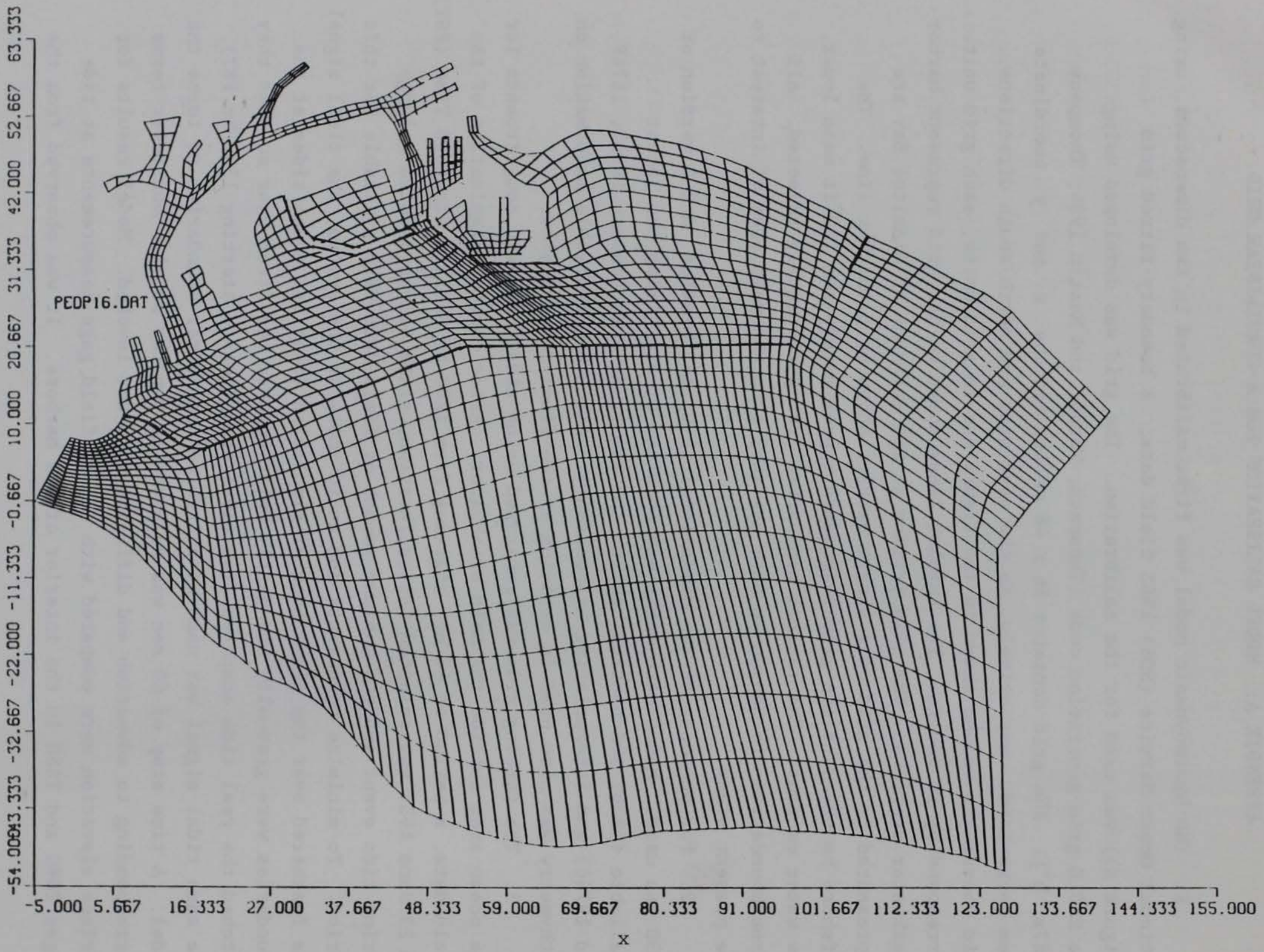

Figure A1. Boundary-fitted grid for San Pedro Bay

comparison that typically the measured and computed tidal ranges were similar, but the measured absolute water levels were higher than model predictions. The difference was on the order of 0.7 ft. Flick and Cayan (1984) reported that the El Nino effect on the southern California coast along with secular sea level rise, and other effects, raised offshore water levels in June and July 1983 by approximately 0.5 to 1.0 ft (0.7 ft at San Diego). Since this effect is not included in the tidal signal generated from constituents, the tidal elevation signal applied at the model boundaries was shifted upward by 0.7 ft, and the model was re-run. A good match was obtained between computed and measured tidal elevations at gages T660 and T680 (Figures A2 and A3) with respect to both magnitude and phase.

4. After the test plan to be investigated was delivered, additional grids were developed to incorporate a grid structure in which all future test plans could be represented. In attempting the detailed calibration process for these grids, it was discovered the skewness of some grid cells caused significant numerical problems that could not be easily overcome (without substantial applied research and development relative to the grid generation program). The weakness in the approach was the inability to develop a practical engineering grid on which stable computations could be made. This fact led to the decision to adopt the dense rectilinear grid used in previous studies of San Pedro Bay (Seabergh and Outlaw 1984).

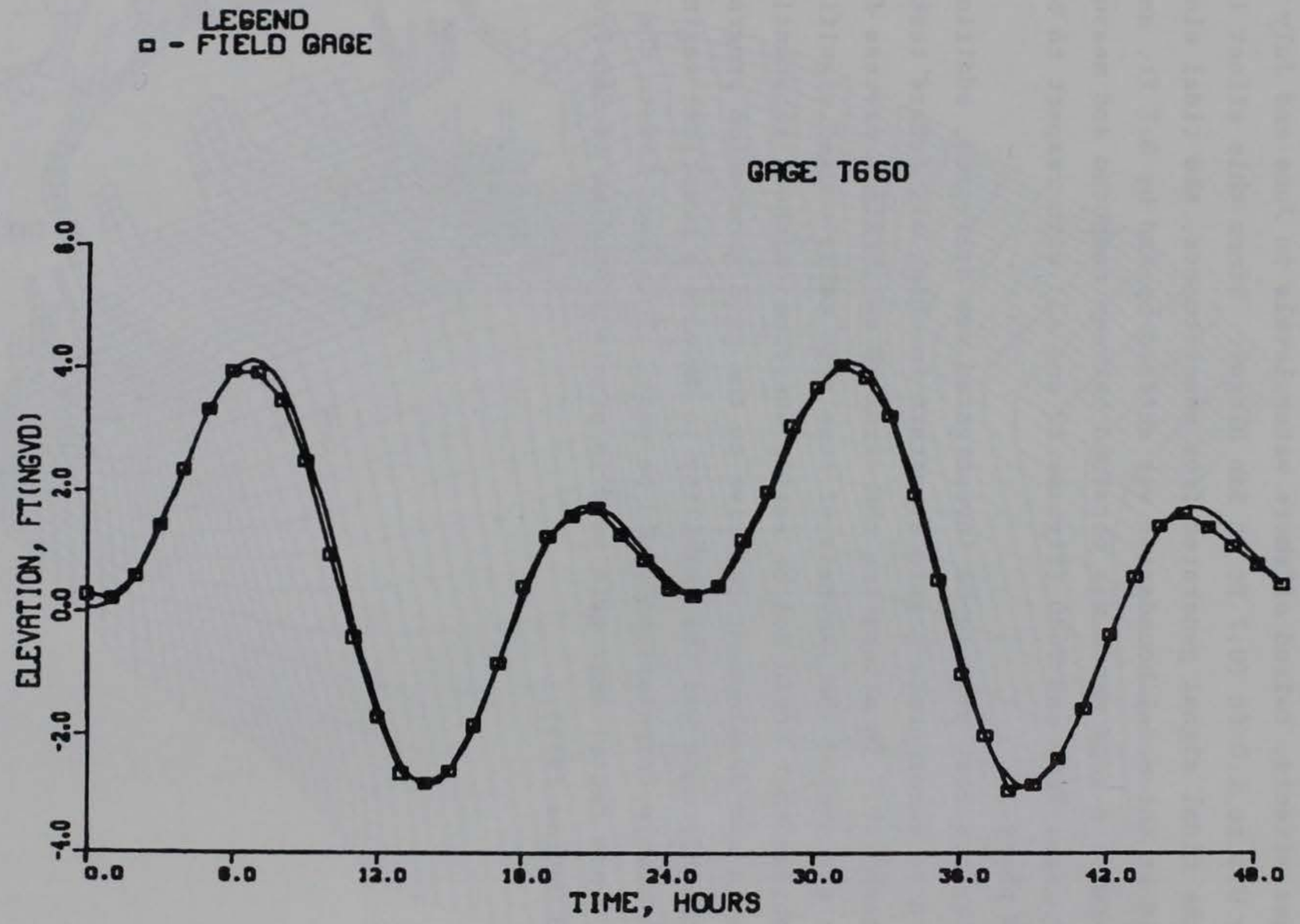

Figure A2. Computed versus observed tidal elevation at Los Angeles Berth 60

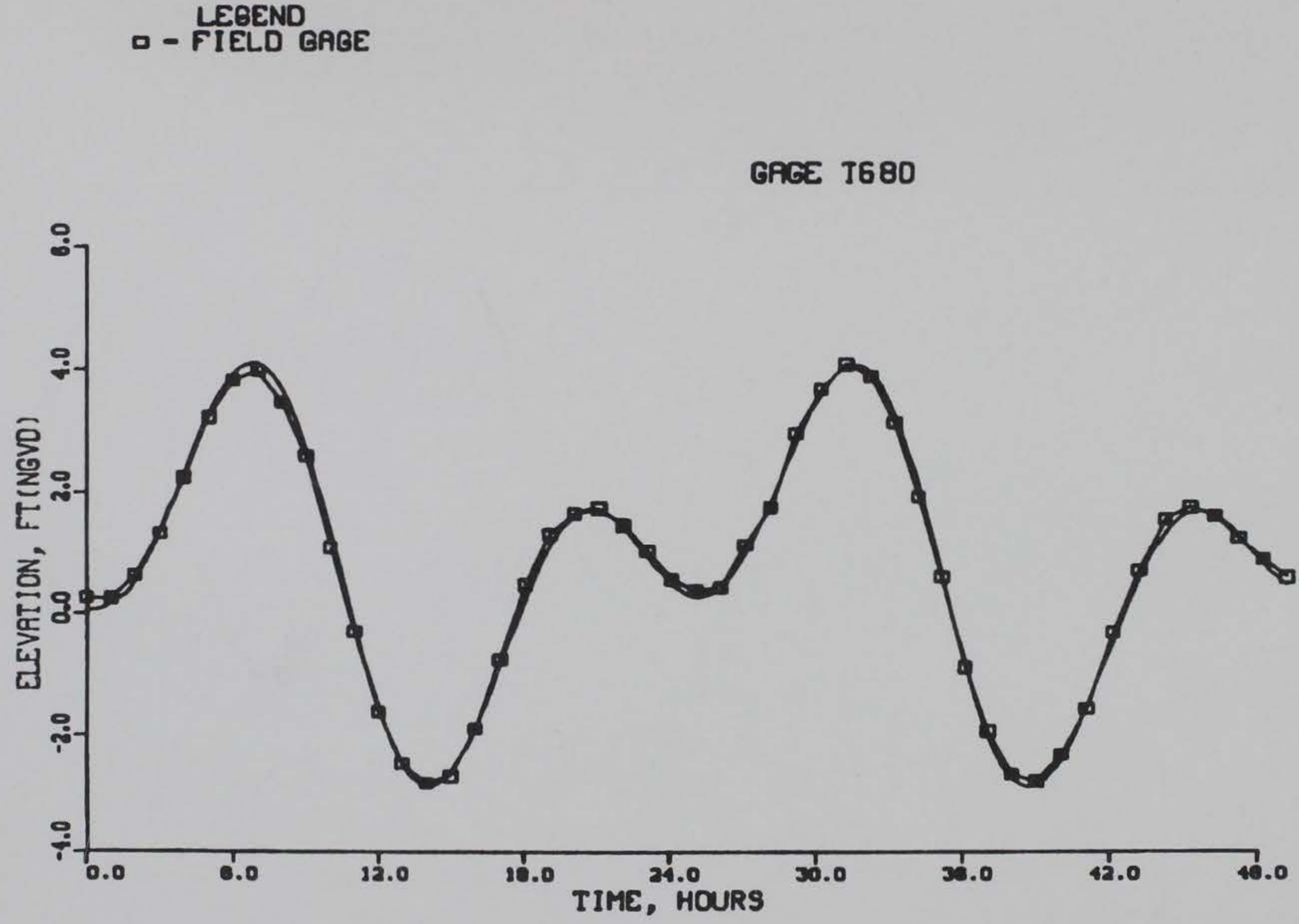

Figure A3. Computed versus observed tidal elevation at Long Beach Pier 2 in West Basin